Abstract Volume
7th Swiss Geoscience Meeting

Neuchâtel, 20th – 21st November 2009

sc | nat

Geosciences
Platform of the Swiss Academy of Sciences

chyn
Centre d'hydrogéologie

7th Swiss Geoscience Meeting, Neuchâtel 2009

Table of contents

http://geoscience-meeting.scnatweb.ch

Organisation

Host Institution

Centre of Hydrogeology of the University of Neuchâtel (Chyn)

Patronnage

Platform Geosciences, Swiss Academy of Sciences

Program Committee

Daniel Ariztegui
Peter Baumgartner
Judit Becze-Deak
Gilles Borel
Thomas Breu
Lionel Cavin
Pierre Dèzes
Hans-Rudolf Egli
Charles Fierz
Karl Föllmi
Alain Geiger
Bernard Grobéty
Martin Hoelzle
Hans Hurni
Adrian Jakob
Eduard Kissling
Rainer Kündig
Ronald Kozel
Neil Mancktelow
Franziska Nyffenegger
Nils Oesterling
Adrian Pfiffner
Marcel Pfiffner
Rolf Philipona
Frank Preusser
Eric Reusser
Bruno Schädler
Urs Schaltegger
Manfred Thüring
Helmut Weissert
Urs Wiesmann
Adrian Wiget
Eric Zechner
François Zwahlen

Local Organizing Committee

François Zwahlen (President)
Sabine Erb
Nico Goldscheider
Philippe Renard
Mario Schirmer

Participating Societies and Organisations

Commission for Research Partnerships with Developping Countries (KFPE)

Commission of Oceanography and Limnology (COL)

International Geographical Union, Commission Geography and Public Policy (IGU)

International Union of Geological Sciences, Swiss Committee (IUGS)

Kommission der Schweizerischen Paläontologischen Abhandlungen (KSPA)

NCCR North-South

Open Source Geospatial Foundation (OSGeo)

Schweizerische Geotechnische Kommission (SGTK)

Swiss Academic Society for Environmental Research and Ecology (SAGUF)

Swiss Agency for Development and Cooperation

Swiss Association of Geologists (CHGEOL)

Swiss Federal Institute of Aquatic Science and Technology (EAWAG)

Swiss Geodetic Commission (SGC)

Swiss Geography Association (SGV)

Swiss Geological Society (SGG/SGS)

Swiss Geological Survey (swisstopo)

Swiss Geomorphological Society (SGGm/SSGm)

Swiss Geophysical Commission (SGPK)

Swiss Hydrological Commission (CHy)

Swiss Society for Hydrogeology SGH

Swiss Society for Hydrology and Limnology (SGHL / SSHL)

Swiss Meteorological Society (SGM)

Swiss National Science Foundation

Swiss Paleontological Society (SPG/SPS)

Swisspeace Foundation

Swiss Society for Quaternary Research (CH-QUAT)

Swiss Snow, Ice and Permafrost Society (SIP)

Swiss Society of Mineralogy Petrography (SMPG / SSMP)

Plenary Session, Friday November 20th

Water Across Boundaries

Espace Louis-Agassiz 1, Aula des Jeunes-Rives, Neuchâtel

14:00 - 14:15	François Zwahlen President SGM 2009	Opening address
14:15 - 14:45	Gordon Young President IAHS	Scientific understanding: essential for sound water resources management (Joint IUGG-CH & IUGS-CH Union Lecture)
14:45 - 15:15	Janet Hering EAWAG	Geochemical Perspectives on Water Quality
15:15	**Coffee break**	
15:45 - 16:15	Steven Ingebritsen United States Geological Survey, USGS	The Role of Groundwater in Geologic Processes
16:15 - 16:45	Robert Cramer Conseil d'Etat de Genève	L'eau : élément fédérateur de la politique transfrontalière
16: 45 - 16:50	*Musical Interlude*	
16:50 - 17:40	Helmut Weissert Bernard Grobéty Pierre Gander Christian Meyer Martin Hoelzle Gilles Borel Daniele Biaggi Christoph Heinrich	Communications Platform Geosciences Presentation SGM 2010 in Fribourg Communication Erlebnis Geologie 2010 Swiss Commission of Palaeontology Prize Swiss Snow, Ice and Permafrost Society Prize Swiss Geological Society Award CHGEOL Award Paul Niggli Medal
17:40 - 17:45	*Musical Interlude*	
17:45 - 18:00		Nexans Award
18:00 - 18:05	*Musical Interlude*	
18:05 - 19:30		Aperitif & Posters
20:00	**Swiss Geoscience Party** = "Cocktail Dînatoire" on a boat in the port of Neuchâtel (reservation required)	

0. Plenary Session

1

Geochemical Perspectives On Water Quality

Janet G. Hering

eawag, Überlandstrasse 133, Dübendorf, Switzerland
janet.hering@eawag.ch

As a sustainable source of safe drinking water, groundwater has many advantages over surface water, most notable its natural protection from the pathogens that are a leading cause of child mortality in developing countries. As tragically illustrated in South and Southeast Asia, however, consumption of groundwater can also pose health risks due to exposure to geogenic contaminants. This presentation will examine the biogeochemical controls on groundwater quality, particularly the concentration of the geogenic contaminants arsenic and fluoride. The occurrence and mobility of geogenic contaminants will be discussed in terms of the composition of geological source materials and the biogeochemical processes by which geogenic contaminants are mobilized and sequestered.

2

The Role of Groundwater in Geologic Processes

S.E. Ingebritsen

U.S. Geological Survey, Menlo Park, California, USA

Historically, interest in groundwater and other subsurface fluids was confined to a few specific disciplines in the earth sciences, notably groundwater hydrology, soil physics, engineering geology, petroleum geology, and petroleum engineering. These disciplines tended to be “applied” in nature, with practitioners concentrating on the immediate and practical problems of water supply, water quality, mine dewatering, deformation under structural loads, and the location and recovery of fluid hydrocarbons. This situation has changed over the past few decades. Hydrogeologists and geologists are now actively exploring the role of groundwater and other subsurface fluids in such fundamental geologic processes as crustal heat transfer, ore deposition, hydrocarbon migration, earthquakes, tectonic deformation, diagenesis, and metamorphism. This talk will emphasize (1) the links between groundwater processes and deformation, seismicity, and permeability and (2) recent advances in understanding of fluid flow and heat transfer at the mid-ocean ridge.

3

Scientific understanding: essential for sound water resources management

Gordon Young

President, International Association of Hydrological Sciences

The presentation looks at water from the perspectives of the freshwater hydrologist and the manager of water resources and examines the theme of the meeting – "Water across boundaries" – from a number of different view points.

Hydrological sciences are placed within the broader context of earth sciences and various "boundaries" are considered:

- between hydrology and atmospheric and ocean sciences;
- between hydrology and the biological sciences;
- between hydrology and volcanic activity.

Within hydrology various "boundaries" are considered:

- between the various phases of water – solid, liquid and gaseous;
- between surface waters, soil moisture and groundwaters.

The interactions between hydrology and human activities are then considered both from the impact of humans on the hydrological cycle through changes in land surface characteristics, through the impact of dams and diversions and through the introduction of pollutants from a variety of sources into the hydrological system.

Water managers must be concerned with a number of human needs for water which must always be balanced by consideration of impacts on the natural environment. They must bridge the divides between hydrological knowledge and understanding and the need to manage wisely for the betterment of the human condition and must learn to use hydrological knowledge to better inform their management decisions. They must also think across the "boundaries" between the various uses and challenges of water:

- Water for the basic human needs of food security and health;
- Water for social development;
- Water for economic development – the need for water for energy and for industry;
- Water security from floods and droughts and pollution spills;
- Water for the essential maintenance of natural ecosystems.

Thus they need to consider the management of water challenges in an integrated fashion – this is the rationale for Integrated Water Resources Management; a mental challenge to cross sectoral boundaries.

The challenges for the water managers do not end here; water almost always flows across administrative boundaries whether these be at the very local level between neighbouring houses or settlements, or at provincial or state level (The Cantonal level in the case of Switzerland) or at international level. And the flow of water is not only on the surface of the land but also within aquifers at depth. Not only does water physically flow across administrative boundaries but there are divides between the bureaucracies at these various administrative levels – and those "boundaries" must also be crossed.

Lastly the water manager must bridge the divides between actions within the "water box", ie the need to think holistically when considering the suite of water uses and challenges, and the positioning of water issues within the much broader framework of social and economic development. These last divides are perhaps the most difficult navigate.

1. Water across (scientific) boundaries

Eduard Hoehn, Adrian Jakob, Ronald Kozel, Urs Mäder, Bruno Schädler, Mario Schirmer

Swiss Hydrological Commission CHy, Swiss Society for Hydrogeology SGH, Swiss Society for Hydrology and Limnology SGHL, Rock-Water Interaction Group, Uni Bern, Eawag Swiss Federal Institute of Aquatic Science and Technology

1.27 Marzocchi R., Pera S.: Groundwater and tunneling: implementation of a geochemical monitoring network in the southern Switzerland

1.28 MBock P., Loizeau J.-L.: Dynamics of colloid concentrations in a small river related to hydrological conditions and land use

1.29 Molnar P., Perona P., Burlando P.: Water disturbance as the organizer of riparian vegetation

1.30 Nitsche M., Badoux A., Turiwski J.M., Rickenmann D.: Calculating bedload transport rates in Swiss mountain streams using new roughness approaches

1.31 Niwa N., Rossi L., Chèvre N.: Pollution des eaux: la santé est-elle un levier pour mettre en place une gestion intégrée à l'echelle du basin versant?

1.32 Preisig G., Perrochet P.: Effective stress and fracture permeability in regional groundwater flow: numerical comparison of analytical formulas

1.33 Rickenmann D.: Debris flows, landslides, and sediment transport in mountain catchments

1.34 Schill E., Abdelfettah Y., Altwegg P., Baillieux P.: Characterisation of geothermal reservoirs using 3D geological modelling and gravity

1.35 Schnegg P.-A.: Field Fluorometer for Simultaneous Detection of 3 Colourless Tracers

1.36 Schwank M., Völksch I., Mätzler Ch., Stähli M.: Recent Research on the Remote Retrieval of Soil Moisture from Space with Microwave Radiometry

1.37 Sinreich M., v. Lützenkirchen V., Matousek F., Kozel R.: Groundwater Resources in Switzerland

1.38 Steinmann M., Pourret O.: The role of the colloidal pool for transport and fractionation of the rare earth elements in stream water

1.39 Tonolla M.: Microbial communities in the steep gradients of the meromictic lake Cadagno

1.40 Vennemann T., Fontana D., Paychere S., Ambadiang P., Piffarerio R., Favre L.: Dissolved inorganic carbon and its stable isotope composition as a tracer of geo-, bio-, and anthropogenic sources of carbon

1.41 Vogt T., Schneider P., Schirmer M., Cirpka O.A.: High-resolution temperature measurements at the river – groundwater interface: Quantification of seepage rates using fiber-optic Distributed Temperature Sensing

1.42 von Fumetti S., Gusich V., Nagel P.: Natural springs - the living passage between groundwater and surface water

1.43 Waber N.H.: Porewater as an archive of the palaeo-hydrogeology during the Holocene and Pleistocene

1.44 Wanner Ch., Schenker F., Eggenberger U.: In-situ Remediation of Polluted Groundwater: A Transdisciplinary Approach

1.45 Weis Ph., Driesner Th., Coumou D., Heinrich Ch.A.: On the physical hydrology of hydrothermal systems at mid-ocean ridges

1.46 Wüest A., Jarc L., Pasche N., Schmid M: One lake, two countries and a lot of methane - the concept for a viable extraction of an unusual resource

1.1

Caractérisation hydrodynamique des principaux types de sol

A. Alaoui & R. Weingartner

Groupe d'hydrologie, université de Berne, Hallerstrasse 12, 3012 Berne, Suisse (alaoui@giub.unibe.ch)

La caractérisation hydrodynamique des principaux types de sol suisses n'est pas encore appréhendée. Elle dépend non seulement du type du sol et de ses propriétés physiques mais surtout de sa structure fonctionnelle. L'aspect hydrodynamique du sol n'est abordé que par un angle théorique ou numérique. Dans cette perspective, nous avons oeuvré pour mettre au point une méthode robuste et fiable pour estimer quantitativement le flux à travers la zone non saturée et définir le risque lié au type d'écoulement (Alaoui et al., 2003).
Le but de cette étude est la caractérisation hydrodynamique des principaux types de sol à potentiel agricole pour l'estimation du flux d'eau transitant vers les eaux souterraines permettant de procéder à une évaluation de leur degré de vulnérabilité.
La méthode utilisée dans cette étude est jugée robuste pour deux principales raisons: i) les mesures de la teneur à partir desquelles le modèle MACRO (Jarvis, 1994) a été calibré sont très précises (intervalle de temps de mesure varie entre 1 et 5 minutes) et très denses (effectuées le long du profile du sol tous les 10 cm) et ii) le modèle utilisé est basé sur les principes physiques du sol. De ce fait, les calculs de simulation sont fiables et peuvent être extrapolés à d'autres sols similaires (de même type et même texture).
Les sols étudiés présentent un risque de pollution certain en cas d'application de pesticides ou herbicides quand ils sont humides ou très humides comme c'est le cas des sols bruns et sols bruns acides.
Les sols bruns lessivés peuvent présenter ce risque en état sec et humide.
Quant aux sols à gley, ils présentent un risque de pollution relatif s'ils sont secs. Le risque augmente avec l'humidité. Quand ces sols sont sur des nappes phréatiques fluctuantes, les eaux souterraines peuvent être contaminées par ruissellement vers les rivières si le sol est en pente ou par percolation verticale vers l'eau de la nappe qui remonte rapidement en surface dans le cas d'une plaine.
Ces résultats montrent en général que les sols ne présentent pas de risque majeur quand ils sont très secs. Le cas échéant, les pesticides et herbicides pourraient être appliquées durant ces périodes pour autant que ces sols ne subissent pas d'averses durant les jours qui suivent cette application.
Il est urgent d'établir une carte pédologique au niveau suisse qui tiendra compte du type de sol, de sa texture et du risque de pollution qu'il présente en cas d'utilisation d'herbicides ou de pesticides. Cette carte servira aux pratiquants dans les domaines du sol et de l'hydrologie. La présente étude est en faite à la base de cette cartographie et devra s'étendre aux sols agricoles de culture différente. L'impact de la culture sur la structure du sol devrait être alors évalué

REFERENCES

Alaoui, A, Germann, P, Jarvis, N, Acutis, M., 2003. Dual-porosity and Kinematic Wave Approaches to assess the degree of preferential flow in an unsaturated soil. Hydrol Sciences J. 48(3):455–472

Jarvis, N., 1994. The MACRO model Version 3.1 – Technical description and sample simulations. Reports and Dissertations no. 19, Department of Soil Science, Swedish University of Agricultural Sciences, Uppsala, Sweden, 51 pp

1.2

Insights from coupled thermal-hydraulic-chemical modelling of geochemical processes in carbonate and silicate-dominated reservoirs within deep geothermal systems

Alt-Epping Peter, Waber H. Niklaus & Diamond, Larryn W.

Institute of Geological Sciences, Rock–Water Interaction Group, University of Bern, Baltzerstrasse 1-3, CH-3012 Bern (alt-epping@geo.unibe.ch)

We use coupled thermal-hydraulic-chemical models patterned after the geothermal systems at Bad Blumau, Austria, and Basel, Switzerland to track the fate of fluids that originate from a carbonate and a silicate-dominated geothermal reservoir,

respectively, on their passage through the geothermal system. We use numerical simulations to explore 1) geochemical conditions in the undisturbed reservoir, 2) chemical and hydrological implications of reinjecting the used fluid into the reservoir, 3) mineral scaling and the rate at which it occurs and 4) borehole corrosion and geochemical fingerprints indicating incipient corrosion.

The composition of the fluid in the reservoir is buffered by the mineralogy of the aquifer rock at local temperature and pressure conditions. Changes in pressure and conductive temperature during ascent and descent of the fluid induce changes in mineral solubilities. Oversaturated minerals may cause scaling within the borehole. The precipitation of mineral phases in the borehole is primarily dictated by the composition of the reservoir fluid. The distribution of minerals is a function of the flow and reaction rates. Mineral scaling within the borehole changes the fluid composition and may gradually clog the borehole, thereby obstructing fluid flow. Because different minerals exhibit different solubilities as a function of temperature, the mineral assemblages that precipitate in the production well are distinct from those in the injection well. For instance, if the fluid in the reservoir is saturated in silica, then the prograde solubility behaviour of silica favours its precipitation in the production well. Conversely, carbonate minerals tend to precipitate in the injection well owing to their retrograde solubility behaviour. However, calculating the distribution of mineral phases is complicated by the fact that the precipitation of some minerals is kinetically controlled, such that they may continue to precipitate far into the injection well (e.g. amorphous silica)

Any modification of the fluid composition caused by mineral precipitation along the fluid's pathway means that the reinjected fluid is no longer in equilibrium with the reservoir rock. Consequently, rock-water interaction and fluid mixing at the base of the injection well drive chemical reactions that cause changes in porosity and permeability of the reservoir rock, potentially compromising the efficiency of the geothermal system.

One concern during geothermal energy production is that of chemical corrosion of the borehole casing. For a range of "what-if" scenarios we explore the effect of corrosion on the fluid composition and on mineral precipitation to identify chemical fingerprints that could be used as corrosion indicators. Once suitable indicators are identified, incipient corrosion could be detected early on during regular chemical monitoring. Corrosion of the casing is typically associated with the release of Fe and H_2 into the circulating fluid. However, the implications of this release depend on the local chemical conditions where corrosion occurs. For instance, elevated H_2 in the fluid is a corrosion indicator only if it is not involved in subsequent redox reactions. Similarly, low H_2 concentrations do not rule out possible corrosion.

In general, the interpretation of a fluid or a mineral sample requires the understanding of chemical processes that occur along the flowpath throughout the geothermal system. If direct observations are not possible, then this understanding can only be achieved through numerical simulations that integrate and couple fluid flow, heat transport and chemical reactions within one theoretical framework. Our simulations demonstrate that these models are useful for quantifying the impact and minimizing the risk that chemical reactions may have on the productivity and sustainability of a geothermal system.

1.3

Transfer of solutes under forested watersheds

Babić Domagoj*, Jenni Robert**, Zwahlen François*

*Centre of Hydrogeology and Geothermics (CHYN), Institute of Geology and Hydrogeology, University of Neuchâtel, Rue Emile-Argand 11, 2009 Neuchâtel, Switzerland
**Bureau Nouvelle Forêt sàrl, Rte de la Fonderie 8c, 1700 Fribourg, Switzerland

The ALPEAU project aims to strengthen the protecting role of forests when it comes to sustainable water resource management and quality. Thus, several forested watersheds were chosen. The Gorges de l'Areuse watershed is located over the Swiss Jura mountains karstik system, whereas the Jorat forest and the Mont Gibloux are situated on the Swiss Plateau, mainly characterized by sandstone formations.

The main goal of this study is to assess the fate of contaminants, such as nitrates and pesticides, on their way down from the forest soil, which physico-chemical features are strongly linked to phytosociological combinations, through the unsaturated and saturated zone down to the system outlet.

In karstic areas, it is important to discriminate between water coming from the soil reservoir, the epikarst (interface between soil and karst), the low permeability volumes (the rock volume between the epikarst and the system outlet) and the

freshly infiltrated rainwater. To do so, gases produced in the soil and dissolved in rainwater will be used. A combined radon, CO_2 and TDGP (total dissolved gas pressure) measurements will be carried out in a water adduction tunnel at the Gorges de l'Areuse test site. Conductivity, temperature, turbidity, DOC (dissolved organic carbon), nitrogen and carbon isotopic composition and dissolved ions will also be part of the survey (Figure 1). Additional artificial tracing experiments will allow to get insight into the travel time, the storage location and the degradation kinetic of dissolved compounds.

Even though the Mont Gibloux test site is set on top of a sandy aquifer, the same method will be applied, if travel times are proved to be under a week. Indeed, radon decays with a half live of about 4 days, whereas CO_2 reacts with carbonate on its way down to the saturated zone.

The main focus on the Jorat forest test site is the environmental fate of cypermethrin, a synthetic insecticide used in timber treatment, oil products used in forest management and their metabolites.
First of all, it is essential to understand the hydrogeological behaviour of the watershed. Thus, a classical physico-chemical follow-up will be established at some chosen water harnessing, completed with comparative tracer tests. Then, wooden piles will be set on treatment sites, treated with cypermethrin (within the range of legal concentrations) and spring water watched over. The experiment will occur under artificial steady state conditions and during heavy rain events, as it is assumed to cause significant infiltration into the aquifer.

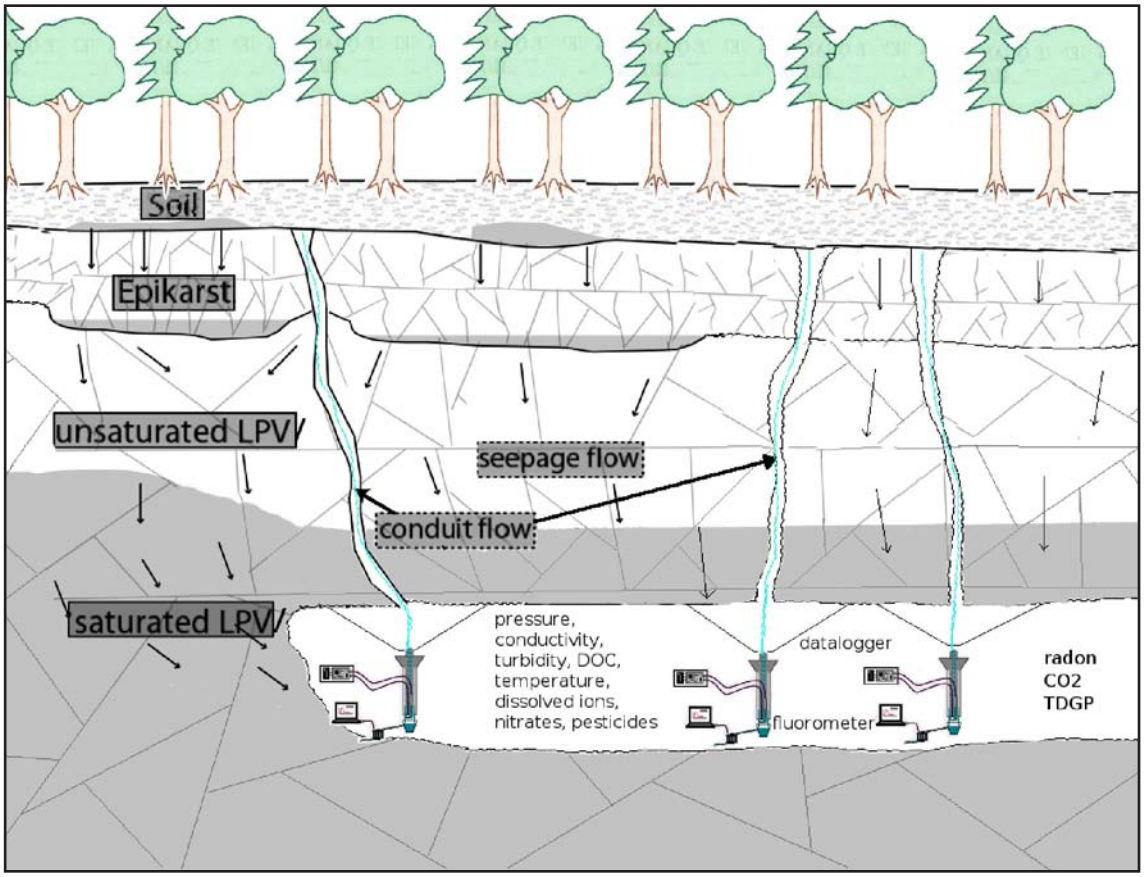

Figure 1. Schematic view of the Gorges de l'Areuse test site (modfied after Savoy L. 2007)

REFERENCES

Perrin, J. 2003: A conceptual model of flow and transport in a karst aquifer based on spatial and temporal variations of natural tracers, Phd thesis, University of Neuchâtel, Switzerland, 227 pages.

Savoy, L. 2007: Use of natural and artificial reactive tracers to investigate the transfer of solutes in karst systems, Phd thesis, University of Neuchâtel, Switzeland, 194 pages.

Surbeck, H. 2003: Radon and CO_2 as natural tracers in Karst Systems, proceedings of ICGG7 (2003), 33-33.

Subeck, H. 2005: Dissolved gases as natural tracers in karst hydrogeology; radon and beyond, proceedings of Multidisciplinary Approach to Karstwater Protection strategy, Unesco Course, Budapest, Hungary.

1.4

Well-head capture zones delineation in transient flow conditions: the use of equivalent steady-state approximations

Badoux Vincent* & Perrochet Pierre**

*AF-Colenco Ltd. Täfernstrasse, 26, CH-5405 Baden (Vincent.badoux@af-consult.com)
**Centre of Hydrogeology and Geothermics, Rue Emile-Argand 11, CH-2000 Neuchâtel (Pierre.perrochet@unine.ch)

The delineation of well-head protection areas S1, S2 and S3 as well as contribution zones Z_u aims to prevent groundwater resources from instantaneous and perennial pollutions. Due to the stress they induce on the land use, these so-called protection schemes cause socio-economic impacts, that becomes non negligible in high-density population area, such as the Swiss Plateau. Therefore the delineation of such protection schemes must be done with care in order to guaranty the protection of the resource on the one hand, while minimizing the overestimation of their size on the other hand.

Aquifers are natural systems that vary with space and time. Such variability will directly influence the way contaminant migrates through the aquifer and indirectly the design of the protection schemes. In practice, characterizing the resource by integrating this variability requires much more effort than using a simple homogeneous medium with steady-state flow conditions. Consequently the delineation of protection schemes is often done using low water steady-state flow conditions, assuming this constitutes a safer approach. However, by applying this simplified methodology, the size of the protection schemes is overestimated and the related socio-economic impacts enhanced.

A new methodology has been developed to identify flow conditions where steady-state approximation is justified or where this approximation should be avoided (Badoux 2007). The ratio between the mean transit time and the fluctuation period appears to be a good criterion to distinguish between these two cases. When this ratio is smaller than 0.5, the size of the protection schemes can be rigorously obtained using high and low water flow conditions. When this ratio is big enough - the exact number is site specific - the protection schemes can be approximated by mean steady-state flow conditions. In between, protection schemes cannot be obtained by any steady-state flow conditions, except if some transport parameters are adapted in an appropriate way.

This methodology has been applied to the Seeland aquifer in Canton Bern.

REFERENCES

Badoux, V. 2007. Analyse des processus advectifs-dispersifs en milieux poreux sous contraintes hydrologiques périodiques. Implications pour la protection des captages d'eaux souterraines. PhD Thesis, CHYN, Univ. Neuchâtel, 293 p.

1.5

Particles in reservoir waters affected by pump storage operations

Bonalumi Matteo*, Anselmetti Flavio*, Kägi Ralf**, Müller Beat*** & Wüest Alfred***

* Eawag, Swiss Federal Institute of Aquatic Science and Technology, Surface Waters – Research and Management, CH–8600 Dübendorf (matteo.bonalumi@eawag.ch)
** Eawag, Urban Water Management, CH–8600 Dübendorf
*** Eawag, Surface Waters – Research and Management, CH–6047 Kastanienbaum

Pumped storage hydroelectricity is used to even out the daily and weekly fluctuations in energy consumption by pumping water to a higher altitude reservoir during low-peak periods, using the excess base-load capacity from coal and nuclear sources. This project investigates the effect of this pump storage operations on particle characteristics in the water column and on resulting sedimentation processes.

Grimselsee (1908 m) and Oberaarsee (2303 m), two reservoirs located in the Bernese Alps, are connected since 1980 by a pump storage unit which exchanges an annual amount of water amounting to several times the volume of the reservoirs. The impact of initial damming was studied recently for downstream areas and in the reservoirs themselves. The partially glaciated

catchments feeding the reservoirs lead to an enormous inflow of inorganic particles during snowmelt in spring, resulting in high turbidity in the reservoirs. Compared to pre-dam conditions, reservoirs retain particles of larger grain size which were previously released to downstream areas (Anselmetti et al., 2007). In addition, it was demonstrated that the shift of runoff from summer to winter affects the light regime and, consequently, the primary production in Lake Brienz (Finger et al. 2007; Jaun et al. 2007).

In order to understand the effect of the increasing pump storage operations on water turbidity and on particle size, water sampling campaigns were performed seasonally in both reservoirs as well as in the power station connecting them. Turbidity seems to correlate strongly with weather conditions and catchment characteristics in summer and with pump storage activity in winter. In summer, Grimselsee was found to be more turbid than Oberaarsee, which has a stronger thermal stratification and whose catchment is less glaciated. In winter, Grimselsee and Oberaarsee show similar conditions. However, turbidity was higher close to the in-/outlets, where both reservoirs are continuously exchanging water.

Hydraulic machines such as turbines cause shear stress and turbulence, which are known to induce flocculation of particles (Blaser & Boller, 1998; Serra et al., 2008). In order to investigate whether this effect occurs in the Grimsel reservoirs, water samples were taken upstream and downstream of the turbines during pump storage and power production regimes. To date, SEM image analyses and particle-counter analyses did not discover any aggregation effect, suggesting that the there is not significant change in particle characteristics from turbine passages.

REFERENCES

Anselmetti, F. S., Bühler, R., Finger, D., Girardclos, A., Lancini, A., Rellstab, C. & Sturm, M. 2007: Effects of Alpine hydropower dams on particle transport and lacustrine sedimentation. Aquatic Sciences, 69, 179-198.

Finger, D., Bossard, P., Schmid, M., Jaun, L., Müller, B., Steiner, D., Schäffer, E., Zeh, M. & Wüest, A. 2007: Effects of alpine hydropower operations on primary production in a downstream lake. Aquatic Sciences, 69, 240-256.

Jaun, L., Finger, D., Zeh, M., Schurter, M. & Wüest, A. 2007: Effects of upstream hydropower operation and oligotrophication on the light-regime of a turbid peri-alpine lake. Aquatic Sciences, 69, 212-226.

Boller, M. & Blaser, S. 1998: Particles under stress. Wat. Sci. Tech., 37 (10), 9-29.

Serra, T., Colomer, J. & Logan, B. E. 2008: Efficiency of different shear devices on flocculation. Water Research, 42 (4-5), 1113-1121

1.6

Sustainable management of urban water: substance flow analysis as a tool

Chèvre Nathalie*, Guignard Cécile*, Bader Hans-Peter**, Scheidegger Ruth**, & Rossi Luca***.

* *IMG - Faculté des Géosciences et de l'Environnement, Université de Lausanne, CH-1015 Lausanne (nathalie.chevre@unil.ch)*
** *Eawag, CH-8600 Dübendorf*
*** *IIE-ECOL, ENAC, EPFL, CH-1015 Lausanne*

Pollutants released by cities into water are of more and more concern as they are suspected of inducing long-term effects on both aquatic organisms and humans (for example, hormonally active substances). The substances found in the urban water cycle have different sources in the urban area and a different fate in the cycle. For example, the pollutants emitted from traffic get to surface water during rain events often without any treatment, and are partially removed from the water cycle by sedimentation; pharmaceuticals resulting from human medical treatments get to surface water mainly through wastewater treatment plants, where they are partly taken out from water. The residual concentrations can re-enter the cycle through drinking water. It is therefore crucial to study the behavior of xenobiotics in the urban water cycle and to get flexible tools for urban water management.

The substance flow analysis (SFA), an extension of the classical material flow analysis originally developed by Baccini & Brunner, has recently been proposed as instrument for phosphorous management in urban water system. SFA is based on the principle of mass balance: a substance enters a closed system and may be transported or transformed in the system and may also leave the system.
To be used as management tool, SFA should be coupled with environmental quality criteria. These values express the maximum concentration, which is tolerable for a given substance in order to protect both human and the environment. Having this limit in mind, one can detect the most problematic flows and take action to diminish them.
In our study, we tested the application of SFA for a large number of classes of xenobiotics, i.e. heavy metals, pharmaceuticals, biocides and cosmetics, to evaluate its use for urban water management. We chose the city of Lausanne as case study as many data were available, on both the sewer system and the water quality.

The city of Lausanne, which is around 42 km² with 130'000 inhabitants. Lausanne is near lake Geneva and its effluents mainly reach this ecosystem, which is a recreational area as well as a source of drinking water for the city. The system itself is described in Figure 1 and illustrated for copper. We considered thirteen inputs of this heavy metal in the water system: drinking water (I_1), roofs (I_2) and houses sides (I_3) runoff, road runoff collecting car brakes (I_4), tires abrasion (I_5), motor oil residues (I_6) and dry deposition (I_{12}), particles from catenaries from trolleybuses (I_7), inputs through trains, i.e. particles from catenaries (I_8), brakes (I_9) and wheels (I_{10}) abrasion, input through boats (I_{11}) and rainwater (I_{13}). Transfer coefficients were estimated based on measurement or hypotheses. For copper, the water quality criterion was given by the Swiss legislation and the sediment quality criterion proposed elsewhere.

The SFA of copper showed that the city of Lausanne releases about 600Kg and 900Kg per year of this heavy metal in respectively the water and the sediments of lake Geneva. These estimations were validated by measurements of copper in the Lake near Lausanne. In the sediments, the continuous enrichment induces high concentrations of this heavy metal, which are above the recommended quality criterion. By using the SFA, we could identify that copper mainly reaches the Lake with stormwater, i.e without being removed by any treatment. The major sources are the catenaries of the trolleybuses and the roofs runoff. A reduction of the contamination of the water system would therefore include actions at this level (for example the treatment of the roofs runoff). SFA was also applied to biocides and pharmaceuticals with interesting results (not shown here).

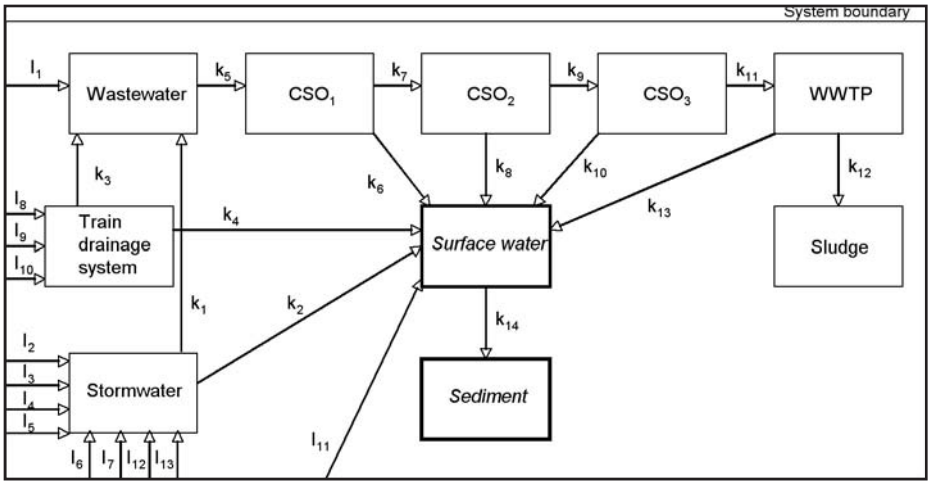

Figure 1: Description of the urbain drainage system of Lausanne and application to copper. The "I" flows stay for "Input". The "k" flows for the transfer coefficients.

REFERENCES

Baccini P., & Brunner P., 1991: Metabolism of the anthroposphere, Springer, Berlin, Germany.

Chèvre N., Guignard C., Rossi L., Pfeifer H.-R., Bader H.-P., and Scheidegger R. Substance flow analysis as a tool for urban water management: the case of copper in Lausanne, Switzerland, Submitted.

MacDonald D., Ingersoll C., and Berger T., 2000: Development and evaluation of consensus-based sediment quality quidelines for freshwater ecosystems, Archives of Environmental Contamination and Toxicology, 39, 20-31.

1.7

Calcite-celestite veins and related past fluid flow through the Mesozoic sedimentary cover at Oftringen, near Olten

de Haller Antoine*, Tarantola Alexandre*, Mazurek Martin* & Spangenberg Jorge**

*RWI, Institute of Geological Sciences, University of Bern, Baltzerstr. 1-3, CH-3012 Bern (DeHaller@geo.unibe.ch)
**Institute of Mineralogy and Geochemistry, University of Lausanne, Building Anthropole, CH-1015 Lausanne

The study is based on core samples from the recently drilled, 719 m deep borehole at Oftringen (near Olten), located in the northwestern Molasse basin, at 1.5 km from the frontal thrust of the Folded Jura (Waber, 2008). Veins of calcite (±celestite, pyrite) occur in the whole Malm sequence (up to 8 veins/m), including the more clay-rich Effingen Member. To date, such an intensity of veining in the Effingen Member has not been found in other deep boreholes located in the Molasse basin. Most of the veins are related to tectonic activity, but clay-filled karst structures are recognized in the upper Geissberg Member

limestone, and a few structures probably related to the diagenetic processes are documented in the Effingen Member. Fluid inclusions show average salinities between 3.3 and 4.4 wt% eq. NaCl in celestite and 2.7 wt% eq. NaCl in calcite. Average homogenization temperatures in calcite fluctuate between 56 and 68 °C, with a broad increase with depth and no correlation with salinity.

Malm whole-rock carbonates have $\delta^{18}O$ values fluctuating within a narrow range, probably determined by equilibrium with seawater (Fig. 1A). Their $^{87}Sr/^{86}Sr$ ratios follow a well-defined depth profile with minimum values in the middle part of the Effingen Member, fitting with Oxfordian seawater (McArthur et al., 2001; Fig. 1B). No correlation is observed between $^{87}Sr/^{86}Sr$ and clay content, and values higher than contemporary seawater might be related to the incorporation of radiogenic detrital carbonate.

The $\delta^{18}O$ values of vein calcite are systematically lower than the corresponding whole rock carbonate (Fig. 1A), consistent with precipitation from seawater at 50 - 70 °C. The $\delta^{34}S$ and $\delta^{18}O$ values of vein celestite follow a bacterial reduction trend pointing to Miocene seawater sulfate. Two vein pyrites gave negative $\delta^{34}S$ values consistent with bacterial sulfate reduction. Calcite and celestite of diagenetic origin have $^{87}Sr/^{86}Sr$ ratios that are indistinguishable from the corresponding whole rock carbonate fraction. In contrast, the $^{87}Sr/^{86}Sr$ ratios of epigenetic vein calcite and celestite show a systematic enrichment in radiogenic Sr compared to the corresponding whole-rock carbonate and require an external Sr source. Only Burdigalian seawater, at the time of Upper Marine Molasse (OMM) deposition, had an $^{87}Sr/^{86}Sr$ ratio high enough to explain the highest value obtained (Fig. 1B).

The rocks of the Malm-Dogger sequence were not pervasively affected by fluids post-dating burial diagenesis, and the influence of such fluids was restricted to open structures. The Molasse basin subsided in the Burdigalian (Kuhlemann and Kempf, 2002; Mazurek et al., 2006), and the veins might record tectonic activity related to this process. Calcite and celestite precipitated from descending seawater due to heating to 50-70°C, while precipitation of pyrite resulted from bacterial reduction of part of the seawater sulfate.

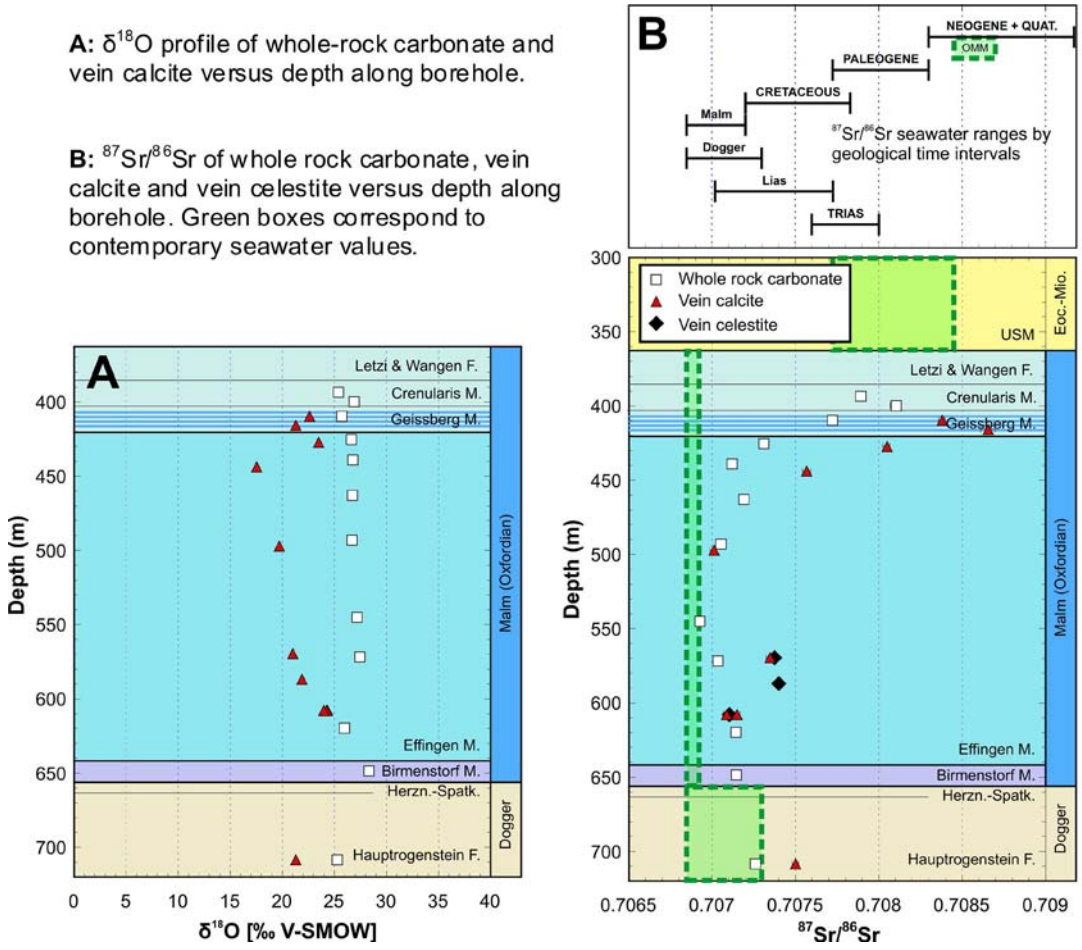

Figure 1. Oxygen and strontium isotopic data.

REFERENCES
Kuhlemann J., & Kempf, O. 2002: Post-Eocene evolution of the North Alpine Foreland Basin and its response to Alpine tectonics. Sed. Geol. 152, 45-78.
McArthur, J.M., Howarth, R.J., & Bailey, T.R. 2001: Strontium isotope stratigraphy: LOWESS Version 3: Best fit to the marine Sr-isotope curve 0-509 Ma and accompanying look-up table for deriving numerical age. J. Geol. 109, 155-170.
Mazurek, M., Hurford, A. J. & Leu, W. 2006: Unravelling the multi-stage burial history of the Swiss Molasse Basin: Integration of apatite fission track, vitrinite reflectance and biomarker isomerisation analysis. Basin Res. 18, 27-50.
Waber, N., ed. 2008: Borehole Oftringen: Mineralogy, Porosimetry, Geochemistry, Pore Water Chemistry. NAGRA Arbeitsbericht NAB-08-18, Nagra, Wettingen, Switzerland.

1.8

Spatial characterization of hydraulic conductivity of the Thurtal-aquifer at the test site Widen

Diem Samuel, Vogt Tobias, Hoehn Eduard

Eawag, Swiss Federal Institute of Aquatic Science and Technology, Überlandstrasse 133, CH-8600 Dübendorf (samuel.diem@eawag.ch)

For many hydrogeological and modeling problems on a scale of the order of 10-100 m, an assessment of the spatial distribution of hydraulic conductivity (h.c.) is of great importance. This is one of the tasks of the ReCorD project (Restored Corridor Dynamics) of CCES (Competence Center Environment and Sustainability of the ETH Domain). This project aims at understanding, how river restoration measures affect river - river corridor - groundwater systems in hydrologic and ecologic terms. The river Thur and the alluvial gravel-and-sand aquifer of the perialpine Thur valley flood plain were chosen for field investigations. In this aquifer, the distribution of h.c. at the required scale has not yet been investigated. Thus, the aim of this Master Thesis is to characterize the hydrogeology of the aquifer at a test site in the central part of the valley (Widen, Felben-Wellhausen/TG), which extends to about 10x20 m (aquifer thickness, 7 m), by using different methods on different scales. Work included logging of core drillings, sieving of the gravel samples (decimeter scale) and the conduction and analysis of a pumping test (decameter scale), flowmeter logs and slug tests (meter scale), with appropriate methods. Except for the slug tests (14 wells), four fully penetrating wells with piezometers of a diameter of 4.5" were used. The analysis of these tests resulted in values of h.c.

The *sieve analyses* (vertical intervals of samples: 0.5 m) were performed with the core material of the four wells. The values of h.c. calculated after Casati (1959) led to small absolute values and a narrow distribution (n=53, μ=-2.73 m/s, σ^2=0.01; where $\mu=\log_{10}$ geometric mean, $\sigma^2=\log_{10}$ variance). The small variability can be explained by the approach of the formula of Casati (1959), taking into account five grain size fractions and assuming absence of the secondary porosity of the material. The small absolute values originate from the calibration of the formula to a specific aquifer. Sieve analyses are well suited for a rough estimate of h.c. of perialpine alluvial gravel-aquifers, with an accuracy of a factor of about 2.
The *pumping test* (pumping well is one of the four wells, head observations in nine additional wells) involves a large aquifer volume. As for all pumping tests, the resulting value of h.c. (here calculated after Neuman (1972, in Kruseman & De Ridder 1991)) is biased by highly conductive zones and corresponds to the upper limit of the spectrum of the natural variability (μ=-1.83 m/s). This value is adequate for large scale investigations.
Flowmeter measurements were carried out at intervals of 0.25 m in the four 4.5"-piezometers. As for all flowmeter tests, an analysis with the method of Javandel & Witherspoon (1969, in Molz 1989) resulted in vertical profiles of relative values of h.c. The relative values can be calibrated to absolute values: Here they are calibrated relative to the mean h.c. of the pumping test, which integrates a large aquifer volume (total of n=29, μ=-1.83 m/s, σ^2=0.14; calculated for an average of 0.5 m intervals). The bias of the result of the pumping test is thus transferred to the results of the flowmeter measurements. The relative profile of h.c. should rather be calibrated with the result of tests that involve only a small aquifer volume, e.g. slug tests in fully penetrating wells, which are hard to realize in a highly conductive aquifer. So flowmeter logs are the adequate method, if the relative vertical distribution of h.c. is of primary importance.
Slug tests. For detailed information about the spatial distribution of h.c. in the order of 10-100 m, which is needed in the ReCorD project for the modeling of groundwater flow, solute and heat transport at small scales, pneumatic multi-level slug tests (with a system of double packers) were applied in 117 intervals of 0.5 m length of 14 piezometers (analyzed after Bouwer and Rice 1979, Springer and Gelhar 1991, in Butler 1998). These experiments resulted in the following distribution of h.c.: n=117, μ=-2.38 m/s, σ^2=0.11.

A statistical evaluation of the values of h.c. from the above methods showed that the results can not be compared. Thus, the choice of the method to assess the distribution of h.c. has to be done according to the problem and the required level of

detail. The slug tests resulted in the best absolute and relative representation of the distribution of h.c., compared to the other three methods: The absolute values of h.c. do not have to be calibrated with the result of a different method, the values of h.c. are accurate and cover most of the natural range of h.c. A statistical comparison of sieve analyses of the Widen test site with those of the whole Thur valley has shown that the distribution of d_{10}, d_{50} and d_{60} grain size fractions are similar in the western part of Thur valley. Probably, the distribution of h.c. assessed for the Widen test site can also be used for the western part of the valley, as this site seems to belong to the same facies. To decrease the work load required for slug tests and to increase the level of detail in h.c. assessments, I recommend a combination of hydraulic testing with high resolution geophysics and the use of tracers. The development of geophysical and tracer methods are an integral part of the ReCorD project.

REFERENCES

Butler, J. J. JR. 1998: The design, performance, and analysis of slug tests. Lewis Publishers.
Casati, A. 1959: Die Durchlässigkeit kiesiger Böden. Monatsbulletin SVGW 6, 120-126.
Kruseman, G. P. & De Ridder, N. A. 1991: Analysis and evaluation of pumping test data. ILRI Publication 47, Second Edition.
Molz, F. J. 1989: The impeller meter for measuring aquifer permeability variations: Evaluation and comparison with other tests. Water Resour. Res. 25 (7), 1677-1683.

1.9

Metal partitioning in aquatic systems: from interdisciplinary research to environmental practice.

Dominik Janusz* & Vignati Davide A.L. **

* *Institut F.-A. Forel, Section de sciences de la Terre et d'environnement, Université de Genève, CP 416, 1290 Versoix – janusz.dominik@unige.ch ,*
** *CNR-IRSA, Via del Mulino 19, 20047 Brugherio (MB), Italy – vignati@irsa.cnr.it*

Knowledge of partitioning of metals is fundamental for understanding their transport and their availability to aquatic organisms. Furthermore, a considerable fraction of metals in rivers, lakes and coastal ocean may be of anthropogenic origin with concentrations approaching the levels considered harmful for aquatic ecosystems. Measuring and, when possible, predicting metal partitioning therefore becomes essential for environmental risk assessment and associated management plans.

Current European and Swiss legislations fix environmental quality standards (EQSs) on metals for the filterable phase; defined as the metal fraction passing through the pores of a 0.45μm filter. A large fraction of "filterable" metals is actually associated with small-size colloids and thus is not truly in solution. Unlike metals in true solution, colloidal metals can be removed from the water column via coagulation and/or aggregation and sedimentation processes. Moreover, metals bound to colloids are not available to some organisms (e.g., algae), but might be available for others (e.g., zooplankton). These discrepancies between fundamental knowledge and current environmental practices raise two major questions: a) Is it possible, and useful, to determine metal partitioning in monitoring programs? b) How can the knowledge of metal partitioning between colloidal and truly dissolved phases be used in environmental assessment?

The published data indicate that metals of low solubility in oxic conditions (e.g., Cr(III), Fe, Mn, Ti, Pb) are predominantly associated with colloids, while metals preferentially forming anionic complexes occur mostly in true solution (e.g., Cr(VI), Mo, U, V). Partitioning of elements occurring as divalent cations (e.g., Cu, Zn, Cd, Ni, Hg) depends largely on physico-chemical conditions of ambient water and on the quantity and quality of colloids.

For the priority elements mentioned in European legislation, the literature data indicate that, in general, Ni and Cd have lower affinity for colloids than Pb and Hg (fig. 1). Note however that a part of the observed variability is caused by persisting technical limitations; i.e. tangential flow filtration (the most widely used technique to separate colloidal and truly dissolved fraction in partitioning studies) not being standardized and prone to artifacts. In such situation, measurement of metal partitioning between colloids and true solution in routine monitoring programs remains unlikely and probably not advisable. Nevertheless, inferring the percentage of truly dissolved fraction from the total filterable fraction has proven to be feasible for some elements (Vignati et al. 2005). Such information can be used to refine models on elements' environmental fate and also provide a more realistic evaluation of toxicity at primary producer level; which is highly relevant to the assessment of ecological risk. Indeed, algal bioassays carried out in the presence of organic colloids, demonstrated decreasing toxicity with increasing fraction of metals bound to colloids (Koukal et al. 2003, 2007).

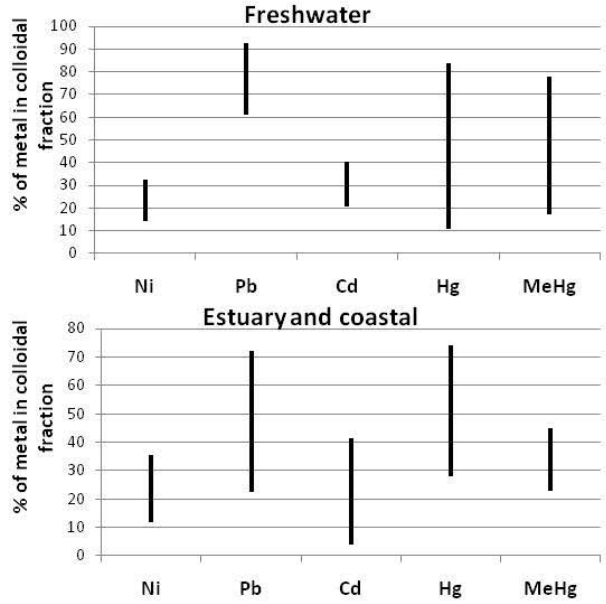

Fig. 1. Percentage of toxic metals associated with the colloidal fraction according to published data from freshwater and estuarine or coastal systems (compiled in Vignati et al. 2009). Bars represent the range between the means of the lower and the upper limits in each study.

REFERENCES

Koukal, B., Guéguen, C., Pardos, M. & Dominik, J. 2003: Influence of humic substances on the toxic effects of cadmium and zinc to the green alga Psedokirchneriella subcapitata. Chemosphere, 53, 953–961.

Koukal, B., Rossé, P., Reinhardt, A., Ferrari, B., Wilkinson, K. J., Loizeau, J.-L. & Dominik, J. 2007: Effect of Pseudokirchneriella subcapitata (Chlorophyceae) exudates on metal toxicity and colloid aggregation. Water Res., 41, 63-70.

Vignati D.A.L., Camusso M. & Dominik J. 2005: Estimation of the truly dissolved concentrations of Cd, Cu, Ni, and Zn in contrasting aquatic environments with a simple empirical model. Ecological Modelling 184, 125–139.

Vignati D.A.L., Valsecchi, S., Polesello, S., Patrolecco, L, & Dominik, J. 2009: Environmental realism and WFD implementation: chemical and ecological relevance of particle-colloid-true solution partitioning of pollutants for surface water monitoring. Trends in Analytical Chemistry, 28, 159-169.

1.10

How water properties control the behaviour of continental and seafloor hydrothermal systems

Driesner Thomas*, Coumou Dingeman** & Weis Philipp*

*Institute of Isotope Geochemistry and Mineral Resources, ETH Zentrum, CH-8092 Zürich (thomas.driesner@erdw.ethz.ch)
**Potsdam Institute for Climate Impact Research, Telegrafenberg A62, D-14412 Potsdam

The flow patterns and thermal evolution in hydrothermal systems are of prime interest to a variety of basic and applied geoscience disciplines ranging from biogeoscience research on life in extreme environments through economic geology to geothermal energy exploration. Due to the extreme temperature-pressure conditions as well as the difficult access to many of these systems (e.g. those at mid-ocean ridges), insight has mostly been gained from numerical simulation.

In the case of continental hydrothermal systems heated by magmatic intrusions, numerical simulation has shown that the system-scale permeability structure is a prime order control on how much the convecting hydrothermal fluid may be heated. This is a result of the different rates with which convection (with the fluid flow rate primarily being controlled by permeability) transports heat away from the source and conduction (in the essentially impermeable hot magmatic source) delivers heat to the fluid (Hayba&Ingebritsen, 1997; Driesner&Geiger, 2007). On the other hand, fluid properties such as the position of the water boiling curve in temperature-pressure space are a major control on the style of hydrothermal fluid flow in the upflow zone.

For mid-ocean ridge hydrothermal systems, recent developments in numerical simulation techniques have revealed that the temperature-pressure-composition dependence of fluid properties such as viscosity, density, and heat capacity is a first order control on hydrothermal system behaviour. For example, by heating water from ambient temperature to to 200°C, viscosity drops by one order of magnitude. This increases the mobility of water by the same amount as a one order of magnitude increase in permeability. Hence, hot water can essentially "by itself" create corridors of high hydraulic conductivity in environments of otherwise homogenous permeability. As a result, strong self-organization effects may occur, the prime example being the recent prediction of pipe-like hydrothermal plumes underlying "black smoker" hydrothermal systems and being surrounded by narrow cylindrical zones of intense, warm recharge (Coumou et al., 2008). Current research focuses on the question to what degree these effects interfere with those resulting from the permeability structure of the crust (see Weis et al., this volume).

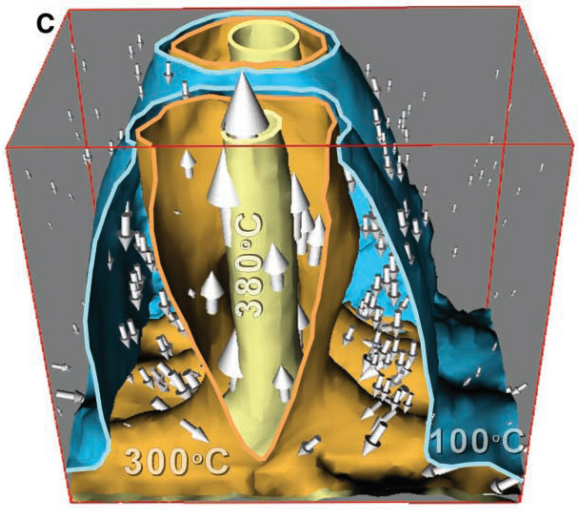

Figure 1. Thermal structure of the hydrothermal plume underlying a mid-ocean ridge black smoker field. A hot central upflow zone with temperatures up to 380°C is surrounded by a narrow recharge zone with temperatures between 100 and 200°C. From Coumou et al. (2008)

For oceanic systems with a homogenous permeability distribution, it can be shown that there is a strong interplay of fluid properties and permeability that determines the system's temperature as well as its ability to convect the incoming heat. Numerical simulations, verified by semi-analytical calculations, show that typical black smoker temperatures can only be achieved when permeability is LESS than about $3x10^{-14}$ m^2. At higher permeabilities, the temperatures are lower since fluid flow rates are too fast to allow stronger heating near the magmatic heat source. Below this permeability, fluid properties limit the maximum temperature of the system to ca. 400°C. Similarly, for typical heat flow rates at the bottom of the system, not all incoming heat can be convected away, and magma eruptions to the seafloor may potentially be the only way to balance the total heat input.

To what degree the influence of fluid properties may play a role in the formation of ore deposits or in the operation of geothermal systems is subject to ongoing research.

REFERENCES

Coumou, D., Driesner, T. & Heinrich, C. A. (2008) The structure and dynamics of mid-ocean ridge hydrothermal systems. Science 321, 1825-1828

Driesner, T. and Geiger, S. (2007) Numerical simulation of multiphase fluid flow in hydrothermal systems. In Fluid-Fluid Interactions (A. Liebscher and C.A. Heinrich, eds.) Reviews in Mineralogy and Geochmistry 65, pp. 187-212

Hayba, D. O., and Ingebritsen, S. E. (1997) Multiphase groundwater flow near cooling plutons. Journal of Geophysical Research 102, 12,235–12,252.

1.11

Tracer tests in urbanised sites: a tool for a better characterisation of groundwater vulnerability in urban areas

Romain Ducommun*, François Zwahlen*

*Centre d'Hydrogéologie et de Géothermie (CHYN), Université de Neuchâtel, Emile-Argand 11, CH-2000 Neuchâtel, romain.ducommun@unine.ch

Vulnerability assessments and mapping methods (Vrba & Zaporozec 1994) are principally designed for natural areas. However, in urban zones, the groundwater recharge is strongly modified, due mainly to sealing of surface and/or presence of subsurface water mains and sewer pipes, which can contribute to recharge, or inversely act as drains for water in saturated and unsaturated zones (Lerner 2002; Thomas & Tellam 2006). As recharge can be considered as a key parameter for vulnerability evaluation (e.g., Aller, Bennett et al. 1987), urban processes which modify groundwater recharge have to be included in any vulnerability assessment of given urban groundwater resources.

In this perspective, multi-tracer tests were carried out at local scale in two urban test sites in Switzerland: Colombier and Neuchâtel. The Colombier test site is located in a low urbanised area, on quaternary glacial sediments forming the Plateau de Planeyse, where a small shallow aquifer is present in the silty formations. The Neuchâtel test site, at the shore of Lake Neuchâtel (Maladière area), is located in a high urbanised area, on highly heterogeneous anthropogenous backfill material and quaternary glacio-lacustrine sediments. The artificial conservative tracers (uranine, sulforhodamine B, duasyne and naphtionate) were injected in sealed and unsealed surfaces, or directly in subsurface rainwater pipes. In both test sites, tracer recovery was monitored in underlying urban aquifers (wells and drainage collectors), and in the downstream part of pipes where the tracer injections were performed.

The recovery results in Colombier and Neuchâtel (example of breakthrough curve in figure 1) pointed out dual role of pipes on recharge (increasing or decreasing recharge), an increase in recharge due to runoff concentration at the boundaries of sealed surfaces, and an increase in recharge due to the presence of artificial backfill materials in the uppermost part of the unsaturated zone. Not surprisingly, increased rates of tracer recovery during wet hydrological periods were observed during the performed tests.

Effects of these various parameters on recharge were further interpreted from a local urban-adapted groundwater vulnerability perspective. Consequently, key factors like the presence of underground pipes (in association with pipe parameters: material, age, hydraulic head, etc), or the local modifications of hydraulic conductivity of soil/subsoil formations by human activity, have to be integrated in urban groundwater vulnerability assessments and mapping methods.

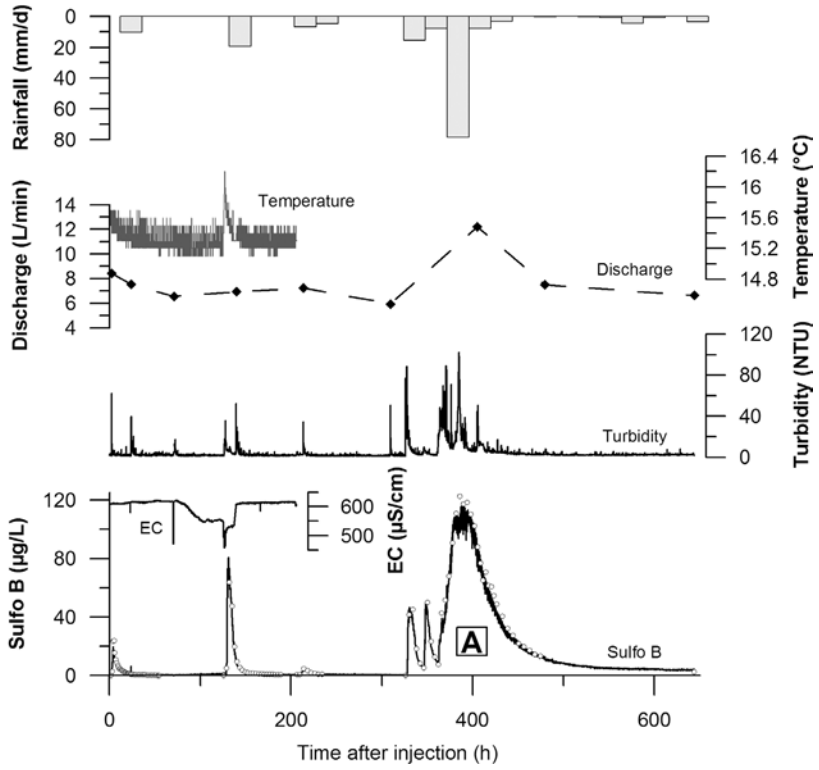

Figure 1. Breakthrough curve for sulforhodamine B (sulfo B) and time-series for electrical conductiity (EC), turbidity, discharge, and water temperature at the Colombier drainage outlet (summer 2007). The major rainfall event (A) and its noticeable related tracer response are indicated.

REFERENCES
Aller, Bennett, et al. 1987: DRASTIC: a standardized system for evaluating groundwater pollution potential using hydrogeological settings. U.S. Environmental Protection Agency (EPA), Ada, Oklahoma, USA.
Lerner 2002: Identifying and quantifying urban recharge: a review. Hydrogeology Journal 10(1): 143.
Thomas and Tellam 2006: Modelling of recharge and pollutant fluxes to urban groundwaters. Science of the Total Environment 360(1-3): 158.
Vrba and Zaporozec, Eds. 1994: Guidebook on Mapping Groundwater Vulnerability. International Contributions to Hydrogeology, vol. 16. Hannover, Heinz Heise GmbH.

1.12

A spectral analysis of rainfall-runoff variability for select Swiss catchments

Tracy Ewen[*,**], Michael Rinderer[*], Thomas Bosshard[**], and Jan Seibert[*]

[**]Institute for Atmospheric and Climate Science, ETH Zurich, Universitätstr. 16, 8092 Zurich.
[*]Department of Geography, University of Zurich, Winterthurerstr. 190, 8057 Zurich, (tracy.ewen@geo.uzh.ch)

Time series analysis can provide useful insight into the complex relationships between variables of interest. In particular, analysis of precipitation and runoff for a particular hydrological catchment allows the physical complexity of the system to be better understood, both spatially and temporally. The Fourier transform is often used to analyse the frequency domain of time series, however, due to the non-stationarity of climatological and hydrological variables, wavelets have been introduced to analyse the spectral properties over time by transforming a time series into two-dimensional time-frequency space.

Wavelets have been used to understand the temporal and spatial variability in complex hydrological systems through an analysis of rainfall and runoff (for e.g., Labat et al., 2000) and to characterise remote watersheds based on runoff data only (Gaucherel, 2002). Cross-wavelet analysis between variables gives further insight into the temporal variability of the relationship (Grinsted et al., 2004) and insight into physical processes governing the system, in particular, the basin response to rainfall, which may help to classify catchments.

Here, we use wavelets to analyse daily precipitation and runoff time series from the Rietholzbach and the Töss catchments in Switzerland to better understand temporal relationships, with a focus on extremes during the past 30 years. We further investigate the spatial relationship between precipitation and runoff and quantify the precipitation contribution from different meteorological stations to total runoff for each catchment. We also discuss the minimal time-scales needed to adequately represent the physical relationships between rainfall and runoff (and hence the climatological signal), which could be applied, for e.g., in order to constrain hydrological impact studies (Bosshard et al., 2009).

REFERENCES
Bosshard, T. Ewen, S. Kotlarski, and C. Schär, 2009: The annual cycle of the climate change signal - An improved method for use in impact studies, Geophysical Research Abstracts, Vol. 11, EGU2009-7095.
Gaucherel, C., 2002: Use of wavelet transform for temporal characterization of remote watersheds, J. Hydrol., 269, 101-121.
Grinsted, A., S. Jevrejeva, J. Moore, 2004: Application of the cross wavelet transform and wavelet coherence to geophysical time series, Nonlinear Proc. Geophys., 11: 561-566.
Labat, D., R. Ababou, A. Mangin, 2000: Rainfall-runoff relations for karstic springs. Part I: convolution and spectral analysis, J. Hydrol., 238, 123-148.

1.13

Gravity-driven Poiseuille-flow in the lithosphere

Peter Germann

Institute of Geography, University of Bern
germann@giub.unibe.ch

Hydro-mechanical concepts of flow in permeable media (like fissured rocks, karst formations, unconsolidated sediments, and soils) are based on laminar flow that is driven by some force (i.e., any combination of the gradients of gravity, density, pressure, osmosis, capillarity, and other potentials), and that encounters resistance (usually expressed as its inverse like permeability or conductivity). Typical length and time intervals are up to kilometres and months in fissured rocks and groundwater systems, tens to hundreds of meters and weeks to days in karst formations and hillslope soils, tens of meters and hours to days in unsaturated and unconsolidated sediments, and single meters and minutes to hours in unsaturated soils. Depending on the problem and the system at hand the dimensionality may vary from one to three, and flow directions may reverse as infiltration/capillary rise in soils may illustrate. In addition, the flow-driving force may alter, for instance, from gravity-dominated infiltration to capillarity-dominated rise of soil moisture and to pressure-dominated flow when the medium becomes water saturated. In view of the many groups of professionals dealing with various kinds of flow and transport in various kinds of permeable media, a variety of concepts and methods have evolved that adapted to the needs of the respective groups. Group-specific adaptations include methods and protocols, time and length scales, system boundaries, and degree of intensity in dealing with spatial variability. For instance, capillarity in the non-saturated root zone of soils is so dominant that soil hydrologists and soil physicists relate water contents, hydraulic gradients and hydraulic conductivities to it. On the other side, the vadose zone (i.e., the non-saturated zone) of unconsolidated sediments between soils and groundwater tables is usually sort of hydraulic and hydrological no-man's land, whereas research on water flow in karst systems and groundwater systems follow their own rules.

A concept of infiltration will be presented that assumes gravity as dominant driving force which is balanced by viscosity. A set of equations evolves that describes the constant velocities of wetting and draining fronts, and that deals with trailing waves. The approach is linear but discontinuous; it does not require a representative elementary volume which is consider as obstacle to the up-scaling of most models. The approach allows for superimposing flows in time and space. Flow fore-casting is easy, however, hind-casting is impossible after flows have joined. From neutron radiography comes experimental evidence that the approach applies to sand layers that are thinner than 1 mm: From sand tank experiments we know that it applies to layers as thick as 2 m. The propagation of wetting front s across 20 m of unconsolidated sediments and across 2 km of fissured granite indicate the applicability of the approach to larger systems. Moreover, it explains conceptually the formation of finger flow in unsaturated porous media.

1.14

A synthesis of available data to analyze the interaction between the Rhône River and its alluvial aquifer

Glenz Damian*, Renard Philippe *, Perrochet Pierre*, Alcolea Andrés*, Alexandre Vogel**

**Université de Neuchâtel, Centre d' Hydrogéologie, Rue Emile Argand 11, CH-2000 Neuchâtel (damianglenz@unine.ch, philippe.renard@unine.ch, pierre.perrochet@unine.ch)*
*** Etat du Valais - Service des routes et des cours d'eau, Projet Rhône, Av. de France 75, CH-1951 Sion (alexandre.vogel@admin.vs.ch)*

Before the first (1863-1894) and second (1930-1960) Rhone corrections, the floods produced by the Rhone River had regularly disastrous effects for the inhabitants. Recent events (1987, 1993 and 2000) revealed major deficiencies in flood protection, which confirmed the necessity of the third regulation project of the Rhône. In addition to flood protection, the project aims at enhancing the ecological aspects of the river (OFEFP/OFEG 2003).

The general approach followed is to widen the riverbed by a factor of at least 1.6. This implies in some sections a lowering of the water level in the river. As the groundwater table of the Rhone alluvial aquifer is partly controlled by the exchanges between the aquifer and the Rhone, the widening of the riverbed may influence the alluvial aquifer. The correction will also modify the geomorphology of the riverbed. This may affect the permeability of the riverbed and thus have an effect on the exchange between the river and the groundwater. For example, a lowering of the groundwater table might induce land

subsidence or cause the drying out of agricultural terrains and involve enhanced irrigation. On the opposite, a rise of the groundwater table might lead to a rise of groundwater in buildings or by swamp formation.

To forecasts those potential impacts, it is necessary to characterize the present situation and to analyse the current state of the exchanges between the river and the aquifer. In a second stage, a numerical groundwater flow model will be used to simulate the main observation and to investigate the possible effects of a modification of the riverbed.

The characterization of the aquifer and the design of the conceptual aquifer model is based on a broad range of sources information such as seismic surveys, boreholes, piezometric head measurements, water analysis, hydraulic tests, etc. So far, the analysis of these data have shown some important aspects.

First, the continuous measurements of piezometric data show that the water table of the alluvial aquifer is highly influenced by the water level of the Rhône river. More precisely, the piezometric maps show that in a large portion of the region, the level of the Rhône is higher than the piezometry. This indicates either recharge conditions or disconnection.The assumption of recharge is in agreement with new maps (e.g. Fig. 1) of the hydrochemical data that were interpolated for this study. Those maps show that low concentrations of the different chemical species are most often measured near the low mineralized Rhône River.

In addition, the comparison of the hydrochemical data with the lithology of the valley slopes indicates places with a groundwater inflow from karstic aquifers.

Finally, the importance of the drainage ditches on the groundwater flow is revealed by the maps of the water chemistry. On those maps, the ditches form clearly recognizable barriers between two types of water (e.g. higher and lower mineralized waters, on both sides of the Canal du Syndicat, Fig. 1).

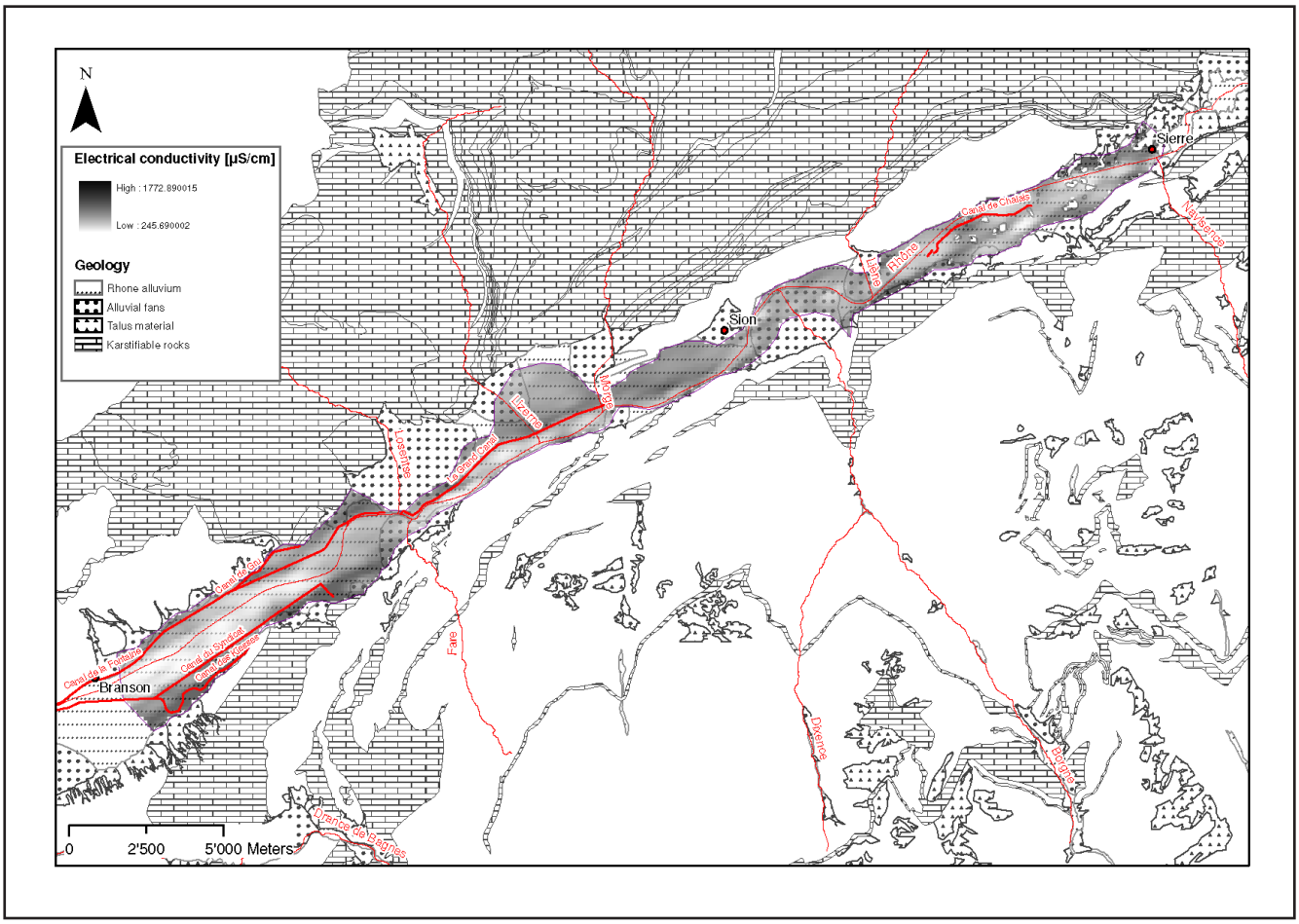

Figure 1. Interpolated map (kriging) of electrical conductivity in the Rhone aquifer between Sierre and Branson (Data: High water levels 1985).

REFERENCES

OFEFP/OFEG, 2003. Cours d'eau suisses. Pour une politique de gestion durable de nos eaux. Berne, 12 pages

1.15

Impacts climatiques sur la recharge d'un système karstique englacé, Tsanfleuron-Sanetsch, Alpes suisses

GREMAUD Vivian*, GOLDSCHEIDER Nico*

Centre d'hydrogéologie et de géothermie, Université de Neuchâtel, Rue Emile Argand 11, 2009 Neuchâtel, Suisse, vivian.gremaud@unine.ch, nico.goldscheider@unine.ch

Les glaciers de haute montagne accumulent une grande quantité d'eau en hiver, contribuant ainsi à la recharge des eaux souterraines durant les saisons chaudes. Actuellement les glaciers alpins sont globalement en retrait et certains vont disparaître dans les 50 prochaines années sous les effets des changements climatiques. La région de Tsanfleuron-Sanetsch dans les Alpes de Suisse occidentale est un site expérimental idéal pour étudier les interactions glacier-aquifère. En effet un glacier au recul très rapide et présentant un risque de disparition prochaine surmonte un aquifère karstique drainé principalement par la source de Glarey et utilisée pour l'approvisionnement en eau potable. De larges surfaces de l'aquifère sont exposées aux précipitions et à la fonte des neiges entre le glacier et ce captage. Ainsi, entre le glacier de Tsanfleuron et sa moraine de 1855 (petit âge glaciaire) la surface du karst a été polie par l'écoulement glaciaire, alors que des lapiaz typiques sont présents sous le cordon morainique. Géologiquement la zone est formée de roches sédimentaires jurassiques à paléogènes, plissée selon un large anticlinal limité au sud par un étroit synclinal au niveau du captage de Glarey. Les relations entre stratigraphie, tectonique, processus de recharge et drainage souterrain de l'aquifère karstique a été étudié par de multiples méthodes, en particulier des essais de traçage et certains paramètres physiques mesurés en continu. La géométrie et structure du glacier de Tsanfleuron ont été étudiées par plusieurs campagnes géophysiques (méthode radio magnétotellurique RMT). Le volume de glace a été estimé à 102 millions de m^3, correspondant à ~93 millions de m3 d'eau liquide disponible pour recharger l'aquifère karstique et le soumettant à une variabilité journalière et saisonnière. L'eau de fonte produite par le glacier influence la géométrie des courbes de restitution et, par conséquent, les flux et le transport dans l'aquifère. Basé sur les prévisions climatiques, un modèle de disponibilité saisonnière de l'eau a été établi. L'hiver et le printemps présenteront un surplus d'eau alors que des périodes de manque d'eau seront à craindre lors de longues périodes sèches en été et automne, l'eau glaciaire étant absente. De plus les précipitations seront plus fortes mais plus rares et la demande en eau plus importante, particulièrement pour l'irrigation.

1.16

Partitioning of total mercury and methylmercury between colloids and true solution in overlying and interstitial waters (Lake Geneva).

Stéphane GUEDRON*, Davide A.L. VIGNATI**, Janusz DOMINIK*.

* *Institut F.-A. Forel, Section de sciences de la Terre et d'environnement, Université de Genève, CP 416, 1290 Versoix (stephane.guedron@unige.ch)*
** *CNR-IRSA, Via del Mulino 19, 20047 Brugherio (MB), Italy*

Mercury is one of the priority metals on the list established by the EU legislation due to its bioaccumulation in the food chain (Morel et al., 1998). Mercury bioaccumulation and biomagnification (i.e., increasing concentrations across trophic levels) are mainly caused by the transformation of inorganic Hg into the organic form methylmercury (MeHg) (Fitzgerald and Lamborg, 2003). As it is the case for many other elements (Vignati et al., 2005), the partitioning of mercury and MeHg largely controls their bioavailability and transfer to the trophic chains. Furthermore, formation of MeHg is particularly active at the sediment water interface thus making the study of Hg and MeHg partitioning in interstitial waters a topic of utmost interest for Hg/MeHg biogeochemical cycles and the associated risk assessment.
In this study, we used tangential flow filtration (TFF) to determine the partitioning of Hg and MeHg between operationally defined colloidal (0.45 μm – 3 kDa) and truly dissolved (< 3 kDa) fractions. Using ultraclean techniques (Cossa and Gobeil, 2000), blank values of 0.1–0.8 ng L^{-1} and < 0.01 ng L^{-1} were obtained for total Hg (HgT) and MeHg, respectively. We also adapted the TFF methodology to process volumes of 60 – 80 mL; corresponding to the amount of interstitial water (IW) recovered from 4 cm of sediment after centrifugation and filtration.
Sediment cores and overlying waters were collected at two sites with contrasting characteristics in Lake Geneva (Switzerland/France). Cores were sliced under nitrogen atmosphere to recover interstitial water. Interstitial water was filtered (0.45 μm) and then ultrafiltered. Total filterable Hg and MeHg concentrations were in the range 3.5–11 ng L^{-1} and 0.061–0.082 ng L^{-1}, respectively. The percentage of Hg and MeHg associated with colloids were similar: 20–35% of total filterable concentrations.

To verify if truly dissolved concentrations of Hg/MeHg could be estimated from the more easily measured total filterable concentrations, we combined our results with data available from literature. No significant correlation between filterable vs. truly dissolved concentrations were found for MMHg. On the other hand, significant Spearman correlations ($R^2 = 0.56$; $N = 30$; $p < 0.01$ for freshwater data and $R^2 = 0.92$; $N = 23$; $p < 0.001$ for oceanic water data) were obtained for total Hg. Our data superimposed rather well to the regression obtained for oceanic waters, rather than to the regression for freshwaters. We therefore surmise that the ligands controlling total Hg partitioning in IW are similar to those in oceanic coastal waters. The validity of this model should obviously be confirmed by future studies, but it opens an intriguing possibility to estimate Hg partitioning in IW and thus to refine the existing biogeochemical models.

REFERENCES

Cossa, D. and Gobeil, C., 2000. Mercury speciation in the Lower St. Lawrence estuary. Can. J. Fish. Aquat. Sci., 57: 138-147.

Fitzgerald, W.F. and Lamborg, C.H., 2003. Geochemistry of mercury in the environment. In: B. Sherwood Lollar (Editor), Treatise on Geochemistry. Elsevier, pp. 107-148.

Morel, F.M.M., Kraepiel, A.M.L. and Amyot, M., 1998. The chemical cycle and bioaccumulation of mercury. Annual Reviews Ecol.Syst., 29: 543-566.

Vignati, D.A.L., Dworak, T., Ferrari, B., Koukal, B., Loizeau, J.L., Minouflet, M., Camusso, M.I., Polesello, S. and Dominik, J., 2005. Assessment of the geochemical role of colloids and their impact on contaminant toxicity in freshwaters: An example from the Lambro-Po system (Italy). Environmental Science & Technology, 39(2): 489-497.

1.17

Trends in streamwater chemistry at the Damma glacier, Switzerland

Hindshaw Ruth*,**, Reynolds Ben*, Wiederhold Jan*,**, Kretzschmar Ruben** & Bourdon Bernard*

*Institute of Isotope Geochemistry and Mineral Resources, Clausiusstrasse 25, CH-8092 Zürich (hindshaw@erdw.ethz.ch)
**Insitute of Biogeochemisty and Pollutant Dynamics, Universitätsstrasse 16, CH-8092

The contribution of silicate weathering to global cationic denudation rates is not known precisely due to the difficulty of separating the weathering from silicate and carbonate minerals. Accurate quantification of in situ silicate mineral weathering rates is required to constrain the carbon cycle. Small, mono-lithological catchments are ideal for elucidating the processes by which silicate rocks weather and how these processes change under varying seasonal conditions.

This work forms part of the multi-disciplinary BigLink Project which is investigating the 10.7 km^2 granitic Damma catchment (Switzerland). The glacier has retreated rapidly, exposing fresh mineral surfaces allowing the initial stages of granite weathering to be studied. Stream waters were sampled for one year, with higher frequency sampling during the summer, in five different locations, in conjunction with high resolution hydrological and meteorological measurements. Selected isotope ratios were analysed in addition to the overall chemical composition to characterise spatial and temporal variations in stream water chemistry.

After correction for atmospheric inputs, daily and seasonal cycles were clearly observed in the cation concentrations. The cyclic trends were independent of dilution and indicated the mixing of at least two distinct sources whose relative proportions changed over seasonal and daily timescales. In order to identify potential end-member sources, porewater and groundwater samples were also analysed. Our data show that these potential end-members are highly variable spatially and temporally.

The different sources reflect differing water-rock interaction times as evinced by variable elemental ratios (e.g. Na/Ca) which were offset from bulk rock ratios. A groundwater contribution with Na/Ca ratios close to bulk rock values is dominant in winter. During increased surface discharge in summer, groundwater contributions are smaller and Na/Ca ratios are offset from those of bulk rock.

This study shows that even in a lithologically well-constrained watershed, large variations in cation flux occur over daily and seasonal timescales, primarily due to changing hydrological conditions. Thus, knowledge of the hydrology of a catchment is essential to quantify cyclic cationic denudation rates, and to estimate silicate weathering rates.

1.18

Processes at and across the interface: Lessons lerned from river groundwater interactions under different hydrologic conditions

Peter Huggenberger

Angewandte und Umweltgeologie, Dept. Umweltwissenschaften, Uni Basel.
Peter.huggenberger@unibas.ch

Canalization of many rivers in the 19th century strongly influenced the economic development and urbanization of most European countries. Together with technical developments in agriculture, a series of environmental problems such as flooding, groundwater pollution and ecological changes, including the decrease of characteristic habitats of riverine landscapes, were created. Most of the river valleys are important groundwater reservoirs, in particular in central Europe. These reservoirs are often highly endangered due to intense agricultural and industrial activities and a dense network of urban areas connected by numerous traffic lines. Additionally, the high permeability of fluvial sediments (esp. fluvial shaped aquifer types of alpine type), the frequently observed lack of a thick protective cover layer and the exchange processes with surface waters result in a high vulnerability of groundwater resources.

Formulated goals for a sustainable development of water resources guide mitigation strategies and consider defined standards, i.e. natural composition of surface waters. Major efforts for future transdisciplinary research, with respect to hydrological regimes (low and high flow) or groundwater flow regimes, will concentrate on the knowledge of the structural dynamics of the river and related groundwater systems. To identify hydrological and hydrogeological system profiles, methodologies to quantify and control these profiles must be developed and applied. This can be achieved by the implementation of management systems that include observation systems and the development of numerical models combined with specific field experiments and scenario development.

The integral of changes in river structures in the catchment (i.e. lack of retention space) has already demonstrated serious consequences during major floods. Due to the experience gained from the hazardous flood events in the last twenty years, the pollution problems and the loss of characteristic riverine landscapes, most countries have adopted a more comprehensive view of rivers. It is recognized that the consideration of processes of river-groundwater interactions are important, which significantly differ for natural and channelized states.

Within this context, positive and negative aspects of river-groundwater interaction for channelized and non-channelized surface waters are investigated. The interaction of surface and subsurface waters is subject to continuous dynamics involving water budgets, water quality and flow patterns. When considering quantitative hydrological aspects of river-groundwater interaction, the transient character of riverbed permeability is an essential factor. Sediment erosion as well as transport and deposition processes are influenced by rivers that are able to exert their natural dynamics. As a consequence, the variance of the riverbed permeability is increased temporarily, influencing infiltration rates and groundwater mixing ratios, as well as residence times for groundwater from different provenance.

To understand the dynamics of river-groundwater interaction, our investigations focus on: (1) the evaluation of transient hydraulic boundary conditions, including the transient character of riverbed permeability and (2) qualitative aspects of surface waters and groundwater. Results from experiments of selected river-reaches are presented, including: (1) adequate observation systems that facilitate the measurement of groundwater parameters at different depths, as well as the definition of sampling strategies, (2) non-destructive geophysical methods (Georadar, Geoelectrics) within the river bed and the riparian zone, as well as (3) subsequent high resolution groundwater flow and transport modeling, including scenario techniques, model calibration and sensitivity analyses. Interaction processes are studied at a regional and a local scale (e.g. Upper Rhine Graben, individual catchment areas, river-reaches and capture zones of extraction wells).

1.19

The fate of organic contaminants at the groundwater-surface water interface

Hunkeler Daniel*, Abe Yumiko*, Aravena Ramon**, Parker Beth*** & Cherry John***

*Centre for Hydrogeology, University of Neuchâtel, Rue Emile Argand 11, CH-2009 Neuchâtel (Daniel.Hunkeler@unine.ch)
**Department of Earth and Environmental Sciences, University of Waterloo, 200 University Avenue West, Waterloo ON N2L 3G1, Canada
***School of Engineering, University of Guelph, Guelph ON N1G 2W1, Canada

Persistent groundwater contaminants with little tendency to sorb to the matrix often travel over extended distances in aquifers and can eventually reach surface water bodies or other groundwater dependent ecosystems. In the vicinity of surface water bodies, sediment quality and redox conditions frequently change and biological activity is enhanced creating additional possibilities for contaminant retention and degradation. To what extent these altered conditions affect the contaminant fate strongly depends on groundwater flow paths, which are often highly complex in vicinity of surface water bodies, and the residence time of groundwater in zones with geochemical conditions suitable for contaminant degradation or retention.

In the presentation, results from two field sites are discussed where a tetrachloroethene (PCE) and a trichloroethene (TCE) plume, respectively discharges to a stream. PCE and TCE are well suited compounds to evaluate the effect of changing geochemical conditions on the contaminant fate since their degradation is highly dependent on the redox conditions. PCE and TCE degrade by reductive dechlorination under moderately reducing conditions, while their degradation products cis-1,2-dichloroethene (cDCE) and vinyl chloride (VC) require strongly reducing conditions for further reductive transformation. Alternatively, cDCE and VC can also be oxidized to CO2 under aerobic and moderately reducing conditions. At the two sites, contaminant transformation was characterized using high resolution sampling and analysis of redox sensitive species, dissolved contaminants, stable isotope ratios of contaminants and microbial parameters.

At the PCE site (Abe et al., 2009), the contaminant plume travelled through a sandy aquifer under confined conditions and discharged into the stream through an approximately 2m thick layer of silty-clayey streambed sediment rich in organic matter (Figure 1a). While no degradation occurred in the sandy aquifer, highly variable degradation was observed in the streambed sediments related to small scale heterogeneities. The degree of degradation reached from no degradation in sandier zones where rapid groundwater discharge occurred to complete reductive dechlorination in clay-rich zones where highly reducing conditions prevailed. The TCE site consisted of an unconfined sandy aquifer (Chapman et al., 2007). In the upgradient part of the site, groundwater travelled at a depth of several meters below ground surface while in the downgradient zone, the water table was close to the surface and contaminants partly migrated through organic carbon rich floodplain sediments where reductive dechlorination occurred (Figure 1b). However, the shallow water table conditions favored groundwater discharge into ponds and creeks. Hence, while the aquifer showed a substantial capacity for contaminant degradation, most of the contaminants traveled via these small creeks to the main stream.

The studies demonstrate that in order to gain insight into the contaminant fate at groundwater-surface water interfaces a good understanding of the geochemical variability and groundwater flow paths is essential. At both sites, zones with favorable conditions for contaminant degradation occurred. However, these zones were partly by-passed and overall only partial elimination of the contaminants occurred. Finally, the study also illustrates the need for high resolution sampling to develop a consistent conceptual model of contaminant migration and degradation at groundwater-surface water interfaces.

a) PCE site

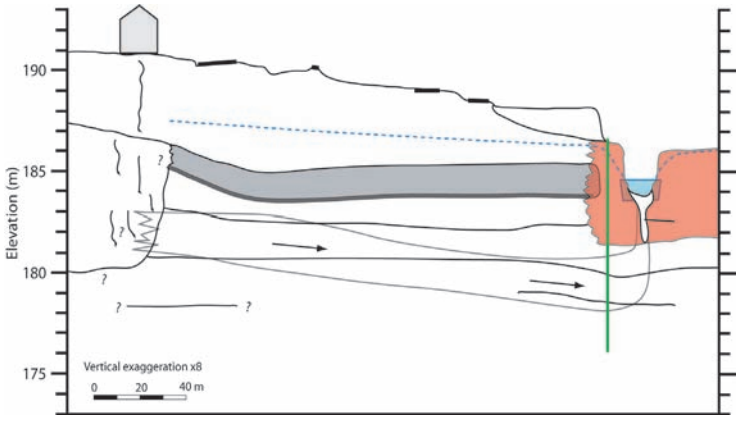

b) TCE site

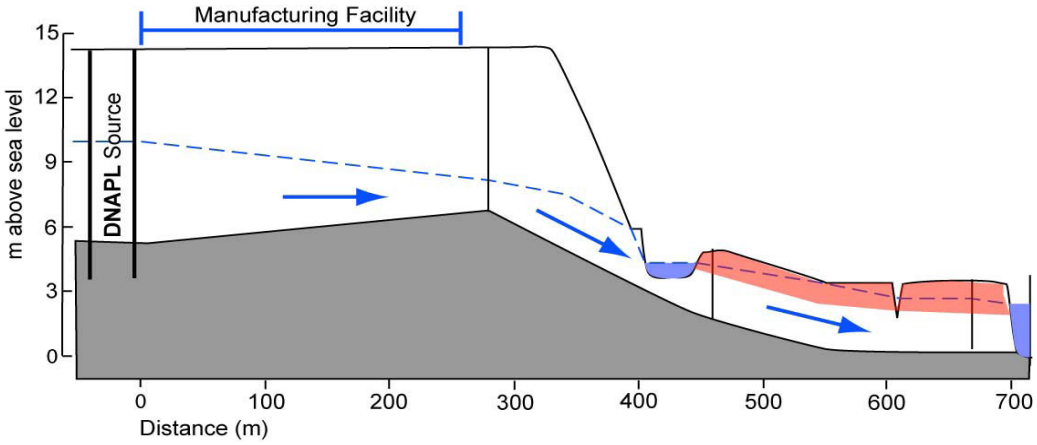

Figure 1: Schematic cross section of the field sites where contaminant plumes discharge into a stream under confined (a) and unconfined (b) conditions.

REFERENCES

Abe, Y., Aravena, R., Parker, B.L. and Hunkeler, D., 2009. Evaluating the fate of chlorianted ethenes in streambed sediments by combining stable isotope, geochemical and microbial methods. J. Contam. Hydrol., 107(1-2): 10-21.

Chapman, S.W., Parker, B.L., Cherry, J.A., Aravena, R. and Hunkeler, D., 2007. Groundwater-surface water interaction and its role on TCE groundwater plume attenuation. J. Contam. Hydrol., 91: 203-232.

1.20

Thoron as a possible marker tracing surface water / groundwater interaction

Huxol, Stephan[1], Hoehn, Eduard[1], Surbeck, Heinz[2], Kipfer, Rolf[1,3]

[21]Eawag, Swiss Federal Institute of Water Science and Technology, CH-8600 Dübendorf, Switzerland (Stephan.huxol@eawag.ch)
[2] Nucfilm Ltd., CH-1792 Cordast, Switzerland
[3] Institute of Isotope Geology and Mineral Resources, Swiss Federal Institute of Technology (ETH) Zürich, Switzerland

Radon (^{222}Rn, half-life 3.6 d) and thoron (^{220}Rn, half-live 55.6 s) are the most long lived isotopes of the noble gas radon. As part of the two natural radioactive decay series of ^{238}U and ^{232}Th, respectively, they are released from minerals to fluids (e. g. soil gas, ground water) by α-decay from their precursors ^{226}Ra and ^{224}Ra, respectively (emanation process). Both radon-isotopes can be found in soil gas. ^{222}Rn has been subject to research for a long time and is well known to occur in aquatic systems, especially in ground water. It is often used as a tracer for assessing residence times of surface waters infiltrating to ground water. In contrast, studies on thoron in aquatic systems are rare. However, thoron is expected to be found in groundwater, too, where it could be used for an assessment of mixing. Also, for assessing upwelling/downwelling processes in the river bed, thoron is a potentially promising tracer.

Up to now, we did not find any thoron in ground water. This is most probably related to the fast decay of thoron, which result in a restricted mobility, and the time-consuming detection system to determine thoron. Further more, the geophysical and geochemical character of the radionuclides of the ^{238}U series is different from that of the ^{232}Th series and, therefore, the appearance of radon in aquatic systems does not necessarily reflect the occurrence of thoron.

In order to conceptually describe the thoron emanation we formulated the following working hypothesis: The precursors of radon and thoron ($^{224, 226, 228}$Ra) are known to be slightly more soluble in anoxic than in groundwater (in oxic water, Ra is only hardly soluble and remain essentially in the solid phase). If such anoxic ground water gets into contact with oxygen, radium tends to co-precipitate with Mn and Fe oxide/hydroxides. As a result, the emanation of thoron to the water phase may be enhanced by radium, which is attached to surface coatings of the precipitates. In order to enhance the sampling procedure, we modulated a conventional sampling system (RAD7, coupled with commercial degassing unit RAD AQUA) by interconnecting an additional closed air loop with adjustable diaphragm pump to decrease the residence times of water and air between sampling and measurement.

Primary results confirm the feasibility of thoron analysis in oxygen-poor springs, especially if iron and manganese precipitates are present. Gamma-spectroscopy of precipitates at the springs's outlet showed the relative high content of thoron precursors and daughter products in the Fe and Mn oxides/hydroxides. Moreover, α-spectrometric analysis showed that thoron precursors and daughters are concentrated on the surface of the precipitates, which further add evidence to our conceptual view of thoron emanation.

1.21

Variability of in situ biodegradation of chlorinated ethenes in a constructed wetland

Imfeld Gwenaël*, Nijenhuis Ivonne*, Nikolausz Marcell** & Richnow Hans H*

*Department of Isotope Biogeochemistry, Helmholtz Centre for Environmental Research - UFZ, Permoserstr. 15, D-04318 Leipzig (gwenael.imfeld@engees.u-strasbg.fr)
*Department of Environmental Biotechnology, Helmholtz Centre for Environmental Research - UFZ, Permoserstr. 15, D-04318 Leipzig

The spatial and temporal biogeochemical development of a model wetland supplied with cis- and trans-1,2-dichloroethene contaminated groundwater was characterized over 430 days by hydrogeochemical and compound-specific isotope analyses (CSIA). The hydrogeochemistry dramatically changed over time from oxic to strongly reducing conditions as emphasized by increasing concentrations of ferrous iron, sulfide, and methane since day 225. δ13C values for transand cis-DCE substantially changed over the flow path and correlated over time with DCE removal. The carbon enrichment factor values (ε) retrieved from the wetland became progressively larger over the investigation period, ranging from -1.7 ± 0.3‰ to -32.6 ± 2.2‰. This indicated that less fractionating DCE oxidation was progressively replaced by reductive dechlorination, associated with a more pronounced isotopic effect and further confirmed by the detection of vinyl chloride and ethene since day 250. This study demonstrates the linkage between hydrogeochemical variability and intrinsic degradation processes and highlights the potential of CSIA to trace the temporal and spatial changes of the dominant degradation mechanism of DCE in natural or engineered systems.

In parallel, the dynamics and composition of microbial communities in the aqueous phase of the model wetland was characterized. PCR-DGGE analysis of water sample obtained from different part of the wetland revealed that changes of the bacterial community structures coincided with a succession of the hydrogeochemical conditions in the wetland, from oxic towards anoxic conditions. During this transition phase, the appearance of vinyl chloride and ethene correlated with the presence of putative dechlorinating bacteria (Dehalococcoides spp., Geobacter spp. and Dehalobacter spp.). Additionally, shift of DCE isotopic composition indicated the progressive prevalence of reductive dechlorination in the wetland. Although the DCE degradation processes varied over time, biodegradation activity was maintained in the wetland system. 16S rRNA gene libraries revealed that Proteobacteria accounted for > 50 % of 16S rRNA genes clone libraries, whereas ~17 % of the sequences from the wetland were related to sulphate reducers. Based on an multiple-method approach, this study illustrates the linkage between microbial community dynamics and composition, changes of hydrochemical conditions and processes of DCE degradation in a wetland system.

1.22

Role of land-atmosphere interactions for climate extremes and trends

Eric B. Jaeger*, Ruth Lorenz* & Sonia I. Seneviratne*

*Institute for Atmospheric and Climate Science, ETH Zurich, Switzerland (eric.jaeger@env.ethz.ch)

Processes acting at the interface between the land surface and the atmosphere have a strong impact on the European summer climate, particularly during extreme years. These processes are to a large extent associated with soil moisture. This presentation provides an overview on recent analyses investigating the role of soil moisture-atmosphere coupling for the European summer climate over the period 1959-2006 using simulations with a regional climate model.

The set of experiments consists of a control simulation with interactive soil moisture, and sensitivity experiments with prescribed soil moisture. Soil moisture-climate interactions are found to have significant effects on temperature extremes

in the experiments, and impacts on precipitation extremes are also identified. Case studies of selected major summer heat waves reveal that the intraseasonal and interannual variability of soil moisture account for 5–30% and 10–40% of the simulated heat wave anomaly, respectively. In addition, is also found that soil moisture has a significant effect on heat wave persistence through soil moisture memory. For extreme precipitation events on the other hand, only the wet day frequency is impacted in the experiments with prescribed soil moisture.

Finally, trends in climate extremes in current climate-change projections, such as an increase in temperature over the whole European continent, as well as a Southern European decrease and Northern European increase in precipitation extremes, can already be detected in simulations for the past decades, and appear at least partly linked to soil moisture-atmosphere feedbacks.

1.23

Swissrivers.ch – Online river forecast prediction

Jordan Frédéric*, Claude Philiponna**, Heller Philippe*

*e-dric.ch eau énergie environnement, Le Grand-chemin 73, CH-1066 EPALINGES (fred.jordan@e-dric.ch)
**Camptocamp SA, PSE A, EPFL, CH-1015 LAUSANNE

Discharge prediction in river basins has become a pluridisciplinary and high-technology topic. The needs for such systems are related to flood management, hydroelectricity market or leisure activities. In this context, swissrivers.ch has been developed to provide everyone, using internet, information about the future discharge in all the main rivers of Switzerland.

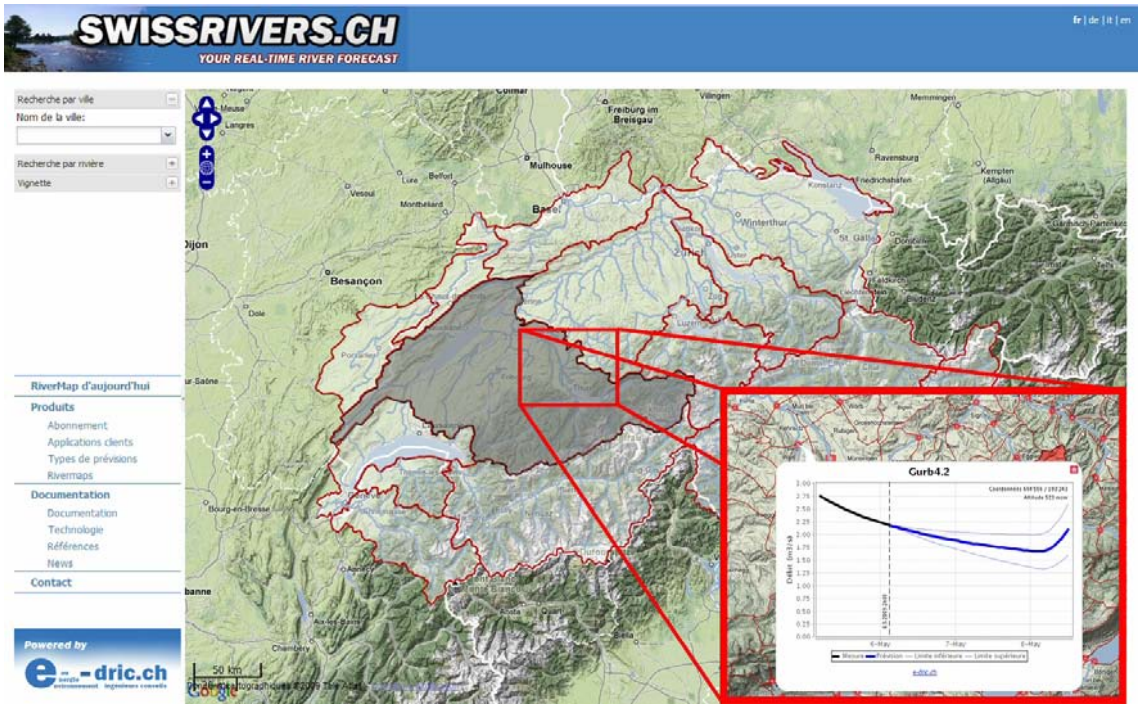

Figure 1. The new web platform www.swissrivers.ch, with a direct geographical access to river discharge predictions.

The new online platform works as follows: numerical weather predictions are provided by the Federal Office for Meteorology and Climatology (Meteoswiss), twice a day and up to 72 hours ahead. Their precipitation and temperature predictions issued from the COSMO-7 model (Schättler, Barbu, 2008) with a 6.6 km horizontal grid mesh are used for an extract over the whole country to calculate the predicted discharges in the sub-basins and in the rivers. In order to optimize the quality of the predicted discharges, the hydrological model is updated 4 times a day: the continuous simulation is automatically modified by comparison between discharge measurements and computed discharges based on meteorological observations over the last 24 hours for each one of the 280 automatic federal gauging stations of Switzerland (BAFU). The objective of this model update is to ensure that the model always simulates realistic discharges in rivers.

The information provided by swissrivers.ch can be freely accessed for 2500 sub-basins and 1500 locations in the swiss rivers. For every selected location, the updated simulation of the last 24h, as well as the discharge prediction for the next 30 hours are presented as a plot.

The system is based on the RS3.0 technology, which allows the automatic data acquisition and storage in a database (weather and discharge observations, numerical weather forecasts), the rainfall-runoff simulation including snowmelt, glacier melt, evaporation, infiltration, surface runoff, river routing as well as flow routing in hydraulic structures (reservoirs, power plants, water diversions, etc...). RS3.0 also allows an automatic publication of the results in a web platform or in a GIS. This technology is based on previous developments realized for the MINERVE Project at the Ecole Polytechnique Fédérale de Lausanne (Jordan et al., 2007, Garcia et al., 2008, Jordan et al., 2008).

The performance of the system has been optimized by a calibration-validation procedure using more than 15 years of hourly data, over 300 control points in Switzerland. However, the model could be improved by integration of new historical and real-time control points, in basins located upstream of large dams and reservoirs.

REFERENCES

Garcia, J., Jordan, F., Dubois, J. & Boillat, J.-L. 2007 : "Routing System II, Modélisation d'écoulements dans des systèmes hydrauliques", Communication LCH n° 32, Ed. Prof. A. Schleiss, Lausanne

Jordan, F. 2007 : "Modèle de prévision et de gestion des crues - Optimisation des opérations des aménagements hydroélectriques à accumulation pour la réduction des débits de crue", Thèse de doctorat n°3711, Ecole Polytechnique Fédérale de Lausanne.

Jordan, F., Garcia Hernandez, J., Dubois, J. & Boillat, J.-L. 2008 : "MINERVE : Modélisation des Intempéries de Nature Extrême du Rhône Valaisan et de leurs Effets", Communication LCH n° 38, ed. A. Schleiss, EPFL, Lausanne

Martinerie, R. 2009 : Numerical Modelling of Stormwater and Wastewater Conveyance System of Lausanne City (Switzerland), Proc., Water Engineering for a Sustainable Environment, 33rd IAHR Congress, Vancover, Canada

Schättler, U., Barbu, C. 2008 : COSMO-Newsletter No.9. pp.87. available through: www.cosmo-model.org > Documentation > Newsletters. Printed at Deutscher Wetterdienst, Offenbach am Main, Germany

1.24

The influence of climate change on the water balance of mesoscale catchments in Switzerland

Köplin Nina*,**, Viviroli Daniel*,**, Weingartner Rolf*,**

*Institute of Geography, University of Bern, Hallerstrasse 12, CH-3012 Bern (nina.koeplin@giub.unibe.ch)
**Oeschger Centre for Climate Change Research, University of Bern, Zähringerstrasse 25, CH-3012 Bern

Recent research shows that the anticipated climate change in Switzerland will result in changing precipitation patterns and increasing temperatures during the first half of the 21st century. Amongst others, the temperature increase will cause an upward shift of the snowline, and precipitation will fall more often as rain than as snow. The combination of these changes will provoke a change in the runoff regime such as an earlier yearly peak flow. While evapotranspiration will generally increase in a future climate, the changes in precipitation amounts will differ seasonally, with increases in winter and decreases in summer (OcCC 2007). The yearly volume of discharge is likely to decrease with the exception of alpine catchments where glaciers will function as reservoirs during the next years (Schädler 2008).

Our main interest lies in the question when and in particular where the system starts tipping over and abovementioned changes show through in the hydrological response of catchments. This issue will be addressed in the framework of the joint research project "Climate Change in Switzerland – Hydrology" (CCHydro) which was initiated by the Federal Office for the Environment (FOEN) and seeks to assess possible effects of climate change on hydrological systems in Switzerland. The heterogeneity of complex mountainous landscapes, however, forbids general statements. Therefore, a multidisciplinary and holistic approach was chosen and the scenarios in use are of high temporal and spatial resolution.

As a first step, hydrological modelling is used to identify and examine catchments that exhibit sensitivity towards a change in climate. For this, we use the process-oriented hydrological modelling system PREVAH (Viviroli et al. 2007). The mesoscale catchments under investigation have a mean area of about 150 km^2. After calibration of the catchments for which measured

discharge records are available, a regionalisation scheme (Viviroli 2007) is used to arrive at a comprehensive set of model parameters for the entire area of Switzerland. Spatially and temporally highly resolved scenarios of the projected climate change until 2050 will then be used to force the model. The scenarios will be scaled down to station data by the Institute for Atmospheric and Climate Science (IAC) at ETH Zurich using the Delta Approach.

As a result, regions exhibiting climate sensitivity in the period 2021 to 2050 will be specified, and possible causal relationships between sensitivity and specific catchment characteristics will be evaluated.

REFERENCES

OcCC 2007: Klimaänderung und die Schweiz 2050. Erwartete Auswirkungen auf Umwelt, Gesellschaft und Wirtschaft. Bern: OcCC.

Schädler, B. 2008: Klimawandel - Geht uns das Wasser aus?, Gas Wasser Abwasser, 10, 763–769.

Viviroli, D. 2007: Ein prozessorientiertes Modellsystem zur Ermittlung seltener Hochwasserabflüsse für ungemessene Einzugsgebiete der Schweiz. Geographica Bernensia G77. Bern: Geographisches Institut der Universität Bern.

Viviroli, D., Gurtz, J. & Zappa, M. 2007: The Hydrological Modelling System PREVAH. Geographica Bernensia P40. Bern: Geographisches Institut der Universität Bern.

1.25

Palaeoenvironmental mapping of the Swiss Rhone river

Laigre Laetitia*, Arnaud-Fassetta Gilles**, Reynard Emmanuel*

** Institut de Géographie, Université de Lausanne, Anthropole, CH-1015 Lausanne (laetitia.laigre@unil.ch)*
*** Département de Géographie, Université Val-de-Marne (Paris 12),*
Avenue du Général de Gaulle 61, F-94010 Créteil Cedex

As many European rivers, the Swiss Rhone river and its floodplain have known several morphological variations after the Little Ice Age that ended around 1850. Based on the concept of the palaeoenvironmental atlas built on the French Rhone river by J.-P. Bravard et al. (2008), palaeoenvironmental mapping has been carried out in the Swiss Rhone river watershed (Laigre 2009). Comparison of historical maps from 1835 to 1996 (Dufour map, Siegfried Atlas, and several editions of national map of Switzerland) shows several events of fluvial metamorphosis (Bravard 1989) of the channel. Until the 1860's, numerous gravel bars, extensive islands and large active zone can be observed. The braided style is the dominant fluvial pattern. Since the end of the 19th century, most of channels are straight, excepted one area – the Finges Forest zone – where a large part of the valley is occupied by an important braided system. Since the 1940's, a channel constriction is observed as well and incision of the present straight channel is progressing.

Analysis of the metamorphosis factors emphasises principally one external variable, which modified the system: human intervention. Channelization of the Rhone river and its tributaries from the late 19th century and gravel extractions have completely modified the natural sedimentary functioning and balance, in a period of reduced sedimentary supply that characterises the end of the Little Ice Age. Moreover, morphological modifications of the fluvial system had impacts on the floodplain landscape evolution and land use in the valley, which was characterised by large woodland and wetland areas until the end of 19th century. Understanding functioning of past environments may be a precious help to anticipate eventual future flood events that cause large damages in the Alpine range.

REFERENCES

Bravard, J.-P. 1989: La métamorphose des rivières des Alpes françaises à la fin du Moyen-Age et à l'époque moderne, Bull. Soc. Géogr. Liège, 25, 145-157.

Bravard J.-P., Provansal M., Arnaud-Fassetta G., Chabbert S., Gaydou P., Dufour S., Richard F., Valleteau S., Melun G. & Passy P. 2008: Un atlas du paléo-environnement de la plaine alluviale du Rhône, de la frontière suisse à la mer. In Desmet M., Magny M., Mocci F. (coord.). Du climat à l'Homme. Dynamique holocène de l'environnement dans le Jura et les Alpes, Collection du Laboratoire EDYTEM, Cahiers de Paléoenvironnement 6 , 101-116.

Laigre L. 2009: Etude diachronique de la dynamique fluviale du Rhône suisse depuis la fin du Petit Age Glaciaire – Cartographie paléoenvironnementale sectorielle de la source au lac Léman, Mémoire de Master, Université Paris 1-Panthéon-Sorbonne.

1.26

Storage and release of water and chemical species in glaciers

Martin Lüthi

Versuchsanstalt für Wasserbau, Hydrologie und Glaziologie (VAW), ETH Zürich, 8092 Zürich (luethi@vaw.baug.ethz.ch)

Glaciers accumulate solid precipitation in form of ice, and with it materials ranging from chemical species to dust and stones. Only under steady climate conditions the release rate of these materials, and water, is constant. Under a varying climate there exist cold periods with reduced release of accumulated water and chemical species, as well as warm periods when water is released at high rate. During the warm periods, high concentrations of chemicals and sediments are released from the glacier. We present results from a transient flow line model of a glacier which allows us to quantify these processes. In a case study on Oberaargletscher we show that persistent organic pollutants (POPs) emitted to the atmosphere in the 1950-1960s were stored in the glacier and are released at high rate during the last decade. Consequently, the concentration of toxic POPs in the proglacial lake are as high as during the time of atmospheric impact, which agrees with measurements in a sediment core.

1.27

Groundwater and tunneling: implementation of a geochemical monitoring network in the southern Switzerland

Marzocchi Roberto* & Pera Sebastian*

* *IST – SUPSI Istituto scienze della Terra, CP 72, CH-6952 Canobbio (roberto.marzocchi@supsi.ch)*

The interaction of tunneling with groundwater is a problem from the environmental as well as the engineering point of view. In fact, tunnel drilling may cause a drawdown of piezometric levels and inflows in tunnels can be a problem during excavation steps. In fractured rock water circulation is strongly influenced by structural elements, such as fault zones, fractures and other discontinuities, and numerical solutions are frequently used in literature (NAGRA since 1985, Ofterdinger et al 1999, Löw et al. 2007). To this purpose various conceptual approaches has been performed to describe and model the groundwater flow through fractured rock masses, ranging from equivalent continuum models to discrete fracture network simulation models. However their application needs many preliminary investigations on the behavior of the groundwater system; moreover these models request a correct calibration, that is very complex, even impossible without a collection of necessary structural and hydrochemical data.

To study large-scale flow systems in fractured rocks of mountainous terrains, a comprehensive study is ongoing close to Lugano using the data produced in one of the main infrastructures actually in construction, the Alptransit Monte Ceneri base tunnel. The main goal of this work is the understanding of how the collection of isotopic and geochemical data, and geophysical techniques (VLF profiles and 2D resistivity surveys), combining with structural and hydrogeological informations, can be used in order to develop hydrogeological conceptual and perhaps numerical models.

In the region surrounding the Monte Ceneri base tunnel there are about 750 springs actually registered in the cantonal database. On the basis of criteria of *(i)* relevance (use and discharge) and *(ii)* distance from the tunnel, a number of springs are be selected for monthly measurements of discharge, electric conductivity, *pH*, and temperature, and water samples are taking to monitor stable isotopes of hydrogen and oxygen (^{2}H, ^{18}O) and tritium (^{3}H), perhaps combined with helium-3.

Furthermore these data will be compared with tunnel inflows informations to perform, within reason, a validation of the model that will be designed taking advantages of these techniques.

In particular, the analysis of stable isotope composition of springs, will reflect their water origin, because spatial (recharge altitude, topography, etc.) and temporal (seasonal) effects in precipitations strongly affect the isotopic composition of meteorological water and consequently of groundwater reservoirs (fig. 1). The analysis of tritium, that is a radioactive isotope, will be used for groundwater dating (fig. 2); using only tritium we will obtain a qualitative indication of water age (young or old groundwater), while tritium combined with helium-3, in case of modern water, will provide us, a “discrete age” for the sampled water.

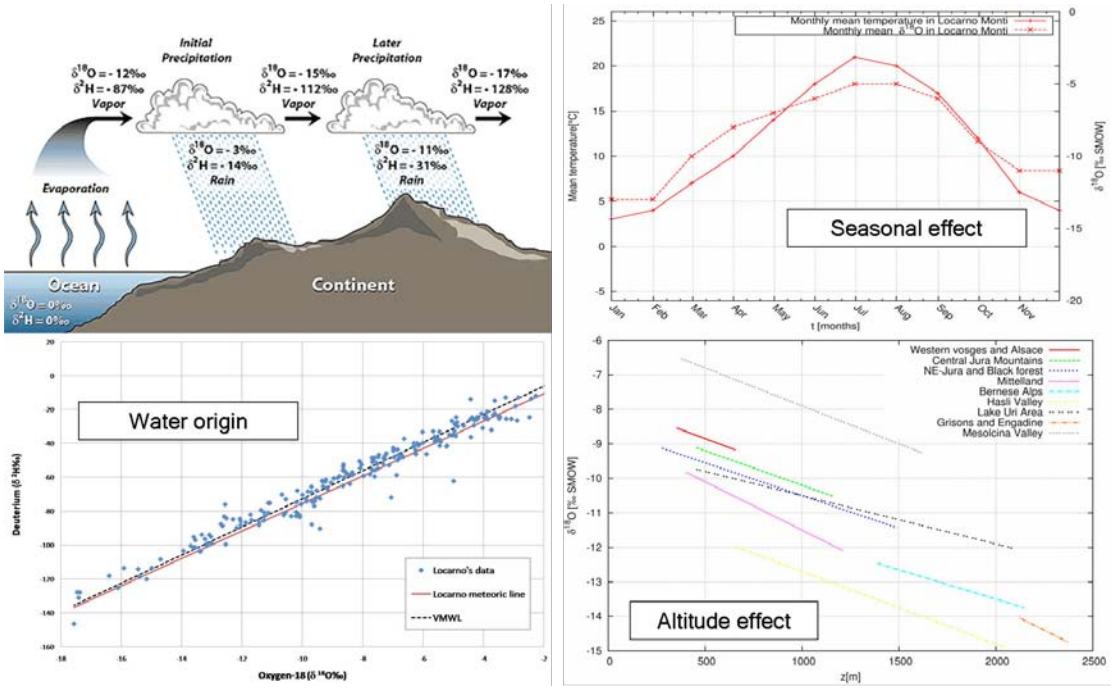

Figure 1. Stable isotopes fractionation: physical processes and relevant registered effects.

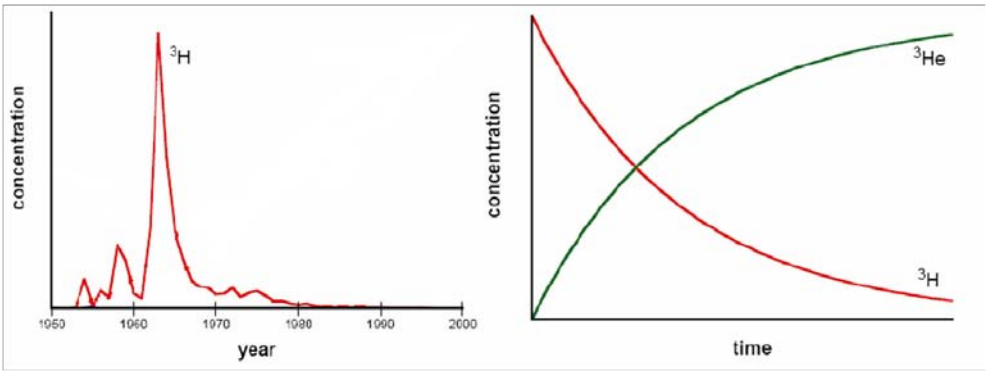

Figure 2. Basic principles of the dating methods with tritium. On the left the registered tritium concentration during last decades, that allows to qualitative distinction between young and old groundwaters. On the right the using of tritium combined with helium-3.

REFERENCES

AA.VV. 1985. Grimsel test site – Overview and test programs, NAGRA technical report 85-46

Löw, S., Lützenkirchen, V., Ofterdinger, U.S., Zangler, C., Eberhardt, E. & Evans, K. 2001. Environmental impacts of tunnels in fractured crystalline rocks of the Central Alps, IAH Selected Papers, Vol. 9, Chapter 34, 507-526

Ofterdinger, U.S. 2001. Ground water flow systems in the Rotondo Granite, Central Alps (Switzerland), Phd thesis of Natural Science, Swiss federal institute of technology (ETH) – Zurich

1.28

Dynamics of colloid concentrations in a small river related to hydrological conditions and land use.

MBock Patrick & Loizeau Jean-Luc

Institut F.-A. Forel, Faculté des sciences, Université de Genève, Route de Suisse 10, CH-1290 Versoix (Jean-Luc.Loizeau@unige.ch)

Colloids play a major role in the transport and bioavailability of contaminants in aquatic environments. Their dynamics in an ecosystem (erosion, transport, aggregation and subsequent settling) is a key parameter to understand the fate and potential impacts of colloid-associated pollutants such as metals or organic pollutants (e.g. Benoit et al. 1994, Irace-Guigand and Aaron 2003). In river systems, colloidal particles are mainly of detrital origin and derived from the erosion of soils and impermeable surfaces in the watershed.

In the present study, the watershed of the Versoix River (France, Switzerland), a tributary of Lake Geneva, has been investigated by sampling water at different sites along the river course, and under various hydrological conditions (low flows, snow melting, small floods). The watershed main characteristics (slope, land use) have been determined at each sampling point and quantified through a GIS-based study. Colloid and particle number and size distributions have been measured in the range 0.05 – 20 μm using a single particle counter (Rossé and Loizeau 2003).

Results show that the size distributions (expressed in number of particles) follow a power law, with very similar slopes, independently of the concentration. At the river mouth, colloid concentrations during small flood conditions were 10 to 100 times higher than during low flows, while suspended matter was only 2 to 3 times higher, and the discharge increased just by a factor two. These large discrepancies in the amplification factors between suspended particles and colloids concentrations reflect the preferential mobilization of easy erodible colloidal particles during rain events. In addition, colloid concentrations also generally increase with the distance from the head waters, for both high and low flows. This likely reflects a continuous colloid source from the river bed itself. However some variations exist in the colloid concentration that may be related to differences in the land cover. The Versoix River watershed is complex, comprising forest, meadows, cultivated fields, industrial and urban surfaces, and wetlands. A careful examination of the colloid concentration evolution along the river course during rain events shows that proportion of urban surfaces and cultivated field are positively correlated to increased colloid concentrations in the river.

As the capacity of colloidal particles to scavenge and subsequently transport contaminant is largely related to their specific surface, the large increase of colloid concentrations during flood implies a much larger potential contaminant load to the receiving water body than that generally observed with pollutant inputs related to suspended particle matter.

REFERENCES

Irace-Guigand, S,and Aaron JJ, 2003. The role of organic colloids in herbicide transfer to rivers: a quantitative study of triazine and phenylurea interactions with colloids. Analytical and Bioanalytical chemistry, 376: 431-435.

Benoit, S.D., Oktay-Marshall, A. Cantu, E.M. Hood, C.H. Coleman, M.O. Corapcioglu and P.H. Santschi, 1994. Partitioning of Cu, Pb, Ag, Zn, Fe, Al, and Mn between filter-retained particles, colloids, and solution in six Texas estuaries, Marine Chemistry 45: 307–336

Rossé, P., and J.-L. Loizeau, 2003. Use of single particle single particle counters for the determination of number and size distribution of colloid in natural surface waters. Colloids and Surfaces A 217:109-120.

1.29

Water disturbance as the organizer of riparian vegetation

Molnar Peter*, Perona Paolo*, Burlando Paolo*

*Institute of Environmental Engineering, ETH Zürich, CH-8093 Zürich (molnar@ifu.baug.ethz.ch, perona@ifu.baug.ethz.ch, paolo.burlando@ethz.ch)

The flow regime plays an important role in the organization of riparian vegetation in natural rivers by creating suitable germination sites, eroding plants and changing the river morphology. An important aspect of the flow regime is the disturbance element, i.e. the seasonal distribution, timing and magnitude of floods. The interactions between water, sediment, and riparian vegetation are most evident in natural unregulated rivers, such as gravel-bed braided streams and sand-bed meandering rivers. Restoration projects in regulated rivers often aim to make room for these natural interactions to take place. Therefore we need to continuously improve the scientific basis to understand the fundamental water-sediment-vegetation interactions and develop new tools and methods to simulate and test them. In this paper we present two new approaches (numerical and laboratory-based) which we are developing in our group and which look at water disturbance as an organizing element of riparian vegetation.

The first numerical approach is a stochastic model for water-sediment-vegetation interactions in a braided gravel-bed stream. This is an approach that models the expansion and contraction of the exposed sediment area in a braided river driven by stochastic flood disturbances and by a deterministic colonization of the exposed sediment banks and bars by riparian vegetation in the time between the floods. The basic model allows us to develop an analytical solution for the probability density function of the exposed sediment area as a function of the flood disturbance parameters and vegetation growth rate (Fig 1) (Perona et al., 2009).

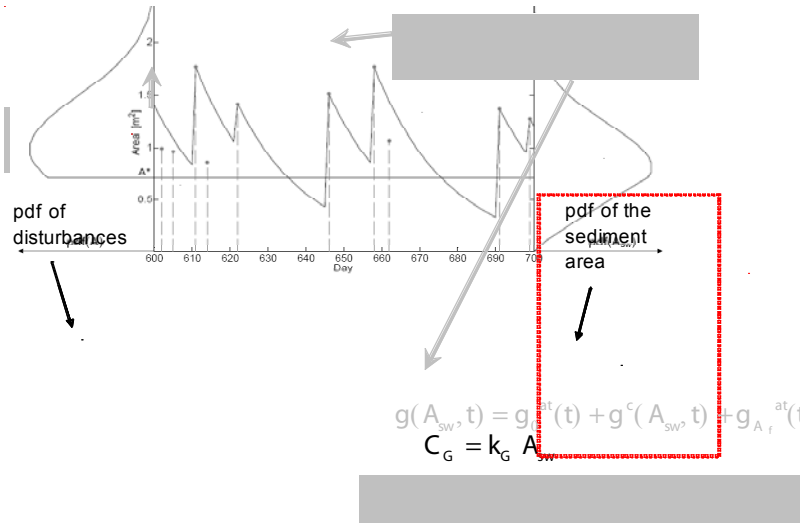

Figure 1. Setup of the process equation for the exposed sediment area A_{sw} and an illustration of the solution for the pdf of A_{sw}.

This simple model may be extended to include successive vegetation stages and their competition for available space on the floodplain (Perona et al., 2008).

The second laboratory approach is an experiment which studies the role of hydrological disturbances on biomass erosion dynamics in a sand-bed flume which is seeded by a fast growing grass. This experiment was conducted at the Total Environment Simulator of the University of Hull under the Hydralab3 EU Programme (Molnar et al., 2009, in preparation). In the experiment we studied the interactions between the disturbances and the growth rate of the vegetation roots and stems. Preliminary results show that the action of fluvial erosion removes systematically plants that are not able to withstand the applied stress, while the non-eroded community continues to grow and develop (Fig 2).

The two presented approaches both illustrate that the water disturbance regime plays an important role in the organization of braided river morphologies and sand bed streams, riparian vegetation, and plant communities. The water disturbance regime and vegetation growth interact and result in a dynamic riparian community. We advocate that this is not a deterministic problem and that the effect of water-sediment-riparian vegetation interactions should be examined in a probabilistic framework both at a large field and small laboratory scale.

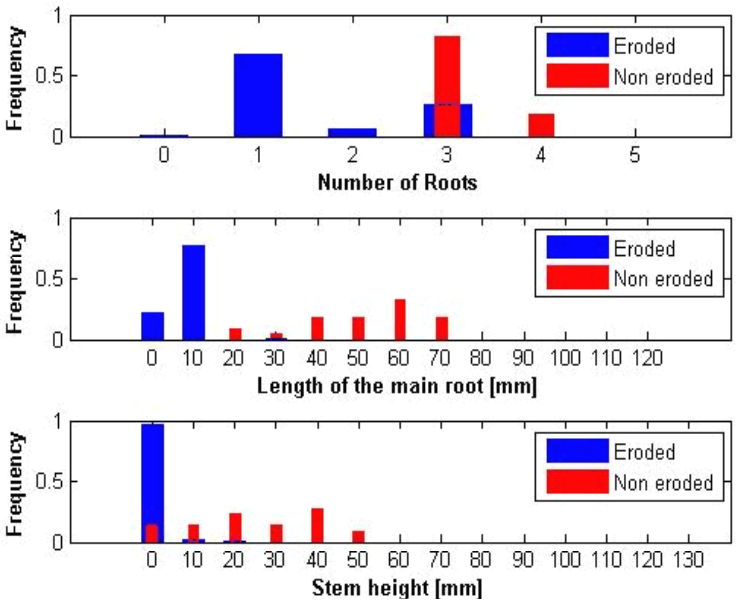

Figure 2. Example of a simulation run with the histograms of the number of roots (top), length of the main root (center) and stem height (bottom) for eroded and non-eroded plants.

REFERENCES

Perona, P., P. Molnar, M. Savina, and P. Burlando (2008). Stochastic sediment-vegetation dynamics in an Alpine braided river, IAHS Publ. 325, 266-274.

Perona, P., P. Molnar, M. Savina, and P. Burlando (2009). An observation-based stochastic model for sediment and vegetation dynamics in the floodplain of an Alpine braided river, Water Resour. Res., doi:10.1029/2008WR007550.

1.30

Calculating bedload transport rates in Swiss mountain streams using new roughness approaches

Manuel Nitsche*, Alexandre Badoux*, Jens M. Turowski*, Dieter Rickenmann*

Swiss Federal Institute for Forest, Snow and Landscape Research WSL, Zuercherstrasse 111, 8903 Birmensdorf, Switzerland (nitsche@wsl.ch)

Most methods for predicting bedload transport do not take into account typical roughness elements of small, steep mountain streams, like step-pool sequences, large boulders or woody debris. However, flow resistance due to such form roughness elements appears to be an important control on bedload transport rates in mountain streams.

Recently, new approaches based on laboratory experiments were proposed to assess flow resistance due to form roughness. They quantify the effects of generalized models of roughness elements to flow resistance. Furthermore, several empirically derived formulae to calculate bedload transport rates including a respective roughness parameter have been published.

The objective of our study is to systematically test these approaches with field observations. For this purpose, we measured the required roughness parameters for seven Swiss mountain streams, with local channel gradients ranging from 1.5 to 16.5 %, and catchment areas from 12 to 43 km^2. We calculated flow resistance and bedload transport for sediment transport events in 2000 and 2005. By comparing calculated and observed data of bedload transport we identified whether and in which range the examined approaches are suitable for application in natural stream conditions.

1.31

Pollution des eaux: la santé est-elle un levier pour mettre en place une gestion intégrée à l'échelle du basin versant?

Niwa Nelly*, Rossi Luca** & Chèvre Nathalie***

* *IPTEH - Faculté des Géosciences et de l'Environnement, Université de Lausanne, CH-1015 Lausanne (nelly. niwa@unil.ch)*
** *IIE-ECOL, ENAC, EPFL, CH-1015 Lausanne (luca.rossi@epfl.ch)*
*** *IMG - Faculté des Géosciences et de l'Environnement, Université de Lausanne, CH-1015 Lausanne (nathalie.chevre@unil.ch)*

La problématique des polluants comme les pesticides, médicaments, cosmétiques, dans les eaux de surface est de plus en plus actuelle. Non pas que ces micropolluants soient des substances nouvelles, mais plutôt que les techniques d'analyse chimique se perfectionnant, on découvre de plus en plus de substances chimiques dans le milieu aquatique. Il semble également que ces substances ne soient pas sans conséquences sur l'homme et l'environnement puisqu'on leur attribue des effets cancérigènes ou de diminution de la fertilité.

Dans une optique de gestion durable des ressources en eau, il est donc indispensable de prendre en compte l'aspect des micropolluants. Cependant, cette pollution est très difficile à maîtriser car elle n'est pas confinée dans un endroit clos. Les substances sont souvent transportées sur de longues distances et peuvent ainsi engendrer des effets loin de leur source d'émission. A titre d'exemple, des rejets industriels dans le Valais ont conduit à une contamination du Léman par certains pesticides et médicaments qui se retrouvaient ensuite dans les eaux brutes des stations de pompage autour du Léman. Cette pollution est aussi difficile à limiter car si des quotas peuvent êtres définis par secteurs, la somme globale des substances de tous les secteurs peut vite donner lieu à une pollution ayant des conséquences importantes sur l'environnement. Enfin, cette pollution est complexe car l'association entre différentes substances peut aussi donner lieu à des cocktails détonants.

Pour minimiser le risque pour l'homme et l'environnement des micropolluants, il est donc indispensable de passer à une gestion « intégrée» de l'eau qui prenne en compte les acteurs et leur organisation à une échelle régionale. Au travers d'un jeu de rôle organisé dans le cadre d'une formation post-grade, nous avons tenté d'explorer comment la santé pourrait être (ou ne pas être) un levier pour mettre en place cette gestion intégrée et en quoi cela pourrait conduire à revisiter les pratiques de l'aménagement du territoire.

La brève analyse que nous avons mené du jeu de rôles nous permet de mettre en exergue trois conclusions principales:
La première, c'est que la santé est un levier particulièrement pertinent pour déclencher une prise de conscience du problème et permet d'amorcer de façon très rapide une démarche visant à le résoudre. En cela, la santé semble être un élément déclencheur et catalyseur du processus.

La seconde, c'est que la santé est un thème sensible dont il est très difficile de déterminer et d'assumer la responsabilité. Pour autant, cette complexité engendre aussi la prise de conscience de la nécessitée de mettre en place un processus collectif. La santé permet donc de rassembler et de dynamiser une démarche collective, globale et intégrée.

Enfin, la troisième, c'est que le processus entier ne peut entièrement reposer sur l'argument de la santé. En effet, il semble que la santé, même si elle représente un enjeu fort, peut être vite en concurrence avec d'autres enjeux, particulièrement avec les enjeux économiques. Il en résulte alors souvent la mise en place de solutions réduites, « end of pipe », qui ne correspondent plus à l'objectif de départ, à savoir : une solution globale et intégrée.

Pour conclure, il nous parait important de souligner à nouveau que si le jeu de rôle est un outil très intéressant pour analyser des processus, il ne remplace en aucun cas l'étude de cas réels. En effet, il s'agit d'une situation simplifiée, accélérée dans le temps et avec des acteurs factices. Néanmoins, il est intéressant de constater que les situations décrites dans le jeu de rôles se retrouvent souvent dans des cas réels.

REFERENCES

Edder P, Ortelli D, and Ramseier S, 2006 : Métaux et micropolluants organiques. Rapp. Comm. int. prot. eaux Léman contre pollut. Campagne 2005. CIPEL (Commission pour la protection des eaux du Léman): Lausanne. p. 65-87.

Niwa N, Rossi L, Chèvre N. Micropolluants dans les eaux: la sante sera-t-elle un levier suffisant pour mettre en place une gestion intégrée ?. Chapitre de livre CEAT. A paraître.

1.32

Effective stress and fracture permeability in regional groundwater flow: numerical comparison of analytical formulas

Preisig Giona* & Perrochet Pierre

*Centre of Hydrogeology, Emile-Argand 11, CH-2009 Neuchâtel (giona.preisig@unine.ch)

The dependency of fracture permeability on effective stress is a subject well known and has been intensively studied last decades. In regional and deep groundwater flow system underground draining structures as tunnels, cause a diminution of pore pressure leading to an increasing effective stress and a decreasing permeability. One approach consists to insert constitutive laws relating effective stress to permeability in Darcy's law, which is used to evaluate 3D regional simulations of discharge rates, pressure distributions and flow paths. This approach gain in accuracy as compared to the classical ones which consider constant permeability field. However, the type and parameterization of the constitutive law influence the final result.

In this work, three different model functions relating effective stress to permeability are implemented in the tensor form of Darcy's law, and compared by means of numerical experiments. Two of these functions were derived from experimental works (Louis 1969; Walsh 1981), the other one was theoretically derived from Hooke's law. Numerical simulations are all based on an initial fractured hydrostatic system where an underground draining structure is activated, causing a steady-state saturated flow from the upper boundary condition (surface) to the lower boundary condition (underground structure). The governing non linear equations are solved using the finite element method.

In the three cases, results show that the introduction of stress-dependent permeabilities in Darcy's law leads to discharge rates significantly lower than those calculated with the classical approach. This is explained by a decreasing permeability due to an increasing effective stress, particularly in the vicinity of the deep draining structure. Louis' experimental model yields the largest difference and has the deficiency of not considering the vertical stress term, while Walsh's model is difficult to solve numerically due to higher order non linearities. The elasto-statistical model analytically derived from Hooke's law seems to be better adapted for solving such problems and yields differences which are somewhat smaller than the two others.

REFERENCES

Louis C. 1969: A study of groundwater flow in jointed rock and its influence on the stability of rock masses. Technical Report No 10, 9/69, Rock Mechanics, Imperial College, UK.

Walsh J.B. 1981: Effect of pore pressure and confining pressure on fracture permeability. Int. J. Rock Mech. Min. Sci. Geomech. Abstr., 18: 429 – 435.

1.33

Debris flows, landslides, and sediment transport in mountain catchments

Rickenmann Dieter*

* Swiss Federal Research Institute WSL, Zürcherstrasse 111, CH-8903 Birmensdorf (rickenmann@wsl.ch)

In mountain headwater catchments with steep channels and hillslopes, floods are often associated with sediment transport and/or with debris flows. Possible interactions between debris flows, shallow landslides and fluvial sediment transport in steep streams are illustrated Figure 1. These processes often occur during high-intensity or long-duration rainstorms, possibly combined with snowmelt, resulting in slope instabilities, sediment transporting flows and floods. These processes are often associated with damage to houses or infrastructure, particularly along the channel network, and may involve also casualties.

Debris flows typically occur in steep headwater catchments. A torrent catchment is characterised by sporadic and sudden high discharges of both water and sediments, and it typically comprises a catchment area less than about 25 km2. The channel gradient may vary from more than 60 % to a few % in the fan area. The torrent system and debris-flow occurrence can be characterised by three main zones: The headwater area or initiation zone where the flow is triggered, the transit zone (gully and channels) where entrainment of more solid material may occur, and the debris fan area where often major deposition takes place. Debris flows in the Alps may involve total sediment volumes of up to some hundred thousand cubic metres. The sediment may be supplied from point sources such as landslides or from incision of the torrent bed by vertical and lateral erosion. The total event magnitude is often used as a rough indication to characterise the intensity of a debris flow. This parameter largely influences the flow behaviour in the channel and – in the case of overtopping - the extent of the affected areas on the fan. Debris flows may deliver important quantities of sediment to the receiving mountain river.

In contrast to lowland gravel bed rivers, relatively few studies were made on sediment transport in steep headwater channels, with stream gradients steeper than about 5 %. Sediment transport dynamics in these channels may be quite different from low-gradient channels. There is often a strong interaction between hillslope processes and the channel network. Sediment transport may be supply limited rather than controlled by the sediment transport capacity for a given discharge and channel conditions. Steep headwater streams are characterised by a wide range of sediment sizes and temporally- and spatially-variable sediment sources. Bed morphology and channel structures may be influenced by the presence of large boulders, woody debris and bedrock constrictions. This can result in large variations in channel geometry, streamflow velocity and roughness, and thus the application of theoretical sediment transport equations may be problematic. Also, quantitative measurements of sediment and bedload transport in steep streams are very limited.

In this presentation an overview will be given on the processes debris flows, shallow landslides and fluvial sediment transport. A particular focus will be the discussion of interactions between these processes. Although a number of methods have been proposed to predict and describe the initiation and flow behaviour of debris flows and sediment transporting flows in mountain streams, quantitative predictions for hazard assessment are still difficult in many cases. The application of some methods will be illustrated using some examples from past flood and rainstorm events.

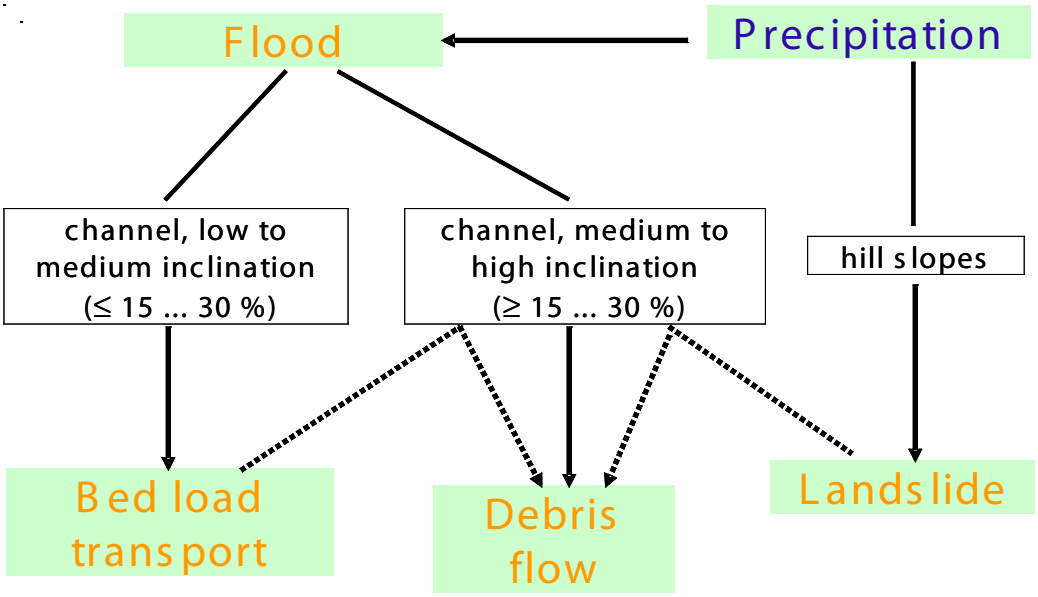

Figure 1: Occurrence of debris flows, shallow landslides and fluvial sediment transport in steep mountain streams.

1.34

Characterisation of geothermal reservoirs using 3D geological modelling and gravity

Schill Eva*, Abdelfettah Yassine*, Altwegg Pierrik*, Baillieux Paul*

Laboratoire de Géothermie - CREGE, Université de Neuchâtel, Rue Emile Argand 11, CH-2009, Neuchâtel, Suisse (paul.baillieux@unine.ch)

The productivity of geothermal resources depend on different parameters mainly the reservoir temperature, the hydraulic conductivity and the stress field. It has been realized in different studies that the hydraulic conductivity of the reservoir is the dominant factor (e.g. Best Practice Handbook for the Development of Unconventional Geothermal Resources with a Focus on Enhanced Geothermal Systems, 2008). This study is part of the long-term research of the Laboratory of Geothermics at Neuchâtel with the objective to develop a methodology to investigate permeability from geophysical exploration. The aim of this study is to develop a method to characterize the porosity from gravity inversion combined with 3D geological modeling.

Gravity measurements provide information on the density of subsurface units either by forward modeling or inversion. And it is well known that the density of the subsurface can be either controlled by lithological changes or changes in porosity (Pruis & Johnson 1998). Furthermore, when the geological area is well known, the 3D gravity inversion is well constraint so it provides accurate result and best densities values are obtained. For porosity, one among the relationships which exist between the density and porosity can be used (e.g. Johnson et al., 2000).

In the geothermal area of Soultz the combination of 3D geology and gravity inversion has revealed density changes in the granitic basement (Figure 1) which can be related to both changes in the granitic facies to the North of the geothermal site and to porosity in the horst structure, where the reservoir is located (Schill *et al.*, subm). Synthetic models for other deep geothermal reservoirs such as St. Gall (Switzerland) provide further indication on the possibilities to deduce porosity from gravity forward modeling. The example from Soultz shows, however, that only if the geological structures are well known and can be assumed as fix in the gravity inversion, the estimation of density changes caused by porosity are possible.

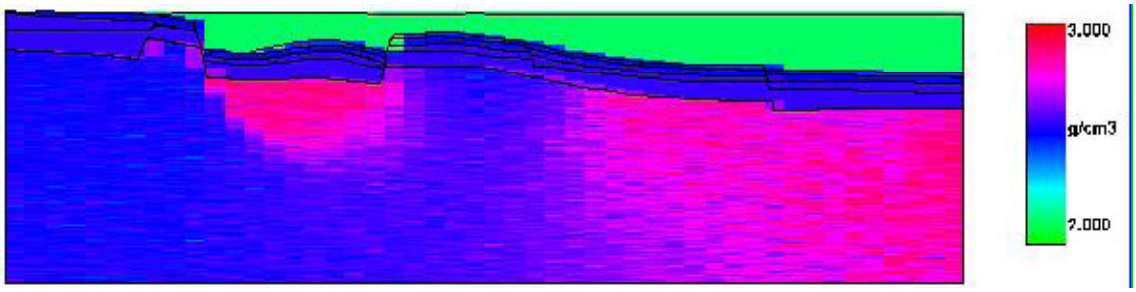

Figure 1: Mean density distribution resulting from inversion of gravity data for a representative E-W profile across the geothermal reservoir of Soultz-sous-Forêts. (E-W extension 29 km, altidude a.s.l.: -8000 to 250 m).

REFERENCES

Schill, E., Geiermann, J. & Kümmeritz, J., subm. 2-D Magnetotellurics and gravity at the geothermal site at Soultz-sous-Forêts. in World Geothermal Congress 2010, pp. 1390, Bali, Indonesia.

Johnson, P.H., Pruis, M. J. & Van Patten, D., Density and Porosity of the Upper Oceanic Crust from Seafloor Gravity Measurements, Geophy. Res. Lett. 27(7), 1053-1056, 2000.

Pruis, M .P. & Johnson H.P. , Porosity of very young oceanic crust from sea floor gravity measurements, G eophys. Res. Lett., 25, 1959-1962, 1998.

1.35

Field Fluorometer for Simultaneous Detection of 3 Colourless Tracers

Schnegg Pierre-André

Centre d'Hydrogéologie et de Géothermie CHYN, Rue Emile Argand 11, CH-2009 Neuchâtel (pierre.schnegg@unine.ch)

We have designed flow-through field fluorometers for simultaneous detection of two or three invisible, colourless tracers, since there is an increasing interest for “blind” tracer tests.

Although most dye tracers used in hydrogeology are harmless to the environment (Behrens et al. 2001, FOEN Report 2002) their visible and indiscreet impact on the population remains a source of annoyance for the field hydrogeologist.

The recent appearance of small, inexpensive LEDs radiating UV light made it possible the excitation of colourless tracers of the naphthalene family.

A few years ago, companies could not always afford multi-tracer tests because laboratory expenses increase with the number of tracers. Today, thanks to the field fluorometer, multi-tracing is the rule (Schnegg and Doerfliger 1997). However, a successful separation of tracers by the field fluorometer presupposes dissimilar spectral characteristics of each tracer (Schnegg 2003). Careful selection of the set of tracers remains mandatory.

The field fluorometer conveniently replaces the water sampler. With this instrument there is no need for frequent sample collection and subsequent laboratory analysis of the samples. Very high time resolution is also of great interest. However, the separation of two or three different dye tracers cannot be performed at the resolution achievable in the laboratory with a spectro-fluorometer. The optics of the field fluorometer is characterized by pass-band filters. To separate 2 or 3 dyes in a multi-tracer test, the fluorometer requires as many light sources (usually LEDs) as tracers, and detectors. Each optical channel is equipped with adequate optical filters. The unknown concentrations of each tracer are obtained by resolving in real-time a system of 2 or 3 linear equations (Schnegg 2003).

For optimal tracer separation, the determinant of the system of equations must be as large as possible. Low values of the determinant indicate inadequate association of tracers of similar excitation/emission spectra. For example, there is no chance to separate a cocktail of rhodamine B, G or WT. Even the sophisticated laboratory instrument will have trouble performing the separation.

Most frequently dye tracers used are: Uranine, eosine, naphtionate, sulforhodamine B, amidorhodamine G, rhodamine WT, duasyne, tinopal, amino G acid (Käss 1998). The problem with most of them is the visual impact in surface or drinking water, particularly near the point of injection (disappearance at concentrations below 10 μg/L). Two of them, naphtionate and amino G acid are much more discreet in the environment. This is because their excitation band is located in the UV part of the spectrum, and their emission is close to the short wavelength limit of visible light.
A field test was carried out in a surface stream (100 L/s) over a distance of 300 metres. Yellow duasyne, a third, hardly visible tracer, was used jointly with the two other tracers. Quantities of 1 and 10 mg of each tracer were injected in turn at 2 minutes interval, so that the breakthrough curves would overlap, allowing thus for testing the separation method. The figure shows the three breakthrough curves after mathematical separation. As expected, they display the same shape and height. Careful calibration of the fluorometer is important for achieving perfect separation.

REFERENCES

Behrens, H., Beims, U., Dieter, H., Dietze, G., Eikmann, T., Grummt, T., Hanisch, H., Henseling, H., Käß, W., Kerndorff, H., Leibundgut, C., Müller-Wegener, U., Rönnefahrt, I., Scharenberg, B., Schleyer, R., Schloz, W., & Tilkes, F. 2001: Toxicological and ecotoxicological assessment of water tracers, Hydrogeology Journal 9, 321–325. DOI 10.1007/s100400100126.

FOEN, Arbeitsgruppe Tracer der Schweizerischen Gesellschaft für Hydrogeologie SGH. 2002: Einsatz künstlicher Tracer in der Hydrogeologie Praxishilfe. Utilisation des traceurs artificiels en hydrogéologie, Guide pratique. Berichte des BWG, Serie Geologie Nr. 3 – Bern. Available at http://www.bafu.admin.ch/hydrologie/01835/02126/index.html?lang=en

Käss, W. 1998 : Tracing technique in Geohydrology. Balkema, Rotterdam.

Schnegg, P.-A., & Doerfliger, N. 1997: An inexpensive flow-through field fluorometer. Proceedings of the Sixième colloque d'hydrologie en pays calcaire et milieu fissuré, la Chaux-de-Fonds.

Schnegg, P.-A., 2003: A new field fluorometer for Multi-tracer tests and turbidity measurement applied to hydrogeological problems, Proc. 8th International Congress of the Brazilian Geophysical Society, Rio de Janeiro.

1.36

Recent Research on the Remote Retrieval of Soil Moisture from Space with Microwave Radiometry

Schwank Mike*, Völksch Ingo *, Mätzler Christian ** & Stähli Manfred*

* *Swiss Federal Institute for Forest, Snow and Landscape Research, Zürcherstrasse 111, 8903 Birmensdorf, Switzerland, (mike.schwank@wsl.ch)*
** *Institute of Applied Physics, University of Bern, Sidlerstrasse 5, 3012 Bern, Switzerland.*

L-band (1 - 2 GHz) microwave radiometry is a remote sensing technique to monitor soil moisture over land surfaces. The European Space Agency's (ESA) Soil Moisture and Ocean Salinity (SMOS) radiometer mission aims at providing global maps of soil moisture, with accuracy better than 0.04 m3m-3 every 3 days, with a spatial resolution of approximately 40 km. Monitoring the large scale moisture dynamics at the boundary between the deep bulk soil and the atmosphere provides essential information both for terrestrial and atmospheric modellers. Performing ground based radiometer campaigns before the mission launch, during the commissioning phase and during the operative SMOS mission is important for validating the satellite data and for the further improvement of the used radiative transfer models.
This presentation is an example of research at the boundary between soil hydrology and remote sensing. It starts with an overview of the SMOS mission followed by an outline of the basic concepts behind remote moisture retrieval from passive L-band radiation. Then the results from a selection of ground based microwave campaigns performed within the ETH domain during the last 7 years are presented. Furthermore, the design of an L-band radiometer is shown which was built for ESA to perform further ground based experiments during the SMOS commissioning and operative phase.

1.37

Groundwater resources in Switzerland

Sinreich Michael*, v. Lützenkirchen Volker**, Matousek Federico**
& Kozel Ronald*

Bundesamt für Umwelt BAFU, Sektion Hydrogeologie, CH-3003 Bern (michael.sinreich@bafu.admin.ch)
**Matousek, Baumann & Niggli AG, Geologiebüro, CH-5401 Baden*

Groundwater is an invisible but crucial component of the water cycle. It feeds surface streams as well as aquatic ecosystems, and is the main drinking water resource in many countries. Switzerland is rich in groundwater due to favourable climatic, hydrological and hydrogeological conditions, i.e. high recharge. More than 80% of Swiss drinking water requirements are met by groundwater, and groundwater therefore represents a social and economic asset of national importance. Knowledge about the extent of the resource is essential for sustainable groundwater management. This is of particular interest given the pressure on groundwater resources due to increasing water demand, intense underground engineering activities, and climate change.

The Groundwater Resources Map of Switzerland on a 1:500,000 scale presents the yield of near-surface groundwater resources in a qualitative manner. The map provides an inventory of hydrogeological units, subdivided according to high, moderate and low productivity, which is determined mainly by aquifer thickness and permeability. However, this map does not provide quantitative information in terms of the volume or the safe yield of groundwater resources. While the *groundwater volume* describes how much groundwater is available in the underground, the *safe yield* is defined as how much groundwater is renewable and can thus be used in a long-term and sustainable manner. Both parameters are crucial for managing groundwater resources. To date, however, they have not been assessed in Switzerland on a national basis.

A study was therefore conducted to evaluate the volume and safe yield of Swiss groundwater resources. Specific approaches were developed in order to provide estimates for both parameters for the main aquifer types encountered (i.e. porous, fissured and karstified rock) and based on the Groundwater Resources Map. This study was performed in co-operation with the Institute of Environmental Engineering and the Geological Institute of the ETHZ (Swiss Federal Institute of Technology Zurich), and the Swiss Institute of Speleology and Karstology SISKA.

Highly productive porous aquifers along large river valleys represent the main drinking water resources in Switzerland. The groundwater volume stored in such aquifers was assessed by considering aquifer geometry and porosity. Estimating safe

yields, however, is more problematic as these aquifers are fed to a large extent by the infiltration of river water. In this case, a modelling approach for an extraction scenario along a river with typical aquifer characteristics provided maximum withdrawal rates. For porous aquifers not connected to surface streams, estimates of safe yield were derived solely from recharge by precipitation.
In fissured aquifers, groundwater fills the pores and open fractures in the weathered part of consolidated rock. Estimates of groundwater volume in fissured aquifers were made from tunnel inflow measurements at selected sites in crystalline alpine rocks. As fissured and karstified aquifers are discharged naturally by springs, discharge data from representative spring inventories were used to evaluate the safe yield for both aquifer types. Finally, a geological-tectonic approach enabled estimates of the groundwater volume in the saturated zone of karstified aquifers, whereas this value is largely determined by the depth to which karst groundwater is regarded as suitable for water supply.

1.38

The role of the colloidal pool for transport and fractionation of the rare earth elements in stream water

Steinmann Marc* & Pourret Olivier**

*UMR 6249 Chrono-environnement, Université de Franche-Comté, F-25030 Besançon cedex (marc.steinmann@univ-fcomte.fr)
**Département Géosciences, Institut Polytechnique LaSalle Beauvais, F-60026 Beauvais cedex (olivier.pourret@lasalle-beauvais.fr)

The rare earth elements (REE) are a powerful tool for the study of trace metal behavior in surface and groundwaters because of their specific atomic structure and their coherent chemical properties throughout the REE group. Fractionation of REE distribution patterns in water samples have in the past been used to monitor processes such as surface and solution complexation or to identify precipitation and dissolution of specific mineral phases (Gaillardet *et al.*, 2003 and cit. therein). Recent studies have shown that the REE of the <0.45 or <0.22 μm fraction of surface and groundwaters are mainly present in colloidal form rather than truly dissolved (Gaillardet *et al.*, 2003 and cit. therein). Colloids are organic or inorganic microscopic phases in a size range of about 0.1 nm to 0.2 μm. For the Kalix river in northern Sweden it has been demonstrated that colloids are more abundant in summer and that the REE-bearing colloidal fraction is composed of Fe/Mn-oxyhydroxides and organic matter (Andersson *et al.*, 2006). These authors furthermore show that in winter small (~ 3 nm) organic-rich colloids, and larger (~ 10-12 nm) Fe/Mn-oxyhydroxide colloids can be distinguished, whereas combined Fe/Mn-organic matter colloids of about 3 nm in size occur during spring and summer. The detailed analysis of the winter colloids reveals that the light REE (La-Sm, LREE) are preferentially associated with Fe/Mn colloids, whereas the heavy REE (Dy-Lu, HREE) have stronger affinity for organic colloids (Andersson *et al.*, 2006). This distinction of the colloidal REE fraction into a organic matter and a Fe/Mn-oxyhydroxide controlled pool is confirmed by experimental studies (Pourret *et al.*, 2007a).

Recently, Steinmann & Stille (2008) have reported for 0.45 μm filtered stream water samples from the french Massif Central a continuously growing depletion of the LREE from upstream to downstream over a flow distance of less than 10 km (Fig. 1). The authors furthermore showed that this evolution is linked with the saturation index (SI) for Fe-oxyhydroxide (goethite, Fig. 2): The stream waters have REE distribution patterns similar to the basaltic bedrock upstream, where the samples are strongly oversaturated with respect to goethite (SI up to 8). During downflow, the SI value for goethite diminishes and the LREE depletion develops. Steinmann & Stille (2008) have interpreted this evolution with the presence of Fe/Mn-bearing colloids that grow during downflow and finally precipitate as Fe/Mn-oxyhydroxide particles. The preferential scavenging of the LREE by these precipitates could explain the observed depletion of the LREE in the < 0.45 μm fraction.

The scope of the present study is to verify the hypothesis of Steinmann & Stille (2008) by direct analysis of the colloidal fraction on new samples sampled in September 2009 in the same field site by using the ultracentifugal procedure described by Pourret *et al.* (2007a) to separate the colloids. This new analytical approach has been completed with computer modeling in order to evaluate in more detail the competition between organic and inorganic colloids on REE transport and fractionation in stream water. Interactions with organic colloids were described using Model VI and the further refined REE parameters described by Pourret *et al.* (2007b). Adsorption of the REE onto oxyhydroxide colloids was modeled using a surface complexation model integrated into PHREEQC.

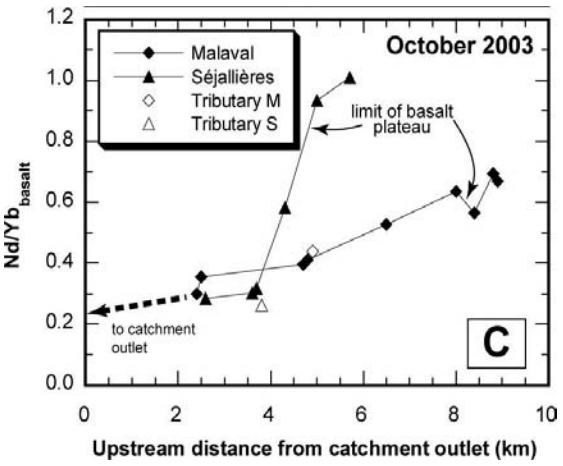

Fig. 1 : Evolution of LREE depletion with distance monitored by bedrock normalised Nd/Yb ratios in the < 0.45 μm stream water fraction (figure from Steinmann & Stille, 2008)

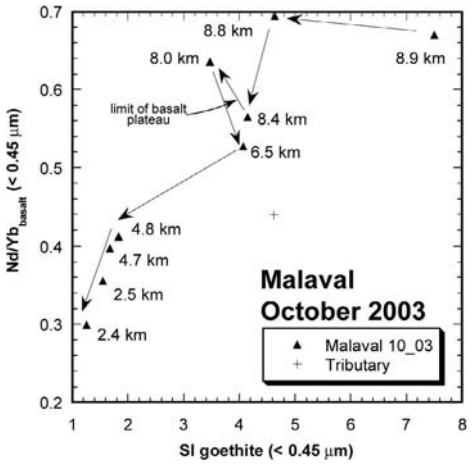

Fig. 2 : Link between Nd/Yb ratios the saturation index (SI) for goethite. Note the regular evolution with flow distance (figure from Steinmann & Stille, 2008)

REFERENCES

Andersson, K., Dahlqvist, R., Turner, D., Stolpe, B., Larsson, T., Ingri, J. & Andersson, P., 2006: Colloidal rare earth elements in a boreal river: Changing sources and distributions during the spring flood. Geochim. Cosmochim. Acta 70, 3261-3274.

Gaillardet, J., Viers, J. & Dupré, B., 2003: Trace elements in river waters. In: Drever, J., Turekian, K. (Eds.), Surface and ground water, weathering, and soils. Elsevier, pp. 225-272.

Pourret, O., Dia, A., Davranche, M., Gruau, G., Hénin, O. & Angée, M., 2007a: Organo-colloidal control on major- and trace-element partitioning in shallow groundwaters: Confronting ultrafiltration and modelling. Applied Geochem. 22, 1568-1582.

Pourret, O., Davranche, M., Gruau, G. & Dia, A., 2007b: Organic complexation of rare earth elements in natural waters: Evaluating model calculations from ultrafiltration data. Geochim. Cosmochim. Acta 71, 2718-2735.

Steinmann, M. & Stille, P., 2008: Controls on transport and fractionation of the rare earth elements in stream water of a mixed basaltic-granitic catchment basin (Massif Central, France). Chem. Geol. 254, 1-18.

1.39

Microbial communities in the steep gradients of the meromictic lake Cadagno

Mauro Tonolla[1,2]

[1)] *Microbial ecology group, Microbiology Unit, Plant biologx Dept. Universtity of Geneva c/o Istituto cantonale di microbiologia (ICM), Via Mirasole 22A, CH-6500 Bellinzona &*
[2)] *Alpine Biology Center (ABC), Piora, CH-6777 Quinto*

Lake Cadagno is a crenogenic meromictic lake located in the catchment area of a dolomite vein rich in gypsum in the Piora Valley in the southern Alps of Switzerland. This lake is characterized by a compact chemocline at 12 m depth with high concentrations of sulfate, steep gradients of oxygen, sulfide and light and a turbidity maximum that correlates to large numbers of bacteria mostly belonging to anerobic phototrophic sulfur bacteria and sulfate reducing bacteria. Population analyses in water samples obtained from the chemocline have been performed regularly during the last 20 years using molecular methods as well as cultivation techniques. The 16S rDNA based clone library obtained from samples of the monimolimnion and the anoxic sediments of the meromictic Lake Cadagno allowed for the development of specific oligonucleotide probes and accurate FISH (fluorescent *in situ* hybridization) distribution analysis of bacterial populations. Phototrophic sulfur bacteria (*Lamprocystis, Thiodictyon*) forming syntrophic aggregates with sulfate reducing bacteria (*Desulfocapsa*) dominated the chemocline whereas members of the genus *Desulfomonile* were prominent in the monimolimnion and in the first centi-

meters of the sediments. In deeper sediment layers methanogenic archaea and SRB were detected by FISH.
Moreover, in the chemocline, spatio-temporal analysis of bacterial populations over 2 decades revealed an initial dominance of Chromatiaceae (*C. okenii, Lamprocystis, Thiodictyon)*, after 2001, a clonal population of *Chlorobium clathratiforme* became dominant. This major change in community structure in the chemocline was probably due to extreme climatic events in autumn of the years 1999 and 2000 causing deep mixing of the waterbody which were accompanied by changes in profiles of turbidity and photosynthetically available radiation, as well as for sulfide concentrations and light intensity. Overall, these findings suggest that the temporary disruption of the chemocline may have altered environmental niches and populations in subsequent years.

REFERENCES:
Tonolla et al. (1998) Documenta Ist. ital. Idrobiol. 63: 31-44.
Bensadoun et al. (1998) Doc. Ist. ital. Idrobiol. 63: 45-51.
Tonolla et al. (1999) Appl. Environ. Microbiol. 65: 1325-1330
Tonolla et al. (2000) Appl. Environ. Microbiol. 66: 820-824.
Tonolla et al. (2003) FEMS Microbiol. Ecol. 43: 89-98.
Peduzzi et al. (2003) FEMS Microbiol. Ecol. 45: 29-37.
Peduzzi et al. (2003) Aquat. Microb. Ecol. 30: 295-302.
Tonolla et al. (2004) J. Limnol. 63(2): 157-166.
Tonolla M., et al.. (2005) FEMS Microbiology Ecology 53: 235–244.
Tonolla M. et al. (2005) Appl. Environ. Microbiol. 71: 3544-3550.
Decristophoris P.M.A. et al. (2009) J. Limnol., 68(1): 16-24.
Gregersen L.H. et al. (2009 Jul 1. [Epub ahead of print]) FEMS Microbiology Ecology

1.40

Dissolved inorganic carbon and its stable isotope composition as a tracer of geo-, bio-, and anthropogenic sources of carbon

Vennemann Torsten*, Fontana Daniela*, Paychere Sophie*, Ambadiang Pierre*, Piffarerio Raffaella*, and Favre Laurie*.

Institut de Minéralogie et Géochimie, Université de Lausanne, CH-1015 Lausanne (Torsten.Vennemann@unil.ch)

The concentration and carbon isotope composition of dissolved inorganic carbon (DIC), in addition to the oxygen and hydrogen isotope compositions of water as well as the major dissolved cations and anions have been analyzed seasonally for several rivers, lakes, dams used as sources for hydroelectric energy, and effluents from a number of waste water treatment plants (WWT) in Western Switzerland. The aim is to evaluate the DIC and its isotopic composition as a tracer for the geologic, biologic and anthropogenic contributions of carbon to the rivers and lakes.

The upper reaches of the Rhone and the Sarine typically have Alpine catchments characterized by thin or no soil covers with only sparse vegetation. Glacial melt waters and surface runoff make up the bulk of the water sources in their upper reaches. Further downstream other tributaries, themselves often being melt water fed but many also being exploited for hydroelectric power and thus with a number of dams along their course, join these rivers. In addition, the vegetation and soil cover increases downstream in parallel with the agricultural exploitation, population density, and the number of WWT plants that generally pass their treated waste waters directly into the rivers. In contrast, rivers draining the Jura mountains do not have a glacial melt water source, nor are there major hydroelectric systems coupled to the river systems investigated.

The difference in geology of the catchment as well as the soil cover thickness and hence biologic activity in the soil are reflected by the C isotope composition of the DIC. $\delta^{13}C$ values are as high as −2.5‰ in the upper source reaches of the Rhone and the Sarine, reflecting predominant uptake of carbon from atmospheric CO_2. Further downstream, $\delta^{13}C$ values decrease towards −5 to −11.5‰, compatible with a higher input of soil-, plant-derived CO_2. The $\delta^{13}C$ values of DIC are higher (−5 to −8.5‰) if carbonate relative to silicate rocks dominate the catchment, unless the agricultural activity is intense. The latter is the case for the rivers draining the largely carbonate-dominated Jura (for example the Venoge), which have $\delta^{13}C$ values of between −11 to −13‰. The $\delta^{13}C$ values are also higher for all lakes and dams along the rivers, indicating an additional exchange with atmospheric CO_2 for water masses exposed to the atmosphere for longer periods. For smaller lakes, the $\delta^{13}C$ values correspond to those of the riverine inputs though. For larger lakes the $\delta^{13}C$ values of the DIC may also be used as tracers of the mixing processes between riverine input and the lake (Fig. 1).

The $\delta^{13}C$ values in the rivers are generally lower in winter and spring compared to summer and fall, indicating a higher biological activity within the water column during the warmer periods. The differences are most notable in dams and lakes, where vertical profiles are also well-established within the upper 5 to 10 m of the water column as a result of increasing photosynthesis during the warmer periods (Fig. 1).

Contributions of organic carbon from WWT plants are clearly marked by 0.5 to 3‰ lower $\delta^{13}C$ values for DIC directly downstream of the effluents, with the treated waste waters having values that may be as low as −27‰. Such sources may also clearly be expressed by differences in H- and O-isotope compositions of the waters relative to the river or lake waters, as well as their sodium, potassium and nitrate contents, as well as the isotopic composition of the latter.

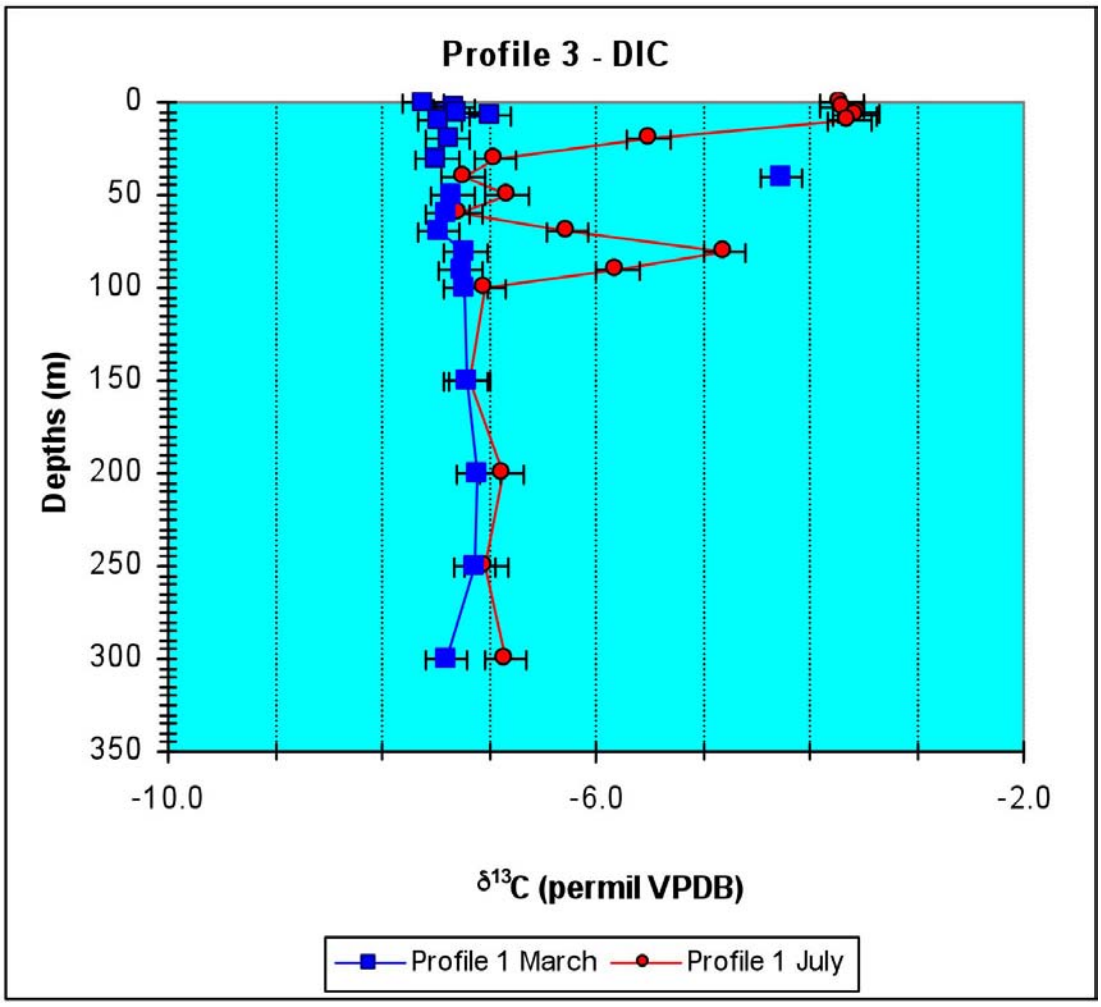

Figure 1: δ13C values of DIC in a depth profile in the deepest part of Lake Geneva (approximately in the center of the lake). Note the high values at the surface during the summer (July 2005 profile) compared to the winter (March 2005 profile) typically indicating the bioproductivity in the photic zone during summer. Higher values at depths of 50 to 100 m represent mixtures of the Rhone water rich in 13C descending to these depths within the lake, three months after a complete overturn of the lake at the end of February.

1.41

High-resolution temperature measurements at the river – groundwater interface: Quantification of seepage rates using fiber-optic Distributed Temperature Sensing

T. Vogt*, P. Schneider*, M. Schirmer*, O. A. Cirpka**

* *Eawag - Swiss Federal Institute of Aquatic Science and Technology, Überlandstrasse 133, CH-8600 Dübendorf (tobias.vogt@eawag.ch)*
** *University of Tübingen, Center for Applied Geoscience, Sigwartstr. 10, D-72076 Tübingen*

In recent years, the transition zone between surface water bodies and groundwater, known as the hyporheic zone, has been identified as crucial for the ecological status of the open-water body and the quality of groundwater. The hyporheic exchange processes vary both in time and space. For the assessment of water quality of both water bodies reliable models and measurements of the exchange rates and their variability are needed.

A wide range of methods and materials exist to estimate water fluxes between surface water and groundwater. Due to advances in sensor technique and data loggers, work on heat as a tracer in hydrological systems has increased recently, especially with focus on surface water – groundwater interaction. A new promising method is Distributed Temperature Sensing (DTS). DTS is based on the temperature dependence of Raman scattering. Light from a laser pulse is scattered along an optical fibre of up to several km length, which is the sensor of the DTS system. By sampling the back-scattered light with high temporal resolution, the temperature along the fibre can be measured with high accuracy (0.1 K) and high spatial resolution (1 m). We used DTS at a test side at River Thur in North-East Switzerland (TG). Here, the river is losing.

For estimation of seepage rates we measured highly resolved vertical temperature profiles in the river bed. To this end, we wrapped an optical fibre around a piezometer tube and measured the temperature distribution along the fibre. Due to the wrapping, we obtained a vertical resolution of approximately 5 mm. We analyzed the temperature time series by means of Dynamic Harmonic Regression as presented by Keery et al. (2007). From the travel time and attenuation of the diurnal signal, we estimated the apparent velocity and diffusivity of temperature propagation, which then can be used to quantify infiltration rates. A particular strength of the new measurement technique lies in the high spatial and temporal resolution, enabling us to detect non-uniformity and temporal changes in vertical water fluxes.

REFERENCES

J. Keery, A. Binley, N. Crook and J.W.N. Smith (2007) Temporal and spatial variability of groundwater–surface water fluxes: Development and application of an analytical method using temperature time series, Journal of Hydrology, 336, 1-16.

1.42

Natural springs – the living passage between groundwater and surface water

Von Fumetti Stefanie*, Gusich Valeria * & Nagel Peter*

**Institut für Biogeographie (NLU), Universität Basel, St. Johanns-Vorstadt 10, CH-4056 Basel (stefanie.vonfumetti@unibas.ch)*

Natural springs are unique ecosystems that provide specific abiotic conditions, and they are stepping-stones between groundwater and surface water. They appear in the landscape in various forms and are especially obvious in alpine regions. Springs are habitats for many freshwater organisms, which partly show a strong adaptation to the specific conditions in springs. As an alpine country Switzerland is rich of springs, but not many are still in a natural or at least near natural condition. Despite their importance as unique habitats and despite their endangered situation they were not well studied until a few years ago. At the Institute of Biogeography from the University of Basel we investigate natural springs in the northern part of Switzerland and adjacent regions. The distribution of the spring fauna and the influence of abiotic parameters, especially discharge, are the main topics of our research. A first approach to a faunistic spring typology shows differences between springs based on the dominant feeding habits of the macrozoobenthic species. They are related to abiotic parameters like substrate composition. Our goal is a spring typology for the whole country based on faunistic data. And also the colonisation of springs is an important part of our research. In a one-year field experiment in artificial springs we investigated the colonisation rate and the preferences of different substrates by macrozoobenthic organisms. Mesoscale analyses show that the colonisation occurs rapidly from the adjacent headwater and that the organisms prefer different substrate types for their settlement.

1.43

Porewater as an archive of the palaeo-hydrogeology during the Holocene and Pleistocene

Waber H. Niklaus

Institute of Geological Sciences, Rock–Water Interaction Group, University of Bern, Baltzerstrasse 1-3, CH-3012 Bern (waber@geo.unibe.ch)

Fractured rocks comprise two different hydraulic regimes: The first regime constitutes the water-conducting zones related to regional and/or local fracture networks where groundwater flow takes place. It is characterised by a hydraulic transmissivity of mostly above 10^{-9} m^2/s and solute transport takes place by advection. The second regime constitutes the low permeable rock matrix with the porewater residing in its connected pore space. Here, the hydraulic transmissivity is low to very low (<< 10^{-10} m^2/s) and solute transport is increasingly dominated by diffusion. The mass of porewater present in the rock matrix is, however, larger than in the fracture network even in crystalline rocks with a connected porosity of less than 1 Vol.%.

Porewater in the rock matrix and groundwater in the fracture network always tend to reach chemical and isotopic equilibrium. If solute transport in the rock matrix can be shown to occur by diffusion, then a chemical and isotopic signature established in the porewater at a certain time might be preserved over geologic time periods. Thus, porewater may act as an archive of the past fracture groundwater composition(s) and therefore of the palaeo-hydrogeological history of a site. The degree of the preservation of such signatures depends on: 1) the distance of the porewater sample from the nearest water-conducting fracture in three dimensions, 2) the solute transport properties of the rock (i.e. diffusion coefficient, porosity), and 3) the period of constant boundary conditions (i.e. constant fracture groundwater composition). The frequent climatic and hydrogeologic changes during the Holocene and Pleistocene and related compositional changes in the fracture groundwater resulted in superimposed signatures in the porewater. These can be unravelled to a large degree by the investigation of different, largely independent natural tracers in the porewater.

Porewater in granitic and monzodioritic rocks from Laxemar-Oskarshamn, central Sweden, are of different chemical and isotopic composition in bedrock characterised by high transmissivity and a high frequency of water-conducting fractures at shallow to intermediate depth (0-400 m b.s.l.), and bedrock characterised by low transmissivity and a low frequency of water-conducting fractures at greater depth (400 -1000 m b.s.l.). In the more transmissive, shallower interval, porewater is of a general Na-HCO_3 chemical type with a Cl^- concentration of less than 1 g/kgH_2O. The oxygen and hydrogen isotope composition indicates a formation from meteoric infiltration under different climatic conditions. Combined with the distance between porewater sample and nearest water-conducting fracture in the borehole and the quantitative modelling of the natural tracer profiles (Cl^-, $\delta^{18}O$, δ^2H) sampled at high resolution in one of the boreholes, the porewater signatures in the first few metres from a fracture may be explained in terms of exchange with Holocene fracture groundwater of present-day type, of Holocene

thermal maximum type (at about 7-4 ka BP) and of glacial (late Weichselian) or glacio-lacustrine (Baltic Ice Lake, 15-11.5 ka BP; Ancylus Lake, 10.8-9.5 ka BP) type. Exchange with fracture groundwater composed of present-day brackish water of the Baltic Sea is limited and absent for the earlier Baltic Sea stages (Yoldia, 11.5-10.8 ka BP; saline Littorina, 8.5-7 ka BP). Farther away from water-conducting fractures, Na-HCO_3 type porewater signatures with low Cl^- concentrations indicate an evolution from Pleistocene fracture groundwater of warm climate origin (possibly Eemian Interglacial) and cold climate periods (early Weichselian or older). Cold climate influence from the last glaciation with $\delta^{18}O$ values around -14‰ VSMOW occurs between about 135-350 m depth and down to about 500 m depth depending on borehole.

At intermediate depth levels below the Na-HCO_3 type porewater a change to higher mineralised porewater of a general Na-Ca-SO_4 and Ca-Na-SO_4 chemical type occurs. Depending on borehole location this porewater type occurs from about 430 m and 620m depth over a restricted interval of about 120 m. The change coincides with a marked decrease in transmissivity, in the frequency of water-conducting features and the transition zone from Ävrö granite to quartz monzodiorite. Highly variable Cl^- concentrations (2.5 to 7.6 g/kgH_2O) and water isotope compositions ($\delta^{18}O$ about -2‰ to -13‰ VSMOW) are associated with high concentrations of Ca^{2+} and SO_4^{2-} up to gypsum saturation. Chemical and isotopic composition of these porewater types cannot be explained by interaction with a known type of fracture groundwater and more advanced rock-water interaction. They appear to have formed from interaction with cryogenic brines that formed during permafrost conditions and which migrated downwards in the fractures by buoyancy effects. The large distance to the nearest water-conducting fracture of this porewater type suggests that these signatures have been established before the Last Glacial Maximum.

At greater depth there occur again more dilute porewaters of Na-HCO_3 type and Na-Ca-Cl-(HCO_3) type. Here, Cl- contents vary between about 0.5 to 3 g/kgH_2O and associated $\delta^{18}O$ values of between about -8‰ to -11‰ VSMOW. Porewaters below 820 m are then of a Na-Ca-Cl type with Cl^- concentrations of more than 8 g/kgH_2O, but low SO_4^{2-} concentrations and an oxygen isotope composition generally enriched in ^{18}O compared to the more shallow porewaters. At these low-transmissivity depths, the porewaters display complex, superimposed signatures that cannot be resolved based on the present data. In the deepest samples, however, a component of a deep saline brine seems to be present similar as observed in fractures at even greater depth.

The data indicate that the palaeo-hydrogeological evolution of a site indeed can be re-constructed based on porewater data. In addition, signatures no longer present in the fracture groundwaters can be identified. In the case of cryogenic brines that formed during permafrost conditions, this is of special importance within the framework of the long-term safety assessment of a deep geologic repository for radioactive waste.

1.44

In-situ Remediation of Polluted Groundwater: A Transdisciplinary Approach

Christoph Wanner*, Franz Schenker** & Urs Eggenberger*

*Institut für Geologie, Baltzerstr. 1+3, CH-3012 Bern (christoph.wanner@geo.unibe.ch)
**Geologische Beratungen SCHENKER KORNER + PARTNER GmbH, Büttenenhalde 42, CH-6006 Luzern (franz.schenker@fsgeolog.ch)

Careless handling of environmentally hazardous substances and wastes has left its mark in the geological underground. If substances like persistent organic compounds or heavy metals from contaminated sites migrate into the groundwater, an immediate and sustainable suppression of the source is required. However, in most cases the groundwater in its downstream flow will stay contaminated over a long time. On duty of the society and the environment to provide for safe water, the remediation of polluted groundwater is both an essential and ambitious task.

Consultant geologists in cooperation with chemical laboratories generally are keen now in assessing the type, amount and distribution of contaminants in groundwater. But after one decade of the commitment by law to remediate the "sins of yesterday", the scientific and technical knowledge on approved procedures to clean spoiled groundwater is still poor. On the one hand research institutes mostly experience at laboratory scale only. At the other hand, the party responsible for a contaminated groundwater plume is interested in fast solutions, and not in making expensive attempts without a guaranty of a long lasting achievement.
Researchers from the university and professionals from consulting companies can complement one another in creating new technologies. Research, development and implementation of new technologies can profit from "the Nine Laws of God governing the incubation of something from nothing" (Kelly, 1995). Taking as an example the project to reduce the charge of he-

xavalent chromium with permeable reactive walls (PRB), the way of a successful cooperation using a transdisciplinary approach (Hermanns-Stengele & Schenker, 2000) will be demonstrated.

In designing a PRB as a passive remediation method the crucial aspects are what to take as the reactive material and of course how well the contaminants are treated after the installation of such a PRB.
Batch and column experiments performed in order to chose the best available iron shavings for the PRB Thun showed that shavings with a carbon content of approximately 4% have very good properties concerning the reduction of hexavalent chromium. Interestingly large differences in the reaction rates among various types of iron shavings were observed. Looking at the various shavings under the scanning electron microscope we came up with the conclusion that reaction rates are highly correlated with the nature of the carbon inclusions within the iron matrix of the shavings.
In order to estimate the success of future barrier operations geochemical models are cheap and powerful tools (Steefel, 2005). Using the data of the lab experiments the geochemical reactive transport model and reaction network of Mayer et al. (2001) was calibrated using the modeling software Crunchflow (Steefel, 2005). The calibrated model was used to simulate the hydrodynamics and hydrogeochemistry within the double pile-array of the barrier in 2D. Examples of model outcomes are illustrated in figure 1.

The modelling work clearly points out that the limiting factors in the performance of the PRB are the groundwater flow velocity, the permeability of the piles and the groundwater chemistry.

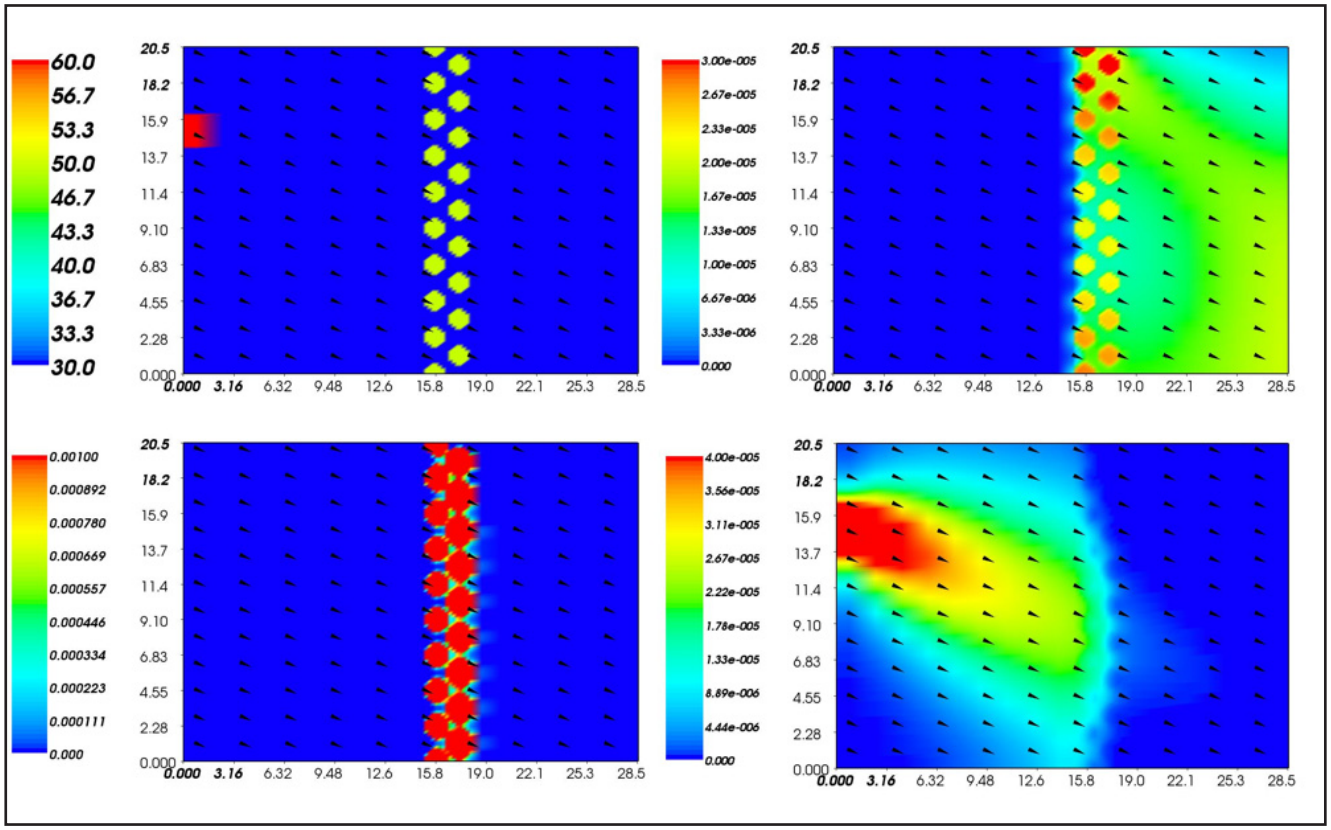

Figure 1. Illustrations of 2D model calculations of the PRB site Thun: Model setup in terms of porosity in the upper left picture, aqueous Fe^{2+} concentrations (mol/l) upper right, green rust precipitation volumes (vol%) bottom left and aqueous Cr^{VI} concentrations (mol/l) bottom right.

REFERENCES

Hermanns-Stengele, R. & Schenker, F. 2000: Groundwater-Remediation with permeable reactive walls – A Transdisciplinary Approach to the sustainable use of the most important natural ressource. In: Transdisciplinarity: Joint Problem-Solving among Science, Technology and Society. Proceedings of the International Transdisciplinarity 2000 Conference, 590- 593.

Kelly, K. (1995): Out of Control: The New Biology of Machines, Social Systems and the Economic World. Reading/ Massachusetts: Addison-Wesley.

Mayer, U. Blowes, D. & Frind E. 2001: Reactive transport modeling of an in situ reactive barrier for the treatment of hexavalent chromium. Water Resources Research 38, 3091-3103.

Steefel C. 2001: Software for modeling multicomponent, multidimensional reactive transport. Lawrence Livermore National Laboratory,Livermore, Ca. UCRL-MA-143182.

Steefel, C. DePaolo, D. & Lichtner P. 2005: Reactive transport modeling: An essential tool and a new research approach for the Earth sciences. Earth and Planetary Science Letters 240, 539–558.

1.45

On the physical hydrology of hydrothermal systems at mid-ocean ridges

Philipp Weis*, Thomas Driesner*, Dim Coumou**, & Christoph A. Heinrich*

* *Institute of Isotope Geochemistry and Mineral Resources, ETH Zurich, Switzerland (philipp.weis@erdw.ethz.ch)*
** *Potsdam Institute for Climate Impact Research, Germany*

Fluid evolution and migration in magmatic hydrothermal systems strongly depend on the physical properties of water. Within the pressure and temperature range given by a specific geologic setting, fluid properties like density and viscosity vary non-linearly by orders of magnitude (Driesner and Heinrich, 2007).

Magmatism at mid-ocean-ridges is predominantly basaltic and acts as a heat source for hydrothermal convection cells. Seawater percolates through the ocean floor into the subsurface, is heated near the magma chamber, travels upward, and vents at the ocean floor, eventually forming black smoker fields.
Numerical simulations in 3D with pure water and a homogeneous permeability have shown that the system naturally forms regularly-spaced pipe-like upflow zones which is well-supported by measurements and observations (Coumou et al., 2008). These simulations further revealed that most of the downflow occurs in the immediate vicinity of the upflow zone where fluids are heated to about 200°C. Compared to the colder fluids at larger distance from the axis, their viscosity is lower by one order of magnitude while they are still relatively dense hence maximizing downward fluid transport. In combination with the ~400°C fluids of the upflow zone, this leads to a mass and energy flux optimization (see also Driesner et al., this volume).

Introducing geological structures to the model geometry adds further complexity to the system but preserves the first order principle described above. Figure 1 shows convection at a mid-ocean ridge system with a deeper gabbroic part overlain by a basaltic layer of higher permeability. The simulations show that a secondary convection cell establishes within the highly permeable basalt layer resulting in a more efficient cooling of the upper part of the upflow zone. Normal faults within the oceanic crust near the ridge axis are often referred to as conduits for enhanced up- or downflow (Fisher, 1998). First numerical simulations introducing normal faults as heterogeneities within the permeability structure of the model geometry have been conducted. Downflow velocities similar to the ones described above only developed in relatively wide normal faults (50m) that have a high permeability contrast to the surrounding rock (up to two orders of magnitude) and are located very close to the ridge axis.

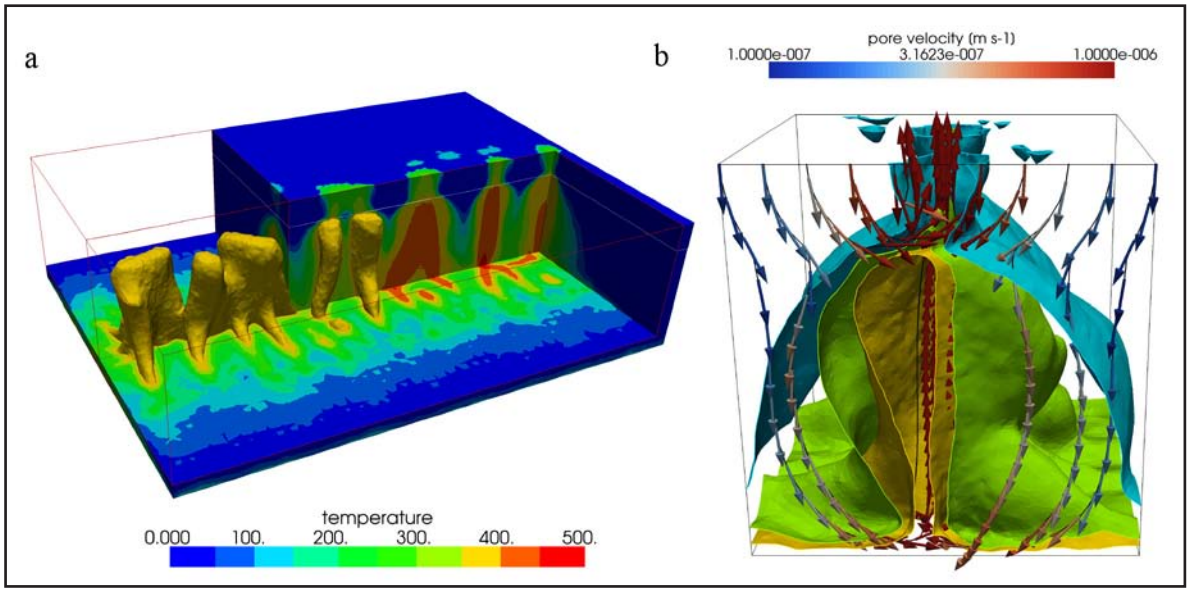

Figure 1. Convection at mid-ocean-ridges self-organizes into hot pipe-like upflow zones (a). Downflow concentrates in the immediate vicinity of the upflow zone as shown by the pore velocities of the selected streamlines (b). The model geometry describes a 1 km deep piece of oceanic crust (3x4 km^2). Constant fluid pressure at the top boundary represents a water depth of 2.5 km and a bell-shaped heat flux at the bottom boundary of a total of 350 MW/km represents an axial magma chamber at depth. The permeability structure consists of a lower gabbroic layer ($k = 3 \times 10^{-14}$ m^2) overlain by a 200 m thick basaltic layer ($k = 10^{-12}$ m^2). Figure 1b is a 1 km^3 excerpt of Figure 1a.

REFERENCES

Coumou, D., T. Driesner, P. Weis, and C.A. Heinrich (2009), Phase-separation, Brine Formation and Salinity Variation at Black Smoker Hydrothermal Systems, J. Geophys. Res., 114, B03212.

Coumou, D., T. Driesner and C.A. Heinrich (2008), The structure and dynamics of mid-ocean ridge hydrothermal systems, Science, 321, 1825-1828.

Driesner, T., and C. A. Heinrich (2007), The system H2O-NaCl. Part I: Correlation formulae for phase relations in temperature-pressure-composition space from 0 to 1000 degrees C, 0 to 5000 bar, and 0 to 1 X-NaCl, Geochimica Et Cosmochimica Acta, 71, 4880-4901.

Fisher, A. (1998), Permeabilty within basaltic oceanic crust, Rev. Geophys. 36, 143-182.

1.46

One lake, two countries and a lot of methane - the concept for a viable extraction of an unusual resource

Alfred Wüest*,**, Lukas Jarc*,**, Natacha Pasche*,** & Martin Schmid*

*Eawag, Swiss Federal Institute of Aquatic Science and Technology, Surface Waters - Research and Management, CH-6047 Kastanienbaum, Switzerland (alfred.wueest@eawag.ch)

** Swiss Federal Institute of Technology, Institute of Biogeochemistry and Pollutant Dynamics, CH-8092 Zürich, Switzerland

The 485 m deep Lake Kivu (Rwanda, DR Congo) is among the most fascinating lakes on earth. Not only does it host a spectacular temperature-salinity staircase of more than 300 interface-layers, it also contains ~60 km^3 of methane and ~300 km^3 of carbon dioxide and is permanently density-stratified by salty, carbon dioxide-rich water released by sub-aquatic springs. Those springs and their chemical composition affect the lake stratification. Especially, the lake-internal nutrient upwelling, strongly depending on the spring discharges, is crucial for algae growth and the subsequent methane production in the deep waters. Over the centuries, methane has accumulated to an amount, which can be economically exploited, but which also poses a risk (limnic eruption like in Lake Nyos) to the riparian ~2 million people. To avoid building-up of such a risk of gas eruption, the two governments have decided to exploit the methane, worth more than $20 billions.

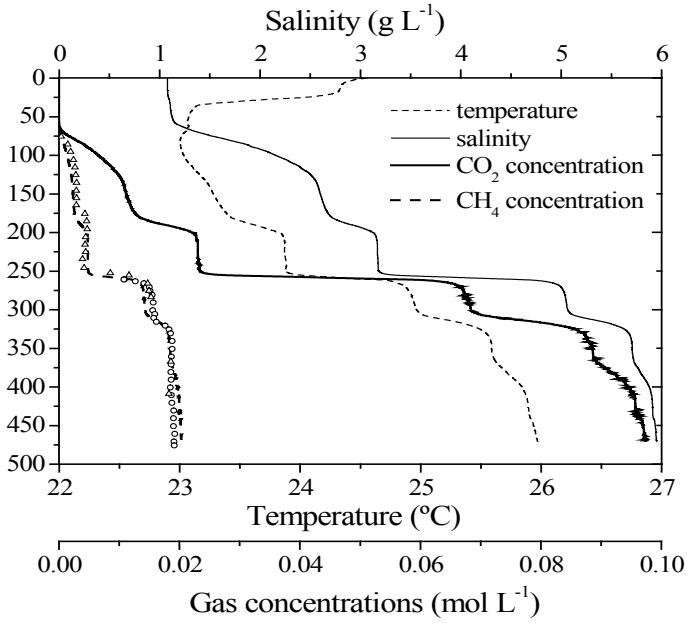

Figure 1. Vertical profiles of temperature, salinity, CH_4 and CO_2, as observed in February 2004 (Schmid et al. 2005). All major water constituents are increasing with depth due to the discharge of deep sub-aquatic springs.

The talk will focus on finding a extraction concept, which (i) lowers the risk of a gas eruption from the lake, (ii) is environmental-friendly and conserves the lake's ecological integrity and (iii) maximizes the economic benefit at the same time.

REFERENCES

Lorke A., Tietze K., Halbwachs M., Wüest A. (2004) Response of Lake Kivu stratification to lava inflow and climate warming. Limnology and Oceanography 49 (3), 778-783.

Muvundja F.A., Pasche N., Bugenyi F.W.B., Isumbisho Mwapu, Müller B., Namugize J-N., Rinta P., Schmid M., Stierli R., Wüest A. (2009) Balancing nutrient inputs to Lake Kivu. Journal of Great Lakes Research 35 (2009) 406–418, doi:10.1016/j.jglr.2009.06.002

Pasche N., Dinkel C., Müller B., Schmid M., Wüest A., Wehrli B. (2009) Physical and biogeochemical limits to internal nutrient loading of meromictic Lake Kivu. Limnology and Oceanography, 54(6), 2009, 1863–1873.

Schmid M., Halbwachs M., Wehrli B., Wüest A. (2005) Weak mixing in Lake Kivu: New insights indicate increasing risk of uncontrolled gas eruption. Geochemistry Geophysics Geosystems 6, Q07009, doi:10.1029/2004GC000892

Schmid M., Tietze K., Halbwachs M., Lorke A., McGinnis D.F., Wüest A. (2003) How hazardous is the gas accumulation in Lake Kivu? Arguments for a risk assessment in light of the Nyiragongo Volcano Eruption of 2002. Acta Vulcanologica 15 (1-2), 115-122.

2. Structural Geology, Tectonics and Geodynamics

Neil Mancktelow, Guido Schreurs, Paul Tackley

Swiss Tectonics Studies Group of the Swiss Geological Society

2.27 Keller T., Kaus B.J.P.: Numerical models of fluid migration in a tectonically active continental crust

2.28 Kilian R., Heilbronner R., Stünitz H., Herwegh M.: Flow mechanisms in granitic ultramylonites

2.29 Lechmann S.M., Schmalholz S.M., Kaus B.J.P., Hetényi G.: Comparing thin-sheet models with three-dimensional numerical models for the India-Asia collision

2.30 Linckens J., Herwegh M., Müntener O.: Strain localization and the importance of second phases in polymineralic mantle shear zones

2.31 Lu G., Kaus B.J.P., Zhao L.: Numerical modelling of craton destruction

2.32 Madonna C., Tisato N., Boutareaud S., Artman B., Burlini L.: New experimental approach to measure seismic wave attenuation of rocks at low frequency

2.33 Malatesta L., Mishin Y., Gerya, T.: The Singularities of Double Subduction Systems

2.34 May D.A., Knepley M.G., Gurnis M.: CitcomSX: Robust preconditioning in CitcomS via PETSc

2.35 Mejri L., Regard V., Carretier S., Brusset S., Dlala M.: Seismotectonic study in Northern Tunisia (exemple: Utique Structure)

2.36 Mettier R.: Numerically modeling current vertical surface motion in the swiss alps from the bottom up - Does the geometry of the orogen dictate how it moves?

2.37 Misra S., Almqvist B.S.G., Burlini L.: Seismic properties of melt-generating metapelites

2.38 Misra S., Tumarkina E., Burlini L., Burg J.-P.: Rheology of metapelites during partial melting and crystallization

2.39 Moix P., Stampfli G.M.: Palaeotethyan, Neotethyan and Pindos series in the Lycian Nappes (SW Turkey): geodynamic implications

2.40 Nagel S., Castelltort S., Mouthereau F., Lin A.T., Willett S.D., Kaus B.J.P.: New constraints on foreland basin development in South-West Taiwan from sequence stratigraphy and flexure modelling

2.41 Negro F., Pellet C.-M., Bousquet R., Beyssac O., Guerra I., Vils F.: Thermal structure and metamorphic evolution of the Piedmont-Ligurian metasediments in the Western-Central Alps

2.42 Nussbaum C., Bossart P.: Influence of faults on the development of Excavation Damaged Zone: the case of the Mont Terri Rock Laboratory

2.43 Pec M., Stünitz H., Heilbronner R.: Transition from frictional to viscous deformation in granitoid fault gouges

2.44 Pleuger J., Mancktelow N.: Structural observations from the Insubric fault between the Valle d'Ossola and Valle d'Orco (NW Italy)

2.45 Rahn M., Wang H.: Apatite FT data from the Triassic Songpan-Garzê flysch, Tibetan Plateau, NW Sichuan, China

2.46 Rami A., Kahlouche S., Khelif M.: Dynamic Topography Determination of the Western Mediterranean Sea from Jason-1 Data

2.47 Ruiz G., Sebti S., Saddiqi O., Negro F., Stuart F., Foeken J., Stockli D., Frizon De Lamotte D.: Mirror denudation pattern on both sides of the Central Atlantic – a trace of the Pangea break-up?

2.48 Schenker F.L., Burg J.-P., Gerya T.: The Eastern Pelagonian metamorphic core complex (northern Greece): Structure and models

2.49 Schmalholz S.M.: Formation of fold nappes in ductile multilayers: insights from numerical simulations

2.50 Smit J., Burg J.-P., Brun J.-P.: Two critical tapers in a single wedge

2.51 Tackley P., Keller T., Armann M., van Heck H., Nakagawa T.: Modelling the thermo-chemical evolution of the interiors of Mercury, Venus, Earth, Mars and super-Earths

2.52 Thielmann M., Kaus B.J.P.: A numerical approach to test lithospheric cross-sections for geodynamic consistency

2.53 Thust A., Heilbronner R., Stuenitz H., Tarantola A., Harald B.: Interaction of H2O rich fluid inclusions and natural quartz crystals in deformation experiments

2.54 Vandelli A., Vachard D., Martini R., Kozur H.W., Moix P., Stampfli G.M.: The Lentas unit in Southern Crete: the base of the Pindos sedimentary series? – New paleontological results

2.55 Vogt K., Gerya, T., Castro A.: Modelling of silicic intrusions in Alpine type orogens

2.56 Zhu G., Gerya T.V., Honda S., Tackley P.J., Yuen, D.A.: Influence of thermal-chemical buoyancy in 3-D mantle wedge

2.1

Tectonic history of the Lut Block in Nehbandan area, Eastern Iran

Bagheri Sasan*, Aref Nejad Marzieh* & Yabaloui Mehdi*

**Department of Geology, University of Sistan and Baluchestan, Zahedan, 98135-674, Iran (sasan_bagheri@yahoo.com)*

We provide new constraints on the tectonic development of the eastern border of the Lut Block based on a geological study of the Nehbandan area (eastern Iran). Several tectonic units and formations provide an insight into the composite tectonic history of the area (Fig. 1). The Deh-Salm Metamorphic Complex maybe represent a Triassic-Jurassic (or older) accretionary wedge. It comprises pelites, psammites and carbonates that enclose some big olistholithes, and deformed layers of peridotite, basic lavas and pyroclastics. A thick siliciclastic deposit (shown on geological maps of the area as the Shemshak Formation) tectonically overlies the Deh-Salm Metamorphic complex. It is composed of large volumes of deep-sea fan turbidites, which deposited over the eastern margin of the Lut Block between the Triassic and Jurassic. Both of aforementioned tectonic units differently underwent a HT/LP metamorphism up to migmatization grades in the late Jurassic (Mahmoodi et al., 2009), which is possibly related to the arc magmatism. The Shah Kuh Granite is late Jurassic in age and pertains to a volcanic arc that developed between the midde and late Jurassic along a northward-dipping, Neo-Tethys subduction zone. Shallow-water volcano-sedimentary sequences exposed close to Mighan village (NW Nehbandan) (Griffis et al., 1992) are interpreted to pertain to the same arc. Since early Cretaceous the platform condition has governed on the eastern edge of the Lut Block up to Paleocene. The Neh Complex includes an ophiolitic mélange and metamorphosed marine sedimentary rocks Senonian to Eocene in age (Tirrul et al., 1983). Igneous rocks found in the mélange are characterized by supra-subduction affinities. We interpret the Neh Complex as a second accretionary prism emplaced along the margin of the Lut Block. Synchronous with the anticlockwise rotation of the southern part of the Lut Block about 90° since the Paleocene up to the Miocene based on paleomagnetic investigations and the Indian/Eurasian collision event, the mélange and Paleogene flysch of the eastern Lut juxtaposed against the Afghan block. Continuous convergence and shearing between the Lut and Afghan Blocks since the Late Eocene created a large and intense deformation and granitization in a NW-SE right-lateral shear system. The youngest tectonic event as the result of the Arabian/Eurasian collision made some more N-NE shear systems such as the West Neh, Nosrat Abad, and Kahurak strike-slip faults as well as several Neogene pull-apart basins at the eastern margin of the Lut block which may be resulted of reactivation of the older faults. Recent seismic activities are the evidence of continuous movement of the latest tectonic regime.

REFERENCES:

Griffis R, Meixner H, Johns G, Abedian N, Behruzi A, Hossein Khan Nazer N, Hamzeh Pour B, Shahriari S, Berberian M, Soheili M, Sahandi M R, and Mohajel M; 1992: Dehsalm Quadrangle map, Scale 1: 250,000, Geological Survey of Iran, Tehran.

Mahmoudi S, Masoudi F, Corfu F and Mehrabi B, 2009 Magmatic and metamorphic history of the Deh Salm metamorphic Complex, Eastern Lut block, (Eastern Iran), from U-Pb geochronology, International Journal of Earth Sciences, in press.

Tirrul, R., Bell, I.R., Griffis, R.J. and Camp, V.E., 1983. The Siatan Suture zone of eastern Iran. Geological Society of America Bulletin, 94: 134-150.

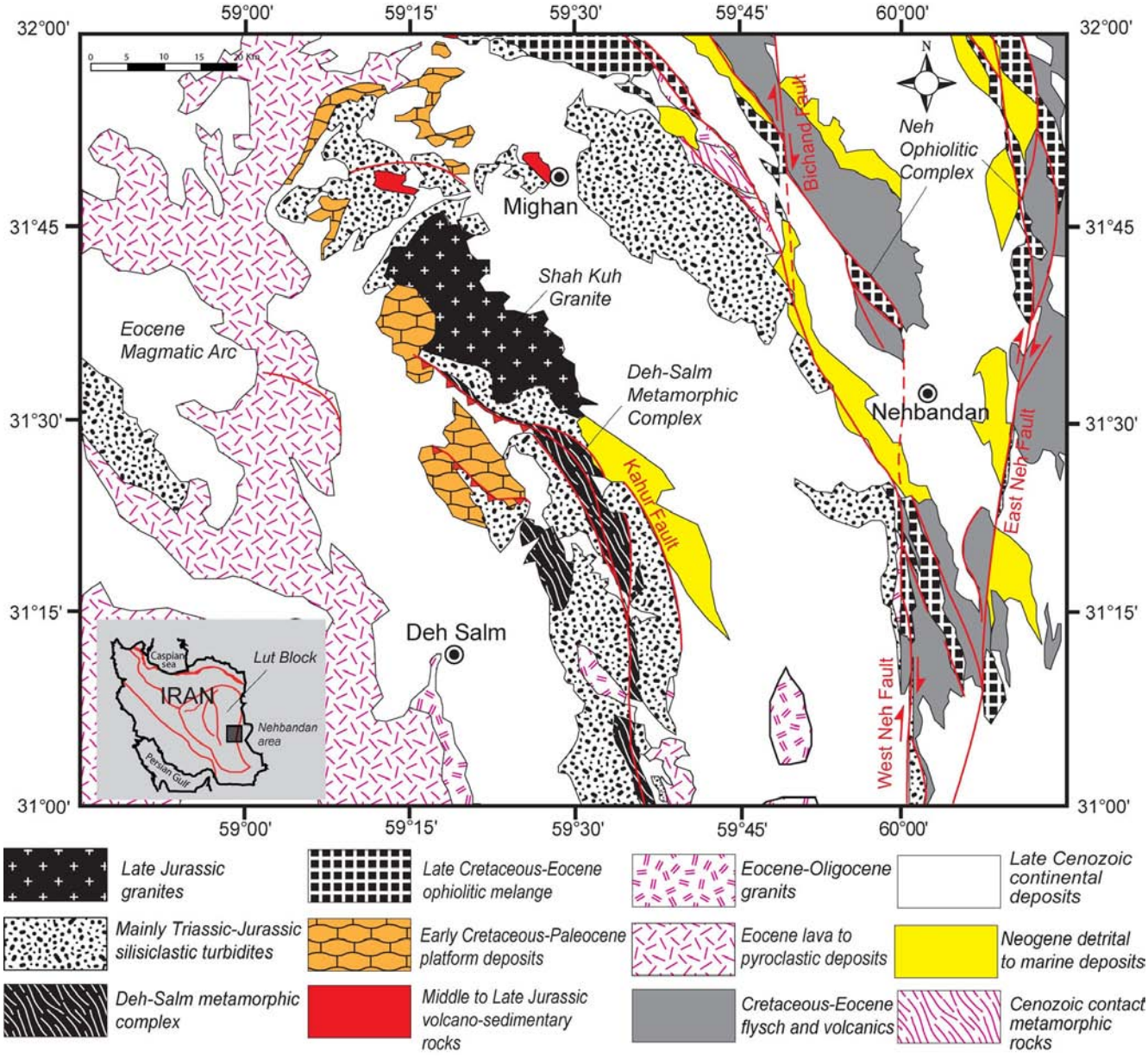

Figure 1. Simplified geological map of the Nehbandan area.

2.2

Neogene tectonics of the Anarak area in Central Iran

Bagheri Sasan*, Buchs David**, Salari Tayebeh* & Nabavi Mehdi*

*Department of Geology, University of Sistan and Baluchestan, Zahedan, 98135-674, Iran
**Research School of Earth Sciences, Australian National University
(sasan_bagheri@yahoo.com)

The Anaraq-Jandaq Terrane comprises a metamorphic assemblage of Carboniferous to Permo-Triassic accreted oceanic island(s) and flysch sediments exposed along the Paleo-Tethys suture in Central Iran (Bagheri & Stampfli 2008). The terrane has recorded a long tectonic history related to early accretionary processes along a Paleo-Tethys margin, closure of the Paleo-Tethys and exhumation in the mid-Triassic, Neo-Tethyan back-arc evolution and, finally, Neogene events that are the focus of this study. The Anaraq-Jandaq Terrane is located along the eastern border of the Ardakan-Kashan Line that extends parallel to the Zagros Thrust in the back-arc area of the Neo-Tethys Uromieh-Dokhtar volcanic arc (Fig. 1). The Line has been interpreted as a dextral shear zone of regional significance (Bagheri, 2007), but additional constraints are still needed to better understand its role in the tectonic evolution of Central Iran.

Structures east of the Ardekan-Kashan Line display several right-stepped en-echelon, double-plunged to half folds that form helicoidal-shapped patterns on a map view (Fig. 1). Large folds and syntethic and antithetic conjugate strike-slip faults occur in basement rocks (e.g. Sylvester, 1988), which are also found in the Anarak area. The largest dextral strike-slip fault system in the Anarak-Jandaq area corresponds to the NW-SE Anarak Shear Zone that is highlighted by a dismemberment of accreted sequences of oceanic island(s). The NE-SW Doruneh Fault is the largest sinistral strike-slip fault in the area and interferes with the Anarak Shear Zone. Two large en-echelon mega-half folds with nearly E-W axial trace have been recognized between the fault and the shear zone. Formation of these folds likely postdates formation of a double plunge antiform found in the Anarak area. The Anarak area is characterized by a recent antiformal pop-up structure (positive flower structure) that comprises several upward diverging thrusted sheets of metamorphic rocks and Tertiary sediments.

Based on preceding observations we divided the Anarak-Jandaq Terrane and adjacent areas into seven structural domains that provide an insight into recent tectonics. Our preliminary results support interpretation of the Ardakan-Kashan Line as a dextral shear zone and suggest that Neogene strain concentrated east of the line as a result to convergence between Arabian and Iranian plates. The convergence led to formation of the Anarak pop-up structure and to reactivation of the exhumation of the Anarak-Jandaq Terrane.

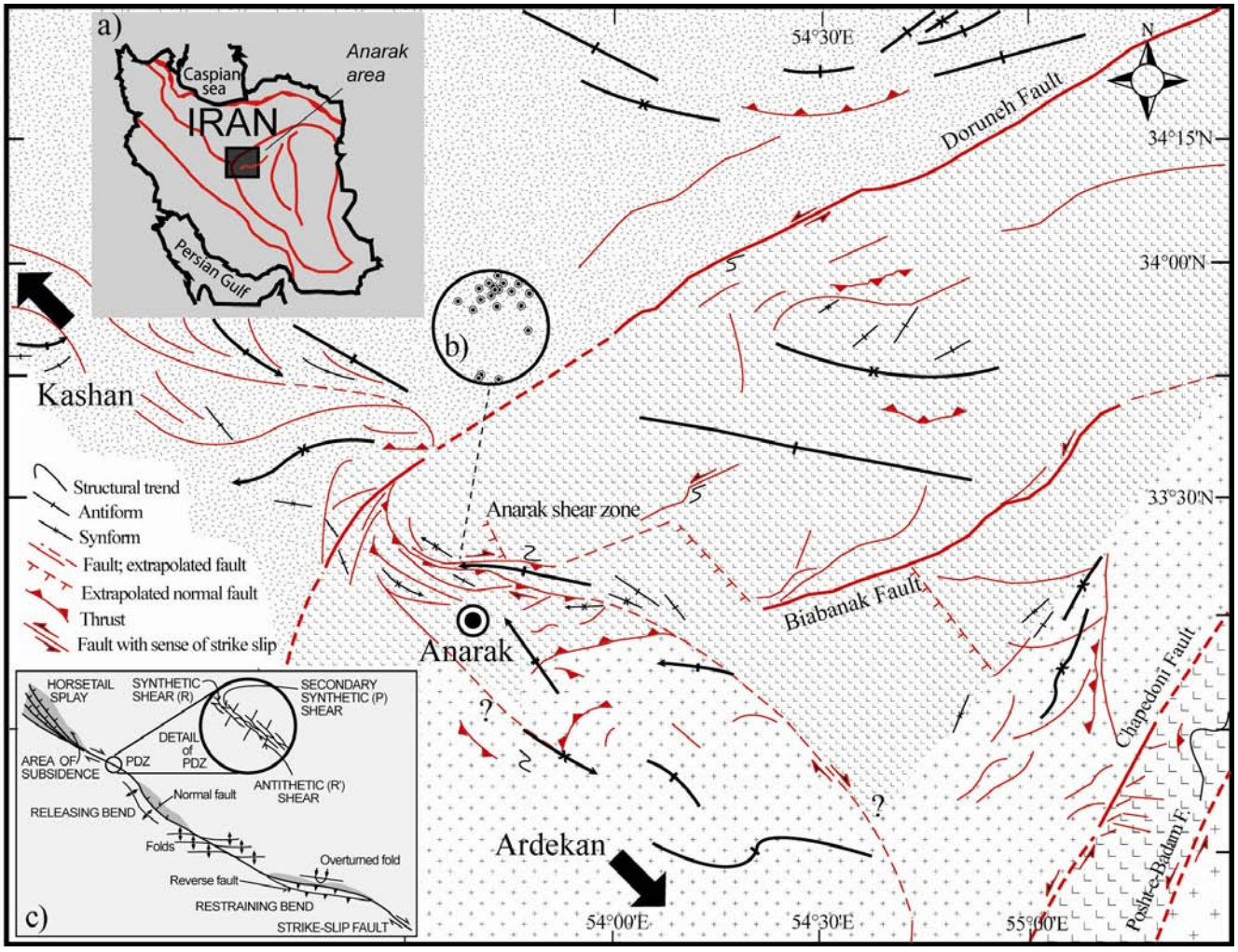

Figure 1: Neogene faults and fold strikes in the Anarak area. a) Tectonic setting of the studied area. b) Stereographic projection of fault planes in the northern Anarak area (poles of fault, lower hemisphere equal-area). c) Spatial arrangement of structures associated with an idealized right-slip fault after Christie-Blick and Biddle (1985).

REFERENCES:

Bagheri, S. 2007: The exotic Paleo-Tethys terrane in central Iran: new geological data from Anarak, Jandaq and posht-e-Badam areas, unpublished Ph.D. thesis, University of Lausanne, Lausanne, Switzerland, 223 pp.

Bagheri, S., & Stampfli, G. M. 2008: The Anarak, Jandaq and Posht-e-Badam metamorphic complexes in central Iran: New geological data, relationships and tectonic implications, Tectonophysics 451:123–155.

Christie-Blick, N. and Biddle, K.T., 1985. Deformation and basin formation along strike-slip faults. In: K.T. Biddle and N. Christie-Blick (Eds.), Strike-slip deformation, basin formation, and sedimentation Society of Economic Paleontologists and Mineralogists Special Publication, p. 1-34.

Sylvester, A.G. 1988: Strike-slip faults, Geological Society of American Bulletin, 100: 1666-1703.

2.3

Khur platform: Tectonic evolution of a part of the Neo-Tethyan back-arc basin in Central Iran

Bagheri Sasan*, Stampfli Gerard **, Moix Patrice **& Bakhshi Mohammad Reza*

*Department of Geology, University of Sistan and Baluchestan, 98135-674 Zahedan, Iran
**Institute of Geology and Paleontology, University of Lausanne, 1015 Lausanne, Switzerland

Tectonically, the Khur region in the NW margin of the Central-East Iranian microcontinent (CEIM) and at the NE side of the Uromieh-Dokhtar magmatic arc is an exceptional area where the Neo-Tethyan back-arc rifting, drifting and collisional stage events are well preserved in the Late Jurassic-Eocene deposits and synchronous igneous and metamorphic rocks. No equivalents of such a thick deposit are known from central Iran (Aistov et al., 1984; Bagheri, 2007). South of the Biabanak fault the terrestrial rift-related Upper Jurassic-Lower Cretaceous Chah Palang and Noghreh Formations unconformably cover the Variscan-Eocimmerian metamorphic rocks (Bagheri and Stampfli 2008) and followed by an enormous thick flyshoid deposit (the post-rift Biabanak shale). The Ar/Ar for micas and U/Pb for single-grain zircons respectively related to the metamorphic and igneous rocks yield the Late Jurassic cooling ages (Bagheri 2007). The second rifting stage occurred south of the Doruneh Fault; there, the Jandaq igneous-metamorphic complex that formed the basement of the tilted blocks is found below the early Late Cretaceous syn-rift formation such as Debarsu. Few tens of kilometers toward the northeast in the Khar Turan area, the early Cretaceous mildly alkaline basalt and orbitolina limestone sequences transitionally change to the Late Cretaceous pelagic deposits. We consider this sequence as a result of sedimentation on the edge of an infant oceanic crust. This sequence is followed by Late Cretaceous-Paleocene Haftooman, Farrokhi and Chupanan formations mainly composed of benthic to pelagic marl and limestone in the Khur area; these nearly 3000 meters marine deposits set down when the Khur platform was being developed during the drifting stage. The thick Eocene-Oligocene flysch of Pish Kuh accompanied by the Late Cretaceous-Paleocene ophiolitic mélanges of Nain-Ashin as well as calc-alkaline volcanic rocks unconformably overlie the platform sequence near the Doruneh Fault. This assemblage could be the products of back-arc closure comparable with the Late Eocene-Oligocene mélange-type rock collections surrounding the CEIM (collisional stage). The Oligocene Lower Red Formation can be regarded as the molasse of this closure event. The Khur platform in view point of stratigraphy and paleontology is very similar to the time-equivalent basin such as Kopeh Dagh and the North Afghan platform in NE Iran; the presence of the Khur platform in Central Iran could be the consequence of counter-clock wise rotation of the CEIM since the Eocene time contemporaneous with the Indian-Eurasian collision.

REFERENCES:

Aistov, L., Melanikov, B., Krivyakin, B., Morozov, L. and Kiristaev, V. (Eds.), 1984. Geology of the Khur Area (central Iran), Explanatory text of the Khur quaderangle map
1:250,000. Geological Survey of Iran, V/O "Technoexport" USSR Ministry of Geology, Reports, TE/No. 20, 1-132, Moscow.

Bagheri, S. 2007: The exotic Paleo-Tethys terrane in central Iran: new geological data from Anarak, Jandaq and posht-e-Badam areas, unpublished Ph.D. thesis, University of Lausanne, Lausanne, Switzerland, 223 pp.

Bagheri, S., & Stampfli, G. M. 2008: The Anarak, Jandaq and Posht-e-Badam metamorphic complexes in central Iran: New geological data, relationships and tectonic implications, Tectonophysics 451:123–155.

Figure 1: Crustal evolution model for Atlantic-type margins utilized for crustal evolution of the Khur platform. (Next Page)

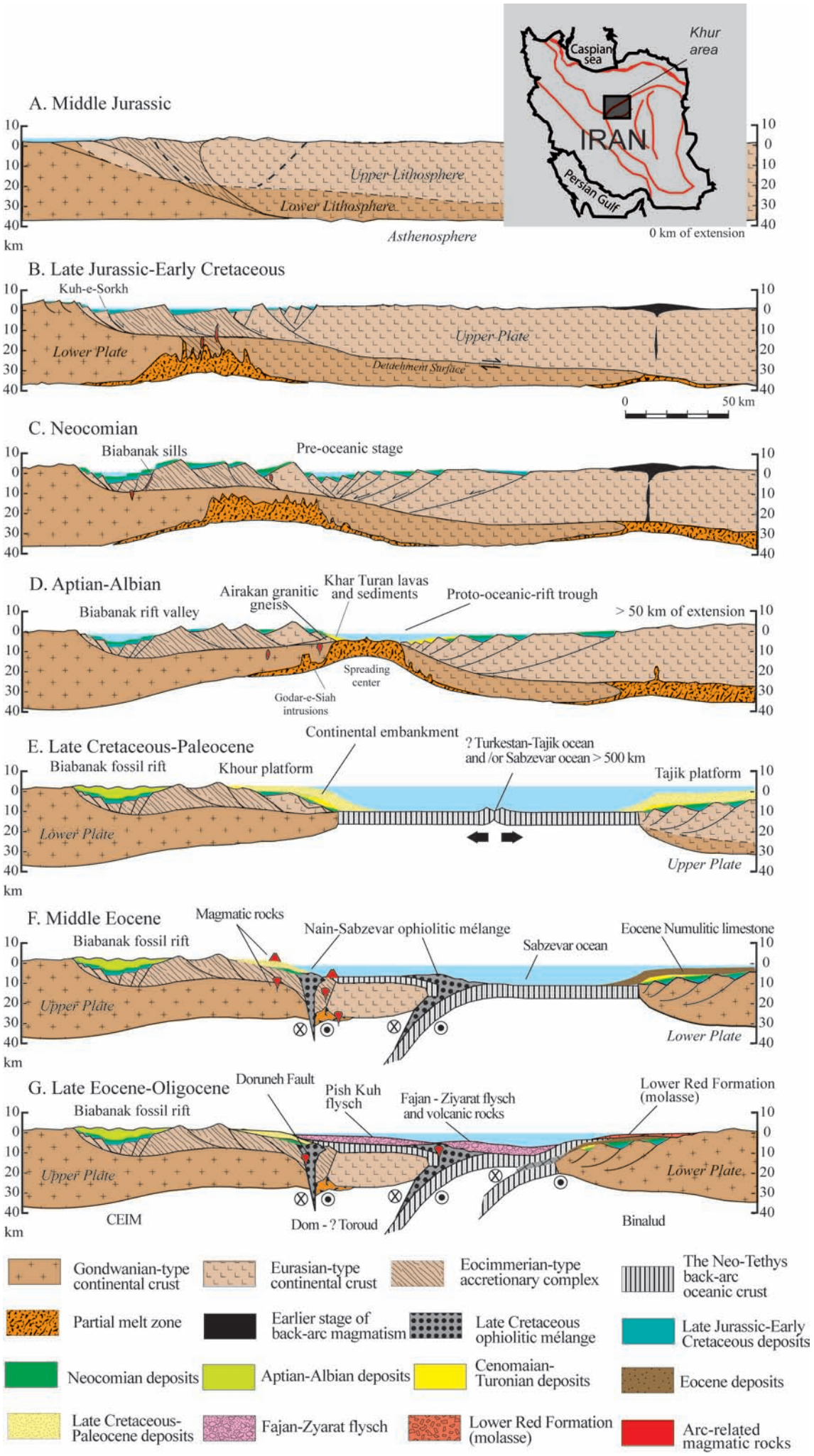
A. Middle Jurassic
Caspian sea
Khur area
IRAN
Persian Gulf
Upper Lithosphere
Lower Lithosphere
Asthenosphere
0 km of extension
km
B. Late Jurassic-Early Cretaceous
Kuh-e-Sorkh
Lower Plate
Upper Plate
Detachment Surface
0
50 km
C. Neocomian
Biabanak sills
Pre-oceanic stage
D. Aptian-Albian
Biabanak rift valley
Airakan granitic gneiss
Khar Turan lavas and sediments
Proto-oceanic-rift trough
> 50 km of extension
Spreading center
Godar-e-Siah intrusions
E. Late Cretaceous-Paleocene
Biabanak fossil rift
Khour platform
Continental embankment
? Turkestan-Tajik ocean and /or Sabzevar ocean > 500 km
Tajik platform
Lower Plate
Upper Plate
km
F. Middle Eocene
Magmatic rocks
Biabanak fossil rift
Nain-Sabzevar ophiolitic mélange
Sabzevar ocean
Eocene Numulitic limestone
Upper Plate
Lower Plate
km
G. Late Eocene-Oligocene
Doruneh Fault
Pish Kuh flysch
Fajan - Ziyarat flysch and volcanic rocks
Lower Red Formation (molasse)
Biabanak fossil rift
Upper Plate
Lower Plate
CEIM
Dom - ? Toroud
Binalud
km
Gondwanian-type continental crust
Eurasian-type continental crust
Eocimmerian-type accretionary complex
The Neo-Tethys back-arc oceanic crust
Partial melt zone
Earlier stage of back-arc magmatism
Late Cretaceous ophiolitic mélange
Late Jurassic-Early Cretaceous deposits
Neocomian deposits
Aptian-Albian deposits
Cenomaian-Turonian deposits
Eocene deposits
Late Cretaceous-Paleocene deposits
Fajan-Zyarat flysch
Lower Red Formation (molasse)
Arc-related magmatic rocks

2.4

Tectonic control of Pb-Zn-Ba-(Sr) deposit at Oued Jebs-Kef Lasfar, northern Tunisia

Jaloul BEJAOUI *, Ahmed SELLAMI **

* *Centre National des Sciences et Technologies Nucléaires, Tunisie, bjaoui_geo@yahoo.fr*
** *Office National des Mines, Tunisie*

The Oued Jebs-Kef Lasfar Pb-Zn-Ba-(Sr) mineralized area is located in the northern Tunisia (60Km from Tunis) and forms part of the diapir zone (Fig.1) which is highly affected by NNW–SSE trending tectonic deformation (Fig.2). The structural analysis carried out in the Oued Jebs-Kef Lasfar deposit reveals the existence of one tectonic phase characterized by a NW-SE (σ1) maximum compression orientation and NE-SW maximum extension trending. The Pb-Zn-Ba-(Sr) mineralization often fills fractures in the calcite matrix within the massive limestone.
The Pb-Zn-Ba-(Sr) event mineralized structures are related to the NW-SE compressive event presumably associated to Alpine convergence (Ben Ayed, 1986). Field observations show some relative chronology corresponding to superimposed striations on fault surfaces and cross-cutting relationships between structures (faults, joints, calcite veins) (Fig.2).
The Cenomanian-Turonian carbonates of the Oued Jebs-Kef Lasfar have been subject to several stylolitisation processes and fracturing events, being subsequently filled by various calcite cements. Based on the described structures and on the regional geological frame, we assume that veins were reulted from the NE–SW extension. These extensional structures are crucial sites for the localization of fluid flow and ore deposition. Such orebodies emplacements are associated with diapirs and are interpreted as the result of a Serravalian-Tortonian gravity-driven fluid circulation event related to late Alpine convergence (Decree et al., 2008).

REFERENCES

Ben Ayed, N.,. (1986)- Évolution tectonique de l'avant-pays de la Chaîne Alpine de la Tunisie du début du Mésozoïque à l'Actuel. Thèse Doctorat ès Sciences, Université Paris-Sud (inédit).

Sophie Decrée, Christian Marignac, Thierry De Putter, Etienne Deloule, Jean-Paul Liégeois and Daniel Demaiffe. (2008) - Pb–Zn mineralization in a Miocene regional extensional context: The case of the Sidi Driss and the Douahria ore deposits (Nefza mining district, northern Tunisia).

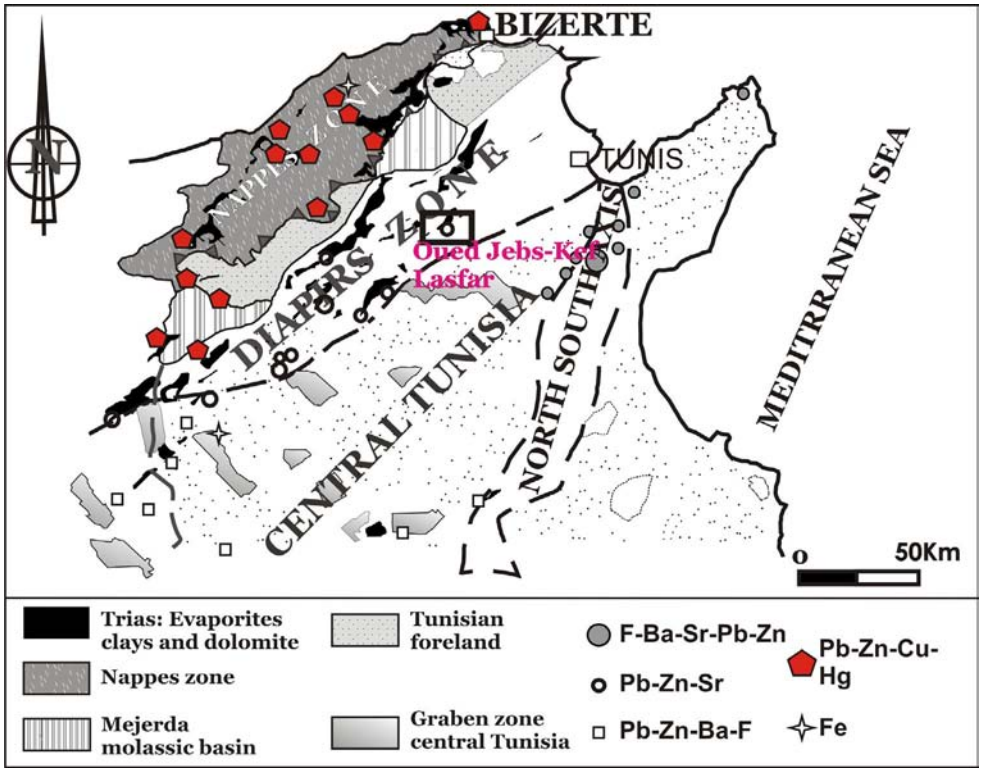

Fig 1. Location of the Oued Jebs ore deposit within the diapirs zone in Tunisian structural map.

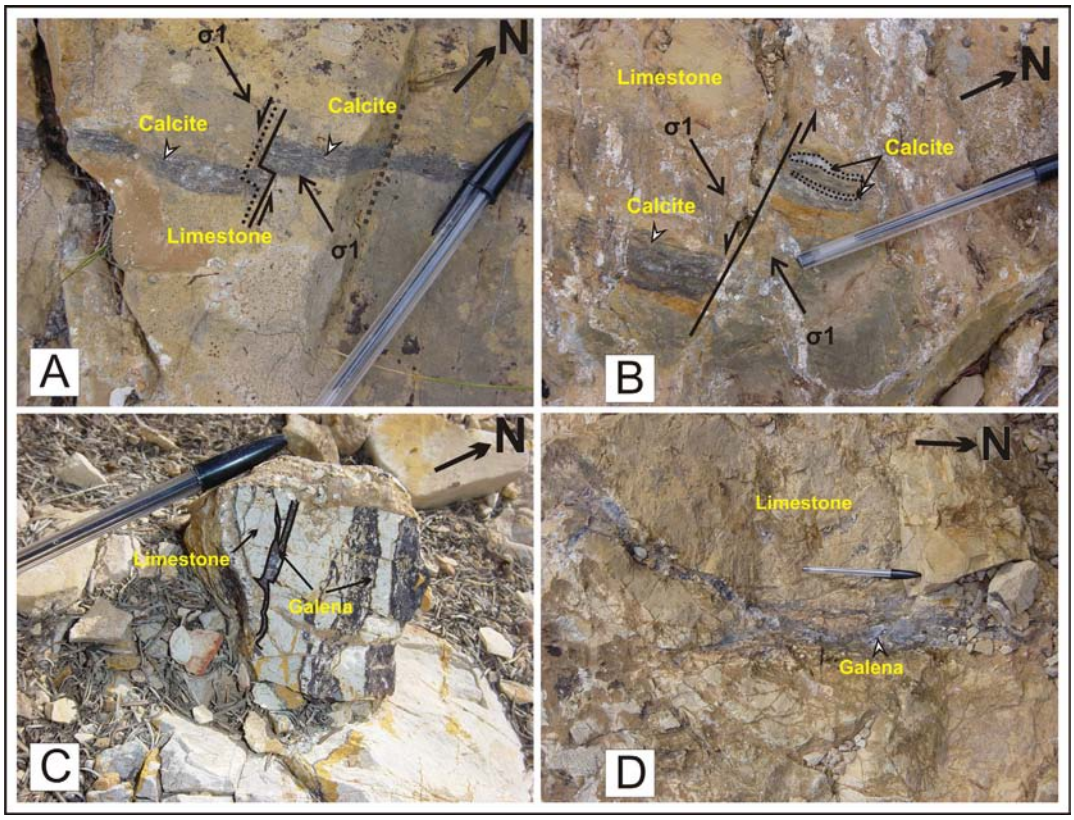

Fig.1- (A) and (B) Cenomanian limestone affected by a minor normal fault associated with extensional fentes collapsed with calcite, (C) sub-parallels veins filled with galena, (D) Cenomanian limestone with two veins generations-filled with galena.

2.5

Polymineralic Mylonites Generated by Chemo-Mechanical Mixing: The Glarus Thrust as an Example

Th. Buckingham, M. Herwegh, O.A. Pfiffner

Institute of Geological Sciences, Bern University, Switzerland

Large-scale shear zones often are characterized by different rock types in the hanging and footwall. The Glarus thrust, as an example, defines a sharp lithological boundary between Permian Verrucano in the hanging and Infrahelvetic sedimentary units in the footwall, separated by a layer of Lochsiten carbonate-tectonite. These tectonites are usually mixtures of silicate and carbonate phases suggesting incorporation of components from footwall and hanging wall. In this way, polymineralic tectonites evolve with ongoing deformation, becoming more and more impure owing to two different mixing processes: fluid-assisted (i) predominantly mechanical and (ii) combined chemo-mechanical mixing.

(i) In the case of pure mechanical mixing on the meso-scale, brittle fracturing and the formation of microshear zones oblique to the shear plane allow shearing of surrounding host material into the carbonate tectonite. Thus, hybrid tectonites may evolve with viscous granular flow inducing a further, dispersed (see ii) mechanical mixing. In the Lochsiten carbonate-tectonite synkinematic calcite veins suggest that this process must have occurred under the presence of fluids, which may have enhanced the formation of the brittle fractures by hydrofracturing.

(ii) Chemo-mechanical mixing is based on the dissolution of mineral phases that are unstable in the surrounding host rocks. The activity of granular flow in the fault rock has two important effects: First the formation of grain-scale cavities promotes the pumping of surrounding fluids into the tectonite, followed by precipitation of second-phase minerals in the newly formed cavities. In this process, homogeneous mixtures of fine-grained calcite matrix and silicate (e.g. feldspars) second-phases develop.

Pure calcite mylonites formed in the aforementioned synkinematic veins become continuously impurified by the two mixing processes, which allows granular flow (diffusion creep) to dominate deformation. Both observed processes persist during the activity of the large-scale shear zone as a function of surrounding wall rocks and local fluid availability. With ongoing exhumation induced-cooling, however, strain is more localized and the active shear zone becomes narrower. Our observations suggest that these two suggested mixing processes are active until the final stages of thrusting when brittle conditions prevail.

2.6

The thermochemical nature of the upper mantle: an interdisciplinary approach

Fabio Cammarano*, Paul Tackley*, Takashi Nakagawa*, Lars Stixrude**, Carolina Lithgow-Bertelloni**, Wenbo Xu***, Barbara Romanowicz****

*ETH Zürich, Institute of Geophysics, Geophysical Fluid Dynamics
**University College London, Earth Sciences
***Michigan University, Earth Sciences
****UC Berkeley, Earth Science, Berkeley Seismological Laboratory

Most of the upper mantle is inaccessible to direct sampling and its physical conditions are indirectly determined from the interpretation of seismic data based on insights from mineral physics. The conjecture of the upper mantle as a well-mixed, homogeneous composition has been recently challenged from a new family of geodynamic models which includes a two-phase (MORB and Harzburgite) mixture which does not equilibrate during mantle evolution (e.g., Tackley et al., 2005). The co-existence of separated rock assemblages cannot be discarded, indeed, considering the low chemical diffusivities of mantle materials. At the same time, the physical interpretation of long period seismic waveforms found that composition should change with depth (below ~250km) at a global scale (Cammarano and Romanowicz, 2007). Here, we show the results of a recent re-interpretation of global seismic data based on a state-of-the-art mineral physics model.
The model is based on knowledge of material properties at high temperatures and pressures. In particular, elastic properties are computed with a recent self-consistent thermodynamical model, based on a six oxides (NCFMAS) system. We model the P, T and frequency dependency of anelasticity by using the model Q5 (Cammarano et al., 2003), based on the Arrhenius law as expected of thermally activated processes. We adopt a non-linear procedure to invert normal modes for possible thermal or compositional structures of the upper mantle. We consider both equilibrium assemblages and mechanical mixtures of MORB and Harzburgite.
We found further evidence that composition should become richer in MORB content below 250 km and we found that only a mechanical mixture is able to fit the seismic data. Standing to our mineral physics model, the required compositional gradient with depth is even too high (for realistic thermal structures). An increase in grain size with depth could play role as well. Future work will push even further such an interdisciplinary approach, trying to extend our interpretation to other geophysical observables and couple the results with models of the thermochemical evolution of the upper mantle.

2.7

Tectonics of the western Gran Sasso d'Italia (Central Apennines)

Giovanni Luca Cardello*, Daniel Bernoulli** & Carlo Doglioni***

* ETH-Zürich, ** Basel University, *** Sapienza University, Rome,

During Jurassic-Cretaceous times, the area of the central Apennines was part of a large, Bahamian-type carbonate platform–basin system, whereby the area of the Gran Sasso was situated between the carbonate platform of Latium and the Abruzzi in the west and the deep basinal area of Marche-Umbria to the east. This transitional area experienced 1. Early Jurassic rifting of the Adriatic margin, leading to the opening of the Ligurian branch of Tethys; 2. prolonged thermal subsidence of the carbonate-platform slope and base-of-slope in the Jurassic–Cretaceous; 3. decollement along Triassic evaporates, thrusting and folding during the Neogene formation of the arc of Gran Sasso and 4. post-nappe normal faulting persisting to this date.
Mapping of the western part of the E–W-trending ridge of the Gran Sasso d'Italia, the highest elevation of the Apennines (2914 m), has yielded the following results:
1 – The early Jurassic rifting event led to the segmentation of the platform slope into structural highs (Corno Grande, Monte and Acqua San Franco) and basins (Pizzo Intermesoli, M. Corvo) as suggested by the pronounced differences in thickness of the early–middle Liassic syn-rift sediments (Corniola Formation). Whereas the Acqua San Franco structural high in the west was buried during the Toarcian, the Corno Grande high in the east persisted throughout Mesozoic times at least into the early Tertiary. The longevity and possible tectonic reactivation of the submarine topography, inherited from early Liassic rifting, persisted way into Jurassic–Cretaceous as suggested by the pronounced differences in thickness of the Jurassic (Corno

Piccolo Formation) and Cretaceous (Cefalone and M. Corvo Formations) base-of-slope sediments derived from the Abruzzi carbonate platform, and sequences punctuated by stratigraphic gaps on the highs.
2 – During the Tertiary orogeny of the Apennines, the inherited Mesozoic structures evolved into N-S trending transfer zones between the individual thrusts and folds over- and underthrusting the more external *Laga unit*. The axis of the frontal anticline and the related thrust of Gran Sasso plunge westward with a parallel decrease in shortening. The tip line of the blind thrust related to the frontal fault-propagation fold becomes deeper and more internal moving westward, according to a gradual transfer of shortening toward the adjacent recess. The E-W trending arm of the Gran Sasso arc experienced a component of left-lateral transpression as expected from the NE-ward propagation of the central Apennines accretionary wedge. The propagation of the arc occurred during deposition of the Messinian Laga Flysch Formation as shown by the growth structures in the latter.
3 – The backlimb of the frontal fault-propagation fold indicates that the entire structure has been tilted after its development. We speculate that this has been generated by a deeper ramp of a backthrust, forming a triangle zone affecting the entire E-W trending Gran Sasso range. This would explain the about 15 km long, regionally diffuse monocline of the Gran Sasso range toward the foreland.
4 – Normal faults cut across the previously tilted internal limb, as shown by the cut-off angle of the faults relative to bedding; Most of them show morphologic evidence of present-day activity, but only part of the displacement observed is due to the Pleistocene-Holocene extension because of the poly-phase role of the main fault systems. According to surficial fault rupture height, the *Tre Selle* normal fault as most of the other normal faults could generate earthquakes of Mw>6.5. The *Tre Selle* fault is clearly linked to the *Assergi Fault* by the *Campo Imperatore Fault* that has transtensive characteristics and an en-échélon orientation, functioning as a link between the two former fault systems.

2.8

Neogene transtensional tectonic evolution of the central Helvetic nappes: preliminary results

Giovanni Luca Cardello* & Neil Mancktelow*

* *Geologisches Institut, ETH-Zürich, CH-8092 Zürich*

The Helvetic nappe stack in the Rawyl depression between the Aar and Mont Blanc massifs is affected by oblique transtensional normal faults developed or reactivated during the Neogene. One field season of mapping of the main fault structures in the Rawyl-Audannes area has provided the following main results.
1. Three preferential orientations normal fault sets are observed, striking E-W, NW, and NE.
2. The NE-striking set dips mainly to the SE and, from relative age relationships of associated veins, is the oldest. Paleotectonic features exposed in Plaine des Roses, Plaine Morte and Les Audannes suggest this set was already active during Cretaceous sedimentation. The Upper Cretaceous stratigraphic sequence is influenced by paleo-escarpments that clearly define the orientation of the paleo-faults. These surfaces are marked in many places by karstification and silicification of the surface, sedimentary dykes and the onlap of basinal younger formations. Some of these faults have been subsequently reactivated during Neogene syn- and post-collisional extension.
3. The E-W and NW-striking systems locally show an initial mylonitic shear-zone stage overprinted by cataclastic faulting, especially in more competent units such as the Schrattenkalk Fm.
4. The E-W and NW-striking faults were broadly coeval, as indicated in the Rawyl-Plaine Morte area by many examples of branching and bending of one set into the other and by the similar displacement directions.
5. Calcite slickenlines and fibres on the Neogene fault planes indicate two main stretching directions. The older one is WSW-directed and generally plunges around 30°, whereas the younger one plunges to the south, with a steeper, mainly dip-slip movement.
6. Crosscutting vein relationships and bending of vein tails planes indicate a counter-clockwise rotation of the stretching direction, from WSW toward S.
7. The WSW–directed orogen-parallel stretching is similar in orientation to that associated with the Simplon-Rhone Fault Zone and is probably coeval, implying possible activity throughout much of the Miocene.

2.9

Sedimentology of Early Pliocene Sandstones in the South-Western Taiwan foreland: implications for basin physiography at the onset of collision.

Castelltort Sébastien*, Nagel Stefan*, Mouthereau Frédéric**, Lin Andrew Tien-shun***, Wetzel Andreas****, Kaus Boris*, Willett Sean*, Chiang Shao-ping*** & Chiu Wei-Yi***

ETH-Zürich, Sonneggstrasse 5, 8092 Zürich (sebastien.castelltort@erdw.ethz.ch)
** Université Pierre et Marie Curie, Place Jussieu, 75252 Paris*
*** Basin Research Group, National Central University, Jonghli, Taiwan*
**** Geological and Paleontological Institute, University of Basel, Bernoullistr. 32, 4056 Basel*

Foreland basins develop at the front of orogens and are filled by sediments derived from the eroding mountain range. As such, their stratigraphic architecture and subsidence history contain a record of mountain building. In Taiwan, the western foreland basin results from the flexure of the EUR lithosphere provoked by thrust loading of units onto the Chinese margin. Field work, seismic profiles and borehole data acquired by oil companies document extensively the development of the basin (Lin et al., 2003). It is composed of a succession of stages recording the progressive filling of the basin after an under-filled stage at the initiation of load-induced subsidence. This general sequence of facies in Taiwan is at the origin of the classical model of foreland basin filling sequence popularized by Covey (1986) in a special IAS volume on Foreland Basins and has since been applied worldwide. However, while the under-filled stage can be clearly recognised on the field, the pre-foreland series (early Kueichulin and before) and the assumed early foreland series that can be observed on the cratonward side of the basin both indicate relatively shallow water environments and are both fed by the Chinese margin through their history. Thus, no obvious changes in sedimentary environments and composition clearly mark the initiation of subsidence. This problem is also reflected in the different ages to which different authors attribute the initiation of foreland basin subsidence. When and where did the load induced subsidence start in Taiwan ? It is crucial to solve this issue because it conditions our understanding of the tectonic history of collision in Taiwan, the type-orogen for theories of critical wedges.

The Basin Research group in Taiwan, Tectonics laboratory in Paris and both Geophysical Fluid Dynamics and Earth Surface Dynamics groups at ETH tackle this issue together and from different approaches.

In this work we present our sedimentological analysis of the Pliocene Tawo and Ailiachao sandstones in the Yujing and Yucyongping areas, situated at or near the transition from passive margin to foreland basin subsidence.
We show that they probably correspond to hyperpycnal turbidites in relatively shallow water pro-delta environments similar to modern deposition in the Yellow Sea. Through time-series analysis of rhythmic beds we show that a remarkable feature is the strong, potentially misleading, influence of tide currents in shaping these deposits. We incorporate these informations into restored paleogeographical hypotheses for this time period using estimated quantities of shortening in the foreland fold-and-thrust belt and show that the Chinese continental margin at this time displayed an important promontory towards the ocean. This could explain why the collision seems to have started before than usually inferred based on reconstructions assuming a cylindrical linear continental margin and extrapolating to the past the modern high-rates of convergence.

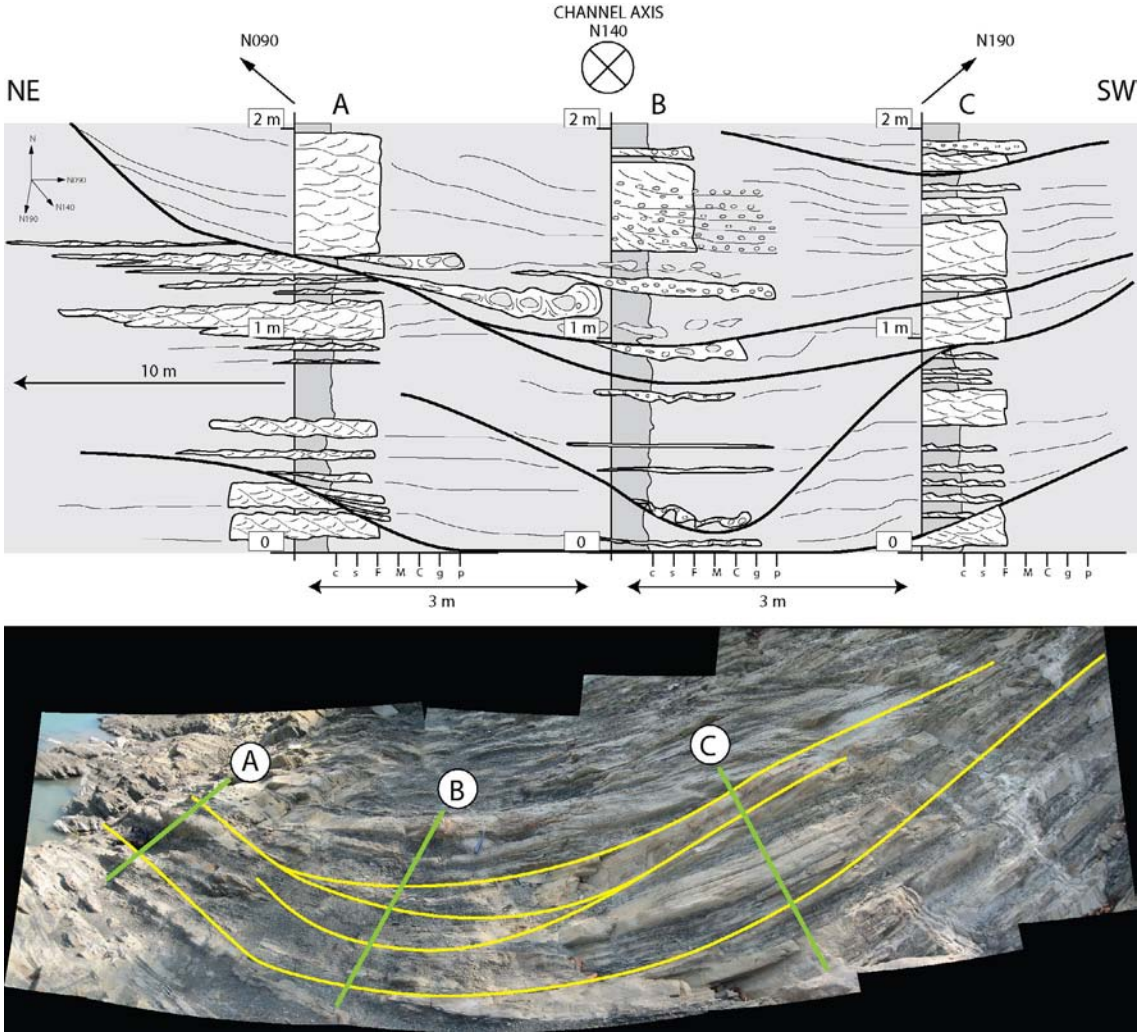

Figure 1. Detailed description of a channel-levee system in shallow turbidites of the Ailiaochao formation in the Pliocene of south-central Taiwan.

REFERENCES

Covey, M. (1986) - The evolution of foreland basins to steady state: evidence from the western Taiwan foreland basin, in Foreland Basins, edited by P. A. Allen and P. Homewood, Spec. Publs int. Ass. Sediment., 8, 77 – 90.

Lin, A. T., Watts A. B. & Hesselbo S. P. (2003) - Cenozoic stratigraphy and subsidence history of the South China Sea margin in the Taiwan region. Basin Research, 15 (4), 453-478.

Funding: This project is funded by Swiss National Funds grant #2-77295-08.

2.10

One-sided subduction in self-consistent models of global mantle convection: the importance of a free surface and a weak crustal layer

Crameri Fabio, Tackley Paul, Meilick Irena, Gerya Taras, Kaus Boris & Keller Tobias

Institut für Geophysik, ETH Zürich, Switzerland (fabio.crameri@erdw.ethz.ch)

Previous dynamical models of global mantle convection indicated that a visco-plastic rheology is successful in generating plate tectonics-like behaviour self-consistently (Moresi et al., 1998; van Heck and Tackley, 2008). Yet, these models fail to create Earth-like plate tectonics: so far in all published models subduction is two-sided and more or less symmetric, whereas terrestrial subduction is one-sided and characterized by a distinctive asymmetry.

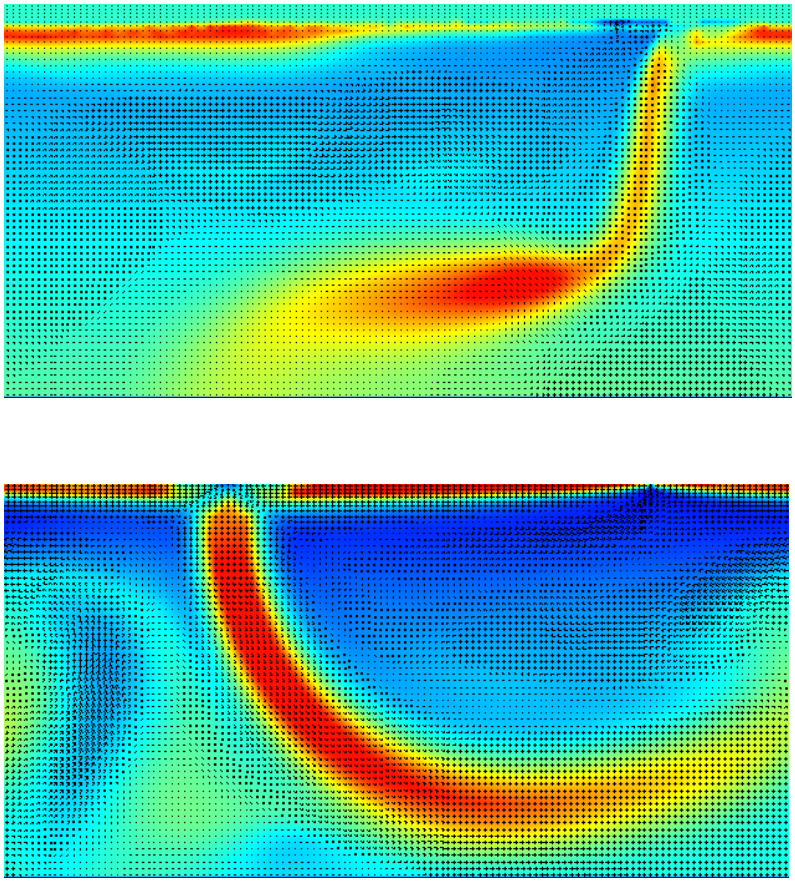

Figure 1. Viscosity fields for convection with a strongly temperature-dependent visco-plastic rheology and (top) a free surface or (bottom) a free-slip surface.

One simplification used in previous models is that of a free-slip upper boundary, in which the shear stress is zero but the vertical position of the boundary is fixed. In contrast, subduction zones display some of the largest variations in surface topography on Earth. For the case of a slab that is initially placed at the surface and allowed to freely subduct, Schmeling et al. (2008) showed that it is necessary to include a proper free surface in numerical models in order to reproduce laboratory results. According to their benchmark study, mimicking a free surface by a low viscosity, zero density layer on top of the crust is an adequate approach. For this reason, we have implemented such a "sticky air layer" in our global numerical model.

We here study the effect of a free surface on the mode of subduction in 2D and 3D global, fully dynamic mantle convection models with self-consistent plate tectonics. For this we use the finite volume multigrid code StagYY (Tackley, 2008) with strongly temperature-dependent viscosity, ductile and/or brittle plastic yielding, and non-diffusive tracers tracking compositional variations (the 'air' layer in this case).

We observe that indeed, a free surface leads to single-sided subduction, whereas identical models with a free slip upper boundary develop double-sided subduction (Figure 1). A free surface is thus an essential ingredient to obtain realistic subduction behaviour in numerical models, probably because it allows the slab to bend in a natural manner.

Although the above models appear one-sided from the temperature or viscosity fields, there is strong mechanical coupling between the slab and the mantle wedge that makes them mechanically double-sided. Regional models of subduction (Gerya et al, 2008) indicate that one requirement for stable one-sided subduction is a low strength interface between the plates achieved by the presence of metamorphic fluids in the subduction channel. Such a lubrication layer consisting of weak hydrated sediments accommodates stable one-sided subduction by strain localization, while the absence of a weak shear zone leads to mechanically two-sided subduction since in this case the plastic strength of the entire plates needs to be sufficiently low to allow for subduction.

In conclusion, a free surface is the key ingredient to obtain thermally one-sided subduction, while additionally including a weak crust is essential to obtain subduction that is both mechanically and thermally one-sided.

REFERENCES

Moresi, L., & Solomatov V. 1998: Mantle convection with a brittle lithosphere - Thoughts on the global tectonic styles of the Earth and Venus. Geophys. J. Int. 133, 669-682.

van Heck, H. & Tackley P. J. 2008: Planforms of self-consistently generated plate tectonics in 3-D spherical geometry. Geophys. Res. Lett. 35, doi:10.1029/2008GL035190.

Schmeling, H., Babeyko A., Enns A., Faccenna C., Funiciello F., Gerya T., Golabek G., Grigull S., Kaus B. J. P., Morra G., Schmalholz S. & van Hunen J. 2008: A benchmark comparison of spontaneous subduction models – towards a free surface: Phys. Earth Planet. Int. 171, 198-223.

Tackley, P. J. 2008: Modelling compressible mantle convection with large viscosity contrasts in a three-dimensional spherical shell using the yin-yang grid. Phys. Earth Planet. Int., doi:10.1016/j.pepi.2008.08.005.

Gerya, T. V., Connolly J. A. D. & Yuen, D. A. 2008: Why is terrestrial subduction one-sided? Geology 36, 43-46.

2.11

Parameters that control the formation of lithospheric-scale shear zones

Crameri Fabio*, Kaus Boris J.P.* & Tackley Paul J.*

**Institute of Geophysics, ETH Zurich, Schafmattstrasse 30, CH-8093 Zürich (fcrameri@student.ethz.ch)*

Shear-heating induced localization might be an important process for subduction initiation. Kaus & Podladchikov (2006) showed with the help of numerical simulations that for some parameters, localization occurs and for other parameter choices, localization does not take place. Thereby, either homogeneous thickening or buckling compensates the deformation. Thermally activated thrusting in contrast to these two mechanisms is preferred for a relatively cold lithosphere. In addition to the thermal structure of the lithosphere, the deformation mode is also determined by the initial rheological structure and by the shortening rates [*Burg and Schmalholz*, 2008].

Here, numerous 2-D simulations (>100 #) are performed to distinguish these regions by changing the parameters that influence the shear heating process. The 2-D simulations are performed using a MATLAB-based finite element code. The standard simulations used for this work model a lithosphere consisting of an upper crust, a lower crust plus an upper mantle part. First, only temperature and strain rate are changed during systematic simulations, followed by changes in the rheology. Additional 2-D simulations have been performed in which the mantle thickness was increased or in which the initial geometry (for example crustal thickness) was changed.

In addition, a fast 1-D finite difference code was developed, that exactly reproduces the results of the 2-D code for laterally homogeneous cases. For the same input parameters, it computes information of temporal changes of both the temperature and strength profile of the Earth's upper part due to shear-heating. Even more important, it further supplies information for the occurrence of localization after comparing and validating its results with the 2-D simulations. As a powerful tool, this 1-D code can finally be used to predict the occurrence of shear localization for given input parameters. This thus yields new insights in the occurrence of shear localization in a compressed lithosphere.

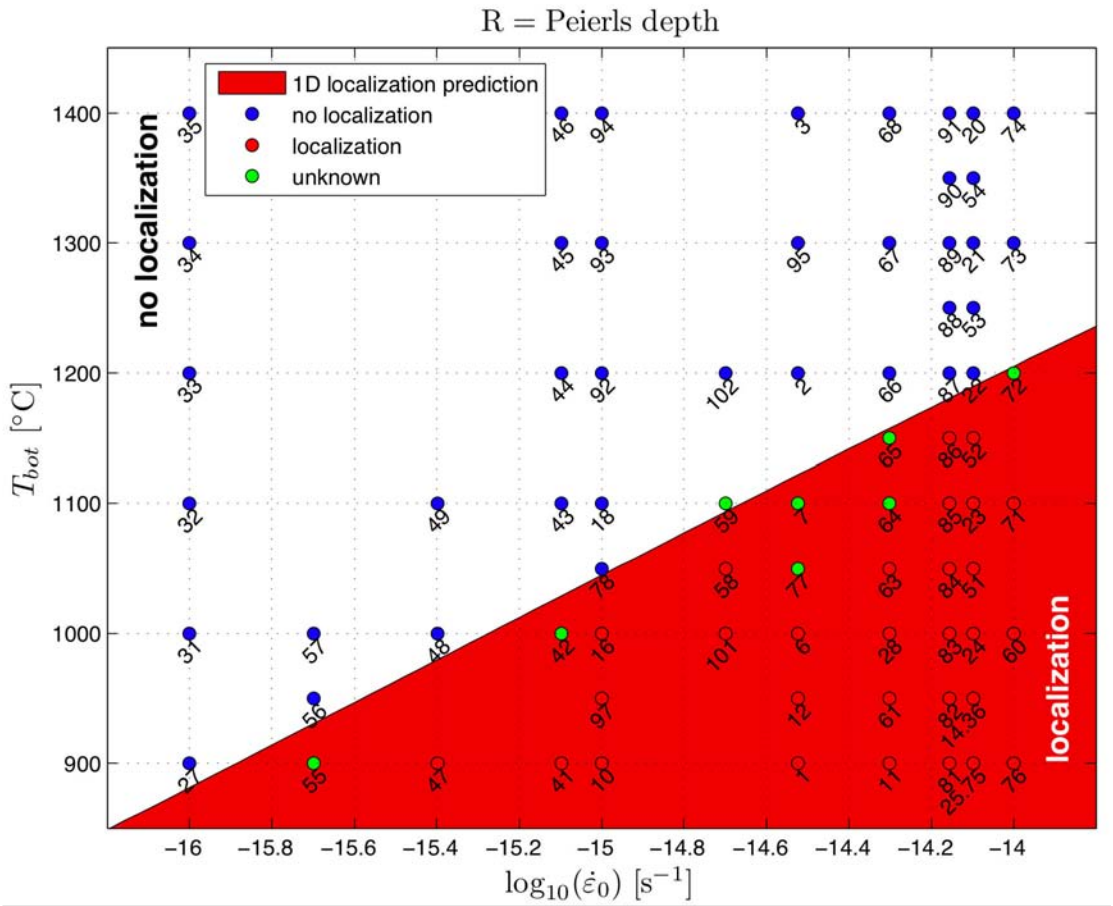

Figure 1. Localization prediction of 1-D code (red area) are compared to 2-D simulation results shown as points and indicating no localization (blue), localization (red) and unknown (green).

REFERENCES

Burg, J. P., and S. M. Schmalholz (2008), Viscous heating allows thrusting to overcome crustal-scale buckling: Numerical investigation with application to the Himalayan syntaxes, Earth and Planetary Science Letters, 274(1-2), 189-203.

Kaus, B. J. P., and Y. Y. Podladchikov (2006), Initiation of localized shear zones in viscoelastoplastic rocks, Journal of Geophysical Research-Solid Earth, 111(B4).

2.12

Twin meteorite impact craters in Thessaly (Central Greece) of Holocene age

Dietrich Volker J.* & Gartzos Efthimios**

*Institute for Mineralogy and Petrography, Swiss Federal Institute of Technology, CH-8092 Zurich, Switzerland (volker.dietrich@erdw.ethz.ch)
**Laboratory of Mineralogy-Geology, Agricultural University of Athens, GR-118 55 Athens, Greece

Two circular permanent lakes of 150 and 250 m in diameter and 12 and 16m depth, respectively, occur 250 m apart from each other in the agricultural fields SW of the town of Almyros (Thessaly). The basement beneath the alluvial cover consists of Mesozoic marly limestones, schists, phyllites, cherts, as well as of slices of radiolarites, serpentinites and meta-basalts (Marinos et al. 1962). The lakes were regarded as dolines due to the occurrence of karst phenomena in the equivalent tectonic units in the surrounding Othris mountains. Another hypothesis as volcanic maar-type diatremes has been suggested on the basis of the existence of small Cenozoic volcanic centers in the wider area (Marinou 1962), however without any evidence for ejected volcanic material.
The suspicion of an origin due to meteorite impact arose with the availability of a high-resolution Google earth satellite image. The lakes exhibit significant sickle-shaped halos up to 30 m high. The ages of the lakes can be assumed on their fresh morphological character as Holocene and bracketed between approximately 12 500 and 9000 to 7000 years BP; the latter age comes from remnants of an Early Neolithic settlement adjacent to the larger lake (Papathanassopoulos 1996).

During two reconnaissance investigations a considerable amount of angular to rounded pebbles were found in the sandy-silty clay of the shores as well as in the halos. No volcanic material was found.
The angular to irregular rounded yellowish to orange and partially black-coated pebbles vary from mm to approximately one decimeter in size. They are made up of: heterogeneous carbonaceous fine-breccias, more or less homogeneous carbonaceous pebbles, in few cases with fusiform and cone shapes as well as quartz, red radiolarite, and very occasionally serpentinite and meta-basalt fragments.

Textures that can be interpreted as evidence for shock-melted carbonates (e.g. in Graup 1999; review in Osinski et al. 2008):

1) *Carbonate quench textures*.
The homogeneous carbonaceous grains and pebbles display distinctive feathery (spinifex) textures of calcite. They are coarser towards the inner parts and progressively finer towards the rims. In addition, fine spinifex crystals cover the walls of "spider-type" radial and concentric cracks, which originate from the inner parts of the pebbles and are filled with euhedral calcite. Many fine spherules (< 100 µm to a few mm) are entirely filled with feathery calcite.

2) Carbonate spherules
Many fine-breccias contain numerous carbonate spherules, which occur as individual spherules and show in several cases coalescent bounding. In most cases the spherules display reaction rims and coronas of submicroscopic fine mineral assemblages. These spherules are not "secondary vesicle fillings", since they are made up of very fine-grained to cryptocrystalline carbonate with "schlieren" and spinifex textures.

3) *Planar microstructures in quartz and calcite* (e.g. in Trepmann 2008)
Small fragmental quartz grains of up to 100 µm are very abundant in the fine-breccias, homogenous carbonaceous pebbles and spherules. In all cases, they show undulate extinction and Boehm lamellae, which are results of tectonic deformation. However, in some cases "planar fractures (PFs)" are also present. Real "planar deformation features (PDFs)" have not been found.

Carbonate chemistry
Several pebbles with relatively homogeneous fine-grained and feathery calcite groundmass were analyzed with XRF method to obtain their bulk chemical composition. The major elements show a rather marly limestone composition with SiO_2 30-35 wt.%, CaO 28-32 wt.%, Al_2O_3 5-6 wt.%, K_2O 0.6-0.7 wt.%, TiO_2 0.35-0.45 wt.% and a low MgO 0.6-0.9 wt.%. The trace elements display rather low concentrations: Rb 25-35 ppm, Sr 35-65 ppm, Ba 130-400 ppm, Nb 5-6 ppm, low values of LREE; Cr 110-160 ppm, Ni 50-65 ppm and Zn 40-50 ppm. The only unusual enrichment exists in Y with 30-70 ppm. Such a composition supports an origin of the pebbles from marly limestones, but differs dramatically from the composition of carbonatitic globules from volcanic diatremes in the ultra-alkaline Province north of Rome (Stoppa & Lupini 1993).

Conclusion
The petrographic and chemical evidence of the collected fine-breccias and pebbles leads to the interpretation of the material as "impact fall back breccias and carbonatitic tectites due to meteoritic impact, although up to now no meteorite fragments have been found. According to the size of the crater lakes the dimensions of the meteorite, which might have split into two fragments, should have been about 10-30 m before reaching the surface. The temperature and pressure of the impact may have been sufficient to decompose and melt the limestones followed by quenching during cooling and decompression to form the carbonatitic pebbles and spherules.

REFERENCES
Graup, G. 1999: Carbonate-silicate liquid immiscibility upon impact melting: Ries Crater Germany. Meteoritics & Planetary Science, 34, 425-438.
Marinos, G. 1962: Sur deux volcans embryonnaires du type mare, prés d'Almyros-Thessalie. Bulletin Geological Society of Greece, 5, 1, 108-114.
Marinos, G., Anastopoulos, J., Maratos, G., Melidonis, N. & Andronopoulos, B. 1962: Geological Map of Greece 1 : 50 000, Sheet Almyros. Institute for Geology and Subsurface Research, Athen.
Osinski, G.R., Spray, J.G. & Grieve 2008: Impact melting in sedimentary target rocks: An assessment. In: Evans, K.R., Horton, J.W. Jr., King, D.T. Jr. & Morrow, J.R. eds., The Sedimentary Record of Meteorite Impacts. Geological Society of America Special Paper, 437, 1-8.
Stoppa, F. & Lupini, L. 1993: Mineralogy and petrology of the Polino Monticellite Caleiocarbonatite (Central Italy). Mineralogy and petrology, 49, 213-231.
Trepmann, C.A. 2008: Shock effects in quartz: Compression versus shear deformation – An example from the Rochechouart impact structure, France. Earth and Planetary Science Letters, 267, 322-332.

2.13

Rheological mechanisms, topographic response, and geodynamic regimes associated with slab breakoff

Duretz Thibault* & Gerya Taras*

**ETH Zürich, Institute of Geophysics, Sonnegstrasse 5, CH-8092 Zurich (thibault.duretz@erdw.ethz.ch)*

A set of numerical experiments were carried out to study the effect of slab breakoff on a subduction-collision system. The numerical code I2VIS (Gerya & Yuen, 2003) used for this purpose allows activation of plasticity, viscous creep and Peierls creep.

A two-dimensional systematic study was performed by varying the oceanic slab age and initial plate convergence rate. In this parameter space, four different end-members were observed where breakoff depth
can range from 40 to 400 km. Different combinations of rheological mechanisms lead to different breakoff modes. Activation of Peierls mechanism generally allows slabs to break faster and shallower.

Each breakoff end-member has its own topographic signal evolution and always display a sharp breakoff signal. Averaged post-breakoff uplift rates ranges between 0,8 km/My for shallow
detachment and 0,2 km/My for deep detachment in foreland and hinterland basins.

Initiation of continental crust subduction was observed when using an oceanic lithosphere older than 30 My. Different exhumation processes such as slab retreat and eduction were observed. Large post-breakoff rebound associated with plate decoupling occurs if the subducted oceanic slab is old enough.

REFERENCES
Gerya, T. V. & Yuen, D. A. 2003: Charaterictics-based marker method with conservative finite-difference schemes for modeling geological flows with strongly variable transport properties. Physics of the Earth an Planetary Interiors 140 (4), 293–318.

2.14

New structural field data from SE of the Mont Blanc massif and preliminary constraints on models of exhumation

Daniel Egli* & Neil Mancktelow*

* *Geologisches Institut, ETH-Zürich, Sonneggstrasse 5, CH-8092 Zürich (daniel.egli@erdw.ethz.ch)*

The kinematics of the exhumation of the Mont Blanc massif is still a controversial topic with various models proposed. Most information on the Neogene exhumation history of Mont Blanc comes from low-temperature thermochronology studies (e. g. Seward & Mancktelow 1994; Leloup et al. 2005; Glotzbach et al. 2008) and there is still lack of detailed structural data. This study provides new detailed information about the deformational history and the exhumation of the Mont Blanc massif and its adjacent cover. We try to estimate the importance of dextral transpressional movements during the uplift of Mont Blanc and its possible link with the Simplon-Rhone fault zone, in order to check a 2D pop-up model against a more 3D dextral transpressive model, developing a positive flower structure. We present here preliminary results of the first field season, which included detailed structural investigations and structural mapping of the south-eastern boundary of the Mont Blanc massif in the Swiss and Italian parts of Val Ferret.

The study area is situated on the south-eastern side of the Mont Blanc massif. Geologically it covers the units of the Mont Blanc massif, the Helvetic and Ultrahelvetic nappes and sediments of the lower Penninic nappes. The Mont Blanc massif is one of the external crystalline massifs, which represent the basement of the former European continental margin and therefore belongs to the Helvetic domain. It mainly consists of pre-Variscan basement and Variscan granitoids. The massif is overlain by the Mesozoic to lower Tertiary sediments of the Helvetics and Ultrahelvetics. These were overridden along the Pennine frontal thrust by sediments of the northern Penninic ocean during the Tertiary Alpine orogeny. The sediments, as well as the crystalline rocks of the Mont Blanc, suffered a polyphase metamorphic and deformational history.

We were able to distinguish 4 generations of folds in the Helvetic, Ultrahelvetic and Penninic sediments of the working area. The appearance of the folds can differ with changing lithologies, but the main characteristics remain the same. We numbered them as regional D1-D4. D1 is only visible as a penetrative cleavage, S1, with some rare relics of isoclinal fold hinges. It is folded by D2, typically forming long-limbed tight to isoclinal folds and often a spaced crenulation cleavage, S2. The S2 cleavage is the main foliation in most parts of the study area and has a relatively constant orientation dipping toward the south-east. The third deformation phase is not found everywhere in the study area. D3 folds form rather short-limbed kinky to wavy folds, often accompanied by a crenulation lineation parallel to the D3 fold axis. If D3 forms an axial plane cleavage, it is quite spaced and subvertical or dipping towards the north-west. These structures could represent a backfold-type structure. The D4 can mainly be found in the black shales between Grand Col de Ferret and Ferret village. They have a typical collapse-type appearance, with subhorizontal axial planes and very kinky hinges and locally result in a north-westward dipping main foliation.

An important aspect of the area is the regional change in orientation of the boundary between the Mont Blanc massif and the overlying sediments. In the area around the southeast portal of the Mont Blanc tunnel (i.e. near Courmayeur), the basement overlies the sediments, the overturned boundary dips ca. 45° toward the north-east, and the contact is often discordant. In the areas more to the north, the dip changes gradually to vertical and finally dips south-east. The basement seems to be thrust eastwards onto the sediments in the Courmayeur area, although no major thrust plane could be detected macroscopically. In the Swiss Val Ferret the contact is concordant and most probably sedimentary. On a mesoscopic scale, we observed that the actual contact between the basement and cover cannot be a very late stage structure because it is slightly folded with a new steep fabric developed in both the sediments and the granite. This foliation is weakly refracted across the boundary. In the slightly higher metamorphic rocks around Petit Col de Ferret, small enclaves of marble are ductiley folded into the basement rocks.

Calcite slickenfibres are quite common in the Helvetic and Ultrahelvetic sediments and have various orientations. The most dominant direction has a dextral strike-slip sense of movement and plunges shallowly toward NE or SW. In the strongly foliated black shales, the fault planes usually correspond with the main foliation whereas in the more competent limestones they make a small angle to the main foliation and generally correspond to Riedel-type faults. More rarely, one can find subvertical slickenfibres showing both thrusting toward the north-west as well as west-side-up movements. These are the only structures found whose kinematics could be directly related to exhumation of the Mont Blanc. The relative age of the different brittle movements is not yet established.

Although an eastward-directed backthrusting of Mont Blanc basement over cover sediments may have occurred, it cannot be the reason for the late Neogene uplift because the contact is subsequently ductiley deformed. A major strike-slip component is found on the eastern boundary of the massif and this movement could well represent a southward continution of the Rhone-Simplon line. However, such transpressive movements are probably not the reason for the uplift of the Mont Blanc, because the shallowly north-eastward plunging fibres showing a dextral sense would rather have a west-side-down vertical component.

REFERENCES
Glotzbach, C., Reinecker J., Danisik, M., Rahn, M., Frisch, W. & C. Spiegel 2008: Neogene exhumation history of the Mont Blanc massif, western Alps, Tectonics, 27.
Leloup, P. H., Arnaud, N., Sobel, E. R. & Lacassin R. 2005: Alpine thermal and structural evolution of the highest external crystalline massif: The Mont
Blanc, Tectonics, 24.
Seward, D & Mancktelow N. S. 1994: Neogene kinematics of the central and western Alps: Evidence from fission-track dating, Geology, 22, 803 – 806.

2.15

Reflection and scattering of Stoneley guided waves at the tips of fluid-filled fractures

Frehner Marcel* and Schmalholz Stefan M.**

* *Department for Geodynamics and Sedimentology, University of Vienna, Althanstrasse 14, 1090 Vienna, Austria (marcel.frehner@univie.ac.at)*
** *Geological Institute, ETH Zurich, Sonneggstrasse 5, 8092 Zurich, Switzerland*

Understanding seismic wave propagation in fractured fluid-rock systems is important for estimating, for example, fluid properties or fracture densities from geophysical measurements. Stoneley guided waves have been used, for example, to explain long-period volcanic tremor signals or to propose potential methods for estimating fluid properties in fractured rocks. In this study, the finite element method is used to model two-dimensional wave propagation in a rock with a finite fluid-filled fracture (Figure 1). The surrounding rock is fully elastic with non-dispersive non-attenuating P- and S-waves. The fluid filling the fracture is elastic in its bulk deformation behavior but viscous in its shear deformation behavior. Therefore, only P-waves can propagate in the fracture, which are dispersive and attenuated. The fracture geometry is resolved in detail by the applied unstructured finite element mesh using triangles.

A Stoneley guided wave is a special wave mode that is bound to and propagates along the fracture with a much smaller velocity than all other waves in the system. In this study, the wave length of the Stoneley guided wave is two orders of magnitude larger than the thickness of the fracture. Its amplitude decreases exponentially away from the fracture, which makes the Stoneley guided wave difficult to detect already a relatively short distances away from the fracture. At the tip of the fracture the Stoneley guided wave is reflected (Figure 1). The amplitude ratio $|R|$ between reflected and incident Stoneley guided wave is calculated from numerical simulations (Figure 2), which depend on the type of fluid filling the fracture (water, oil or hydrocarbon gas), the fracture geometry (elliptical or rectangular) and the presence of a small gas cap at the fracture tip. For an elliptically shaped fracture (aspect ratio of ellipse = 333) the amplitude ratio varies between 75% for oil and water and almost 100% for gas. Although the fracture thickness is two orders of magnitude smaller than the wave length, the shape of the fracture tip influences this ratio significantly. The amplitude ratio of a Stoneley guided wave at the tip of a straight water-filled fracture with a flat fracture tip is around 43%.

The part of the Stoneley guided wave that is not reflected is scattered at the fracture tip and emitted into the surrounding elastic rock as elastic body waves (Figure 1). For fully saturated fractures the radiation of these elastic body waves points in every directions from the fracture tip. In the presence of a small gas-cap at the tip of a fluid-filed fracture the radiation of the elastic body waves is strongly forward directed. The relatively strong reflection at the fracture tip enables the Stoneley guided wave to travel back and forth along a fracture several times before it looses too much of its initial energy. This leads to a periodic radiation of body waves at the fracture tip. The corresponding frequency can be low in relatively small fractures due to the small velocity of Stoneley guided waves. The emitted elastic body waves may allow detecting Stoneley guided wave-related signals at distances away from the fracture where the amplitude of the Stoneley guided wave itself is too small to be detected.

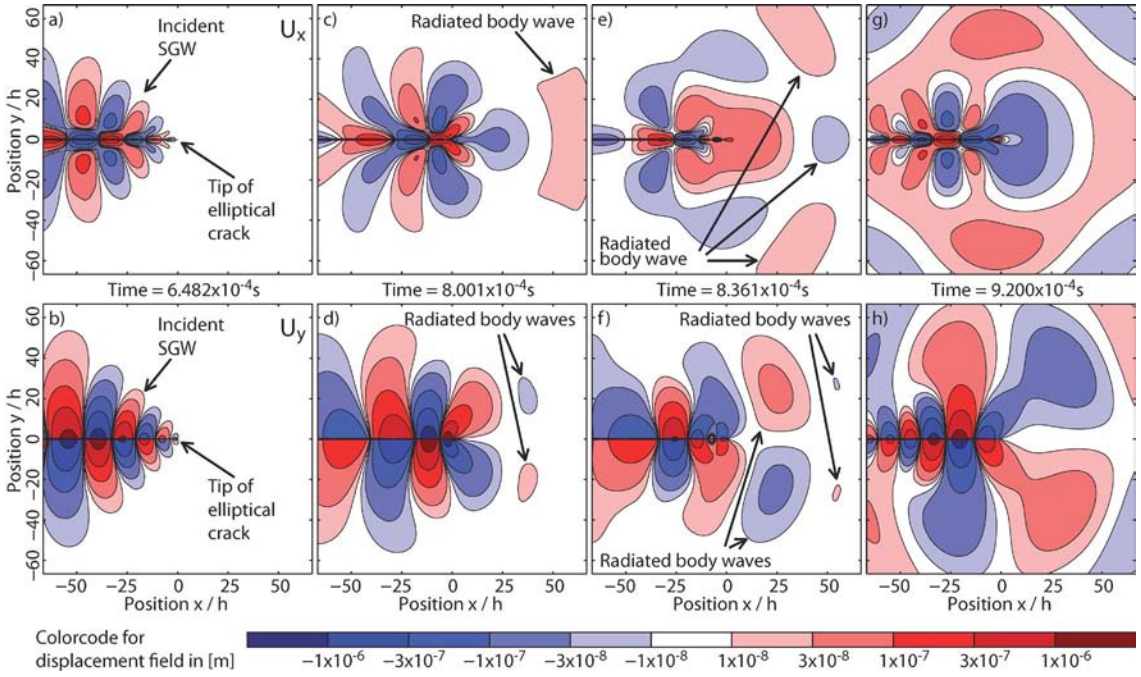

Figure 1: Snapshots of the 2D displacement field of a simulation of a Stoneley guided wave propagating along an elliptical crack filled with water. Upper panels show the horizontal component of the displacement field. Lower panels show the vertical component of the displacement field. Panels from left to right represent progressive points in time. The Stoneley guided wave is partially reflected at the crack tip and elastic P- and S-waves are emitted from the crack tip into the surrounding rock.

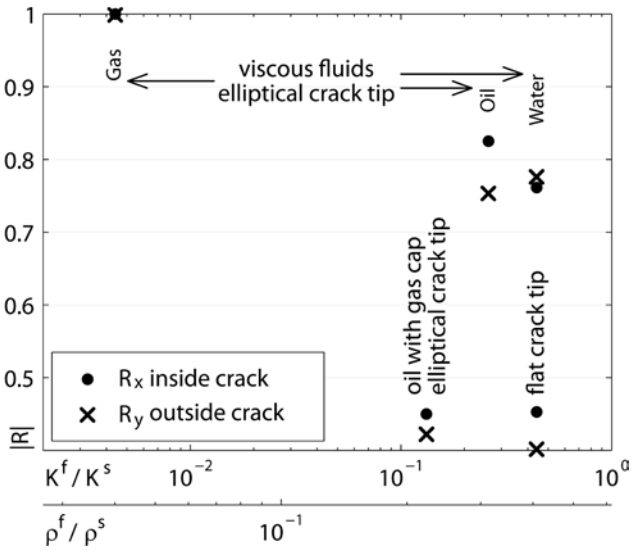

Figure 2: Absolute value of the amplitude ratio |R| between reflected and incident Stoneley guided wave of a Stoneley guided wave that is reflected at the tip of a crack. Rx is calculated from the horizontal displacement-time signals at eight receivers inside the crack. Ry is calculated from the vertical displacement-time signals at six receivers outside the crack. Values labeled “viscous fluids, elliptical crack tip” are derived from simulations of an elliptical crack fully saturated with the corresponding viscous fluid. Values labeled “flat crack tip” are derived from a simulation of a rectangular crack with a flat crack tip fully saturated with viscous water. Values labeled “oil with gas cap, elliptical crack tip” are derived from a simulation of an elliptical crack partially saturated with viscous oil and having a small gas cap at the crack tip.

2.16

Exhumation of a metamorphic complex in a strike-slip setting: observations from the Chugach Metamorphic Complex (CMC), southern Alaska

Deta Gasser*, Emilie Bruand*, Kurt Stüwe*

*Department of Earth Science, Universitätsplatz 2, A-8010 Graz, Austria
(deta.gasser@uni-graz.at

The exhumation of metamorphic rocks to the surface of the Earth is a much discussed subject in modern geodynamics. Models involving channel flow, pure and simple shear extrusion and others have been postulated based on observations in the Central Himalayan Crystalline Complex or the eclogite complexes in the Alps. Most of these models focus on the vertical component in profile view, not considering horizontal movements in plan view.

The CMC of Southern Alaska consists of low-P high-T gneisses that developed during the Eocene in a Cretaceous accretionary prism. They are exhumed from 20-35 km depth between major crustal-scale dextral shear zones (Fig. 1). Lineations are typically parallel to strike and sub-horizontal, indicating that horizontal movement in plan view is a vital part of the exhumation process. In addition, the complex has a particular triangular shape in plan view, indicating that the exhumation history might not be the same all along the complex but might be different in parts of different width of the complex.

In order to understand the nature of the low-P high-T metamorphism in a accretionary setting and its subsequent exhumation history we are currently working on a project combining extended field work, petrological, structural and geochronological methods. During the summers 2008 and 2009 we mapped six key areas covering the whole complex from north to south and from east to west in order to understand the structural and petrological variations all over the complex. We furthermore calculated detailed pressure and temperature conditions that occurred during metamorphism in the different parts of the complex. In order to better understand the timing and the rates at which heating, cooling and exhumation occurred, we apply several geochronological methods such as U-Pb dating of monazites and zircons, ArAr and RbSr dating of biotite and muscovite and zircon fission track dating to rocks from different parts of the complex.

In this contribution we present an overview of the geology of the CMC, results from our field work as well as first geochronological results.

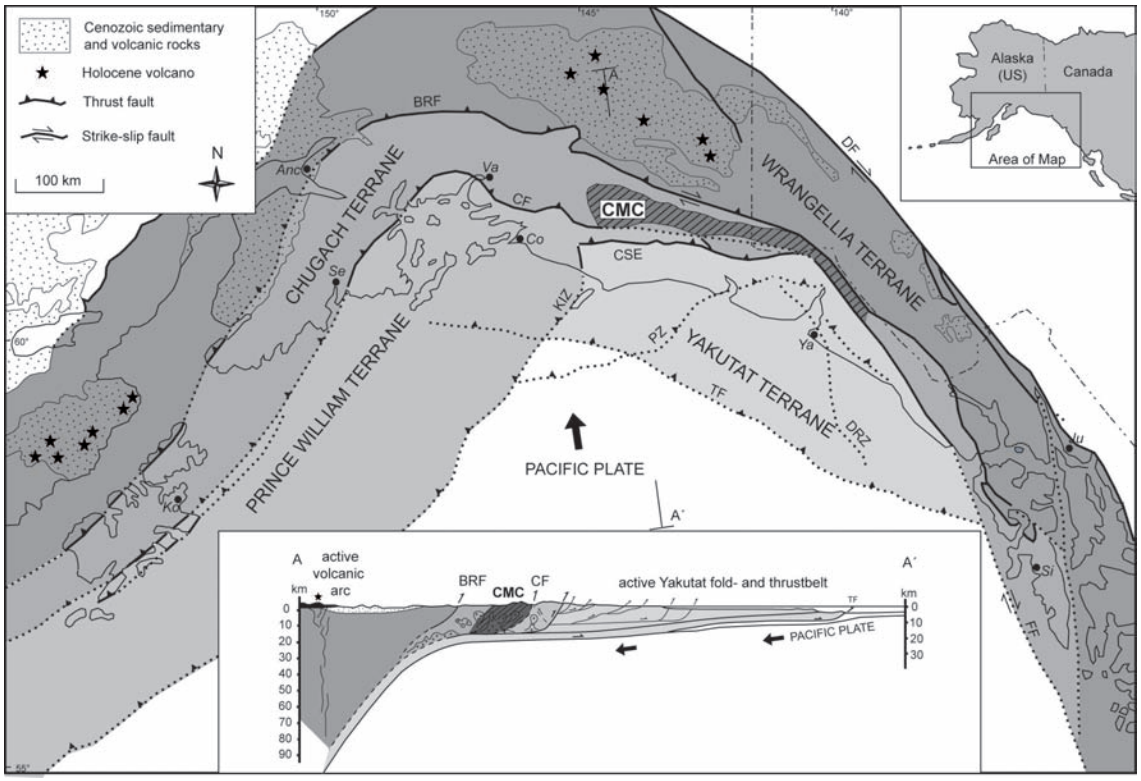

Fig. 1 Tectonic overview map and cross-section of southern Alaska. Abbreviations: CMC Chugach Metamorphic Complex,g TF transition fault, PZ Pamplona zone, KIZ Kayak Island Zone, DRZ Dangerous River Zone, CSE Chugach St Elias Fault, CF Contact Fault, FF Fairweather Fault, BRF Border Ranges Fault, DF Denali Fault.

2.17

The Rezli fault zone: Field observations from a major oblique-slip fault in the Rawil depression, Western Switzerland

Deta Gasser*, Neil Mancktelow**

*Department of Earth Science, Universitätsplatz 2, A-8010 Graz, Austria
(deta.gasser@uni-graz.at)
***Geological Institute, ETH Zürich, CH-8092 Zürich, Switzerland (neil.mancktelow@erdw.ethz.ch)*

In Western Switzerland, the plunge of fold axes and the regional distribution of units in the Helvetic nappes define a broad depression, the Rawil depression, between the crystalline rocks of the Aiguilles Rouge massif to the SW and the Aar massif to the NE. The southern part of this depression, together with the Rhone Valley to the south, belongs to one of the seismically most active regions in Switzerland. Seismogenic faults interpreted from earthquake focal mechanisms strike ENE-WSW to WNW-ESE, with dominant dextral strike-slip and minor normal components and epicentres at depths of < 15 km. In order to understand the post-nappe-stacking, brittle faulting history of this area, we compiled fault data from the literature and existing maps and conducted detailed field work on one exceptionally well-exposed fault zone, the Rezli fault zone (RFZ).

The compilation of data from the literature establishes that, in addition to thrusts related to nappe stacking, the Rawil depression is cross-cut by four sets of brittle faults: (1) SW-NE striking normal faults that strike parallel to the regional fold axis trend, (2) NW-SE striking normal faults and joints that strike perpendicular to the regional fold axis trend, and (3) WNW-ESE striking normal plus dextral oblique-slip faults as well as (4) WSW-ENE striking normal plus dextral oblique-slip faults that both strike oblique to the regional fold axis trend.
Fault set 1 was probably initiated during sedimentation and reactivated during nappe folding and stacking, whereas the other fault sets formed *after* emplacement of the Helvetic nappes.

The RFZ belongs to fault set 3 and is a shallow to moderately-dipping (ca. 30-60°) fault zone with an oblique-slip displacement vector, combining both dextral and normal components. It must have formed in approximately this orientation, because the local orientation of fold axes corresponds to the regional one, as does the generally vertical orientation of extensional joints and veins associated with the regional fault set 2. The fault zone has a maximum horizontal dextral offset component of ca. 300 m and a maximum vertical normal offset component of ca. 200 m.

The fault zone crosscuts four different lithologies: (1) limestone, (2) intercalated marl and limestone, (3) marl and (4) sandstone, and its internal architecture strongly depends on the lithology in which it developed. In the limestone, it consists of veins, stylolites, cataclasites and cemented gouge, in the intercalated marls and limestones of anastomosing shear zones, brittle fractures, veins and folds. In the marls it consists of anastomosing shear zones, pressure solution seams and veins and in the sandstones of coarse breccia and veins. Later, straight, sharp fault planes cross-cut all these features. In all lithologies, common veins and calcite-cemented fault rocks indicate the strong involvement of fluids during faulting.

All three Neogene fault sets (2-4) could have been active under the actual stress field inferred from the current seismicity. This implies that the same mechanisms that formed these fault zones in the past may still persist at depth. The detailed observations from the Rezli fault zone can act as a model for processes still occurring at deeper levels in this seismically active region.

2.18

Influence of rheology and giant impactors on the terrestrial core formation

Golabek Gregor*, Gerya Taras*, Kaus Boris*, Ziethe Ruth**, Moll Gian-Peider*** & Tackley Paul*

**Institut für Geophysik, Sonneggstrasse 5, CH-8092 Zürich (gregor.golabek@erdw.ethz.ch)*
***ESA/ESTEC-SCI-SM, Keplerlaan 1, NL-2201 AZ Noordwijk*
****Institut für Computerwissenschaften, Universitätsstrasse 6, CH-8092 Zürich.*

Knowledge about the terrestrial core formation mechanism is still very limited. Several core formation modes have been proposed: The fracturing mode suggests that a central unmelted region is displaced by a degree one mode from the center

of the accreting body and is fragmented due to the large stresses created by an overlying asymmetric iron layer (Stevenson, 1981). In contrast, core formation via iron diapirs (e.g. Ziethe and Spohn, 2007), which can be formed by giant impacts (e.g. Ricard et al, 2009), have been proposed. We investigate which core formation mode is active under certain conditions.
Therefore we perform 2D simulations using the code I2ELVIS applying the newly developed "spherical-Cartesian" methodology (Gerya and Yuen, 2007). It combines finite differences on a fully staggered rectangular Eulerian grid and Lagrangian marker-in-cell technique for solving momentum, continuity and temperature equations as well as the Poisson equation for gravity potential in a self-gravitating planetary body. In the model, the planetary body is surrounded by a low viscosity massless fluid ("sticky air") to simulate a free surface. We apply a temperature- and stress-dependent viscoplastic rheology inside Mars- to Earth-sized bodies and include heat release due to radioactive decay, shear and adiabatic heating. As initial condition we use stochastically distributed iron diapirs with random sizes in the range of 50 to 100 km radius inside the accreting planet, representing the iron delivered by pre-differentiated impactors.
Additionally, we add a giant impactor core into several models. For simplicity, we neglect the heating of the planetary body by the impact itself. We assume the impactor core to be at rest at the beginning of the simulation.
A systematic investigation of the influence of silicate rheology, temperature and diapir radii on different-sized protoplanets is being performed. We show that depending on the silicate rheology, which is strongly dependent on the water content of olivine (Katayama and Karato, 2008) and the initial temperature profile, plastic yielding and shear localization take place and different regimes of core formation appear: For weak planetary interiors iron diapirs sink in collective groups, similar to already published core formation models (e.g. Ziethe and Spohn, 2007). For highly viscous planets an asymmetric iron layer forms, which surrounds the central part of the planet or a mixture of diapirism and fracturing mechanism develops. Results including large diapirs indicate that for Mars-sized and larger bodies a runaway differentiation process can be induced. We derive scaling laws, which predict the onset of plastic yielding and shear localization in the silicates and of the runaway differentiation process and the associated core formation modes. The final temperature profiles of the different core formation modes are discussed with regard to their influence on the onset of mantle convection.

REFERENCES

Gerya, T.V. & Yuen, D.A. 2007: Robust characteristics method for modelling multiphase visco-elasto-plastic thermo-mechanical problems. Phys. Earth Planet Int., 163, 83-105.

Katayama, I. & Karato, S.-i., 2008: Low-temperature, high-stress deformation of olivine under water-saturated conditions. Phys. Earth Planet. Int., 168, 125–133.

Ricard, Y., Šrámek, O. & Dubuffet, F. 2009: A multiphase model of runaway core-mantle segregation in planetary embryos. Earth Planet. Sci. Lett., 284, 144-150.

Stevenson, D.J. 1981: Models of the Earth's core. Science, 214, 611-619.

Ziethe, R. & Spohn, T. 2007: Two-dimensional stokes flow around a heated cylinder: A possible application for diapirs in the mantle. J. Geophys. Res., 112, B09403.

2.19

Towards self-consistent modelling of the Martian dichotomy: Coupled models of simultaneous core and crust formation

Golabek Gregor*, Keller Tobias*, Gerya Taras* & Connolly James**

*Institut für Geophysik, Sonneggstrasse 5, CH-8092 Zürich (gregor.golabek@erdw.ethz.ch)
**Institut für Mineralogie und Petrologie, Clausiusstrasse 25, CH-8092 Zürich

One of the most striking surface features on Mars is the crustal dichotomy, a large difference in elevation and crustal thickness between the southern highlands and the northern lowlands. The dichotomy is among the oldest geological features on Mars and was formed more than 4.1 Ga ago (Solomon et al., 2005) owing to either exogenic or endogenic processes (e.g. Keller and Tackley, 2009). In order to find an internal origin of the crustal dichotomy, located within a maximum of 400 Ma of planetary differentiation, the thermal state of the planet resulting from core formation needs to be considered. Based on the geochemical analysis of SNC meteorites it was suggested that a primordial crust with up to 45 km thickness can be formed already during the Martian core formation (Norman, 1999). Therefore we suggest that the sinking of iron diapirs delivered by pre-differentiated impactors induced shear heating-related temperature anomalies in the mantle, which fostered the formation of early Martian crust. In this study, we examine parameter sets that will likely cause an onset of hemispherical low-degree mantle convection directly after, and coupled to, an already hemispherically asymmetrical core formation. To test this hypothesis we use a numerical model, where we self-consistently couple the formation of the Martian iron

core to the onset of mantle convection. Peridotite melting is enabled to track melting and crust formation caused by heat released from core formation and radioactive heating.
We perform 2D simulations using the code I2ELVIS applying the recently developed "spherical-Cartesian" methodology (Gerya and Yuen, 2007). It combines finite differences on a fully staggered rectangular Eulerian grid with
Lagrangian marker-in-cell technique to solve momentum, continuity and temperature equations as well as the Poisson equation for gravity potential in a self-gravitating planetary body. In our model setup, the planet is surrounded by a low viscosity, massless fluid ("sticky air") to simulate a free surface. We apply a temperature- and stress-dependent viscoplastic rheology inside a Mars-sized planet. Radioactive and shear-heating as well as consumption of latent heat by silicate melting are taken into account. The depth of neutral buoyancy of silicate melt with respect to solid silicates is determined by the difference in compressibility of the liquid and solid phase. To self-consistently simulate the silicate phase changes expected inside a Mars-sized body, we employ the thermodynamical Perple_X database (Connolly, 2005). As initial condition, we apply randomly distributed iron diapirs with 75 km radius inside the planet, representing the cores of stochastically distributed impactors characteristic for the late accretion stage of terrestrial planets. Additionally, we explore the effect of one giant impactor core on the planetary evolution.
Results indicate that the presence of a large impactor core induces hemispherically asymmetrical core formation. Furthermore, the amplitude of shear heating anomalies generally well exceeds the solidus of primitive mantle
material. The formation of a considerable amount of silicate melt is observed. Some of the generated melt segregates to the surface to form primordial crust, whereas negatively buoyant melt from deeper sources sinks to the CMB. The hemispherical asymmetry in temperature induced by a giant impactor works in favour of an onset of low-degree mantle convection after core formation. Such a hemispherical convection geometry might subsequently be sustained by phase-dependent viscosity (Keller and Tackley, 2009), and thus harbour an early development of a dichotomous crustal thickness distribution.

REFERENCES

Connolly, J.A.D. 2005: Computation of phase equilibria by linear programming: A tool for geodynamic modeling and its application to subduction zone decarbonation. Earth Planet. Sci. Lett., 236, 524– 541.

Gerya, T.V. & Yuen, D.A. 2007: Robust characteristics method for modelling multiphase visco-elasto-plastic thermo-mechanical problems. Phys. Earth Planet Int., 163, 83-105.

Keller, T. & Tackley, P.J. 2009: Towards self-consistent modelling of the Martian dichotomy: The influence of one-ridge convection on crustal thickness distribution. Icarus, 202, 429–443.

Norman, M.D. 1999: The composition and thickness of the crust of Mars estimated from rare Earth elements and neodymium-isotopic compositions of Martian meteorites. Meteorit. Planet. Sci., 34, 439–449.

Solomon S.C., Aharonson, O., Aurnou J.M., Banerdt W.B., Carr M.H., et al. 2005 : New perspectives on ancient Mars. Science, 307,1214–20.

2.20

Integrated U/Pb, (U-Th)/He and oxygen stable isotope study on zircon of a normal fault zone of the western Alps, Switzerland

I. Guerra*, D. Stockli**, F. Corfu***, F. Negro****, N. Mancktelow***** and T. Vennemann*

*Institut de Minéralogie et Géochimie, Université de Lausanne, Anthropole, CH-1015 Lausanne, Switzerland (ivan.guerra@unil.ch)
**Department of Geology, University of Kansas, 1475 Jayhawk Boulevard, Lawrence KS 66045-7613, USA
***Department of Geosciences, University of Oslo, Sem Sælands vei 1 Blindern, 0316 Oslo, Norway
****Centre d'Hydrogéologie et Géothermie, Université de Neuchâtel, Emile-Argand 11, CH-2009 Neuchâtel, Switzerland
*****Geologisches Institut, ETH Zürich, Sonneggstrasse 5, CH-8092 Zürich, Switzerland

Small, euhedral zircons (up to 80 μm in length) were found in late hematite- and quartz-rich veins of the Arolla area (western Alps, Switzerland), crosscutting two different types of Alpine units: the Dent Blanche Klippe and the Tsaté Nappe. These zircons – together with zircons in the relative host rocks – have been investigated for their U/Pb, (U-Th)/He, and oxygen isotope compositions in order to determine the thermal history of this portion of the Alps via the cooling path of these minerals.

U/Pb analysis indicates that the zircons – both in the late veins and in the host rock - have absolute radiometric ages clustering around 270 - 280 Ma, which is the accepted age for intrusive rocks from the Austroalpine Dent Blanche units but which is in apparent contrast with the interpretation of the Tsaté Nappe as an ophiolitic remnant of the Jurassic Liguro-Piemontais Ocean. The other conclusion of these U/Pb analyses is that the zircons in the late veins are all inherited from the host rock.

The same samples were investigated with the (U-Th)/He method. First results indicate that the cooling ages for the host rocks are different compared to the cooling ages for the zircons in late veins: in particular the calculated cooling age for the Arolla gneiss is 25.5 ± 2.0 Ma, while the cooling age for the associated mineralized fault plane is 17.7 ± 1.4 Ma. The cooling ages for the Tsaté metagabbro cluster around 30 Ma with one important exception at 311.8 ± 36.9 Ma that needs to be further investigated.

Oxygen stable isotope fractionations between quartz and hematite in the same late veins correspond to temperatures of about 170°C. The proximity of the calculated emplacement temperature for late veins and the lower accepted closure temperature for zircon in the (U-Th)/He system (~180°C, Reiners et al., 2004) imply that the age of 17.7 ± 1.4 Ma can be interpreted as the formation age of this late brittle fracture.

Further analyses on the two units are in progress and focus on two main directions: 1) analysis of other mineralized normal fault planes to compare their cooling age with the cooling age of their respective host rock, and 2) cooling age determinations on the host rocks to better understand the regional thermal path of this portion of the Alps, which is so far poorly understood.

REFERENCES

Reiners, P. W., Spell, t. L., Nicolescu, S. and Zanetti, K. A. (2004): Zircon (U-Th)/He thermochronometry: He diffusion and comparisons with $^{40}Ar/^{39}Ar$ dating. Geochim. Cosmochim. Acta 68, 1857-1887.

2.21

Quaternary fluvial patterns on the in-land Makran accretionary wedge (SE IRAN)

Haghipour Negar*,**, Burg Jean-Pierre*, Kober Florian* & Zeilinger Gerold ***

Geological Institute, ETH Zurich, Sonneggstrasse 5, CH-8092 Zurich (negar.haghipour@erdw.ethz.ch)
**Geological Survey of Iran, Meraj Avenue, Azadi Square, P.O. Box 13185-1494,Tehran, Iran*
***Institute für Geowissenschaften, Universität Postdam, D-14476 Golm, Deutschland*

We document the five most important drainage basins of the Iranian Makran and their fluvial terraces to investigate the surface record of the on-going Makran subduction zone. We compare stream profiles extracted from 30m resolution DEM-Aster images using a slope-area model for the main channel of each catchment.
The five studied rivers are transverse and flow from the northern crest line of the accretionary wedge to the coastal plain, in the south. The stream-profiles show a convex-up pattern that suggests disequilibrium in the western and eastern parts of the subduction zone, in Iran; this is in contrast with the central part, where one river has the concave-up profile expected from an equilibrium state. The knick-zones along all river profiles coincide with major faults and folds rather than lithological changes. The results from slope-area data, steepness index (Ks) and concavity index ( ) suggest a spatially variable surface uplift. The southward divergence of the projected strath terraces of 2 of these rivers further indicates differential bedrock uplift in the south compared to the more homogeneous northern inner Makran.
Field mapping of the fluvial terraces, complemented by information from aerial photos, topographic maps and height correlation, reveals 5 regional terrace levels.
Temporal correlation of these five levels, using terrestrial cosmogenic nuclides (TCN) dating method, is in progress. This time information will constrain the
reconstruction of the paleo- valleys of the studied rivers and will provide a frame for precise estimates of the surface uplift rate, incision rate and the tectonic significance of vertical surface movements on accretionary wedges.

2.22

Strain localization in quartz mylonites of the Simplon Fault, Central Alps

Härtel Mike*& Herwegh Marco*

Institut for Geoscience, University of Bern, Baltzerstrasse 1+3

The Simplon Fault zone (SFZ) is a major detachment fault between the Upper and Lower Penninic Units in the Central Alps and comprises mylonitic microstructures deformed under the presence of water (Mancktelow & Pennacchioni 2004 and references therein) at metamorphic conditions ranging from lower greenschist facies (N) to upper amphibolite facies conditions in a water rich environment (S). In order to study strain localization history in this large-scale structure, different sample series were collected along profiles across the Simplon fault to investigate the changes in dynamic recrystallization mechanisms, coupling of quartz grain size, presence of second phases and crystallographic preferred orientation (CPO). In the case of pure quartz mylonites (former qtz veins and qtz lenses), ribbon grains occur within a 900 meter wide high strain zone. The recrystallized grain size in this fault zone generally is reduced compared to the undeformed veins, but the degree of grain size reduction varies strongly. In terms of dynamic recrystallization, the smallest grain sizes correlate with bulging recrystallization and subgrain rotation recrystallization. However, also combinations of grain boundary migration recrystallization either with bulging nucleation or subgrain rotation occur. In such microfabrics, the mean recrystallized grain size is relatively large. Interestingly, these grain size changes are not systematically as a function of distance to the fault contact but rather occur in form of different domains. In terms of CPO, a strengthening is observed towards the contact except at the contact itself, were the occurrence of cataclasites induced a CPO weakening. Based on these observations, and previous studies of Hirth & Tullis (1992) and Stipp et al. (2002), we suggest that the observed changes in grain size and recrystallization mechanism are related to a cooling-induced strain localization during progressive deformation. The fact that high temperature microstructures are juxtaposed to low temperature microstructures indicates an overprint of the old high-temperature deformation history under lower temperature conditions. Interestingly, this later strain localization did not result in a symmetric strain localization pattern in the large-scale shear zone but rather shows local variations, eventually pointing to episodic changes in the spatial distribution of deformation during the evolution of the Simplon fault.

REFERENCES

Hirth, G. and Tullis, J., 1992: Dislocation creep regimes in quartz aggregates. J. Struct. Geol., 14(2): 145-159.

Mancktelow, N.S. and Pennacchioni, G., 2004: The influence of grain boundary fluids on the microstructure of quartz-feldspar mylonites. Journal of Structural Geology, 26(1): 47-69.

Stipp, M., Stünitz, H., Heilbronner, R. and Schmid, S.M., 2002: Dynamic recrystallization of quartz: correlation between natural and experimental conditions. In: S. de Meer, M.R. Drury, J.H.P. de Bresser and G.M. Pennock (Editors), Deformation Mechanisms, Rheology and Tectonics: Current Status and Future Perspectives. Special Publications. Geological Society, London, pp. 171-190.

2.23

Petrography and geochemistry of upper mantle and lower crust of supra-subduction (?) ophiolites in the Makran, SE Iran

Hunziker Daniela*, Burg Jean-Pierre*, Bouilhol Pierre**, Jafar Omrani***

Geological Institute, Structural Geology and Tectonics, ETH Zurich, Sonneggstrasse 5, NO E69, CH-8092 Zurich (daniela.hunziker@erdw.ethz.ch)
**Department of Earth, Atmospheric and Planetary Science, Massachusetts Institute of Technology, 77 Massachusetts Avenue Cambridge, MA02139, USA*
***Geological Survey of Iran, Meraj Avenue, Azadi Square, P.O.Box 13185-1494, Tehran, Iran*

Ophiolites archive tectonic and chemical processes in oceanic lithosphere from its crystallization to accretionary stages during obduction and/or continental collision. The origin of ophiolites is subject to discuss since they can evolve in various geotectonic settings whose discrimination is challenging.

Despite excellent outcrop conditions and exposure of a complete sequence, the Remeshk/Mokhtaramabad and Fannuj/Maskutan ophiolitic complexes in the Southeast Iranian Makran area have been very scarcely surveyed. These ophiolites are situated along the northern boundary of the inner Makran accretionary wedge, above the active subduction of the Arabian plate beneath the Eurasia. We present first results on structures, petrography, geochemistry and geochronology of these ophiolites. The ultimate goal is to reconstruct their original geotectonic setting, the magmatic processes that produced them and the tectonic evolution of the area.

Temporal and structural relations between the different lithologies have been established and detailed cross sections illustrate our preliminary map, much more precise than previous ones. The extensive ultramafic complexes comprise a lower, harzburgite-dominated unit with few lherzolites overlain by dunites. Pyroxene-bearing peridotites show typical features of tectonized mantle deformed at sub-solidus conditions. The olivine chemistry (xMg = 0.90-0.91, NiO content of 0.4-0.45wt%) indicates that they represent ophiolitic upper mantle. Most dunites are characterized by cumulate textures in olivine and a slightly lower xMg = 0.88-0.89 and NiO content of 0.27-0.35wt%. Dunites are locally impregnated by plagioclase-rich melts with minor amounts of clinopyroxene and intruded by many gabbroic dykes, which mark the transition zone between mantle and crust.
The gabbroic sequence above the dunites displays increasingly differentiated rocks originated from the same magma source, upward in the following order: troctolite - olivine gabbro – gabbro - anorthositic dykes - diabase. These rocks are later intruded by plagiogranites and hornblende-gabbros whose association with the ophiolites is not clarified. Bulk rock and mineral compositions show oceanic features of a fast spreading MOR, but some indicate crystallization in a supra-subduction realm. Trace element analyses and geochronology will constrain the evolution of the Makran ophiolites.

2.24

Brittle deformation bands in the sandstones of the Western Swiss Molasse Basin

Ibele, Tobias*, Matzenauer, Eva*, Mosar, Jon*

*Département de Géosciences Université de Fribourg, Chemin du Musée 6, CH-1700 Fribourg (tobias.ibele@unifr.ch)

Brittle deformation in porous sandstone was described to take place as cataclasis on a grain size scale, forming deformation bands (DB) (Aydin 1978). These brittle deformation bands typically are a few mm wide zones of reduced porosity as a result of reduced grain sizes by fracturing. The denser packing of the angular subgrains leads to strain hardening and subsequently ongoing deformation creates new DBs sub-parallel to the initial ones. Increasing strain is compensated by several anastamosing DBs forming deformation band shear zones (DBSZ) which are up to several tens of centimetres wide and often end up with a discrete slip surface (Aydin & Johnson 1978). The process of forming brittle DBs was described to take place in porous sandstones of the upper few km of the crust as well as in unconsolidated clastic sediments near the surface (Cashman & Cashman 2000).

In our study DBs turned out to be a prominent tectonic structure in the Western Swiss Molasse basin that together with slickensides in fault zones take up a considerable amount of deformation. Although they are hitherto undescribed from the area, they are abundant in the sandstones of the Lower Freshwater and Upper Marine Molasse (USM and OMM). During structural fieldwork we frequently found single DBs, large DBSZs with and without slip-planes and networks of DBSZs that intersect and offset each other indicating successive events.
Investigation of thin sections showed typical zones of fractured grains as well as very fine fault gauges with a poorly evolved foliation. Some of the DBs are found to be cemented by calcite but most of them are formed by unconsolidated fault gauges, which is suggestive to a relative low depth and/or recent time of their formation. In one case a synkinematicley grown white mica associated with a SC structure was found to fill the core of a DB, pointing towards special conditions during deformation including fluids and probably a certain burial depth. Furthermore such white mica offers the opportunity of quantitative dating but feasibility is still unclear in our case.

Within networks of DBSZ some of the crosscutting relationships are systematic with respect to orientation but are not systematic with respective chronology to time sequence, indicating a contemporaneous evolution as Riedel systems. The orientation and kinematics of the mapped DBs correlates well with the ones elaborated from slickensides in the study area as they are right-lateral when striking WNW-ESE and left-lateral when striking N-S. They deform in a strike slip regime with NW-SE compression that started in the upper Miocene and persists until recent times.

REFERENCES

Aydin, A. 1978: Small faults formed as deformation bands in sandstone, Pure and Applied Geophysics 116, 913-930.
Aydin, A. & Johnson, A.M. 1978: Development of faults as zones of deformation bands and as slip surfaces in sandstone, Pure and Applied Geophysics 116, 931-942.
Cashman, S. & Cashman, K. 2000: Cataclasis and deformation-band formation in unconsolidated marine terrace sand, Humboldt County, California, Geology 28, 2, 111-114.

2.25

Lateral fold identification in Northern Tunisia Thrust Belt front

*Aridhi Kais, **Mohamed Abdoullah Ould Bagga, *Saâdi Abdeljaouad, *Fouad Zargouni and ***Eric Mercier

*Faculty of Sciences of Tunisia, Department of Geology, 2092 Tunis-El Manar I -Tunisia (Aridhikais@Gmail.com).
** Faculty of Sciences of Gabès, Department of earth sciences, City Riadh Zrig-1030 - Gabès -Tunisia.
*** Science and Technical Faculty of Nantes - France.

Tectonic transport of sedimentary sequences led to their deformation in fault-related-folds known in the tectonic style as "ramp folds". Some of these folds called frontal ramp folds, strike transversally to the thrust transport, whereas the lateral folds, develop parallel to this direction. However, the presence of fold axis oriented at a high angle with respect to the transport direction may reflect various deformation kinematics and mechanisms, as highlighted by Wilkerson et al. (2002) and Frizon de Lamotte et al., (1995).

In the Tunisian thrust and fold belt, (fig.1) the fault related folds were recognized only in a recent date, Oueld Bagga et al., (2006). And the fold structures were all interpreted as frontal folds. In this work we will evidence by mean of two field examples, the presence of lateral folds and we will discuss the geometrical features suggesting their formation kinematics. The first example is ilustrated by the Aïn el Bey structure, which belong to the external edge of the northern Tunisian belt; the second example concerns a local structure in the Numidian thrust sheet (fig.2-3).

In this setting, we will show that these fold orientations with respect to the transport direction, their limb dip variation, the thrust fault migration, the existence of bed cut-off as well as sedimentary criteria, suggest all that these folds are related to pre-existing synsedimentary faults that were reactivated during the tectonic inversion as lateral ramp faults.

We will as well show that the previous structural and sedimentary data are not suitable with lateral fold formation as a consequence of superimposed tectonic strain, or a drug along strike faults or a decrease of the slip magnitude along the frontal faults.

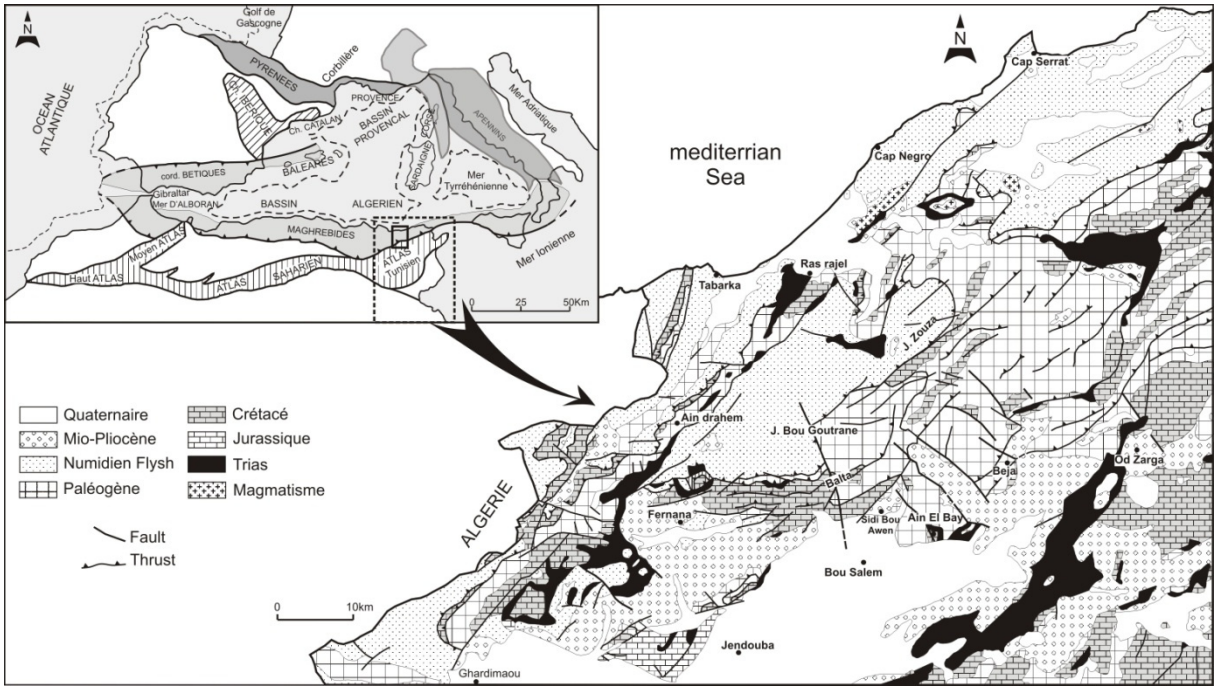

Fig.1: Alpine geology belt (Durand DELGA, 1980) and area of study localization (extracted to geological map of Tunisia 1/500000), modified

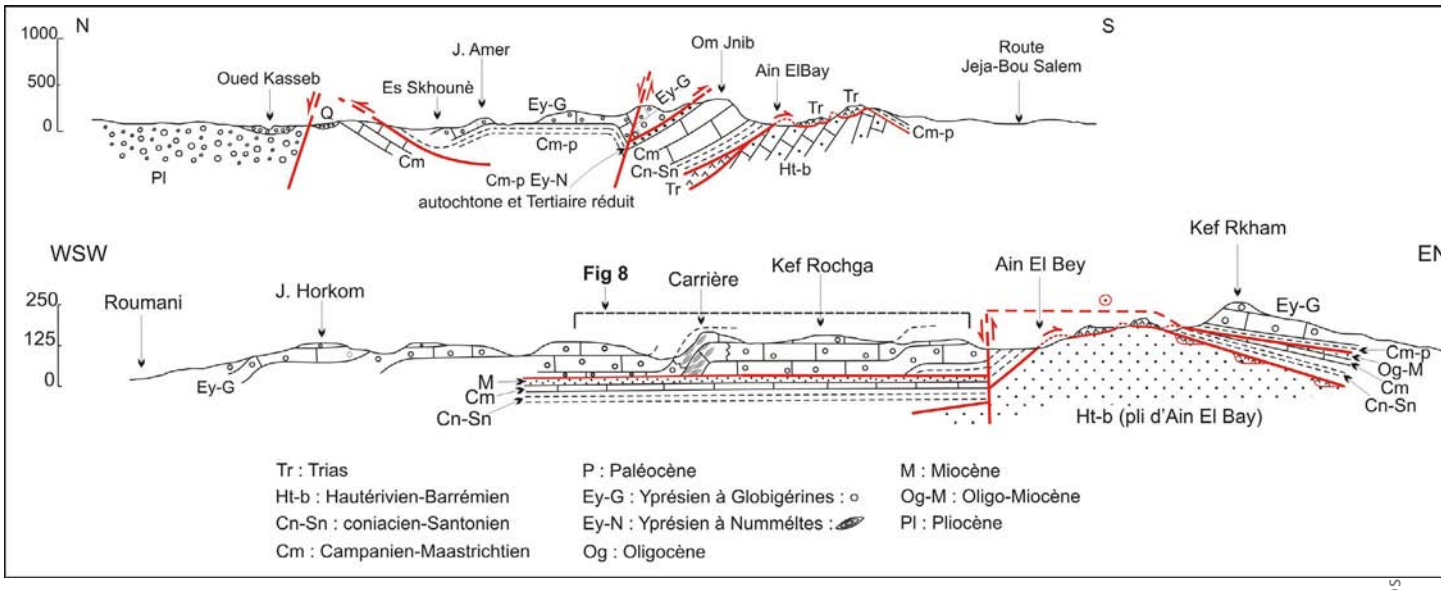

Fig.2: transverse and longitudinal Section on the level of Ain El Bey struc-

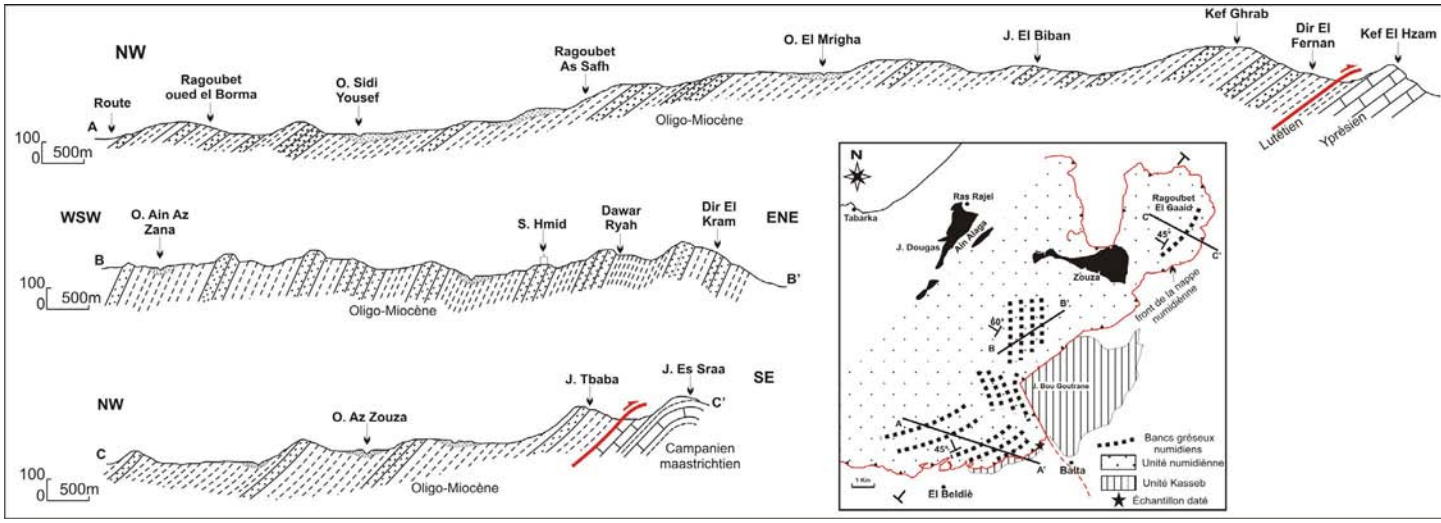

Fig.3: sections in the Numidian thrust sheet

REFERENCE

M. Scott Wilkerson, Ted Apotria and Tammer Farid, (2002): Interpreting the geologic map expression of contractional fault related fold terminations: lateral/oblique ramps versus displacement gradients. Journal of structural geology, 2002, vol. 24, no4, pp. 593-607.

Frizon de Lamotte and JEAN-CLAUDE GUEZOU, (1995): Distinguishing lateral folds in thrust-systems; examples from Corbihres (SW France) and Betic Cordilleras (SE Spain). Journal of Structural Geology, 1995, Vol. 17, No. 2, pp. 233 to 244.

Mohamed Abdoullah Ould Bagga, Saâdi Abdeljaouad and Eric Mercier, (2006): La « zone des nappes » de Tunisie : une marge méso-cénozoïque en blocs basculés modérément inversée (région de Taberka/Jendouba ; Tunisie nord-occidentale), Bulletin de la Société Géologique de France; May 2006; v. 177; no. 3; p. 145-154.

2.26

Insights in the dynamics of free subduction from semi-analytical and numerical models.

Kaus Boris J.P.*,**, Becker, Thorsten W.

*Geophysical Fluid Dynamics, Department of Earth Sciences, Schaffmattstrasse 30, CH-8093 Zurich (boris.kaus@erdw.ethz.ch)
**University of Southern California, Los Angeles, USA.

Subduction zone dynamics has been extensively studied with laboratory models in which a dense, high viscosity slab sinks into a less dense and less viscous mantle.

Recently, it was found that these laboratory results could be reproduced with numerical models if the upper boundary condition is a true free surface, or if a weak 'sticky-air' layer is employed [Schmeling et al, 2008].

Yet, our insight in the dynamics of subduction remains somewhat limited and no scaling law exists that *predicts* slab velocity (or slab behavior) as a function of slab thickness, slab/mantle viscosity ratio and slab/mantle density difference. Existing scaling laws, such as the approach of Conrad and Hager [1999, JGR], rely on knowing the radius of curvature of subducting slabs, which is a parameter that is typically known only *after* an experiment has been performed.

For this reason, we here perform additional 2D numerical simulations in which we address the effects of numerics (resolution, time step), initial geometry (slab tip length and angle), and rheology on subduction dynamics in the presence of a free surface.

Results confirm earlier findings that slab dynamics is to a large extend controlled by the effective viscosity contrast between slab and mantle. Two main deformation modes exist as a function of viscosity contrast: the 'drip' or 'Rayleigh-Taylor' mode occurs for viscosity contrasts smaller than about 100, and is dominated by slab-stretching and non-constant horizontal plate velocities (which are significantly larger towards the trench). The 'plate' mode, on the other hand, occurs for viscosity contrasts larger than 500 and is characterized by slabs that do not change their initial length during subduction. Horizontal plate velocities are homogeneous along the slab top and bending occurs in the trench area, with a bending radius that depends on viscosity contrast and slab thickness. In the plate mode, the initial slab tip length and angle have a significant effect on the initial subduction rate. After the slab tip reached a depth of several hundreds of km, however, subduction velocities are largely independent on the initial geometry and are described by a modified Stokes law.

We developed a semi-analytical subduction model by combining this velocity parameterization with thin viscous sheet equations. It is demonstrated that good agreement exists between numerical and analytical models, both in terms of geometry and in terms of temporal evolution.

In a next step, the analytical model was employed to derive scaling laws for slab radius, which scales as 1/3 to the viscosity contrast, but is nearly linearly dependent on slab thickness. A consequence of this is that slab-dissipation is no more then about 25 percent of the dissipation in the mantle. Moreover, it can be demonstrated that stretching dominates slab bending for slab-mantle viscosity contrasts of less than about 100 (with a weak dependence of slab thickness), in agreement with the numerical simulations.

The semi-analytical results are used to derive a phase diagram for slab-dynamics on Earth, which predicts several subduction modes to exist, if a viscosity increase at the 660 km phase transition is present, in agreement with preliminary numerical simulations.

2.27

Numerical models of fluid migration in a tectonically active continental crust

Keller Tobias, Kaus Boris J. P.

Institute of Geophysics, ETH Zürich, Sonneggstr. 5, CH-8092 Zürich (keller@erdw.ethz.ch)

The flow of a low viscosity fluid through the pore space of a rigid matrix is described by Darcy's law, stating that the Darcy flux q_D is given by

$$\underline{q}_D = \Phi^*(\underline{v}_f - \underline{v}_s) = - k_\Phi/\eta_f * \nabla P_{ex}$$

, where Φ is the porosity of the rigid matrix, $\underline{v}_f$ and $\underline{v}_s$ the fluid and solid velocities, k_Φ the permeability of the matrix, η_f the dynamic fluid viscosity and ∇P_{ex} the gradient of the excess fluid pressure (fluid pressure exceeding hydrostatic pressure).

We investigate the behaviour of a two phase-system involving partial melt percolating through a continental crust, which itself is being deformed according to viscoelastoplastic incompressible Stokes flow. To do so, we assume that the fluid pressure is equal to the solid pressure and therefore we can take $\nabla P_{ex} = \nabla P_{sol} - \rho_f g$. The solid compaction term usually present in coupled Stokes-Darcy problems is neglected here, since the compaction length scale for parameters relevant to our problem is on the order of 0.1-1 km, which is below our numerical resolution.

The numerical setup involves a continental crust of 20-30 km thickness overlying the mantle lithosphere. At the lithosphere-asthenosphere boundary, we introduce a source region of partial melt, either cylindrical or uniformly distributed. The subsequent percolation of melt through the crust is computed depending as a function of dynamic pressure which evolves while the crust is tectonically deformed in either extensional or compressional regime.

First results indicate that both the geometry and spatial evolution of high porosity channels are strongly related to the regional stress field. We observe vertical channels for extensional tectonics and horizontal ones in compressional environments. Additionally, the darcy flux tends to be concentrated in plastic fault zones developing in the upper crust.

In a more general sense the results indicate that partial melt originating in the upper mantle can produce stress-related high-porosity zones while percolating through a tectonically active continental crust. Where brittle faults are present, porous flow can be concentrated towards them. One possible application of this type of models could be the emplacement of hydrated slab melts into the overriding plate in an ocean-continent collision zone.

2.28

Flow mechanisms in granitic ultramylonites

Rüdiger Kilian*, Renée Heilbronner*, Holger Stünitz**, Marco Herwegh****

*Geological Institute, University Basel, Switzerland (ruediger.kilian@unibas.ch)
**Geological Institute, University Tromsø, Norway;
***Institute of Geological Sciences, University Bern, Switzerland

In the Gran Paradiso metagranodiorite small scale ductile shear zones developed at lower amphibolite facies conditions. Along the strain gradient from the host rock to the center of the shear zone we observe the transition from mm-sized, (1) non-recrystallized igneous quartz grains to (2) entirely recrystallized, polycrystalline quartz aggregates, to (3) planar, polycrystalline quartz layers to (4) dispersed quartz grains in a polymineralic matrix.
In the higher strain parts (3) the matrix consists of a mixture of plagioclase, K-feldspar and biotite (+/- white mica). Quartz is the more competent rheological phase which is demonstrated by the geometrical relation of the quartz clasts and the matrix. Published experimentally derived flow laws also support this interpretation.
With increasing strain, aggregates become elongated and form layers of decreasing thickness alternating with matrix layers. The dominant slip system is basal <a> leading to a strong texture with a c-axis peripheral maximum slightly rotated with the sense of shear with respect to the local foliation as the reference frame. A shape preferred orientation develops corresponding to the c-axis orientation. The grain size remains constant throughout the strain gradient with a mean equivalent diameter of about 100 μm (volume weighted).
In the most highly strained parts (4) a phase mixture develops with homogeneously dispersed quartz grains. The texture of the quartz is weakened, the shape preferred orientation systematically changes from a monoclinic to an orthorhombic geometry and the quartz grain size decreases to a mean equivalent diameter of 60 μm (volume weighted).
The microstructural development with increasing strain is associated with a change from dislocation creep in quartz aggregates to granular flow. We present a model for the process of disintegration of quartz aggregates and the coeval grain size reduction. The dominant deformation mechanism is grain boundary sliding accommodated by solution transfer. We conclude that the quartz grain size reduction is primarily achieved by phase boundary migration, nucleation and growth. The disintegration of aggregates and the dispersion of grains reflect that processes involved during dislocation creep can not accommodate grain scale strain incompatibilities in quartz at the stress level imposed by the matrix.

2.29

Comparing thin-sheet models with three-dimensional numerical models for the India-Asia collision

Lechmann Sarah M.*, Schmalholz Stefan M.*, Kaus Boris J. P.** & Hetényi György***

*Geologisches Institut, Sonneggstrasse 5, CH-8092 Zürich (sarah.lechmann@erdw.ethz.ch)
**Institut für Geophysik, Sonneggstrasse 5, CH-8092 Zürich
***Institut für Mineralogie und Petrographie, Clausiusstrasse 25, CH-8092 Zürich

Knowledge about the tectonic evolution of the Tibetan Plateau is still incomplete and many open questions remain concerning the deformation style of the crustal thickening, causing the abnormally high elevation of the Tibetan Plateau. Different models have been suggested explaining the crustal thickening by (1) homogeneous, continuous deformation using thin-sheet models, (2) discrete movement along thrusts developing crustal wedges and (3) lateral crustal flow due to pressure gradients resulting from topography. Most existing numerical models are not fully three-dimensional (3D) (e.g. thin-sheet models) and assume a certain deformation style a priori, which makes it difficult to judge the applicability of such constrained models to the formation of the Tibetan Plateau.
We present a comparison of deformation styles during continent indentation resulting from a fully 3D numerical model and a thin-sheet model. The rheology for both models is power-law. The 3D model consists of four layers representing a simplified lithosphere: strong upper crust, weak lower crust, strong upper mantle and weak lower mantle. From the effective viscosity distribution of the 3D model a vertically averaged effective viscosity is calculated and used for the thin-sheet model to make direct comparisons between the two models.

Simulating indentation is achieved by assigning a tripartite velocity profile at one lateral boundary: A constant horizontal velocity is applied at one section. The velocity then gradually decreases towards zero, applying a cosine-function. The last section of the indenting boundary is fixed. The other three lateral boundaries show free slip. The 3D model additionally exhibits a free surface and a bottom boundary allowing free slip.

In the 3D model folding and lower crustal flow can take place, which are two deformation styles that are ignored in the thin-sheet model. We quantify the differences in the velocity field resulting from the two models. We focus on areas around the indentation corners (the so-called syntaxes) because there the differences in both models are expected to be largest. Also, the Himalayan syntaxes are full 3D structures where 3D deformation effects are expected to be strongest.
Applications of the 3D model together with available geophysical data to the Himalayan syntaxes and the India-Asia collision are discussed.

2.30

Strain localization and the importance of second phases in polymineralic mantle shear zones

Linckens jolien*, Herwegh Marco*, Müntener Othmar**

* *Institute of Geological Sciences, Baltzerstrasse 1+3, CH-3012 Bern (linckens@geo.unibe.ch)*
** *Institute of Mineralogy and Geochemistry, l'Anthropole, CH-1015 Lausanne*

Localization of deformation in shear zones is a common feature in the Earth's crust and upper mantle (e.g., thrusts, strike slip faults). The evolution of such high strain zones is often long lasting, incorporating variations in physical (e.g. P, T) and chemical conditions with time. As previously inferred from studies on peridotite shear zones, second phases (e.g. spinel, pyroxenes) can be important in localizing strain as they can keep the olivine matrix grain size small. The influence of second phases on the olivine grain size and their affect on strain localization has not yet been quantified in detail.
To determine the importance of second phases in localizing strain in the mantle, three different peridotite shear zones (Wadi Hilti, Oman; Othris, Greece and Lanzo, Italy) were analyzed and compared. In the case of the Oman and Lanzo peridotite, a range of microstructures, from porphyroclastic tectonites to ultramylonites were investigated. These microstructures are related to continuous localization under retrograde conditions. In addition, mylonite samples of the Othris peridotite were analyzed.
Similar to previous studies performed on calcite mylonites, each of the different mantle microstructures can be subdivided into two different microfabric types: (a) second phase controlled microstructures, where the olivine grain size increases with increasing Zener parameter (Z = dp/fp; second phase grain size/second phase volume fraction) (b) recrystallization controlled microstructures, where the olivine grain size shows no dependence on the second-phase content and remains constant with increasing Z. The olivine grain size for both microfabric types becomes smaller with decreasing temperature and strain rate. The different peridotite shear zones show the same relation between the Zener parameter and the olivine grain size when the deformation conditions (e.g. temperature and strain rate) were the same. From a geodynamic point of view, Zener trends can therefore be applied as a tool to determine the deformation conditions and their variations in space and time in case of mantle rocks.
The CPO of olivine in the different microstructures weakens going from porphyroclastic tectonites to ultramylonites and also with decreasing Zener parameter. This indicates that, with ongoing strain localization and with increasing second-phase content, diffusion creep becomes more important as deformation mechanism.
The combination of the Zener trend with olivine deformation mechanism maps and CPO is a good method to assess the importance of second phases on strain localization. In this way the dominant deformation mechanism and strain rate in the different microstructures can be derived. The analysis of the peridotite shear zones shows that when there is a switch in dominant deformation mechanism between pure olivine and polymineralic layers or when both are deformed by grain size sensitive deformation, the strain rate is up to an order of magnitude larger in the polymineralic layers.

2.31

Numerical modeling of craton destruction

Gang Lu [1], Boris Kaus [2], Liang Zhao[1]

1 Institute of Geology and Geophysics, Chinese Academy of Sciences, Beijing, China
2 Geophysical Fluid Dynamics, Department of Earth Sciences, ETH,8092,Switzerland

Archean cratons are characterized by a cold, thick, stable lithosphere keel. The North China Craton(NCC),however, is an anomaly. The eastern NCC experienced significant lithospheric thinning in the Late Mesozoic to Cenozoic. In order to understand the mechanisms of lithospheric thinning, we performed a set of geodynamic experiments using MILAMIN_VEP, which is based on the finite element method.
The setup involves a flat homogeneous lithosphere with a thickness of 190km. The influences of (a) lithosphere extension, (b) upper mantle convection and (c) thermal anomaly beneath lithosphere are investigated separately or simultaneously. In the cases of (a), a push velocity is imposed to extend the lithosphere while the end of lithosphere is replaced by material with low viscosity. In the cases of (b), thermal anomalies at the bottom of the model are used to start the convection. In cases of (c), high temperature anomalies are imposed just beneath the lithosphere.
We conclude from our initial experiments that: (A) simple extension can thin the whole lithosphere homogeneously at the beginning and break the lithosphere by a normal fault finally, (B) downwellings dominate convection after about 10Myrs, independent of the initial magnitude of the temperature anomaly. The bottom of lithosphere can be partly destroyed at certain places where stable downwelling forms, and gets thicken again after the downwelling disappears, (C) a simple high temperature anomaly beneath lithosphere has little influence to the lithosphere thinning. It is thus suggested that extension is a candidate mechanism of destroying a craton.

2.32

New experimental approach to measure seismic wave attenuation of rocks at low frequency

Claudio Madonna*, Nicola Tisato*, Sébastien Boutareaud*, Brad Artman** and Luigi Burlini*

**Structural Geology and Tectonics, Sonneggstrasse 5, 8092 Zurich (claudio.madonna@erdw.ethz.ch)*
***Spectraseis AG , Giessereistrasse 5, 8005 Zurich*

We describe a new experimental approach to accurately characterize attenuation in fluid-bearing porous rock samples.
A new apparatus has been developed and built in order to measure attenuation (1/Q) of seismic P-waves passing through a rock sample in the low frequency regime (0.1 Hz - 50 Hz), employing the stress-strain method in an internally heated gas apparatus (Paterson rig).
Stress is measured with a load cell of 1000 N full scale with a resolution of 0.01 N. Strain is measured with high-sensitive LVDTs of 1 mm full scale and a resolution of 10^{-9} m. This new apparatus differs from previous ones in that it can measure the bulk attenuation of a non-isotropic, non-homogeneous 50-to-100 mm length sample by avoiding strain gauges.
The quality factor Q is obtained from the time shift between the sinusoidal stress, which is mechanically applied at the bottom of the sample, and the sinusoidal strain response measured on the top of the sample.
We present a sketch of the apparatus and we include a discussion of some of the problems encountered while building the apparatus; we further discuss recent improvements. In addition, we present preliminary results and the corresponding digital signal processing on aluminium (as standard) and Berea-sandstone partially saturated with oil and water and characterized by means of tomographic images.
This new technique can be used to accurately establish a catalog of 1/Q values as a function of in-situ rock properties. In particular, future studies using this apparatus will investigate the effects of different fluid properties on 1/Q. Such new, accurate measurements will be important in passive and active seismic investigations on fluid-bearing rocks.

2.33

The Singularities of double subduction systems

Malatesta, Luca*; Mishin, Yury*; Gerya, Taras V.*

*Institute of Geophysics, ETH-Zurich, Sonneggstrasse 5, 8092 Zurich, Switzerland

Among the tectonic processes occurring at the surface of the Earth, the double subduction systems are some of the less studied. By double subduction system, we understand a configuration in which the force of a one or two-sided accretion is translated in two distinct subductions next to each other dipping in the same direction. They are relevant for both modern (Izu-Bonin-Marianas and Ryukyu arcs, Hall (1997)) and ancient tectonics (western Himalayas, Burg (2006)). Next to their documentation in the field, few experiments have been performed to understand their dynamics. The first and only numerical modeling of the problem until the present research has been successful in determining the dynamics of a simple model (Mishin, 2008). We performed further experiments with the same 2D coupled petrological-thermomechanical code (Gerya and Yuen, 2003) but in a more complex setup. It encompassed an oceanic plate containing two weak zones and bound with two continental plates, one of which moving constantly towards the other. We studied the effects of four key-parameters: the age of the oceanic plate, the activation volume of the dislocation creep, the composition of the oceanic crust and the length of the first subducting slab (figure 1). The experiments led us to the conclusion that (A) the age of an oceanic plate and the activation volume influence the subductions system as follow: they are (i) linearly and proportionally related to the break-off time and (ii) inversely proportional to the roll-back power. (B) The relative thickness of gabbro in the crust has distinct effects on the dipping slab: it is (i) inversely proportional to the break-off time and (ii) proportional to the 660 km entry angle (C) The subduction regime (advancing, penetrating or retreating mode) depends on the slab entry angle in the 660 km discontinuity zone. The entry angle sums up the other parameters. Key angles determining the different regimes were determined for a given slab length. (D) the length of the first subducted slab impacts the geometry of the global system but does not change its dynamics. (E) Simultaneous subductions cannot be obtained in a one-sided accretion with the investigated model, further elements – absent from the modeling – should account for it. (F) The subduction regime and orientation (i) can be possibly regained through the study of sedimentation record but (ii) is not coherently linked to the style of the final orogeny. (G) Double subduction systems lead to a complex basin evolution of fore- and back-arcs and pro- and retro-forelands, and to a specific override pattern which can mislead the interpretation of the subduction orientation.

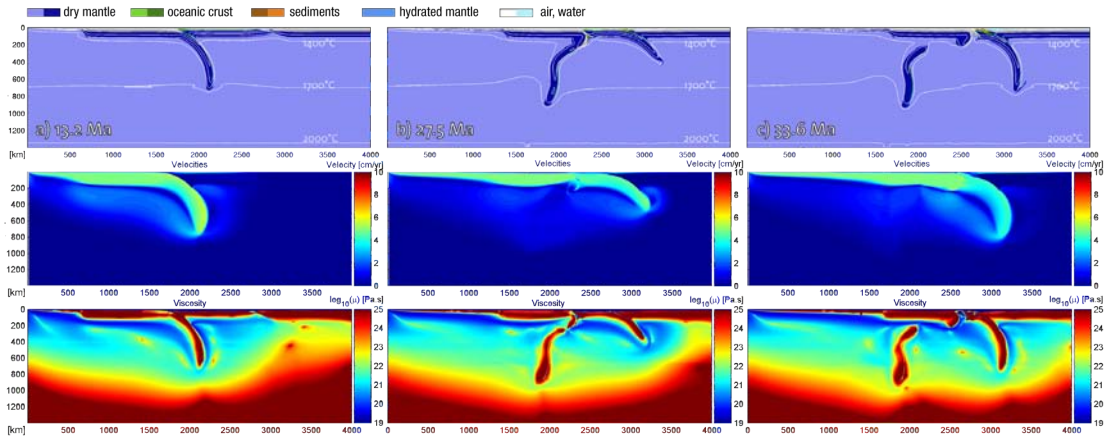

Figure 1. Evolution in three steps of a double subduction numerical model. With the chemical composition in the first row, the velocity in the second and the viscosity in the third.

REFERENCES

J.-P. Burg. Two orogenic systems and a transform-transfer fault in the Himalayas: evidence and consequence. Earth Science Frontiers, 13:27-46, 2006.

T. V. Gerya and D. A. Yuen. Characteristics-based marker-in-cell method with conservative finite-difference schemes for modelling geological flows with strongly variable transport properties. Physics of the Earth and Planetary Interiors, 140:295-320, 2003.

R. Hall. Cenozoic plate tectonic reconstructions of SE Asia. Geological Society London Special Publication, 126:11-23, 1997.

Y. Mishin, T. V. Gerya, J.-P. Burg, and J. A. Connoly. Dynamics of double subductions: Numerical modeling. Physics of the Earth and Planetary Interiors, 171-280-195, 2008.

2.34

CitcomSX: Robust preconditioning in CitcomS via PETSc

Dave A. May*, Matthew G. Knepley**, Mike Gurnis***

* *Department of Earth Sciences, ETH Zurich, Zurich, Switzerland (dave.mayhem23@gmail.com)*
** *Computation Institute, University of Chicago, Chicago, IL, USA (knepley@gmail.com)*
*** *Computational Infrastructure for Geodynamics, California Institute of Technology, Pasadena, CA, USA (gurnis@gps.caltech.edu).*

The use of numerical simulations to study convection in the mantle has a long and rich history in geodynamics. The Citcom family of mantle convection codes are in wide spread use through out the geodynamics community. Since the inception of the original Cartesian version written by Louis Moresi in the early 1990's, many variants have been developed. Two important contributions were made by Shijie Zhong in the form of the parallel 3D Cartesian version and the parallel, full spherical version.

The Computational Infrastructure for Geodynamics (CIG) have been providing maintenance and support for CitcomS over the last 5 years. The CIG effort to provide a community mantle convection code has resulted in several developments to CitcomS. These include the addition of new physics (rheology, compressibility), coupling with other software, the inclusion of additional geologically relevant input/outputs and improved portability. Such improvements have seen a further increase in the development and usage of this particular version of Citcom. Today, CitcomS is routinely used to solve mantle convection and subduction models with approximately one hundred million unknowns on large distributed memory clusters.

Many advances have been made in both numerical linear algebra and the software encapsulating these mathematical concepts since the development of the original Citcom. However, the solver used by all Citcom software has remained largely unchanged from the original version. Incorporating modern techniques into CitcomS has the potential to greatly improve the flexibility and robustness of the iterative methods used to solve the underlying saddle point problem. Here we describe how PETSc (http://www.mcs.anl.gov/petsc), a flexible linear algebra package, has been integrated into CitcomS in a non-invasive fashion which i) preserves all the pre-existing functionality and ii) enables a rich infrastructure of preconditioned Krylov methods to be used to solve the discrete Stokes flow problem. The "extension" of the solver capabilities in CitcomS has prompted this version to be referred to as CitcomSX.

We demonstrate the advantages of CitcomSX by comparing the convergence rate and solution time of the new Stokes solver with the original CitcomS approach. We utilise a scaled BFBt preconditioner which is constructed via the assumption of the existence of an approximate commutator as a preconditioner for the Schur complement. The BFBt preconditioner is composed of smaller sub-problems for which efficient, robust and scalable multilevel methods exist. Here we demonstrate that the scaled BFBt we utilise is robust and yields convergence rates largely independent of the element resolution and the viscosity contrast. Using this preconditioner, we can accommodate higher viscosity contrasts than were possible with the original CitcomS solver. The test problems used for these comparisons include simulations of variable viscosity mantle convection (regional, full spherical) and slab subduction (regional).

2.35

Seismotectonic study in Northern Tunisia (exemple: Utique Structure)

Lassaad Mejri[1,2,4,5], Vincent Regard[1,2,3], Sébastien Carretier[1,2,3], Stéphane Brusset[1,2,3], Mahmoud Dlala[5]

[1.] *Université de Toulouse ; UPS (OMP) ; LMTG ; 14 Av Edouard Belin, F-31400 Toulouse, France*
[2.] *CNRS ; LMTG ; F-31400 Toulouse, France*
[3.] *IRD ; LMTG ; F-31400 Toulouse, France*
[4.] *CNSTN, Pôle technologique 2020 Sidi Thabet, Ariana, Tunisie*
[5.] *Université de Tunis El Manar ; Faculté des Sciences de Tunis, 1060 Tunis, Tunisie*

The present-day seismicity at northeastern Tunisia reported from permanent networks is of low to moderate magnitude. However, earthquakes are mentioned in the literature, specially a destructive one in the antique city of Utique. Geologic, seismic, and neotectonic investigations in this area shows that Utique fold is closely related to the recent tectonic activity in this region. Data show that Utique fold is built on an E-W fault, and we found evidence of activity of this fault in the past 20 ky. Seismic section and balanced cross section shows that it was affected by two phases of compressional deformation. The

first one is occurred during Miocene and caused folding over a passive ramp in Triassic sediment. The timing of the second one is unclear because of low definition of seismic data in its uppermost part: it clearly occurred after Serravalian. A total shortening of 690 m has been measured indicating an average shortening rate of 0.14 mm/yr since the beginning of Pliocene. As already mentioned, compression must have begun early in Pleistocene (1.8 My); this leads to a most likely value for shortening rate of 0.38 mm/yr, corresponding to ~8% of the current shortening in Tunisia (~4.5 mm/yr in a direction N145°E between stable Africa and Sardinia after a compilation of results from D'Agostino and Selvaggi [15] and Hollenstein et al.). Field observations of surface faulting, debris of less than 2000 years old pottery reworked and possibly tilted calcareous nodules at the fault zone suggest that the main compressional phase continues up to present.

Utique fault outcrops in a gully ~5 m wide and ~5m deep. The gully seems to have experienced a complicated story with a first incision stage followed by recent filling and renewed incision that continues currently. A fault plane was found, displaying important variations in trend and dip; the average values being a N150°E trend and an 80°N dip, with uncertainties evaluated to be ~20°. The fault offsets clearly some conglomerates made of Pliocene marine formation reworking and gray clay levels, observed elsewhere lying on top of calcrete. It is mantled by the recent gully infilling made of angular debris, which could have been affected by the fault. In between, a non continuous formation made of clay and calcrete-derived sands could be observed; it is apparently faulted and contains a piece of pottery, less than 2000 years-old after an archeologist expertise (Slim Khosrof, National Institute of Patrimony, Tunis, personal communication)

Our data show definitively the late Pleistocene–Holocene activity of the Utique Fault; and we can predict the earthquake recurrence interval which should be of ~10^3-10^4yr. This makes the Utique fault propagation fold an important structure when regarding seismological hazard of the 1.5M people Tunis City, located 35 km to the south. This high seismic risk zone deserves to be taken into account during the establishment of important regional development programs and in the application of seismic building code.

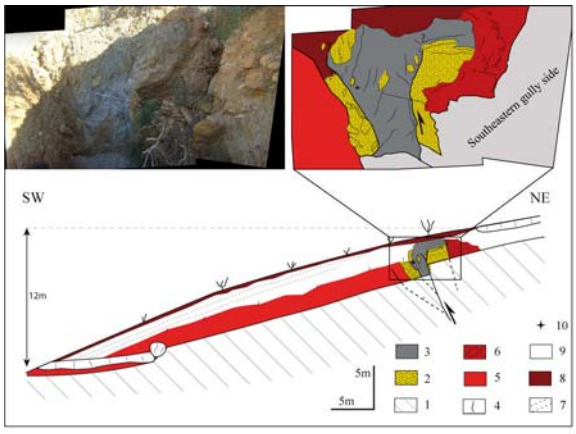

Figure 6: utique fault outcrop with photography of the main fault plane; aggrandissement in top corresponds to the zone of fault, on the right the corresponding photograph. Main lithological formations, in likely tratigraphic order: (1) gully basement; (2) sandstones and conglomerates mainly made of pliocene strata pieces 3) gray clays; (4) calcareous crust; (5) red clays with calcareous nodules; (6) recent conglomerates; 7) colluvial wedge; (8) soil; (9) undetermined; (10) approximative pottery location

Figure 6: affleurement de la faille d'utique avec un cliché du plan de faille majeur; l'aggrandissement en haut correspond à la zone de faille, à droite la photo correspondante. Les principales formations ont données dans l'ordre stratigraphique a priori : (1) partie basale ; (2) sables et conglomerats issus du émantèlement du pliocène; (3) argiles grises ; (4) croûte calcaire ; (5) argiles rouges ; (6) débris récents ; 7) colluvions ; (8) sol ; (9) lithologie indéterminée ; (10) position approximative du tesson échantillonné.

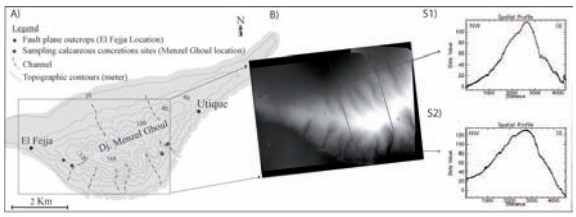

Figure 7: Topographic Utique Structure representation; A) sampling sites and fault plane outcrops, B) Digital Elevation Model and spatial profile representation.

Figure 7: Représentation topographique de la structure d'Utique ; A) localisation des sites d'échantillonnageet de l'affleurement de la faille, B) modèle numérique de terrain,avec des profiles spatiales à travers l'anticlinal d'Utique

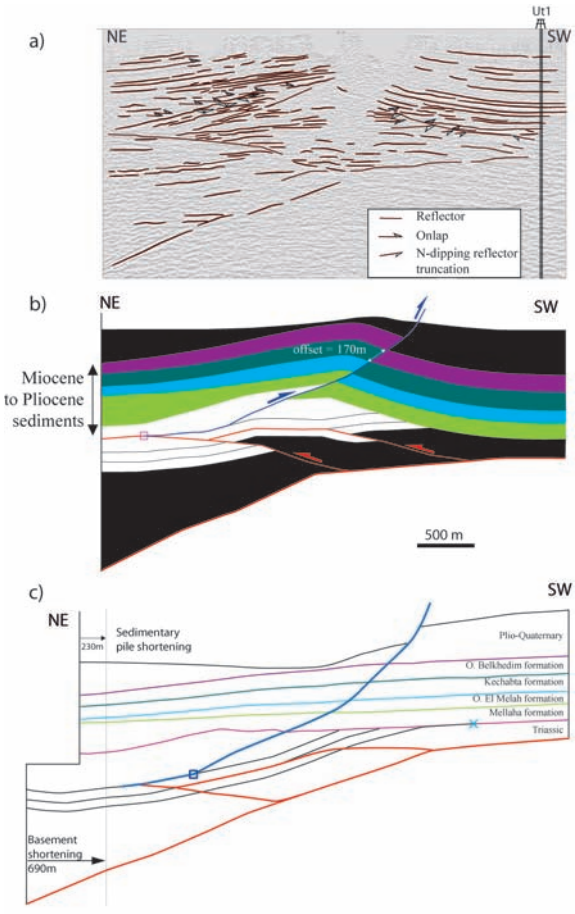

Figure 5: a) seismic profile interpretation (no vertical exaggeration); b) Cross-section in Utique structure drawn after seismic line L1 and slip rate measurement; c) Unfolding cross-section back to lowermost Miocene

Figure 5: a) interprétation du profil sismique (pas d'exagération verticale); b) coupe équilibré de la structure d'Utique et estimation du raccourcissement ; c) dépliage de la coupe jusqu'au Miocène inférieur.

2.36

Numerically modeling current vertical surface motion in the swiss alps from the bottom up - Does the geometry of the orogen dictate how it moves?

Mettier Ralph*

Institut für Geologie, Baltzerstrasse 1-3, CH-3012 Bern (mettier@geo.unibe.ch)

Apart from the obvious topographical features, the ongoing surface motion is one of the most easily accessible and best quantifiable characteristics of a typical alpine-style orogen. However, it is often unclear as to how many different processes, such as i.e. isostatic adjustment effects, contribute to the observed motion, and how much is simply a consequence of the ongoing shortening.
Recent advances in several methods, such as enhanced GPS measurements, Interferometric Synthetic Aperture Radar (InSAR) and fission track (FT) dating, as well as precise leveling can now provide us with a good description of the vertical motion at present and in fairly recent history of the orogen. This in-turn, provides us with fresh, and often much needed, criteria for calibrating our conceptual and numerical models of orogenesis and the involved processes.
We present a series of finite element models, that attempt to reproduced the observed vertical surface motion on a roughly north-south cross section of the Swiss Alps. While fairly simple as far as rheology, thermodynamics and various other aspects are concerned, the geometry of the cross sections is of high complexity, representing individual tectonic units such as the Aar- and Gotthard massifs, the Helvetic and Penninic nappe structures as well as the underlying subduction of the european crust.
The models simulate a short span of accelerated time, with a fixed rate of shortening prescribed by the boundary conditions. The resulting motion at the surface of the model, as well as the internal deformation of the individual tectonic units is then examined, interpreted and compared to their real-world counterparts. The model series incorporates variations in the chosen physical descriptions of the materials, deforming both purely elastic and partially elasto-plastic, as well as in the description of the frictional behaviour at the interfaces between units. Further parameter variations within these model sub-series provide insight into the relative relevance of these parameters.
Perhaps unexpected, considering the simplicity of the models, the results exhibit good correlation with the data obtained from real-world measurements. This leads us to speculate that the underlying geometry may well be the dominant factor in describing the behaviour of such an orogen.

2.37

Seismic properties of melt-generating metapelites

Santanu Misra*, Bjarne Sven Gustav Almqvist** and Luigi Burlini*

*Geological Institute, **Institute of Geophysics; ETH Zurich, CH-8092, Switzerland*

We performed ultrasonic pulse transmission measurements on synthetic rocks of pelitic composition to identify their seismic properties and determine the complete elastic tensor during partial melt generation. Experiments were conducted at 750°C and 300MPa confining pressure on cylindrical samples of quartz-muscovite aggregates (1:1 by volume) having an internal, transversely isotropic planar fabric and ~ 24% porosity. The velocities of compressional waves (V_p) and extensional waves (V_E) were measured continuously for 6 hours at different frequencies (0.1, 1.0 and 3.0 MHz) with waves propagating at 0, 45 and 90° with respect to the axis of symmetry of the samples. Shear-wave (V_s) velocities were determined indirectly, based on the V_E and V_P. In the beginning of the experiments the reduction of porosity with confining pressure and temperature lead to an increase of the seismic velocities compared to room pressure and temperature. V_p decreased by 200-400 m/s with the onset of melt generation, which started after 1.5 hours of the experiment. A complex behaviour of the seismic velocities was observed with increasing melt generation and nucleation of new crystals. The seismic anisotropy varies for the duration of the experiment, and is dependent on the sample history (i.e., porosity reduction, melt generation, crystal nucleation).These experimental results can suitably be applied to geophysical investigation of the lower crust where partial melting is an important geological process.

2.38

Rheology of metapelites during partial melting and crystallization

Santanu Misra, Elizaveta Tumarkina, Luigi Burlini and Jean-Pierre Burg

Structural Geology and Tectonics Group, Geological Institute, ETH, Sonneggstrasse 5, Zurich 8092, Switzerland

This study investigates the rheological behaviour of metapelitic rocks at depth where they undergo synkinematic partial melting and subsequent crystallization during progressive deformation. Torsion experiments were performed on synthetic pelitic rock samples at 300 MPa confining pressure and 750°C temperature with a constant strain rate ($\dot{\gamma} = 3x10^{-4}$) for a range of finite shear strains (γ = 0.5-15). Partial melting started a relatively low shear strains (γ = 2-4), which was coupled with strong strain softening (~ 60%) in the creep behaviour. With further shearing (γ = 4-10) the creep turned to be steady state flow with nucleation of tiny, new crystals. At higher shears (γ = 10-15), new mineral phases started growing at the expense of partial melts, which resulted in weak strain hardening and finally, brittle failure of the sample at the same pressure-temperature.

The stress exponent values (*n*) were continuously increasing from 3 to 28 with progressive deformation indicating a transition from power to exponential flow law (power Law Breaking). Depending on the melt and solid proportions in the system the speculated four stages of percolation thresholds during partial melting and crystallization of lithosphere were established by the experimental data.

2.39

Palaeotethyan, Neotethyan and Pindos series in the Lycian Nappes (SW Turkey): geodynamic implications

Moix Patrice & Stampfli Gérard M.

Institut de Géologie et de Paléontologie, Université de Lausanne, Bâtiment Anthropole, CH-1015 Lausanne (Patrice.Moix@unil.ch)

For a long time, the idea of a continuum between the Hellenides in Greece and the Taurides in Turkey has been discussed (e.g., Brunn et al., 1976). This was principally based on correlations between the platform series of the external parts of the Hellenides-Taurides system, as well as similarities between sedimentary sequences in southwestern Turkey and in the Dodecanese islands (e.g., Bernoulli et al., 1974). In southwestern Turkey, the Lycian Nappes occupy a large area between the Beydağları platform to the southeast and the Menderes Massif to the northwest. It has been demonstrated that the Lycian Nappes are derived from the Izmir-Ankara belt and represent allochthonous parts of the northern passive margin of the Anatolian terrane (Moix et al., 2008). Because of their location between the Hellenic system to the west and the Tauric one to the east, the Lycian Nappes and their para-autochthonous series are a key area. The Tavas Nappe forms the lowermost unit in the Lycian pile and is classically subdivided into the Karadağ, Teke Dere, Köyceğiz and Haticeana units (de Graciansky, 1972). Detailed fieldwork supported by numerous micropalaeontological evaluations make obvious that the Tavas Nappe is in reality highly composite.

The lowermost Karadağ unit consists of a platform succession ranging from the Late Devonian to the Late Triassic. A large hiatus outlined by the deposition of sandstone and quartzite exists between the Sakmarian and the Middle Triassic. The Carnian is marked by a general deepening of the platform preceding shortly the deposition of a wildflysch-like formation. The discovery of the Cordevolian (early Carnian) *Pseudofurnishius murcianus murcianus* van den Boogaard conodont fauna on top of the platform and in the first limestone beds interstratified at the base of the siliciclastic formation is of crucial importance. This fauna characterizes the Sephardic province and is a typical indicator for the Neotethyan domain sensu stricto. The Palaeozoic succession of the Karadağ unit is a typical shallow-water Gondwana type shelf development and can be compared to similar sections in the Alborz range in northeastern Iran. The large hiatus during the Permian could be seen as a rift shoulder related to the Neotethyan (= East-Mediterranean) rifting. Consequently, the Karadağ unit likely belongs to the Cimmerian Taurus terrane and was part of the northern passive margin of the Neotethys.

The Karadağ unit is always found structurally below the Teke Dere unit, this superposition being a possible result of the Late Triassic Eo-Cimmerian orogenic event. The Teke Dere unit includes several slices composing the most complete Palaeotethyan succession in Turkey. It comprises Kasimovian OIB-type basalts and associated platform and slope sediments representing a Palaeotethyan seamount, Carboniferous MORB-type basalts, an Early Carboniferous siliciclastic series stratigraphically overlain by Middle Permian limestones, and a Middle Permian arc sequence. Both the platform limestones associated to the

seamount and the dolostones above the Early Carboniferous siliciclastic series yielded shallow-marine microfauna and microflora sharing strong biogeographical affinities with the northern Palaeotethyan borders. Palaeotethyan remnants found as subduction-accretionary complexes or reworked during the Eo-Cimmerian orogenic event provide a strong mean to identify and locate the Palaeotethyan suture zone.

The thick Mesozoic sequence, formed by the Köyceğiz and Haticeana series (both of them belonging to the same palaeogeographic realm), occupies a high structural position above the Karadağ and Teke Dere units. The base of the series comprises Late Triassic continental red arkosic sandstones and conglomerates. This molasse-like sedimentation is followed by Liassic shallow-marine limestone and includes a late Liassic Ammonitico Rosso. The sedimentation continues with late Liassic to Maastrichtian pelagic micrites, cherty micrites and calciturbidites. It is then unconformably overlain by a late Palaeocene to Lutetian flysch. At places, Late Triassic volcanic rocks (transitional MORB-type) associated to pelagic limestones, turbiditic sandstones, and calcareous sandstones alternating with volcaniclastic sediments form the lowermost exposure of the Köyceğiz series. This sedimentological evolution is in many points similar to Pindos-like series found now in southern Turkey and in the Dodecanese islands. These series originated in the Huğlu-Pindos Ocean, along the northern passive margin of the Anatolian (Turkey) and Sitia-Pindos (Greece) terranes (Moix et al., 2007).

In conclusion, the Tavas Nappe includes more or less dismembered units belonging to the Palaeotethyan, Neotethyan and Huğlu-Pindos realms. The Karadağ unit belongs to the Neotethys (= East-Mediterranean) domain, the Teke Dere succession is composed of several thrust sheets of Palaeotethyan origin, and the Köyceğiz and Haticeana series are related to the Huğlu-Pindos oceanic domain. The identification of such remnants in the Lycian Nappes and their comparisons with adjacent areas offer efficient tools to make accurate geological correlations between Greece and Turkey.

REFERENCES

Bernoulli, D., de Graciansky, P.-C. and Monod, O., 1974. The extension of the Lycian Nappes (SW Turkey) into the southeastern Aegean Islands. Eclogae Geologicae Helvetiae, 67(1): 39-90.

Brunn, J.H., Argyriadis, I., Ricou, L.-E., Poisson, A., Marcoux, J., de Graciansky, P.-C., 1976. Eléments majeurs de liaison entre Taurides et Hellénides. Bulletin de la Société Géologique de France, 18(2): 481-497.

Graciansky de, P.-C., 1972. Recherches géologiques dans le Taurus Lycien. PhD Thesis, Paris Sud - Centre d'Orsay, Paris, 762 pp.

Moix, P., Kozur, H.W., Stampfli, G.M. and Mostler, H., 2007. New palaeontological, biostratigraphical and palaeogeographical results from the Triassic of the Mersin mélange, SE Turkey. In: S.G. Lucas and J.A. Spielmann (Editors), The global Triassic. New Mexico Museum of Natural History and Science Bulletin v. 41, Albuquerque, pp. 282-311.

Moix, P., Beccaletto, L., Kozur, H.W., Hochard, C., Rosselet, F. and Stampfli, G.M., 2008a. A new classification of the Turkish terranes and sutures and its implication for the paleotectonic history of the region. Tectonophysics, 451(1-4): 7-39.

2.40

New constraints on foreland basin development in South-West Taiwan from sequence stratigraphy and flexure modelling

Stefan Nagel*, Sébastien Castelltort*, Frederic Mouthereau**, Andrew T. Lin***, Sean D. Willett* & Boris Kaus*

Eidgenössische Technische Hochschule (ETH) Zürich, Sonneggstrasse 5, 8092 Zurich, Switzerland, stefan.nagel@erdw.ethz.ch

** Université Pierre et Marie Curie - Paris VI, Laboratoire de Tectonique - CNRS UMR 7072, Barre 46-45 Niveau 2 - Case 129, 4, Place Jussieu F-75252 Paris Cedex 05 France*

*** National Central University, Basin Research Group, Earth Science Dep. No.300, Jhongda Rd., Jhongli City, Taoyuan County 32001, Taiwan(R.O.C.)*

The island of Taiwan is situated on the boundary between the Philippine Sea Plate and the Eurasian plate and has long been put forward as a textbook example of an Arc-Continent collision. Oblique arc-continent collision began during the late Miocene and has resulted in progressive migration of active deformation and foreland basin development from north to south. Thus the northern part of the foreland basin is dominated by shallow marine and nonmarine deposits, whereas the southern part of the foreland basin is dominated by deeper marine deposits (Covey, 1984). The foreland basin system of Western Taiwan recorded infill from both the Chinese Mainland as well as from the emerging Taiwan Island. Furthermore, the high rates of convergence, high rate of rock uplift and the wet, stormy climate of the sub-tropical typhoon belt combine to produce erosion and sediment yield rates amongst the highest in the world. Today, the Taiwan Strait is about 150 to 200

km wide and around 70 m deep. However, the timing of the development of the foreland basin and subsequent change of direction of paleocurrent is not yet well-defined. Different authors described a basal unconformity on seismic profiles offshore Taiwan, which was dated ±6.5 Ma (late Miocene), but has not yet been supported by onshore observations.
We analysed two Pliocene Formations in the Central (Meishan County) and South part (Tsengwen Reservoir) of Taiwan: the Kueichulin Formation (Tawo Sandstone Member) and the Ailiaochiao Formation. We conducted several lithofacies (e.g. heavy minerals, thin sections, etc.) and biostratigraphical analysis in order to understand the regional sequence stratigraphy and to be able to set up a paleoenvironmental interpretation of the studied area. The Tawo Sandstone Member basically consists of wavy, lenticular and flaser bedded, thin laminated Silt- and Mudstones interbedded with small, fine to medium grained sandstones (thickness: 10 cm to 5 m). The siltstone facies shows rhythmic variations in laminae thickness with conspicuous bidirectional current ripples indicating a tidal influence. The sandstone facies are (in places) dominated by bioturbation and physical sedimentary structures, such as scoured surfaces with lag deposits, low-angle cross-lamination, flaser and wavy bedding on top. The trace-fossil assemblage includes structures
typical of both the Skolithos and Cruziana
ichnofacies, characterizing a shallow-marine (shoreface) environment in which high-energy and low-energy settings coexisted. Similar lithofacies have been described from tidally influenced continental shelf environments in South Korea and China.

The Ailiaochiao Formation more to the South consists of fine laminated siltstone and interbedded mudstone layers. They are unconformably incised by numerous fine grained sandstone layers forming cut-and-fill structures with distinct climbing ripples in two opposite directions within a wider channel. In the middle of the channel axis exist conspicuous conglomerates with fine grained sandy matrix containing mud clasts and forams. Bioturbation is commonly very rare.
The successive sedimentation of the Chinshui Shale (and the equivalent Maopu Shale respectively), commonly interpreted as deeper marine sediments, indicates a formative Transgression event. The associated sea level rise is interpreted as the onset of load induced subsidence by the growing orogen. We interpret the two sections as transition from a shallow marine, tidally influenced environment with (protected) lagoons and estuaries passing into a channel-levee system in proximal parts of a growing prodelta.
The spatio-temporal history of the Western foreland basin is interpreted as an evolution from an “under-filled” stage with marine depositional environments deepening upwards and relatively low sedimentation rates (Kueichulin fm and lower Chinshui fm) toward an “over-filled” stage marked by the filling of the basin with progressively shallower environments upwards and eventually becoming continental.
The project will focus on the high-resolution stratigraphic record of the collision in the western foreland basin by compiling published and unpublished data, collecting new field observations and using subsurface seismic imaging in the basin in order to reconstruct paleogeography, depositional environment, and tectonic and sediment-transport controls on depositional patterns. These results will serve as input to stratigraphic and 3D deformation models to constrain the development of the orogen and its southward propagation. The results of this study will provide important evidence for the space and time evolution of the orogen-related loading of the foreland.

REFERENCES

Covey, M., 1984: Sedimentary and tectonic evolution of the western Taiwan Foredeep, Unpublished Ph.D. thesis

Covey, M., 1984: Lithofacies analysis and basin reconstruction, Plio-Pleistocene Western Taiwan Foredeep, Petroleum Geology of Taiwan, Vol. 20, pp. 53-83

Lin, A. T., A. B. Watts and S. P. Hesselbo, 2003: Cenozoic stratigraphy and subsidence history of the South China Sea margin in the Taiwan region. Basin Research, 15 (4), 453-478.

Mouthereau, F., and O. Lacombe, 2006: Inversion of the Paleogene Chinese continental margin and thick-skinned deformation in the Western Foreland of Taiwan, Journal of Structural Geology, 28, 1977-1993.

Funding: This project is funded by Swiss National Funds grant #2-77295-08.

2.41

Thermal structure and metamorphic evolution of the Piedmont-Ligurian metasediments in the Western-Central Alps

Negro François*, Pellet Clara-Marine*,**, Bousquet Romain**, Beyssac Olivier***, Guerra Ivan****, Vils Flurin*****

* *Institut de Géologie et d'Hydrogéologie, Université de Neuchâtel, Rue E. Argand 11, CH-2009 Neuchâtel (francois.negro@unine.ch)*
** *Institut für Geowissenschaften, Universität Potsdam, Germany*
*** *Laboratoire de Géologie, Ecole Normale Supérieure, Paris, France*
**** *Institut de Minéralogie et Géochimie, Université de Lausanne, L'Anthropole, CH-1015 Lausanne*
***** *Department of Earth Sciences, University of Bristol, UK*

The Western-Central Alps, located between the Simplon and the Aosta-Ranzolla faults, represent a "transition" zone where many paleogeographic domains were continuously accreted within the alpine orogenic wedge. Within this orogenic wedge, the Piedmont-Ligurian oceanic domain recorded blueschist to eclogite metamorphic conditions during the Alpine orogeny. The Piedmont-Ligurian zone, is classically divided, according to their metamorphic evolution, into a LP (greenschist to blueschist facies) unit (Combin zone), and a HP to UHP unit (Zermatt-Saas nappe). The contact between both zone is supposed is a major detachment fault (Combin fault). Although P-T conditions are quite well known in the Zermatt-Saas nappe, quantitative constraints are lacking in the Combin zone.

We investigated the temperature record in the oceanic metasediments of the Piedmont-Ligurian units, using Raman spectroscopy of carbonaceous material. This method allows quantifying the maximum temperature, and therefore the peak of metamorphism, without being affected by the retrograde evolution. The aim of this study was to (1) estimate the peak temperature reached within each unit (2) compare the temperature record between the different units. We additionally characterized the metamorphic assemblages in the metasediments of both units. Samples were collected in the metasediments of the Combin zone north and south of the Dent Blanche massif, and in the Zermatt-Saas nappe in the area of Zermatt and Lago di Cignana to estimate the temperature gap across the Combin fault.

In the Combin nappe, temperatures range between 430-500°C, and are very coherent in the northern and southern parts of the Dent Blanche. In the Zermatt-Saas nappe, temperatures are similar to the ones obtained in the Combin nappe, also in the range 450-530°C, and the temperature gap is significantly lower than it is proposed in the literature. However, mineral assemblages are not well preserved in the Combin nappe compared to the Zermatt-Saas nappe, which could be explained by intense retrogression.

We compare these temperatures with the metamorphic assemblages observed in the different units and discuss these results in the frame of the tectono-metamorphic evolution of the high-pressure low-temperature oceanic units from the Western-Central Alps.

2.42

Influence of faults on the development of Excavation Damaged Zone: the case of the Mont Terri Rock Laboratory

Nussbaum Christophe* & Bossart Paul*

**Federal Office of Topography swisstopo, Fabrique de Chaux, CH-2882 St-Ursanne (christophe.nussbaum@swisstopo.ch)*

One concern in the research on waste disposal in argillaceous rocks is the understanding of processes controlling the development of the Excavation Damaged Zone (EDZ). The geometry and kinematics of the EDZ fracture network provide a valuable input for this problematic. However, the Mont Terri site is characterised by a complex tectonic setting made of numerous faults with different orientations and dips. These pre-existing faults or inherited structures, related to the Jura thrust-and fold belt and to the Rhine-Bresse transverse zone, strongly interfere on the creation of EDZ fractures. Numerous field observations indicate that tectonic faults control the initiation and localisation of EDZ fractures. For this reason, it is crucial to have a perfect knowledge of the tectonic pattern. Systematic small-scale mapping of the tunnel walls, floor and adjacent niches provides basic information about the geometry and kinematics of the geological fractures intersected in the underground rock laboratory. The observed tectonic faults can be divided into three different fault systems (Nussbaum & Bossart, 2008): i) SSE dipping faults (mainly formed by bedding-parallel slip during the folding of the Mont Terri anticline); ii) low

angle SW dipping fault planes and flat-lying SSE to S dipping fault planes and iii) N to NNE trending steeply inclined sinistral strike-slip faults. The three fault systems identified in the Mont Terri rock laboratory can be integrated into the surrounding map-scale structures in a coherent way.

The development and geometry of EDZ fracture network depend largely on the excavation direction in respect with the pre-existing faults. Tunnel orientation in respect with the bedding seems to play an important role due to the rock anisotropy. When the drift excavation is normal to the bedding and faults planes dipping with 45° to SSE, the chance to initiate EDZ fractures is quite limited since the rock anisotropy structure is perfectly oriented in the Coulomb criteria failure direction. These weakness planes are reactivated as shear fractures. Secondary EDZ fractures may develop below these fault planes. In turn, in sections where faults are scarce, whatever the excavation direction, well-developed EDZ fracture network is observed. However, Depending on the facies which is excavated, the occurrence of EDZ fractures may significantly change. In fact, the Opalinus Clay in the Mont Terri rock laboratory may be divided into three main facies: a shaly facies in the lower part of the formation (argillaceous and marly shales with micas and nodular, bioturbated layers of marls or with mm-thick layers of sandstones), a sandy facies in the middle and upper part of the formation (marly shales with layers of sandstones and bioturbated limestones, or with lenses of grey, sandy limestones and mm-thick layers of white sandstones with pyrite; and a thin carbonate-rich, sandy facies in the middle of the formation (calcareous sandstones intercalated with bioturbated limestone beds, the latter showing a high detrital quartz content). These facies are characterised by different uniaxial compressive strengths. The shaly facies presents the lower values of strengths, 10.5 MPa parallel to the bedding and 25.6 MPa normal to the bedding. This may be a reason to explain the occurrence of well-developed EDZ fracture network in gallery section excavated through the shaly facies. In turn, EDZ fractures in the sandy facies, characterised by an average value of uniaxial compressive strength of 35 MPa, are very scarce.

In conclusion, the pre-existing natural discontinuities such as well developed, inclined bedding planes and faults, seem to act as limiting structures (Figure 1). Mechanical characteristics of the facies which are excavated also influence the generation of EDZ fractures.

Figure 1. Relationship between a low angle natural thrust fault (upper) which limits a set of subvertical extensional EDZ fractures characterised by plumose structures (Photo: Comet, Photoshopping Zürich)

REFERENCES

Nussbaum, Ch. and Bossart, P. Geology. In Mont Terri Rock Laboratory. Project, Programme 1996 to 2007 and Results. (2008). Ed: Bossart, P. & Thury, M.: – Rep. Swiss Geol. Surv. 3.

2.43

Transition from frictional to viscous deformation in granitoid fault gouges

Peč Matěj *, Stünitz Holger **, Heilbronner Renée*

*Geologisch-Paläontologisches Institut, Bernoullistrasse 32, CH-4056 Basel (matej.pec@unibas.ch)
** Institutt for geologi, Universitetet i Tromsø, Dramsveien 201, 9037 Tromsø, Norway

Frictional movement on faults produces extremely fine-grained fault gouges and increases the permeability, thus enabling fluid flow. The fine grain size, together with the presence of fluids, is a potential precursor for the transition from frictional to viscous deformation in the fault gouge.

In order to investigate this switch in the dominant deformation mechanism, we performed a series of simple shear deformation experiments in a Griggs deformation apparatus. Crushed Verzasca Gneiss powder (grain size < 200 μm) with 0.2 wt% water added was placed between forcing blocks cut at 45° and weld-sealed in gold and platinum jackets. All the experiments were run at 500 MPa confining pressure and 300°C or 500°C.

The fine grain size is produced during the first part of the experiments by fast deformation (strain rate = 10^{-4} and 10^{-3} s^{-1}) to a gamma-value of up to 2.5. The material consists of a fine-grained gouge with a porosity of around 1%. Angular, extremely fine-grained particles (< 50 nm in size) are distributed throughout the shear zone. The amount of fine-grained material increases towards shear bands that develop at low angles to the shear zone boundary.

In the second part of the experiments we stopped the deformation at peak differential stress and allowed the stresses to relax over one week (case A). Alternatively, we lowered the peak differential stress to a level close to the confining pressure and kept it constant for one week (case B).

In case A experiments, we observe slow (creep) strain rates (as low as 10^{-8} sec^{-1}) and a temperature dependence of the creep rate. The stress drop of samples deformed at 500°C is larger (~200 MPa) and the displacement is higher (0.141 mm) compared to the samples deformed at 300°C (80 MPa and 0.110 mm, respectively). In case B, the amount of displacement accommodated by the samples is far smaller (total 0.01 mm at 500°C), it is at the limit of measurements that can be resolved with our current apparatus.

The microstructures in both case A and B experiments (fig. 1) are strikingly different from those deformed by friction only (fig. 2). We observe the disappearance of the finest grain size fraction, appearance of lobate interconnected grain boundaries and the cementation of multiple grains into bigger ones.

From these observations, together with the observed temperature dependence, we infer that the samples were deformed by solution – precipitation-creep processes. The exact nature of the creep deformation is difficult to assess at this stage, because the stress levels necessary to achieve creep in the experiments, so far, are above the Goetze criterion.

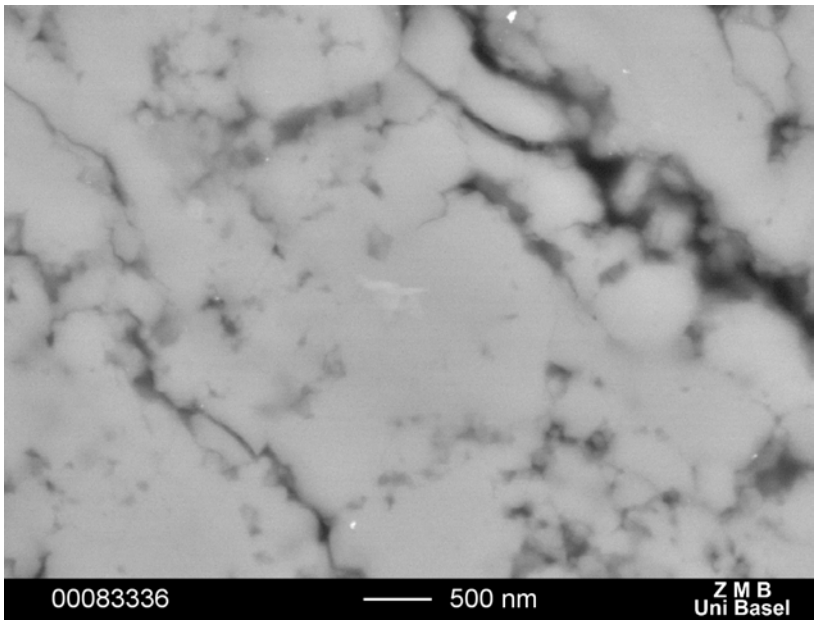

Figure 1: Fault gouge deformed by creep

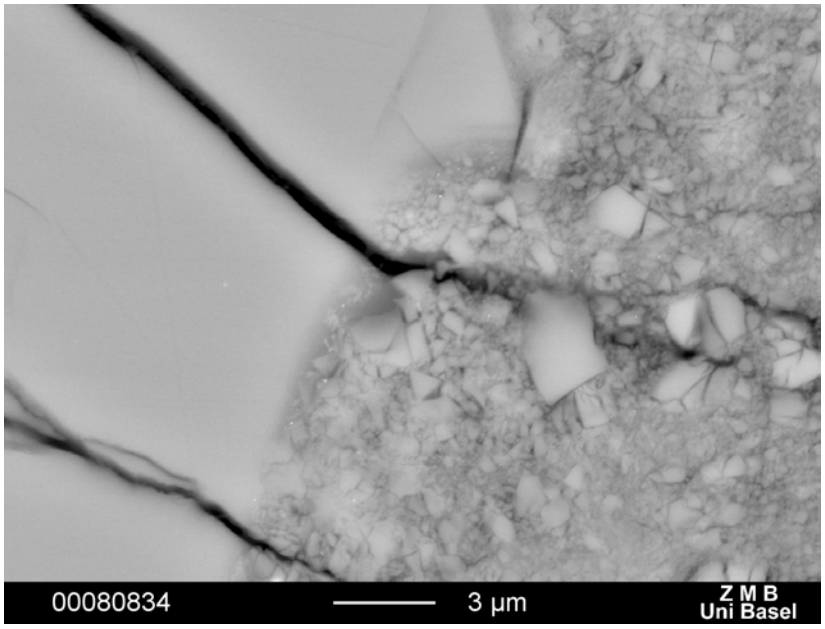

Figure 2: Fault gouge deformed by friction only

2.44

Structural observations from the Insubric fault between the Valle d'Ossola and Valle d'Orco (NW Italy)

Pleuger Jan* & Mancktelow Neil*

Geologisches Institut, ETH Zürich, Sonneggstraße 5, CH-8092 Zürich

The Palaeogene to Miocene Insubric fault zone (IFZ) separates the South Alpine domain from units that have been subducted during Alpine orogeny. From Valle d'Ossola to somewhat N of Serra d'Ivrea, the Southern Alps are typically represented by the Ivrea zone and the adjacent NW block by the Sesia zone. Further SW, the IFZ splits into the Internal and External Canavese faults (ICF and ECF). The Canvese zone *s.str.* occupies the position between the ECF and ICF and thus between the Sesia and Ivrea zones. Carbonatic lenses occuring sporadically further NE are referred to as Canavese *s.l.*.

The vertical displacement along the IFZ varies along strike and is largest S of the Lepontine dome. The horizontal displacement is estimated as ca. 30 km by Müller et al. (2001) and ca. 100 km by Schmid & Kissling (2004). The IFZ rocks show spatial and temporal variations in displacement sense and direction and of metamorphic conditions during movement.

Our observations from Valle d'Ossola largely agree with those of Schmid et al. (1987). The IFZ is a several hundred metres thick, moderately to steeply NW-dipping greenschist-facies mylonite zone, mostly with a NW-side-up shear sense. The NW-side-up mylonites are an axial-planar foliation S_1 of a first Insubric fold generation F_1. In the southern part of the IFZ, F_1 and S_1 are overprinted by a second fold generation F_2. Coming from the NW, F_2 first appears with axes that are parallel to a gently NE-plunging intersection lineation between S_1 and the F_2 axial-planar foliation S_2. As the intensity of D_2 increases toward the SE, the lineation clearly becomes a stretching lineation, the orientation plunges more steeply NE, and is associated with a SE-side-up and dextral shear sense.

Further SW in Valle Strona and Valle Mastallone, the volume of SE-side-up mylonites exceeds that of NW-side-up mylonites. In Valle Strona, the NW-side-up mylonites are more internal (SE) with respect to the SE-side-up mylonites contrary to what is observed in Valle d'Ossola and Valle Mastallone where the latter are mainly confined to mylonites derived from an Ivrea zone protolith. In Valle Mastallone, two generations of SE-side-up mylonites exist. The older generation, found near Rimella, has a NE-SW-trending stretching lineation and a dextral plus south-side-up shear sense. The dominant younger generation has an approximately down-dip (NW) orientation of the stretching lineation. These SE-side-up mylonites are locally overprinted by small-scale ductile to brittle, gently S-dipping, fault zones with a SE-directed normal sense of movement, and by a NNE-SSW-trending and steeply dipping sinistral mylonitic to cataclastic fault zone near Fobello.

Still further SW in Valle Sessera, cataclastic Insubric deformation becomes dominant over ductile shearing in terms of the affected rock volumes. The South Alpine rocks are locally affected by lower greenschist-facies mylonite zones. These are mostly only a few metres thick and both dextral and sinistral displacement senses are observed. The most characteristic cataclasite consists of a several tens of metres thick breccia with quartz-rich mylonite fragments. This mylonite is either com-

pletely reworked in the breccia or still preserved below the Early Oligocene andesites that are exposed between the breccia and the Sesia zone. The andesites occur along the IFZ from Valle Sessera to the S, until close to the Serra d'Ivrea. It is noteworthy that basement xenoliths within the andesites are exclusively derived from the Sesia zone, which implies uplift of the Southern Alps relative to the Sesia zone after andesite deposition. The breccia immediately SE of the andesites and the kakirites between the breccia and Ivrea zone probably developed during this uplift.

S of the Serra d'Ivrea, deformation along the ECF and ICF was mostly brittle. At the ECF, only rocks that can deform ductilely under relatively low temperatures, such as calcschist and serpentinite, were mylonitised. Such mylonites generally reflect W-side-up faulting with negligible horizontal components. Strike-slip faulting was mostly accommodated by later brittle faulting along the ECF. While the displacement sense of strike-slip motions along the ECF is ambiguous, the brittle to brittle-ductile fault rocks of the ICF consistently show combined E-side-up and dextral displacement.

The kinematic variations along-strike and across the IFZ may be integrated into the following simplified pattern. Vertical motions prevailed earlier in the IFZ history while strike-slip displacement became later more important. The combined displacement along the ECF and ICF resulted in a lowering of the Canavese zone *s.str.* with respect to both the Sesia and Ivrea zones. NE of Serra d'Ivrea, this lowering resulted in the downward disappearence of the Canavese zone, except for the sporadic carbonatic lenses of Canavese *s.l.*. Across the IFZ, the difference in metamorphic grade of fault rocks derived from the Sesia and Ivrea zones appears moderate. Therefore, the net vertical displacement between the two, resulting from the combination of NW-side-up and SE-side-up faulting, was probably also moderate. A large part of the exhumation of the high-temperature metamorphic rocks of the Lepontine dome may in fact be related to updoming in the core of the Vanzone antiform, rather than backthrusting along the IFZ. The amount of strike-slip displacement increases from SW to NE. While it is unclear if sinistral or dextral shearing prevailed in the Canavese, in Valle d'Ossola only dextral mylonites are found (though with varying horizontal components). Considering that the dominant D_1 N-side-up mylonites exposed there formed entirely under greenschist-facies conditions, without any synkinematic transition from higher or to lower metamorphic grade, the horizontal displacement of the D_1 and D_2 mylonites is unlikely to exceed a few tens of kilometres.

REFERENCES

Müller, W., Prosser, G., Mancktelow, N. S., Villa, I. M., Kelley, S. P., Viola, G. & Oberli, F. 2001: Geochronological constraints on the evolution of the Periadriatic Fault System (Alps). Int. J. Earth Sci., 90, 623-653.

Schmid S. M. & Kissling, E. 2000: The arc of the western Alps in the light of geophysical data on deep crustal structure. Tectonics, 19, 62-85.

Schmid S. M., Zingg, A. & Handy, M. 1987: The kinematics of movements along the Insubric Line and the emplacement of the Ivrea Zone. Tectonophysics, 135, 47-66.

2.45

Apatite FT data from the Triassic Songpan-Garzê flysch, Tibetan Plateau, NW Sichuan, China

Rahn Meinert* & Wang Hejing **

*ENSI, 5232 Villigen-ENSI, Switzerland (meinert.rahn@ensi.ch)
**School of Earth and Space Sciences, Peking University, Beijing 100871, P. R. China

Triassic flysches of the Songpan-Garzê orogen in Sichuan, Central China, cover an area of 5 times the size of Switzerland. Outcrops are located in the easternmost Tibetan Plateau, bordered to the west by the Longmenshan fault, site of the 2008 Wenchuan earthquake (Hao et al. 2009) Accumulated flysch sediments reach thicknesses of 15 km and have undergone upper diagenetic to lowermost greenschist facies conditions soon after deposition. The metamorphic and later exhumation history of the flysches was investigated by means of illite crystallinity (IC) e.g. Wang et al. 2008) and apatite fission track (FT) dating, with one sample profile extending across the Longmenshan fault system into the Sichuan basin.

48 apatite FT samples cover an age range between 3 and 136 Ma, suggesting that all samples are at least partially annealed (the youngest dated sediments are Jurassic). A marked correlation between IC and FT data reveal that the differences in recorded metamorphic grade at the present-day surface were significantly caused by differential exhumation, i.e. the structural evolution of the former flysch basin. One sample group of Late Miocene FT ages within the flysch coincides with a regional increase in metamorphic grade up to greenschist facies conditions.

Vertical profiles were investigated to study the tectono-thermal structure of the flysches during metamorphism and exhu-

mation. One vertical profile (2400-4100 m) shows a linear trend corresponding to a FT age gradient of 42 myr per km altitude. Regarding its track length and illite crystallinity data, the profile pattern is recognized as the lower part of an exhumed partial annealing zone. The lower end of the partial annealing zone is estimated at appr. 15 Ma, corroborated by the presence of similar ages further N. From the vertical thickness of the partial annealing zone (> 3km), the thermal gradient during apatite age reset must have been < 20°/km.

Two sample groups with reset Late Miocene to Pliocene apatite FT ages next to faults of the Longmenshan fault system confirm vertical offset of the eastern side blocks by tectonic activity. Areas of strong differential uplift contrast with the locality of the 2008 Wenchuan earthquake along the main fault line. Young uplift is here found further west of the main fault, where also a series of former earthquakes of slightly lower magnitude was recorded in the past.

REFERENCES

Hao K. X., Si, H., Fujiwara, H. & Ozawa T. 2009: Coseismic surface-ruptures and crustal deformations of the 2008 Wenchuan earthquake Mw 7.9, China, Geophysical Research Letters, doi:10.1029/2009GL037971.

Wang, H., Rahn, M., Tao, X., Zheng, N., Xu, T. 2008: Diagenesis and metamorphism of Triassic Flysch along profile Zoige-Lushan, Northwest Sichuan, China. Acta Geologica Sinica 82, 917–926.

2.46

Dynamic Topography Determination of the Western Mediterranean Sea from Jason-1 Data

Rami Ali*, Kahlouche Salem*, Khelif Mhamed**

(*) Centre of Space Techniques, PO Box 13, Arzew 31200 Oran Algeria (rami_alidz@yahoo.fr)
(**) Abou Bakr Belkaid University, Faculty of Science Engineering 13000 Tlemcen Algeria

The ocean has a major impact on earthly life and domestic needs; the emergence of satellite altimetry allows us a large contribution for most applications and oceanographic activities. In particular, the sea dynamic topography, which is the distance separates the geoid and the sea surface height and that reflects the dynamics of the ocean, is a primordial oceanography unknown.

The processing of jason-1 satellite data permit us to determinate the Mediterranean surface height, while using the global model of geoid "EGM2008" obtained from a combined data (GRACE, Terrestrial and altimetric measurements,....) we can calculate the sea dynamic topography.

The comparison of the obtained results with the data transmitted in the message of Jason-1 satellite allowed us the validation of the methodological approach developed.

REFERENCES

Darwin, G.H. (1883). Report on the Harmonic Analysis of Tidal Observation, Brit. Ass. for Adv. Sci. Rep.

Kahlouche, S., A. Rami, S.A. Ben Ahmed Daho (2003). Topex Altimetric Mean Sea Level and Gravimetric Geoid in the North of Algeria, International Association of Geodesy Symposia, Springer Verlag 126, PP ....– ISSN 0939-9585.

Lefevre, F. (2000). Modélisation des marées océaniques à l'échelle globale: assimilation de données in situ et altimétriques, Thèse d'état.

Newton, I. (1687). Philosophiae Naturalis Principia Mathematica, London.

Rami, A., Khelif, M., Kahlouche, S., Dennoukri., T. (2006). Estimation of the Sea State Bias Effect on the Altimetric Measurements Using a Parametric Model, In: Proc of the Symposium 15th Years of Progress in Radar Atimetry, SP-614 ESA Publication Division – ISBN 92-9092-925-1– ISSN 1609-042X.

2.47

Mirror denudation pattern on both sides of the Central Atlantic – a trace of the Pangea break-up?

Ruiz Geoffrey*, Sebti Samira**, Saddiqi Omar**, Negro François*, Stuart Fin***, Foeken Jurgen****, Stockli Dani*****, Frizon De Lamotte Dominique******

* IGH, E. Argand 11, CH-2009 Neuchatel (geoffrey.ruiz@unine.ch)
** Faculté des Sciences, Ain Chock, Casablanca-Morocco
*** SUERC, Glasgow-UK
**** FALW, Vrije Universiteit Amsterdam-NL
***** Dpt of Geology, Uni. Kansas - USA
****** Uni. Cergy-Pontoise-France

The target area of this project is the WSW- ENE oriented intra-continental Atlas chain in Morocco located between the West Africa Craton and the Betic-Rif system. It is a key natural laboratory because it 1) is the southernmost expression of Alpine deformation in Africa, and 2) encompasses Pre-Cambrian to recent evolution of the region. The presence of high surface elevations today in the High-Atlas (>4000m) and Anti-Atlas (>2500m) to the south is subject to discussions because there is little quantitative data available at present. Phases of uplift are thus ill constrained as places where the associated erosion products were accumulated.

To better constrain the most recent orogenic growth of the Atlas chain, we selected a section located to the SW of Morocco, and investigated the time-Temperature paths from the different morpho-structural domains using low-temperature thermochronology analyses. These are Fission-Track analysis on Apatite (120-60°C), Zircon (270-210°C) and U-Th/He analysis still on Apatite (80-45°C) and Zircon (200-170°C) minerals. Results are much contrasted from one domain to the other: Pre-Cambrian bedrocks from the Anti-Atlas domain yield old thermochronological Fission-Track ages on zircon (380-300 Ma) and apatite (180-120 Ma) minerals that are associated with slightly younger (U-Th)/He ages on apatite (150-110 Ma). U-Th/He ages on apatite from the High-Atlas are much younger (~35-5 Ma) with a clear alpine signature. Apatite Fission-Track ages from the Meseta region further north are also relatively old ranging between 200 and 140 Ma.

We here concentrate on the interpretation of old thermochronological ages from the Meseta and Anti-Atlas regions leaving the Alpine signal for another contribution. There are two direct, possibly inter fingering, interpretations for the preservation of such old thermal record in the Anti-Atlas and Meseta regions. First they remained “stable” being unaffected by 'Alpine' deformation that took place in the High-Atlas. Second, they are being affected “now” but no level with such record is yet exposed. Thermal modelling was performed to decipher between the 2 scenarios using our new thermochronological and available geological constraints. Models suggest that the first scenario is most likely with a clear Triassic to Late Jurassic phase of heating until ~100-90°C that was followed by a phase of cooling until the Middle Cretaceous. These results suggest that the Meseta was buried by a 2-3 kilometres thick sedimentary pile until ~180 Ma and as a result that the concept of a topographic high limiting the Tethysian from the Atlantic has to be reconsidered. Further, denudation patterns from the mirror image of the Atlas system on the other side of the Atlantic ocean are almost identical (Grist and Zentilli, 2003) suggesting that the patterns we constrained for the Triassic until Middle Cretaceous in SW Morocco have to be related to the break-up of the Pangea and oceanization in the Central Atlantic from ~180 Ma.

REFERENCES

Grist, A.M., & Zentilli, M. (2003). Post-Paleocene Cooling in the Southern Canadian Atlantic Region: Evidence from Apatite Fission Track Models. Canadian Journal of Earh Sciences, 40 (9), 1279-1297.

2.48

The Eastern Pelagonian metamorphic core complex (northern Greece): Structure and models

Schenker Filippo Luca*, Burg Jean-Pierre, Gerya Taras.

ETHZ, Department of Earth sciences, Sonneggstrasse 5, CH-8092 Zürich
**(filippo.schenker@erdw.ethz.ch)*

Geological mapping revealed a migmatitic dome in the footwall of a low angle detachment in the eastern Pelagonian region, to the north and east of the Aliakmon River artificial lake, in Greece. The dome dimensions are about 20 x 15 km with the long axis striking NNW-SSE. All lithologies show a penetrative foliation striking mainly NW-SE and dipping NE or SW, according to the dome flank. On the foliation plane a NE-SW stretching lineation is associated with sense of shear indicators. Systematic measurements average as follows: i) Top-to-the-SW sense of shear: Direction: 254°±15; Plunge: 12°±9, ii) Top-to-the-NE sense of shear: Direction: 47°±17; Plunge: 15°±13.
While the top-to-the-SW sense of shear is regional, top-to-the-NE shear refers to relatively narrow (20 to 100 m) shear zones. The most spectacular of these shear zones juxtaposes highly migmatitic orthogneisses against non migmatitic ones. In the migmatitic core both biotite orthogneisses and amphibolites (former basaltic dykes that have intruded into the crystalline basement) have undergone partial melting. Melting of the metagranite locally produced garnet + amphibole + melt, which would indicate Pressure-temperature conditions of 10-20 kb and <800-900°C respectively under water-saturated conditions. Zircon U-Pb dating from a migmatite on the northwestern flank of the dome suggests that melting took place at 137±1 Ma [Anders, 2007].
The results were the basis for numerical modelling of migmatite domes in extensional setting. We employed I2ELVIS, a numerical 2D computer code designed for visco-elasto-plastic rheology and using conservative finite differences method [Gerya, 2003a]. The model domain is 300 km wide and 160 km deep. It consists of four rheological layers representing upper crust, lower crust, lithospheric mantle and asthenospheric mantle. Changing parameters as extension rate, lithosphere thickness and geotherms points to the importance of partial melting in the lower crustal: (1) it maintains a flat Moho and (2) positive buoyancy of molten rocks enhances doming. PTt paths of model points are used to discriminate thermo-mechanical scenari of migmatitic core complexes.

REFERENCES

Anders, B., Reischmann, T. & Kostopoulos, D. 2007: Zircon geochronology of basement rocks from the Pelagonian Zone, Greece: constraints on the pre-Alpine evolution of the westernmost Internal Hellenides, Int J Earth Sci (Geol Rundsch), 96, 639-661.

Gerya, T. V. & Yuen, D. A. 2003a: Characteristics-based marker-in-cell method with conservative finite-differences schemes for modeling geological flows with strongly variable transport proprieties. Physics of the Earth and Planetary Interiors, 140, 295-320.

2.49

Formation of fold nappes in ductile multilayers: insights from numerical simulations

Schmalholz Stefan Markus

ETH Zurich, Geologisches Institut, Sonneggstrasse 5, CH-8032 Zurich (schmalholz@erdw.ethz.ch)

Fold nappes are large-scale recumbant folds that have most likely formed by dominantly ductile deformation. In the Western Swiss Alps, the Middle and Lower Penninic basement nappes as well as the Helvetic ones display, in most cases, the typical geometry and stratigraphy of fold nappes with a normal flank, a frontal part and an overturned limb (Escher et al., 1993). In contrast to fold nappes, thrust sheets lack an overturned limb and are characterised by a basal thrust or detachment surface (e.g. Epard and Escher, 1996). In the Swiss Alps, the core of fold nappes often consists of metamorphic basement surrounded by a sedimentary cover (e.g. Escher et al., 1993; Epard and Escher, 1996). Examples are the Morcle-Mont-Blanc nappe or the Antigorio nappe (e.g. Escher et al., 1993). Although fold nappes are frequent in the Swiss Alps and are a prominent feature in many mountain belts, there are only few studies that investigated the mechanical deformation processes acting during

the formation of fold nappes. Therefore, there are still many open questions concerning the controlling far-field deformation field (simple or pure shear), the rheology (e.g. Newtonian viscous, power-law or viscoplastic) and the impact of heterogeneities (e.g. effective viscosity ratio within sedimentary cover).

I present first results of finite element models simulating the formation of fold nappes in ductile multilayers. In these models the sedimentary cover is modelled with ductile multilayers exhibiting a power-law rheology and the basement is modelled with one thick layer having also a power-law rheology. The far-field deformation field is assumed to be simple-shear. The applied finite element method employs a Lagrangian formulation with re-meshing where the numerical grid is deformed with the calculated velocity field. This method ensures that the boundaries between the different layers (i.e. sedimentary units and basement) are accurately resolved during the entire large strain deformation.

Figure 1 presents the result of one particular simulation. Although the model is relatively simple the results already show several interesting features: a) the sedimentary layers are detached from the basement at several locations, b) folds of different size and order are formed, c) fold axial planes with different orientations are formed during one continuous deformation phase and d) recumbent folds with overturned limbs more or less parallel to the far-field simple shear direction are formed. Furthermore, in the middle of the model the multilayers formed a fold nappe which has an overturned limb, a frontal part and a normal limb.

The applicability of the presented numerical models to natural fold nappes in the Swiss Alps is discussed. Also, modelling approaches for a more realistic numerical modelling of fold nappes in the Swiss Alps are presented.

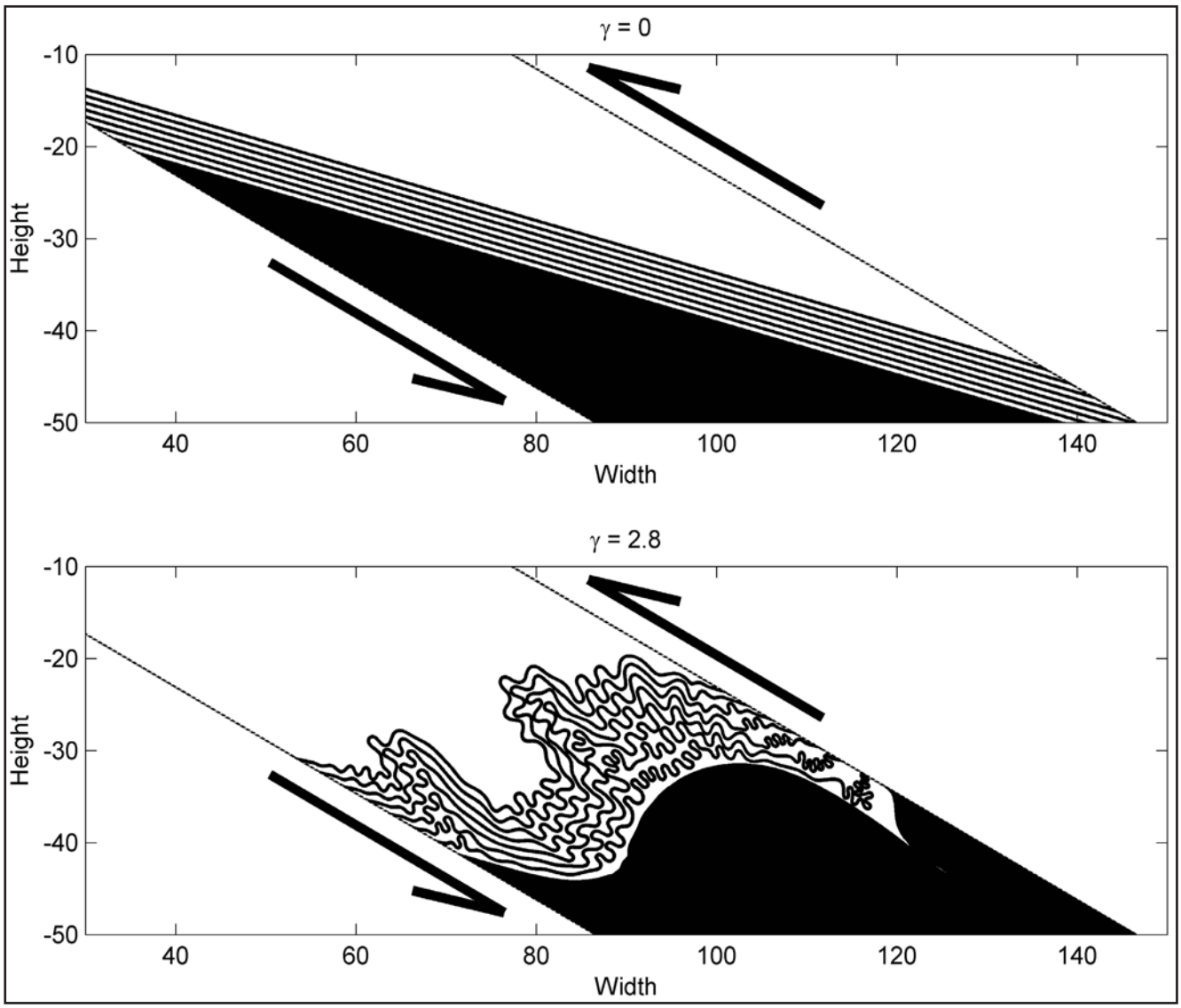

Figure 1. Numerical result for multilayer folding under far-field simple shear. A) Initial geometry. B) Geometry for a shear strain of 2.8.

REFERENCES

Escher, A., Masson, H. & Steck, A. 1993: Nappe geometry in the Western Swiss Alps, J. Struct. Geol., 15, 501-509.

Epard, J.-L. & Escher, A. 1996: Transition from basement to cover: a geometric model, J. Struct. Geol., 18, 533-548.

2.50

Two critical tapers in a single wedge

Jeroen Smit*, Jean-Pierre Burg* and Jean-Pierre Brun**

*ETH Zurich, Geological Institute, Sonneggstrasse 5, 8092 Zurich
** Géosciences Rennes, Université de Rennes 1, Campus de Beaulieu, Bat 15, 35042 Rennes, France

Thrust involving a ductile décollement (e.g. salt, over-pressured shales) like Zagros, Jura, Pakistan Salt Ranges, Cascades and Makran have in common a small cross-sectional taper, attributed to large thrust spacing and fast frontward propagation above the ductile décollement. Such a low cross-sectional taper has been analytically explained by approximating the ductile layer as a horizon with negligible shear strength.
We tested the development of thrust wedges involving a ductile basal décollement of uniform shear strength by means of laboratory experiments. The model consists of a sand layer with initial wedge geometry and a basal ductile décollement of constant thickness and shear strength made of silicone putty. 30% of bulk shortening is applied to the wedge at constant velocity. Thrusting starts in the middle of the wedge, followed by in-sequence frontward propagation. The back part of the wedge, between backstop and the closest thrust, remains undeformed; it passively advances over the base without internal deformation.
It appears that both domains have different critical tapers. The inner domain is in a critical state from the onset of shortening (i.e. the initial wedge is already critical), while the frontal domain steadily acquires a state of critical taper by thrusting. This result is at variance with the classical assumption that shortening of a wedge made of homogeneous layers creates a single critical taper. The experimental thrust wedges do show other features characteristic for weak décollement wedges like narrow cross-sectional taper, large thrust spacing and variety in thrust geometries. Application of the results to natural thrust wedges like the Jura Mountains could shed new light on their development and geometry at depth.

2.51

Modelling the thermo-chemical evolution of the interiors of Mercury, Venus, Earth, Mars and super-Earths

Tackley Paul, Keller Tobias, Armann Marina, van Heck Hein, Nakagawa Takashi

Institut für Geophysik, ETH Zürich, Sonneggstrasse 5, 8092 Zürich (ptackley@ethz.ch)

The latest generation of the global 3-D spherical convection model StagYY [Tackley, PEPI 2008] allows the direct computation of a planet's thermo-chemical evolution, including self-consistent lithospheric behavior (e.g., rigid lid, plate tectonics, or episodic plate tectonics [van Heck and Tackley, GRL 2008]), chemical differentiation induced by melting, large viscosity variations, a parameterized core heat balance, and a realistic treatment of phase diagrams and material properties. The latter has recently been added using free energy minimization to compute stable phases as a function of temperature, pressure, and composition as expressed by ratios of the five main oxides, and thus avoids the need for increasingly complicated and ad hoc parameterizations of phase transitions. Global models allow the computation of planetary secular cooling including prediction of how the core heat flux varies with time hence the evolution of the geodynamo, and possible transitions in plate tectonic mode. Modern supercomputers and clusters allow increasingly higher resolution, with up to 1.2 billion unknowns possible on only 32 dual-processor nodes of an opteron cluster. In ongoing research, this tool is being applied to understand the evolution of Earth, Mars, Venus, Mercury, and super-Earths. Studying several bodies using an integrated approach facilitates a more systematic and holistic understanding of planetary behaviour both inside and outside our solar system.

Our Mars models [T. Keller and P.J. Tackley, Icarus 2009] show that with an appropriate viscosity profile, convection rapidly develops a 'one ridge' planform consisting of a single ridge-like upwelling and small-scale downwellings below a stagnant lid, and that this produces a dichotomous crustal distribution that bears a striking first-order resemblance to the crustal distribution on Mars. The actual boundary of the crustal dichotomy on Mars is not hemispherical but rather like the seam on a tennis ball, and this is reproduced by our models, with the highland region being located above the upwelling. Furthermore, the elevation difference between the highland and lowland regions is very similar to that on Mars, although the average crustal thickness is higher than thought to be appropriate for Mars. In some calculations, the location of the upwelling subsequently migrates to the edge of the highland region, providing an explanation for Tharsis. Melting is found to have a dramatic influence on thermal evolution particularly during the early stages.

With our Venus models we are studing the modes of heat loss, the origin of the inferred surface age and understanding the admittance (gravity/topography) ratio. Of particular interest is whether a smooth evolution can satisfy the various observational constraints, or whether episodic or catastrophic behaviour is needed, as has been hypothesised by some authors. Simulations in which the lithosphere remains stagnant over the entire history indicate that over time, the crust becomes at least as thick as the mechanical lithosphere, and delamination occurs from its base. The dominant heat transport mechanism is magmatic. A thick crust is a quite robust feature of these calculations. Higher mantle viscosity results in larger topographic variations, thicker crust and lithosphere and higher admittance ratios; to match those of Venus, the upper mantle reference viscosity is about 10^{20} Pa s and internal convection is quite vigorous. The most successful results in matching observations are those in which the evolution is episodic, being in stagnant lid mode for most of the evolution but with 2-3 bursts of activity caused by lithospheric overturn. If the last burst of activity occurs ~1 Ga before present, then the present day tends to display low magmatic rates and mostly conductive heat transport, consistent with observations. In ongoing work we are examining the effect of crustal rheology and a more accurate melting treatment.

Due to the absence of an atmosphere and proximity to the Sun, Mercury's surface temperature varies laterally by several 100s K, even when averaged over long time periods. The dominant variation in time-averaged surface T occurs from pole to equator (~225 K). Here we demonstrate, using models of mantle convection in a 3-D spherical shell, that this stationary lateral variation in surface temperature has a small but significant influence on mantle convection and on the lateral variation of heat flux across the core-mantle boundary (CMB). We evaluate the possible observational signature of this laterally-varying convection in terms of boundary topography, stress distribution, gravity and moment of inertia tensor. In future we plan to test whether the lateral variation in CMB flux is capable of driving a thermal wind dynamo, i.e., weak dynamo action with no internally-driven core convective motions.

The discovery of extra-solar planets with terrestrial composition and sizes up to twice that of Earth, so-called "super-Earths", has prompted interest in their possible mantle dynamics and evolution. The pressure at the core-mantle boundary (CMB) of a 2* Earth-sized super-Earth is about four times the pressure at Earth's CMB, which has a strong effect on physical properties such as thermal expansivity, diffusivity and viscosity. The mantle of such a super-Earth would be made mostly of post-perovskite (PPv), which has different physical properties than perovskite, the major mineral of Earth's lower mantle. Here we use the newly-computed rheological parameters for PPv, computed using density function theory [Ammann, Brodholt and Dobson, 2008] in simulations of super-Earths of up to twice Earth size. The models assume a compressible anelastic approximation that includes the depth-dependence of material parameters. Rheological parameters for minerals other than PPv are based on those for perovskite. Plastic yielding at low pressures facilitates plate-like lithospheric behaviour. Results demonstrate that super-Earths are equally likely or more likely than an equivalent Earth-sized planet to be undergoing plate tectonics, and that the low viscosity of PPv has a strong and previously unseen effects on the mantle dynamics of super-Earths.

2.52

A numerical approach to test lithospheric cross-sections for geodynamic consistency

Thielmann Marcel*, Kaus Boris J.P.*

*(2) Geophysical Fluid Dynamics, Department of Earth Sciences, Sonneggstrasse 5, ETH Zurich, Zurich,

Cross sections though active mountainbelts are usually constrained by a range of geophysical and geological data, but the resulting interpretations are not necessarily geodynamically consistent. To better understand the thermomechanical behaviour of such collision zones it is of major importance to combine knowledge about the geometrical, the density and the inferred viscosity structure of those zones. Constraints on the geometry can be obtained by reflection seismics, refraction seismics or seismic tomography. Constraints on the density come from gravimetrical methods. Effective rheological parameters of the lithosphere, however, are much less known. Laboratory experiments on creep of rocks, extrapolated to natural conditions, yield several orders of magnitude variation in the effective viscosity. Better constraining the effective viscosity of the lithosphere is however crucial, since variations in these parameters might result in drastically different lithospheric dynamics.
For this reason, we here develop and test an approach that employs 2D thermomechanical viscoplastic geodynamics codes. Rather than studying the long-term deformation of the lithosphere, as is typically done with such codes, we here focus on the present-day structure of the lithosphere. The main assumptions are: 1) the present day geometry of the lithosphere (in particular surface topography and Moho depth) is reasonably well known. 2) Far-field plate velocities are known (from plate models or GPS measurements). The lithosphere is then divided into several layers. By varying the effective viscosity and

density of each of the layers, we can study the effects of changing these parameters on gravity, surface velocity, stress-distribution, and mantle flow.
A comparison of modelled data with observations would thus -in principle- give geodynamic constraints on the rheology of the lithosphere. Before applying it to real data, however, it is necessary to study the theoretical power of the methodology. For this reason we here apply the method to snapshots obtained from synthetic (million-year timescale) forward runs.

2.53

Interaction of H2O rich fluid inclusions and natural quartz crystals in deformation experiments

Thust Anja*, Heilbronner Renee*, Stuenitz Holger**, Tarantola Alexandre*** & Harald Behrens****

*Geologisch-Paläontologisches Institut, Bernoullistrasse 32, CH-4056 Basel (anja.thust@unibas.ch)
**Institutt for geologi, Universitetet i Tromsø, Dramsveien 201, N-9037 Tromsø
*** Faculté des Sciences, Université Henri-Poincaré, 54506 Vandoeuvre-lès-Nancy, France
****Institut für Mineralogie Universität Hannover, Callinstraße 3, D-30167 Hannover

The effect of H_2O on the strength of quartz is well known and has been discussed many times in the literatur (e.g. Grigge & Blacic 1965, Kronenberg & Tullis 1984, Kronenberg 1994). Here we study the H_2O interactions between natural dry quartz and H_2O rich fluid inclusions during deformation in the solid medium Griggs apparatus. The deformation experiments took place under a range of confining pressures (700MPa up to 1500 MPa), mostly at 900°C and strain rates of ~ 10^{-6} s^{-1}. We deformed cylinders of single crystal quartz that were cored in two different orientations (1) normal to one of the prism planes and (2) 45° to <a> and 45° to <c> (O^+ orientation). The strengths of the samples vary from 84 MPa up to 414 MPa, with the majority between 150 MPa and 220 MPa. Low strength can be explained by the formation of newly recrystallized grains and deformation by dislocation creep, higher strength correlates with a lower H_2O content and less deformation of the sample.
The H_2O rich fluid inclusions contain different chlorides like antarticite ($CaCl_2 \cdot 6H_2O$) and hydrohalite ($NaCl \cdot 2H_2O$), measured with micro thermometry; they range in size from 50 μm to 700 μm. After deformation the inclusions are more homogeneously distributed throughout the sample and dramatically reduced in size (< 0.1μm). Regions with a large change in size of fluid inclusions are the regions with the highest concentration of deformation (Fig.1). There is also a difference in fluid homogenisation for the two different orientations. In crystals with orientation normal {m}, the fluid distribution is more homogeneous and to a finer scale than in crystals of O^+ orientation.
After deformation the salinity of the fluid inclusions is increased, from ~10.6 wt.% equivalent NaCl up to ~12 wt.% equivalent NaCl.
The release of H_2O from fluid inclusions is an important process for crystal plastic deformation. Fluid inclusion rupture, micro cracking and the fast crack healing at these temperatures promote the distribution of H_2O through the quartz and influences the strength of the material.

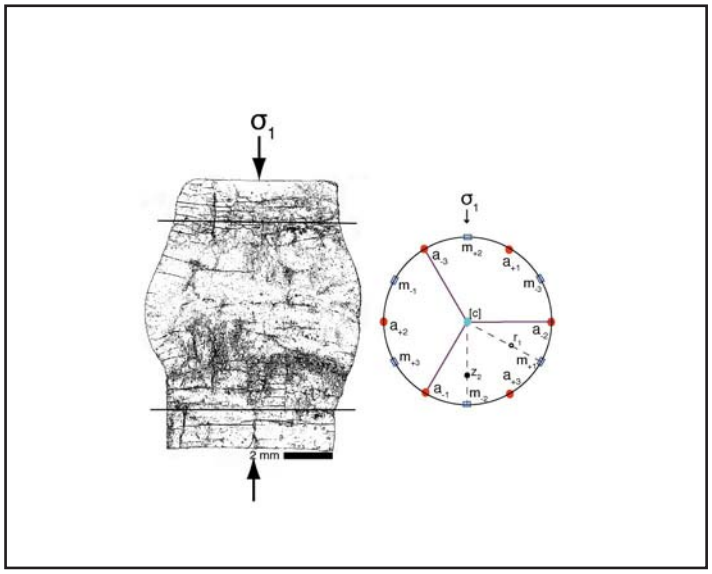

Figure1: Deformed sample in orientation normal to {m} (see stereoplot), the lines separate the highly deformed part in the middle, with a high fluid inclusion density from the +/- undeformed part at the ends.

2.54

The Lentas unit in Southern Crete: the base of the Pindos sedimentary series? – New paleontological results

Vandelli Alessia*, Vachard Daniel**, Martini Rossana***, Kozur Heinz W.****, Moix Patrice*, Stampfli Gérard M.*

* *Institut de Géologie et de Paléontologie, Université de Lausanne, Anthropole building, CH-1015 Lausanne (alessia.vandelli@unil.ch)*
** *Université des Sciences et Technologies de Lille 1, F-59655 Villeneuve d'Ascq Cedex, France*
*** *Département de Géologie et Paléontologie, Université de Genève, rue des Maraîchers 13, CH-1205 Genève*
**** *Rézsü u. 83, H-1029 Budapest, Hungary*

Crete is constituted by a complex nappe structure. Based on their tectonostratigraphic position and their tectonometamorphic history, these allochthonous units were subdivided into the upper and lower nappes, separated by a detachment fault. In the studied area in southern Crete, only the upper nappes are represented. In a structurally ascending order, these are (1) the Tripolitza platform, (2) the hemipelagic to pelagic Pindos domain, (3) the Arvi unit, (4) the Lentas series, (5) the Miamou mélange, (6) the metamorphic Asteroussia nappe and (7) the uppermost ophiolitic nappe (e.g., Davi & Bonneau, 1985). This tectonic pile could actually be prone to modifications. Our preliminary results focus on the Lentas and the Pindos units (Fig. 1).

In the Lentas series, reworked pebbles in a conglomerate above shallow-marine limestones yielded the first occurrence of late Kungurian (latest Early Permian) foraminifers and carbonate algae in Greece. *Praelikanella cretae* Vachard, Vandelli & Moix n. gen., n. sp. and *Uragiellopsis bonneauii* Vachard, Vandelli & Moix n. sp. are newly established. The identified assemblage belongs to the *Misellina parvicostata* Zone and has a North Paleotethyan signature. The pelagic limestones interstratified with siltstones and turbiditic sandstones with plants yielded several conodonts species typical for the Lacian (early Norian) *Epigondolella rigoi* Zone and the Sevatian (late Norian) *Mockina bidentata* Zone.

In the pelagic limestones at the base of the Pindos series (Fig. 1), we identified Late Triassic (Carnian-Norian) foraminifers including *Duostomina* sp., *Duotaxis* sp., *Endoteba* ex gr. *controversa* Vachard & Razgallah, *E.* ex gr. *obturata* (Brönnimann & Zaninetti), *Glomospira* sp., *Ophthalmidium* spp., *Trochammina* sp., *Glomospira* sp., Miliolidae and Nodosariidae. In the same succession, a conodont assemblage belonging to the *Mockina bidentata* Zone was sampled.

Our paleontological results in combination with field observations indicate a possible link between the Lentas and the Pindos successions. Because of ages and facies similarities with equivalent series in Greece and Turkey, we propose that the Lentas series forms the base of the Pindos sequence. Furthermore, we suggest that the pelagic limestones of the Pindos domain are an equivalent of the Drimos Fm., while the pelagic limestones alternating with sandstones and conglomerates in the Lentas sequence correspond to the Priolithos Fm. (cf. Degnan & Robertson, 1998). These series belonging to the passive margin of the Pindos Ocean are found all over the eastern Mediterranean area: the Pindos-Olonos series in the Peloponnese and in continental Greece, the Ethia and Mangassa series in Crete, the Köyce iz series in the Lycian Nappes, the Hu lu series in the Bey ehir-Hoyran Nappes and the Mersin mélange (all in Turkey). All of these nappes likely belong to the same paleogeographic domain (Hu lu-Pindos Ocean, Moix et al., 2007). In addition, the shallow marine late Kungurian sediments of Paleotethyan affinity reworked in the Lentas unit is compatible with the presence of reworked pelagic Famennian conodonts at the base of the Mangassa series in eastern Crete (Bonneau & Aubouin, 1987).

In conclusion, the Lentas and Pindos units belong to the same paleogeographic realm and represent the synrift series and the development of the passive margin of the Hu lu-Pindos Ocean, a back-arc basin of the Paleotethys.

REFERENCES

Bonneau, M., Aubouin,J., 1987. Des fossiles dévoniens remaniés dans le Trias supérieur de la zone du Pinde en Crète (Grèce) : indications sur la nature du substratum anté-Permien des zone helléniques externes. C. R. Acad. Sc. Paris, t. 304, Série II, n°2

Davi, E., Bonneau, M., 1985. Geological map of Greece, Andiskarion sheet 1:50000. Institute of Geology and Mineral Exploration (IGME).

Degnan, P.J., Robertson A.H.F., 1998. Mesozoic-Early Tertiary passive margin evolution of the Pindos Ocean (NW Peloponnese, Greece). Sedimentary Geology 117, 33-70.

Moix, P., Kozur, H.W., Stampfli, G.M. & Mostler, H., 2007. New palaeontological, biostratigraphic and palaeogeographic results from the Triassic of the Mersin Mélange, SE Turkey. In: Lucas, S.G. & Spielmann, J.A. (eds.). The Global Triassic. New Mexico Museum of Natural History and Science, Bull., 41, 282-311.

Vachard, D., Vandelli, A. & Moix, P., 2009: Discovery of the late Kungurian (latest Early Permian) in southern Crete (Greece); geological consequences. Geobios (submitted).

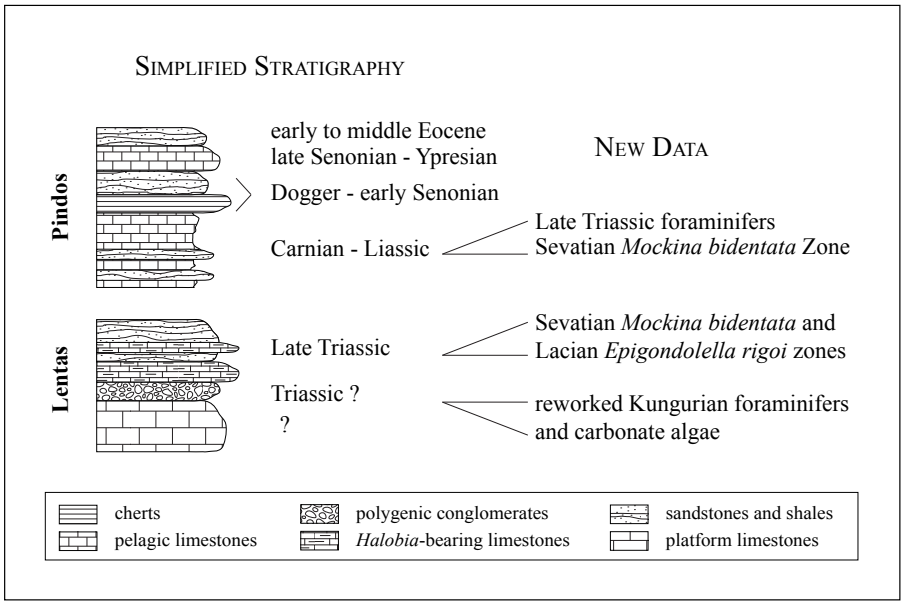

Fig. 1: Synthetic stratigraphic column of the Lentas and Pindos units

2.55

Modelling of silicic intrusions in Alpine type orogens

Vogt Katharina*, Gerya Taras*,**, Castro Antonio***

*Department of Earth Sciences, ETH Zürich, Sonneggstr. 5, 8092 Zürich, Switzerland (katharina.vogt@erdw.ethz.ch)
**Department of Geology, Moscow State University, 119199 Moscow, Russia
***Department of Geology, University of Huelva, 21071 Huelva, Spain

The emplacement of huge intrusive bodies such as batholiths is a fundamental issue in geology. To improve our understanding of the dynamics of batholith emplacements under an active continental margin, a set of numerical experiments have been performed using a 2D geochemical – petrological – thermomechanical numerical model. Based on finite differences and marker in cell techniques, the model simulates subduction of an oceanic plate beneath an active continental margin. The model includes spontaneous slab retreat and bending, dehydration of subducted crust, aqueous fluid transport, partial melting, melt extraction and melt emplacement.

A systematic parameter study has been carried out by varying the rheological weakening effect imposed by fluids and melts. Aqueous fluids percolating from the subducting slab into the mantle wedge mainly affect the forearc region, whereas extracted melts propagating from the mantle wedge toward the surface have a major impact on the lithosphere below the arc.

The results indicate that several tectonic regimes exist, some of which show the development of silicic plumes. It was found that the rheological weakening effect of melts and fluids is of major importance for the formation and emplacement of silicic plumes. As a function of fluid and melt weakening, silicic plumes may (1) ascend and intrude into the crust, (2) extend horizontally and remain beneath the continental lithosphere (underplating) or (3) be emplaced at a later stage. Strong fluid related weakening promotes stacking of sediments and therefore results in a large accretion wedge. In this case, insufficient sediments are being subducted and plumes do not form. Small amounts of fluid weakening, on the other hand, results in strong coupling of the subducting and overriding plates in a collision-like subduction setting. In this case, large quantities of sediments are being subducted and sedimentary plumes are formed. However, if the continental lithosphere is insufficiently weakened by extracted melts, these sedimentary plumes cannot ascend.

Our results thus suggest that batholiths may be the result of the emplacement of silicic plumes into the crust and their emplacement dynamics is strongly affected by the rheological weakening effect of fluids and melts.

2.56

Influence of thermal-chemical buoyancy in 3-D mantle wedge

Guizhi Zhu*, Taras V. Gerya*,**, Satoru Honda***, Paul Tackley*, David A. Yuen****

*Department of Geoscience, Swiss Federal Institute of Technology (ETH Zurich), CH-8092 Zurich, Switzerland (guizhi.zhu@erdw.ethz.ch)
**Adjunct Professor of Geology Department, Moscow State University, 119899 Moscow, Russia
***Earthquake Research Institute, University of Tokyo, Tokyo 113-0032, Japan
****University of Minnesota, Minneapolis, MN 55455-0219,USA

We use 3-D petrological-thermomechanical numerical simulations to investigate hydrous, partially molten, cold plumes originated from the subducting slab, which is favored by the lowered density and weakened rheological properties of the overlying mantle caused by the fluid release from the subducting slab.

The simulations were carried out with the I3ELVIS code [Gerya,2009], which is based on a multi-grid approach combined with marker-in-cell methods and conservative finite-difference schemes. The dynamics of the partially molten plumes is investigated in rheology-density space of the plumes, including the effective viscosity of the partially molten rocks and the density contrast due to compositional difference.

Lowered viscosity of the partially molten rocks atop the subducting slab favors the development of the cold plumes. Indeed,the plumes of 10^{19} Pa s viscosity are more powerful once the plumes start since they start later and accumulate more buoyancy than those of 10^{18} Pa s viscosity. Moreover, the notable difference in plume behaviors arises depending on the limitation for the melt-related density contrast (which simulates variable degree of melt extraction). Particularly, sheet-like plumes tend not to develop directly away from the subducting slab, but to move upwards along the slab if the density contrast is limited to 50-100 kg/m^3. Three patterns of plumes (finger-like plumes that form sheet-like structure parallel to the trench; ridge-like structures perpendicular to the trench; flattened wave-like instabilities propagating upwards along the upper surface of the slab and forming zig-zag patterns parallel to the trench) shown in previous work [Zhu, et al., in revision] occur for the models with density contrast >200 kg/m^3 and 10^{19} Pa s viscosity of partially molten rocks. Finger-like plumes develop in all of our models with density contrast >50 kg/m^3.
As a possible application of our 3-D numerical study to natural magmatic phenomena, we also compare space-time melt productivity pattern computed from the models with the distribution and evolution of volcanic activities in the intraoceanic setting.

REFERENCES

Gerya, T. V. 2009: Introduction to numerical geodynamic modelling, Cambridge University Press (in press), Chapter 14 and 15.

Zhu, G., Gerya, T.V., Yuen, D., Honda, S.,Yoshida,T.,Connolly,J.A.D. 2009: 3-D dynamics of hydrous thermal-chemical plumes in oceanic subduction zones. Geochem. Geophys. Geosyst. (in revision)

3. Mineralogy-Petrology-Geochemistry

Bernard Grobéty, Eric Reusser

Swiss Society of Mineralogy and Petrology (SSMP)

3.22 Márquez-Zavalía F., Heinrich C.A., Meier D.: Ore fluid evolution in a volcanic-hosted epithermal ore deposit: Farallón Negro, Argentina

3.23 Mattsson H., Bosshard S.: Columnar jointing and the formation of "chisel-marks" in the Hrossadalur lava flow, northern Iceland

3.24 Mattsson H., Reusser E.: Baggalútar from Hvalfjördur, SW Iceland: Volcanic spherulites or not?

3.25 Monnard H, Manzella I., Phillips J., Bonadonna C.: Convective Instabilities in Volcanic Clouds

3.26 Monsef I., Rahgoshay M., Emami M.H., Shafaii M.: Geochemical constraints on the development of a Mesozoic volcanotectonic arc and fore-arc basin in the Sanandaj-Sirjan Zone, south Iran

3.27 Monsef R., Emami M., Rashidnejad Omran N.: Transtensional basin system in Central Iranian Volcanic Belt

3.28 Moulas E., Kostopoulos D.: Metamorphic evolution of a kyanite-eclogite from Thermes, Rhodope Massif, Greece

3.29 Pistone M., Caricchi L., Burlini L., Ulmer P.: Rheological properties of crystal- and bubble-bearing silicic magmas: preliminary experimental results

3.30 Regis D., Manzotti P., Boston K., Cenki-Tok B., Robyr M., Rubatto D., Thomsen T., Engi M.: Complexities in the high pressure metamorphic history of the central Sesia Zone near Cima di Bonze (NW Italy)

3.31 Reitsma M., Schaltegger U., Spikings R., Carlotto V.: The temporal evolution of the Mitu group, south-east Peru - first U-Pb age data.

3.32 Rosa A., Sanchez-Valle C., Wang J., Saikia A.: Single-crystal elastic properties of superhydrous phase B determined by Brillouin scattering spectroscopy

3.33 Scalisi R., Costantini L., Bonadonna C., Di Muro A.: The influence of volatiles in basaltic explosive eruptions: the example of the Chaimilla eruption (3.1 Ka, Villarrica Volcano, Chile).

3.34 Semytkivska N., Ulmer P.: An experimental study in the system Fe-Mg-Ti-Cr-Si-O±Al: ilmenite solid solution as a function of pressure and temperature

3.35 Sergeev D., Dijkstra A.: Pyroxenite veins in the Jurassic Pindos Ophiolite (NW Greece): cm-scale mantle heterogeneity preserved in MORB-source peridotites

3.36 Shafaii H., Stern R., Rahgoshay M.: The Zagros Collision Zone: Petrological and geodynamical constraints on Inner and Outer Zagros Ophiolitic Belt

3.37 Skopelitis Al., Bachmann O.: The transition from cold-wet to hotter-drier rhyolites in subduction zones: the case of the Kos-Nisyros-Yali volcanic center, Aegean arc, Greece

3.38 Tercier-Waeber M.-L., Hezard T., Masson M.: Dynamics of Cd, Pb and Cu cycling in a stream under contrasting photobenthic biofilm activity and hydrological conditions.

3.39 Thomsen T., Pettke T., Allaz J., Engi M.: LAMBERN – software U-Pb, Th-Pb and Pb-Pb age dating by LA-ICP-MS analysis

3.40 Trittschack R., Grobéty B.: First insights into the dehydration of lizardite

3.41 Tsunematsu K., Bonadonna C., Falcone J.L., Chopard B.: Analytical and numerical description of tephra deposition: the example of two large explosive eruptions of Cotopaxi Volcano, Ecuador

3.42 Udry A., Müntener O.: Petrology of mafic-ultramafic complexes within the Archean Lewisian complex of NW Scotland

3.43 Vils F., Dijkstra A., Pelletier L., Ludwig T., Kalt A.: Iridium-strip heater glass pellets: Effects of fusion temperature and time on Li, Be and B content

3.44 Voegelin A., Samankassou, E., Nägler T.: Molybdenum isotopes in modern corals: investigation into their potential as redox proxy of bygone oceans

3.45 Wang J., Sanchez-Valle C., Stalder R.: Effect of minor elements (H^+ and Al^{3+}) on the elastic properties of orthopyroxenes

3.46 Wiederkehr M., Bousquet R., Masafumi S., Ziemann M., Berger A., Schmid S.: Deciphering the Alpine orogenic evolution from subduction to collisional thermal overprint: Raman spectroscopy and 40Ar/39Ar age constraints from the Valaisan Ocean (Central Alps)

3.47 Zurfluh F., Hofmann B., Gnos E., Eggenberger U., Opitz C.: Approximate terrestrial age dating of meteorites by use of handheld XRF

3.1

Apport des donnees des rayon x, de crystallographie et des inclusions fluides dans la determination de l'origine et la composition mineralogiques de la serie barytine -celestite du gisement d'Ain Allega. Tunisie septentrionale.

ABIDI Riadh *; SLIM-SHIMI Najet ** ; HATIRA Nouri *; MEJRI Zouhaier *

*: *Faculté des sciences de Bizerte, département de géologie, Jarzouna-Bizerte.7021. Tunisie.*
**: *Faculté des sciences mathématiques, physiques naturelles de Tunis. Campus Universitaire. 1060 Tunis. Tunisie.*
E.mail :abidi1riadh@yahoo.com ; najetshimi@yahoo.fr ; nouri_hatira@yahoo.fr ; mejrizouhair@yahoo.fr

Le gisement d'Ain Allega et de type « Cap-rocks » est situé sur la bordure orientale du diapir d'Ain Allega. La minéralisation est discordante par apport à la roche encaissante, elle se présente sous forme de ciment des brèches, sous forme de remplissage des fractures et des cavités de dissolution et sous forme de remplacement de la roche encaissante (Dolomie d'âge triasique). ce gisement présent une simple minéralisation composé par la galène, la saphalerite, la marcasite et la pyrite avec une gangue représenté par la barytine, la célestite, la dolomite, la calcite et le quartz. L'étude pétrographique des minéraux de la série barytine – célestite montre qu'ils possèdent plusieurs faciès en particulier microfibreux, saccharoïde, fibrolamellaire et prismatique.

L'étude radiocristallographique des minéraux de cette série barytine célestite ((Ba_X, Sr_{1-X}) SO_4) avec X [0-1]) prouve qu'on a une variété d'espèces de minéraux dont on a barytine pure (100% $BaSO_4$) abondant, célestite pur (100% $SrSO_4$) abondant, barytine srantianfère (85 to 96.5 % $BaSO_4$) minoritaire et célestite-baryfère (95% $SrSO_4$) minoritaire. Ces minéraux varie entre eux selon le degré de substitution de strontium (Sr) par le baryum (Ba) dans la celestite ($SrSO_4$) et le degré de substitution de baryum par le strontium dans la barytine ($BaSO_4$). Cette substitution est très bien visible dans les diffractogrammes au rayons X des minéraux de cette série qui est matérialisé par la variation de la position, l'intensité et la morphologie des raies 200, 011, 113, 312 de la barytine et la barytine strantianitère et les rais 410, 401 et 122 de la célestite et la célestite baryfére et aussi variation de la distance réticulaire du pic principal de la barytine de 3.44 à 3.42 pour la barytine strantianitère (fig.1).

L'étude des inclusions fluides contenues dans la célestite pur a montré que les inclusions primaire et secondaire monophasées à liquide sont les plus abondantes. Les mesures microthermométriques prouve que le fluide minéralisateur est d'origine hydrothermale et qui est caractérisé par une température d'homogénéisation élevais (180°C) et une salinité moyenne à élevais (16 % poids éq NaCl). Le rapport entre la température d'homogénéisation et la salinité (fig. 2) indique que la saumure de basin avec une certaine introduction de fluide de mélange magmatique - météorique était responsable de la minéralisation de minerai d'Ain Allega. La salinité élevée de cette solution ait résulté de la lixiviation et la dissolution des unités évaporitiques du Trias.

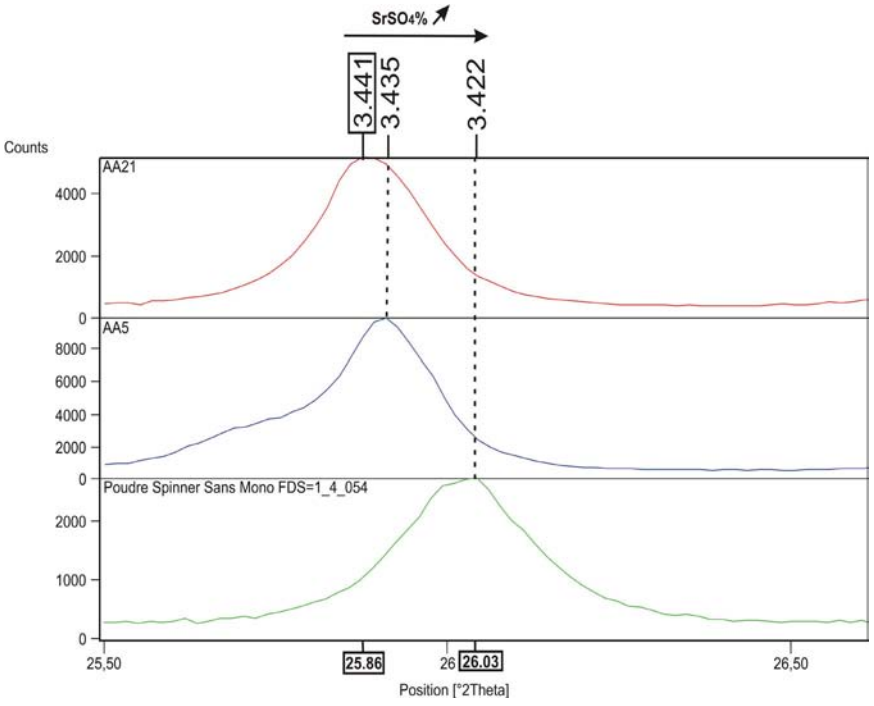

Figure. 1. Variation de la position du pic principal de la barytine en fonction du degré de substitution de Baryum par Strontium dans la barytine.

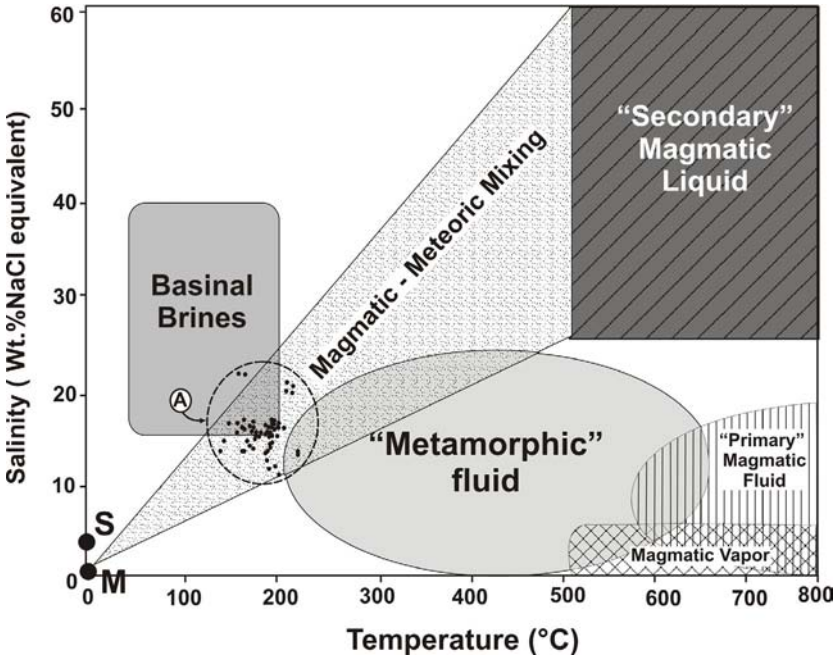

Figure.2. Diagramme de corrélation binaire température –salinité des inclusion fluides dans la célestite du gisement d'Ain Allega

3.2

Tephra Stratigraphy of the May, 2008, Chaiten Eruption, Chile

F. Alfano1, C. Bonadonna1, A. C. M. Volentik2, C. B. Connor3, S. F. L. Watt4, D. M. Pyle4, L. J. Connor3

1. Department of Mineralogy, University of Geneva, rue des Maraichers 13, CH-1205 Geneva, Switzerland.
2. Department of Geology and Geophysics, Volcanology, Geochemistry and Petrology University of Hawai'I, 1680 East-West Road, POST 614B, Honolulu, HI 96822
3. Department of Geology - SCA 528, University of South Florida, 4202 E. Fowler Ave., Tampa, FL, 33620, USA.
4. Department of Earth Sciences, University of Oxford, Parks Road, OX1 3PR, UK

Abstract. On May 2 2008 Mount Chaiten, located in the southern Chile, on the northern sector of Patagonia, after only 36 hours of precursory seismic activity, interrupted a long period of quiescence of more than 9000 years, producing his first historical eruption and causing the spontaneous evacuation of Chaiten village, located few km from the vent. The 2008 eruption of Chaiten is considered to be the largest volcanic event since the eruption of Hudson volcano (Chile) in 1991, and the first rhyolitic event since the eruption of Novarupta (Alaska) in 1912. The activity was characterized by several explosive events associated with plumes up to 20 km a.s.l. The products have been dispersed in a wide area (more than 200 km of distance from the crater), with the finest ash reaching the Atlantic coast of Argentina. Satellite images clearly show the developing of the counterclockwise rotation of the dispersal axis from SSE to NNE related to a shift in wind direction. Our field observations in the medial area (5-20 km from the vent) indicate that the May 2008 tephra deposit consists of numerous layers, most of which can be correlated with individual small explosions and subsequent fallout events. These layers vary from extremely fine-grained tephra to layers of lapilli and large blocks, composed of both juvenile and lithic material. In distal area (>200 km), the fallout deposit consists only of white to grey fine and coarse ash, eventually containing some accretionary lapilli. Although the May 2008 eruption was of moderate volume, tephra fallout had a substantial impact in terms of generation of lahars (in proximal-medial area, up to 20 km far from the vent), damage to vegetation (i.e. forests and crops) and remobilization of fine ash with effects to human and animals health. In this work we propose a reconstruction of the stratigraphy of the first events, which took place between 2nd and 8th May 2008 and a first physical characterization of the eruption. The medial stratigraphy associated with the four main explosive events could be recognized: 2nd-3rd May, 4th-5th May, 6th-7th May and 8th May, with an estimated cumulative volume of 0.118±0.057 km^3 (integration of power-law fitting) For the last event, represented by a layer composed mainly of lithic lapilli and blocks (>2 mm), an isopleth map was compiled and the associated plume height was determined. The plume is estimated to be about 19 km, when calculated considering the average of the geometric mean of the three axes of the 5 maximum clasts, and about 17 km, when calculated considering the geometric mean of the three axes of the 50th percentile clast. These values are close to the satellite observations for the event of the 8th May (i.e.about 20 km a.s.l.).

3.3

Metamorphic evolution of the Qinling Group, Qinling belt, east central China

Bader Thomas*, Franz Leander*, de Capitani Christian*, Ratschbacher Lothar**, Hacker Bradley R.***, Weise Carsten**, Wiesinger Maria**, Popp Michael**

*Mineralogisch-Petrographisches Institut, Universität Basel, CH-4056 Basel
(thomas.bader@unibas.ch)
**Institut für Geologie, Technische Universität Bergakademie Freiberg, D-09599 Freiberg
*** Geological Sciences, University of California, Santa Barbara, CA-93106

The Qinling Group, part of the Upper Proterozoic-Triassic Qinling belt, mainly comprises felsic gneisses, amphibolites and marbles. It can be subdivided into two parts. The northern margin experienced a Cambrian ultrahigh-pressure metamorphism as evident by the occurrence of diamond inclusions in metamorphic zircon (Yang et al., 2003). The central-southern part was affected by migmatisation within a Devonian magmatic arc caused by a northward trending subduction zone facing the Qinling orogen (Ratschbacher et al., 2003, for a review). Few data on the metamorphic evolution of the southern part of the Qinling Group were published by You et al. (1993) while such data are lacking for the northern margin. In the current study, we present new petrologic data for both parts derived by means of equilibrium phase calculations and conventional geothermobarometry combined with $^{40}Ar/^{39}Ar$ and Th/Pb geochronology.

Eclogites from the Northern margin of the Qinling Group are fine to medium-grained, weakly foliated rocks that occur as lenses with diameters up to 2m mantled by phengite gneisses. Texturally, our samples give indications for the UHP event by numerous radial cracks around quartz inclusions in garnet pointing to former coesite. The assemblage of the pressure peak comprises garnet (core) – omphacite – coesite – phengite – rutile. However, modelling using the DOMINO program and the application of conventional geothermobarometers yielded quartz-eclogite facies conditions of ~ 600 °C at 1.8-2.2 GPa representing an early exhumation stage. The exhumation history of the eclogitic rocks is further constrained by the late amphibolite facies mineral assemblage garnet (rim) – amphibole – plagioclase – quartz – ilmenite pointing to ~650 °C at 1.0-1.4 GPa. This was verified by conventional thermobarometry on garnet amphibolite 75221 C and garnet gneiss 75214D from the same unit pointing to 630-660°C at 1.0 GPa (fig. 1, left).

The central and southern parts of the Qinling Group reveal high-grade metamorphic PT conditions as evident by migmatisation of felsic gneisses. Peak metamorphic assemblages in metapelitic gneisses comprise garnet – plagioclase – K feldspar – quartz – sillimanite – ilmenite and garnet – hornblende – plagioclase – quartz – ilmenite in metabasites. PT estimates using the DOMINO program and conventional geothermobarometry point to 600-730 °C at 0.3-0.7 GPa (fig. 1, right). The lower PT conditions are interpreted to indicate a retrograde development of the metamorphism. No indication of eclogite facies metamorphism was found in the gneisses and amphibolites. However, the finding of a small body of strongly overprinted spinel peridotite in the southern part of this profile, which had re-equilibrated to 630-670 °C (i.e. identical temperatures to the surrounding gneisses and amphibolites), points to a probable early HP event.

$^{40}Ar/^{39}Ar$ dating of phengites from the northern margin of the Qinling Group yields 470±1 Ma. Significantly younger ages were obtained by dating metamorphic monazite (Th/Pb, 340-395 Ma), hornblende ($^{40}Ar/^{39}Ar$, 373-395 Ma) and biotite ($^{40}Ar/^{39}Ar$, 330-390 Ma) from the central and southern Qinling Group.

These findings prove that the exhumation of the UHP metamorphics took place in Early- to Mid-Ordovician. The rocks of the central-southern Qinling Group underwent a Devonian ultra metamorphism in the middle crust within a magmatic arc setting with high heat flow. Further investigations will show, how both subunits had been juxtaposed.

REFERENCES

Ratschbacher, L., Hacker, B.R., Calvert, A., Webb, L.E., Grimmer, J.C., McWilliams, M., Ireland, T., Dong, S. & Hu, J. 2003: Tectonics of the Qinling Belt (Central China): Tectonostratigraphy, geochronology, and deformation history. Tectonophysics 366, 1-53.

Yang, J., Xu, Z., Dobrzhinetskaya, L. F., Green II, H. W., Pei, X., Shi, R., Wu, C., Wooden, J. L., Zhang, J., Wan, Y., Li, H., 2003: Discovery of metamorphic diamonds in central China: an indication of a > 4000-km-long zone of deep subduction resulting from multiple continental collisions. Terra Nova, 15, 370-379.

You, Z., Han, Y., Suo, S., Chen, N. & Zhong, Z., 1993: Metamorphic history and tectonic evolution of the Qinling Complex, eastern Qinling Mountains, China. Journal of metamorphic Geology, 11, 549-560.

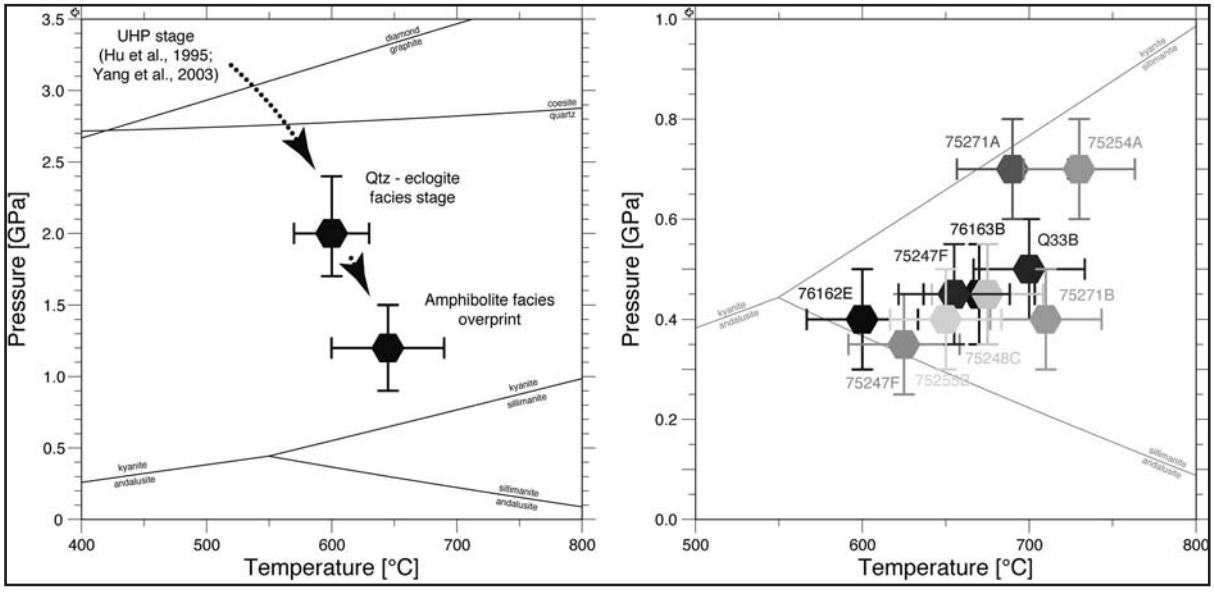

Figure 1: left: Metamorphic development of the northern margin of the Qinling Group. Right: PT estimates of the central-southern Qinling Group.

3.4

Stable isotopes in precipitation as proxies for the Neogene topographic and climatic evolution of the Alps

Bauer Kerstin*,**, Vennemann Torsten*, Mulch Andreas**

*Institut de Minéralogie et Géochimie, Anthropole, Université de Lausanne, CH-1015 Lausanne, Switzerland (Kerstin.Bauer@unil.ch)
** Institut für Geologie, Leibniz Universität Hannover, Callinstr. 30, 30167 Hannover, Germany

The paleoelevation of a mountain belt is an important parameter to understand its evolution and sets constraints on uplift and erosion rates and also on the paleoclimate. A quantitative tool to determine this is the altitude effect on the stable isotope composition of precipitation, since the $\delta^{18}O$ and δD values in precipitation decrease with elevation.

Precipitation of the past can be preserved in surface-formed hydrous silicates and also, after infiltration via faults and shear zones, in metamorphic minerals which interacted with meteoric water and/or trapped this water as fluid inclusions.

This study aims to reconstruct the changes in isotopic composition of precipitation and thus palaeoelevation of the European Alps during the Miocene. Therefore, isotopic compositions of minerals derived from surface alteration and/or fault gauges of different localities in the Alps will be studied.

To obtain a correction for the climatic conditions which can also change the $^{18}O/^{16}O$ and D/H ratios, low elevation material from the Alpine foreland covering the same time period will also be analyzed. Clay minerals from the Molasse basin appear to be promising material and paleoclimate information derived for sea level conditions from several of these layers already exist from studies of marine fossils.

Additionally, samples will be analyzed from present soil horizons to further examine the local dependences of isotopic variations with elevation and the uptake of the isotopic composition from rainwater into the minerals formed.

REFERENCES

Janz, H. & Vennemann, T. W., 2005: Isotopic composition (O, C, Sr and Nd) and trace element ratios (Sr/Ca, Mg/Ca) of Miocene marine and brackish ostracods from North Alpine foreland deposits (Germany and Austria) as indicators for paleoclimate. Palaeogeography, Palaeoclimatology, Palaeoecology 225 (2005), 216-247.

Kocsis, L., Vennemann, T. W., Hegner, E., Fontignie, D., & Tütken, T., 2009: Constraints on Miocene oceanography and climate in the Western and Central Paratethys: O-, Sr-, and Nd-isotope compositions of marine fish and mammal remains. Palaeogeography, Palaeoclimatology, Palaeoecology 271 (2009), 117-129.

Mulch, A., Teyssier, C., Cosca, M. A., Vanderhaeghe, O., & Vennemann, T. W., 2004: Reconstructing paleoelevation in eroded orogens. Geology 32, 6 (2004), 525-528.

Mulch, A. & Chamberlain C. P., 2007: Stable Isotope Paleoaltimetry in Orogenic Belts – The Silicate Record in Surface and Crustal Geological Archives. Reviews in Mineralogy & Geochemistry 66 (2007), 89-118.

3.5

Mineralogy, Fluid inclusions and sulphur isotope investigation of the Pb-Zn-Ba-(Sr) deposits at Oued Jebs-Kef Lasfar, North Tunisia

Jaloul BEJAOUI *, Ahmed SELLAMI ** and S. A. SKAGGS ***

* *Centre National des Sciences et Technologies Nucléaires, Tunisie, bjaoui_geo@yahoo.fr*
** *Office National des Mines, Tunisie*
*** *Department of Geology, University of Georgia, 210 Field St, Athens, GA 30602, USA*

The Oued Jebs-Kef Lasfar Pb-Ba-Zn-(Sr) deposit is located in northern Tunisia, 60 Km from Tunis (Fig.1). Sulfides mineralization is mainly associated with Cenomanian-Turonian inter-layered limestone and marls of the Cretaceous, which replace carbonate, cemented breccias and cavities (Fig.2).

The geology of the area is dominated by massive limestone and marly limestone units of Cretaceous age, which are extensively folded. The ore deposit consists of a system of mineralized veins and breccias, extending over an area of 15 km^2. The ore-hosting limestone layers are characterized by a strong kaolinite enrichment, in amounts directly related to the proportion of the ore minerals.

The mineralization lies mainly within the organic-rich black shale succession of the Bahloul Formation (Cenomanian-Turonian) and to a lesser extent along the transition zone between Triassic and Cretaceous), where zebra-textured celestite layers also occur (Fig. 3). The celestite-calcite rhythmites, whose structure is caused by grain size variation, occur mainly around the rising salt diapirs.

Kaolinite is associated with hydrothermal mineralization and occurs in the paragenesis of the sulfides in breccias (Fig.3).

The mineralogical characteristics of kaolinite were determined by X-ray powder diffraction and they are 7,15A° (d001) and 3,57A°(d002) and is attenuated after heating. Treatment with ethyl-glycol had no effect.

Fluid inclusions were investigated in hydrothermal barite associated with sphalerite and galena. All the observed fluid inclusions are two-phase liquid and vapor inclusions, but the aqueous fluid inclusions in barite which could be analysed, range in size from 20 to 100 μm.

Primary inclusions exhibit homogenization temperature (Th) mean values ranging from 110°C to 140°C, with salinities of 14 to 18 wt. % NaCl equiv. The microthermometric data are in agreement with those measured in the Jebel Ajered Pb-Zn-Ba ore deposit (Bejaoui et al., 2008).

Microthermometric data of fluid inclusions reveal the involvement of basinal brines in mineralization of Oued Jebs. $\delta^{34}S$ values in sphalerite and galena at Oued Jebs-Kef Lasfar range from 0.7‰ to 5.3‰. These positive values suggest an origin from evaporite sulfates, followed by thermochemical reduction (Claypool et al., 1980).

The present fluid inclusions study demonstrates the involvement of basinal brines in mineralization of Oued Jebs-Kef Lasfar.

Key words: basinal brines - Oued Jebs-Kef Lasfar - Fluid inclusions- Pb-Zn-Ba-(Sr).

Acknowledgments
We are grateful to Pr. Maria BONI for helpful comments and suggestions.

REFERENCES

Bejaoui J., Bouhlel S., Cardellach E., and Piqué À. (2008) - Mineralogy and fluid inclusion study of carbonate hosted Pb-Zn-Ba-(Cu) deposits in Jebel Ajered, Central Tunisia. 6 Swiss Geoscience Meeting (SGM) 2008, 173-175.

Claypool G.E, Holseer W.H., Kaplan I.R., Sakai H., and Zak I. (1980) - The age curve of sulphur and oxygen isotopes in marine sulphate and their mutual interpretation. Chem. Geol., 28, 163-187.

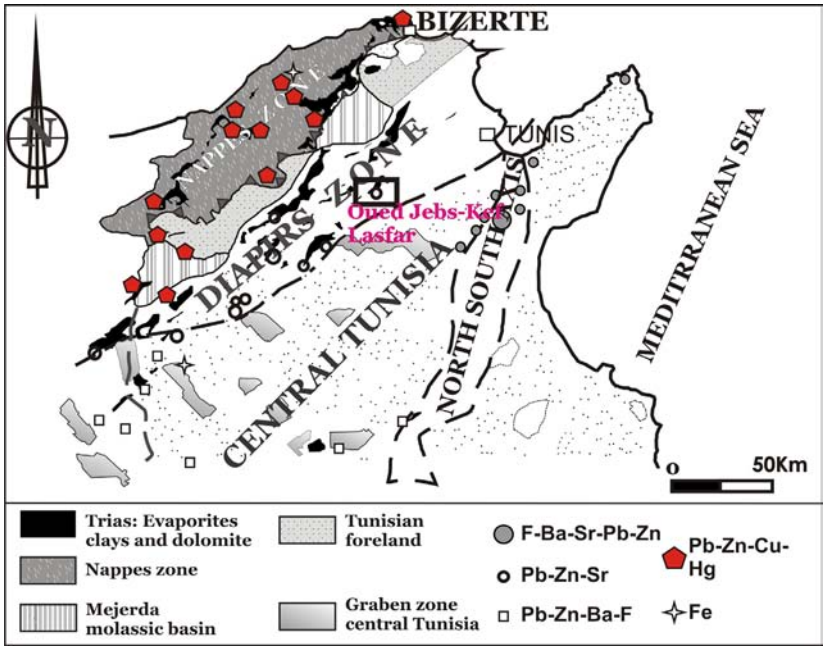

Fig 1. Location of the Oued Jebs ore deposit within the diapirs zone in Tunisian structural map.

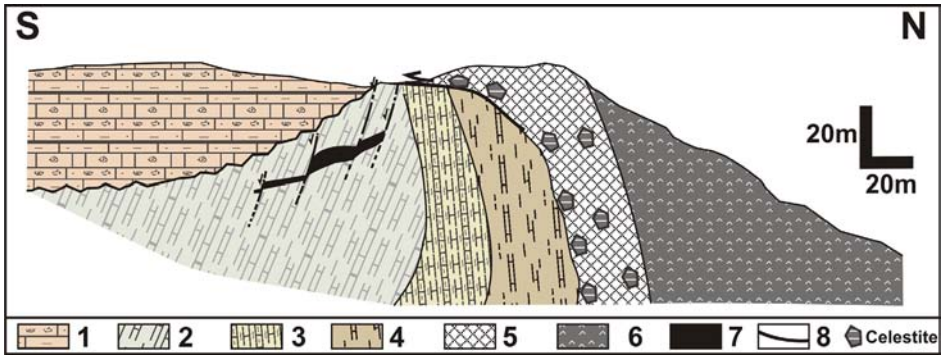

Fig 2. Cross section of Oued Jebs Pb-Zn-Ba-(Sr) ore deposits. : 1 Eocene: bioclastic limestone and marls, 2 Cenomanian-Turonian: marly limestone, 3 Albian: marl and limestone, 4 Aptian: carbonate series within silty clay layers. 5 transition zone: marls and dolomite-rich "zebra" celestite, 6 Trias: evaporites, 7: Pb-Zn-Ba-(Sr) orebodies, 8 faults.

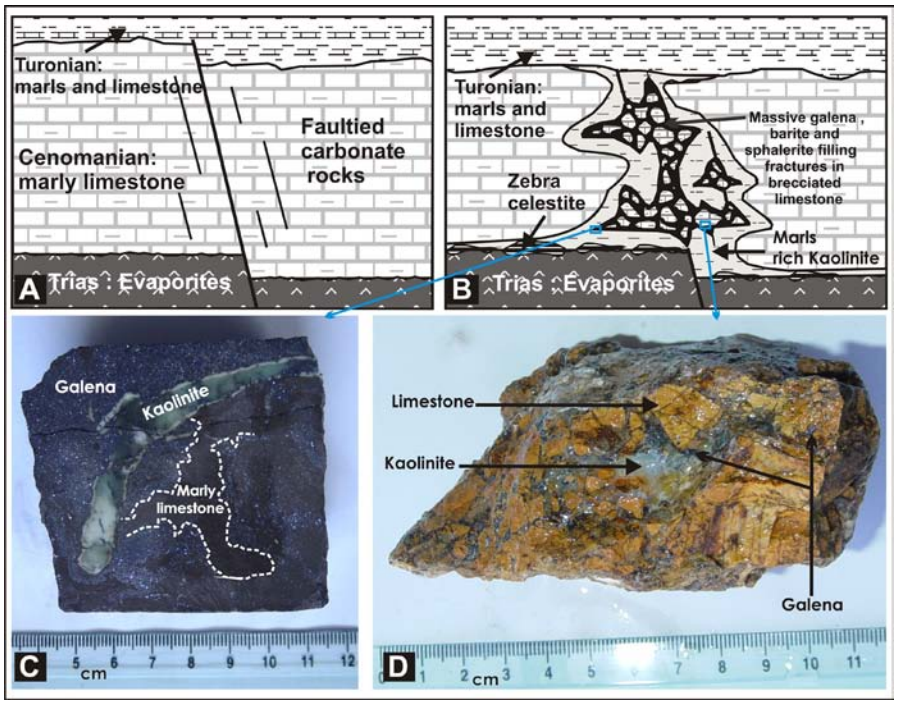

Fig 3. A Cenomanian limestone affected by fault and fractures, B Mosaic breccias cemented by sulfides mineralization, C Marls rich in kaolinite mineralized with massive galena, D Mosaic breccias cemented with kaolinite and disseminated galena.

3.6

Geology and geochronology of the Ilo batholith of southern coastal Peru

Boekhout Flora*, Thierry Sempere**, Richard Spikings*, Urs Schaltegger*

*Earth and Environmental Sciences, Rue de Maraîchers 13, CH-1205 Genève
**IRD et LMTG, 14 Avenue Edouard Belin, 31400 Toulouse, France

In Southern coastal Peru the so-called Ilo batholith is emplaced in the 'Chocolate' formation, of Early to Middle Jurassic age, that comprises more than 1000 m of basaltic and andesitic flows, agglomerates and breccias. Previous workers have correlated the dioritic to granodioritic rocks of this intrusion with the 'Coastal Batholith' of Cretaceous to Paleogene age. However, K-Ar and Ar-Ar geochronology of plutonic rocks near the city of Ilo point to Early Jurassic ages (Clark et al. 1999, Sánchez 1983a). This part of the plutonic assemblage was thus emplaced prior to the initiation of 'Coastal batholith' emplacement.
Mafic and felsic granitoid magmas are intimately associated, as reflected by the emplacement of mixed diorite-granodiorite units. Also, mafic and felsic magma mingling north of Ilo have been observed, e.g. globular enclaves of diorite in granodiorite, elongated inclusions, both basaltic and composite (basaltic/dacitic) synplutonic dikes: thus no simple mafic to felsic intrusive sequence prevailed during batholith construction.
Our aim is to describe and interpret the history of the Ilo batholith and to discuss how the magmatic history of this batholith fits into the framework of magma genesis and modes of emplacement along the active Andean margin. This first occurence of large volumes of plutonic rocks may well represent the first stages of Andean subduction (Oliveros et al. 2006).
A combination of field observations, zircon U-Pb (LA-ICP-MS and CA-ID-TIMS) data, and element geochemistry of the batholith will be used to distinguish between different magmatic pulses and their duration. Additional Sr, Nd, Pb, Hf isotope studies will be carried out, specifying the magmatic source of the different pulses of plutonic activity.

Eastward tilting of 20-30° has exposed a complete cross-section of the batholith in map view with an north-northeastward paleo-up direction, revealing that the Ilo batholith has a tabular shape: We are therefore able to study the contact with the Chocolate formation above and below the batholith, including a sampling campaign along several cross sections through the batholith for dating and geochemical analyses.
In addition to samples from the batholith itself, clastic sedimentary rocks above and below the batholith have been sampled in order to determine their maximum depositional age by dating detrital zircons using LA-ICP-MS. In this case the same or very similar detrital zircon populations should be found in both locations (below and above the tabular plutonic body), as they were originally juxtaposed.

Preliminary data of 3 samples dated by U-Pb TIMS show a pulse of magmatism at ~164 Ma with an epsilon Hf ranging from +4 to +6.9 indicating a depleted mantle source typical of continental margin settings. The geochemical data suggest a calc-alkaline magma source.
McBride et al (1983) postulated two intrusive pulses on the basis of six conventional K- Ar dates on four granitoid samples in the Ilo area of Late Jurassic (ca. 151 – 159 Ma) and mid- Cretaceous (96 – 111 Ma). Sánchez (1983a) obtained similar Albian K-Ar dates for several granodioritic samples northeast of Ilo but also found Early to Middle Jurassic dates (196-182 Ma) for two dioritic rocks from the coastal zone.
Our preliminary data might indicate another magmatic pulse, or show a longer duration of one of the previously decribed pulses.

REFERENCES

Clark Alan H, Farrar Edward, Kontak Daniel J., Langridge Robert J. 1999: Geological an Geochronological Constraints on the Metallogenic Evolution of the Andes of Southeastern Peru, Economic Geology, 85, 1520-1583.

Oliveros Veronica, Féraud Gilbert, Aguirre Luis, Fronari Michel, Morata Diego 2006 : The Early Andean Magmatic Province (EAMP) : 40Ar/39Ar dating on Mesozoic volcanic and plutonic rocks from the Coastal Cordillera, northern Chile, Journal of Voclanology and Geothermal Research, 157, 311-330.

McBride, S.L., Robertson, R.C.R., Clark, A.H., and Farrar, E. 1983: Magmatism and metallogenetic episodes in the northern tin belt 'Cordillera Real' Bolivia, Geol. Rundschau, 72, 685 – 713.

Sánchez, A. W., 1983: Edades K-Ar en rocas intrusivas del area de Ilo, Dpto. de Moquegua, Geol. Soc. Peru Bol, 71, 183 – 192.

3.7

Melt inclusions from Volcan Llaima (38.7°S, Andean Southern Volcanic Zone, Chile): Insights into shallow magma storage and crystallization

Bouvet de Maisonneuve Caroline*, Dungan Michael*, Bachmann Olivier** & Burgisser Alain***

* *Département de Minéralogie, Rue des Maraîchers 13, CH-1205 Genève (caroline.bouvet@unige.ch, Michael.Dungan@unige.ch)*
** *University of Washington, Earth and Space Sciences, Seattle, WA 98195-1310 (bachmano@u.washington.edu)*
*** *Institut des Sciences de la Terre d'Orléans - CNRS, Fr-45071 Orléans (burgisse@cnrs-orleans.fr)*

Olivine-hosted melt inclusions in scoria from four large historic eruptions of Llaima are used to elucidate processes of magma differentiation, recharge, mixing, and eruption triggering. These deposits were produced as violent Strombolian eruptions of crystal-rich mafic magma (<6 wt% MgO; 25-45% plag+oliv±cpx) associated with voluminous lava flows. Major element melt inclusion compositions are highly diverse in single samples (50-58 wt% SiO_2; 6-3 wt% MgO). These overlap with the whole-rock data trend defined by the entire volcano up to 53-55% SiO_2, but more evolved compositions form a divergent, linear trend up to >2 wt% TiO_2 with Al_2O_3 as low as 12.5 wt% at 57-58 wt% SiO_2, compared to 1.2-1.4 wt% TiO_2 and 16-17 wt% Al_2O_3 at 58 wt% SiO_2 in most Llaima andesitic magmas. The evolved extension of the melt inclusion trend is inferred to be the product of shallow evolution of interstitial melt during the formation of crystal mush as a consequence of degassing and decompression crystallization following magma stagnation. The suppression of FeTi-oxide stability and the dominance of plagioclase crystallization are consistent with low-P dry conditions. These observations are in accord with relatively low H_2O (dominantly 1-3.5 wt%) and CO_2 (dominantly 0-300 ppm) contents in melt inclusions (SIMS-ASU), which yield saturation pressures of ~300-500 bars (<2 km). H_2O and CO_2 contents do not correlate with major element melt composition, and melt inclusion fluid-saturation pressures do not correlate systematically with fractionation indices such as K_2O or Mg#. Corollaries to these observations are that degassed matrix glasses attached to many of these olivines are commonly less evolved than corresponding melt inclusions (generally in equilibrium with host olivines), olivine core compositions in single samples are diverse (Fo_{69-83}), and many of these olivines are reversely zoned to rims of Fo_{77-79}. The absence of correlated degassing and magma evolution trends in historic Llaima magmas suggests that they are stored as multiple bodies created by a higher frequency of magma replenishment in comparison to the frequency of large eruptions. This temporal-spatial disconnection leads to isolated evolution and degassing of discrete magma batches, followed by assembly just prior to eruption. Injection of relatively hot and mafic gas-rich magma is probably the triggering mechanism, in accord with and higher Olivine-Melt temperatures recorded by relatively primitive matrix glasses.

3.8

Unzipping of crystal mush as a rapid mechanism to remobilize and homogenize magma bodies

Burgisser Alain*, Bergantz George**

* *ISTO, CNRS - University of Orléans, 1a rue de la Férollerie, 45071 Orléans cedex 2, France (burgisse@cnrs-orleans.fr)*
** *Dept. of Earth and Space Sciences, University of Washington, Box 351310, Seattle, WA 98195-1310 USA*

The largest products of magmatic activity on Earth, the great bodies of granite and their corresponding large eruptions, have a dual nature: homogeneity at the large scale and spatial and temporal heterogeneity at the small scale. This duality calls for a mechanism that *1)* removes selectively the large-scale heterogeneities associated with the incremental assembly of these magmatic systems and *2)* occurs rapidly despite crystal-rich, viscous conditions seemingly resistant to mixing.

We present a simple dynamic template can unify a wide range of seemingly contradictory observations from both large plutonic bodies and volcanic systems by a mechanism of rapid remobilization ("unzipping") of highly viscous crystal-rich mushes. We demonstrate that this remobilization can lead to rapid overturn and produce the observed juxtaposition of magmatic materials with very disparate ages and complex chemical zoning. What is novel about our model is the recognition that the process has two stages. Initially a stiff mushy magma is reheated from below producing a reduction in crystallinity that leads to the growth of a subjacent buoyant mobile layer. A second stage occurs when the thickening mobile layer

becomes sufficiently buoyant to penetrate the overlying viscous mushy magma and produce rapid overturn of the entire system. This process exports homogenized material from the lower mobile layer to the top of the system, and leads to partial overturn within the viscous mush itself as an additional mechanism of mixing.

The agreement between calculated and observed unzipping rates for historical eruptions at Pinatubo and at Montserrat demonstrates both the general applicability of the model and the ability of unzipping to rapidly produce large amounts of mobile magma available for eruption. This mechanism furthers our understanding of the bifurcation between crust building by formation of periodically homogenized plutons and ignimbrite formation by large eruptions.

3.9

Behaviour of allanite during mylonitisation and implications for U-Th-Pb dating: case study at the Mt Mucrone, Italy

Cenki-Tok Bénédicte* , Oliot Emilien**, Thomsen Tonny B.*, Berger Alfons***, Spandler Carl****, Rubatto Daniela*****, Robyr Martin*, Manzotti Paola*, Regis Daniele*, Engi Martin* and Goncalves Philippe**

Uni. Bern, IfG, Baltzerstr. 1+3, 3012 CH-Bern (cenkitok@geo.unibe.ch)
**Uni Franche-Comté, UMR6249, 16 rte de Gray, F-25030 Besançon*
***Uni Copenhagen, Institute for Geography and Geology, Øster Voldgade 10, DK-1350 Copenhagen*
****James Cook University, 101 Angus Smith Dr, QLD 4811 Townsville, Australia*
*****Australian National University, 0200 Canberra, Australia*

Allanite occurs in meta-granodiorite showing different amounts of strain, from undeformed (a) to mylonitic (f). This body intruded the polycyclic Sesia basement at Permian times and underwent HP metamorphism and ductile deformation during the Alpine convergence. We study the effects of deformation on allanite U-Th-Pb apparent ages.
In the mylonitic rock allanite forms mm-size angular grains in a strongly recrystallised matrix and shows exclusively Permian ages, eventhough the grains are intimately linked to Alpine deformation and metamorphism. These grains occur in mm-sized lenses around which the mylonitic foliation flows. In addition to allanite, these lenses are composed of randomly oriented phengite and Ca-rich garnet (up to 30wt%). During mylonitisation these allanite grains were mechanically shielded by a robust mineral (epidote) that subsequently broke down to garnet and phengite.
The undeformed rock gives insight into allanite forming reaction. Relics of Permian magmatic monazite are found exclusively in the undeformed samples where the magmatic textures and minerals are largely preserved. Coronas of allanite, thorite and apatite surround monazite relics indicating the reaction: monazite + plagioclase + fluid —> allanite + apatite + thorite. These textures are located at the contact where magmatic biotite and plagioclase breakdown to form the HP assemblage phengite and garnet.
Alpine allanite is found in the undeformed rock. It is much smaller (ca. 200 μm), present fragmented textures with satellite neocrystals, is rich in Sr (up to 2wt%) and has a positive Eu anomaly. In medium strain rocks small (< 20 μm) Sr-rich rims around Permian allanite can be found. This indicates that Alpine allanite crystalisation is clearly associated to plagioclase breakdown (plagioclase + H2O —> jadeite + zoisite + quartz) and must have been triggered by local fluid present conditions.
The interpretation of these complex textures, microstructures and ages needs superposition of at least two events. At Permian times, mm-sized allanite rimed by epidote most probably formed in late magmatic fractures associated to fluid circulation. At Alpine times, these fractures play the role of precursor heterogeneities where ductile deformation is localized. Allanite in the mylonite is mechanically and chemically shielded during the Alpine event.
Allanite is a robust chronometer. However in case of superposition of deformation events, its Pb isotope composition may not record all the events seen by the rock. Reworking of old structures during the Alpine orogeny has to be taken into account when interpreting ages on allanite in deformed rocks. A deeper look into textures and structures – that can be misleading at a first glance – is necessary to understand the significance of U-Th-Pb in situ ages in polycyclic rocks.

3.10

Rapid transition to long-lived deep crustal magmatic maturation and the formation of giant porphyry-related mineralization (Yanacocha, Peru)

Chiaradia Massimo*, Merino Daniel*, Spikings Richard*

*Département de Minéralogie, Rue des Maraîchers 13, 1205-Genève (Massimo.Chiaradia@unige.ch)

An expanding amount of literature over the previous decade reports the occurrence of magmatic rocks with geochemical features of adakites (or adakite-like; i.e., high Sr/Y, low Yb) in association with major porphyry Cu-Au and porphyry-related epithermal deposits, and a twofold scientific debate has developed about this question: on one hand the genesis of adakite-like rock is controversial; on the other the meaning itself of the association of porphyry-type deposits with adakite-like rocks is debated.

Rocks with adakite-like features are considered to be the result, among others, of slab melting and slab melt-mantle wedge interactions (e.g., Defant and Drummond, 1990), of mafic lower crustal melting (e.g., Atherton and Petford, 1993), or of high-pressure fractional crystallization accompanied or not by the assimilation and melting of lower crust (e.g., Chiaradia et al., 2009). Discrimination between these processes is not straightforward, which has led to controversy on the origin of rocks with adakite-like signatures in many Phanerozoic arc systems. The debated origin of these rocks has propagated into contrasting models explaining the mechanisms of the association between adakite-like rocks and porphyry-type deposits in various Phanerozoic arc environments and post-collisional zones (e.g., review of Richards and Kerrich, 2007). Any hypothesis accounting for the relationships between adakite-like rocks and porphyry-type deposits should be based on a thorough petrogenetic study that is tightly coupled with the temporal evolution of magmatic rocks and their relationships with mineralization.

Here we report geochronologic, geochemical and isotopic data from adakite-like porphyritic rocks associated with the giant high-sulfidation system of Yanacocha, northern Peru, which is the world's largest gold deposit of this type. Mineralization is associated with porphyritic intrusions distributed along a ~8 km long NE-trending magmatic structural corridor. Eight of these intrusions investigated in this study range in age from 12.4 to 8.4 Ma and show systematic chemical and isotopic changes through time. In particular, rocks become systematically more felsic (andesite to rhyodacite), adakite-like and isotopically crust-contaminated through time, with a rapid transition from non adakitic to strongly adakite-like signatures occurring at about 12 Ma and within a time interval of <0.5 Ma.

Based on petrography, mineral and rock chemistry and isotopic compositions the Yanacocha intrusive magmas are interpreted to be the result of recharge assimilation fractional crystallization (RAFC) processes occurring at different crustal levels, involving amphibole-clinopyroxene-garnet fractionation at deeper levels, leading to more or less strong adakite-like signatures, and plagioclase-amphibole fractionation at shallower levels. Systematic geochemical and isotopic changes through time, coupled with plagioclase zoning and amphibole geobarometry suggest that the evolution of the magmatic system occurred through interaction of andesitic melts with an increasing length of the crustal column and shifted progressively through time towards shallower crustal levels as indicated by a decrease in adakitic indices between 11-8.4 Ma (although the rocks remained strongly adakite-like throughout) and by overall decreasing minimal pressures of amphibole crystallization.

This evolution was possibly the result of a steadily increasing compression associated with the Quechua II orogenic phase (12-10 Ma) that, by progressively slowing down magma ascent, forced magmas to evolve at a series of intermediate level chambers between the lower and upper crust. Increased compression during the Quechua II orogenic phase might have been related to the onset of subduction of the buoyant Inca oceanic plateau, estimated to occur at ~12 Ma (Gutscher et al., 1999), i.e., the same time of the onset of the rapid transition from "normal" to adakite-like signatures.

The giant Yanacocha ore system developed in coincidence with the ensuing ~3.6 My-long intrusion of adakite-like magmas formed by the above processes into a small upper crustal volume (corresponding to a surface area of ~5 km*5 km). This suggests that large-scale geodynamic processes leading to prolonged magmatic evolution at deep crustal levels might be a first-order control on the formation of giant porphyry-type systems, as is also indicated by similar magmatic evolutions in other porphyry-systems worldwide. How this occurs in detail (e.g., generation of volatile- and metal-rich oxidized magmas through high-pressure fractionation, recycling of sulfide-rich cumulates in the lower crust, focussed and long-lived magmatic input into a small upper crustal volume) requires additional investigation.

REFERENCES
Atherton, M.P., & Petford, N. 1993: Generation of sodium-rich magmas from newly underplated basaltic crust. Nature, 362, 144-146.
Chiaradia, M., Müntener, O., Beate, B., & Fontignie, D. 2009: Adakite-like volcanism of Ecuador: lower crust magmatic evolution and recycling. Contributions to Mineralogy and Petrology, in press, DOI 10.1007/s00410-009-0397-2.
Defant, M.J., & Drummond, M.S. 1990: Derivation of some modern arc magmas by melting of young subducted lithosphere. Nature, 347, 662-665.
Gutscher, M.-A., Olivet, J.-L., Aslanian, D., Maury, R., & Eissen, J.-P. 1999: The "lost Inca Plateau": Cause of flat subduction beneath Peru?. Earth and Planetary Science Letters, 171, 335-341.
Richards, J.P., & Kerrich, R. 2007: Adakite-like rocks: their diverse origins and questionable role in metallogenesis. Economic Geology, 102, 537-576.

3.11

Complex evolution of a highly explosive basaltic-andesite eruption of Villarrica volcano, Chile: the Chaimilla deposit

Costantini Licia*, Pioli Laura*, Longchamp Celine**, Bonadonna Costanza* & Clavero Jorge***

*Département de Minéralogie, Rue de Maraîchers 13, CH-1205 Genève (licia.costantini@unige.ch)
**Institute of Geomatics and Risk Analysis, Amphipôle - CH-1015 Lausanne
***Servicio Nacional de Geologia y Mineria (Sernageomin), Chile

Villarrica is a 2847-m-high basaltic-andesitic stratovolcano located in the southern Chilean Andes. It is one of the most active volcanoes in South America and it has been active for 600 ka producing about 60 eruptions in the last 450 years.
Although its historical eruptive activity has been mainly effusive and weakly explosive, with more than 30 known eruptions in the last century, Villarrica volcano also had large postglacial explosive behaviour, which produced pyroclastic density currents and tephra fallout from both the central vent and flank parasitic pyroclastic cones (Clavero and Moreno 2004). The two known largest-volume eruptions are the Licán and Pucón ignimbrites (13.8 and 3.6 ka respectively), which produced widespread pyroclastic density currents and are likely associated to caldera formation. The best-preserved and widely dispersed pyroclastic fallout is the Chaimilla deposit, which was erupted after the caldera-forming Pucón ignimbrite (~3.1 ka). After the last large eruption (1984-85), the Villarrica activity has been characterized by continuous degassing and sporadic bubble bursts (Witter et al., 2004; Gurioli et al., 2008).

We present the stratigraphy of Chaimilla deposit combined with the grain size, componentry, density, vesicularity and groundmass textures of juvenile products from selected fallout beds. These data are used to estimate the erupted volume and to constrain the eruption dynamics and evolution with time of this uncommon, but highly dangerous, type of activity of Villarrica volcano.

Based on lithological and textural features, we divided the Chaimilla deposit into 4 main eruption phases: Basal, Lower, Middle and Upper phases, which consist of several units (units A-J). Both fallout and pyroclastic density current units are present. The dispersal maps of different eruptive units are characterized by a weak variation on the dispersal axis (being the unit C dispersed mainly northward and the unit H north-westward), suggesting a change in wind direction during the eruption.
We estimated the erupted volume of the main fallout units and our results indicate that Chaimilla deposit was generated by a large-magnitude eruption (VEI 4).
Grain size distribution of both Lower and Upper fallout samples show a unimodal distribution, ranging from -5 to 9 , with the fraction >4 (<63 μm) always ≤1 wt%. Unit F (Middle phase) has a slightly bimodal grain size distribution and significant amount of fine ash. Samples from the Basal phase have instead a strongly bimodal grain size distribution, with a predominance of ash fraction. Juvenile component predominates in all the Chaimilla deposit, and lithic content decreases from bottom to top of the deposit, suggesting that the beginning of the eruption was characterized by the opening of a closed vent.

While the grain size distribution of Lower and Upper phase of Chaimilla eruption is always unimodal, density distribution of juvenile samples shows a strong bimodal character, whose bimodality is higher in the Lower phase with respect to the Upper phase. We identified two different clast populations: population 1 is the lightest one, having mode between 1.0 and 1.2 gr/cm^3. Population 2 represents the densest clasts with a mode ranging between 1.4 and 1.8 gr/cm^3. Clast microtextures

are different in the two populations: clasts from population 1 have spherical- to irregular-shaped bubbles and moderately crystallized groundmass (~40 vol%), while population 2 has clasts characterized by strongly irregular to collapsed bubbles and highly crystallized groundmass (~60 vol%).

Our eruption model implies the arrival of new magma (represented by clast population 1) into a stagnant, degassed magma body which was accumulated at shallow level (clast population 2). The new magma body exsolved volatiles that could not easily escape through the conduit due to presence of stagnant body. This caused gas pressure to build up, triggering the explosive eruption. The eruption started with multiple ash-rich explosions leading to vent opening (Basal phase). The following Lower phase marked the onset of the first highly explosive phase of the eruption, with final vent opening and crater widening, as marked by decreasing lithic content from bottom to top of the deposit. The Lower phase deposit was generated by a pulsating, plume column, which instability was probably due to the large amount of the dense clast population 2. The plume column collapsed completely during the Middle phase, which is in fact characterised by series of pyroclastic density current deposits. With the oncoming of the Upper phase, the plume column built up again and remained sustained producing a thick fallout bed predominantly constitued of low-density clast population 1. The eruption ended with thick series pyroclastic density currents which marked the total collapse of the eruptive column.

REFERENCES

Clavero, J. & Moreno, H. 2004. Evolution of Villarica Volcano, in Villarica Volcano (39.5˚S), southern Andes, Chile. In: Lara LE, Clavero JE (eds) Villarrica Volcano (39.5S) southern Andes, Chile. Gobierno de Chile, Servicio Nacional de Geología y Minería, pp 17-27

Gurioli L, Harris AJL, Houghton BF, Polacci M, Ripepe M (2008) Textural and geophysical characterization of explosive basaltic activity at Villarrica volcano. Journal of Geophysical Research 113:doi:10.1029/2007JB005328

Witter JB, Kress VC, Delmelle P, Stix J (2004) Volatile degassing, petrology, and magma dynamics of the Villarrica lava lake, southern Chile. Journal of Volcanology and Geothermal Research, 134, 303-337

3.12

Pumice, a window into the volcanic conduit

Degruyter Wim*, Dufek Josef**, Bachmann Olivier***,*

*Section des Sciences de la Terre et de l'Environnement, 13 Rue des Maraîchers, CH-1205, Genève (wim.degruyter@unige.ch)
**School of Earth and Atmospheric Sciences, 311 Ferst Drive, Georgia Institute of Technology, Atlanta, GA 30332 (USA)
*** Department of Earth and Space Sciences, Mailstop 351310, University of Washington, Seattle, WA 98195-1310 (USA)*

To better understand pumice microtextures and stress distribution within the volcanic conduit, a numerical study is performed using passive tracers to map the type and amount of shear in different parts of the conduit. During an explosive eruption pumices are formed by fragmenting the rising magmatic foam (i.e. highly vesicular magma). Provided they are quenched fast enough, pumices reflect the state of the magma just prior to fragmentation and their microtextures carry information on the stresses applied during magma ascent. Numerous deposits contain both tube pumice, with highly elongated vesicles and frothy pumice, with nearly spherical vesicles showing evidence that they were exposed to different stresses during magma ascent (e.g. Kos Plateau Tuff and Campanian Ignimbrite). The main aim of this investigation is to determine the strain histories of magmatic parcels that eventually become pumice

We have modified the Multiphase Flow with Interphase Exchanges (MFIX) code to simulate a two-phase (bubbles and magma), two-dimensional, isothermal flow with disequilibrium bubble growth. We include a rheology model depending on water content with outlet expansion into the atmosphere. Furthermore, different fragmentation criteria (i.e. critical gas volume fraction, strain rate and gas overpressure) are examined. Strain histories are investigated by releasing passive tracers within simulated magma rise, which record the pure and simple shear strain rates during ascent. The range of accumulated stresses at fragmentation shown by the passive tracers can then be linked to the range of different microtextures found within pumices.

3.13

Hornblende fractionation and peraluminous tonalite: an example of the Chelan Complex, Washington Cascades, USA

Dessimoz Mathias*, Othmar Müntener*

* *Institut de minéralogie et géochimie, Université de Lausanne, 1015 Dorigny (mathias.dessimoz@unil.ch)*

Over the last years numerous experimental studies on the role of H_2O were performed to understand how crustal differentiation occurs at high pressure under water (under)saturated conditions similar to what is expected in island arcs. These experiments emphasize the role of silica poor phases such as garnet and amphibole at high pressure on the differentiation of basaltic melt. Here we present results from a study on the Chelan Complex (Western U.S) to evaluate the role of hornblende in the formation of felsic plutonic rocks.
The Chelan complex is a deep plutonic complex exposed in the North Cascades Core at the southern end of the northwest trending Chelan block. It represents one of the deeper exposures (30 km) of the Cascadian arc and could therefore help to improve our understanding of which processes occur in the deep part of a continental arc and the fractionation processes of wet mafic magmas at high pressure.

The Chelan Complex is composed by tonalite, gabbros, ultramafic rocks and “migmatite”. Field observations, in particular comb layers, pegmatitic gabbros and igneous breccias indicate that the magmatic origin is well preserved along the entire complex. While subsolidus deformation occurs locally, most of the rocks are deformed in presence of a silicate melt, as indicated by a pervasive magmatic foliation well developed in the tonalite as well as some shear zones filled with sillicic melt and few magmatic folds.

The pressure of emplacement of the complex is bracketed between 0.6 Gpa and 1.5 Gpa by the widespread occurrence of primary epidote in tonalite and gabbros and by the absence of garnet. However, the formation of pyroxene spinel symplectites after olivine and plagioclase and Al-Ti systematics in hornblende indicate emplacement pressures of about 1.0 Gpa followed by isobaric cooling to 700°C at 1.0 Gpa.

Idiomorphic amphibole and interstitial plagioclase in gabbros, lack of negative Eu anomaly in amphibole and increase of Zr/Ti suggest early amphibole rather than plagioclase fractionation.

Whole rock chemistry performed on hornblendite, hornblende gabbros, diorite, tonalite and mafic dykes display continuous trends for various oxides and are coherent with an evolution through magmatic processes. The different behaviour of major elements could be reproduced successfully by a simple crystal fractionation model, in agreement with proportion and composition of cumulates observed in the field (ultramafic, hornblendite and gabbros) and mineral composition measured.

Textural observations, modelling and results of high pressure experiments indicate that hornblende is the main phase controlling the differentiation of the Chelan complex at high pressure and high water pressure. We hypothesize that peraluminous tonalite with high Sr/Y could be derived from a basaltic melt by hornblende fractionation and assimilation of crustal material is thus not required.

3.14

Peridotites on Macquarie Island: evidence for anciently-depleted domains in the Earth's mantle pointing to global Proterozoic melting 'events'?

Dijkstra, Arjan H.*

**Institut de Géologie, d'Hydrogéologie et de Géothermie, Université de Neuchâtel, CP 158, 2009, Neuchâtel*

Macquarie Island in the Southern Ocean is a fragment of Miocene ocean crust underlain by mantle peridotites that was uplifted and exposed above sea-level. Petrological and geochemical analysis has shown that the mantle rocks are too refractory to be the source residue of the overlying crustal rocks. For instance, the peridotites contain essentially no residual clinopyroxene, suggesting very high degrees of partial melting and melt extraction. Melting models involving trace elements suggest that the peridotites have seen in excess of 20% near-fractional melting.

Osmium isotope analysis of whole rock samples of peridotites from Macquarie Island yielded very unradiogenic $^{187}Os/^{188}Os$ ratios of 0.1194-0.1229. These values are much lower than typical values obtained on abyssal peridotites. They indicate a long-lived Re-depletion. Re-depletion model ages are Proterozoic (0.7-1.2 Ga). These results confirm that there is no simple genetic link between the Miocene crust and the mantle rocks exposed on Macquarie Island, but that the mantle rocks are a fragment of mantle that has recorded an old melting event, without any subsequent refertilization.

Ultra-refractory peridotites are also known from the 15-20° Fracture Zone (Mid-Atlantic Ridge) and the Izu-Bonin-Mariana fore-arc, and they are found as xenoliths from beneath Kerguelen Island and Hawaii. In all these cases, the ultra-refractory peridotites also gave old Re-depletion ages. The Macquarie Island peridotites are probably samples of an anciently-depleted, ultra-refractory mantle reservoir that has global significance, but that has generally been overlooked so far because of its sterility, i.e., its inability to further produce basalt.

The most tentative aspect of the, admittedly very limited, data-set of Os isotope ratios of ultra-refractory peridotites from the localities listed above is that they seem to point to two global melting events in the Proterozoic, around 0.8 and 1.2 Ga (based on Re-depletion ages). The possible geological significance of these events will be explored in my contribution.

REFERENCES

Dijkstra, A.H., Sergeev, D.S., Spandler, C.A., Pettke, T., Meisel,T., and Cawood, P.A. Ultra-refractory peridotites on Macquarie Island and the case for anciently-depleted domains in the Earth's mantle. Accepted for publication in Journal of Petrology, 2009.

3.15

Sphalerite mineralisation in Bajocian shallow-water carbonates in the Swiss Jura Mountains related to extensional synsedimentary tectonics during the Middle-Late Jurassic.

Natalia Efimenko*, Jorge E. Spangenberg**, Jens Schneider***, Massimo Chiaradia****, Thierry Adatte*, Virginie Matera***** and Karl B. Föllmi*

Institut de Géologie et Paléontologie, Université de Lausanne, 1015 Lausanne, Switzerland (natalia.efimenko@unil.ch)
Institut de Minéralogie et Géochimie, Université de Lausanne, 1015 Lausanne, Switzerland
Département of Earth and Environmental Sciences, Katholieke Universiteit Leuven, Celestijnenlaan 200E, 3001 Heverlee, Belgium
Département de Minéralogie, Université de Genève, 1205 Genève, Switzerland
Institut de Géologie et d'Hydrogéologie, Université de Neuchâtel, 2007 Neuchâtel, Switzerland

Disseminated sphalerite mineralisation occurs in Triassic and Jurassic carbonates in the Swiss Jura Mountains (e.g. Holenweg, 1969; Hofmann, 1989). We report new results from an ongoing study on cadmium-rich (up to 1.8 wt.%) sphalerite (ZnS) found in oolithic carbonates of Bajocian age at Lausen, Auenstein and Pratteln (Canton Basel Land). These oolithic carbonates of the "Hauptrogenstein" formation contain elevated concentrations of Cd (up to 21.4 ppm; Rambeau, 2006) and Zn (up to 207 ppm; Jacquat et al., 2009). We aim to understand how these metals were incorporated into the rock and the conditions of sphalerite formation by using thin-section microscopy, XRD, ICP-MS, LA-ICPMS, EMP, cathodoluminescence, sulphur isotopes, and Rb-Sr/Pb-Pb isotopic dating and tracing.

Cd and Zn enrichments are mostly associated with permeable oolithic carbonate lithologies. High concentrations of Cd and Zn in less permeable rocks (marls, micritic carbonates) appear to be fault-controlled. For example, in marly basinal deposits of the Klingnau Formation (coeval in age to the Hauptrogenstein formation) at Holderbank, Cd concentrations are low at 0,03 ppm but attain up to 0.5 ppm near faults. Likewise, Zn increases from 20 to 300 ppm towards these faults. This Cd and Zn zonation suggests that the circulating fluids were rich in Cd and Zn compared to the primary hostrock, and mainly focussed by faults systems or by permeable rock units.

The distribution of Zn and Cd concentrations in the oolithic carbonate rocks is highly heterogeneous. This appears to be related to porosity differences, and probably to difference in the distribution of Zn- and Cd-bearing phases within the rock. Zinc was shown to be associated with calcite, goethite and sphalerite (Jacquat et al., 2009). Cadmium is most likely adsorbed onto the surface of oolithic carbonate grains (Rambeau, 2006), goethite, clay minerals, pyrite, and within the sphalerite crystals. The preferential correlation of Cd with Zn in carbonate rock may be related to the high concentration of Cd in sphalerite. Nevertheless, Cd concentration does not systematically correlate with Zn. This may be explained by the different behaviour of these two metals during their retention onto mineral phases (goethite, clay minerals, pyrite, carbonate). At

Lausen, Cd concentration decreases from 12 to 0.03 ppm and Zn from 2000 ppm to 12 ppm within few centimetres from reduced grey portions to more altered yellowish parts of the rock. Spalerite microcrystals and framboidal pyrite were observed in grey unaltered parts. No sphalerite was observed in the altered rock portions, where pyrite was oxidized.
This suggests that Cd and Zn were remobilised during the weathering processes.
XRD analyses of sphalerite crystals revealed the presence of both sphalerite and wurtzite. The existence of wurtzite indicates bacterial activity involved in ZnS crystallisation at low temperatures (less than 60-80°). The negative $\delta^{34}S$ values of sphalerites (−22.3 to −5.3‰) point to bacterial sulfate reduction (BSR) as the main source of reduced sulfur. A contribution of sulfide from sedimentary pyrite cannot be excluded.
Direct Rb-Sr dating of selected sphalerite samples from Auenstein yields an upper Middle Jurassic (Bathonian) isochron age of 162 ± 4 Ma which is interpreted to record sphalerite formation during a period of widespread tectonothermal activity related to the opening of the North Atlantic and Tethyan oceans. These syn-sedimentary tectonics also influenced the paleotopography and facies distribution, which were spatially related to reactivated Paleozoic faults (e.g. Allenbach, 2001). Therefore, we propose a model of cadmium and zinc enrichment in the carbonate rocks by deep-sourced fluids during multistage tectonic processes in the region related to an extensional regime during the Jurassic. The Pb isotopic composition of sphalerite is very uniform, indicating an isotopically well-homogenized fluid system. Comparative Pb isotope patterns may point to lead sources located in granitic and metamorphic basement rocks exposed in the southern Black Forest farther north. Lead may have scavenged, mixed and homogenized from Pb-isotopically distinct crystalline basement rock types by fluids during the Bathonian to yield a Pb isotope signature compatible with carbonated-hosted sphalerite in the Swiss Jura.
Sphalerite precipitation may be related to the active bacterial sulphate reduction. The zonation of Cd and Zn in carbonate rocks seems to be controlled by the distribution of facies and the existence of faults. During the Tertiary, tectonic activity in Jura Mountains area may have triggered oxidative alteration of sulfides, formation of iron oxy-hydroxides, and remobilisation of Cd and Zn.

REFERENCES

Allenbach R. P. 2001: Synsedimentary tectonics in an epicontinental sea: a new interpretation of the Oxfordian basin of northern Switzerland. Eclogae Geologicae Helvetiae, 94, 265-287.

Hofmann B. 1989: Erzmineralien in paläozoischen, mesozoischen und tertären Sedimenten der Nordschweiz und Südwestdeutschlands. Schweiz. Mineralogische und Petrographische Mitteilungen, 69, 345-357.

Holenweg H. 1969: Mineralparagenesen im Schweizer Jura. Schweizer Strahler, 3, 303-308.

Jacquat O., Voegelin A., Juillot F. & Kretzschmar R. 2009: Chages in Zn speciation during soil formation from Zn-rich limestones. Geochimica et Cosmochimica Acta, 73, 5554-5571.

Rambeau C. 2006: Cadmium anomalies in jurassic carbonates (Bajocian, Oxfordian) in western and southern Europe. PhD thesis, University of Neuchâtel, 179 p. (unpubl.).

3.16

Modeling the evolution of geothermal reservoirs in deep fractured rocks: Coupling chemistry to heat and fluid transport

Hingerl Ferdinand F. *,**, Wagner Thomas **, Kulik Dmitrii A. *, Kosakowski Georg*, Driesner Thomas**, Thomsen Kaj*** & Heinrich Christoph A. **

Paul Scherrer Institut, 5232 Villigen PSI, Switzerland, (ferdinand.hingerl@psi.ch)
Institute of Isotope Geochemistry and Mineral Resources, ETH Zurich, Switzerland
***Technical University of Denmark, 2800 Kgs. Lyngby, Denmark*

A consortium of research groups from ETH Zurich, the Paul Scherrer Institut, EPF Lausanne, and the University of Bonn, cooperate in the **CCES** program **GEOTHERM** (www.geotherm.ethz.ch) aimed at performing basic research on key aspects of Enhanced Geothermal Systems (EGSs). Our task within the program consists of modeling the fluid–rock interaction and scale formation during geothermal heat extraction. In particular, we are developing advanced software that should realistically simulate the long term (years to decades) evolution of the permeability and heat exchange efficiency in an EGS reservoir.

Our simulations are anchored on theoretical investigations of the interplay of chemical processes (mineral dissolution and precipitation in rock fractures and technical installations) with the flow of the reactive fluid through a geometrically complex and changing fracture network. Modeling of this integrative scenario is performed by coupling a chemical equilibrium

solver with algorithms that simulate the mass and heat transport and geometrical phenomena. The chemical solvers are commonly based on a Law-of-Mass-Action (LMA) method, whereas in our work, the complementary Gibbs-Energy-Minimization (GEM) code package GEM-Selektor (http://gems.web.psi.ch) is used. GEM chemical solvers can compute phase speciation in more chemically plausible systems than it can be done using LMA solvers, especially when many highly non-ideal solutions are involved.

The EGS reservoir is characterized by variable (up to high) salinity and elevated temperature and pressure, which is a challenge on the calculation of aqueous speciation. For this reason, in addition to several variants of Debye-Huckel equation, we have implemented the Pitzer (Harvie et al. 1984) and the EUNIQUAC (Thomsen & Rasmussen 1999) aqueous activity model, both applicable to mixed electrolyte systems at high ionic strength. Compared with the conventional Pitzer model, EUNIQUAC requires fewer empirical fit parameters (only binary interaction parameters needed) and uses simpler and more stable temperature and pressure extrapolations. This results in an increase in computation speed, which is of crucial importance when performing coupled long term simulations of geothermal reservoirs.

In order to successfully apply the implemented electrolyte solution models, we are currently compiling a thermodynamic database and extend it with relevant Pitzer and EUNIQUAC parameters for calculating mineral solubility in a wide range of temperatures, pressures and ionic strength as applicable to geothermal fluids. We have also implemented the Soave-Redlich-Kwong (Soave 1972) and Peng-Robinson (Peng and Robinson 1976) equations of state for non-ideal gas mixtures, which will enable simultaneous calculations of gas solubility and boiling processes.

The standalone GEM numerical kernel of the GEM-Selektor code (abbreviated GEMIPM2K) was already successfully coupled to the Thermo-Hydro-Mechanical (THM) code GeoSys/Rockflow (Shao et al. 2009). Further coupling with the advanced TH code CSMP++ (Coumou 2008; http://csmp.ese.imperial.ac.uk/wiki/Home) is foreseen within the project. The novel coupled codes utilizing GEMIPM2K will be used within a benchmarking study, testing the efficiency, the numerical stability, and the sensitivity of the results to different numerical procedures and geochemical approaches, last but not not least to the impact of the choice of a thermodynamic data set. As the concluding step, we intend to construct a conceptual model for the geochemical water-rock interaction processes including the formation of mineral scales and the corrosion of pipes in wells at the Basel EGSs site.

REFERENCES

Bruno J., Bosbach D., Kulik D., Navrotsky A. 2007: Chemical thermodynamics of solid solutions of interest in radioactive waste management:A state-of-the art report, Chemical Thermodynamics Series, 10, Paris, OECD, 266 p.

Coumou, D. , **Matthäi, S., Geiger , S., and Driesner, T.** 2008. Computers & Geoscience, Volume 34, Issue 12, pp 1697-1707

Harvie, E.H., Moller, N., Weare, J.H. 1984. The prediction of mineral solubilities in natural waters: The Na-K-Mg-Ca-H-Cl-SO_4-OH-HCO_3-CO_3-CO_2-H2O systemto high ionic strengths at 25°C. Geochim. Cosmochim. Acta Vol. 48, pp. 723-751.

Karpov, I.K., Chudnenko, K.V., Kulik, D.A. 1997. Modeling chemical mass transfer in geochemical processes: thermodynamic relations, conditions of equilibria, and numerical algorithms. American Journal of Science 297: 767-806.

Karpov I.K., Chudnenko, K.V., Kulik, D.A., Avchenko, O.V., and Bychinski, V.A. 2001. Minimization of Gibbs free energy in geochemical systems by convex programming. Geochemistry International 39, no. 11: 1108-1119.

Kulik, D., Berner, U., and Curti, E. 2004. Modelling chemical equilibrium partitioning with the GEMS-PSI code. In: PSI Scientific Report 2003 / Volume IV, Nuclear Energy and Safety (Eds. B.Smith and B.Gschwend), Paul Scherrer Institut, Villigen, p.109-122.

Kulik D.A. 2006a. Classic adsorption isotherms incorporated in modern surface complexation models: Implications for sorption of actinides. Radiochimica Acta 94, no. 9-11: 765-778.

Peng, D.Y., Robinson, D.N. (1976) A new two-constant equation of state. INd. Eng. Chem. Fundam., 15, 59-64.

Soave, G. (1972) Equilibrium constants from a modified Redlich-Kwong equation of state. Chem. Eng. Sci. 27, 1197-1203.

Shao, H., Dmytrieva, S. V., Kolditz, O., Kulik, D. A., Pfingsten, W., Kosakowski, G. 2009. Modeling reactive transport in non-ideal aqueous - solid solution system. Applied Geochemistry 24, 1287-1300.

Thomsen, K., Rasmussen, P. 1999. Modeling of Vapor-Liquid-Solid Equilibria in Gas – Aqueous Electrolyte Systems. Chem. Eng. Sci., 54, 1787-1802.

3.17

The mafic – granitic connection of the Torres del Paine laccolith, Patagonia

J. Leuthold1, O. Müntener1, L. Baumgartner1, B. Putlitz1, M. Ovtcharova2, Urs Schaltegger2, Massimo Chiaradia2

1 IMG-UNIL, CH-1015 Lausanne, Switzerland (julien.leuthold@unil.ch)
2 Mineralogy – UNIGE, CH-1205 Geneva, Switzerland

We have conducted a field, petrological and geochronological study of a bimodal intrusive complex from the Torres del Paine laccolith, Patagonia, Chile. The goal of this study is to understand how various types of mafic rocks evolve at shallow pressure and how they are related in space and time to the various granitic sheets. From field relations it is evident that the granite intruded as a series of sheets, with the oldest pulse on top and the youngest at the base of the laccolith. High precision U-Pb dating on single zircons (Michel et al. Geology 2008) is in agreement with field relations and yielded 12.59±0.02 for the oldest and 12.51±0.03 for the youngest granite dated.
The granites are underlain by a series of mafic sills composed of hornblende-gabbros and diorites. We distinguish two types of hornblende gabbros that are chemically similar but clearly different with respect to their mineral crystallization sequence. However, the contacts between the different mafic rocks are ductile as illustrated by mafic enclaves in diorite or ascent of small diorite diapirs into overlaying hornblende gabbros, indicating (near-) simultaneous emplacement of most of the mafic rocks.
Bulk rock chemistry suggests that the mafic and granitic rocks follow a high – K calcalkaline to shoshonitic differentiation trend. Liquid compositions calculated from Laser Ablation ICP-MS trace element analysis of cumulate minerals indicate that the mafic rocks crystallized from a K-rich basaltic to shoshonitic magma. Intercumulus minerals show equilibrium with a granodioritic to granitic melt, that is similar to Paine granites. Preliminary isotope dilution – thermal ionization mass spectrometry on zircons from one gabbro and one diorite yielded 12.40±0.04 and 12.447±0.013 Ma, which is about 60'000 years younger than the youngest granite dated so far. This would suggest that a large volume of the laccolith grows downwards, with younger and more mafic sheets at the bottom of the complex. The youngest granites that cut the entire complex, however, await precise dating.

REFERENCES
Michel et al. (2008), Geology 36/6, 459-462

3.18

Bromine speciation and partitioning in high pressure aqueous fluids and silicate melts: implication for the behavior of halogens in subduction zones

M. Louvel*, C. Sanchez-Valle*, W.J. Malfait*, G.S. Pokrovski**, C.N. Borca***, D. Grolimund***

**Institute for Mineralogy and Petrology, ETH Zurich, CH-8092 Zurich, Switzerland. (marion.louvel@erdw.ethz.ch)*
***CNRS, Laboratoire des Mecanismes et Transferts en Geologie, F-31400 Toulouse, France.*
****Swiss Light Source, CH-5232 Villigen PSI, Switzerland.*

Although halogens are minor volatiles in the Earth's crust, they are important tracers of magmatic and degassing processes and provide insights about subsurface magma movement and eruption likelihood in subduction-related volcanism [1]. Additionally, their ability to complex with other elements has also considerable implications on the formation and distribution of ore deposits [2]. Prerequisite for an efficient use of halogens as geological tracers is an adequate knowledge of their solubility and distribution between aqueous fluids and silicate melts, as well as their speciation in subduction zone fluids. Experimental data on the solubility and fluid-melt partitioning behavior of halogens is however limited to pressures below 0.3 GPa [3,4] and virtually no data is available on their speciation in high-pressure fluids.
In order to investigate the behavior of halogens in sub-arc environments, X-ray absorption (XAFS) and X-ray fluorescence (XRF) spectroscopy measurements were conducted in a hydrothermal diamond-anvil cell (HDAC-[5]) up to 850 °C and 1.5(1) GPa in Bromine-rich fluids equilibrated with silicate melts. Bromine was used as an analog for chlorine suitable for X-ray fluore-

scence measurements through the diamond windows of the HDAC. Experiments were conducted at the X05-LA MicroXAS beamline of the Swiss Light Source (Switzerland). Pressure in the sample chamber was monitored from the PVT equation of state of a chip of gold added to the experimental volume. Br fluid-melt partition coefficients in the haplogranite-H_2O system were determined by XRF spectroscopy. Br speciation was investigated using XAFS over a wide range of P-T and bulk compositions, ranging from pure NaBr aqueous solutions (3wt% Br) to alkali-SiO_2-rich solutions, water-saturated $Na_2Si_2O_5$ and haplogranititic melts and supercritical fluids (25wt% $Na_2Si_2O_5$ and 10wt% haplogranite).
The combined results of these experiments provide valuable information on the partitioning behavior and structural environment of Br in high-pressure fluids. Br strongly partitions into the aqueous fluid phase, in agreement with the results of Bureau et al. [6] in quench experiments. Partition coefficients $D^{fluid/melt}$ are close to 25 at 650 °C – 1.0(1) GPa but decrease with increasing P-T, as the system approaches miscibility. The XAFS data reveal changes in the local structure around Br as chemical complexity increases in the system from NaBr solutions to alkali-rich SiO_2 fluids, suggesting the complexation of Br with Na, Si and Al. The implications of these results for the behavior of Br and halogens in subduction zone fluids will be discussed.

REFERENCES
[1]Aiuppa et al (2008), Chem. Geol. 263, 1-18.[2]Hedenquist&Lowenstern (1994), Nature 370, 519-527.[3]Webster (1992), Geoch. Cosmo. Act. 56, 679-687.[4]Bureau&Metrich (2003), Geoch. Cosmo. Act. 67, 1689-1697.[5]Bassett et al (1993), Rev. Sci. Inst. 64, 2340-2345.[6]Bureau et al (2000), Earth. Planet. Sci. Lett. 183, 51-60.

3.19

Compositional dependent compressibility of dissolved water in silicate glasses revealed by Brillouin scattering on haplogranitic and basaltic glasses

Wim J. Malfait*, Carmen Sanchez-Valle*, Paola Ardia*,** & Etienne Médard***

*Institute for Mineralogy and Petrology, ETH Zurich, CH-8092 Zurich (wim.malfait@erdw.ethz.ch)
**Dept. of Geology and Geophysics, University of Minnesota, MN 55455 Minneapolis, USA
***Laboratoire Magmas et Volcans, Université Blaise-Pascal-CNRS, OPGC, F-63038 Clermont-Ferrand

The density of hydrous magmas is a key control on the timescales and outcome of many igneous processes, *e.g.* the crystal settling velocities in a magma chamber and the emplacement depth of intrusions. Unfortunately, direct density measurements on hydrous liquids at magmatic temperatures and pressures are experimentally challenging and as a result, very few experimental data are available. At atmospheric pressure and room temperature, the partial molar volume of water in silicate glasses and melts seems to be independent of the bulk composition of the glass (Richet and Polian, 1998). Encouraged by this constant partial molar volume at room conditions and because of the lack of sufficient experimental constraints, current density models for hydrous magmatic liquids (*e.g.* Ochs and Lange, 1999) assume that the partial molar volume of the dissolved water at high temperature and pressure is also independent of melt composition. This assumption, however, has never been experimentally confirmed.

In order to verify if the partial molar volume of water remains independent of magma composition at elevated pressures, we have determined the sound wave velocities and bulk modulus (K_S) of a series of hydrous haplogranitic and basaltic glasses, quenched at different pressures, using Brillouin spectroscopy. The compressional wave (V_P) and shear wave velocities (V_S) systematically decrease with the addition of water. The partial molar K_S of water, and hence the compressibility, is different for different magma compositions. This implies that the partial molar volume of water will not be independent of melt composition at elevated pressure. These results suggest that the density model of Ochs and Lange (1999) may have limited applicability at elevated pressure. The development of more robust density models for hydrous magmatic liquids cannot proceed until additional in situ, high pressure and temperature measurements of melt density, thermal expansion and/or compressibility are available.

REFERENCES
Ochs, F.A., and Lange, R.A. (1999) The density of hydrous magmatic liquids. Science, 283, 1314.
Richet, P., and Polian, A. (1998) Water as a dense icelike component in silicate glasses. Science, 281, 396-398.

3.20

PVTx properties of high pressure aqueous fluids by Brillouin scattering spectroscopy

Mantegazzi Davide*, Sanchez-Valle Carmen*, Reusser Eric*, Driesner Thomas**

*Inst. for Mineralogy and Petrology, ETH Zurich, CH-8092 Zurich, (davide.mantegazzi@erdw.ethz.ch)
** Inst. of Isotope Geochemistry and Mineral Resources, ETH Zurich, CH-8092 Zurich

Aqueous fluids play a very important role in many geological processes in the Earth's crust and mantle. Typical examples of fluid mediated geological events are: the magma production in the mantle wedge beneath active volcanoes at subduction zones, metamorphic reactions involving fluid phases, the hydrothermal alteration of the seafloor, the transport of chemical components and the related ore deposits formation.

Studies on Fluid Inclusions (FI) have pointed out that fluids in the ternary system H_2O – NaCl – CO_2 can be considered as good approximation for natural geological fluids.

In order to quantitatively model fluid-rock interactions, thermodynamic data on minerals and fluids at geologically relevant P-T conditions are necessary. While these data are available for the most rock-forming minerals, this is not the case for aqueous fluids different than pure H_2O. For example, the equations of state (EoS) of H_2O – NaCl fluids are restricted to 0.5 GPa. Therefore, the interpretation of fluid related deep geological processes requires the extrapolation of thermodynamic properties over an order in magnitude in pressure. In addition, the knowledge of the thermodynamic properties of fluids in the ternary system H_2O – NaCl – CO_2 is essential for understanding and modeling the FI data.

In this contribution we present the PVTx properties of different aqueous fluids up to high P-T conditions, calculated from sound velocity measurements using Brillouin scattering spectroscopy. All experiments were conducted in an externally heated membrane-type diamond anvil cell (mDAC).

Brillouin scattering spectroscopy allows the direct measurement of the velocity of acoustic waves propagating in a material (fluid or solid). The collected sound velocities V_p are used to determine the EoS (P, T,x) of the analyzed fluids.
The results are combined with previous experimental and theoretical EoS to obtain a continuous model from low to high P-T conditions, providing a database for the thermodynamic properties of the most relevant aqueous systems involved in fluid-mediated geological processes.
Figure 1 shows the comparison between the EoS (P, T,x) of different H_2O – NaCl mixtures. At 2 GPa the solution with 5.5 wt% NaCl is 5.2% denser than pure water, while at 3 GPa the solution with 14.9 wt% NaCl is 9.6% denser than water. With increasing pressure the difference in density between water and chloride-rich solutions is increasing.

REFERENCES

Abramson, E., & Brown, M.J. 2004: Equation of state of water based on speeds of sound measured in the diamond-anvil cell. Geochim. Cosmochim. Acta 68, 1827-1835.

Driesner, T. 2007: The system H2O-NaCl. Part II: Correlations for molar volume, enthalpy, and isobaric heat capacity from 0 to 1000 degrees C, 1 to 5000 bar, and 0 to 1 X-NaCl. Geochim. Cosmochim. Acta 71, 4902-4919.

Sanchez-Valle, C., & Bass, J. D. 2007: Equation of state of fluids from sound velocity measurements in the diamond anvil cell using Brillouin scattering spectroscopy. Geochim. Cosmochim. Acta 71, A873-A873.

Wagner, W., & Pruss, A. 2002: The IAPWS formulation 1995 for the thermodynamic properties of ordinary water substance for general and scientific use. J. Phys. Chem. Ref. Data 31, 387–535.

Figure 1. EoS (P, T, X) for H2O – NaCl mixtures with different salt concentrations as a function of pressure along the 200°C isotherm. All these EoS have been determined with the same experimental technique. Data for the 14.9 and 5.5 wt% NaCl solutions are from this work; densities for the 0 wt% NaCl mixture are taken from Sanchez-Valle and Bass (2007).

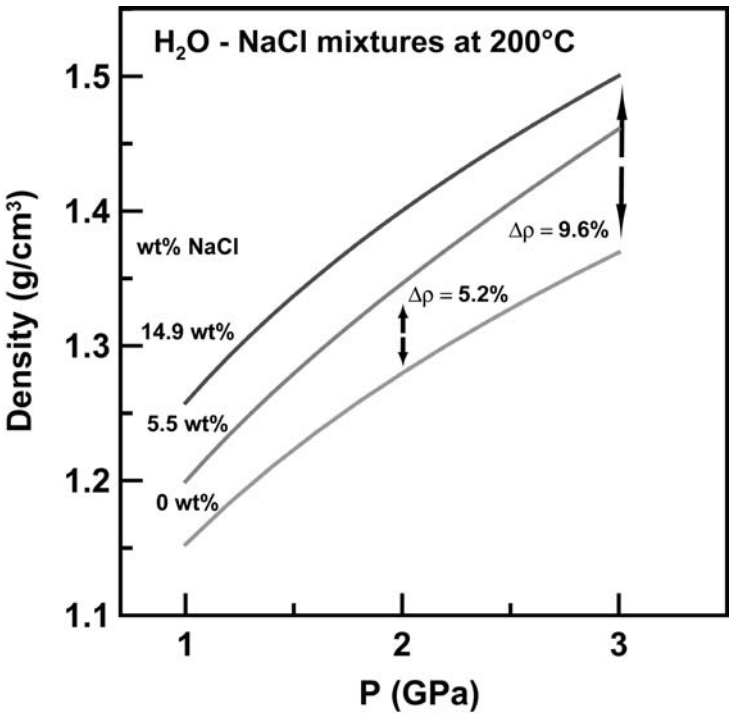

3.21

Evidence of Jurassic rifting in the Dent Blanche nappe (near Cignana, Italy)

Paola Manzotti*, Daniele Regis*, Benedicte Cenki-Tok*, Martin Robyr*, Tonny B. Thomsen*, Daniela Rubatto**, Michele Zucali*** & Martin Engi*

*University of Bern, Baltzerstrasse 1+3, 3012 CH-Bern (manzotti@geo.unibe.ch)
**The Australian National University, Mills road, Canberra, ACT, 0200 Australia
***Dipartimento di Scienze della Terra «Ardito Desio», Università degli Studi di Milano, via Mangiagalli 34, 20133 I-Milano

The Roisan Zone is considered to be the Mesozoic metasedimentary cover of the Dent Blanche nappe (Austroalpine domain, Western Italian Alps; Diehl et al., 1952). It is dismembered into metric to hectometric bands and pods of marbles, dolomitic breccias with a phyllitic matrix, calcschist, micaschist, chlorite schist, impure and manganoan quartzites.

In the Roisan Zone we found the Alpine record to be heterogeneous; the metamorphic imprint indicates low temperature and intermediate pressure, locally this is associated with superimposed mylonitic foliations. Four evolutionary stages have been reconstructed by meso- and microstructural analysis. Pre-stage 1 is a pre-Alpine event recognised only at the microscale. During stage 1 a well differentiated millimetric foliation develops, whereas D2 structures consist of isoclinical folds, transposing the S1 foliation into a new, pervasive S2. D3 structures mainly consist of isoclinal folds: this stage is not always associated with the development of a new foliation.

Within the Roisan Zone, particularly near Cignana, we investigated cross-cutting relationships between metamorphic and deformational signatures. In Mn-quartzite and marble a relative temporal sequence was deduced. Titanite and allanite were singled out for U-Th-Pb dating. Allanite from Mn-quartzites occurs as subhedral crystals and displays irregular zoning in LREE, Ca, Fe, and Mg. SHRIMP and LA-ICP-MS analyses did not yield the metamorphic Alpine age expected on the basis of petrographic and structural observations. The analyzed generation of allanite grains shows Permian ages (between 350 and 290 Ma).

Titanite in marble occurs as abundant subhedral to anhedral crystals (mostly fractured and/or deformed), locally sub-parallel to the foliation. BSE images, qualitative X-ray elemental maps, and EMP spot analysis show weak regular to irregular zoning in Al, Ti and Ca. SHRIMP U-Pb analysis of titanite domains with various Al contents yield apparent spot $^{206}Pb/^{238}U$ ages scattering between 284 and 160 Ma.

The younger ages of titanite are tentatively interpreted as reflecting an extensional regime that preceded the Alpine collision. Further work is underway now to clarify whether zoning of LREE, Ca, Fe and Mg in allanite and variations of Al, Ti and Ca in titanite grains may partly reflect changes in fluid compositions in a metasomatic-hydrothermal system associated with extension, possibly in an oceanic environment.

REFERENCES

Diehl, E.A., Masson, R., Stutz, A.H. 1952: Contributo alla conoscenza del ricoprimento della Dent Blanche. Memorie degli Istituti di Geologia e Mineralogia dell'università di Padova 17, 1-52.

3.22

Ore fluid evolution in a volcanic-hosted epithermal ore deposit: Farallón Negro, Argentina.

Márquez-Zavalía, M. Florencia*, Heinrich, Christoph A.**, Meier, Dimitri**

*IANIGLA, CCT Mendoza, CONICET, CC 330, (5500) Mendoza, Argentina (mzavalia@mendoza-conicet.gov.ar)
**Isotope Geochemistry and Mineral Resources, Federal Institute of Technology, ETH Zentrum NO, CH-8092, Zurich, Switzerland

The Farallón Negro mineral deposit is located in Catamarca province, Argentina, at 27º19´S and 66º40´W. This low sulfidation epithermal gold deposit belongs to the Farallón Negro mining district, along with other epithermal (e.g., Capillitas, Cerro Atajo) and porphyry deposits such as Bajo de la Alumbrera and Agua Rica. This cluster of Cu-Au mineral deposits are genetically linked to a Miocene volcanic complex with a suite of rocks of high-K calk-alcaline to shoshonitic affinities known as Farallón Negro Volcanic Complex (FNVC). Many authors interpreted the whole complex as the remnant of a large andesitic volcano (e.g., Halter et al., 2004; Proffett, 2003; Ulrich et al., 2002; and references therein), though Harris et al. (2006) present some contradicting evidences.

Alto de la Blenda area, where this study was focused, is one of the two main suits of veins of the Farallón Negro mineral deposit. The main veins of Alto de la Blenda are: Laboreo, Esperanza and Esperanza SE. The W part of Laboreo vein is hosted in andesite and the rest of that vein and the other two are hosted in monzonite. They are more than 1000 m long, 1 to 6 m wide, with grades up to 7 g/t Au and 200 g/t Ag (Montenegro & Morales, 2004).

There were recognized four stages of the mineralization with 7 generation of quartz. **Stage I** is represented by the earliest quartz recognized (Q1) in the deposit, present as fragments in a breccia, it is bluish grey in colour and occurs along with fragments of whitish carbonate (Cb1) and scarce disseminated pyrite. **Stage II** corresponds to the breccia, which is cemented by a second generation of quartz (Q2), grey in colour, interlayered with bands of creamy carbonate (Cb2) and associated with free Au, sulphides (pyrite, galena, chalcopyrite, sphalerite) and Cu, Ag, Au and Pb sulphosalts. At the end of this stage, quartz (Q3) in colourless crystals up to 1 cm long fills the remaining open spaces and vugs. **Stage III** is represented by a younger generation of grey quartz (Q4), associated with pink and yellowish carbonate (Cb3) and chalcopyrite and Ag minerals. It occurs parallel to the breccia and frequently crosscutting it. At the end of this stage, small cavities are filled with quartz crystals (Q5) that frequently develop a layered base on which grow transparent, colourless crystals up to 2 cm long, developing comb textures. In some areas, **Stage IV** is present, where the last two generations of quartz can be recognized. The first one (Q6) is scarce and occurs with white (and pink?) layered carbonate (Cb4), mostly oxidized (cryptomelane and pyrolusite >> manganite, manjiroite and "wad") and galena, chalcopyrite and sphalerite generally scarce. Sometimes the association Q6+Cb4 is parallel to the whole sequence and other times crosscuts it. The youngest quartz (Q7) fills the open spaces and develops colourless crystals up to 1 cm long. In several areas of the deposit, localized brecciation affects different parts of the sequence.

Preliminary fluid inclusion results give ranges of homogenization temperatures from 200 to 270ºC, and salinities from 3.40 to 4.70 NaCl equiv. for Esperanza vein and similar homogenization temperatures but lower salinities for Laboreo vein. The first results of microanalyses by LA-ICPMS, performed in primary aqueous fluid inclusions trapped in quartz, show concentrations of ppm-levels of Au and hundreds of ppm of Cu. The highest values of Au concentrations were found in Q2 and Q3, belonging to the second stage of the mineralization, while the highest Cu values came from samples with Q6 and Q7, corresponding to the last stage of the mineralization (Stage IV). Other ore forming elements were also analyzed and all results will be informed in detail when the study is completed. There were as well investigated the aqueous fluids of the late veins, with Au-Ag-bearing quartz+Mn-carbonate+base-metal minerals, found in the Bajo de la Alumbrera open pit (Meier, 2008; Meier et al. 2008) Though the results are still preliminary, the research in progress shows the first saline epithermal fluids in a low-to

intermediate sulfidation epithermal system containing significantly higher metal concentrations than fluids in any active geothermal system (e.g., Simmons and Bronwn, 2006). These very high metal concentrations (ppm-levels of Au and hundreds of ppm of Cu) in the fluid indicate that even low- to intermediate-sulfidation economic vein deposits do not form from convecting groundwater alone, but from injection of vapor-derived magmatic fluid.

REFERENCES

Halter, W.E., Bain, N., Becker, K., Heinrich, C.A., Landtwing, M., VonQuadt, A., Clark, A.H., Sasso, A.M., Bissig, T. & Tosdal, R.M. 2004: From andesitic volcanism to the formation of a porphyry Cu-Au mineralizing magma chamber: the Farallon Negro Volcanic Complex, northwestern Argentina: Journal of Volcanology and Geothermal Research, 136, 1-30.

Harris, A.C., Bryan, S.E. & Holcombe, R.J. 2006: Volcanic setting of the Bajo de la Alumbrera porphyry Cu-Au deposit, Farallon Negro Volcanics, Northwest Argentina: Economic Geology, 101, 71-94.

Meier, D. 2008: Low salinity fluids at the Bajo de la Alumbrera porphyry Cu-Au deposit, Argentina. MSc thesis. Inst. Isotope Geochemistry and Mineral Resources, Dept. Earth Sc., ETH-Zürich, Swiss Federal Institute Technology.

Meier, D. , Heinrich, C.A., Guilong, M. & Márquez-Zavalia, M.F. 2008: Low salinity fluids at the Bajo de la Alumbrera porphyry Cu-Au deposit, Argentina. Swiss Geoscience Meeting.

Montenegro, N. & Morales, F. 2004: Distrito mineralizado Farallón Negro. YMAD, Belén, Catamarca, Argentina. In: Márquez-Zavalía, M.F. (Ed.) Curso Latinoamericano de Metalogenia UNESCO-SEG 2004. Guía de Campo: 83-99.

Proffett, J.M. 2003: Geology of the Bajo de la Alumbrera porphyry copper-gold deposit, Argentina: Economic Geology, 98, 1535-1574.

Ulrich, T., Günther, D. &Heinrich, C.A. 2002: The Evolution of a porphyry Cu-Au deposit, based on LA-ICP-MS analysis of fluid inclusions: Bajo de la Alumbrera, Argentina: Economic Geology, 97, 1889-1920.

Simmons, S.F. & Bronwn, K.L. 2006: Gold in magmatic hydrothermal solutions and the rapid formation of a giant ore deposit. Science, 314, 5797, 288-291.

3.23

Baggalútar from Hvalfjörður, SW Iceland: Volcanic spherulites or not?

Mattsson Hannes B.*, Reusser Eric*

**Institute for Mineralogy and Petrology, Department of Earth Sciences, ETH Zürich, Clausiusstrasse 25, CH-8092 Zürich (hannes.mattsson@erdw.ethz.ch)*

Baggalútar form well-rounded spherules, ranging between 0.5-3 cm in diameter, and occur either as single spherules or aggregates containing up to 10 individual spherules joined together. They are relatively common on beaches along the Atlantic coast in Hvalfjör ur (SW Iceland).In literature, Baggalútar have commonly been explained as being volcanic spherulites (Saemundsson and Gunnlaugsson, 1999). However, Baggalútar lack the internal structure characteristic for volcanic spherulites which commonly involves radial growth of feldspar and quartz needles as silicic glass devitrifies. They are not accretionary lapilli as these commonly form by accretion of fine ash around a nucleii in an onion-like texture. Neither are they consistent with being marine concretions, which are characterized by concentric internal textures.

In thin section, only random internal texture can be observed and the Baggalútar is composed of a fine-grained groundmass with abundant rounded voids which have been infilled with secondary minerals (mainly thomsonite, heulandite and natrolite). XRD and SEM analyses show that the groundmass is composed of lath-shaped plagioclase (An-rich), augitic clinopyroxene and titanomagnetite in various proportions (Fig.1). The overall mineralogy of the Baggalútar is therefore consistent with being basaltic. Furthermore, the internal texture suggests that it could be basaltic ash, in which the vesicles have been infilled by zeolite minerals at a later stage.

However, a few things about the occurrence of Baggalútar remain enigmatic:

1. Absence of phenocrysts. In five investigated thin sections only two small clinopyroxene phenocrysts could be found, and all spherules have a fine-grained homogeneous texture strongly reminiscent of quenching.
2. What causes the well-rounded shape? This is in contrast to the randomly oriented internal structure of the spherules. If only single Baggalútar are considered, their well-rounded shapes could potentially be attributed to marine abrasion. However, this does not explain the occurrence of multi-spherule aggregates in which each spherule is well-rounded.
3. Where do they come from? So far no outcrop has been found in Hvalfjör ur in which the Baggalútar occurs in situ, and finding such an outcrop may help to shed light on their formation.

REFERENCES
Saemundsson, K. & Gunnlaugsson, E. 1999: Islenska steinabokin, Mal og Menning, Reykjavik, pp. 233.

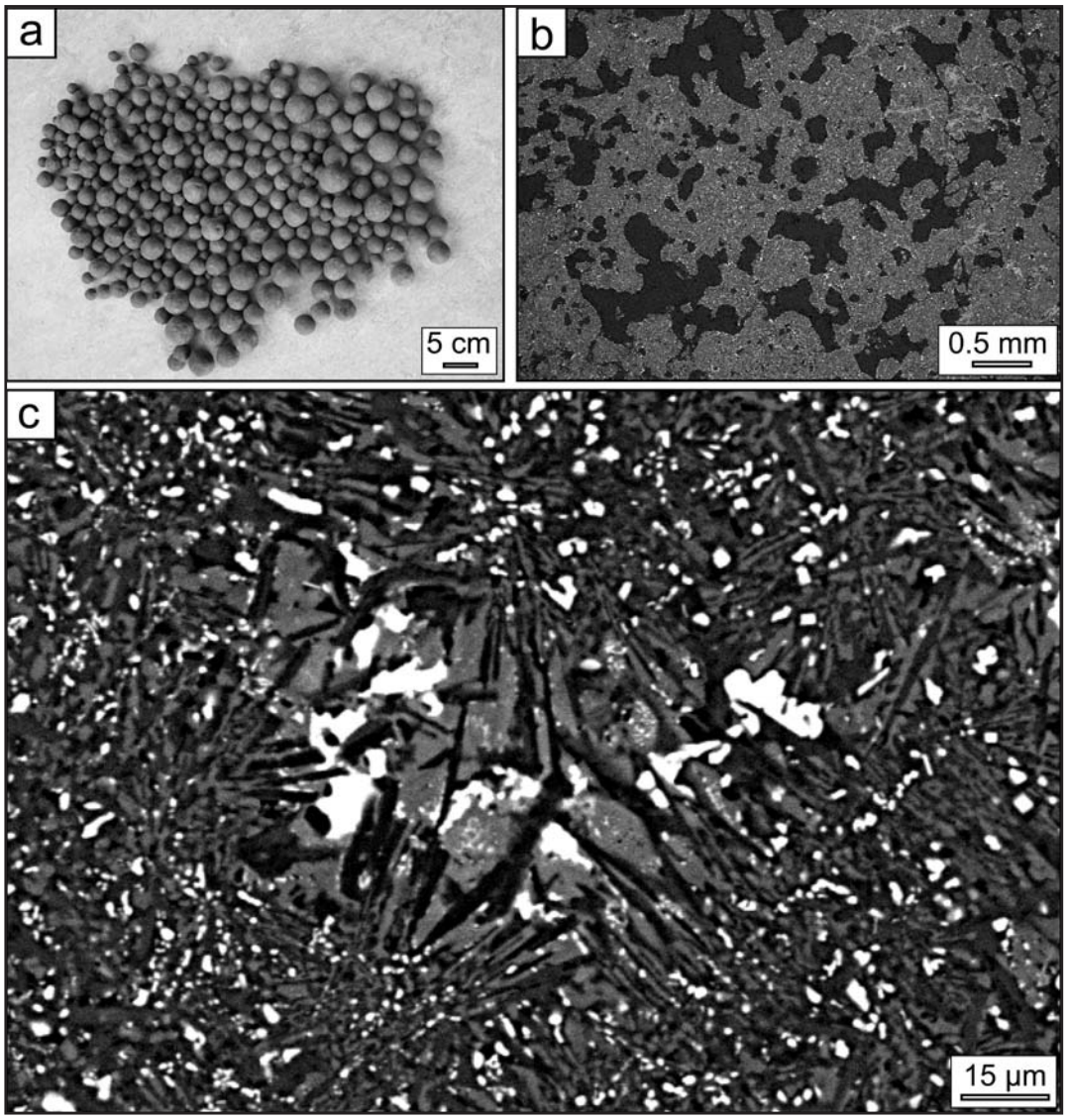

Fig. 1. Characteristics of Baggalútar at different magnifications. (a) A collection of hand specimens. (b) SEM image showing homogeneous internal texture with vesicles infilled by zeolites. (c) Close-up SEM image of the groundmass comprising plagioclase (lath-shaped, dark), clinopyroxene (grey) and titanomagnetite (white).

3.24

Columnar jointing and the formation of "chisel-marks" in the Hrossadalur lava flow, northern Iceland

Mattsson Hannes B.*, Bosshard Sonja*

Institute for Mineralogy and Petrology, Department of Earth Sciences, ETH Zürich, Clausiusstrasse 25, CH-8092 Zürich (hannes.mattsson@erdw.ethz.ch)

Columnar jointing and "chisel-marks" are common features in thick, slowly cooled, basaltic lavas. The fracturing to form columnar jointing is commonly attributed to thermoelastic strain creating a local tensile stress, which results in the formation of joints organized into columns with a polygonal cross-section and large aspect ratio (length/diameter).The chisel marks, on the other hand, are striae oriented perpendicular to the main axis of the column and reflects a stepwise crack propagation as the lavas cool.

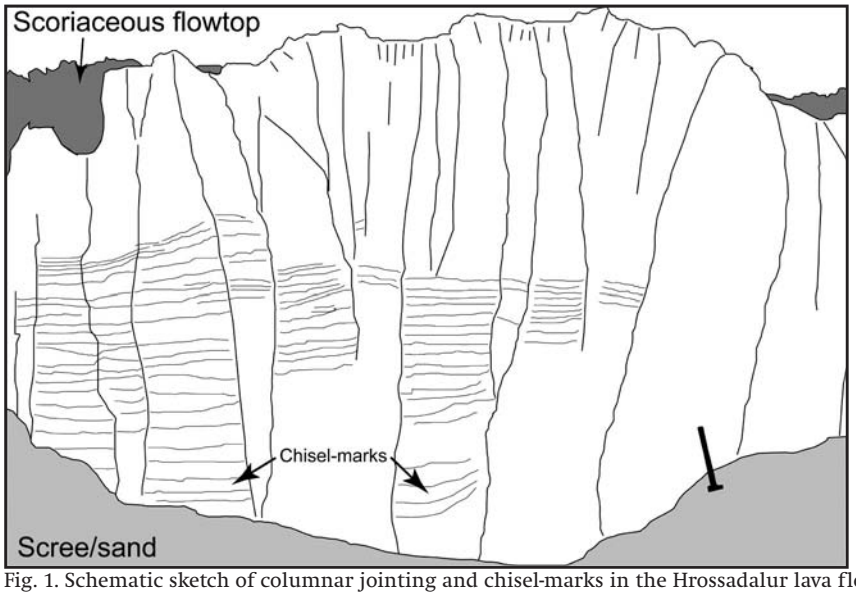

Fig. 1. Schematic sketch of columnar jointing and chisel-marks in the Hrossadalur lava flow. Hammer for scale.

At Hrossadalur in northern Iceland a 200 m long cross-section of a ponded, columnar-jointed, basaltic lava flow is exposed in a normal fault belonging to the much larger Krafla fissure swarm. The total thickness of the Hrossadalur lava flow exceeds 10 m, and display an internal morphology characteristic for p-type pahoehoe with a vesicular upper crust and a dense interior. Close to the top of the lava flow small-scale columnar jointing is abundant (although poorly developed). In this part of the flow chisel marks are absent. Starting roughly 0.8-1.5 m from the top of the flow (i.e. the cooling surface), columnar joints are fewer and larger in size and chisel-marks start to form (Fig. 1). The initial spacing between individual chisel marks is small (a few cm). However, the spacing of the chisel-marks shows a systematic increase with depth into the interior of the flow (in cases exceeding 25 cm near the central part of the flow). The base of the exposed section is composed of a massive part, where columnar jointing and chisel marks are absent. Instead concentric arrangement of vesicles and flow foliation indicate that this portion of the lava flow was occupied by lava tubes.

Measurements of the spacing of chisel-marks at Hrossadalur, in combination with observations of crack propagation in active Hawaiian lava flows (Hon et al., 1994), suggests that the spacing represents the effective thickness of the viscoelastic part of the crust as a lava flow progressively cools and solidifies. The fracture propagation is incremental, going from the brittle crust (<800°C), through the viscoelastic layer (800-1070°C), to the molten interior (>1070°C). After one step of fracture propagation, the flow needs to cool to build up sufficient thermoelastic strain to promote another cycle of crack-propagation.

Tentative modeling of conductive cooling (Carslaw and Jaeger, 1959) involving a change of state (molten to solid), shows good agreement between the time-dependant thickness of viscoelastic crust and the measured spacing of chisel-marks at Hrossadalur. Thus, the spacing of the chisel marks present in columnar jointed basalts can effectively be used to constrain the cooling history of slowly solidifying lava lakes and intrusions as well as lava flows.

REFERENCES

Carslaw, H.S. & Jaeger, J.C. 1959: Conduction of heat in solids, 2nd Ed., Oxford Univ. Press, New York, pp. 510

Hon, K., Kauahikaua, J., Denlinger, R. & Mackay K. 1994: Emplacement and inflation of pahoehoe sheet flows: Observations and measurements of active lava flows on Kilauea volcano, Hawaii, Geological Society of America Bulletin, 106, 351-370.

3.25

Convective instabilities in Volcanic Clouds

Monnard Hélène*, Manzella Irene*, Jeremy Phillips**, Costanza Bonadonna*

*Department of Mineralogy, University of Geneva, Rue des Maraîchers 13, CH-1205 Genève (hmonnard@gmail.com)
**Department of Earth Sciences, Centre for Environmental and Geophysical Flows, University of Bristol, UK

Convective instabilities driven by particle sedimentation may play an important role in the particle dispersal from volcanic plumes (e.g. Figure 1). Such instabilities occur in density stratified fluids and they are characterised by the formation of fingers. When a particle laden fluid is situated above a denser fluid, the two layers are initially stable. With the particle settling, a thickening interface layer becomes gravitationally unstable and fingers could start develop.
Many experiments have been carried out to characterize this process (e.g. Chen 1997; Hoyal et al. 1999; Völtz et al 2000). However, not many experiments were carried out to investigate convective instabilities in a volcanic setting (e.g. Carey 1997). In addition, numerical models used to describe tephra dispersal do not account for convective instabilities.
We have performed laboratory experiments to investigate the dynamics of this phenomenon and its effects on the rate of particle sedimentation from the bottom of the volcanic plume and deposition at the bed.

The experiments were carried out in a Plexiglas tank of a size of 30cm width x 7.5cm depth x 50cm height (see Figure 2a), where a removable and flexible PET sheet is placed at 25 cm height to separate two different layers of fluid and ensure an initially sharp interface. The upper part is filled up to 13.5 cm with a lighter suspension of water and particles, the lower part is filled with a denser sugar and water solution. The upper layer is strongly mixed before each experiment to ensure an initially uniform concentration. Experiments consist in removing the separation and analyzing the formation of fingers. Each experiment is filmed by a HD camera. A process of calibration has been carried out to correlate the different grey levels of a film image to different level of concentration.

After the removal of the separation, if we consider the upper layer to behave as a simple quiescent suspension, we could expect its mean concentration to decrease linearly with time as follows:

$$C(t) = C_0 - \frac{C_0 w_s t}{h}$$

Preliminary observations showed us that this is not the case for our experiments (see Figure 2b). As a matter of fact, the concentration values start decreasing after a certain time following the opening of the separation. This could be due to the fact that the linear model does not take into account the accumulation of particles at the interface between the two layers at different densities, which actually causes gravitational instabilities. These first considerations confirm the fact that convective instabilities influence the rate of sedimentation and consequently underline the need to develop new and complete analytical expressions to improve modelling of sedimentation from buoyant plumes.

Figure 1: Examples of fingering generated at the base of horizontally-spreading volcanic clouds (Eruption of Montserrat, 1997. Photo by Costanza Bonadonna).

(a)

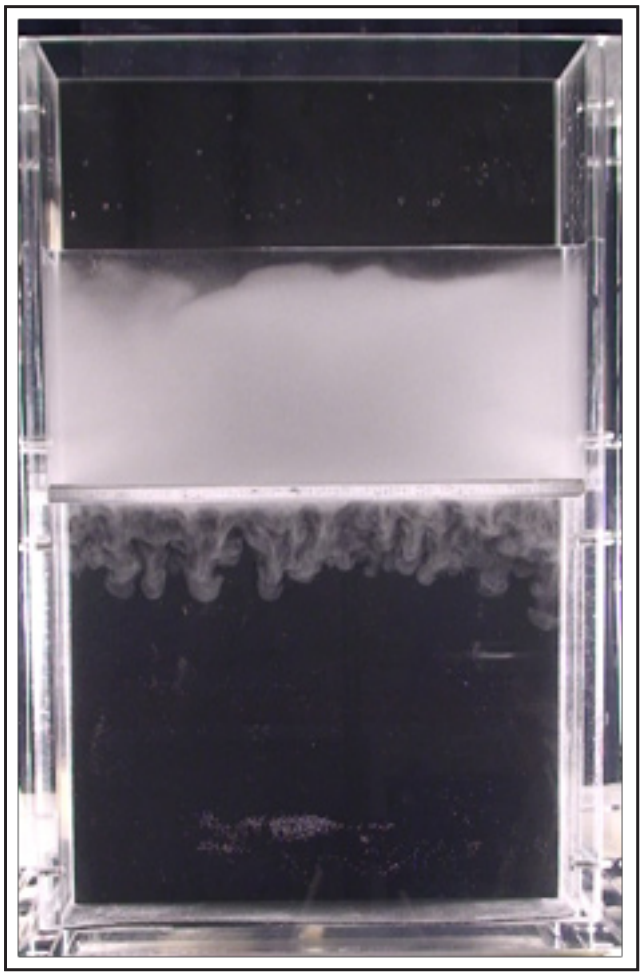

(b)

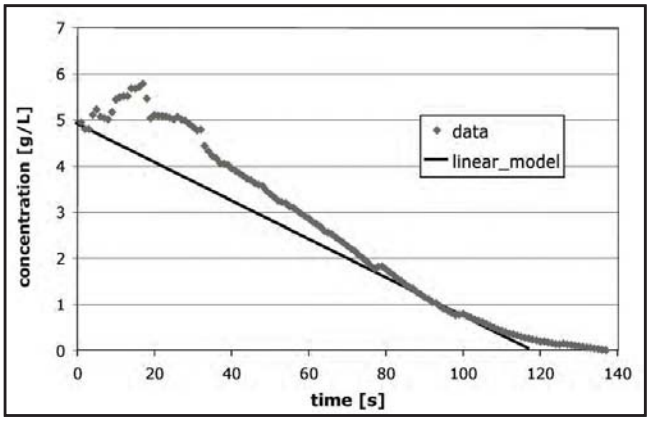

Figure 2: (a) The experimental set-up, a Plexiglas tank of 30x7.5x50 cm after the banner is removed. (b) Mean concentration for the upper layer as a function of time for an initial concentration of 4.9 g/L compared with the linear model.

REFERENCES

Carey, S. N. 1997: Influence of convective sedimentation on the formation of widespread tephra fall layers in the deep sea. Geology, 25(9), 839-842.

Chen, C. F. 1997: Particle flux through sediment fingers, Deep Sea Research Part I. Oceanographic Research Papers, 44(9-10), 1645-1654.

Hoyal, D. C. J. D., et al. 1999: Settling-driven convection: A mechanism of sedimentation from stratified fluids. J. Geophys. Res., 104.

Voltz, C., et al. 2000: Finger-like patterns in sedimenting water-sand suspensions. Physics Reports, 337, 117-138.

3.26

Geochemical constraints on the development of a Mesozoic volcano-tectonic arc and fore-arc basin in the Sanandaj-Sirjan Zone, south Iran

Monsef Iman*, Rahgoshay Mohammad*, Emami Mohammad-Hashem** & Shafaii Moghadam Hadi***

*Shahid Beheshti University, Faculty of Earth Sciences, Tehran, Iran (iman_monsef@yahoo.com)
**Research Institue for Earth Sciences, Geological Survey of Iran, Teharn, Iran
***Damghan University of Basic Sciences, School of Earth Sciences, Damghan, Iran

The tectonic history of the Neo-Tethyan region in Iran was begun by the creation of the oceanic lithosphere with rifting between the Central Iranian Block and Gondwana (Arabia) during Late Permian-Early Triassic time. The subduction of the Neo-Tethys starts to the south of the Central Iranian Block at Late Triassic–Late Jurassic time. This subduction phase led to presence of volcanic activities and emplacement of intrusive bodies within the Sanandaj-Sirjan Zone (Fig. 1). Therefore the Sanandaj-Sirjan Zone behaved as an active continental margin, witness by the presence of calc-alkaline arc-related magmatism. The Sanandaj-Sirjan Magmatic Arc is composed mainly of a Mesozoic magmatism including lava (basalt, andesite and dacitic tuff) and plutonic rocks (granite, granodiorite and quartz monzonite), alternating with limestones and Orbitolina limestone.

About a same time during subduction of the Neo-Tethys, rifting along the Sanandaj-Sirjan Zone took place, resulting in opening of a Late Triassic to Early Jurassic transtensional fore–arc basin called the Hajiabad–Esfandagheh Color Melange Zone (Fig. 1). This zone contains abundant ultramafics with chromite deposits, partly preserved volcano–sedimentary sequences with pillow lavas, Globotruncana–bearing red marls and radiolarites, and exotic marbles, amphibolites and minor blueschists. Volcanic rocks have a mixture of dominantly arc-like (calc-alkaline) and subordinate MORB-like compositional features.

The emplacement of Color Melange Zone took place during the Early to Late Cretaceous as a result of collisional and continental subduction of the Gondwana (Arabia) beneath the Central Iranian Block along the Main Zagros Thrust Belt. The Zagros orogen is a young Tertiary collision belt generally considered a recent analogue of the Himalayan orogenic belt.

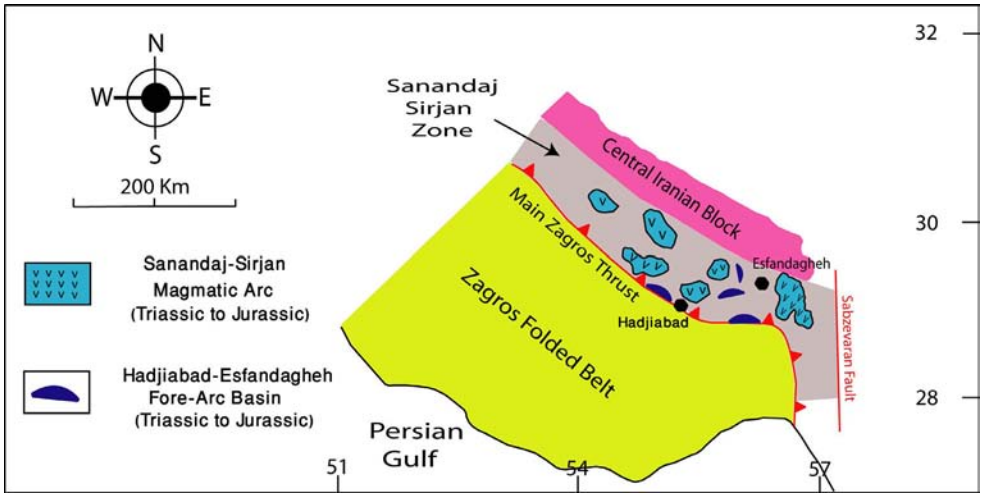

Figure 1. Simplified structural sketch map of south Iran. The locations of major structural zones consisting of Sanandaj-Sirjan Zone, Central Iranian Block, Main Zagros Thrust and Zagros Folded Belt are indicated.

REFERENCES

Agard, P., Monie, P., Gerber, W., Omrani, J., Molinaro, M., Meyer, B., Labrousse, L., Vrielynck, B., Jolivet, L. & Yamato, P., 2006: Transient, synobduction exhumation of Zagros blueschists inferred from P-T, deformation, time, and kinematic constraints: Implications for Neotethyan wedge dynamics. Journal of Geophysical Research, 111, B11401, 1-28.

Ewart, A., Collerson, K.D., Regelous, M., Wendt, J.I. & Niu, Y., 1998: Geochemical evolution within the Tonga-Kermadec-Lau arc-back arc systems: the role of varying mantle wedge composition in space and time. Journal of Petrology, 39, 331-368.

McCulloch, M.T. & Gamble, J.A., 1991: Geochemical and geodynamical constraints on subduction zone magmatism. Earth and Planetary Science Letters, 102, 358-375.

Pearce, J.A., 1980: Geochemical evidence for the genesis and eruptive setting of lavas from Tethyan ophiolites. In: Panayiotou, A., (Eds.), Ophiolites. Procceding International Ophiolite Symposium, Nicosia, Geological Survey Department, 261-272.

3.27

Transtensional basin system in Central Iranian Volcanic Belt

R. Monsef *, M.H. Emami**, N. Rashidnejad Omran***

* ISLAMIC AZAD UNIVERSITY,ESTAHBAN BRANCH,IRAN (zaos13000@yahoo.com)
**RESEARCH INSTITUE FOR EARTH SCIENCES, GEOLOGICAL SURVEY OF IRAN.
*** GEOLOGY DEPARTMANT BASIC SCIENCE FACULTY, TARBIAT MODARES UNIVERSITY,PO. 14115-111,TEHRAN

Urumieh-Dokhtar magmatic zone (UDMZ) has been considered as a place for the main magmatic activities in the Central Iranian continent in the Cenozoic(mainly in eocene).Magmatism is spatially and temporally associated with Alpine-Himalaya collisional tectonics. Explosive activities in Paleogene and early Neogene were commonly from fissure eruptions and feeder dikes had a domonant role for creation of thick sequences of magmatic and pyroclastic rocks. The Slafchegan to Delijan region covers an area about 500 sq. It is characterized by a number of sub parallel mountains and depressions, running NW-SE belongs to Neogene.centeral vent eruptions caused for creation of strata-volcanoes in the study area and varient of volcanic domes in continental environment. The Neogene volcanic activities are divided into two phases: At the first stage (Ngv_1), volcanic rocks contain basalt to andesite-basalt as lava or pyroclastic materials.The explosive event was followed by the volcanic to subvolcanic associations of Ngv_2 with products of mainly andesitic to rhyiolitic composition. The volcanic domes of Ngv_2 and their diverse modes of emplacement are especially characteristic of this phase as Kuh-e-Aleh (fig.1). Petrography,Geochemistry and mineral chemistry data confirm the presence of transtensional regions along the Urumieh-Dokhtar magmatic zone(UDMZ), opened during Paleogene and early Neogene due to the collision of the Arabia platform and Central Iranian continent. At Tertiary time, the time span between the Laramidian and Mio-Pliocene phase is related to the opening up of the basins (intercontinental rift), the extensional phenomenon moving slowly at the end of the Eocene and the beginning of the Oligocene. Local Nogene volcanism due to transtensional regions happens in Oligo-Miocene. The closing of the basins, or compressional period, began with the Mio- Pliocene movement which caused the folding and uplifting.

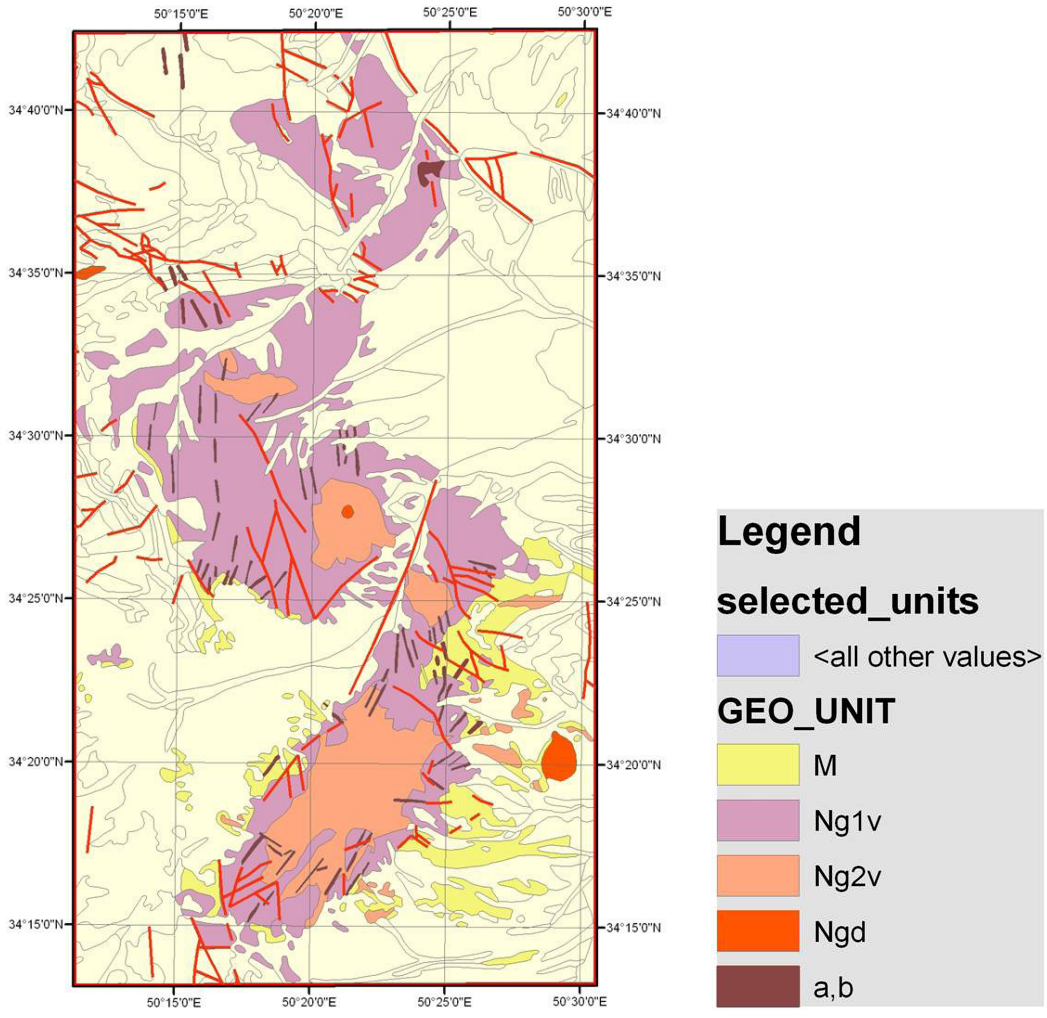

Figure 1. Geological our view map of Neogene volcanic activities.1:25000

REFERENCES
Emami. M.H., 1981, Geologie de la region de Qom-Aran (Iran) contribution a l etude dynamique et geochimique du volcanisme tertiaire de l Iran Central, These Doctorat Etat Grenoble, 489
Ricou, L.E., 1994. Tethys reconstructed plates, continental fragments and their boundaries since 260 Ma from Central America to South – eastern Asia. Geodynamica Acta (Paris) 7.
Verdel, Charles, 2009, Cenozoic Geology of Iran: An integretad study of extensional tectonics and related volcanism, Thesis doctor of philosophy,California Institute for Technology.

3.28

Metamorphic evolution of a kyanite-eclogite from Thermes, Rhodope Massif, Greece.

Moulas Evangelos*, Kostopoulos Dimitrios**

*Geologisches Institut, ETH Zürich, Sonnegstrasse 5, 8092 Zurich, Switzerland (moulase@student.ethz.ch)
**Department of Mineralogy and Petrology, Faculty of Geology and Geoenvironment, School of Sciences, National and Kapodistrian University of Athens, 157 84 Athens, Greece*

The Rhodope Massif in northern Greece is a recently identified ultrahigh-pressure metamorphic (UHPM) province comprising garnetiferous metapelites and eclogites with microdiamond inclusions. These rocks preserve evidence of melting (T>1100°C; P>7 GPa) in a Jurassic subduction zone and a complex reheating history at the base of the crust in the early Tertiary.

A kyanite-eclogite from the Thermes area reveals the pressure-temperature-time path followed by the Rhodope UHPM rocks. Textures involving phengitic mica indicate melting at high confining pressures. Quartz inclusions in kyanite show multi-polygonal domains and radial cracks suggesting former coesite, hence P conditions >2.7 GPa (at about 700°C).

Clinopyroxene formed under UHP conditions was replaced by diopside + plagioclase symplectites whereas kyanite was replaced by corundum + plagioclase symplectites during decompression. The latter reaction occurred in locally silica undersaturated domains of the rock (Godard & Mabit 1998). Large porphyroblastic amphiboles with taramitic cores mantled by pargasitic compositions attest amphibole formation via hydration reactions in the eclogite-facies and later decompression to the amphibolites facies.

Subsequent granulitisation proceeded via reactions between i) garnet porphyroblasts and matrix diopside to form coronas of plagioclase + ilmenite + magnetite + sodic gedrite around garnet, ii) corundum and diopside to form spinel + plagioclase symplectites after kyanite and iii) kyanite, spinel and corundum to form sapphirine (Liati & Seidel 1996). These imply that conditions of approximately 1.5 GPa at T>800°C were attained, possibly associated with a second-stage partial melting episode. Zircon geochronology using SHRIMP revealed a middle Eocene age (~42 Ma) for granulite formation. This age, in conjunction with the coeval age of apophyses of the Skaloti granite in the area, is consistent with the general history of the Rhodope Massif undergoing general exhumation and crustal collapse in Eocene times.

REFERENCES
Godard, G. & Mabit, J.-L. 1998: Peraluminus sapphirine formed during retrogression of a kyanite-bearing eclogite from Pays de Léon, Armorican Massif, France, Lithos 43, 15-29.
Liati, A. & Seidel, E. 1996: Metamorphic evolution and geochemistry of kyanite eclogites in central Rhodope, northern Greece, Contrib. Mineral. Petrol. 123, 293-307.

3.29

Rheological properties of crystal- and bubble-bearing silicic magmas: preliminary experimental results

Pistone Mattia *, Caricchi Luca **, Burlini Luigi ***, Ulmer Peter *

* *ETH-Institute for Mineralogy and Petrology, Clausiusstrasse 25, CH-8092 Zurich, Switzerland (mattia.pistone@erdw.ethz.ch; peter.ulmer@erdw.ethz.ch)*
** *University of Bristol, Wills Memorial Building - Queen's Road, BS8 1RJ Bristol (ca.luca@live.com)*
*** *ETH-Geological Institute, Sonneggstrasse 5, CH-8092 Zurich, Switzerland (luigi.burlini@erdw.ethz.ch)*

Natural magmas are mixtures of silicate melts, crystals and gas bubbles. The viscosity of such multi-phase mixtures is the single most important property controlling the eruptive behavior of volcanoes. The rheological behavior and the physical properties of magmas depend primarily on the viscosity of the silicate melt and on the relative contents of crystals and bubbles (Caricchi et al. 2007; Llewellin & Manga 2005) as well as on the interactions between these three phases.
The shape and size distribution of crystals has been demonstrated to influence significantly the variation of viscosity with respect to the crystal fraction. In addition, the non-Newtonian behavior of magmas (viscosity decreases with increasing deformation rate) has been associated to the geometrical ordering of suspended particles in the magma (Caricchi et al. 2007; Costa et al. 2009).

Bubbles exert contrasting effects on the rheological behavior of magmas depending on applied stress conditions. Deforming bubbles cause the viscosity to decrease while spherical gas vesicles behave as crystals, thus increasing the magma viscosity.
We present novel experimental results on the rheological behavior of magmas composed of liquid and both, gas-pressurized bubbles and crystals, deformed at magmatic pressures and temperatures. This study aims to constrain the dependence of rheological and physical properties of magmas on the viscosity of the silicate melt, on the relative contents of crystals and bubbles and on the interactions between these three phases.
The starting material constitutes of a haplogranitic melt containing variable amounts of H_2O (2.68 wt% and 5.25 wt%) and CO_2 (2.06 wt% and 4.97 wt%) and different proportions of quartz crystals (between 24 and 65 vol%; 63-125 μm in diameter) and bubbles (between 7 and 22 vol%; 5-150 μm in diameter).
The experiments were performed in simple shear using a HT-HP internally-heated Paterson-type rock deformation apparatus (Paterson & Olgaard, 2000) at strain rates ranging between $5{\cdot}10^{-5}$ s^{-1} and $1{\cdot}10^{-3}$ s^{-1}, at a pressure of 200 MPa and temperatures between 773 and 923 K.

At these temperature and strain rate conditions the silicate melt behaves as a Newtonian liquid (Webb & Dingwell, 1990). Consequently, non-Newtonian effects can entirely be related to the presence of bubbles and crystals. In all experimental runs a marked weakening behavior (decrease of stress with increasing strain) was observed.
Back-scattered electron images were acquired on external portions of the samples, where the simple shear configuration is best appreciated. These images clearly highlight the presence of melt-enriched portions of the samples were bubbles are strongly deformed. In contrast, in regions surrounding these melt-enriched bands, bubbles are almost spherical testifying that these portions of the material suffered a significantly lower amount of deformation. Locally, deformed bubbles between crystals resulting from local stress concentration generated by the solid particles can be observed. The measured weakening is most probably related to the generation of melt-enriched shear bands. The localization of deformation in these lower viscosity regions results in a decrease of viscosity with increasing strain (shear thinning effects).

These preliminary experimental results serve to guide our ongoing experimental efforts to finally obtain rheological laws for crystal and bubble bearing magmas to simulate and predict volcanic eruptions from shallow magma reservoirs and volcanic conduits.

REFERENCES

Caricchi, L., Burlini, L., Ulmer, P., Gerya, T., Vassalli, M. & Papale, P. 2007: Non-Newtonian rheology of crystal-bearing magmas and implications for magma ascent dynamics. Earth Planet. Sci. Lett. 264, 402-419.

Costa, A., Caricchi, L. & Bagdassarov, N.S. 2009: A model for the rheology of particle-bearing suspensions and partially molten rocks. Geochem. Geophys. Geosyst. 10, 1-13.

Llewellin, E.W. & Manga, A. 2005: Bubble suspension rheology and implications for conduit flow. J. Volcanol. Geotherm. Res. 143, 205–217.

Paterson, M.S. & Olgaard, D.L. 2000: Rock deformation tests to large shear strains in torsion. J. Struct. Geol. 22, 1341-1358.

Webb, S.L. & Dingwell D.B. 1990: Non-Newtonian rheology of igneous melts at high stresses and strain rates: experimental results for rhyolite, andesite, basalt and nephelinite. J. Geophys. Res. 95 (B10), 15695-15701.

3.30

Complexities in the high pressure metamorphic history of the central Sesia Zone near Cima di Bonze (NW Italy)

Daniele Regis*, Paola Manzotti*, Katherine Boston**, Benedicte Cenki-Tok*, Martin Robyr*, Daniela Rubatto**, Tonny Thomsen*, Martin Engi*

*University of Bern, Baltzerstrasse 3, CH-3012 Bern, Switzerland (regis@geo.unibe.ch)
**The Australian National University, Mills road, Canberra, ACT, 0200 Australia

The central Sesia-Lanzo Zone includes a narrow, continuously surfacing unit, which was termed Monometamorphic Cover Complex (MCC) by Venturini (1995). The MCC comprises: (a) the *Bonze Unit*, composed of basic rocks (metagabbros and glaucophane-eclogites), found in tectonic contact with (b) metasediments (calcschists, metamarls, impure quartzites) of the *Scalaro Unit*. The contacts between this body and the two large basement blocks of the Sesia Zone are clearly tectonic and mostly predate the eclogitic metamorphism.

Rubatto et al. (1999) showed that gabbros of the Bonze Unit had intruded the crystalline basement in the early Carboniferous. Blasto-mylonitic metagabbros contain local relics of brown hornblende; these may reflect pre-Alpine metamorphism (amphibolite facies?). However, no relics of a pre-Alpine stage have been found in the metasediments of the Scalaro Unit. This unit is thus a good target for structurally controlled petrochronology of the Alpine evolution in the central Sesia Zone.

We report results of detailed structural, petrographic, chemical and geochronological work carried out in the Cima Bonze region, with a focus on impure quartzites of the poly-deformed Scalaro Unit. A pervasive HP planar structure (S2 foliation) dominates in the area studied and in the samples analysed. Several generations of metamorphic allanite and LREE-rich epidote occur, providing a robust (Th-Pb, U-Pb) chronometer that can be intimately linked to the petrological and micro-structural evolution. Three growth zones with variable REE and U-Th contents were recognized in these allanites, and retrogressive tiny rims of clinozoisite/epidote were often observed. Phase relations between allanite and other REE-rich phases were carefully studied and yield a very clear and interesting sequence. Epidote often includes relics of monazite, thorite, apatite and xenotime. The phase relations indicate the reaction: monazite + fluid à allanite + thorite + apatite. Large crystals of xenotime forming coronas on zircon are associated with small crystals of thorite and REE-poor allanite.

SHRIMP U-Th-Pb *in situ* dating of the three growth zones consistently yield three different Alpine ages (from 83 Ma to 65 Ma). Preliminary LA-ICP-MS data on the same samples confirm the ion probe results. Further electron microprobe dating is underway on monazite and thorite to understand their relations to allanite and to unravel whether the early monazite is a prograde or a detrital phase.

These results have important implications on the Alpine HP-evolution of the Sesia Zone as a whole. A detailed PTDt-path is presently being be worked out, but the preliminary data in any case indicate a complex, protracted reaction sequence producing allanite over at least 10 m.y. This may serve to explain at least some of the complex Ar-Ar age patterns found by Venturini (1995).

REFERENCES

Rubatto D., Gebauer D., Compagnoni R. 1999: Dating of eclogite-facies zircons: the age of Alpine metamorphism in the Sesia-Lanzo Zone (Western Alps). Earth Planet. Sci. Letters 167, 141-158.

Venturini G. 1995: Geology, geochemistry and geochronology of the inner central Sesia Zone (Western Alps – Italy). Mémoires de Géologie, Lausanne, 25, 148 pp.

3.31

The temporal evolution of the Mitu group, south-east Peru – first U-Pb age data.

Reitsma Mariël*, Schaltegger Urs*, Spikings Richard*, Carlotto Victor**

*Earth and Environmental Sciences, Rue des Maraîchers 13, CH-1205 Genève
**INGEMMET, Av. Canada 1470 San Borja, Lima, Peru

The Eastern Cordillera of southern Peru formed along a crustal zone that has been active as part of the western Gondwana margin since the middle Paleozoic. The present study investigates the Mitu Group of south-east Peru in the area of Abancay-Cusco-Sicuani-Titicaca. This unit comprises continental clastic sediments deposited in syn-sedimentary basins during an extensional period in Permo-Triassic times and has not benefitted from a thorough geochemical-geochronological investigation so far. One of the main reasons for this lack of data is a complex structure of the graben system, tectonically complicated by compressional inversion of the extensional basins during Andean orogeny. Due to dominating coarse-grained clastics, the Mitu Group is devoid of fossils and its age is only poorly bracketed to be Permo -Triassic based on its stratigraphic relation to the underlying Copacabana and overlying Pucara groups. The upper levels of the Copacabana have been constrained by palynology to the Artinskian (Doubinger and Marocco, 1981). However, a hiatus may be observed between the Copacabana and the Mitu groups in most places, rendering the age estimate of the basal Mitu imprecise. The Pucara Group, regarded by Rosas et al. (2007) as thermal sag after Mitu extension, is attributed to the late Triassic - early Jurassic on the basis of ammonite fossils and U-Pb zircon ages from ash beds (Schaltegger et al., 2008). The aim of this study is to provide more accurate and precise age constraints for the age and duration of the Mitu Group by using U-Pb geochronology of volcanic zircon in rhyolitic lavas, and of detrital zircon in clastic sediments. For andesitic volcanic lithologies, age approximations will be obtained by Ar-Ar techniques applied to amphibole and groundmass samples.

Field data were obtained from a long and apparently complete section through the Mitu, situated 120km SE of Cusco near the city of Sicuani. This section consists of typical Mitu deposits; continental red beds, breccias and andesitic lavas. However, a zircon-bearing rhyolitic lava at the bottom gives us the opportunity to date the start of Mitu sedimentation by U-Pb ID-TIMS; this analysis will provide a precise age for the base of the Mitu group for the first time. In the Sicuani area the Mitu unconformably overlies the Ambo group, suggesting that the entire Copacabana is missing. Laser-ablation ICP-MS U-Pb data of detrial zircons from a sandstone just below the unconformity indicate a maximum age of latest Carboniferous (303Ma) for the underlying Ambo group. This maximum age overlaps with the palynological age of the lower Copacabana (Azcuy et al., 2002), raising the question whether the Ambo and Copacabana are truly diachronous or just coeval units of different sedimentary facies associations.
In another section, 100km W of Cusco, near the city of Abancay, we found Mitu sediments overlying the Copacabana Group. Here the Copacabana contains well preserved plant fossils of the lycopsids family also found elsewhere in Peru and Bolivia. Lack of acidic volcanism during Mitu extension in this region prevents from dating of lavas using the U-Pb method. The detrital zircon population in a sandstone in the lowermost part of the Mitu was analysed for U-Pb ages, using LA-ICP-MS techniques. The youngest zircons in the population are around 235 Ma hence providing a maximum age for the onset of Mitu group sedimentation. The Artinskian age for the upper Copacabana from Doubinger and Marocco (1981) has also been obtained from the Abancay region, establishing a hiatus of some 50 Myrs between the two units. The Mitu Group is intruded by a 220 Ma granite body (Lipa and Saraiva, 2008) indicating significant burial of the sediments at this time.
500km SE of Cusco, on the Bolivian shores of lake Titicaca, the Ambo Group features plant fossils of the Lycopsids family like those found in the Copacabana near Abancay. Our detrital zircon LA-ICPMS study on a quartz arenite just below the fossils indicates a maximum U-Pb age of 343Ma. However a zircon-bearing ash bed will allow for more precise calibration of the fossil age by ID-TIMS techniques. The zircon U-Pb data will provide a test whether the Copacabana and the Ambo group are indeed diachronous or just lateral variations of a sedimentary system.

REFERENCES

Azcuy, C.L., Di Pasquo, M. & Valdivia Ampuero, H. 2002: Late Carboniferous miospores from the Tarma Formation, Pongo de Mainique, Peru. Review of palaeobotany and palynology 118, 1-28.

Doubinger, J., and Marocco, R. 1981 : Contenu Palynologique du Groupe Copacabana (Permien Inférieur et Moyen) sur la bordure Sud de la Cordillère de Vilcabamba, région de Cuzco (Pérou). International Journal of Earth Sciences 70, 1086-1099.

Lipa Salas, V. & Saraiva Dos Santos, T. 2008: Geocronologia y evolucion tectonica del pluton Abancay-Apurimac-Peru. XIII Latin-American geological congress: Lima, Peru.

Rosas, S., Fontboté, L. & Tankard, A. 2007: Tectonic evolution and paleogeography of the Mesozoic Pucara Basin, central Peru. Journal of South American Earth Sciences 24, 1-24.

Schaltegger, U., Guex, J., Bartolini, A., Schoene, B. & Ovtcharova, M. 2008: Precise U-Pb age constraints for end-Triassic mass extinction, its correlation to volcanism and Hettangian post-extension recovery. Earth and Planetary science letters 267, 266-275.

3.32

Single-crystal elastic properties of superhydrous phase B determined by Brillouin scattering spectroscopy

Rosa Angelika D.*, Sanchez-Valle Carmen*, Wang Jingyun* & Saikia Ashima*

Institute for Mineralogy and Petrology, ETH Zurich, Zurich 8092, Switzerland (angelika.rosa@erdw.ethz.ch)

Superhydrous phase B, $Mg_{10}Si_3O_{18}H_4$, (here referred to as ShyB) belongs to the group of DHMS phases (dense hydrous magnesium silicates), that are likely the most important water reservoirs in deep subducted slabs.
In order to formulate accurate mineralogical and compositional models of subducted slabs and to interpret seismic observation in this area, precisely measured elasticity data at relevant P-T conditions are needed but are not often available.

In this contribution we present results of Brillouin scattering measurements of the sound velocities and single-crystal elastic properties of ShyB at ambient conditions. Brillouin scattering is one of the most powerful and precise method to investigate the elastic properties of single-crystals and polycrystalline samples of small size. The ShyB single-crystals used here were synthesised in a Walker module multi anvil press of 1000 ton at IMP, Zurich at 20 GPa and 1200 ^{0}C. The Voigt-Reuss-Hill average for the adiabatic bulk and shear moduli are Ks = 150(3) GPa and μ = 98(2) GPa, respectively. The present results are in good agreement with a previous Brillouin scattering study by Pacalo & Weidner (1996) [1]. The bulk modulus obtained in this study is also in good agreement with the results of a previous single-crystal PV study [2] but resolve discrepancies between previous compressional studies using powdered samples [3,4]. The results show that the aggregate compressional and shear wave velocities of ShyB (V_P = 9.17(9) and V_S = 5.43(4) km/s) are the lowest among coexisting phases in subducted peridoties, including Mg-Perovskite, hydrous Ringwoodite or Ferropericlase. The velocity distribution calculated from the best-fit elastic model of ShyB reveals a nearly isotropic seismic behaviour of ShyB at room conditions. The compressional anisotropy (A_P) is only 6.6% while slightly higher shear anisotropy (A_S) of 11.6 % is observed. If the moderated anisotropy of ShyB is maintained at high P-T, the strong seismic anisotropy observed in subducted slabs below the transition zone, may not be related to the presence of ShyB.

REFERENCES

[1] Pacalo, R.E.G. and Weidner, D.J. 1996: Elasticity of superhydrous B. Physics and Chemistry of Minerals, 23, 520-525.
[2] Kudoh, Y., Nagase, T., Ohta, S., Sasaki, S., Kanzaki, M., and Tanaka, M. 1994: Crystal structure and compressibility of superhydrous phase B, Mg20Si6H8O36. In S.C. Schmidt, J.W. Shaner, G.A. Samara, and M. Ross, Eds. High-Pressure Science and Technology, Am. Inst. Phys. Conf. Proc., 309, p. 469-472.
[3] Inoue, T., Higo, Y., Yamada, A., Irifune, T. &Funakoshi, K. 2006: High-pressure and high-temperature stability and equation of state of superhydrous phase B by insitu X-ray diffraction. In S.D. Jacobsen, and S. Van der Lee, Eds. Earth Deep Water Cycle, p. 147-157. AGU, Washington DC.
[4] Litasov, K.D., Ohtani, E., Ghosh, S., Nishihara, Y., Suzuki, A. and Funakoshi, K. 2007: Thermal equation of state of superhydrous phase B to 27 GPa and 1373 K. Physics of the Earth and Planetary Interiors, 164, 142-160.

3.33

The influence of volatiles in basaltic explosive eruptions: the example of the Chaimilla eruption (3.1 Ka, Villarrica Volcano, Chile).

Scalisi Rosalinda1, Costantini Licia1, Bonadonna Costanza1, Di Muro Andrea2

1Section des sciences de la Terre et de l'environnement 13, Rue des Maraichers, Ch-1025 Genève (s.linda84@tiscali.it)
2Laboratoire de physique et chimie des systèmes volcaniques, IPGP-Paris VI, Paris, France

Villarrica is a basaltic-andesite stratovolcano located in the Southern Chilean Andes. It is one of the most active volcanoes in South America associated with east-dipping subduction of the Nazca plate beneath the South American plate. Although its historical eruptive activity has been mainly effusive, in its history Villarrica volcano had also explosive behavior producing both large pyroclastic density currents and tephra fallout. The largest-volume eruptions are the Lìcan Ignimbrite (~10Km^3, ~14,000 BP) and Pùcon Ignimbrite (~5Km^3, ~3500BP) (Witter et al., 2004), both of basaltic-andesite composition. The most re-

cent pyroclastic density current occurred ~1620 BP (Moreno et al., 1994). After the last eruption (1984-1985), Villarrica volcano has had a continuous passive degassing activity from the summit lava lake (Witter et al., 2004).
In this project we have investigated the initial condition of Villarrica magma storage reservoir and the role of different volatile species in controlling the eruption dynamics of Chaimilla deposit (~3,100 BP), which is the best preserved and most widely dispersed tephra fallout of Villarrica volcano. This is done by a detailed petrographical and geochemical study of olivine-hosted melt inclusions and of all the phases present in the system (i.e. minerals and glass matrix).

The petrographical and geochemical study has been carried out at the University of Geneva and Lausanne (for EMP analysis) with the exception of H_2O and CO_2 analyses of melt inclusions which was done at the Laboratory Pierre Sùe (Paris, France) using both FTIR and RAMAN techniques.

Our preliminary results show that the magma chemistry did not change during the evolution of the eruption (SiO_2 content of whole rock is ~53 wt% and SiO_2 content of melt inclusion varies between 52 and 56 wt%) with exception of the uppermost fallout layers, which show a slightly more primitive composition (SiO_2 content of whole rock is ~52 wt% and SiO_2 content of melt inclusion is ~51 wt%). Pre-eruptive H_2O content is relatively high (~2-3 wt%) for a basaltic magma, but this high content has been frequently found in other high-explosive basaltic eruptions (e.g. Metrich et al.,2004; Spilliaert et al., 2006; Roggensack et al., 1997). In addition Chaimilla melt inclusions do not contain CO_2 suggesting a relatively shallow magma reservoir.

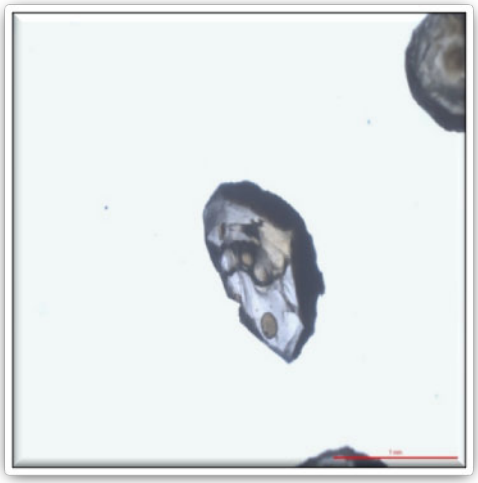

A

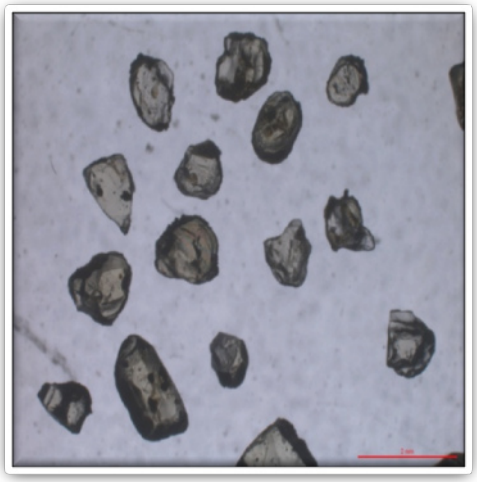

B

Fig A: melt inclusion present in olivine (Samples from Chaimilla scorias, Villarrica volcano, Chile). Fig B: different olivine crystals of Chaimilla deposit.

REFERENCES

Métrich N, Allard A, Spilliaert A, Andronico D, Burton M (2004). 2001 flank eruption of the alkali- -and volatile-rich primitive basalt responsible for Mount Etna. Earth and Planetary Science Letters, 228, 1-17.

Moreno H, Clavero J, Lara L. (1994). Actividad explosiva post-glacial del volcano Villarrica , Andes del Sur. Septimo congreso geologico chileno. Universidad de concepcion. Conception, Chile, 329-333.

Roggensack K, Hervig RL, McKnight SB, Williams SN (1997). Explosive basaltic volcanism from Cerro Negro volcano: Influence of volatiles on eruptive style. Science, 277, 1639-1642.

Spilliaert N, Allard P, Metrich N, Sobolev AV (2006). Melt inclusion record of the conditions of ascent, degassing and extrusion of volatile-rich alkali basalt during the powerful 2002 flank eruption of Mount Etna (Italy). Journal of Geophysical Research 111:doi: 10.1029/2005JB003934.

Witter J.B, Kress V.C, Delmelle P, Stix J (2004). Volatile degassing, petrology, and magma dynamics of the Villarrica Lava Lake, Southern Chile. Journal of Volcanology and Geothermal Research, 134, 303-337.

3.34

An experimental study in the system Fe-Mg-Ti-Cr-Si-O±Al: ilmenite solid solution as a function of pressure and temperature

Semytkivska Nina*, Ulmer Peter*

Department of Earth Science. ETH Zurich, Clausiusstr.25, 8092 Zurich

With the aim of improving the experimental basis of the calibration in the system Mg-Fe-Ti-Cr-Al-Si-O, we done experimental study with particular attention to picro-ilmenite.
Experiments were performed at temperature of 1000-1400 ^{o}C and pressure of 2.5, 3.5, and 5 GPa using different bulk compositions with variable Mg/Fe, Cr/Al ratios, and silica activity under relatively reducing conditions by employing graphite containers sealed into Pt-capsule. Experiments were run in solid-media piston cylinders and multi-anvil apparatus for durations of 30-120 hours.
Different phase paragenesis was observed at our experimental products. Bulk composition has a marked effect on the phase paragenesis, in particular, stability of the phases is influenced by the Mg# of the system. Ilmenite is stable together with olivine + orthopyroxene + spinel at bulk XMg of 0.73 (tab. 1, 2). rutile + olivine + opx + spinel are coexisting phases at a bulk X_{Mg} of 0.85 . Composition with lower SiO2 contents and low XMg values are characterized by the presence of three oxides: ilmenite + rutile + spinel coexisting with olivine and opx. Compositions with high X_{Mg} (0.85) and lower SiO_2 contents result in the disappearance of opx and rutile; present phases are olivine + spinel + ilmenite.

The experimental data set was used to determine equilibrium fractionation of Fe and Mg between coexisting ol and ilm, and applied to formulate model for ilmenite solid solution and intended to provide a new version of ilmenite-olivine an exchange geothermometer that could be applicable to the Cr-rich assemblage.

3.35

Pyroxenite veins in the Jurassic Pindos Ophiolite (NW Greece): cm-scale mantle heterogeneity preserved in MORB-source peridotites

Dmitry S. Sergeev*,**, Arjan H. Dijkstra*

*Université de Neuchâtel, Institut de Géologie et d'Hydrogéologie, Switzerland (dmitry.sergeev@unine.ch)
**Université de Lausanne, Institut de Minéralogie et Géochimie, Switzerland*

Geochemical and isotopic differences between different types of MORB are commonly attributed to heterogeneity in the mantle source. One of the major factors that can cause such heterogeneity is the presence of recycled ocean crust. We believe that traces of such heterogeneities can be preserved in pyroxenite veins in ophiolitic peridotite bodies. The Dramala Complex in the Pindos ophiolite (NW Greece) is a peridotite body with a mid-ocean ridge character, where we found a km-sized structural domain with coarse-grained mantle tectonites and 1-10 cm thick pyroxenite veins. Pyroxenites are concordant to the high temperature deformation structures in the host peridotites and show metamorphic, replacive textures in thin sections.

We measured Highly Siderophile Elements (HSE, i.e., Os, Ir, Ru, Pt, Pd, Re) and Os isotope ratios in whole rock pyroxenites and wall-rock peridotites. Pyroxenites were carefully cut from the enclosing peridotites. HSE patterns in both cases have identical character; some small differences in incompatible HSE concentrations (Pt, Pd, Re) occur due to the presence of sulphides in pyroxenites. Peridotites have chondritic to subchondritic $^{187}Os/^{188}Os$ ratios (0.1196-0.1291), whereas the pyroxenites are all significantly more radiogenic ($^{187}Os/^{188}Os$=0.1418-0.1980). These difference cannot simply be explained by differences in Re/Os ratios between peridotites and pyroxenites. Geochemical and petrographic data show that concordant pyroxenites represents relics of replacive pyroxenites formed melt-rock reaction between pyroxene-saturated melts and peridotite.

The fact that pyroxenite layers are parallel to the foliation in high-temperature deformed peridotite tells us about their early-stage origin. Based on textures and HSE concentrations, we propose that pyroxenites exposed now are replacive products

of SiO_2-rich melts, derived from the melting of old mafic layers within the peridotites, with very radiogenic $^{187}Os/^{188}Os$ isotope ratios, since no other source of high $^{187}Os/^{188}Os$ isotope ratio is likely to exist in these rocks. Moreover we suggest that the melt did not generally migrate over large distances perpendicular to the pyroxenites, i.e., that the pyroxenites are essentially the wall-rock of the old mafic layers. If our interpretation is correct, then these are the first traces of isotopic mantle heterogeneity in residual MORB-source mantle observed so far. The presence of pyroxenites with superchondritic Os isotope ratios in the mantle can explain why estimates for $^{187}Os/^{188}Os$ isotope ratios of depleted mantle rocks are generally subchondritic.

3.36

The Zagros Collision Zone: Petrological and geodynamical constraints on Inner and Outer Zagros Ophiolitic Belt

Hadi Shafaii Moghadam *, Robert J. Stern **, Mohamad Rahgoshay ***

*School of Earth Sciences, Damghan University of Basic Sciences, Damghan, Iran, E-mail: hshafaii@dubs.ac.ir
** Geosciences Department, University of Texas at Dallas, Richardson, TX 75083-0688, USA
***Faculty of Earth Sciences, Shahid Beheshti University, Tehran, Iran

Despite broad affinities to other ophiolites in the Tethyan Mediterranean-Oman ophiolite belt, the upper Cretaceous ophiolites of SW Iran remain relatively unknown in terms of geochemistry, petrogenesis and tectono-magmatic evolution. Zagros ophiolites comprise two parallel belts, including Inner Zagros Ophiolitic Belt (IB), along the SW periphery of the Central Iranian block and Outer Zagros Ophiolitic Belt (OB), south of Main Zagros Thrust Fault. IB and OB ophiolites formed at the same time: IB hornblende gabbros yield a K/Ar age of 93 Ma whereas OB diabases and hornblende gabbros yield Ar/Ar ages of 86-93 Ma, similar to ages of other ophiolites of the Mediterranean-Oman belt (Oman ~95 Ma, Cyprus ~90-94Ma). Pelagic limestones resting conformably on IB and OB ophiolites are Turonian-Maastrichtian (93.5-65.5 Ma). Several lines of evidence such as high Cr content of harzburgite spinel and flat REE patterns of the lavas with negative Nb-Ta anomalies from both inner and outer belt Zagros ophiolites indicate formation above a subduction zone, also similar to other Tethyan Oman-Mediterranean ophiolites. These similarities in ophiolite ages and tectonic setting suggest that the Oman-Mediterranean ophiolite belt represents a remarkably coherent lithospheric block. The parallel alignment of Zagros ophiolites between the Urumieh-Dokhtar arc and the Zagros fold-and-thrust belt (accretionary prism), further suggests that IB and OB ophiolites may be exposed limbs of a deformed anticlinoria, and represent fore-arc basement. In this interpretation, IB and OB represent inner and outer portions of the Late Cretaceous Iranian fore-arc, developed over an incipient N-dipping subduction zone on the southern Eurasian margin. The Zagros fold-and-thrust best is an accretionary prism that formed by off-scraping of Arabian Plate sediments, and the Urumieh-Dokhtar arc is an Andean-type arc that is waning as the region transitions from subduction to collision.

3.37

The transition from cold-wet to hotter-drier rhyolites in subduction zones: the case of the Kos-Nisyros-Yali volcanic center, Aegean arc, Greece

Skopelitis Alexandra*, Bachmann Olivier**

*Earth and environmental science, Rue des Maraîchers 13, CH-1205 Genève, (Alexandra.Nowak@unige.ch)
**University of Washington, Earth and Space Sciences Seattle, WA 98195-1310 (bachmano.@u.washington.edu)

The complexity of magmatic chamber mechanisms are extensively studied but not completely understood. Several parameters, such as temperature, pressure, melt composition and cristallinity, can modify rheology, geochemistry, and geometry of the chamber and therefore have an important influence on the type and style of eruption. Magma viscosity is strongly linked with water content, crystal content and temperature.

Two kinds of rhyolites have been defined in the literature (Christiansen 2005): the first kind is cold (<750 °C) and oxidized (NNO+1) whereas the second kind is hotter (≥850 °C) and more reduced (~NNO or lower). Although both are at or near volatile saturation in shallow crustal magma chambers, the cold-oxidized type is obviously more water-rich, as it contains biotite and lacks pyroxene. The wet type is usually found in subduction zone settings, whereas the drier type is more characteristic of hot spot and extensional environments where mantle melting occurs by adiabatic decompression.

The present study shows that both types of rhyolites can be found in the same locality in the Aegean Arc in Greece (Fig. 1). We compared rhyolitic pumices of the Kos Plateau Tuff (KPT eruption age: 160 ky, (Smith et al. 1996)) from Kos Island to Nisyros and Yali, two southernmost islands. The rocks chemistry shows evolved compositions with an average around 70 %wt SiO_2 for Nisyros and 75-76 %wt SiO_2 for KPT and Yali.

The caldera-forming KPT erupted from a shallow (1.5-2.5 kb) near-solidus (~670-700 °C) and oxidized (NNO+1) magma chamber that was saturated with a water-rich gas phase. The following eruptions from Nisyros and Yali were in contrast, 100-150 °C hotter, less oxidized (~NNO) and mainly contained plagioclase and clinopyroxene (although Yali does contain minor quartz and sanidine as well). The reason for this shift from wet to drier rhyolites can be due to either (1) a change in parental basalt composition (drier basalts leading to drier rhyolites) or (2) an efficient degassing event induced by the caldera-forming event. More studies, including experiment work to reconstruct the temperature-pressure conditions before eruptions, are needed to better understand which scenario contributed to the observed shift in these rhyolites.

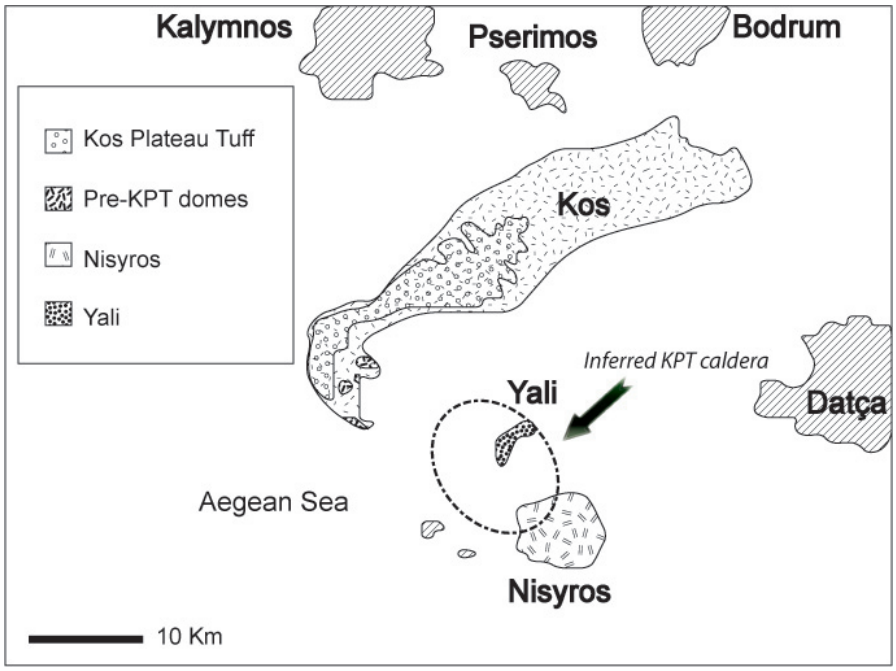

Figure 1. Simplified map of Kos, Nisyros and Yali. (Modified after Allen, 2001)

REFERENCES

Allen, S.R. 2001: Reconstruction of a major caldera-forming eruption from pyroclastic deposit characteristics: Kos Plateau Tuff, eastern Aegean Sea. Journal of Volcanology and Geothermal Research 105, 141-162.

Christiansen, E.-H. 2005: Contrasting processes in silicic magma chambers; evidence from very large volume ignimbrites. Geological Magazine 142(6), 669-981.

Seymour, K.S. & Lalonde, A. 1991: Monitoring oxygen fugacity conditions in pre, syn- and postcaldera magma chamber of Nisyros volcano, Aegean island arc, Greece. Journal of Volcanology and Geothermal Research 46, 231-240.

Smith, P. E., York, D., Chen, Y. & Evensen, N.M. 1996: Single crystal 40Ar/39Ar dating of a Late Quaternary paroxysm on Kos, Greece: Concordance of terrestrial and marine ages. Geophysical Research Letters 23, 3047-3050.

Volentik, A., Vanderkluysen, L., Principe, C. & Hunziker, J.C. 2005: Stratigraphy of Nisyros volcano (Greece). The geology, geochemistry and evolution of Nisyros Volcano (Greece). Implications for the volcanic hazards. Mémoires de Géologie (Lausanne), 26-66.

3.38

Dynamics of Cd, Pb and Cu cycling in a stream under contrasting photo-benthic biofilm activity and hydrological conditions

Tercier-Waeber Mary-Lou*, **, Hezard Teddy* & Masson Matthieu**

*CABE – Department of Inorganic, Analytical and Applied Chemistry, University of Geneva, Sciences II, 30 Quai E.-Ansermet, CH-1211 Geneva 4 (Marie-Louise.Tercier@unige.ch)
**Institut F.-A. Forel, University of Geneva, 10 Route de Suisse, CH-1290 Versoix

The past decade studies performed in rivers and streams demonstrated that many trace metal and metalloid experience diurnal cycles, with total dissolved metal concentrations often changing one- to five-fold during a 24h period. However, most of these studies were performed in summer under low-flow conditions. Moreover, samples were collected hourly by hand for later laboratory analysis. This laborious sample collection and processing approach limits hourly sampling to 1–3 days at maximum. More frequent analysis is required to understand the seasonal occurrence and amplitude of diel metal cycles, and the processes controlling these cycles.

With this goal in mind, we applied an automated voltammetric analyzer to study, at time scale of hour and under contrasting bio-chemical and hydrological conditions, the diurnal evolution of Cd, Cu and Pb in the Riou-Mort river (France) impacted by polymetallic pollution resulting from former open-cast coal mining and ore treatment. This analyzer is based on a bioanalogic microsensor which allows in situ real-time monitoring of the dynamic fraction, i.e. the potentially bioavailable fraction, of the target analytes. In parallel, T, pH, dissolved oxygen and conductivity were monitored in situ and water samples were collected for complementary analyses of the water composition.

Several original results were obtained. The data revealed that, in the studied river, the diurnal cycles of the Cd, Cu and Pb dynamic species were controlled by redox and sorption effects induced by either: pH diurnal cycle linked to metabolic activity of benthic biofilms; photoreduction of colloidal Mn oxides; and/or biofilm exudation of extracellular polymeric substances. We also observed that: the dynamic fraction of a given cationic metal can show diurnal cycle with opposite trends depending on the bio-chemical conditions; the trends of the diurnal dynamic metal species cycles may be different that those reported for the dissolved metal species. The importance of these findings will be discussed in the context of interpreting existing data banks, assessing metal ecotoxicity impact, and designing more appropriate monitoring control strategies.

REFERENCES

Tercier-Waeber, M.-L. & Taillefert, M. 2008: Remote in situ voltammetric techniques to characterize the biogeochemical cycling of trace metals in aquatic systems. J. Environ. Monit.,10, 30-54.

Tercier-Waeber, M.-L., Hezard, T., Masson, M., & Schäfer J. 2009: In situ monioring of the diurnal cycling of dynamic metal species in a stream under contrasting photobenthic biofilm activity and hydrological conditions, Env. Sci. Technol., DOI: 10.1021/es900247y.

3.39

LAMBERN – software for U-Pb, Th-Pb and Pb-Pb age dating by LA-ICP-MS analysis

Thomsen Tonny B.*, Pettke Thomas*, Allaz Julien*** & Engi Martin*

* University of Bern, Institute of Geological Sciences, Baltzerstrasse 1+3, CH-3012. (thomsen@geo.unibe.ch)
** University of Massachusetts Amherst, Department of Geosciences, 611 North Pleasant Street, USA

For U-Pb, Th-Pb and Pb-Pb age dating, the LA-ICP-MS offers a cost reducing and time efficient technique compared to e.g. TIMS and SIMS, by which a bulk of data with a moderate precision (typically <2 %) can be obtained in a very short time (e.g. 50-100 ages in 1-2 days). To compare the obtained data, standardized protocols accepted by the LA-ICP-MS age dating community and associated software able to handle and calculate ages from the various solid phases are required. At present, little soft-

ware is available (e.g. LAMTRACE, GLITTER, Lamdate, PEPITA, ComPbCorr, PbI; summarized in Ko ler & Sylvester, 2003 and Košler et al., 2008). Some of these assume no initial Pb present (LAMTRACE, GLITTER), however, some geologically relevant minerals such as allanite, titanite, rutile and perovskite may contain a significant proportion of common Pb. Other approaches rely on a nebulization-induced spike bracketing technique (Lamdate), an approach that is not employed in all laboratories.

Thus, we present here a transparent, step-by-step Excel-based data reduction procedure for in-situ solid state U-Th-Pb-based age determinations by LA-ICP-MS. The software (called LAMBERN) is able to handle all solid phases with sufficient U, Th and Pb content for age dating by LA-ICP-MS, including phases with a significant common Pb proportion. The software offers full control in all steps of the consecutive and flexible data reduction approach (includes several options for data correction and age calculation procedure). All data treatment, age calculation and error propagation are carried out in a single Excel file. Various diagrams, including time-intensity, time-ratio, sensitivity, ablation yield, Concordia, Tera-Wasserburg are generated. The output can be read directly by IsoPlotEx (Ludwig, 2003) for additional plotting and calculations.

LAMBERN employs a standard-sample-standard bracketing approach with a maximum of 20 individual analyses imported through an integrated VBA macro of xl, txt or csv files (from Elan, Thermo Finnigan Element2 or ThermoX). Time intervals for background and signal are selected by the user. Screening of the signals for extreme values (technically induced "outliers") and for signals of poor quality (e.g. from time-dependant fractionation) is carried out through time-intensity and time-ratio diagrams and includes an option for the rejection of data from a tolerated relative standard deviation ( ) specified by the user. The rejection of data includes entire sweeps.

Options for the data correction is specified in the setup parameters section and include background correction, mercury interference correction (of ^{204}Hg on ^{204}Pb), correction for instrumental mass bias (Linear, Power and Exponential Laws, Russell and Baxter formulations), detector drift and 3 different common Pb correction routines (measured 204 and the "207Pb" and "208Pb" corrections). Matrix effects calibration can be applied if required. Selection is done between (i) non-matched matrix based on e.g. NIST SRM-610 glass or (ii) matrix matching employing one or more (in-house) reference materials of known age (e.g. Harvard91500 zircon for analysis of zircons of unknown age).

At present, the robustness of the screening and calculation procedures in LAMBERN are being tested through analyses of standard zircons (91500zircon, Temora-1, Plesovice), allanites (AVC, CAP, Tara, Daibosatsu, Bona, Sissonne), titanite and monazite (in-house standards). In general, the accuracy of non-matrix matched calibration routines for zircon, allanite and in part titanite report up to 30% deviation from "true" ages (e.g. TIMS, SIMS). Thus, matrix-matched calibration is employed. At the time of reporting, LAMBERN has been in use by only a handful of test-users, thus is a "beta" version.

REFERENCES

Košler J., Forst L. & Sláma J. (2008) LamDate and LamTool: spreadsheet-based data reduc-tion for laser ablation ICP–MS 315. In Sylvester P. (ad) Laser Ablation–ICP–MS in the Earth Sciences, Current Practices and outstanding issues, Appendix A4: Software for Reduction of LA–ICP–MS Data. MAC Short Course Series 40, 305-306.

Košler, J. & Sylvester, P. 2003. Present trends and the future of zircon in geochronology: la-ser ablation ICPMS. Reviews in Mineralogy & Geochemistry, 53, 243-275.

Ludwig, K.R. (2003) IsoplotEx v. 3.0. Berkeley Geochronological Center.

3.40

First insights into the dehydration of lizardite

Trittschack Roy & Grobéty Bernard

University of Fribourg, Department of Geosciences, Chemin du Musée 6, CH-1700 Fribourg (roy.trittschack@unifr.ch)

Lizardite $Mg_3Si_2O_5(OH)_4$ is a trioctahedral 1:1 phyllosilicate, which belongs together with chrysotile and antigorite to the serpentine mineral group. The structure of lizardite, based on simple flat lying T-O, is much simpler compared to the corrugated and cylindrical structures of antigorite and chrysotile respectively. Lizardite is, therefore, the logic starting point in an attempt to understand the dehydration processes and rates of this mineral group.

The aim of this study is to understand the rate determining steps and the kinetics of the dehydration of lizardite. The dehydration implies the deprotonation of part of the hydroxyl groups and recombination of the hydrogen ion with neighbouring hydroxyl groups to form a water molecule. The second step is the transport of the water molecule out to the surface. High-temperature experiments like in-situ HT-XRD and in-situ IR spectroscopy are ideally suited to investigate the structural changes during the reaction. Exploratory IR experiments and XRD studies on lizardite under room conditions gave starting temperatures for the dehydration between 500°C and 550°C which lies in the range of former investigations by Brindley & Zussman (1957) and Frank et al. (2005). The initial product of dehydration is amorphous, which crystallizes after a certain time

to forsterite followed by enstatite. Assuming proportionality between the integral intensity of hkl-peaks and the amount of lizardite present, the reaction rate can be extracted from the rate of intensity decrease. The data will be treated with the conventional Avrami method as well as the so called "time to a given fraction" (TGF) method. One major advantage of the TGF method is the possibility to discover changes in the activation energy E_a during the course of dehydration (Putnis, 1992). Known values for the activation energy of lizardite derived from differential thermal analyses (DTA) and lying around 350kJ mol^{-1} (Weber & Greer, 1965), which is rather large compared with other phyllosilicates with values around 200kJ mol^{-1}.

REFERENCES

Brindley, G.W. & Zussman, J. 1957: A structural study of the thermal transformation of serpentine minerals to forsterite. American Mineralogist, Vol. 42(7-8), 461-474.

Frank, M.R., Earnest, D.J., Candela, P.A., Wylie, A.G., Wilmot, M.S. & Maglio, S.J. 2005 (abstract): Experimental study of the thermal decomposition of lizardite up to 973K, Salt Lake City Annual Meeting 2005

Putnis, A. 1992: Introduction to Mineral Sciences, Campridge University Press, 457 p.

Weber, J.N. & Greer, R.T. 1965: Dehydration of serpentine - Heat of reaction and reaction kinetics at PH2O=1 Atm. American Mineralogist, Vol. 50(3-4), 450-464.

3.41

Analytical and numerical description of tephra deposition: the example of two large explosive eruptions of Cotopaxi Volcano, Ecuador

Tsunematsu Kae*, Bonadonna Costanza*, Falcone Jean-Luc** & Chopard Bastien**

*Département de Minéralogie, Université de Genève, Rue de Maraîchaire 13, CH-1205 Genève

** Département d'Informatique, Université de Genève, Battelle, Building A, Carouge; 7 route de Drize, CH-1227 Carouge

The downwind and crosswind tephra deposition was studied in detail for two large explosive eruptions of Cotopaxi volcano, Ecuador (a pumiceous unit, Layer 3, and a scoriaceous unit, Layer 5; Barberi et al. 1995). The two eruptions were characterized by a similar plume height, i.e. 28 ± 2 km for Layer 3 and 28 ±0 km for Layer 5, but Layer 3 was characterized by a larger volume, i.e. 1.5 km^3 for Layer 3 and 0.3 km^3 for Layer 5 (Biass and Bonadonna, submitted). The two layers are characterized by similar total grain size distribution (Md_Φ: ~-2), but Layer 3 tephra was advected by a stronger wind (28 m/s for Layer 3 and 21 m/s for Layer 5). As a result, crosswind variation of grain size is consistent for the two layers, but at any given distance from vent downwind deposition is coarser for Layer 3 (Figure 1). The increase rate of Md_Φ is about 0.2 for both layers (Figure 1a).

We have implemented both the model of Bonadonna and Phillips (2003) for tephra dispersal from strong volcanic plumes and the Cellular Automata model of Tsunematsu et al. (2008) to describe crosswind tephra deposition based on a Gaussian distribution. In addition, we have also implemented the model of Tsunematsu et al. (2008) to account for sedimentation from the bottom of the umbrella cloud as supposed to a point-source particle considering the following equation (Bonadonna and Phillips 2003):

$$M = M_0 \exp - \left\{ \int_{x_0}^{x} \frac{w}{Q} dx \right\} \quad (1)$$

where M (kg) is the total mass of particles of a given size fraction at the bottom of the spreading current, M_0 (kg) is the initial mass injected into the spreading current, Q is the volumetric flow rate, v is the terminal velocity of the particle of given grain size, w is the maximum crosswind width and x is the distance from the plume. Both the model of Bonadonna and Phillips (2003) and Tsunematsu et al. (2008) had shown good agreement with tephra deposition observed along the dispersal axis for a number of eruptions. However, the crosswind deposition had not been investigated in detail.

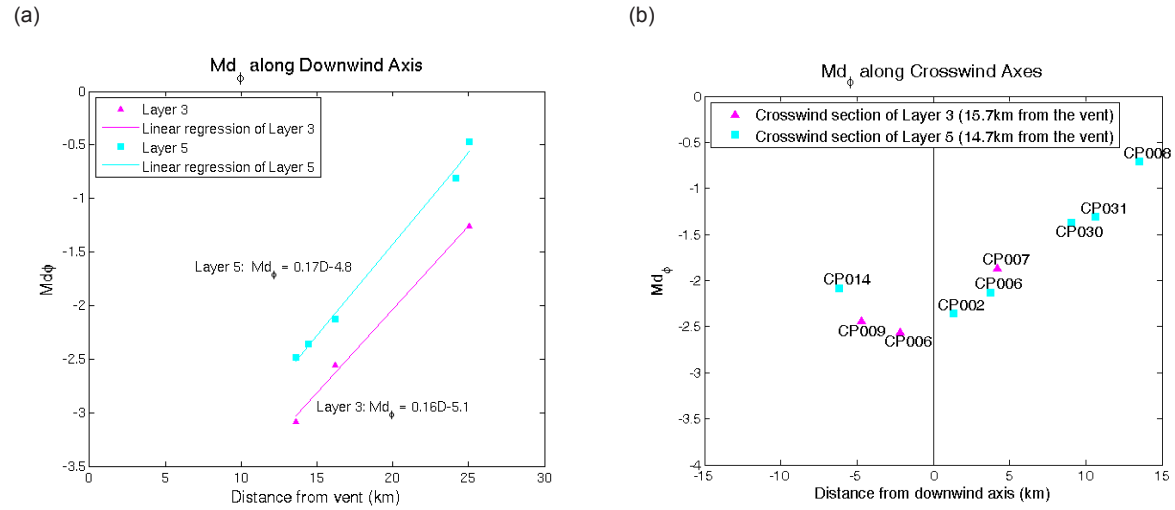

Figure 1. Median of grain size distribution along downwind axes (a) and crosswind axes (b). Pink triangles are data for Layer 3 and blue squares are data for Layer 5. For the downwind data, linear regressions are calculated for each layer. Pink line is for Layer 3 and blue line is for Layer 5.

REFERENCES

Barberi, F., Coltelli, M., Frullani, A., Rosi M., & Almeida, E. 1995: Chronology and dispersal characteristics of recently (last 5000 years) erupted tephra of Cotopaxi (Ecuador): implications for long-term eruptive forecasting. JVGR, 69, 217-239.

Biass S. & Bonadonna C., (in preparation) A quantitative uncertainty assessment of eruptive parameters derived from tephra deposits.

Bonadonna C. & Phillips J. C. 2003: Sedimentation from strong volcanic plumes. JGR. 108. B7, 2340, doi:10.1029/2002JB002034.

Tsunematsu K, Falcone JL, Bonadonna C & Chopard B. 2008: Applying a Cellular Automata Method for the Study of Transport and Deposition of Volcanic Particles H. Lecture Notes in Computer Science (LNCS). vol. 5191, 393-400.

3.42

Petrology of mafic-ultramafic complexes within the Archean Lewisian complex of NW Scotland

Udry Arya*, Müntener Othmar*,

* *Institute of Mineralogy and Geochemistry, University of Lausanne, Anthropole, CH-1015 Lausanne (arya.udry@unil.ch)*

The Lewisian complex is a fragment of the ancient Laurentian continental mass, the southern extension, which is now buried beneath the metasediments of the Scottish highlands. The Archean gneisses of the Lewisian complex represent a long, and complex part of Earth history.

The area of interest is in Northwestern Scotland, between Loch Laxford and Loch Inver. The terrain consists mostly of banded gneisses with a variety of basic to ultrabasic bodies. The gneisses are banded with alternating acid and mafic layers. Granulite facies parageneses are common. Large bodies of ultrabasic rocks contain variable proportions of olivine, pyroxene, spinel, plagioclase and hornblende, whereas basic bodies are essentially made of pyroxene, hornblende, plagioclase and garnet bearing assemblages. This study focuses on two of these complexes near Drumbeg and near Scourie. These bodies are described as layered 'meta' intrusives and are embedded within tonalitic to granodioritic gneisses.

Isotopic studies indicate that the gneisses derived from magmas that separated from the mantle about 2.9 Ga (Moorbath and al. 1969; Hamilton and al. 1979) and the high grade metamorphism was completed by about 2.7 Ga (Chapman and Moorbath 1977). Later dikes (Scourie dikes) are dated at 2.4 Ga (Chapman 1979), followed by retrograde amphibolite facies metamorphism and injection of granites and pegmatites at about 1.8 Ga. (Johnstone and Mykura 1989).

Several hypotheses have been put forward about the formation of those ultramafic and mafic bodies, but it has been demonstrated that voluminous granodiorite and tonalite surrounding rocks are of calc-alkaline affinity, which is generally inferred to be important in subduction zone environments. After Park and Tarney (1987), gneisses represents continental crust formed during subduction and the mafic-ultramafic association represents material intercalated tectonically during processes of crustal generation, probably from subducting ocean floor. This interpretation might be debated. We evaluate the hypothesis whether such rock associations could be related to crystallization from H_2O-rich magmas within an Archean

subduction zone environment, or alternatively, whether they could be related to metamorphosed dry plutonic rocks within the Archean crust, by applying new mapping and systematically investigating mineral chemical major and trace element data.
It is entirely unknown, whether primary igneous phases are still present (e.g. Sills et al. 1982) and apparent granulite facies "metamorphic" textures mask the igneous crystallisation history of this high pressure rocks. However, with the application of new in-situ methods such as Laser Ablation ICP-MS, new results on the main minerals and whole rocks were obtained. In addition, we will determine in-situ the major and trace element distribution of the major mineral phases that should provide additional constraints on the equilibration history of these rocks. We focus on elements distributions and garnets zonations and try to evaluate a magmatic vs metamorphic origin.
We present preliminary results on the thermal evolution of mafic-ultramafic systems within granulite facies host rocks. Testing the hypothesis of an arc origin is not only an important question for a better understanding of the Archean Lewisian complex, but much more so for the importance how subduction processes worked in the Archean.

REFERENCES

Chapman, H.J. (1979): 2390 M.yr Rb-Sr whole rock isochron for the Scourie dykes of NW Scotland. Nature, 277, 642

Chapman H.J., Moorbath S. (1977): Lead isotope measurements from the oldest recognized Lewisian gneisses of north-west Scotland. Nature, 268, 41-42

Hamilton P.J., Evensen N.M., O'Nions R.K., Tarney J. (1979): Sm-Nd systematics of Lewisian gneisses : implications for the origin of granulites. Nature, 277, 25-28

Johnstone, G.S. and Mykura, W. (1989): British regional geology: the northern Highlands of Scotland (4th edition). British Geological Survey, pp219

Moorbath S., Welke H., Gale N.H. (1969): The significance of lead isotope studies in ancient, high grade metamorphic basement complexes, as exemplified by the Lewisian rocks of Northwest Scotland. Earth Planet Sci Lett, 6, 245-256

Park, R.G. and Tarney, J. (1987): The Lewisian complex : a typical Precambrian high-grade terrain? Evolution of the Lewisian and comparable Precambrian high grade terrains, Geological Society Publication, 27, 13-25

Sills, J.D., Savage, D., Watson, J.V., and Windley, B.F. (1982): Layered ultramafic-gabbro bodies in the Lewisian of northwest Scotland: geochemistry and petrogenesis. Earth and Planetary Science Letters, 58, 345-360

3.43

Iridium-strip heater glass pellets: Effects of fusion temperature and time on Li, Be and B content

Vils Flurin*, Dijkstra Arjan*, Laure Pelletier*, Thomas Ludwig** & Angelika Kalt*

*Institut de Géologie et d'Hyrogéologie, Rue Emile-Argand 11, Cp158, 2009-Neuchâtel (flurin.vils@unine.ch)
**Institut für Geowissenschaften, Im Neuenheimer Feld 236, D-69120 Heidelberg

To solve a broad range of geochemical problems, precise and accurate whole rock and trace element analyses are required. Especially in the case of low abundant elements like Li, Be and B, which are widely used as tracers of alteration, subduction and recycling processes in the Earth, this is a critical issue. For in-situ mineral measurements of these elements, secondary ion mass spectrometry (SIMS) is probably the most sensitive and most accurate. A method that allows to analyse whole rock light element concentrations using SIMS would be extremely powerful and would dramatically increase sample throughput. However, a method to measure whole rock contents of all three light elements together is missing so far.
An Iridium-strip heater provides a flux free method to fuse directly homogeneous glass pellets from powdered rocks. These pellets can be investigated for major and light elements using microbeam (electron, ion or laser) methods. We have conducted experiments under different fusion temperatures (1500-1800°C) and time (30-240 s) on selected samples representing a wide variety of Li (0.91 to 56.5 μg/g), Be (0.24 to 3.5 μg/g) and B content (2.18 to 12 μg/g). We studied the behaviour of the three elements with respect to the different compositions, fusion time and temperature.
Homogeneity within the fused glasses is generally reached under the studied conditions for most elements. Electron microprobe measures and element distribution maps confirm this homogeneity. Light element measurements showed homogeneous behaviour for Li and Be (RSD of 3%, 6% respectively), but B is significantly less homogeneous (average RSD of 31%). Heating time dependent loss of Li, Be and B occurs throughout all studied samples, but Be and Li loss is always within analytical errors of the used methods (generally <10%). Significant B loss during fusion is found in almost every sample. In general, B is showing highly volatile behaviour, and at 1800°C most B has evaporated. Clearly, flux-less preparation of whole rock glasses is not a viable method for B analysis because of its volatility, but the method is well-suited for Li and Be.

3.44

Molybdenum isotopes in modern corals: investigation into their potential as redox proxy of bygone oceans

Voegelin, Andrea R.*, Samankassou, Elias* & Nägler, Thomas F.**

* *Département de Géologie et Paléontologie, Université de Genève, Rue des Maraîchaire 13, CH-1205 Genève (andrea.voegelin@unige.ch)*
** Institut für Geologie, Universität Bern, Baltzerstrasse 1+3, CH-3012 Bern

Periods of marine O_2 deficiency are important features of Earth history, in particular for climate and the evolution of life. The oxygenation state of paleo-environments is closely connected to the cycling of redox sensitive elements. Hence, the interpretation of past changes in oceanic redox chemistry depends on the identification of geochemical proxies which provide a reliable fingerprint of past seawater compositions.

In recent years the molybdenum isotope system has attracted significant attention and has proven to be useful in the investigation of the extent of sea-floor anoxia in the geological past (e.g. Arnold et al., 2004, Wille et al., 2008, Pearce et al., 2008). Carbonate rocks have just recently been introduced as promising new Mo isotope archive (Voegelin et al., 2009). It was shown that Mo uptake into non-skeletal carbonate precipitates is accompanied by minor isotope fractionation. Consequently, they were proposed as a monitor of the ambient fluid composition, which, under favorable conditions, may closely reflect the ocean water $\delta^{98/95}$Mo of bygone oceans. The application of skeletal carbonate is complicated by biologically controlled isotope fractionation, which may completely obliterate the original ocean water signature (Voegelin, 2009). So far, only well preserved modern aragonitic corals have revealed to exhibit a consistently small offset from seawater. They may thus provide the means to obtain a well dated and nearly continuous reconstruction of the Mo isotopic composition of past oceans from the Holocene as far back as Ordovician times. Their application as paleo-oceanographic tool, however, depends on the preservation of an ocean water signature during diagenetic processes, especially the replacement of meta-stable skeletal aragonite with calcite.

This study investigates unaltered coral matrices and diagenetically modified material in order to assess possible post-depositional Mo isotope and trace element exchange processes and their implications for the future use of corals as Mo archive.

REFERENCES

Arnold, G. L., Anbar, A. D., Barling, J. & Lyons, T. W, 2004: Molybdenum isotope evidence for widespread anoxia in mid-Proterozoic oceans. Science, 304, 87-90.

Pearce, C. R., Cohen, A. S., Coe, A. L. & Burton, K. W., 2008: Molybdenum isotope evidence for global ocean anoxia coupled with perturbations to the carbon cycle during the early Jurassic. Geology, 26 (3), 231-234.

Voegelin, A. R., Nägler, T. F., Samankassou, E. & Villa, I. M., 2009: Molybdenum isotopic composition of modern and Carboniferous carbonates. Chemical Geology, 265, 488-498.

Wille, M., Nägler, T. F., Lehmann, B., Schröder, S. & Kramers, J. D., 2008: Hydrogen suphide release to surface waters t the Precambrian/Cambrian boundary. Nature, 453, 767-7.

3.45

Effect of minor elements (H^+ and Al^{3+}) on the elastic properties of orthopyroxenes

Jingyun Wang*, Carmen Sanchez-Valle* & Roland Stalder**

* *ETH, Inst Mineral & Petrol, CH-8092 Zurich (jingyun.wang@erdw.ethz.ch)*
** *Innsbruck Univ, Inst Mineral & Petrog, A-6020 Innsbruck, Austria*

Orthopyroxenes (Opx), along with olivine, garnets and clinopyroxenes, are major components of the upper mantle. Knowledge of the changes in seismic velocities and elastic properties of Opx as a function of composition is therefore essential to build up mineralogical models of the upper mantle and to interpret heterogeneities in the mantle revealed by high-

resolution seismic tomographic images. While the elastic properties of Mg- and Fe-end-members have received much attention over the past years, the influence of minor element substitutions on the elastic properties of orthopyroxenes has been less investigated.

Here we present Brillouin scattering measurements of the single-crystal elastic properties of synthetic hydrous aluminum-free and hydrous aluminum-bearing orthopyroxenes (hereafter referred to as HyOpx and AlOpx, respectively) under ambient conditions. The samples were synthesized at 2.5 GPa and 1150 °C in piston-cylinder apparatus. HyOpx contains minor amounts of H^+ (280 ppm H_2O) while AlOpx has a similar Al_2O_3 content (6.3 wt%) to that of natural Opx, and minor amounts of H^+ (1500 ppm H_2O), and Fe (0.26wt% FeO). The aggregate bulk (K_S) and shear (μ) elastic moduli of HyOpx, K_S = 108.5(9) GPa and μ = 77.0(4) GPa, are indistinguishable from those of anhydrous orthoenstatite. The results suggest that incorporation of H_2O up to 280 ppm has no significant influence on elastic properties of $MgSiO_3$-orthoenstatite. The aggregate elastic moduli of AlOpx, K_S = 126.2(1.2) GPa and μ = 81.3(8) GPa, are respectively 14.7 and 6% higher than those of pure $MgSiO_3$-orthoenstatite. These results confirm that the stiffening of the bulk modulus reported in natural Opx relative to Mg-end-members is mainly due to the substitution of Al for smaller Si in tetrahedral sites. This conclusion is supported by the strong increase in the C_{33} elastic constant upon Al substitution that reflects the stiffening of the tetrahedral chains running along c-axis. Consequently, the aggregate velocities of AlOpx, V_P = 8.50(9) km/s and V_S = 5.01(6) km/s, are 7% and 4% higher than those of the magnesian end-member. The results indicate that Al has the strongest effect on the seismic velocities of Opx of all minor elements and may be taken into account to refine compositional and mineralogical models of the upper mantle.

3.46

Deciphering the Alpine orogenic and thermal evolution from subduction to collision: Raman spectroscopy and 40Ar/39Ar age constraints from the Valaisan Ocean (Central Alps)

Wiederkehr Michael*, Bousquet Romain**, Sudo Masafumi**, Ziemann Martin A.**, Berger Alfons*** & Schmid Stefan M.****

*Bundesamt für Landestopografie swisstopo, Landesgeologie, Seftigenstrasse 264, CH-3084 Wabern, Switzerland (michael.wiederkehr@swisstopo.ch)
**Institut für Geowissenschaften, Universität Potsdam, Karl-Liebknecht-Strasse 24/25, D-14476 Potsdam/Golm, Germany
***Institut for Geografi og Geologi, Københavns Universitet, Øster Voldgade 10, DK-1350 København K, Denmark
****Institut für Geologische Wissenschaften, Freie Universität, Malteserstrasse 74-100, D-12249 Berlin, Germany

The metasediments of the Valaisan Ocean and the adjacent distal European margin, exposed between the Pizzo Molare/Passo di Lucomagno area and the Prättigau half-window show a remarkable metamorphic gradient: Carpholite bearing assemblages in the east indicate pressure dominated blueschist facies metamorphism. Further west the same units are characterized by a temperature dominated Barrovian amphibolite facies metamorphism ("Lepontine" metamorphism). The relationships between deformation and metamorphism indicate two distinct metamorphic events: a late-stage Barrowian ("Lepontine") event clearly overprints an earlier HP/LT event. This is independently confirmed by a bimodal P-T path (Wiederkehr et al., 2008). To unravel this poly-metamorphic evolution we performed detailed investigations of carbonaceous matter by Raman spectroscopy in order to monitor the spatial distribution of peak-metamorphic temperatures. Additionally, we performed $^{40}Ar/^{39}Ar$ dating of mica by using in-situ and step-wise-heating techniques in order to decipher the temporal relationships between these two metamorphic events. The new data yield important insight regarding the transition from subduction to collision, both on the scale of the tectonic units derived from the Valaisan paleogeographical domain and on the scale of the entire orogenic belt.

The results of Raman spectroscopy, performed on a total of 214 samples, allow for high resolution mapping of the maximum metamorphic temperatures reached in these samples in three dimensions. Such three-dimensional mapping of the isotemperature contours in map and profile view faithfully reflects the present-day distribution of peak-metamorphic temperatures. The temperature gradients resulted from a superposition of at least three distinct metamorphic events (Wiederkehr et al., submitted). (1) Within the northeastern rim of the Lepontine dome - both along and across strike - the isotemperature contours in the 450-570 °C temperature interval are associated with the collision-related late-stage Barrow-type event. They clearly cut across nappe contacts and mega-folds deforming such older tectonic contacts. (2) Further to the NE the 350-425 °C isotemperature contours reflect temperatures reached during an earlier blueschist facies event and/or subsequent near-isothermal decompression. They are folded by large-scale post-nappe stacking mega-folds. (3) A substantial "temperature jump" across the tectonic contact between the frontal Adula nappe complex (500-520 °C) and the surrounding Valaisan-de-

rived metasediments (410-430 °C) indicates that, in contrast to the postulates raised by earlier studies, equilibration of temperatures during the late-stage Lepontine event is incomplete in this area.

The dating of high-pressure metamorphism, subsequent retrogression and final Barrow-type overprint was obtained by $^{40}Ar/^{39}Ar$ dating of biotite and different white mica generations that are all well characterized in terms of mineral chemistry, texture and associated mineral assemblages (Wiederkehr et al., in press). Four distinct age populations of white mica record peak-pressure conditions at 42-40 Ma, followed by several stages of a retrograde metamorphic evolution, predominantly decompression, between 36 and 25 Ma. Biotite isotopic analyses yield consistent apparent ages that cluster around 18-16 Ma for the Barrow-type thermal overprint that was associated with the temperature increase that followed decompression. The isotopic data reveal a significant time gap in the order of some 20 Ma between the subduction-related HP/LT event (42-40 Ma) and the later collision-related MP/MT Barrovian overprint (19-18 Ma). This substantial time gap, together with the age constraints on white mica reflecting the retrograde metamorphic evolution of the HP/LT stage, support the notion of a poly-metamorphic evolution associated with a bimodal P-T path. Amphibolite facies Barrow-type overprint of the NE Lepontine dome clearly represents a separate heating pulse that post-dates isothermal decompression after the high-pressure stage. This indicates that it is the accretion of vast amounts of European continental crust forming the present-day Lepontine dome that provides high radiogenic heat production responsible for amphibolite facies metamorphism (Bousquet et al., 2008]. This heating is an entirely conductive and therefore rather slow process.

REFERENCES

Bousquet, R., Oberhänsli, R., Goffé, B., Wiederkehr, M., Koller, F., Schmid, S.M., Schuster, R., Engi, M., Berger, A. & Martinotti, G. 2008: Metamorphism of metasediments at the scale of an orogen: A key to the Tertiary geodynamic evolution of the Alps. In: S. Siegesmund et al. (eds.) Tectonic Aspects of the Alpine-Dinaride-Carpathian system, Geol. Soc. Special Publ., 298, 393-411.

Wiederkehr, M., Bousquet, R., Schmid, S.M. & Berger, A. 2008: From subduction to collision: Thermal overprint of HP/LT meta-sediments in the north-eastern Lepontine Dome (Swiss Alps) and consequences regarding the tectono-metamorphic evolution of the Alpine orogenic wedge. In: N. Froitzheim & S.M. Schmid (eds.) Orogenic processes in the Alpine collision zone, Swiss J. Geosci., 101(Suppl), S127-S155.

Wiederkehr, M., Sudo, M., Bousquet, R., Berger, A. & Schmid, S.M. in press: Alpine orogenic evolution from subduction to collisional thermal overprint: 40Ar/39Ar age constraints from the Valaisan Ocean (Central Alps), Tectonics.

Wiederkehr, M., Bousquet, R., Ziemann M.A., Berger, A. & Schmid, S.M. submitted: 3-D assessment of peak-metamorphic conditions by Raman spectroscopy of carbonaceous material: an example from the margin of the Lepontine dome (Swiss Central Alps), submitted to Contrib. Mineral. Petrol.

3.47

Approximate terrestrial age dating of meteorites by use of handheld XRF

Zurfluh Florian*, Hofmann Beda**, Gnos Edwin***, Eggenberger Urs* & Opitz Christoph**

*Institut für Geologie, Baltzerstrasse 1+3, CH-3012 Bern (florian.zurfluh@geo.unibe.ch)
**Naturhistorisches Museum Bern, Bernastrasse 15, CH-3005 Bern
***Muséum d'Histoire naturelle, route de Malagnou 1, CP 6434, CH-1211 Genève

During a large project for systematic meteorite search in the hot desert of the Sultanate of Oman we have so far collected 5237 samples that represent ~550 fall events. This is, besides the Antarctic collection, the largest well-characterised meteorite population. Our main goals are to evaluate statistically our finds and study the weathering and contamination effects of the samples during their terrestrial residence. For these purposes we need to know how long the meteorites are on earth. Usually the terrestrial age is determined by ^{14}C measurements (e.g. Jull 2006). But these analyses are time consuming and there is no chance to measure all collected samples. Former studies have shown a continuous uptake of Sr and Ba during the terrestrial sojourn of meteorites (e.g. Al-Kathiri et al. 2005). We try to calibrate an age scale for fast dating of Omani meteorites by use of Sr contents measured with handheld XRF.

We use a Niton XL3t-600 handheld XRF analyser for fast and non-destructive measurements of nearly all elements between K and U, with a special focus on Fe, Mn, Ni, Ca and the weathering proxy Sr. This instrument has a predefined measurement mode for trace elements in medium concentrations. Tests with international and own meteorite standards measured with ICP-MS and handheld XRF confirmed an accuracy of Sr measurements with this "soil mode" within a derivation of ± 13 % at counting times of 120 seconds. Initial Sr contents in ordinary chondrites, the most abundant group of meteorites, are between 10 and 11.1 ppm (Wasson & Kallemeyn 1988) whereas they can reach values of several thousand ppm during weathering and contamination.
Another effect might be useful for relative dating: in hot deserts occurs an accumulation of Mn-rich material during exposure time on some rocks. It is also possible to quantify this desert varnish with handheld XRF.

Measurements were performed on cut- (C), exposed- (E) and buried-surfaces (V) of meteorites from five large strewn fields and some individual samples collected on two major meteorite recovery surfaces in the Sultanate of Oman, the Dhofar (Dho)/ Shisr region and Jiddat al Harasis (JaH)/Sayh al Uhaymir (SaU). The influence of the soil is evident but a lot of analysis of Omani desert soil samples delivered low variations for Sr concentrations somewhere between 250 to 350 ppm (Al-Kathiri et al. 2005). From each strewn field seven to 25 samples were analysed on the three mentioned surfaces (C,E and V). Each surface was measured for at least three times to minimise effects of local inhomogeneities.

The results of this survey were compared with ^{14}C ages from Al-Kathiri et al. (2005). The samples from the youngest strewn field, SaU001, have in general the lowest Sr contents. As one would expect the highest values are measured on the outer surfaces (V) of the samples that were buried in the soil, approve the contamination of the meteorites with Sr from the soil. The young and medium age samples (SaU001, JaH073 & JaH091) have high differences between the outer (E, V) and the interior (C) Sr concentrations whereas the older samples (Shisr015 & Dho005) have a more balanced ratio between the surfaces. A continuous diffusion of Sr from the exterior to the interior is a plausible explanation for this effect.
The cut surfaces deliver the best values for an approximate age dating. There is an inconsistency between the Sr contents at the cut surface and the ^{14}C age of the two JaH strewn fields. Since these are extremely large strewn fields, shielding effects could have falsified the radiocarbon age (Gnos et al. 2006, 2009). The younger "Sr age" of the JaH091 is supported by a general lower degree of weathering observed in thin section. Additionally the JaH073 samples have a more elevated Mn enrichment on the exposed surfaces that indicates a thicker desert varnish and therefore longer residence time in the desert.

With a combined study of the weathering grade observed in thin section, fast measurement by handheld XRF of Sr on cut surfaces and the degree of Mn enrichment on exposed surfaces it should be possible to estimate approximate the terrestrial ages of Omani meteorites.

REFERENCES

Al-Kathiri, A., Hofmann B. A., Jull A. J. T., and Gnos E. 2005: Weathering of meteorites from Oman: Correlation of chemical/ mineralogical weathering proxies with 14C terrestrial ages and the influence of soil chemistry, Meteoritics & Planetary Science, 40, 1215-1239.

Gnos, E., Eggimann M. R., Al-Kathiri A. and Hofmann B. A. 2006: The JaH091 strewn field, Meteoritics & Planetary Science 41 Suppl., A64

Gnos, E., Lorenzetti S. R., Eugster O., Jull A. J. T., Hofmann B. A., Al-Kathiri A and Eggimann M. R. 2009: The Jiddat al Harasis 073 strewn field, Sultanate of Oman, Meteoritics & Planetary Science 44, Nr 3, 375-387

Jull, T. 2006: Terrestrial Ages of Meteorites. In Meteorites and the Early Solar System II (eds. D. S. Lauretta and H. Y. McSween), pp. 889-905. University of Arizona Press, Tucson.

Wasson, J.T. & Kallemeyn G.W. 1988: Compositions of chondrites, Phil.Trans.R.Soc.Lond. A325, 535-544

4. Open Cryosphere session

M. Hoelzle, A. Bauder, B. Krummenacher, C. Lambiel, M. Lüthi, M. Phillips, J. Schweizer, M. Schwikowski

Swiss Snow, Ice and Permafrost Society

4.1

Flow dynamics of the steep part of Triftgletscher (Switzerland)

Dalban Canassy Pierre[1], Funk Martin[1]

[1] *Laboratory of Hydraulics, Hydrology and Glaciology (VAW), ETH Zurich, CH-8092 Zurich, Switzerland (dalban@vaw.baug.ethz.ch)*

Several studies on hanging glaciers have been tried to highliht possible precursors before break offs. If satisfactory results have been obtained on cold glaciers, it seems that break off mechanisms are different for those which are temperate, such as the Triftgletscher, Switzerland (Gadmertal, Bernese Alps).

Due to the disapearance of a huge amount of ice in its lower part during the last decades, the steep part of Triftgletscher was destabilized, and a pro-glacial lake appeared. Studies showed that a release of an ice mass with more than one million m3 could create a wave triggering a flood in the downglacier valley (Gadmertal).

To improve our understanding about ice break offs of temperate hanging glaciers, we have monitored the ice fall of Triftgletscher using different ways : Two automatic cameras with a trigger time every three hours, permit to perform the computation of the surface motions, and three seismic sensors, which permit to detect and locate seismic events associated with iceqakes.

The aim is to combine seismic and photogrammetric results and correlate the seismic activity with changes in the observed ice surface motions, in order to foresee possible break offs.

First results showed that time periods characterized by the highest surface velocities also have the biggest amount of seismic events. Thus there seems to be a relationship between displacements in the steep part and seismic activity, and that seismicity can be used as a forecast tool. We also noticed that there were more events during night than during day time. This indicates that basal drainage activity plays an important role in the ice motions. We located events in different parts of the serac fall : cracks due to crevasses opening near the surface, and yet unknown events in the lower part because of falling of ice blocks. The next step is to detect and locate events from stick and slip motion, which could characterize precursor motions to break offs, and to do a validation by using the terrestrial photogrammetry.

News results about stick and slip motion characterization and photogrammetric results will be presented.

4.2

Electrical Resistivity Tomography Monitoring of permafrost within the PERMOS network

Delaloye Reynald[1], Hauck Christian[1], Hilbich Christin[2], Lambiel Christophe[3], Morard Sebastien[1], Scapozza Cristian[3]

[1]*Department of Geosciences, Geography Unit, University of Fribourg, Chemin du Musée 4, 1700 Fribourg*
[2]*Glaciology, Geomorphodynamics & Geochronology, Physical Geography Division, Department of Geography, University of Zurich, Winterthurerstrasse 190, 8057 Zurich, and Department of Geography, University of Jena, Germany (chilbich@geo.uzh.ch)*
[3]*Faculté des géosciences et de l'environnement, Institut de Géographie, IGUL Quartier UNIL-Dorigny, Bâtiment Anthropole, 1015 Lausanne*

The PERMOS network (Permafrost Monitoring Switzerland) started in 2000 and aims at a long-term observation of mountain permafrost. It currently comprises more than 20 sites where the thermal evolution of the ground and/or the ground surface is monitored. Besides the surface and subsurface temperatures the ice content of the frozen ground is not only a key parameter controlling slope stability in periglacial environments but also an important input parameter for permafrost models.

Addressing the necessity for a method to monitor the long-term evolution of the ground ice content in mountain permafrost in the context of global warming, an Electrical Resistivity Tomography Monitoring (ERTM) network was initiated in the framework of PERMOS in 2005. In contrast to single geophysical surveys the so-called time-lapse approach of repeated measurements serves to overcome the common problem of the often ambiguous interpretation of absolute resistivity values. The ERTM approach is based on the assumption, that temporal changes in the measured electrical resistivity provide information on changes in the subsurface ice and water content.

Following a pilot study on the Schilthorn crest, running since 1999, a network of four permanent geoelectric profiles was established in 2005/2006 at three further sites (Murtèl rockglacier, Stockhorn rock plateau, Lapires talus slope) to evaluate the potential of permafrost monitoring by repeated geoelectrical measurements. Based on the good results ERTM is now an operational element of the PERMOS programme and a number of new permanent profiles was installed during the last years. The network now comprises 14 permanent ERTM profiles at 10 sites in Switzerland, including bedrock sites (Schilthorn, Stockhorn), rock glaciers (Murtèl, Gianda Grischa, Rechy), talus slopes (Lapires, Les Attelas, Dreveneuse, Creux du Van, Arolla), and an ice-cored moraine (Gentianes).

First results of this unique network indicate a huge potential of the ERTM approach to detect and characterise climate induced ground ice degradation. The observed 2-dimensional resistivity changes reveal spatially more detailed information than 1D borehole temperatures and contribute to an increased understanding of the response of different permafrost landforms to climate change.

4.3

Icequakes as precursors of ice avalanches

Jérome Faillettaz[1], Martin Funk[1] & Didier Sornette[2,3]

[1] VAW, ETH Zürich, Laboratory of Hydraulics, Hydrology and Glaciology, Switzerland (faillettaz@vaw.baug.ethz.ch)
[2]Department of Management, Technology and Economics, ETH Zürich
[3]Department of Earth Sciences, ETH Zürich

A hanging glacier at the east face of Weisshorn broke off in 2005. We were able to monitor and measure surface motion and icequake activity for 21 days up to three days prior to the break-off.

Results are presented from the analysis of seismic waves generated by the glacier during the rupture maturation process. Three types of precursory signals of the imminent catastrophic rupture were identified:

i) an increasing seismic activity within the glacier
ii) a change in the size-frequency distribution of icequake energy, and
iii) a log-periodic oscillating behaviour superimposed on power law acceleration of the inverse of waiting time between two icequakes.

The analysis of the seismic activity gave indications of the rupture process and led to the identification of two regimes: a stable one where events are isolated and non correlated which is characteristic of diffuse damage, and an unstable and dangerous one in which events become synchronized and large icequakes are triggered.

4.4

How much ice is stored by the Swiss glaciers?

Daniel Farinotti[1], Matthias Huss[1,2], Andreas Bauder[1] & Martin Funk[1]

[1]Laboratory of Hydraulics, Hydrology and Glaciology (VAW), ETH-Zurich, CH-8092 Zurich (farinotti@vaw.baug.ethz.ch)
[2] Department of Geosciences, University of Fribourg, CH-1700 Fribourg

Glaciers are characteristic features of mountain environments and play an important role in various aspects. They are a key element of the water cycle, being thus important for hydropower production or agricultural exploitation, and epitomize the "untouched environment", being precious for tourism industry. With the ongoing climate warming, the retreat of mountain glaciers is of major concern and studies assessing future glacier changes and related impacts recently received increasing interest. Such predictions necessarily need the present ice volume as initial condition and for transient modelling, the ice thickness distribution has to be known.

Recently, Farinotti et al. (2009a) developed a method based on mass conservation and principles of the ice flow dynamics for inferring the ice thickness distribution of a glacier from the inversion of the surface topography. We applied the method to 62 glaciers in the Swiss Alps, including all ice masses larger than 3 km^2 in surface area, using direct ice thickness measurements to constrain the model parameters. The resulting set of ice volumes were referenced to the year 1999 by means of a time series of glacier mass balance (Farinotti et al.,2009b, Huss et al., 2008) and used to calibrate a volume-area scaling relation (Bahr et al., 1997). The obtained relation was then applied to the glaciers contained in the Swiss Glacier Inventory 2000 (Paul, 2007) in order to estimate the total glacier ice volume in the Swiss Alps.

In 1999, the glacierized area in the Swiss Alps was 1063±10 km^2, with 67% covered by glaciers larger than 3 km^2. For the Swiss Alps, we infer a total glacier ice volume of 74±9 km^3 (Farinotti et al., 2009b). Nearly one quarter of this volume is stored in the hydrological basin of the Massa river, which comprises the three large glaciers Grosser Aletschgletscher, Mittelaletschgletscher and Oberaletschgletscher (Fig. 1). According to the time series of glacier mass balance, the ice volume in the Swiss Alps decreased by 12% between 1999 and 2008. The extraordinarily warm summer of 2003 caused a ice volume loss of about 3.5%.

Figure 1. Inferred ice thickness distribution in the hydrological basin of the Massa river. Available radio-echo sounding profiles are shown. Hatched areas are analysed using a scaling relation (Figure taken from Farinotti et al., 2009b).

REFERENCES

Bahr, D.B., Meier, M.F. and Peckham, S.D., 1997. The physical basis of glacier volume–area scaling. Journal of Geophysical Research 102 (B9), 20355-20362.

Farinotti, D. , Huss, M., Bauder, A., Funk, M. and Truffer, M., 2009a, A method to estimate the ice volume and ice-thickness distribution of alpine glaciers. Journal of Glaciology, 55 (191), 422-430.

Farinotti, D., Huss, M., Bauder, A. and Funk, M., 2009b. An estimate of the glacier ice volume in the Swiss Alps. Global and Planetary Change, 68, 225-231.

Huss, M., Bauder, A., Funk, M. and Hock, R., 2008. Determination of the seasonal mass balance of four Alpine glaciers since 1865. Journal of Geophysical Research, 113, F01015.

Paul, F., 2007. The new Swiss Glacier Inventory 2000 - Application of Remote Sensing and GIS. Schriftenreihe Physische Geographie, Vol. 52, University of Zurich. 210 pp.

4.5

Surface snow modeling at Dome C, Antarctica

Groot Zwaaftink Christine[1], Cagnati Anselmo[2], Crepaz Andrea[2], Fierz Charles[1], Lehning Michael[1], Valt Mauro[2]

[1]WSL Institute for Snow and Avalanche Research SLF, Davos, Switzerland
[2]*ARPAV CVA, Arabba di Livinallongo, Italy*

Modeling effectively surface snow compaction in Antarctica is of great interest for a better understanding of exchange processes between the snow surface and the atmosphere as well as their relevance to surface mass balance. At Dome C, we measured water equivalent of solid precipitation collected about 0.8 m above the snow surface. The density of this collected snow varies roughly from 50 to 300 kg m-3 with a mean around 80 kg m-3. On the other hand, the measured density over the top 10 cm of the snow cover being about 300 kg m-3, this layer roughly represents the mean yearly accumulation at Dome C, for which detailed snow profiles, continuous records of snow temperatures, and a two year meteorological data set are available. There are some observations of drifting snow effects and we expect wind to play a major role in this densification process.

Extensive qualitative descriptions of the snow deposition process exist in literature but no detailed quantitative study. Adjusting its settings to the extreme Antarctic climate, we use SNOWPACK, a flexible, modular snow cover model to simulate snow cover evolution. The influence of the wind on rapid densification is parameterized by means of an event driven snow deposition. This results in a more realistic snow cover with a pronounced stratigraphy, evident in snow density and grain sizes.

Other mechanisms which we try to include are the influence of water vapor deposition and sublimation at the surface, for example.

We will discuss implications from our results for future studies with respect to both modeling and in situ measurements relating to this very important process.

4.6

Integrative cryospheric research - an example in the Swiss Alps

Hauck Christian, Hoelzle Martin, Huss Matthias, Salzmann Nadine, Scherler Martin, Schneider Sina

Alpine Cryosphere and Geomorphology (ACAG), Department of Geosciences, University of Fribourg, Chemin du Musée 4, CH-1700 Fribourg

As climate is changing and the discussion on impacts and adaptation are emerging rapidly in the scientific and political dialogue, it becomes even more critical to observe, analyse and understand important components of the climate system in an integrated manner. Observations are the indispensable precondition to improve process understanding. Moreover, only with a reliable and consistent data baseline, models can be verified and the uncertainty in projections of future changes can be assessed.

The high-mountain cryosphere is particularly sensitive to changes in the atmospheric conditions with several feedback mechanisms on various spatial and temporal scales. At the same time, also the cryospheric components, snow, ice and permafrost, interrelate which leads to non-linear responses to climate change. A typical example is the differing effect of the snow cover for glacier mass balance variability and ground isolation over permafrost occurrences. It is therefore critical to advance integrated measurement and analysis concepts for all cryospheric components of high-mountain environments.

The recently formed new research group 'Alpine Cryosphere and Geomorphology (ACAG)' at the University of Fribourg is aiming at actively advancing integrated investigation in high-mountain environments. The area 'Stockhorn-Findelgletscher' near Zermatt, Valais, has been chosen to become a 'poster child' of integrated cryospheric research where various measurement and modelling approaches are applied. Measurements include all components of the energy balance, spatial distribution of snow accumulation, glacier mass balance, permafrost ground temperatures down to 100m, geophysical monitoring of ice and water content and ground surface temperatures (e.g. Gruber et al. 2004, Machguth et al. 2006, Hilbich et al. 2008). In addition, new model approaches to determine the response of glacier mass balance (Findelgletscher), active layer depth (permafrost Stockhorn) and evolution of ground ice content are used to analyse the impact of climate change on glaciers and permafrost and their respective differences (e.g. Hauck et al. 2008).

Our presentation will focus on some of the main research activities in the Stockhorn-Findelgletscher area and give examples for integrating the scientific activities.

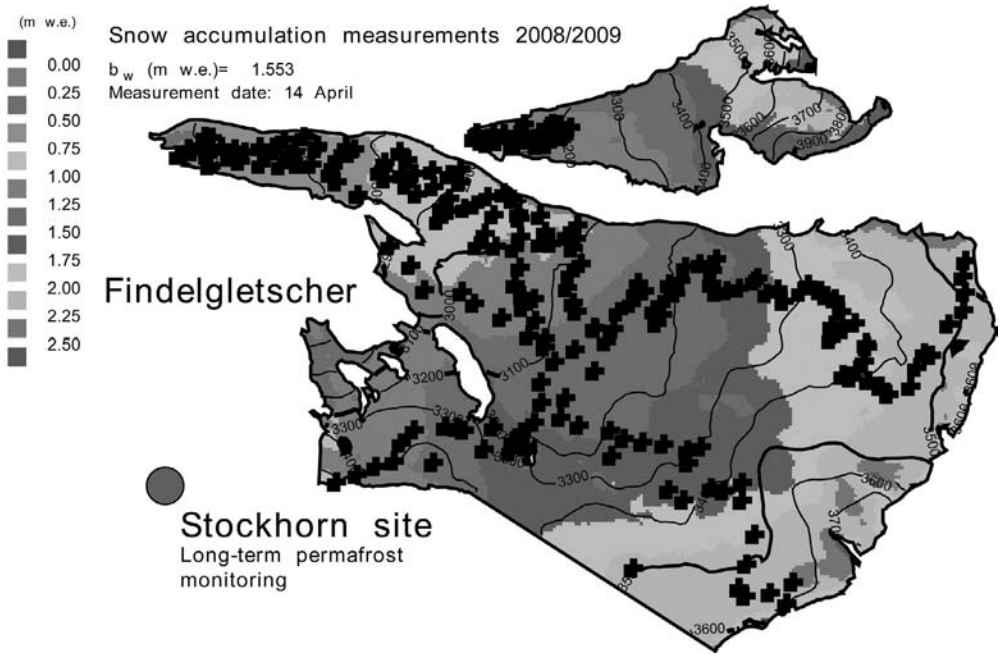

Figure 1. Findelgletscher and Stockhorn permafrost monitoring site. First results of the distributed snow accumulation measurements in April 2009 are shown. Crosses indicate snow probings, the inferred distribution of the snow water equivalent is shown in grey scales.

REFERENCES

Gruber, S., L. King, T. Kohl, T. Herz, W. Haeberli, & M. Hoelzle. 2004. Interpretation of geothermal profiles perturbed by topography: The Alpine permafrost boreholes at Stockhorn Plateau, Switzerland. Permafrost Periglacial Processes, 15, 349-357.

Hauck, C., Bach, M. & Hilbich, C. 2008. A 4-phase model to quantify subsurface ice and water content in permafrost regions based on geophysical data sets. Proceedings of the 9th International Conference on Permafrost, Fairbanks, Alaska, 1, 675-680.

Hilbich, C., Hauck, C., Delaloye, R. & Hoelzle, M. 2008. A geoelectric monitoring network and resistivity-temperature relationships of different mountain permafrost sites in the Swiss Alps. Proceedings Ninth International Conference on Permafrost, Fairbanks, Vol. 1, Kane D.L. and Hinkel K.M. (eds), Institute of Northern Engineering, University of Alaska Fairbanks, 699-704.

Machguth, H., Eisen, O., Paul, F. & Hoelzle, M., 2006. Strong spatial variability of snow accumulation observed with helicopter-borne GPR on two adjacent Alpine glaciers. Geophysical Research Letters, 33 (L13503): doi:10.1029/2006GL026576

4.7

Large scatter and multidecadal fluctuations in the 20th century mass loss of 30 Swiss glaciers

Huss Matthias[1],[2], Bauder Andreas[2] & Funk Martin[2]

[1] *Department of Geosciences, University of Fribourg, 1700 Fribourg, Switzerland (matthias.huss@unifr.ch)*
[2] *Laboratory of Hydraulics, Hydrology and Glaciology (VAW), ETH Zürich, 8092 Zürich, Switzerland*

The ongoing retreat of mountain glaciers strongly impacts on the hydrological cycle, might cause economic losses in alpine regions and is expected to dominate eustatic sea level rise over the next century. Long-term time series of glacier mass balance represent a key to projecting future glacier changes and understanding the glacier-climate linkage. However, mass balance is measured on only a few glaciers, and the records typically are only some decades long.

Here, we present thirty new time series of glacier surface mass balance, accumulation and melt over the past 100 years in the Swiss Alps. The data set includes different glacier sizes, exposures and regions, and thus constitutes the first long-term mass balance time series being representative on a mountain range scale. Our results are based on a comprehensive set of field data and modelling. For each glacier, up to 10 high-accuracy digital elevation models (DEMs) were established providing ice volume changes in subdecadal to semicentennial periods. In addition, more than 8000 direct observations of annual mass balance and winter accumulation are available. This data base was used to constrain a distributed temperature-index model (Hock, 1999; Huss et al., 2008) driven by daily air temperature and precipitation for the period 1908-2008.

All glaciers show considerable mass loss, but rates differ strongly between individual glaciers (Fig. 1). 100-year cumulative mass balance varies between −11 m water equivalent (Allalingletscher) and −65 m w.e. (Griesgletscher). These strong differences in the response of glacier mass balance to changes in climate forcing are attributed to an interaction of several complex processes. Large and flat glaciers tend to have more negative mass balance due to their long reaction time. Positive and negative albedo feed-back mechanisms, as well as changing winter precipitation, variable on smaller spatial scales than air temperatures, might also explain some of the differences.

Mass loss is particularly rapid in the 1940s and late 1980s to present, while short periods of mass gain occurred in the 1910s and late 1970s (Fig. 1). This indicates that glacier mass loss over the 20th century was not linear, but exhibits important long-term variations. We find oscillations in the rate of glacier mass loss in the Swiss Alps with a period of 65 years. Glacier mass balance is significantly anticorrelated to the Atlantic Multidecadal Oscillation (AMO) index which refers to anomalies in the sea surface temperature in the North Atlantic. We thus propose a link between Atlantic Ocean circulation and Alpine glacier mass loss.

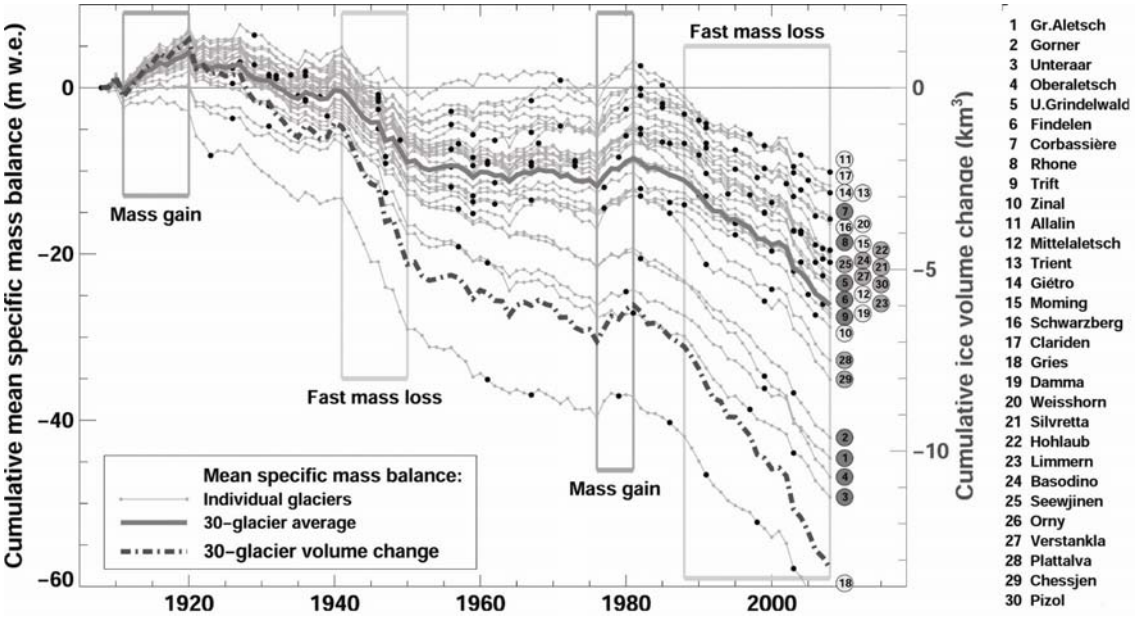

Figure 1. Time series of cumulative mean specific annual mass balance of 30 Swiss glaciers in the 20th century. Black dots indicate the dates of DEMs. The solid line represents the arithmetic 30-glacier average. Glacier names and numbers are arranged according to descending glacier size. The dash-dotted line shows the cumulative total volume change of the 30 glaciers (right-hand side axis). Two short periods with mass gain and two periods with fast mass loss are marked.

REFERENCES

Hock, R., 1999. A distributed temperature-index ice- and snowmelt model including potential direct solar radiation. Journal of Glaciology, 45, 101–111.

Huss, M., Bauder, A., Funk, M. & Hock, R., 2008. Determination of the seasonal mass balance of four Alpine glaciers since 1865. Journal of Geophysical Research, 113, F01015.

4.8
Mass balance monitoring on Pizolgletscher

Huss Matthias [1,2]

[1] *Department of Geosciences, University of Fribourg, 1700 Fribourg, Switzerland (matthias.huss@unifr.ch)*
[2] *Laboratory of Hydraulics, Hydrology and Glaciology (VAW), ETH Zürich, 8092 Zürich, Switzerland*

Very small glaciers are rarely subject of glaciological studies. Although these glaciers only cover a limited fraction of the glacierized area in the Alps, their number is considerable. According to glacier inventory data, 82% of the Swiss glaciers are smaller than 0.5 km^2. So far, the mass balance of glaciers in this important size class was never investigated in Switzerland.

In 2006 a new mass balance monitoring program on the very small Pizolgletscher, north-eastern Swiss Alps, was started. Pizolgletscher has an area of currently 0.08 km^2 and is a relatively steep, north-exposed cirque glacier (Fig. 1). The monitoring program consists of two field surveys, one in April and one in September, and will be continued over the next years. During the winter survey the spatial distribution of snow accumulation is determined by up to 100 snow probings on a dense network and snow density measurements in a snow pit. Three stakes drilled into the ice provide information about the annual mass balance (Fig 1a). In addition, the changes in glacier area and ice volume are known in subdecadal intervals from seven photogrammetric surveys since 1968 providing high-accuracy digital elevation models.

Based on the seasonal in-situ measurements glacier-wide mass balance is determined using a novel method. A distributed mass balance model with daily time steps is tuned to match both the measured snow water equivalent in spring and the annual mass balance at the stakes (Huss, 2009). The observed accumulation distribution is used to constrain the model in space. This method allows an optimal exploitation of the field data, the determination of mass balance over fixed time periods and, thus, the comparison of different years.

In the two first years of the survey Pizolgletscher was subjected to strong mass loss. The annual mass balance in 2006/2007 was −1.60 m water equivalent (w.e.) and in 2007/2008 −0.83 m w.e. The winter accumulation was low in 2007 with an early onset of the melting season. In April 2008 and 2009, however, average snow depths of almost 5 metres were measured, counteracting the high air temperatures of the following summer. The spatial pattern of snow deposition on Pizolgletscher is highly variable and importantly determined by wind (Fig. 1b). Consequently, glacier advance is due to an apposition of firn in front of the glacier tongue, and is not related to a dynamic reaction of ice flow. Pizolgletscher can, thus, change its area and length rapidly, which is illustrated by the length change measurements carried out since the late 19th century.

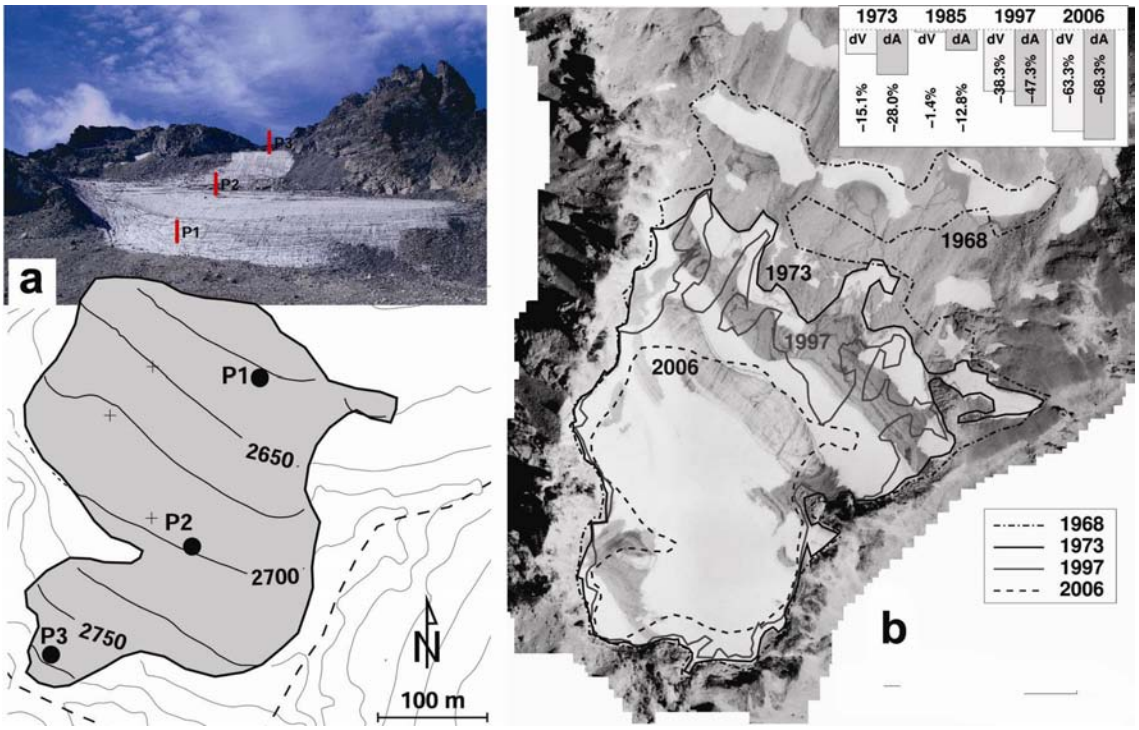

Figure 1. (a) Front view and map of Pizolgletscher. The position of the mass balance stakes is shown. (b) Orthophotograph of Pizolgletscher taken in September 1973. Lines indicate glacier extent in 1968, 1973, 1997 and 2006. The inhomogeneous distribution of snow is well visible. The inset shows the change in glacier area (dA) and volume (dV) relative to the year 1968.

Between 1968 and 2006 Pizolgletscher has lost more than 60% of its area and volume, most of the decrease taking place over the last two decades (inset in Fig. 1b). Extrapolating this loss into the future is, however, unreliable, as the glacier will retreat by degrees into a more protected cirque with high accumulation rates, seeking for a new equilibrium. Based on the observed ice volume changes, the seasonal mass balance over the last 40 years was reconstructed according to Huss et al. (2008). The cumulative mass balance is −17 m w.e., which is consistent with other mass balance records in the Swiss Alps (e.g. Silvrettagletscher). A short period of moderate mass gains in the late 1970s is followed by strong mass loss, in particular since 2003.

The first results of the new mass balance monitoring program on Pizolgletscher are promising and have revealed interesting insights into the response of small glaciers to climate warming, in particular their high sensitivity to accumulation changes and the importance of the spatial distribution of snow deposition.

REFERENCES

Huss, M., Bauder, A., Funk, M. & Hock, R., 2008. Determination of the seasonal mass balance of four Alpine glaciers since 1865. Journal of Geophysical Research, 113, F01015.

Huss, M, 2009. Past and Future Changes in Glacier Mass Balance, Chap. A.1. Dissertation No. 18230, ETH Zürich, 218 pp.

4.9

Ice wastage on the Kerguelen Islands (49°S, 69°E) between 1963 and 2006

Raymond Le Bris[2],Etienne Berthier[1], Laure Mabileau[1], Laurent Testut[3], and Frédérique Rémy[1]

[1]*LEGOS, CNRS, Toulouse, France.*
[2]*Department of Geography, University of Zurich, Zurich, Switzerland. (rlebris@geo.uzh.ch)*
[3]*LEGOS, Université de Toulouse, Toulouse, France.*

The glaciers and ice caps located around the Antarctic and Greenland ice sheets contain a significant fraction of the land ice on Earth (Dyurgerov & Meier. 2005). Difficult to access, their response to climatic fluctuations and their recent evolution are poorly known (Gordon et al. 2008). Because the behavior of these ice masses also constitutes a genuine climatic indicator, the objective of this study is to assess the changes of the extent and volume of glaciers and ice caps on Kerguelen Island during the last forty years (Berthier et al. 2009). This study is also a contribution to the GLIMS initiative (Raup et al. 2007)

Based on archived data (e.g. IGN map published in 1967, glaciological campaigns carried out in the 1970s) and on recent satellite data (Landsat, SPOT, SRTM, ICESat), we define successive outlines of the principal outlet glaciers to measure the pace of the retreat of the Cook Ice Cap. In order to understand the response of the Ice Cap to climatic forcing, we also analyzed the climatic data recorded by the Météo France station in Port aux Français.

The results reveal that all glaciers have retreated since 1965 although a strong variability exists from one outlet glacier to another. One striking result is the East/West asymmetry of the glacier retreat: west-flowing glaciers have lost 11.4% of their area while east-flowing glacier lost 28.2%. The dramatic retreat on the eastern side is illustrated by the retreat of Explorer's Glacier front by 3150 m +/-162 m since 1965 or an average of 75 m/yr. Furthermore, the Ampère Glacier thinned on average by 125 m +/-16 m in the frontal area, about -4.8 m/yr. (cf. also Vallon 1977). Locally, the mean thinning rate during the last 40 years reached as much as 10 m/yr.

In total, the ice cap lost 20% of its surface area over a period of thirty-eight years (1965-2003). The Cook Ice Cap is in recession since nearly one century and this trend accelerated since the years 1960-70 (Frenot et al. 1993).
The analysis of most recent satellite images (from the years 2003 to 2007) shows that the retreat continues today with the same speed or even slightly faster.

The ice cap is thus far from its state of balance. If the current climatic conditions prevail (high temperatures and a relatively low level of precipitation) or if they are even amplified in the future, it might be possible that the ice cap will totally disappear.

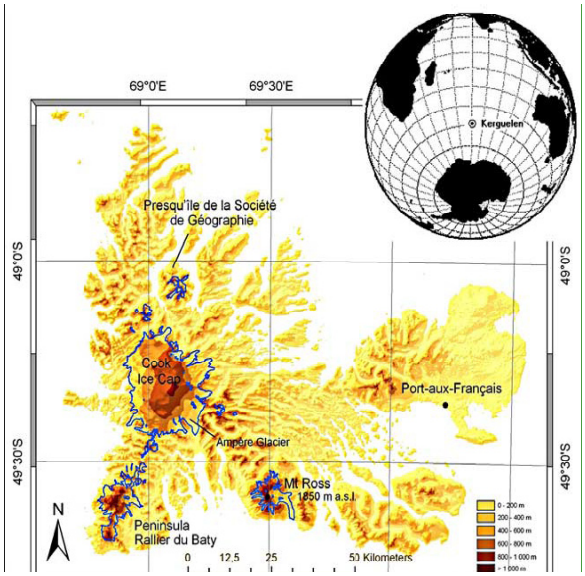

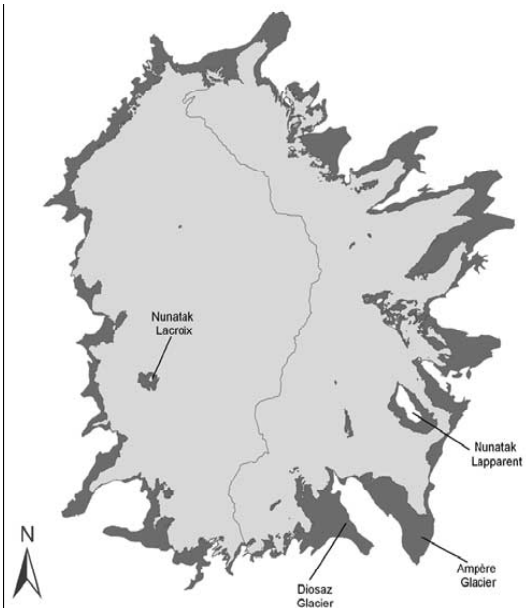

Figure 1. Topography of the Kerguelen Islands. The four main glacierized regions and the base station (Portaux-Français) are also indicated. The small globe identifies the location of the island in the South Indian Ocean.

Figure 2. East-west asymmetry of the Cook Ice Cap shrinkage.
The dark gray represents ice-covered areas that disappeared between 1963 and 2001.

REFERENCES

Berthier, E., Y. Arnaud, C. Vincent, and F. Remy (2006), Biases of SRTM in high-mountain areas: Implications for the monitoring of glacier volume changes, Geophys. Res. Lett., 33, L08502, doi:10.1029/2006GL025862.

Dyurgerov, M. B., and M. F. Meier (2005), Glaciers and the Changing Earth System: A 2004 Snapshot, 117 pp., Inst. of Arctic and Alp. Res., Univ. of Colo., Boulder.

Frenot, Y., J.-C. Gloaguen, G. Picot, J. Bougère, and D. Benjamin (1993), Azorella selago Hook. used to estimate glacier fluctuations and climatic history in the Kerguelen Islands over the last two centuries, Oecologia, 95, 140– 144.

Gordon, J. E., V. M. Haynes, and A. Hubbard (2008), Recent glacier changes and climate trends on South Georgia, Global Planet. Change, 60(1–2), 72–84, doi:10.1016/j.gloplacha.2006.07.037.

Raup, B., et al. (2007), Remote sensing and GIS technology in the Global Land Ice Measurements from Space (GLIMS) project, Comput. Geosci., 33(1), 104–125, doi:10.1016/j.cageo.2006.05.015.

Vallon, M. (1977a), Bilan de masse et fluctuations récentes du glacier Ampère (Iles Kerguelen, TAAF), Z. Gletscherkd. Glazialgeol., 13, 55– 85.

4.10

Observation and analysis of two wet-snow avalanche cycles

Christoph Mitterer, Rebecca Mott, Michael Schirmer, Jürg Schweizer

WSL Institute for Snow and Avalanche Research SLF, Flüelastrasse 11, CH-7260 Davos Dorf (mitterer@slf.ch)

The formation of wet-snow avalanches as well as the snowpack processes leading to wet-snow instabilities are poorly understood. Forecasting wet-snow avalanches is a great challenge and poses great difficulties for local authorities. Better knowledge about the processes leading to wet-snow instabilities is therefore very important. During the winters of 2007-2008 and 2008-2009 two distinct wet-snow avalanche cycles occurred in the surroundings of Davos, Switzerland. We analyzed meteorological data, in-situ snowpack information and mapped avalanche extent. In addition, the snow cover model SNOWPACK was used to fill the gap where snowpack data, such as volumetric water or snow temperature, were not available. Snowpack information for different elevation bands were modelled by using a constant lapse-rate for air temperature and incoming long wave radiation. The analysis focused on the causes of instability: loading and/or weakening due to water infiltration. The full energy balance was calculated using meteorological data and extrapolated to the investigation area using the model ALPINE3D. Both avalanche cycles occurred in a short period of time. The 2007-2008 avalanche cycle was characterized by short periods of warming and additional loading by snowfall and input of melt water due to rain. For the 2008-2009 wet-snow avalanche cycle, on the other hand, distinct warming and solar radiation were probably responsible for a higher production of melt water. Terrain parameters such as aspect and slope angle combined with liquid water infiltration patterns were crucial during the second wet-snow avalanche cycle. Snowpack data suggest that in the first year snow stratigraphy favoured the formation of weak layers, whereas for the second year snow stratigraphy may have favoured a gradual ripening of snowpack leading to a weakening of the basal layers.

4.11

Shear experiments with snow samples

Ingrid Reiweger[1], Robert Ernst[1], Jürg Schweizer[1], Jürg Dual[2]

[1] *WSL Institute for Snow and Avalanche Research SLF, Davos, Switzerland (reiweger@slf.ch)*
[2] *Institute of Mechanical Systems, ETH Zürich, Switzerland*

Natural dry-snow slab avalanches start with a failure within a weak snow layer. In order to understand the mechanical behaviour and the failure mechanism, we performed loading experiments with homogeneous and layered snow samples under controlled conditions in a cold laboratory. For simulating loading conditions similar to the natural snow pack, we designed and built an apparatus where a snow sample can be tilted by a 'slope angle' and is loaded via the gravitational force. The deformation within the snow sample was measured optically with a pattern recognition algorithm (PIV). Shortly before macroscopic failure (breaking of the whole sample) we observed a concentration of deformation (softening) within the weak layer. Additionally, we measure acoustic emissions during the shear experiments to quantify the microscopic failure (breaking of bonds) in the snow sample before the complete failure. Our results support the assumption that the dominating mechanisms for snow deformation are the competing processes of breaking and sintering of bonds between grains. Results from PIV clearly showed that when a layered snow sample was subjected to a constant slow loading rate, the deformation was concentrated within the weak layer. This has often been assumed but has not been documented so far. Preliminary results of the acoustic emission measurements of the homogeneous samples indicated that the AE may hint on the micromechanics during deformation.

4.12

A viscoelastic constitutive relation describing primary and secondary creep and solid elastic behaviour of ice

Riesen Patrick[1], Hutter Kolumban[1], Funk Martin[1]

[1]*Versuchsanstalt für Wasserbau, Hydrologie und Glaziologie (VAW), ETH Zürich, CH-8092 Zürich*

The flow of glacier ice is widely treated by a stress-strain relation commonly referred to as Glen's flow law. The Glen flow law is a pure viscous relation, hence a certain amount of stress immediately corresponds to deformation (i.e. strain rate), independent of time and possible relaxation. This behaviour is appropriate for stationary (secondary) creep of ice. However, recent detailed ice flow measurements on Gornergletscher, Switzerland, performed during the drainage of a glacier dammed lake, have identified particular unexplained flow changes where significant variations occur within a few hours to several days. It was suggested that elastic effects may play a role in such a rapid response of glacier ice. From an engineering point of view, the loads required to produce displacements of the ice similar to those observed, is on the order of several 10^5 Pa. In this range, linear viscoelastic behaviour of ice may be inappropriate and one must consider non-linear viscoelastic response of the ice. However, many experiments and creep tests conducted in the past have shown non-stationary (primary) creep to be effective for approximate durations of a few hours to a few days. We therefore conjecture that primary creep plays a role in short-time glacier flow variations. To test our hypothesis and elucidate the influence of possible viscoelastic effects, we constructed a constitutive relation which is able to reproduce primary and secondary creep as well as elastic effects. A modified Rivlin-Eriksen fluid model, where the stress is related to both strain rate and strain accelerations is used to describe primary and secondary creep of the ice. We couple the viscous fluid model with a non-linear elastic Kelvin-type stress-strain relation to enable the material to exhibit elastic behaviour of a solid. The constitutive relation obeys thermodynamic requirements. The transient response in ice flow is thus assigned to the effects of viscoelastic relaxation and primary creep. The decoupled formulation allows to study those effects separately or in combination. Some first numerical results using the finite element method have been obtained for two glaciological benchmark problems of (i) flow in a channel and (ii) flow over an inclined slab.

4.13

Coupling of ERT and thermal modelling to monitor permafrost without boreholes

Rings Jörg[1], Hauck Christian[2], Hilbich Christin[3]

[1] *ICG 4 Agrosphere, Forschungszentrum Jülich, Germany*
[2] *Alpine Cryosphere and Geomorphology (ACAG), Department of Geosciences, University of Fribourg, Chemin du Musée 4, CH-1700 Fribourg*
[3] *Glaciology, Geomorphodynamics & Geochronology, Department of Geography, University of Zurich, Winterthurerstr. 190, CH-8057 Zurich*

Geophysical methods, and especially the Electrical Resistivity Tomography (ERT) method, are being recognised as standard tools for the detection and monitoring of permafrost, since recent advances in data acquisition and processing have made their application worthwhile even though some effort has to be made to ensure good data quality and reliable inversion results (Hilbich et al. 2009). In many scientific studies borehole temperature data serve as ground truth for the geophysical results, enabling a thorough and rigorous assessment of the quality of the approach. Furthermore, ERT yields 2- and 3-dimensional data of the subsurface and is sensitive to the unfrozen water and ice content, which is complementary to the 1-dimensional temperature measurements in boreholes.

On the other hand, the non-invasiveness of the geophysical surveys and the corresponding low costs and minimal disturbance of the system to be monitored is usually seen as the major advantage of geophysics as opposed to boreholes. For future autonomous and widespread monitoring systems for permafrost (similar to the snow and meteo station networks), a purely geophysical approach is envisaged. However, ERT measures the electrical resistivity of the subsurface, which has to be related to ice content or temperature. Common approaches use petrophysical relationships (such as the well-known Archie's Law) to relate the measured resistivity changes to saturation and ice content changes or temperature (Hauck et al. 2008). But without ground truth data from boreholes or extensive laboratory calibration using subsurface material, the exact nature of the site-specific petrophysical relationship cannot be determined.

In this contribution, we introduce a filtering approach combined with coupled modelling of thermal conduction and ERT to predict subsurface temperatures based on ERT monitoring data without the need for borehole or laboratory data. We use sequential Bayesian filtering or particle filtering (see e.g. Arulampalam et al. 2002), which has the advantage of continuously providing probability distributions of state (temperature) and parameters (e.g. thermal conductivity) whenever measurements become available. A particle filter approximates these distributions by a set of discrete, weighted particles. Initial state and parameter are drawn from prior distributions and thermal conduction is modelled independently for each particle. The modelled change in temperature is transferred to change in resistivity by a linear relation, and an ERT forward model is used to simulate the system response. Then, the particles are weighted according to the agreement between measured and modelled ERT response. A re-sampling routine is used to ensure that, over time, the particles gravitate towards the posterior distributions of state and parameter.

To test the approach, modelled and observed ground temperatures were compared at the high-altitude permafrost station on Schilthorn, Berner Oberland/Swiss Alps. First results using automated ERT monitoring data from the PERMOS (Permafrost Monitoring Switzerland) network show a good performance during a 3-month period in spring and summer 2009. Improvements can be achieved by using more sophisticated thermal models and by iterative procedures to determine the (vertically variable) material properties of the subsurface, such as porosity and thermal conductivity.

REFERENCES

Arulampalam, M.S., Maskell, S., Gordon, N. & Clappt, T. 2002. A tutorial on particle filters for online nonlinear/non-Gaussian Bayesian tracking, IEEE Transactions on Signal Processing, 50, 174-188.

Hilbich, C., Marescot, L., Hauck, C., Loke, M.H. & Mäusbacher, R. 2009. Applicability of ERT monitoring to coarse blocky and ice-rich permafrost landforms. Permafrost and Periglacial Processes 20 (3), 269-284.

Hauck, C., Bach, M. & Hilbich, C. 2008. A 4-phase model to quantify subsurface ice and water content in permafrost regions based on geophysical data sets. Proceedings of the 9th International Conference on Permafrost, Fairbanks, Alaska, 1, 675-680.

4.14

The polythermal structure of Grenzgletscher (Swiss Alps)

Claudia Ryser[1], Martin Lüthi[1], Norbert Blindow[2], Sonja Suckro[2]

[1] *Versuchsanstalt für Wasserbau, Hydrologie und Glaziologie (VAW), ETH-Zürich, 8092 Zürich, Switzerland (ryser@vaw.baug.ethz.ch)*
[2] *Institut für Geophysik der Westfälischen Wilhelms- Universität Münster, 48149 Münster, Germany*

With a combination of borehole measurements and helicopter-borne ice radar, the temperature distribution in the lower part of the polythermal Grenzgletscher (Swiss Alps) was investigated. Vertical temperature profiles were measured in 12 deep boreholes. Cold ice was found in a central flow band in the Grenzgletscher branch, where the coldest ice (-2.6 °C) was found in 60 - 75m depth. The cold ice occupies 80-90% of the ice thickness of 200 - 320m, and is laterally conned to a band of +/-200m from the central flow line. The ice is temperate close to the bed and towards the margins. Comparison of ice radar soundings acquired with the UMAIR georadar with borehole temperatures shows that low-backscatter zones coincide with ice at temperatures more than 0.5K below the pressure melting temperature. The low-backscatter zones are thus used to map the distribution of cold ice on the whole lower glacier. The cold ice advected from the accumulation causes a zone of persistent superficial meltwater streams and lakes.

4.15

Simulation of high mountainous discharge: how much information do we need?

Schaefli, Bettina[1] and Huss, Matthias[2]

[1] *Water Resources Section, Faculty of Civil Engineering and Geosciences, Delft University of Technology, 2600GA Delft, The Netherlands (b.schaefli@tudelft.nl)*
[2] *Laboratory of Hydraulics, Hydrology and Glaciology (VAW), ETH Zurich, 8092 Zurich. Now at: Alpine Cryosphere and Geomorphology, Department of Geosciences, University of Fribourg, 1700 Fribourg, Switzerland*

For the management of water resources, the hydrologic cycle of high mountainous catchments is frequently simulated with very simple precipitation-discharge models representing the snow accumulation and ablation behavior of a very complex environment with a set of lumped equations accounting only for altitudinal temperature and precipitation differences. These models are generally calibrated so that the model reproduces as closely as possible a series of observed discharge measurements. The question inevitably arises whether long term predictions of such a calibrated model are actually reliable, since knowing that a model performs well for historic situations does by no means imply that it will perform well for future, considerably modified catchment conditions. A first, although not sufficient step to answer this question, is investigating whether with such a model, we are "getting the right answers for the right reasons". In glacierized catchments, this would for example imply that a precipitation-runoff model should not just mimic observed discharge but also reproduce the glacier mass balance.

In this study, we show how much observed information we need to reliably calibrate a hydrological model for a high mountainous catchment. Based on glacio-hydrological data from the Rhone glacier catchment, we analyze how well a simple conceptual precipitation-runoff model (GSM-SOCONT, Schaefli et al., 2005) can reproduce seasonal glacier mass balance data and in a second step, how much information is required to achieve a reliable model calibration. Here, we focus on the question whether observed discharge is sufficient or whether we need annual or even seasonal glacier mass balance data.

For this particular catchment, a detailed reproduction of observed seasonal balances requires a modification of the accumulation and ablation module of GSM-SOCONT. The model only accounts for altitudinal differences of the meteorological conditions and e.g. not for wind drift or exposition. As our results show, introducing seasonal accumulation and ablation parameters is sufficient to enable this simple model to reproduce observed seasonal balances (Fig. 1) and annual net balances (Fig. 2). Furthermore, our results suggest that calibrating the hydrological model exclusively on discharge can lead to wrong representations of the intra-annual accumulation and ablation processes and, thus, to a bias in long term glacier mass balance simulations (Fig. 2). Adding only a few annual net balance observations considerably reduces this bias. Calibrating exclusively on annual net balance data can, in turn, lead to wrong seasonal mass balance simulations (not shown).

Even if these results are case study specific, our conclusions give valuable new insights into the benefit of different types of observations for calibrating hydrological models in high alpine catchments.

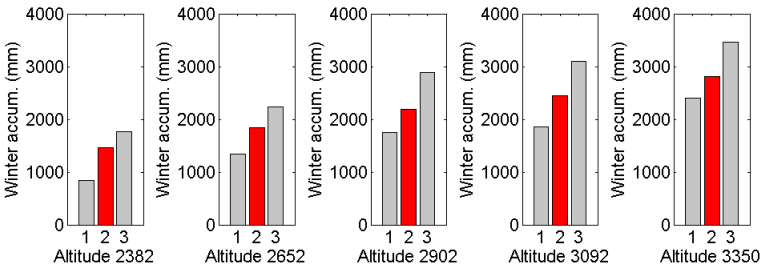

Figure 1: Winter mass balance for 5 elevation bands (winter 1979 / 1980); grey bars: 10% and 90 % percentiles of all observed point mass balances (Funk, 1985), red bars: simulated mean mass balance (modified GSM-SOCONT with seasonal accumulation and ablation parameters).

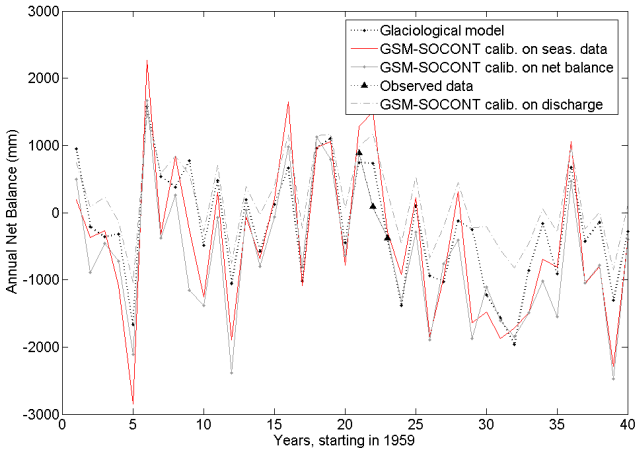

Figure 2. Comparison of annual net balance simulations obtained with the detailed glaciological model presented in (Huss et al., 2008) and with the simple hydrological model GSM-SOCONT (with seasonal accumulation and ablation parameters), calibrated on seasonal data, on net balance data (Funk, 1985) or on discharge.

REFERENCES

Funk, M.: Räumliche Verteilung der Massenbilanz auf dem Rhonegletscher und ihre Beziehung zu Klimaelementen, Eidgenössische Technische Hochschule Zürich, Zürich, 183 pp., 1985.

Huss, M., Bauder, A., Funk, M., and Hock, R.: Determination of the seasonal mass balance of four Alpine glaciers since 1865, Journal of Geophysical Research, 113, F01015, 10.1029/2007JF000803, 2008.

Schaefli, B., Hingray, B., Niggli, M., and Musy, A.: A conceptual glacio-hydrological model for high mountainous catchments, Hydrology and Earth System Sciences, 9, 95 - 109, 2005.

4.16

Impact of snowmelt on zero curtain and thaw layer depth for different subsurface textures. Field and modeling- based studies at the Murtél-Chastelets area.

Schneider Sina, Scherler Martin

Alpine Cryosphere and Geomorphology (ACAG), Department of Geosciences, University of Fribourg, Chemin du Musée 4, CH-1700 Fribourg

The summer zero curtain phase, a time period characterized by consumption of latent heat in an isothermal soil region at temperatures near the melting point, is of high importance for the thermal regime of permafrost.

It is assumed that the main cause for the initialisation of the summer zero curtain is the thawing of the snow pack and thus the infiltration of melt water into the frozen active layer. Furthermore we assume that the evolution of the zero curtain depends on the texture of subsurface.

Borehole temperature measurements from our field site Murtél-Chastelets show that on fine grained material the isothermal region is much thicker than in coarse blocky material. In addition we use a numerical heat and mass transfer model to further investigate the infiltration processes on these different substrates.

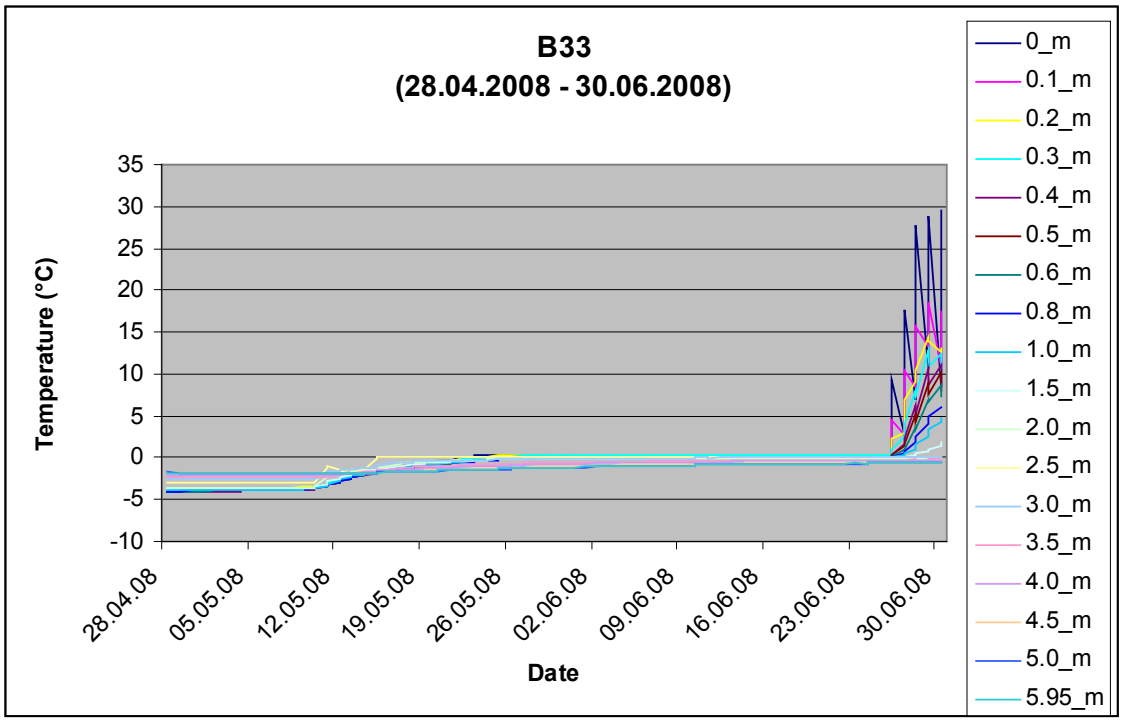

Figure 1.: Zero curtain of borehole B33 (coarse blocky material) during spring 2008

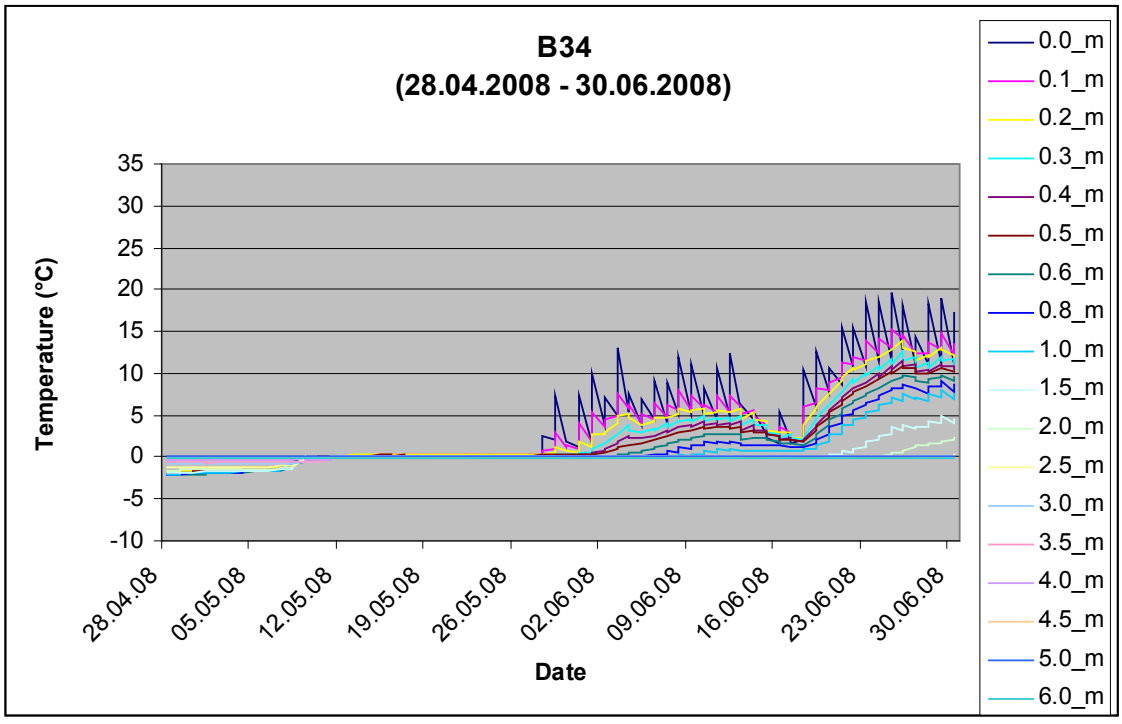

Figure 2.: Zero curtain of borehole B34 (fine grained material) during spring 2008

REFERENCES:

Outcalt, S., F. E. Nelson, and K. M. Hinkel (1990). The Zero-Curtain Effect: Heat and Mass Transfer Across an Isothermal Region in Freezing Soil. Water Resources Research 26 (7), 1509-1516.

Kane, D. L. and J. Stein (1983). Water Movement Into Seasonally Frozen Soils. Water Resources Research 19 (6), 1547-1557.

4.17

Using XPD for determining physical rock parameters of permafrost materials

Tilo Schneider [1], Ildiko Katona-Serneels[2]

[1] *Institut für Geowissenschaften, Burgweg 11, 07749 Jena, Germany*
[2] *Department of Geoscience, Chemin du Musée 6, CH - 1700 Fribourg, Switzerland*

Permafrost occurs in different substrates. Variability in rock type, porosity, block size distribution and weathering attitude determines morphology, dynamic and ice content of rock glaciers and talus slopes.
To analyze these conditions geophysical techniques such as geoelectrics and seismics are adequate methods to determine properties of the shallow surface in permafrost regions. Even though values for the physical characteristics of the prevailing rocks can usually be found in literature, they may vary over a wide range. In order to calculate more detailed models of the subsurface the physical rock parameters like electrical resistivity and acoustic impedance have to be known very well. Determining the physical characteristics of single minerals may therefore limit the uncertainties of the whole geophysical rock analysis.

At typical permafrost monitoring sites, such as the Murtèl/Chastelets area in the Eastern Swiss Alps, several drill cores and rock samples were collected and analyzed using X-Ray Powder Diffractometry. By this, it is possible to determine the mineral composition of the rocks in the investigation area. In addition, a Reed-Field analysis was used to calculate the quantity of the respective mineral content. This enables to determine mean physical rock properties in the subsurface which then can be used to improve geophysical modeling. The XPD analysis is a fast and exact method to determine the mineral content in rock samples qualitatively and quantitatively.

In this study rock samples from three different permafrost areas in the Swiss Alps have been analyzed. All three sites (Murtèl/Chastelets (GR), Schilthorn (BE), Stockhorn (VS)) are included in the Swiss permafrost monitoring network PERMOS, where borehole temperatures, meteorological data and geophysical data are being collected extensively. In our contribution we will present results from the mineral analysis and compare them to geophysical parameters observed at the three sites.

4.18

A systematic approach to quantify the performance of SNOWPACK

Steinkogler Walter[1],[2], Fierz Charles[1], Lehning Michael[1], Obleitner Friedrich[2]

[1]*WSL Institute for Snow and Avalanche Research SLF, Flüelastrasse 11, CH-7260 Davos Dorf (Steinkogler@slf.ch)*
[2]*Institute of Meteorology and Geophysics, Innsbruck University, Innrain 52, A-6020 Innsbruck*

New snow settlement in the very first hours and days after a snowfall has not yet been fully understood. Modelling errors at this initial stage propagate through a whole winter season, thus affecting a correct modelling of crucial snow cover properties such as density, temperature distribution and snow depth.

Up to now, parameter tuning for settling in SNOWPACK (Lehning & Fierz, 2008) has mainly been done by visual comparison of modelled with measured settling curves. This can be accomplished by tracking model layers that correspond to positions of combined settlement and temperature sensors (snow harps). As a result, verification of model performance with in situ measurements is possible. Here comprehensive data sets obtained during a number of snowfall periods are used. Based on these observations we present a systematic approach to assess the performance of the model. Sensitivity studies allow to locate the most important model parameters which influence the settlement of deposited snow. Our approach offers the possibility to visualise and quantify the performance of different model runs. In particular, we will present such an analysis both during and a few days after snow falls.

REFERENCES

Lehning, M., & Fierz C., 2008: Assessment of snow transport in avalanche terrain. Cold Reg. Sci. Technol., 51(2-3), 240–252.

4.19

Mass balance of Brewster Glacier, New Zealand, modelled over three decades

Dorothea Stumm[1], Fitzsimons Sean J[1], Cullen Nicolas J[1], Hoelzle Martin[2], Machguth Horst[3], Anderson Brian[4] & Mackintosh Andrew[5]

[1]*Department of Geography University of Otago, PO Box 56, Dunedin, New Zealand (dorothea.stumm@geography.otago.ac.nz)*
[2]*Department of Geosciences, University of Fribourg, Chemin de musée 4, 1700 Fribourg*
[3]*Department of Geography, University of Zurich, Winterthurerstr. 190, 8057 Zurich*
[4] *Antarctic Research Centre, Victoria University of Wellington, PO Box 600 Wellington, New Zealand*
[5] *School of Geography, Environment and Earth Science, Victoria University of Wellington, PO Box 600 Wellington, New Zealand*

The aim of this study was to model the mass balance and snowlines on Brewster Glacier for the past three decades, by using a distributed mass balance model (Oerlemans, 2001; Machguth et al., 2006).

The mass balance model is based on the energy balance, and runs with meteorological input data. Input data are an interpolated climate dataset from the National Institute of Water and Atmospheric Research (NIWA), and the ERA-40 re-analysis dataset from the European Centre for Medium-Range Weather Forecasts (ECMWF). Direct mass balance measurements, which were initiated in 2004, provided data to calibrate the model. These measurements were collected with the glaciological method that includes stake and snowpit measurements. For model validation, we used the annual end-of-summer snowline (EOSS) records from the Glacier Snowline Survey (Chinn, 1995; Willsman et al.,2008), which document the evolution of the Brewster Glacier excellently since 1978. After calibrating the mass balance model, the mass balance and snowlines were simulated for the past three decades. The modelling results were then compared to the yearly EOSS records.

The mass balance model performed well with the interpolated NIWA dataset for the calibration period. But for the previous 30 years, the model calculations did not correspond well to the EOSS records. Therefore, the model input dataset was exchanged with the ERA-40 re-analysis data. The results compared much better to the EOSS records, and fit better with mass balance estimates from a parameterisation scheme (Haeberli & Hoelzle 1995) and a GPS mass balance survey (Willis et al., 2008). Furthermore, mass balance trends were modelled well. However, spatial resolution of the ERA-40 data set is very coarse, and we suggest testing in future studies whether the performance of mass balance modelling can be improved by applying finer resolution Regional Climate Model data driven from re-analysis.

REFERENCES

Chinn, T. J. 1995: Glacier Fluctuations in the Southern Alps of New Zealand determined from Snowline Elevations. Arctic and Alpine Research, 27(2), 187-198.

Haeberli,W. & Hoelzle, M. 1995: Application of inventory data for estimating characteristics of and regional climate change effects on mountain glaciers - a pilot study with the European Alps. Annals of Glaciology, 21, 206-212.

Machguth, H., Paul, F., Hoelzle, M. & Haeberli, W. 2006: Distributed glacier mass balance modelling as an important component of modern multi-level glacier monitoring. Annals of Glaciology, 335-343.

Oerlemans, J. 2001: Glaciers and Climate Change. A.A. Balkema Publishers, Lisse/Abingdon/Exton (PA)/Tokyo.

Willis, I., Lawson, W., Owens, I., Jacobel, B. & Autridge, J. 2008: Subglacial drainage system structure and morphology of Brewster Glacier, New Zealand. Hydrological Processes, DOI: 10.1002/hyp.7146.

Willsman, A., Salinger, M. J. & Chinn, T. J. 2008: Glacier Snowline Survey 2008. Technical report, National Institute of Water and Atmospheric Research Ltd.

4.20

Natural and anthropogenic primary aerosols record from an Alpine ice core (Colle Gnifetti, Swiss Alps).

Florian Thevenon[1], Flavio S. Anselmetti[2], Stefano M. Bernasconi[3] & Margit Schwikowski[4]

[1]*Institut F.-A. Forel, Université de Genève, CH-1290 Versoix (Florian.Thevenon@unige.ch)*
[2] *Eawag, Swiss Federal Institute of Aquatic Science and Technology, CH-8600 Dübendorf*
[3] *Geological Institute, ETH Zurich, CH-8092 Zurich*
[4] *Paul Scherrer Institut, CH-5232 Villigen*

The Colle Gnifetti glacier, located in the Monte Rosa massif (Swiss-Italian border, 4455 m a.s.l.), satisfactory conserves the accumulation history of summer precipitation chemistry and climatic conditions over relatively long time-period (i.e. a few hundred years). In fact, the Colle Gnifetti glacier is characterized by a high ice-thickness (about 60 to 130 m) and a low net snow accumulation of about 30 cm water equivalent per year (weq.), resulting from the preferential wind erosion of dry winter snow.

Considering that 1) the anthropogenic aerosols are mostly deposited in summer, when polluted air is transported up to high altitudes by convection, and that 2) due to its orographical position in the Southern Alpine chain, the Colle Gnifetti glacier is strongly influenced by air masses advected from southerly directions, the Colle Gnifetti summer archives therefore offer a unique possibility for reconstructing i) regional (pre-)industrial carbonaceous aerosol emissions, and ii) changes in the dynamic of the southwesterly dust-laden winds from the Sahara.

The Colle Gnifetti ice core analysis demonstrates that the elemental black carbon (BC) aerosol record is independent of the large-scale climatic control affecting the transport of mineral dust to the Southern Alps, but primarily reflects regional-scale anthropogenic activity (Thevenon et al., 2009). More precisely, the $\delta^{13}C$ composition of BC suggests that wood combustion was the main source of preindustrial atmospheric BC emissions. Moreover, biomass burning activity and especially C_4 grassland burning abruptly dropped between 1560 and 1750 (Figure 1), suggesting that agricultural practices strongly decreased in Europe during this cold period of the 'Little Ice Age'. Unlike the BC deposition, the mineral dust transport to the summits of the Southern Alps is primarily controlled by large-scale climatic patterns (i.e. drier winter in North Africa and stronger North Atlantic southwesterlies), leading to transport of massive dust plumes from the Sahara around 1560-1685, 1775-1785, and after 1860. In contrast, the periods of low Saharan dust deposition around 1515-1560, 1690-1770 and 1790-1850 may indicate weaker meridional atmospheric circulation at that times, leading to colder and drier spring/summer conditions over Western and Central Europe.

REFERENCE

Thevenon, F., F. S. Anselmetti, S. M. Bernasconi, and M. Schwikowski (2009). Mineral dust and elemental black carbon records from an Alpine ice core (Colle Gnifetti glacier) over the last millennium. J. Geophys. Res., 114, D17102, doi:10.1029/2008JD011490.

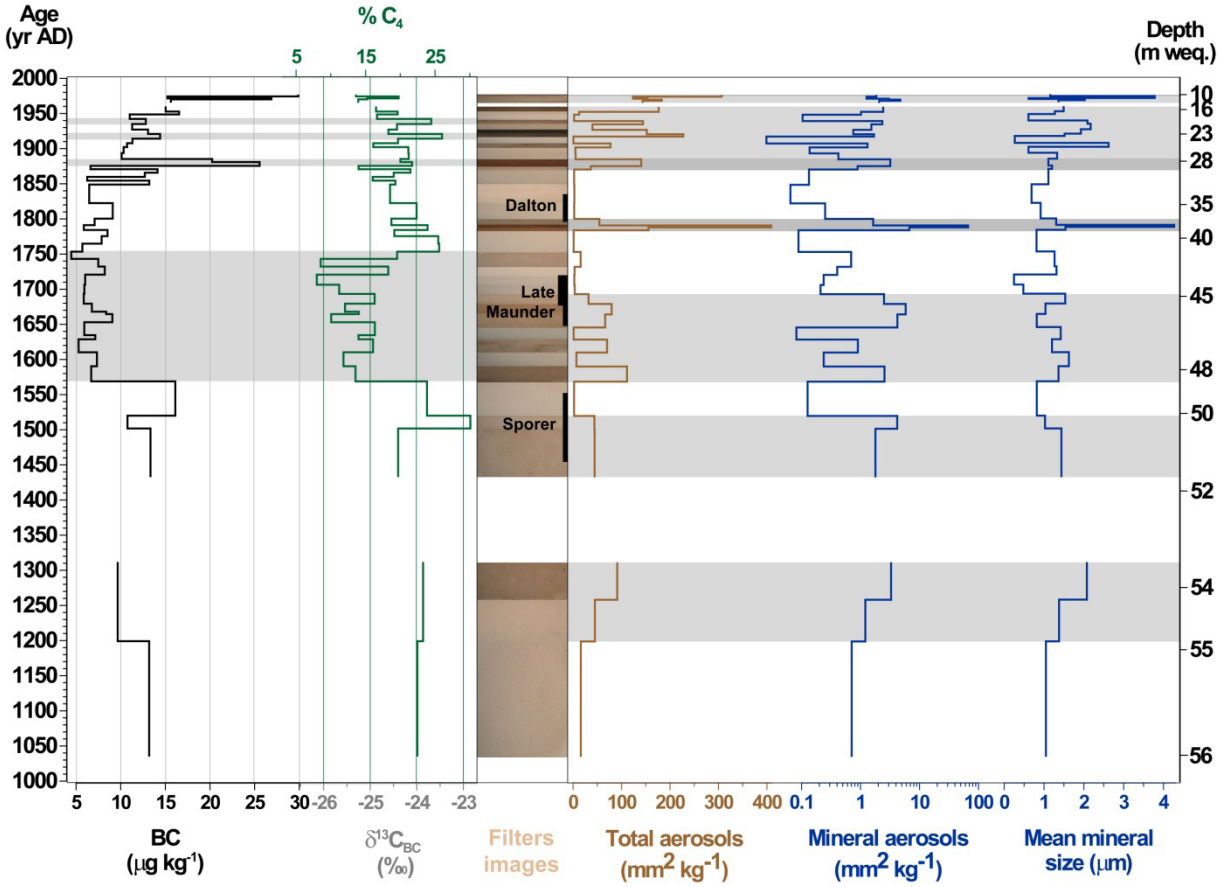

Figure 1. The last millennium record of black carbon (BC) concentration and the associated $\delta^{13}C_{BC}$ composition, as a function of age (year A.D.; left axis) and depth (meter water equivalent, m weq; right axis). The digital images of the filters, the total and mineral aerosol records, and the mean diameter of the mineral fraction. The three last major solar anomalous periods, the Spörer, the (Late) Maunder, and the Dalton Minima, are reported for comparison (Thevenon et al., 2009). (Next Page)

4.21

Impacts of climate change on 22 south-eastern Swiss glaciers from 1900 until 2100

Usselmann Stephanie [1], Huss Matthias [1,2] & Bauder Andreas [1]

[1] *Laboratory of Hydraulics, Hydrology and Glaciology (VAW), ETH Zürich, CH-8092 Zürich (usselmas@vaw.baug.ethz.ch)*
[2] *Department of Geosciences, University of Fribourg, CH-1700 Fribourg*

Since the 1850s, the end of the Little Ice Age, Alpine glaciers have suffered major losses of ice volume. The impact of climate change on glaciers is reflected most clearly in their surface mass balance. Therefore, a reconstruction of mass balance time series of different glaciers during the last century is important for a better understanding of the response of Alpine glaciers to current global warming.

In this study, the temporal and spatial changes of 22 glaciers in the south-eastern Swiss Alps are analyzed between 1900 and 2008 using different types of field data and distributed modelling. The investigated glaciers cover a wide range of glacier area and ice volume, as well as exposure and slope. This allows investigation of differences in the response of individual glaciers to climate change in a relatively small region.

Seasonal mass balance time series of glaciers have been calculated for the period 1900 – 2008 using a distributed accumulation and temperature-index melt model (Huss et al., 2008). The model is calibrated using observed ice volume changes in multidecadal periods. In order to calculate the volume change, two successive digital elevation models (DEMs) are compared

to each other. The basis for these DEMs are (i) terrestrial topographic surveys, (ii) photogrammetric analysis of aerial photographs, and (iii) already existing datasets, as DHM25 (swisstopo) and SRTM (NASA). In-situ point measurements of annual mass balance and winter accumulation, available for some glaciers, as well as long-term discharge records for the three major catchments in the study region are used for model validation.

Since 1900 the changes in glacier area and volume are consistently negative. Between the 1930s and the end of the last century the area of the 22 investigated glaciers decreased by about 24%. Over the last century (1900 – 1999) the regional ice volume has decreased by 30%, with strong differences between individual glaciers (20 – 60%). The rate of 100-year mass loss strongly differs between adjacent glaciers. Whereas large valley glaciers (e.g. Vadrec del Forno) show cumulative mass balances of up to -70m w.e., smaller and steeper glaciers (e.g. Vadret da Palü) exhibit less negative mass balances of around -15m w.e. (Fig. 1).
Using regional climate scenarios (Frei, 2007), future glacier retreat is simulated transiently for all glaciers over the 21st century. We project glacier area changes between -80% and -100% and volume changes between -70% and -100% with strong impacts on the water cycle (Fig. 2).

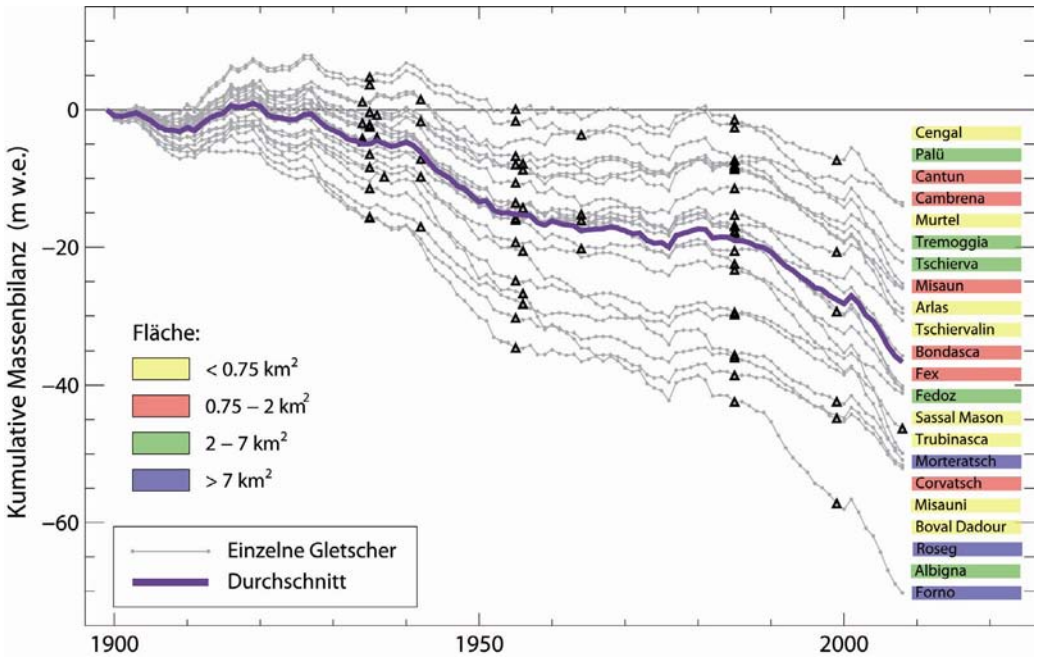

Figure 1. Cumulative series of mean specific mass balance of the 22 investigated glaciers from 1900 to 2008. Time series for the individual glaciers are displayed in grey; triangles indicate the dates of DEMs. The solid violet line represents the arithmetic average for the investigated glaciers. Glacier names are given at the right-hand side and colours indicate glacier size (Usselmann, 2009).

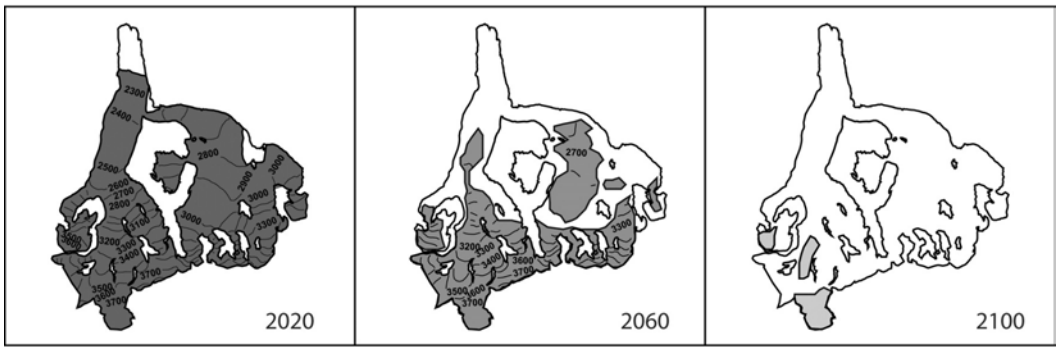

Figure 2. Simulated future evolution of Vadret da Morteratsch until 2100. Glacier extent is shown for the years 2020, 2060 and 2100 for the most likely climate scenario. Glacier extent in the year 2008 is shown (Usselmann, 2009).

REFERENCES

Frei, C., 2008. Die Klimazukunft der Schweiz. In: Klimaänderung und die Schweiz 2050 – Erwartete Auswirkungen auf Umwelt, Gesellschaft und Wirtschaft. Beratendes Organ für Fragen der Klimaänderung (OcCC): 12–16, http://www.occc.ch.

Huss, M., Bauder, A., Funk, M. & Hock, R., 2008. Determination of the seasonal mass balance of four Alpine glaciers since 1865. Journal of Geophysical Research, 113, F01015.

Usselmann, S., 2009. Schweizer Gletscher im Wandel von Klima und Zeit. Diplomarbeit, Friedrich-Alexander-Universität Erlangen-Nürnberg, pp. 179.

4.22

Understanding rapid dynamic changes of marine Greenland outlet glaciers from numerical modeling

Andreas Vieli[1 2], Faezeh M. Nick[3]

[1] *VAW, Glaziologie, ETH Zuerich, Gloriastr 37/39, CH-8092 Zuerich*
[2] *Department of Geography, Durham University, South Road, Durham DH1 3LE, UK (andreas.vieli@Durham.ac.uk.ch)*
[3]*GEUS, Ostervolgade 10, DK-1350, Copenhagen, DK*

Recent rapid dynamic changes of Greenland's outlet glaciers raised concerns over the contribution to future sea level rise. These dynamic changes seem to be linked to the warming trend in Greenland, but the mechanisms that link climate and ice dynamics are poorly understood, and current numerical models of ice sheets are not able to simulate these changes realistically. These dynamic changes therefore provide major uncertainties in the predictions of mass loss from the Greenland ice sheet. We developed a numerical ice-flow model that reproduces the observed rapid changes in Helheim Glacier, one of Greenland's largest outlet glaciers. Our simulations show that the ice acceleration, thinning and retreat begin at the ocean terminating calving front and then propagate rapidly upstream through dynamic coupling along the glacier. We find that these changes are unlikely to be caused by basal lubrication through enhanced surface melt from the recent atmospheric warming and that mass loss is amplified by a deep basal overdeepening at the bed. Importantly, the modelling further shows that such tidewater outlet glaciers are extremely sensitive to changing boundary conditions at the calving terminus and dynamically adjust extremely rapidly. This implies that the recent rapid mass loss of Greenland's outlet glaciers may reflect short-term variations in climate or ocean conditions and should not be extrapolated into the future.

4.23

Hazard assessment investigations in connection with the formation of a lake on the tongue of the Unterer Grindelwaldgletscher, Bernese Alps, Switzerland

Mauro A. Werder[1], Andreas Bauder[1], Hans-Rudolf Keusen[2], Martin Funk[1]

[1]*VAW, ETH Zurich, CH-8092 Zurich, Switzerland (werder@vaw.baug.ethz.ch)*
[2]*GEOTEST AG, Birkenstrasse 15, CH-3052 Zollikofen, Switzerland*

The surface level of the Unterer Grindelwaldgletscher glacier tongue has subsided by more than 200\,m over the last 150 years. The surface lowering is not uniform over the glacier tongue but depends on the thickness of the uneven debris cover, which led to the formation of a depression on the tongue. A lake has formed in this basin, for the first time in 2005, which can drain rapidly leading to a so-called glacier lake outburst flood. The lake basin has been increasing in size at an alarming rate and, in 2008 it reached a volume which poses a significant flooding threat to the communities downstream, as was exemplified by an outburst of the lake in May 2008. We extrapolated the future evolution of the lake basin based on surface lowering rates in 2004–2008. We tuned a model with the measured hydrograph from 2008 and ran it with the extrapolated lake volumes to simulate such a lake outburst and estimated possible future flood hydrographs. We discuss the rapidly increasing risk for Grindelwald and other communities, the reasons why in 2009 no rapid lake drainage occurred, as well as the installation of an early warning system and the construction of a 2.1km long drainage tunnel.

4.24

Analysis of temporal and spatial snow depth changes in a steep rock face

Vanessa Wirz , Michael Schirmer, Michael Lehning

WSL-Institut für Schnee- und Lawinenforschung SLF, Flüelastrasse 11, CH-7260 Davos Dorf (wirz@slf.ch)

The presence of snow in steep alpine terrain affects many phenomena, e.g. water management, snow avalanches or permafrost distribution. Hence good knowledge on spatial and temporal distribution of snow in steep alpine terrain is of high importance. Inaccessibility and alpine dangers in very steep terrain are the main reasons for lack of studies on snow depth in those areas. The main goal of this study is to get more detailed information about the amount and distribution of snow in very steep terrain and to better understand the relevant processes and factors, which affect snow accumulation, redistribution, erosion and ablation in steep rock faces. For this purpose, a high resolution terrestrial Laser Scanner (TLS) was used producing precise snow height digital surface models. We collected surface data without snow, before and after significant snowfall or wind drift events and during the ablation period. We then generated digital surface models (DSM) for each observation period. The summer scan under the total absence of snow allowed us to provide a digital elevation model (DEM) and to calculate absolute snow depth. Relative snow depth changes can be extracted by the comparison of different winter scans. In addition to the laser scans, orthophotos were taken with a digital camera.

In a first step we could show that with TLS reliable information on surface data of a steep rocky surface can be achieved. In comparison to a flat field point measurement the mean snow depth in the rock face was smaller during the entire winter, but trends of snow depth changes were similar. We observed repeating accumulation and ablation patterns in the rock face, while maximum snow depth loss occurred always at those places with maximum snow depth gain. Furthermore, increasing snow depth resulted in a decrease of high slope angles. Further analyses should involve the statistical relation of spatial and temporal distribution of snow depth to (i) terrain features e.g. slope angle, aspect or curvature and (ii) resulting surface processes derived from spatial distributed model outputs e.g. radiation, wind fields or blowing and drifting snow.

5. Meteorology and climatology

Rolf Philipona, Markus Furger

Swiss Meteorological Society

5.1

Magnitude and altitude dependence of Swiss temperature trends: local and large-scale influences

Ceppi Paulo, Scherrer Simon C., Appenzeller Christof

Climate Services, Federal Office of Meteorology and Climatology (MeteoSwiss), Zürich, Switzerland (Paulo.Ceppi@meteoswiss.ch)

Even though the increase in Central European temperatures over the last decades is undisputed, the altitude dependence of warming trends is still subject to many uncertainties. While most reanalyses and model projections indicate an increase of warming effects with altitude in the mid-latitude lower to middle troposphere (see IPCC 2007), studies based on observations yield less clear results, sometimes in contradiction with model-based analyses (e.g. Bradley et al. 2004, Appenzeller et al. 2008). Furthermore, the nature and effects of the physical processes responsible for the altitude dependence of the trends are only partly known and require further investigation.

This paper aims at estimating current temperature trends in Switzerland and at assessing their altitude dependence. We applied trend analysis methods to a new gridded Swiss temperature dataset, generated at MeteoSwiss from station-based homogenised temperature records for the time period 1959-2008 (Begert et al. 2005). Using different temporal resolutions

(yearly, seasonal and monthly), we investigated the magnitude of recent warming and its altitude dependence. From the results of the trend analysis, we attempted to identify possible physical mechanisms (e.g. large scale dynamics or local factors such as snow pack or fog) explaining the vertical dependence of the temperature trends.

Our results indicate that yearly trends are positive and statistically significant at the 95% level for all of Switzerland, with values between 0.23 and 0.44°C per decade. However, seasonal variations are considerable. The trends are strongest in summer (0.34 to 0.62°C/decade) and weakest in autumn (-0.02 to 0.38°C/decade). Using multiple regression models, we show that global temperature variations and changes in large scale dynamics cannot explain the full amplitude of the observed temperature trends in Switzerland. This indicates that smaller scale and local effects might play an important role.

The temperature trends show some altitude dependence, but the importance of this effect is strongly dependent on season. While yearly trends show a slight tendency towards decreasing magnitudes with altitude, there is a much clearer signal in early spring and autumn, with trends being much stronger in lowland regions than in the mountains (see Fig. 1).

Furthermore, our observations show that during spring, the strongest warming signal propagates towards higher altitudes with time, following the 0°C isotherm and the increasing altitude of the snow line. This is consistent with findings in other mountainous regions (Pepin & Lundquist 2008). The observed height dependences in spring have been interpreted as resulting from reduced snow cover, implying changes in surface albedo and surface energy budget. The stronger trends at low altitudes in autumn are still under investigation. Potential mechanisms leading to this difference are a decrease in fog day frequency in the lowlands over the last decades and/or changes in foehn frequency, at least in the main foehn regions.

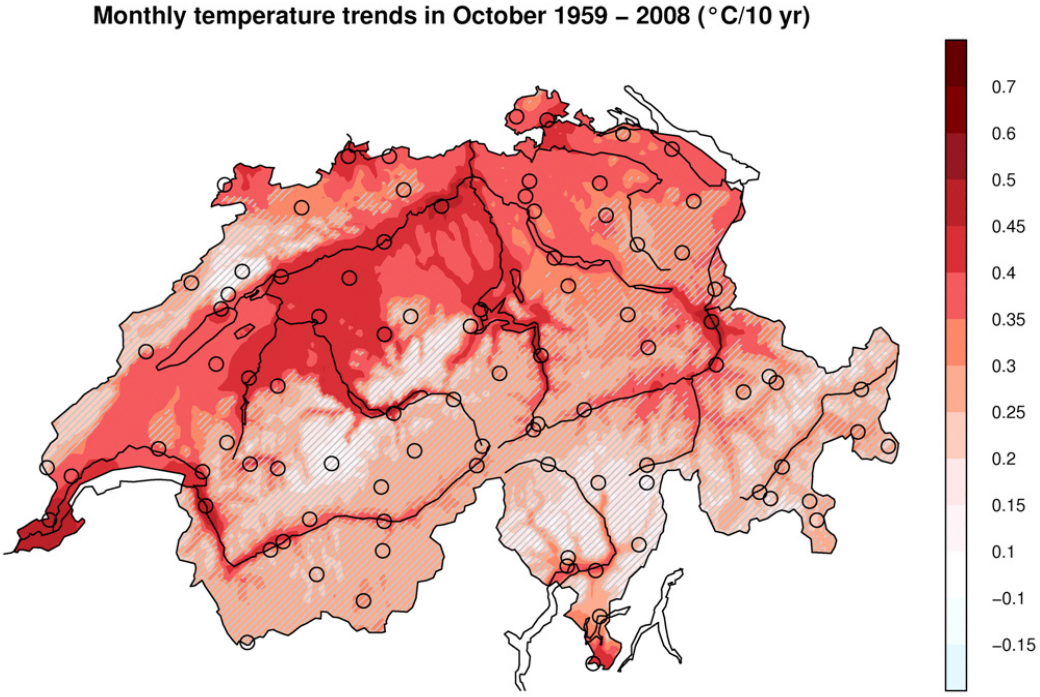

Figure 1. Temperature trends (°C/decade) in October from 1959 to 2008. Shading denotes non-significant trends at the 95% level. Note that the trends exhibit a clear altitude dependence with higher values at lower stations.

REFERENCES

Appenzeller, C., Begert, M., Zenklusen, E. & Scherrer, S. C. 2008. Monitoring climate at Jungfraujoch in the high Swiss Alpine region. Science of the Total Environment, 391(2-3):262-268.

Begert, M., Schlegel, T. & Kirchhofer, W. 2005. Homogeneous temperature and precipitation series of Switzerland from 1864 to 2000. Int. J. Climatology, 25(1):65-80.

Bradley, R. S., Keimig, F. T. & Diaz, H. F. 2004. Projected temperature changes along the American cordillera and the planned GCOS network. Geophysical Research Lett., 31(16).

Pepin, N. C. & Lundquist, J. D. 2008. Temperature trends at high elevations: Patterns across the globe. Geophysical Research Lett., 35(14).

IPCC 2007. Climate Change 2007: The Physical Science Basis. Contribution of Working Group I to the Fourth Assessment Report of the Intergovernmental Panel on Climate Change. Cambridge University Press.

5.2

Decadal variability of aerosol optical depth in Europe and its relationship to the global dimming and brightening and the shift in the NAO

Marc Chiacchio[1], Tracy Ewen[1,3], Martin Wild1, Mian Chin[2], Thomas Diehl[2]

[1] *Institute for Atmospheric and Climate Science ETH, Zurich, Switzerland*
[2] *NASA Goddard Space Flight Center, Greenbelt, Maryland, USA*
[3] *Department of Geography, University of Zurich, Zurich, Switzerland*

Trends of aerosol optical depth from the Goddard Chemistry Aerosol Radiation and Transport (GOCART) Model are detected according to their annual and seasonal temporal resolution for the period 1979-2007. During this time aerosol emissions in Europe have declined due to environmental regulations imposed to control air pollution. By doing so it is believed that this has affected the amount of solar radiation that reaches the surface of the Earth, which has upset the surface radiative balance, hence, global dimming and brightening. Though clouds have also played a role to the decadal changes in surface solar radiation, the inter-relationship between these variables are still not well known and their role among one another has not yet been quantified. Through various statistical techniques we show the role that aerosols play on the global dimming and brightening according to a seasonal analysis as well as their role on the related atmospheric circulation that is dominant in Europe, such as the North Atlantic Oscillation (NAO). It is well established that the NAO mainly affects the climate in Europe in winter. In recent decades, large changes in the NAO have occurred with a large positive trend in the index after about 1980, and it has accounted for much of the warming in Europe. This large positive trend in the NAO also occurs at the same time that aerosol emissions in Europe were greatest, which might imply that they could be contributing to the changes in the NAO and controlling the solar radiation on a decadal scale.

5.3

Pacific North American climate variability and links to the North Atlantic

Tracy Ewen[1],[2] & Stefan Brönnimann[2]

[2]*Institute for Atmospheric and Climate Science, ETH Zurich, Universitätstr. 16, 8092 Zurich.*
[1]*Department of Geography, University of Zurich, Winterthurerstr. 190, 8057 Zurich, (tracy.ewen@geo.uzh.ch)*

Climate variability in the Pacific-North American region is often analysed in terms of a few dominant modes of variability, such as the PNA and PDO. While the PNA predominantly characterises variability on seasonal to interannual time scales, the PDO is often used to characterise decadal scale variability. Similarly, variability in the North Atlantic European sector is analysed in terms of the NAO (seasonal-to-decadal) and AMO (decadal-to-centennial).

Until recently, the PNA index has only been available back to 1948, as it is defined based on 500 hPa geopotential height data. Using historical upper-air data, we have reconstructed a monthly index back to 1920 (Ewen et al., 2008), which now allows decadal-scale variability to be assessed. We analyse this index together with ENSO (NINO3.4), PDO, NAO, and AMO indices in the time-frequency domain and further assess the stationarity and phase relationship of the indices. We find stable relations between the PNA and all other indices, but at different time scales. ENSO and PNA show coherent behaviour in the 4-8 year period. We also find coherent low-frequency variability (for periods longer than 10 yrs) between the PNA and PDO. The correlation between PNA and NAO is weak (but significant) in late winter, and time intervals with significant coherency are found on the interannual scale but also on the interdecadal scale. Finally, we analyse periods of coherency between the indices in terms of their climatic significance, in particular to the Arctic warming during the 1930s and the North American Dust Bowl drought in the 1920s (Brönnimann et al, 2009).

REFERENCES

Brönnimann, S., T. Griesser, A. Stickler, T. Ewen, A.N. Grant, A.M. Fischer, M. Schraner, T. Peter, E. Rozanov, T. Ross, 2009: Exceptional atmospheric circulation during the Dust Bowl, to appear in Geophys. Res. Lett., 36, L08802, doi:10.1029/2009GL037612.

Ewen, T., S. Brönnimann and J. Annis, 2008: An extended Pacific North American index from upper air historical data back to 1922. J. Climate, 21 (6), 1295-1308.

5.4

Assessment of extreme precipitation in Switzerland with statistical analyses

Fallot Jean-Michel[1], Hertig Jacques-André[2]

[1]*Institut de Géographie, Université de Lausanne, Dorigny-Anthropole, CH-1015 Lausanne (Jean-Michel.Fallot@unil.ch)*
[2]*Hertig&Lador SA, Grand Rue 38, CH-1176 St Livres*

Extreme precipitation and flood events produce the greatest damages due to natural hazards in Switzerland. Extreme precipitation amounts for a return period of 500 years are generally used for calculating the ideal dimensions of protection structure against floodings. The Swiss Federal Institute for Forest, Snow and Landscape Research (WSL) calculated these extreme precipitation values from statistical analyses carried out on rainfall time series at about 300 locations in Switzerland over the period 1901-1970 (Zeller et al., 1980).
Several studies show that frequency of strong precipitation has increased in Switzerland and in the world with the global climate warming (Fallot, 2000 ; Frei et al., 2000; IPCC, 2007): For this reason, daily (24-hour) extreme precipitation values for a return period of 500 years were recalculated from Gumbel analyses carried out on rainfall time series measured at 429 locations in Switzerland over the period 1961-2008.
Previous studies show that Gumbel analyses give the best results for estimating daily extreme precipitation values in Switzerland for a return period of 100 or 500 years (Zeller et al., 1980). Our study shows that these extreme values can be well estimated at most locations (75%) in Switzerland from such analyses. On the other hand, daily extreme precipitation values are more or less underestimated for a small number of stations (7%).
Results of these new analyses also reveal that daily extreme precipitation values estimated for a return period of 500 years over the period 1961-2008 are in average 14% higher than similar values calculated for the period 1901-1970. For 31% of stations, daily extreme precipitation values for a return period of 500 years estimated from rainfall time series over the period 1901-1970 only correspond to extreme values for a return period of 100 years for time series over the period 1961-2008. This confirms that extreme precipitation values have increased and they could cast a doubt over the ideal dimensions of protection structure against flooding in some area in Switzerland.
Figure 1 shows that daily extreme precipitation values for a return period of 500 years are much higher south of the Alps (up to 560 mm in 24 hours) due to its high exposure to wet and warm air mass coming from Mediterranean Sea.

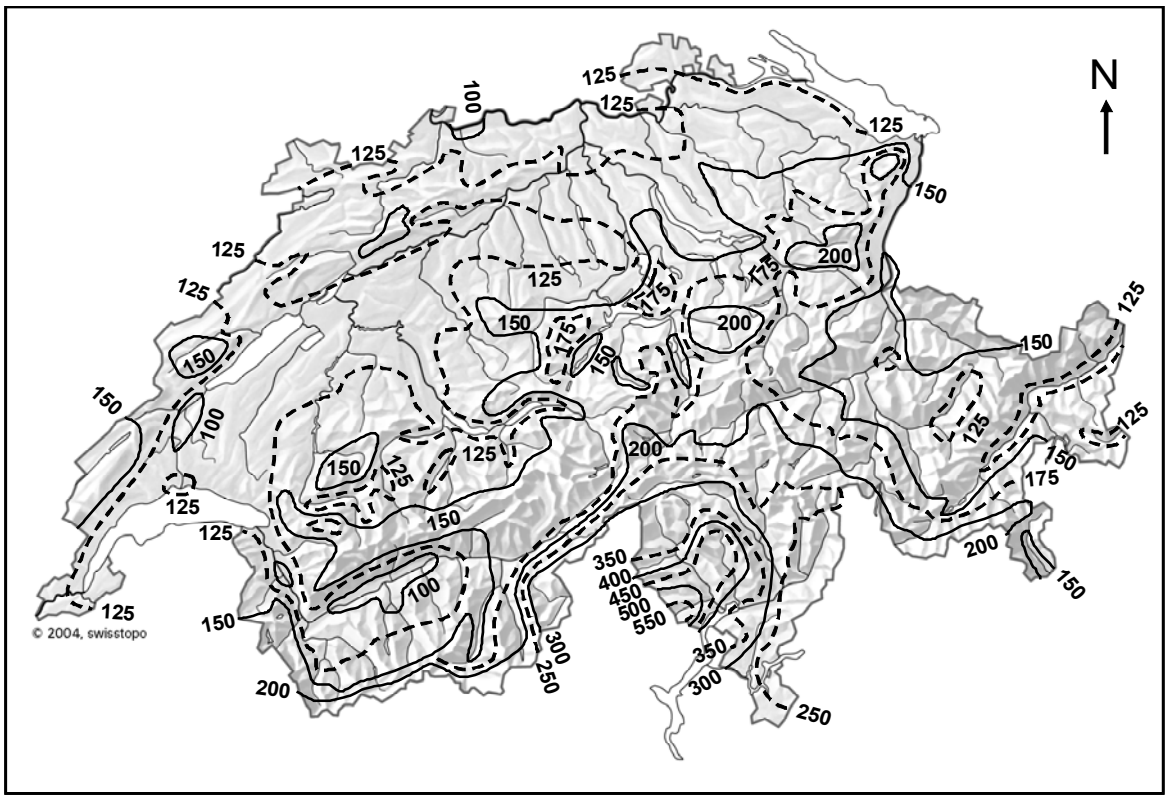

Figure 1. Daily (24-hour) extreme precipitation for a return period of 500 years estimated in Switzerland from Gumbel analyses carried out on rainfall time series at 429 locations over the period 1961-2008.

However, extreme precipitation values can only be known at precise locations from Gumbel analyses. But these values strongly vary within a catchment area in a complex topography what can affect floods calculations. Thus, a three-dimensional meteorological model was developed for calculating extreme winds and precipitation every 2 km at the horizontal scale (Audouard et al., 2006). Results of this model were compared with daily extreme precipitation values for a return period of 500 years estimated from rainfall time series over period 1961-2008. This comparison shows a quite good agreement between the model and extreme values estimated from field measurements, but they are also several differences due to some approximations in the model.

REFERENCES

Audouard A., Hertig J.-A., Fallot J.-M., 2006: Modélisation des précipitations extrêmes en Suisse. Actes du 19ème colloque de l'Association Internationale de Climatologie, Epernay, 6-9-9.2006, p. 83-88.

Fallot J.-M., 2000: Evolution du nombre de jours avec des précipitations abondantes en Suisse durant le 20ème siècle. Publications de l'Association Internationale de Climatologie, 13, 100-108.

Frei C., Davies H.C., Gurtz J., Schär C., 2000: Climate dynamics and extreme precipitation and floods events in Central Europe. Integrated Assessment, 1, 281-299.

IPCC, 2007: Climate Change 2007. The physical science basis. Working Group 1 to the fourth Assessment Report of Intergovernmental Panel on Climate Change (IPCC), Cambridge University Press, Cambridge, UK, 996 p.

Zeller J., Geiger H., Roethlisberg G., 1980: Starkniederschläge des schweizerischen Alpen- und Alpenrand-Gebiet. Eidgenössische Forschungsanstalt für Wald, Schnee und Landschaft (WSL), Birmensdorf.

5.5

Soil moisture monitoring and soil moisture impact on convective precipitation in orographic terrain

Hauck Christian[1], Krauss Liane[2], Barthlott Christian[2]

[1]*Department of Geosciences, University of Fribourg, Chemin du Musée 4, 1700 Fribourg*
[2]*Institute for Meteorology and Climate Research, Karlsruhe Institute of Technology, Germany*

Soil moisture is an important parameter in the soil-atmosphere system, which influences the hydrology as well as the availability of moisture in the planetary boundary layer (PBL). The latter is mainly controlled by the energy balance at the Earth's surface, large-scale advection, and advection on the mesoscale exhibiting a daily cycle. At least in situations with low synoptic forcing, the PBL characteristics and their impacts on the triggering and/or dynamics of convective storms are strongly influenced by the partitioning of available radiation energy into sensible and latent heat which itself is determined by soil moisture.

Whereas previous observational and modelling studies demonstrated that soil moisture can indeed strongly contribute to the variability of surface temperature and precipitation over flat terrain, the influence of soil moisture on convection initiation and precipitation in complex terrain has not been investigated in detail.
In this contribution we will show results of a data set from a soil moisture network within the orographically complex terrain of the Black Forest/Rhine Valley in Southwestern Germany, which was installed in the framework of the international COPS campaign (Convective and Orographically-induced Precipitation Study). In addition to soil moisture, soil temperature, and data from energy balance, radiosonde station and precipitation networks are available to analyse the impact of soil moisture on convective precipitation (Wulfmeyer et al. 2008, Kottmeier et al. 2008). Model studies using a nonhydrostatic limited-area atmospheric prediction model (COSMO-DE) are used to compare modelled and observed soil moisture and precipitation fields.

The soil moisture monitoring network consists of more than 50 stations and 160 single sensors measuring vertical profiles of soil moisture (5, 20 and 50 cm depth). Based on regional differences between 4 distinct regions within the investigation area soil moisture is analysed regarding their variability with respect to soil texture properties, altitude and exposition (luv/lee). Each sensor (newly developed low-cost sensor SISOMOP) was calibrated according to the properties of the soil. A thorough analysis of the soil at the various soil moisture stations shows that the actual soil textures often differ from the ones used for the respective grid point in the operational soil model COSMO/TERRA. Consequently, first results from a comparison between simulated and measured soil moisture values show strong differences with a mean bias around 20-30% for most of the stations and measurement depths.

Even though it is generally assumed that the impact of the interaction processes between soil surface and atmosphere on near-surface variables and PBL characteristics is larger under weak synoptic forcing than for strong synoptic forcing, model simulations and observational evidence revealed that the impact of soil moisture is not systematically higher for boundary-layer forcing mechanisms. In the model sensitivity experiments, the Bowen ratio exhibits a clear dependence to soil moisture conditions, but the soil moisture impact on precipitation is much more complex and depends also on its influence on convective indices, i. e. convective available potential energy (CAPE) and convective inhibition (CIN). A considerable, but not systematic feedback of convective precipitation with soil moisture exists in the complex orography analysed. The results demonstrate the high importance of accurate initial soil moisture fields in numerical weather prediction models.

REFERENCES

Kottmeier, Ch., N. Kalthoff, U. Corsmeier, Ch. Barthlott, J. Van Baelen, A., Behrendt, R. Behrendt, A. Blyth, R. Coulter, S. Crewell, M. Dorninger, C., Flamant, Th. Foken, M. Hagen, C. Hauck, H. Höller, H. Konow, M. Kunz, H., Mahlke, S. Mobbs, E. Richard, R. Steinacker, T. Weckwerth, A. Wieser, & V. Wulfmeyer V. 2008. Mechanismus initiating deep convection over complex terrain during COPS. Meteorol. Z., 17 (6), 931-948.

Wulfmeyer, V., Behrendt, A., Kottmeier, Ch., Corsmeier, U., et. al. 2008. The Convective and Orographically-induced Precipitation Study: A Research and Development Project of the World Weather Research Program for Improving Quantitative Precipitation Forecasting in Low-mountain Regions. Bull. Amer. Meteor. Soc., 89 (10), 1477-1486.

5.6

Aerosol properties of Saharan dust collected at the Jungfraujoch: determined by single particle analysis

Meier Mario Federico[1], Grobéty Bernard[1],[2] & Collaud Coen Martine[3]

[1]*Dept. of Geosciences, University of Fribourg, Chemin du Musée 6, CH-1700 Fribourg (mario.meier@unifr.ch)*
[2]*Fribourg Center for Nanomaterials (FriMat), Univ. of Fribourg, CH-1700 Fribourg*
[3]*MeteoSwiss, Aerological Station, CH-1530 Payerne*

Mineral dust can have a pronounced effect on the optical parameters of the aerosol. During Saharan Dust Events (SDE) an inversion of the wavelength dependence of the Single Scattering Albedo (SSA) is observed (Collaud Coen et al., 2004). The aim of this study is to analyse aerosol particles from a SDE to determine their size distribution between 0.4 and 10 micrometers, their morphology and their mineral composition in relation with the observed optical modifications.

For this purpose PM10 was actively sampled onto Nuclepore® filters at the high altitude research station Jungfraujoch (3580 m.a.s.l.), before and during a very strong SDE which occurred between 26. and 29.5.2008. Calculated back trajectories show that the air masses before the SDE came from the West (France, Southern Spain) and during the SDE from the South. The source region of the mineral dust collected during the SDE was East Libya and Tunisia. The aerosol was, therefore, transported straight across to Mediterranean Sea towards the Alps.

Stereological and chemical single particle analyses were performed by Computer Controlled Scanning Electron Microscopy (CCSEM) coupled with Energy Dispersive Spectroscopy (EDS). With this automated technique it was possible to obtain chemical and morphological parameters of about 2000 particles for each sample. Aerosol particles have also been directly collected with an electrostatic sampling device on carbon coated copper grids for analysis by Transmission Electron Microscopy (TEM).

The mineralogy, determined by CCSEM, was not clearly different for aerosol collected before and during the SDE. All samples are dominated by clay minerals, followed by feldspars, gypsum, quartz and carbonates. Individual, well separated iron oxides, partially suspected as causes for inversion of the wavelength dependence of the SSA, were rare. However, detailed analyses with TEM of particles from the SDE showed that inclusions of iron and titanium oxides within the clay particles are common. The size of these inclusions is between 10 and 200 nm. During the SDE an increase of the total aerosol mass concentration was observed. The values raised from 100-200 ngm^{-3} prior to the SDE to values > 10.000 ngm^{-3}. The particle size distribution shows a clear correlation with the inversion of the SSA wavelength dependence. For all days with negative values of the SSA exponent, the concentration of particles with diameters smaller than 1.5 μm is proportionally to the concentra-

tion of bigger particles enhanced. The mineral type contributing most to this size fraction are clay particles. For particles >1 μm the scattering becomes dominated by geometrical optics. This leads to a wavelength independence of the scattering coefficient.

The results corroborate the previous explanation of the SSA wavelength dependence inversion caused by a relative change in the size distribution of the aerosol particles and by the presence of iron oxides. The iron oxides occur as inclusions with sizes between 10 and 200 nm in clay particles with sizes between 0.5 and 5 μm.

REFERENCES

Collaud Coen, M., Weingartner, E., Schaub, D., Hueglin, C., Corrigan, C., Henning, S., Schwikowski, M. & Baltensperger, U. 2004: Saharan dust events at the Jungfraujoch: detection by wavelength dependence of the single scattering albedo and first climatology analysis, Atmospheric Chemistry and Physics, 4, 2465-2480.

5.7

Selecting and producing climatic data to assess the climate change / human migration nexus

Etienne Piguet[1], Amir Delju[2], Raoul Kaenzig[3]

[1]*Institut de géographie, Université de Neuchâtel, Espace Louis-Agassiz 1, CH-2000 Neuchâtel (Etienne.Piguet@unine.ch)*
[2]*World Meteorological Organization, 7bis av. de la Paix, CH 1211 Genève-2 (adelju@wmo.int)*
[3]*Institut de géographie, Université de Neuchâtel, Espace Louis-Agassiz 1, CH-2000 Neuchâtel (Raoul.Kaenzig@unine.ch)*

Since the IPCC (2007) report mentioned population displacements as a foreseeable consequence of climate change, numerous synthesis papers and case studies have been published about the past, present and future migratory consequences of environmental degradations (Kniveton et al., 2008; Piguet, 2008). A number of international conferences and expert workshops took place and an impressive coordinated research project in 23 regions of the world was achieved (http://www.each-for.eu/). The variety of empirical methods used in these researches is impressive, ranging from qualitative interviews and historical analogies to representative questionnaire surveys, and highly sophisticated quantitative methods.

Several of the existing researches already use climatic data such as rainfall (Barrios et al., 2006), drought frequencies (Henry et al., 2003) or hurricanes frequencies (Afifi and Warner, 2008) but such data are in our view clearly underused up to now. This is due in part to a lack of dialogue between migrations scholars and climatologists / meteorologists. In order to bridge this gap, the paper will present a critical assessment of the different methods used to connect environmental change and migration and of the use of meteorological and climatic data in that context. On that basis, we will present an overview of the data which could be used or should be produced in order to improve the study of the environment/climate change migration nexus

REFERENCES

Afifi, T. and Warner, K. 2008: The Impact of Environmental Degradation on Migrations Flows across Countries. United Nations University - EHS - Working Paper.

Barrios, S., Bertinelli, L. and Strobl, E. 2006: Climatic change and rural–urban migration: The case of sub-Saharan Africa. Journal of Urban Economics 60, 357-371.

Henry, S., Boyle, P. and Lambin, E.F. 2003: Modelling inter-provincial migration in Burkina Faso: the role of socio-demographic and environmental factors. Applied Geography 23, 115-136.

Kniveton, D., Schmidt-Verkerk, K., Smith, C. and Black, R. 2008: Climate Change and Migration: Improving Methodologies to Estimate Flows. Geneva: International Organization for Migration - Migration Research Series 33.

Piguet, E. 2008: Climate change and forced migration. New Issues in Refugee Research - United Nations High Commissioner for Refugees Research Paper.

5.8

Water temperature changes in receiving waters due to the increase of imperviousness: a multidisciplinary assessment approach

Rossi Luca[1], Margot Jonas[1], Hari E. Renata[2]

[1]*Ecole polytechnique fédérale de Lausanne (EPFL), Ecological Engineering Laboratory (ECOL), ENAC - IEE, Station 2, CH-1015 Lausanne (luca.rossi@epfl.ch)*
[2] *Swiss Federal Institute for Aquatic Science and Technology (EAWAG), Department of Systems Analysis, Integrated Assessment, and Modeling (SIAM), Überlandstrasse 133, CH-8600 Dübendorf*

Water temperature is one of the key parameters influencing the chemical equilibrium and development of flora and fauna in aquatic systems. An increase in temperature reduces oxygen solubility, accelerates metabolism, such as photosynthesis or the development of fish eggs, and raises the sensitivity of organisms to toxic substances, parasites and diseases. In urban areas, an increase in water temperature also may result in an increase in toxicity from ammonia discharging from combined sewer overflows [(VSA 2007).

There are numerous causes of temperature changes in receiving waters. Natural causes can include climate (daily, seasonal and long-term changes) (Hari et al. 2006), the presence or absence of near-stream shading, the morphological conditions of the receiving waters or groundwater discharge into the aquatic system. Anthropogenic causes can include discharge from hydro-electric power stations with storage lakes (sudden reservoir drainage causes a sudden temperature drop in the receiving water), discharge of industrial cooling water (which usually heats the receiving water), and urban stormwater discharge during a rain event (Rossi & Hari 2007; Margot 2008). This discharge of urban stormwater during rain events can constitute a temperature problem for receiving waters. In urban areas, this thermal boost is related to the flow regime, the thermal and physical properties of urban surfaces and the removal of riparian vegetation along urban watercourses. These factors increase the amount of thermal energy in urban receiving waters and may lead, particularly in summer, to a short-term spike in the receiving water temperature at the beginning of a rain event. In fact, sealed asphalt surfaces or roofs can reach extremely high temperatures (> 60°C) during extended periods of good weather. A simultaneously low water discharge rate in the receiving waters increases the potentially dangerous thermal effect of the stormwater discharge to indigenous aquatic biota.

In the 1990s, an alarming decline in the catch of brown trout (*Salmo trutta fario L.*) in rivers and streams occurred in Western Europe, including Switzerland (Burkhardt-Holm et al. 2002). The climatic temperature increase is considered to be one of the main driving forces of this decline (Hari et al. 2006). In addition to climatic change, the progressive increase in the area of impervious surfaces (e.g. pavement) caused by urban development leads to stormwater reaching aquatic systems more rapidly, resulting in higher in-stream temperatures than in the past. Swiss anglers suspect that urban stormwater discharge into rivers and streams during rain events may harm the development of certain fish species.

Since legal temperature limits are calculated only over a long-term discharge period (≥ year), they cannot be applied to short-term alterations such as those expected following rain events, thus creating a legal loophole.

This question will be addressed with in this paper. Thresholds are proposed for sensitive habitats during a rain event as assessment criteria to protect the fish in the receiving waters from thermal harm. The thresholds are based on the temperature requirements of brown trout, one of the most important fish native to Swiss rivers and streams. A multidisciplinary assessment approach, including hydrological, physical, biological and ecotoxicological processes will be presented and subsequently validated through the presentation of different case studies of differently sealed surfaces in Switzerland.

REFERENCES

Burkhardt-Holm, P. Peter, A. Segner, H. 2002: Decline of fish catch in Switzerland - Project Fishnet: A balance between analysis and synthesis. Aquat Sci 64:36-54.

Hari, RE. Livingstone, DM. Siber, R. Burkhardt-Holm, P. Güttinger, H. 2006: Consequences of climatic change for water temperature and brown trout populations in Alpine rivers and streams. Global Change Biology 12:10-26.

Margot, J. 2008: Impacts des déversoirs d'orage sur les cours d'eau. Application de la méthodologie STORM et validation par le biais d'analyses écotoxicologiques et chimiques. Master Thesis EPFL, 274 pp + annexes.

Rossi, L. Hari, RE. 2007: Screening procedure to assess the impact of urban stormwater temperature to populations of brown trout in receiving water. Integrated Environmental Assessment and Management Journal 3:383-392.

VSA. 2007: Urban wet-weather discharges in receiving waters: guidelines for the conceptual planning of protection measures (STORM guidelines, available in French, German and Italian). Swiss Water Pollution Control Association, www.vsa.ch, Zürich, Switzerland.

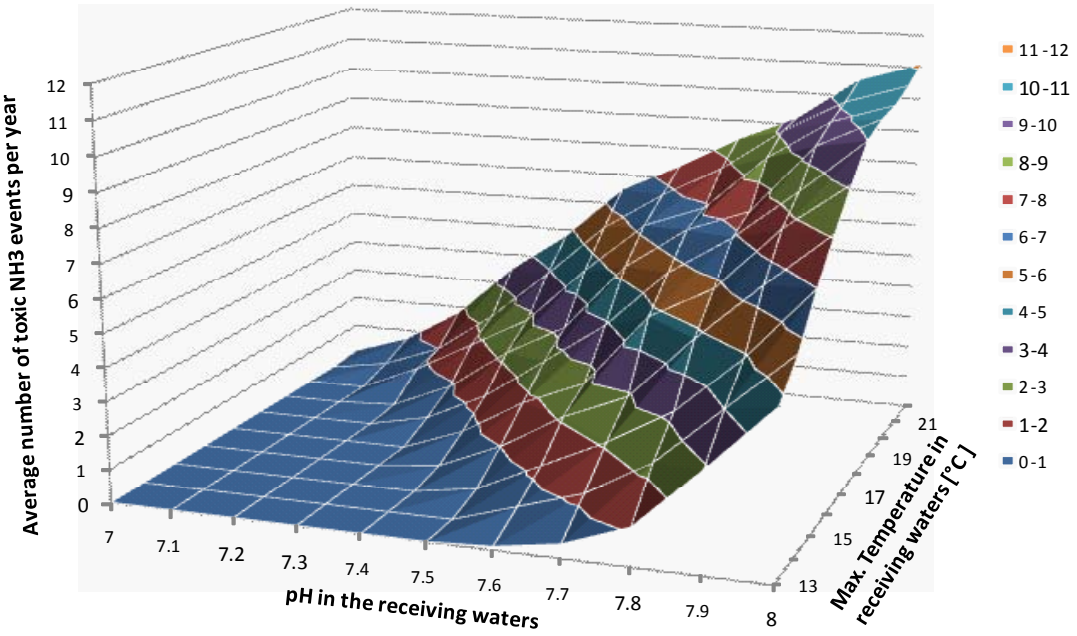

Figure 1. Example of the influence of temperature and pH on the number of critical ammonia toxicity events per year in a stream (Margot, 2008). In Switzerland, one critical event in 5 years is tolerated (VSA 2007).

5.9

Should climate models be evaluated with statistic-based or process-based metrics?

Schaller, Nathalie[1], Mahlstein, Irina[1] & Knutti, Reto[1]

[1] *Institute for Atmospheric and Climate Science, ETH Zurich*

In the discussion on the greenhouse-induced climate change, modifications in the hydrological cycle are of particular interest since they are expected to have severe consequences for societies and ecosystems (IPCC, 2007). Unfortunately, the model spread for precipitation is large and precise statements about future changes in the precipitation patterns are difficult to provide.

The evaluation of climate models is a relatively new research field and thus, so far no standardized metric for defining a climate model's skill has been defined. Recently, some attempts have been made to rank or weight the model's projections (Phillips & Gleckler, 2006, Gleckler et al., 2008, Pincus et al., 2008). Thereby, the favoured way to proceed was to evaluate the model simulations against observations using statistical measures. However, we suspect that depending on the purpose and the variable considered, process-based metrics defined on a regional scale are more suitable to identify the good models than statistical measures defined on a global scale. Here, we compare three different ways of ranking the climate models, namely a statistic-based ranking considering a broad range of climate variables performed by Reichler & Kim (2008), a statistic-based ranking considering only the precipitation field and a process-based ranking consisting of six metrics representing regional features of the modelled precipitation response to climate change. Surprisingly, the multimodel mean performs only average for the process-based ranking, while it outperforms all single models in the statistics-based rankings. The models performing best can be different for each region or zone considered and identifying them each time newly depending on the application may allow for more reliable projections. Further, considering only the five best models for each metric allows for a reduction of the model spread and thus, for more precise information about the future climate state.

REFERENCES

Gleckler, P. J., K. E. Taylor, & C. Doutriaux, 2008: Performance metrics for climate models. Journal Of Geophysical Research-Atmospheres, 113 (D6), D06,104.

IPCC (2007), Climate change, 2007: The physical science basis. Contribution of working group I to the fourth assessment report of the Intergovernmental Panel on Climate Change [Solomon, S., D. Qin, M. Manning, Z. Chen, M. Marquis, K.B. Averyt, M. Tignor & H.L. Miller (eds)], Cambridge University Press, Cambridge, United Kingdom and New York, NY, USA, p. 996.

Phillips, T. J. & P. J. Gleckler, 2006: Evaluation of continental precipitation in 20th century climate simulations: The utility of multimodel statistics. Water Resources Research, 42 (3).
Pincus, R., C. P. Batstone, R. J. P. Hofmann, K. E. Taylor, & P. J. Glecker, 2008: Evaluating the present-day simulation of clouds, precipitation, and radiation in climate models. Journal Of Geophysical Research-Atmospheres, 113 (D14), D14,209.
Reichler, T. & J. Kim, 2008: How well do coupled models simulate today's climate? Bulletin Of The American Meteorological Society, 80(3), 303-311.

5.10

The MeteoSwiss strategy for the renewal of the precipitation measurement network

Catherine Stocker-Mittaz, Christian Häberli, Christoph Frei, Urs Germann[1]

[1]*Federal Office of Meteorology and Climatology MeteoSwiss, Krähbühlstrasse 58, CH-8044 Zürich (catherine.stocker@meteoswiss.ch)*

The requirements for precipitation data have risen in recent years: in particular, meteorologists (eg, for the warning of extreme events) and hydrologists (eg, calculation of the areal precipitation for flood warnings) are depending on precipitation information with both a high spatial and temporal resolution. As a result of the increasing use of precipitation data in forecast models (runoff forecasting, snowpack development, agriculture, etc.) the need for quantitative precipitation fields has increased. For these applications a high absolute accuracy and high spatial / temporal resolution is required and the data need to be available as fast as possible.

The conventional precipitation monitoring network of MeteoSwiss started in December 1863. Precipitation amounts and snow heights are measured manually once per day. Neither the method of observation nor the processing of the data have been substantially adapted to new technologies.

Due to the increased demands, both some cantons and private institutions designed their own measurement networks and operate approximately 300 automatic precipitation stations in Switzerland. In addition, the cantons are increasingly interested in co-operation regarding design and operation of measurement stations and handling of data with MeteoSwiss.

In the context of the rolling requirements review the different observing systems and networks from MeteoSwiss were integrally considered and the MeteoSwiss strategy for the renewal of the precipitation measurement network was developed.

A comparison of the various observing systems, precipitation analysis and products shows the strengths and weaknesses of the possible combinations of the different measurement platforms (automatic surface stations, conventional precipitation measurement network, radar). For applications with the demands of a high spatial and temporal resolution and high absolute accuracy none of the products turns out as appropriate.

Requirements for precipitation information from climatology, meteorology, hydrology and radar technology, together with the resulting strengths and weaknesses of current products, result in a strategy with which the deficiencies of the current monitoring network shall be countered:

- MeteoSwiss provides spatially comprehensive data sets with high temporal resolution (at least hourly) that allow statements about the precipitation patterns in the individual regions for warnings in Switzerland (138).
- MeteoSwiss provides at least in day-resolution data sets that allow statements about the precipitation patterns in areas smaller than the regions for warnings. These records have a higher absolute accuracy than the ones with high temporal resolution.
- MeteoSwiss provides long precipitation data series (also for total and fresh snow height) for statistical evaluations and takes the necessary measures to secure the sites, which are important for the comprehensive monitoring of climatological precipitation conditions (including snow heights) in Switzerland.
- MeteoSwiss offers a standardized product portfolio in which these records can be provided customer-oriented.

Approximately 50 additional, fully equipped (not only precipitation) surface stations, 100 automatic and about 200 conventional precipitation stations result (mostly at sites of the existing precipitation measurement network). The new stations will be built and operated by MeteoSwiss. For specific needs, this network shall be completed with stations of the federal government and the cantons. These additional stations shall be certified and thus receive a status similar to stations of MeteoSwiss (including data storage in the MeteoSwiss data warehouse).

6. Darwin, Evolution and Palaeontology

Lionel Cavin

Schweizerische Paläontologische Gesellschaft (SPG/SPS), Kommission der Schweizerischen Paläontologischen Abhandlungen (KSPA), Swiss Commission of Palaeontology Award

6.1

Late Aquitanian mammals from the Engehalde locality (Bern, Switzerland)

Damien Becker[1], Jean-Pierre Berger[2], Florent Hiard[2], Ursula Menkveld-Gfeller[3], Bastien Mennecart[2], & Laureline Scherler[2,1]

[1]*Section d'archéologie et paléontologie, République et Canton du Jura, Office de la culture, Hôtel des Halles, Case postale 64, 2900 Porrentruy 2, Switzerland (damien.becker@palaeojura.ch)*
[2]*Département de Géosciences, Géologie et Paléontologie, Université de Fribourg, Chemin du Musée 6, 1700 Fribourg, Switzerland*
[3]*Natural History Museum Bern, Bernastrasse 15, 3005 Bern, Switzerland*

Due to the construction of the Swiss national road from Bern to Worblaufen in 1850, the sandy and marly deposits of the Lower Freshwater Molasse (USM) were excavated in Engehalde. Some specimens of vertebrate fossils (turtles, ruminants, suids, and rhinocerotids) and shells of gastropods and bivalves were brought to light by Studer (1850). Then Stehlin (1914) reported the presence of *Palaeochoerus typus*, but the referred material was not found in the historical collection anymore. The same author notified also two ruminants, *Amphitragulus* cf. *elegans* and *Amphitragulus lemanense*. However, as these two taxa are considered synonyms, only *Amphitragulus elegens* is valid. Moreover, many specimens wrongly ascribed to *Amphitragulus elegans* or *Amphitragulus lemanense* in the literature have to be reported to the closer species *Dremotherium feignouxi*. The remains of rhinocerotids were reviewed by Becker (2003) and ascribed to *Diaceratherium lemanense*: some of them display derived morphological characters interpreted as probable intraspecific variations. These historic discoveries allow a first dating to the Aquitanian time.

During the construction of the Neufeld tunnel (2006–2008), the ancient fossil locality of Engehalde was made accessible for a restricted time. The Natural History Museum Bern organized a new palaeontological excavation campaign. The discovered material did not contain new rhinocerotid remains, but yielded essentially specimens of rumiants, composed by teeth and postcranial bones assigned to the "*Dremotherium*–like" group (probably *Dremotherium feignouxi*). The lower left jaw of a mustelid, probably from the genus *Palaeogale*, *Plesictis*, or *Plesiogale*, was the highlight of the new discoveries (Fig. 1). The washing and picking of sediment samples allowed the sorting of charophytes from the group *Stephanochara praeberdotensis* as well as small mammal remains with *Prolagus* sp., *Eucricetodon infralactorensis*, *Peridyromys* sp. and *Cainotherium* sp. (Menkveld-Gfeller & Becker 2008).

Figure 1. Lower left jaw of a mustelid-like predator (fossil length 6 cm)

These new data, in particular the occurence of *Prolagus* sp. and *Eucricetodon infralactorensis*, allow an improved dating of this locality to the late Aquitanian (European Mammal Reference Level MN2; Burkart Engesser, pers. com.). This biostratigraphical interpretation coincides with other well-dated localities reporting similar faunal composition, like the derived form of *Diaceratherium lemanense* (Becker et al. 2009) and the representatives of the *Amphitragulus elegans – Dremotherium feignouxi* group (Gentry et al. 1999). Regarding the palaeosynecology, the referred mammal association does not permit an accurate characterization of the environment of the Bern area during the late Aquitanian. However, the representatives of the *Amphitragulus elegans – Dremotherium feignouxi* group could point to the existence of a wooded environment. Their association with *Diaceratherium lemanense* underlines probably a bushland in a transitional zone between forest and grassland. Moreover, the lithofacies of the trapping sediments (fluvial sands and floodplain marls) indicate an environment probably close to bodies of water or swamps.

REFERENCES
Becker, D. 2003: Paléoécologie et paléoclimats de la Molasse du Jura (Oligo-Miocène): apport des Rhinocerotoidea (Mammalia) et des minéraux argileux. PhD Thesis, University of Fribourg, GeoFocus 9, 327 pp.
Menkveld-Gfeller, U. & Becker, D. 2008: Baustelle Zubringer Neufeld: eine neue alte Fossilfundstelle. Bulletin für angewandte Geologie 13, 107-112.
Becker, D., Bürgin, T., Oberli, U. & Scherler, L. 2009: A juvenile skull of Diaceratherium lemanense (Rhinocerotidae) from the Aquitanian of Eschenbach (eastern Switzerland). Neues Jahrbuch für Geologie und Paläontologie Abhandlungen 254, 5–39.
Gentry, A.W., Rössner, G. E. & Heizmann, E.P.J. 1999: Suborder Ruminantia. In Rössner, G.E. & Heissig, K. (Eds.): The Miocene Land Mammals of Europe. Verlag Dr. Friedrich Pfeil, München, 225–258.
Studer, B. 1850: Über die Süsswassermolasse bei Bern. Mitteilungen der Naturforschenden Gesellschaft in Bern 178, 89–92.

6.2

Smithian ammonoids (Early Triassic): explosive evolutionary radiation following the Permian/Triassic mass extinction1

Brühwiler Thomas[1], Bucher Hugo[1,2], Goudemand Nicolas[1], Ware David[1], Hermann Elke[1]

[1]*Paläontologisches Institut und Museum der Universität Zürich, Karl Schmid-Strasse 4, 8006 Zürich (bruehwiler@pim.uzh.ch)*
[2]*Department of Earth Sciences, ETH, Universitätsstrasse 16, 8092 Zürich*

In the aftermath of the end-Permian mass extinction, ammonoids were among the fastest clades to recover: the recent analysis of a global diversity data set of ammonoid genera from the Late Carboniferous to the Late Triassic shows that Triassic ammonoids actually reached levels of diversity higher than in the Permian less than 2 million years after the PTB (Brayard et al., 2009). The evolution of Early Triassic ammonoids was not a smooth, nor gradual process. It is characterized by the following main features: (i) a very low diversity in the Griesbachian (early Induan), (ii) a moderate diversity increase in the Dienerian (late Induan), (iii) an explosive radiation in the early Smithian (early Olenekian), (iv) a late Smithian extinction event followed by a second explosive radiation in the early Spathian (late Olenekian) (Brayard et al., 2006, 2009).

In order to better understand the Smithian ammonoid radiation we conducted extensive field studies in two classical regions for the Early Triassic, namely the Salt Range (Pakistan) and Spiti (Indian Himalayas). Smithian ammonoids from these regions have been known for more than a century, and these places are the type localities of many taxa (e.g. Waagen, 1895; Krafft & Diener, 1909). Additionally, we studied a section at Tulong (South Tibet) as well as extremely ammonoid-rich exotic blocks of Hallstatt Limestone in the Oman Mountains.

Our abundant, bed-rock-controlled and well-preserved material enables us to revise many classical ammonoid taxa that were previously known only inadequately. Moreover, a large number of new taxa was found, which enables us to define one new family, 18 new genera and about 29 new species. A total of eight successive ammonoid associations can be correlated between our sections (Brühwiler et al., 2007). This high-resolution biochronological scheme for the Smithian of the Northern Indian Margin can be correlated with ammonoid successions from other regions such as South China (Brayard & Bucher, 2008).

Due to the very high evolutionary rates of Early Triassic ammonoids (Brayard et al., 2009) the reconstruction of phylogenetic relationships among Smithian ammonoids is difficult. However, our well-constrained taxonomic and biochronologic data provide new insights on the evolution of several lineages. Furthermore, the ongoing comprehensive study of Dienerian ammonoid faunas from the Salt Range and from Spiti (Ware et al.) will help us to decifer the origin of some Smithian ammonoids.

[1]This research is supported by the Swiss NSF project 200020-113554.

REFERENCES
Brayard, A. & Bucher, H. 2008: Smithian (Early Triassic) ammonoid faunas from northwestern Guangxi (South China): taxonomy and biochronology. Fossils and Strata, 55, 1-179.
Brayard, A., Bucher, H., Escarguel, G., Fluteau, F., Bourquin, S. & Galfetti, T. 2006: The Early Triassic ammonoid recovery: Paleoclimatic significance of diversity gradients. Palaeogeography, Palaeoclimatology, Palaeoecology, 239, 374–395.
Brayard, A., Escarguel, G., Bucher, H., Monnet, C., Brühwiler, T., Goudemand, N., Galfetti, T. & Guex, J., 2009: Good Genes and Good Luck: Ammonoid Diversity and the End-Permian Mass Extinction. Science, 325, 1118-1121.
Brühwiler, T., Bucher, H., Goudemand, N. & Brayard, A. 2007: Smithian (Early Triassic) ammonoid faunas of the Tethys: new preliminary results from Tibet, India, Pakistan and Oman. The global Triassic: New Mexico Museum of Natural History and Science Bulletin, 41.
Krafft, A.v. & Diener, C., 1909: Lower Triassic cephalopoda from Spiti, Malla Johar, and Byans. Palaeontologia Indica, ser. 15, 6, 1-186.
Waagen, W., 1895: Salt-Range fossils. Vol 2: Fossils from the Ceratite Formation. Palaeontologia Indica 13, 1-323.

6.3

Darwinian dinosaurs : missing links or evolutionary failures ?

Eric Buffetaut

CNRS, UMR 8538, Laboratoire de Géologie de l'Ecole Normale Supérieure, 24 rue Lhomond, 75231 Paris Cedex 05, France (eric.buffetaut@sfr.fr)

Charles Darwin did not often mention dinosaurs in his works. In the third edition of *On the origin of species* (1861, p. 346), he alluded to them in a chapter about extinction: "So little is this subject understood, that I have heard surprise repeatedly expressed at such great monsters as the Mastodon and the more ancient Dinosaurians having become extinct; as if mere bodily strength gave victory in the battle of life. Mere size, on the contrary, would in some cases determine quicker extermination from the greater amount of requisite food". Ten years later, in *The descent of man, and selection in relation to sex* (1871, p. 204), he emphasized their evolutionary significance: "Prof. Huxley has made the remarkable discovery, confirmed by Mr. Cope and others, that the old Dinosaurians are intermediate in many important respects between certain reptiles and certain birds—the latter consisting of the ostrich-tribe (itself evidently a widely-diffused remnant of a larger group) and of the Archeopteryx, that strange Secondary bird having a long tail like that of the lizard".

Thus Darwin illustrated two views of dinosaurs that were to become both prevalent and competing until today: icons of extinction, or missing links. The "missing link" interpretation predominated during the last part of the 19th century and the beginning of the 20th, when dinosaurs were widely considered as ancestral to birds, on the basis of osteological resemblance and the discovery of both *Archaeopteryx* and the "toothed birds", *Hesperornis* and *Ichthyornis*, from the Late Cretaceous of the United States. According to this view, dinosaurs, as bird ancestors, had played an important part in the evolution of one of the most successful groups of living vertebrates. This interpretation fell out of favour during the mid-twentieth century, largely because of the influential book by Gerhard Heilmann, *The origin of birds* (1926), in which the purported absence of clavicles in dinosaurs was used to demonstrate that they could not possibly have been ancestral to birds (which possess clavicles) – since "Dollo's law" stipulates that once an organ has been lost in the course of evolution, it cannot reappear again.

As dinosaurs could no longer be seen as ancestral to anything, they had to be considered as some kind of evolutionary dead end, and this interpretation prevailed until the 1970s. The image of the dinosaurs as too large, too slow and too stupid to have been able to survive became prevalent for a large part of the 20th century. This could be seen in terms of natural selection, with large food requirements as a possible disadvantage, as already mentioned by Darwin in 1861, or in terms of non-Darwinian, orthogenetic evolution resulting in non-adaptive transformations detrimental to the organisms involved. The idea that dinosaurs were somehow "doomed" to extinction by rather obscure evolutionary mechanisms became popular for a long time.

Things changed again in the 1970s when dinosaur biology was thoroughly reinterpreted and the image of sluggish, cold-blooded giants was challenged and a new view of dinosaurs as more active, possibly warm-blooded, animals gradually emerged. This went together with a reappraisal of dinosaur-bird relationships, based on new discoveries of small carnivorous dinosaurs and descriptions of new specimens of *Archaeopteryx*, which resulted in a rebirth of the hypothesis of the dinosaurian ancestry of birds. This was strengthened by the discovery of clavicles in many dinosaurs (thus eliminating Heilmann's objection) and by that of the famous "feathered dinosaurs" from the Early Cretaceous of China, which provide extremely strong evidence in favour of a close phylogenetic relationship between small theropod dinosaurs and birds.

In the 1980s, the question of dinosaur extinction also underwent a revival, within the larger framework of catastrophic events at the Cretaceous-Tertiary boundary. The discovery of the major asteroid impact that happened 65 million years ago led to a thorough reconsideration of the possible causes of terminal Cretaceous extinctions, including that of non-avian dinosaurs. Seen as part of major extinction event affecting many groups of organisms in various environments, in all likelihood caused by the impact of an extra-terrestrial object, the disappearance of the dinosaurs could no longer be seen as the result of some mysterious inability to adapt to gradual environmental change. Although the details of dinosaur extinction at the end of the Cretaceous remain to be worked out, the reason for their disappearance is now much clearer than it was before the discovery of the end-Cretaceous impact – and Darwin's original remark about the importance of food resources (or the lack thereof) takes on a new significance in view of current hypotheses about the collapse of food webs following the asteroid impact.

Although the evolutionary significance of dinosaurs, both in terms of extinction and of intermediate forms, was apparent to Darwin, and to quite a few of his followers, including Huxley, in the 19th century, it was underrated during much of the 20th century. It is only since the 1990s that palaeontologists have recognised again that dinosaurs were not simply an extinct group of reptiles, but were in fact the source of one of the major groups of living vertebrates, viz. the birds, and that the demise of non-avian dinosaurs was the result of an exceptional global event, rather than the consequence of some kind of non-adaptive evolution. The example of dinosaurs illustrates well how the outdated concept of "evolutionary failures" has been superseded by a more truly Darwinian interpretation of the fossil record.

REFERENCES
Darwin, C. 1861: *On the origin of species by means of natural selection, or the preservation of favoured races in the struggle for life*. 3rd edition. John Murray, London.
Darwin, C. 1871: *The descent of man, and selection in relation to sex*. John Murray, London.
Heilmann, G. 1926: *The origin of birds*. Witherby, London.

6.4

Diatom assemblage turnover in the NW-Pacific at the 2.73 Ma climate transition

Girault France E. & Thierstein Hans R.

Geological Institute, ETH, Sonneggstrasse 5, CH-8092, Zurich (france.girault@erdw.ethz.ch)

The North Pacific contains a critical diatom sedimentary record of the Cenozoic global cooling history. The most striking part of that record covers the ultimate closure of the Panama Seaway 2.73 Ma ago which was synchronous with the onset of Northern Hemisphere glaciations (NHG). These physical changes were concomitant with an abrupt change in the biological pump efficiency related to the onset of ocean surface water stratification.
The ODP site 882 record (Leg 145) - with its well constrained Neogene paleoceanographic history around the 2.73 Ma transition - provides an excellent basis to test patterns and potential controls of diatom size variability and species dominance. Frustule sizes of centric diatoms have been quantified to better understand the environmental response of these organisms to a drastic and permanent paleoceanographic and climatic change.
Size and morphological characteristics of the centric diatom frustules (diameter >20 μm) were collected for a statistically representative number of specimens (i.e. 250-700) per sample using recently developed automated light microscopy and image analysis techniques.

6.5

Neogene global cooling: diatom size variability in a changing ocean

Girault France E.[1], Weller Andrew F. [1,2] & Thierstein Hans R.

[1] *Geological Institute, ETH, Sonneggstrasse 5, CH-8092, Zurich (france.girault@erdw.ethz.ch)*
[2] *Present address: Geosoft Australia Pty Ltd, 14/100 Railway Road, Subiaco WA 6008, Australia*

Over the past 40 Ma, the development and stepwise expansion of the Antarctic ice-sheet, together with tectonic movements (e.g. closure of the Panama isthmus) have deeply modified the patterns of global circulation and chemical signature of the various water masses (e.g. redistribution of dissolved silica). These changes have also induced the development of oceanic boundaries (e.g. Polar front), directly affecting the evolution of planktic micro-organisms.
Using the widespread record of siliceous microfossils (Southern Ocean, Equatorial Pacific and North Pacific), we have assessed the impacts of these oceanographic reorganizations on diatoms, focusing on size and taxonomic changes and turnovers among centric diatoms over the past 15 Ma.
The ability of diatoms to adapt and survive in a changing ocean has probably been a key for their survival especially over the Neogene, when climatic and oceanographic changes have been the strongest. Similarly, size variability among this group tightly reflects their response to environmental perturbations as well as their taxonomic turnovers that have been driving diatom evolutionary patterns toward highly diverse and endemic communities prevailing in today's oceans.

6.6

Paleobiology of Early Triassic conodonts: implications of newly discovered fused clusters imaged by X-ray synchrotron microtomography

Goudemand Nicolas[1], Orchard Michael[2], Tafforeau Paul[3], Urdy Séverine[1], Brühwiler Thomas[1], Bucher Hugo[1], Brayard Arnaud§, Galfetti Thomas[1], Monnet Claude[1], Lebrun Renaud§§ & Zollikofer Christoph§§

[1]*Paläontologisches Institut und Museum, Universität Zurich, Karl Schmid-Str. 4, 8006 Zürich (goudemand@pim.uzh.ch).*
[2]*Geological Survey of Canada, 101-605 Robson St., Vancouver,BC, V6B 5J3 Canada.*
[3]*European Synchrotron Radiation Facility, 6 rue Jules Horowitz, BP 220, 38043 Grenoble cedex, France.*
§UMR-CNRS 5561 Biogéosciences, Université de Bourgogne, 6 Bd Gabriel, 21000 Dijon, France.
§§Anthropologisches Institut und Museum, Universität Zürich, Winterthurerstrasse 190, 8057 Zürich

Several fused clusters of conodont elements of the Early Triassic genus *Novispathodus* were discovered in limestone beds at the Smithian-Spathian boundary (Luolou Formation., Galfetti *et al*., 2008) from several localities within the Guangxi province of South China. Conodont clusters are groups of morphologically different elements belonging to the same individual, which were somehow cemented together post-mortem. Such specimens of exceptional preservation are extremely rare in the Triassic and these are the first reported for the Early Triassic.

Our fused clusters partially preserve the relative three-dimensional position and orientation of some ramiform, grasping elements. They are therefore extremely important for our understanding of the feeding apparatuses of conodonts.

Because of the intricate geometry of the superposed elements, of their fragility and of their extreme rarity, it is usually tricky to study such specimens. We overcome these problems by performing a propagation phase contrast synchrotron microtomography (Tafforeau *et al*., 2006). A pink beam setup at 17.6 keV, which was very recently developed at the European Synchrotron Radiation Facility on beamline ID19, has been successfully tested on our conodonts. This new technique enables a submicron resolution (0.23µm) with a speed and an overall quality never reached before. Some fused clusters as well as co-occurring isolated elements from the same sample and pertaining to the same multi-element species were scanned using this technique.

Besides taxonomic revision of the Gondolelloidea superfamily (the most significant group of conodonts during Permian and Triassic times), this discovery led us to propose a new functional model.

In our view, the best solution implies the presence of a presumably cartilaginous 'copula', upon which the conodont elements are moving independently, more or less as do dental plates in extant lampreys, but not strictly as proposed by Purnell and Donoghue (1997). We suggest that during retraction towards the caudally located platform (cutting or grinding) elements, the S0 element first has a closing, rotating movement, most probably synchronized with the closure of the M elements, with which it would have performed a pinching, seizing function. This movement is then followed by a sub-straight, dorso-caudally directed translation, by which it would have torn off the prey's 'flesh' and brought it towards the platform elements. The latter movement is accompanied by the closure of the other S elements, channelling the food in the appropriate direction.

Considering that the presence of such 'copula' associated with tongue protractor and retractor muscles has been asserted only for extant cyclostomes (hagfishes and lampreys; Yalden, 1985; Donoghue *et al*., 2000), our new model may provide important insights for deciphering the affinity of conodonts and for our general understanding of the origin of vertebrates.

Acknowledgements
This research is supported by the Swiss NSF project 200020-113554. We acknowledge the European Synchrotron Radiation for provision of synchrotron radiation facilities and for granting access to beamline ID19.

Figure 1. Animated 3d reconstruction of the feeding apparatus of Novispathodus.

REFERENCES

Galfetti, T., Bucher, H., Martini, R., Hochuli, P.A., Weissert, H.,Crasquin-Soleau, S., Brayard, A., Goudemand, N., Brühwiler, T.& Guodun, Kuang 2008. Evolution of Early Triassic outer platform paleoenvironments in the Nanpangjiang Basin

(South China) and their significance for the biotic recovery. Sed. Geol. 204: 36-60.
Tafforeau, P., et al. 2006. Applications of X-ray synchrotron microtomography for non-destructive 3d studies of paleontological specimens. Appl. Phys. A 83: 195-202.
Purnell, M. A.& Donoghue, P. C. J. 1997. Architecture and functional morphology of the skeletal apparatus of Ozarkodinid conodonts. Phil. Trans. R. Soc. Lond. B 352: 1545-64.
Yalden, D. W. 1985. Feeding mechanisms as evidence of cyclostome monophyly. Zool. J. Linn. Soc. 84: 291-300.
Donoghue, P. C. J., Forey, P. L.& Aldridge, R. J. 2000. Conodont affinity and chordate phylogeny. Biol. Rev. 75: 191-251.

6.7

The Devonian Nekton Revolution

Christian Klug[1], Björn Kröger[2], Wolfgang Kiessling[2], Gary L. Mullins[3], Thomas Servais[4], Jiří Frýda[5], Dieter Korn[2] & Sue Turner[6]

[1]Paläontologisches Institut und Museum, Universität Zürich, Karl Schmid-Strasse 4, CH-8006 Zürich, Switzerland, (chklug@pim.uzh.ch)
[2]Museum für Naturkunde, Humboldt-Universität zu Berlin, Invalidenstraße 43, D-10115 Berlin, Germany
[3]Department of Geology, The University of Leicester, University Road, Leicester, LE1 7RH, United Kingdom
[4]Laboratoire de Paléontologie et Paléogéographie du Paléozoïque, UMR 8014 du CNRS, Université des Sciences et Technologies de Lille, SN5 Cité Scientifique, F-59655 Villeneuve d'Ascq, France
[5]Faculty of Environmental Science, Czech University of Life Sciences, Kam cká 129, 165 21 Praha 6 Suchdol, Czech Republic
[6]Queensland Museum, 122 Gerler Rd., Hendra, Queensland 4011, Australia

Impressive discoveries of Neoproterozoic and Early Palaeozoic Fossillagerstaetten drew the attention on evolutionary and ecological processes of these timespans. It almost seemed that, except for some of the "Big Five", nothing essential happened after the Ordovician. Such a scenario is certainly not true.

Contrariwise, some major ecological fluctuations have been recorded from the Devonian, several of which have less prominent Silurian precursors. Famous examples are the radiation of land plants and jawed fish (both known already from the pre-Devonian). During the Devonian, several animal groups conquered the land (various arthropods and possibly tetrapods). Marine invertebrates show significant ecological and morphological changes: Important cephalopod groups such as bactritoids as well as ammonoids evolved and reef growth increased until the Late Devonian crises. Both the global rise and fall of dacryoconarids occurred, graptolites became extinct, and various mollusc clades modified early ontogenetic strategies during the Devonian, documenting a planktonic turnover. In addition, there is a macroecological change in marine faunas from a demersal (swimming close to the sea-floor) and planktonic habit towards a more active nektonic habit.

Various interpretations are at hand to explain this Devonian Nekton Revolution: (1) Demersal and nektonic modes of life were probably initially driven by competition in the diversity-saturated benthic habitats as well as (2) the availability of rich planktonic food resources (as reflected in evolutionary alterations in early ontogenetic stages of many mollusks). Escalatory feedbacks probably promoted the rapid evolution of nekton (jawed fish and some derived cephalopod groups in particular) in the Devonian, as suggested by the sequence and tempo of water-column occupation. Potentially, both these radiations and the Givetian to Famennian mass-extinctions were linked to a pronounced increase in nutrient input to sea surface waters during eutrophication episodes.

6.8

Red trilobites with green eyes from the Devonian of Morocco

Christian Klug[1], Hartmut Schulz[2] and Kenneth De Baets[1]

[1]Paläontologisches Institut und Museum der Universität Zürich, Karl Schmid-Str. 4, CH-8006 Zürich (chklug@pim.uzh.ch)
[2]Institut für Geowissenschaften, Eberhard-Karls-Universität Tübingen, Sigwartstr. 10, D-72076 Tübingen, Germany

Latest Emsian (Early Devonian) sediments at the famous mud-mound- and trilobite-locality Hamar Laghdad (Tafilalt, Morocco) yielded some well preserved, largely red-coloured remains of phacopid trilobites. Closer examination revealed that only the lenses of the eyes of these phacopids are usually greenish in colour. EDX-analyses showed that the lenses retained their original calcitic composition while most of the exoskeleton was silicified. The silicified parts contain elevated concentrations of iron which causes the red colour.

Presumably, the primary porosity of most of the phacopid exoskeleton except the chitinous legs and the lenses was, because of the pore canals, higher than that of the lenses, facilitating the replacement of calcite by other minerals. Furthermore, the presence of organic components in the lenses in combination with a homogeneous distribution of the calcite crystals might have slightly increased the resistance of the lenses towards mineral replacement. The homogeneity of the calcite crystals of the lenses was needed for their optimal optical functionality. These factors probably account for the fact that the eyes retained the calcite which is often greenish in brachiopod shells such as the thick-shelled Middle Devonian *Devonogypa* and *Ivdelinia* from the Maïder Basin while the rest of the trilobite exoskeleton is red. This differential replacement also explains why the lenses are slightly corroded while the rest of the exoskeleton is superficially well preserved. So far, this differential replacement of calcite is only known from the eyes of phacopids. Other trilobite taxa from the same strata and locality have holochroal eyes and thus much smaller lenses which were probably more rapidly replaced by silica. The greenish colour of the lenses might originate from impurities of iron and magnesium; the concentrations of the corresponding ions might have been too low to be detected with the EDX with certainty.

Hamar Laghdad also yielded phacopid exoskeletons with less completely silicified exoskeletons which enabled a detailed reconstruction of the silicification process. Initially, only the outer surface of the exoskeleton and the vicinity of pore canals were silicified. In a second step, the bend in the growth lines of the interlensar sclera were silicified together with the remaining exoskeleton except for the lenses, then the complete interlensar sclera and in the end also the lenses.

6.9

First record of a belemnite preserved with beaks, arms and ink sac from the Nusplingen Lithographic Limestone (Kimmeridgian, SW Germany)

Christian Klug[1], Günter Schweigert[2], Dirk Fuchs[3] and Gerd Dietl[2]

[1]*Paläontologisches Institut und Museum, Karl Schmid-Str. 4, CH-8006 Zürich (chklug@pim.uzh.pim)*
[2]*Staatliches Museum für Naturkunde, Rosenstein 1, D-70191 Stuttgart, Germany*
[3]*Institut für Geowissenschaften, Freie Universität Berlin, Malteserstr. 74-100, D-12249 Berlin, Germany*

A recent discovery of an unusually preserved belemnite from Nusplingen comprises the extraordinarily rare remains of beaks and nearly *in situ* arm-hooks as well as the ink sac and the incomplete phragmocone. So far, *Hibolithes semisulcatus* (Münster, 1830) is the only larger belemnite known from the Nusplingen Lithographic Limestone (Upper Jurassic, Late Kimmeridgian, Beckeri Zone, Ulmense Subzone; SW Germany) which has the same phragmocone shape and size, thus we assign the new specimen to this taxon. The rostrum was probably lost due to a lethal predation attempt in which the prey was killed but not entirely eaten. For the first time, a specimen reveals details of the belemnite beak morphology, which we compare to the beaks of other Jurassic cephalopods. This specimen presently represents the only known rostrum-bearing belemnite of post-Toarcian age which has been preserved with non-mineralised body parts. As *Hibolithes semisulcatus* is known to possess one pair of mega-onychites, the absence of those in the present specimen provides evidence of sexual dimorphism in *Hibolithes semisulcatus.* This phenomenon was previously presumed for all belemnites, but it is known only from *Passaloteuthis* with certainty since the rostrum of the latter is unambiguously associated with an arm crown that occasionally includes one pair of mega-onychites. The imperfect preservation of the belemnite beaks hampers a detailed comparison with other Recent and fossil coleoid beaks. Some morphological characters (low width of the outer lamella, double lateral lobes of the dark parts of rostrum and hood, possibly short internal lamella) of the lower beak of *Hibolithes* more closely resemble Recent decapods than Recent octopods. The upper beak of *Hibolithes* differs in the long, narrow and curved rostrum from those coleoid beaks previously known from Nusplingen. The dark part of the lower beak also shows a unique outline with a short and pointed rostrum, an elongate posteroventral extension and two small rounded sinuses which pointed towards the wings (sometimes similarly developed in Recent *Sepioteuthis*). It appears likely that this beak form is quite characteristic and it might reflect a special diet of the belemnites. Taking their probably high swimming velocity (fins, stream-lined body, and horizontal orientation of the longest body axis) with the arm hooks and the sharp beaks into account, it appears quite likely that belemnites were fast-swimming, effective, medium-sized predators. With the new discovery, Nusplingen now represents the only locality which has yielded complete beak apparatuses from all major Jurassic cephalopod groups.

6.10

The borehole 01983X2854 (Preuschdorf, Upper Rhine Graben, Alsace, France) as a basis of a formal definition of the Upper Pechelbronn Beds (Rupelian)

Lavoyer Thibault, Yerly Bertrand & Berger Jean-Pierre

Département de Géosciences, Géologie et Paléontologie, Université de Fribourg, chemin du Musée 6, 1700 Fribourg, Switzerland

From the middle Eocene to Late Oligocene, an intense lacustrine, brackish and marine sedimentation, documented by salt deposits and oil accumulation, took place in the Upper Rhine Graben (URG), especially in the Pechelbronn Beds (Lower-, Middle- and Upper).

Although these layers were studied, in the past, for the oil industry (Schnaebele 1948) and are a lithostratigraphic unit used in maps and papers concerning the Paleogene of the URG, they have never been formally designated because they almost never crop out at the surface and drifting and drilling materials were often discarded. Nevertheless, the International Stratigraphic Guide (see Murphy and Salvador 1999), demands a type section for each formally named Formation.

Several palaeogeographical reconstitutions and stratigraphic charts for the URG have been published (Berger et al. 2005 a & b). However, the Rupelian deposits were not well defined.

This work presents the first step for a definition of a type section of a type section of the Upper Pechelbronn Beds, with the presentation of several lithofacies and paleontological data.

The studied borehole, 01983X2854 (Preuschdorf, Alsace, France) is a complete cored drilling, about 220m in depth. It was originally made to evaluate a decontamination issue, but has also yielded micropaleontological and sedimentological data. It corresponds to the Upper Pechelbronn Beds with a small part of the Middle Pechelbronn Beds at the base.

The high abundance of ostracods and gastropods in grey marls, corresponding to the 10 lower meters, indicate the top of the Middle Pechelbronn Beds with the Hydrobia Zone. These layers are covered by a succession of marls and sandstone, suggesting a different environment. The lower part of the borehole is consistent with the lithostratigraphic zonation defined by Schnaebele (1948) for his “normal facies” whereas the upper part corresponds to his “freshwater facies”.

The lower part of the borehole has yielded new paleontological data. Diatoms (*Triceratium* sp), charophytes (*Chara* spp., *Rhabdochara* sp.), foraminifers (*Ammodiscus* sp., *Quinqueloculina* sp., *Flintina* sp., *Lenticulina* spp., *Dentalina* sp., *Subreophax elongates*, *Vaginulopsis* spp.), bivalves, gastropods, bryozoans, ostracods (*Grinioneis tribeli*, *Hazelina indigena*, *Hemicyprideis* spp., *Ilyocypris* sp.), insects, echinoderms, fishes and mammals teeth are used as main indicators of biostratigraphy and palaeoecology. The fossil record emphasizes a complex alternation of freshwater, brackish and marine fauna along the whole studied section.

This study is financed by the SNF Project 200020-118025 “Paleontology and Stratigraphy of the Rhine graben during the Paleogene”, and includes parts of the Masters-thesis of B. Yerly “ The transition between the Middle and Upper Pechelbronn Beds in the drilling 1983X2854, Preuschdorf (Rupelian, Upper Rhine Graben, Alsace, France)” (in prep. 2009) and the PhD-thesis of T. Lavoyer “Paleontology and Stratigraphy of the Middle Upper Rhine Graben during the Paleogene: a key-study for the relationships between Rift system, Alpine Orogeny and Paleoclimate” (in progress).

We thank S. Spezzaferri (Uni. Fr., foraminifers), C. Pirkenseer (Uni. Leuven, ostracods) for fossils determination, P. Elsass (BRGM) and M. Kimmel (Geoderis) for providing access to the core drilling.

REFERENCES

Berger, J.-P. et al., 2005a. Paleogeography of the Upper Rhine Graben (URG) and the Swiss Molasse Basin (SMB) from Eocene to Pliocene. International Journal of Earth Sciences, 94(4): 697-710.

Berger J.-P. et al., 2005b. Eocene-Pliocene time scale and stratigraphy of the Upper Rhine Graben (URG) and the Swiss Molasse Basin (SMB). International Journal of Earth Sciences, 94(4): 711-731.

Murphy M.A. & Salvador A. 1999. International Stratigraphic Guide An abridged version. Episodes, Vol. 22, no. 4

Schnaebele R., 1948. Monographie géologique du champ pétrolifère de Pechelbronn. – Mémoires du Service de la Carte géologique d’Alsace et de Lorraine, 7:254 S Strasbourg

6.11

Determination of the paleodiet and the phylogeny of extinct ruminants using Relative Wrap Analysis on mandibles: case of Iberomeryx minor (Mammalia, Artiodactyla)

Bastien Mennecart[1], Damien Becker[2] & Jean-Pierre Berger[1]

[1]*Department of Geosciences – Earth Sciences, ch. du Musée 6, Pérolles, 1700 Fribourg, Switzerland (bastien.mennecart@unifr.ch)*
[2]*Section d'archéologie et paléontologie, République et Canton du Jura, Office de la culture, Hôtel des Halles, Case postale 64, 2900 Porrentruy 2, Switzerland*

The primitive ruminant *Iberomeryx* is essentially known by few dental remains and is still poorly documented. Its phylogeny and palaeobiology stays rather enigmatic. Only two species have been described: the type species *I. parvus* from the Benara locality in Georgia (Gabounia 1966), and the West European species *I. minor* from Itardies, Mounayne, Raynal and Roqueprune 2 in Quercy (Sudre 1987), Montalban in Spain (Golpe-Posse 1974), and Lovagny, Soulce and Beuchille in the Swiss Molasse Basin (Becker et al. 2004). *I. savagei* from India had recently been placed in the new genus *Nalameryx* (Métais et al. 2009). All these localities are dated to the Rupelian and correspond mainly to MP23 (European mammal biozone). Based on the short tooth-crown height and the bunoselenodont pattern of the molars, Sudre (1984) and Becker et al. (2004) proposed a folivore/frugivore diet for *Iberomeryx*.

Based on relative warp analysis (24 landmarks) of 84 extant and fossil ruminant mandibles from 24 genera and 32 species, this study proposes a preliminary discussion on the phylogeny and the diet of the genus *Iberomeryx*. The results permit to differentiate *Pecora* and *Tragulina* on the first axis thanks to the length of the diastema, the length of the premolars and the mandible ankle. As suggested by Sudre (1984), *Iberomeryx* is close to the extant Tragulina by the shape of its mandible. But, this latter is clearly different of those of the Tragulidae, the only extant family in Tragulina. This difference is essentially due to a stockier mandible (condylar process, mandible ramus and *corpus mandibulae*), and a deeper mandibular incisure. Additionally, we observe no diastema and well bunodont teeth. *Iberomeryx* may be considered as a primitive Tragulidae, the only known from the Oligocene, based on the general shape of its mandible and its jaw teeth. Moreover, its diet could not be strictly frugivore, but it could possibly also exceptionally eat some meat matter such as small Hypertragulidae.

This study is supported by the Section d'archéologie et paléontologie (Porrentruy), the University of Fribourg, and the Swiss National Foundation project (115995) on the large mammal evolution in the Swiss Molasse Basin during the Oligocene and Early Miocene.

REFERENCES

Becker, D., Lapaire, F., Picot, L., Engesser, B. & Berger, J.-P. 2004: Biostratigraphie et paléoécologie du gisement à vertébrés de La Beuchille (Oligocène, Jura, Suisse). Revue de Paléobiologie, Vol. spéc. 9, 179-191.

Gabounia, L. 1966: Sur les Mammifères oligocènes du Caucase. Bulletin de la Société Géologique de France 7, 857-869.

Golpe-Posse, J. 1974: Faunas de Yacimientos con Suiformes en el Terciario espanol. Publicaciones des Instituto Provincial de Paleontologia de Sabadell, Paleontologia y Evolucion 8, 1-87.

Métais, G., Welcomme, J.-L- & Ducrocq, S. 2009: New lophiomericyd ruminants from the Oligocene of the Bugti Hills (Balochistan, Pakistan). Journal of Vertebrate Paleontology 29(1), 231-241.

Sudre, J. 1984: Cryptomeryx Schlosser, 1886, tragulidé de l'Oligocène d'Europe; relations du genre et considérations sur l'origine de ruminants. Palaeovertebrata 14, 1-31.

6.12

Macroevolutionary trends of Acrochordiceratidae Arthaber, 1911 (Ammonoidea, Middle Triassic)

Monnet Claude[1], Bucher Hugo[1], Guex Jean[2] & Wasmer Martin[1]

[1]*Paläontologisches Institut und Museum, Universität Zürich, Karl Schmid Strasse 4, CH-8006 Zürich (claude.monnet@pim.uzh.ch, hugo.fr. bucher@pim.uzh.ch, martin.wasmer@gmail.com)*
[2]*Institut de Géologie et Paléontologie, Université de Lausanne, BFSH-2, CH-1015 Lausanne (jean.guex@unil.ch)*

Directed evolution of life through millions of years, such as increasing complexity and increasing adult body size, is one of the most intriguing patterns displayed by fossil lineages. The general tendency for body size to increase during the evolution of a group of animals is known as Cope's rule. Processes and causes of such macroevolutionary trends remain however to be clearly understood (Jablonski 2000). Among fossils, ammonoid shells (marine cephalopods) are well known to experience repetitive macroevolutionary trends of their adult size, geometry and ornamentation (Schindewolf 1940; Haas 1942; Bayer & McGhee 1984; Dommergues 1990; Guex 1992).

This study analyzes the evolutionary trends of the family Acrochordiceratidae Arthaber, 1911, which spanned the upper Early to lower Middle Triassic. Exceptionally large collections of this ammonoid family from North America enable quantitative and statistical analyses of its macroevolutionary trends. This study highlights that (1) the monophyletic clade of Acrochordiceratidae follows the classical evolute to involute evolutionary trend (i.e. increasing coiling of the shell); (2) the lineage also shows a seemingly stepwise increase of its shell adult size (shell diameter); (3) the clade also records increasing complexity of its suture line; and (4) the lineage is also characterized by a prominent increase of the intraspecific variation of its shell morphology, which follows the Buckman's Law of Covariation.

These macroevolutionary trends are statistically robust and seem more or less gradual. Furthermore, they can be considered as non-random with the sustained shift of the mean, the minimum and the maximum of studied shell characters. Such result is usually interpreted as being the effect of a selection pressure on the entire lineage, which leads to infer the presence of one ecological niche common to all species of this mostly anagenetic lineage with moderate evolutionary rates.

Increasing involution of ammonites is usually interpreted by increasing adaptation mostly in terms of improving hydrodynamics. However, this trend in ammonoid geometry can be explained as a case of Cope's rule (increasing adult body size) instead of *ad hoc* functional explanations of coiling, because both shell diameter and shell involution are two possible paths for ammonoids to accommodate increasing body size.

REFERENCES

Bayer, U. & McGhee, G.R. 1984: Iterative evolution of Middle Jurassic ammonite faunas. Lethaia, 17, 1-16.

Dommergues, J.L. 1990. Ammonoids. In: McNamara, K.J. (ed.), Evolutionary trends, Belhaven Press, London, 162-187.

Guex, J. 1992: Origine des sauts évolutifs chez les ammonites. Bulletin de la Société Vaudoise de Sciences Naturelles, 82, 117-144.

Haas, O. 1942: Recurrence of morphologic types and evolutionary cycles in Mesozoic ammonites. Journal of Paleontology, 16, 643-650.

Jablonski, D. 2000. Micro- and macroevolution: scale and hierarchy in evolutionary biology and paleobiology. Paleobiology, 26 (suppl. 4), 15-52.

Schindewolf, O.H. 1940. Konvergenz bei Korallen und Ammoniten. Fortschritte der Geologie und Palaeontologie, 12, 387-491.

Figure. Evolutionary trends represented by late immature shell geometry and suture line for Acrochordiceratidae during the Anisian (Middle Triassic). Global evolutionary trends affecting successive spectra of variants for Acrochordiceratidae are increasing adult shell size, increasing involution, increasing suture complexity, and increasing intraspecific variability. (Next Page)

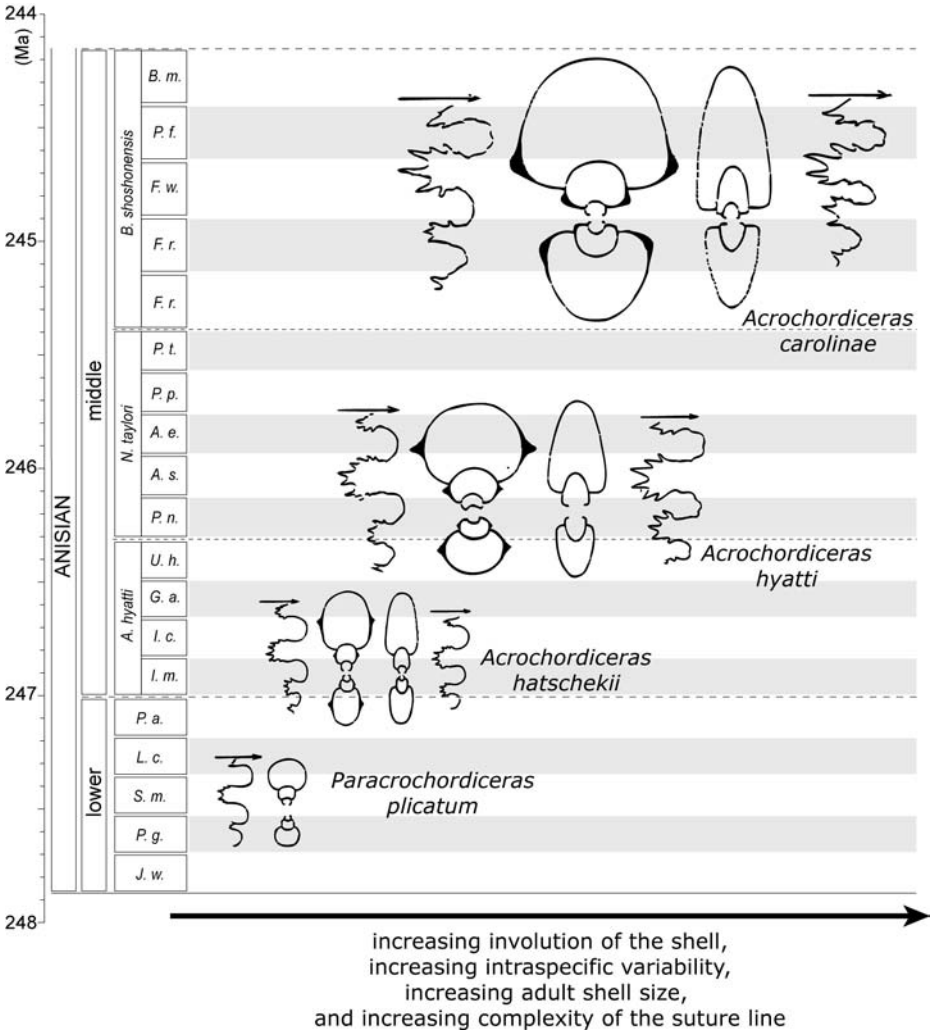

6.13

Reinvestigation of the basal ray-finned fish Birgeria stensioei from the Middle Triassic of Monte San Giorgio (Switzerland) and Besano (Italy)

Romano Carlo[1] & Brinkmann Winand[1]

[1]*Paläontologisches Institut und Museum, Karl Schmid-Strasse 4, CH-8006 Zürich (carlo.romano@pim.uzh.ch; wbrink@pim.uzh.ch)*

The two earlier descriptions and a previous reconstruction of the Middle Triassic actinopterygian *Birgeria stensioei* Aldinger, 1931 from the Besano Formation of Monte San Giorgio (Canton Ticino, Switzerland) and Besano (Lombardy, Italy) relied either on a few fragmentary remains or on a single individual only. Here we present the first study of *B. stensioei* that is based on multiple specimens of this basal ray-finned fish. Sixty-seven specimens have been examined.

The reinvestigation of *B. stensioei* yielded new information at genus and species level. *B. stensioei* predominantly differs from the other species of the genus *Birgeria* Stensiö, 1919 in the arrangement of the bones of the dorsal fin base. While in the other species usually two series of pterygiophores are present throughout the dorsal fin base, only one series of pterygiophores is developed in the anterior part of the dorsal fin root of *B. stensioei*. The caudal peduncle and the caudal fin lobes are more slender and longer than illustrated in the previous reconstruction of *B. stensioei* (see Schwarz 1970). The morphology of the caudal peduncle and fin as well as the aforementioned specialised dorsal fin root indicate that propulsion might have been more advanced in *B. stensioei* compared to the other species of the genus *Birgeria*. *B. stensioei* is furthermore distinguished from most of the other species of *Birgeria* by the degree of ossification of the brain case and the palatoquadrate. As in many other basal actinopterygians, a dermohyal is developed in *B. stensioei* and this bone is probably present in the other species of *Birgeria* as well.

6.14

Terrestrial palaeoclimatical and palaeoenvironmental reconstructions in Northwestern Switzerland: carbon and oxygen isotope compositions of Early Oligocene and Late Pleistocene vertebrate remains.

Scherler Laureline[1],[2], Tütken Thomas[3], Becker Damien[2] & Berger Jean-Pierre[1]

[1]*Department of Geosciences, Institute of Geology, ch. du Musée 6, CH-1700 Fribourg (laureline.scherler@unifr.ch)*
[2]*Section d'archéologie et paléontologie, Hôtel des Halles, CP64, CH-2900 Porrentruy*
[3]*Steinmann Institute, University of Bonn, Poppelsdorfer Schloss, D-53113 Bonn*

Vertebrate remains from two Early Oligocene localities of the Delémont basin (Beuchille and Poillat) and from eight Late Pleistocene doline fillings of the Ajoie Region (Courtedoux-Vâ Tche Tchâ and Boncourt-Grand'Combe) have been excavated along the Transjurane highway (Canton Jura, Northwestern Switzerland). Teeth of large mammals and bones of aquatic reptiles have been analysed for their isotope compositions ($\delta^{18}O_{CO3}$, $\delta^{18}O_{PO4,}$ $\delta^{13}C$) in order to reconstruct the palaeoclimatical and palaeoenvironmental conditions.

The two Early Oligocene localities of Beuchille and Poillat are located in the Jura Molasse ("Molasse alsacienne" Formation) of the Delémont basin (Northern Switzerland). The presence of the small mammal *Blainvillimys avus* and the ruminant *Iberomeryx minor* allows a datation to the mammal zones MP23-24, around 31.5 to 29.0 Ma (Becker et al. 2004). Eight samples of reptile bones (crocodiles and turtles) as well as four samples of sympatric primitive rhinocerotid teeth (*Ronzotherium* sp.) have been analysed. The reptile bones have low $\delta^{18}O_{PO4}$ values (from 13.6‰ to 17.8‰) indicating freshwater environments ($\delta^{18}O_{H2O}$ calculated values averaging -6.15±1.03‰) which are supported by the palaeontological identifications of the turtle remains (*Trionyx* and Testudinidae: freshwater and terrestrial turtles, respectively). A similar $\delta^{18}O_{H2O}$ value of -6.18±1.5‰ is calculated from enamel $\delta^{18}O_{PO4}$ values (18.3±1.3‰) of the rhinocerotid teeth, which presumably reflects the composition of meteoric water. Using a modern-day mean air temperature (MAT)-$\delta^{18}O_{H2O}$ relation for Switzerland a MAT of 18.0±2.5°C for the Early Oligocene could be calculated and was about 8-9°C warmer than today in the Canton Jura (Recent MAT of 8.7°C). This result is in agreement with the palaeotemperature of ~17°C reconstructed from fossil plant remains in the Early Oligocene of Central Europe by Mosbrugger et al. (2005).

The eight Late Pleistocene doline fillings of Boncourt-Grand'Combe (GC) and Courtedoux-Vâ Tche Tchâ (VTA) are located in the Ajoie Region (Northwestern Switzerland) and correspond mainly to loessic and gravel deposits associated with fossil remains. Forty-six teeth of large mammals (*Equus germanicus, Mammuthus primigenius, Coelodonta antiquitatis, Bison priscus*) have been analysed: eight samples from the GC doline filling and thirty-eight from the seven VTA doline fillings. The sedimentary series bearing the mammal remains trapped within the GC doline have been dated by OSL (Optically Stimulated Luminescence) to an age of ~80 ka BP. The mammal remains preserved within the seven VTA dolines have all been discovered in the same sedimentary unit dated to the time interval 45-40 to 35 ka BP (latest Middle Pleniglacial) by OSL and radiocarbon (Becker et al. 2009).

According to the enamel $\delta^{13}C$ values, which are similar in both time periods, the large mammals lived in a C_3 plant-dominated environment as indicated by values ranging from -14.5‰ to -9.2‰ (O'Leary, 1981). The MAT calculated from the $\delta^{18}O_{PO4}$ values of the large mammal assemblage from the GC doline averages 6.0±4.6°C. The MAT calculated for the large mammal assemblage of the younger VTA dolines averages 5.6±4.1°C, showing a quite similar climate. This latter result is concording with the quantified ecology study of the small mammal assemblages of these dolines, which indicates palaeotemperatures averaging 5°C (Oppliger, 2009). These palaeoclimatical values are about 3 to 4°C cooler than today in the Canton Jura. However, some variations in the $\delta^{18}O_{PO4}$ values of the different studied species are observed, and particularly in the VTA dolines: for example the equids show slightly lower $\delta^{18}O_{PO4}$ values (13.09±0.8‰) than the bovids (14.6±1.1‰). The calculated MAT after specific calibrations can thus be very different, ranging from 2.2±2.8°C for the *Equus* remains to 8.8±3.5°C for the *Bison* remains, with a value of 5.8±3.3°C for the *Coelodonta* and 8.7±2.2°C for the *Mammuthus*.

In order to understand this bias a precised sampling of teeth formed before and after the weaning of the foals has been done. It shows that the oxygen isotopic compositions are not affected by the nursing period whereas the carbon isotopes show slightly lower values. The differences in oxygen stable isotope compositions within these Late Pleistocene mammals could then been explained by the sampling method, the mammal physiology and/or ecology, or time averaging. The determination of a palaeotemperature should be more reliable during the Oligocene when the climate was much more stable than in the Pleistocene when brutal climatical changes occurred very frequently.

We thank the Section d'archéologie et paléontologie du Jura, the University of Fribourg and the Swiss National Foundation (project 115995) for financial support.

REFERENCES
Becker, D., Lapaire, F., Picot, L., Engesser, B. & Berger, J.-P. 2004: Biostratigraphie et paléoécologie du gisement à vertébrés de La Beuchille (Oligocène, Jura, Suisse). Revue de Paléobiologie, 9, 179-191.
Becker, D., Aubry, D. & Detrey, J. 2009: Les dolines du Pléistocène supérieur de la combe de "Vâ Tche Tchâ" (Ajoie, Suisse): un piège à restes de mammifères et artéfacts lithiques. Quaternaire, 20, 2, 135-148.
Mosbrugger, V., Utescher, T. and Dilcher, D. L. 2005: Cenozoic continental climatic evolution of Central Europe. PNAS, 102, 14964-14969.
O'Leary, M. H. 1981: Carbon isotopes in photosynthesis. BioScience, 38, 328-336.
Oppliger, J. 2009: La microfaune des dolines du Pléistocène supérieur de la combe de Vâ Tche Tchâ et de la région de Boncourt (Ajoie, Jura, Suisse). Unpublished report, 29pp.

6.15

How do recurrent patterns of covariation in molluscan shells connect to growth dynamics?

Urdy Séverine[1], Goudemand Nicolas[1], Bucher Hugo[1] and Monnet Claude[1]

[1]*Paläontologisches Institut und Museum, Universität Zurich, Karl Schmid-Str. 4, 8006 Zürich (urdy@pim.uzh.ch).*

The comparison of shell shape among and within different clades of molluscs can be informative with regards to the basic rules of accretionary growth. Indeed, patterns of variation of shell shape and its associated growth features (like growth halts) in ammonoids and gastropods suggest that common rules of accretionary growth underlie the morphogenesis of the shell and its evolution in both clades (e.g. Bucher, 1997; Checa & Jimenez-Jimenez, 1997; Checa et al. 2002).
Moreover, in some phylogenetically distant ammonoids species, covariations among the intensity of ornamentation, the lateral compression of the aperture and the degree of whorl overlap have been described (Buckman's laws). It has been suggested that simple growth rules could underlie these evolutionary recurrent patterns of covariation (Hammer & Bucher, 2005a). Similarly, shell characters covary with the spacing between growth halts during the ontogeny of some of these highly variable ammonoids species.
One goal of this study is to explore whether a comparable pattern of covariation is to be found in gastropods as well. We also want to find out whether documentation of modes of growth in gastropods could support the view according to which some recurrent patterns of covariation could reflect basic constraints tied to accretionary growth. Another interest is the relationship among shape, growth rates and age, a point that is difficult, if not impossible to study on ammonoids.
In this study, we investigate the ontogenetic patterns of covariation among aperture shape, intensity of ornamentation and spacing between growth halts in a population of gastropods (*Hexaplex trunculus*, Muricidae) reared under controlled laboratory conditions. All individuals originated from a single egg mass. We describe the growth dynamics of these individuals from the age of approximately 100 days to 550 days after hatching.
This study highlights a covariation among growth rhythm, growth halts spacing, aperture allometry and intensity of ornamentation:
-Variation in shell shape is analysed by geometric morphometrics of landmarks located on the aperture. We document an ontogenetic allometry of aperture, which becomes relatively wider with size. This is consistent with results obtained using elliptic Fourier analysis of aperture contour and traditional biometrics.
-Variation in the 'strength of ornamentation' is related to the mean spacing between growth halts: smoother snails tend to exhibit more closely spaced growth halts. This covariation, as put in evidence here in *H. trunculus*, seems analogous to that observed in some highly variable ammonoids species (e.g. *Gymnotoceras rotelliformis*, *Amaltheus margaritatus*).
-The mean number of growth halts per month is related to the global shape of the growth curve and to the mean spacing between growth halts: the more frequent the growth 'pulses', the shorter the time spent on a growth halt (down to nearly continuous growth), the more linear the growth curve and the smaller the growth segments between successive growth halts.
Additionally, we develop a growth vector model (Urdy et al., 2009) in order to simulate the formation of growth halts phenomenologically (Fig.1). This model is able to account for some patterns of covariation among specimens. In particular, variation in growth rhythm is regarded as critical in generating the observed covariation between growth halts spacing and ornamentation. Based on these simulations, we suggest that this covariation mainly results from simple scaling among the aperture dimensions and the lengths of shell segments between successive growth halts. Then, the important structuration of phenotypic variation in some ammonoids species could be a generic outcome of underlying variation in growth rhythm.

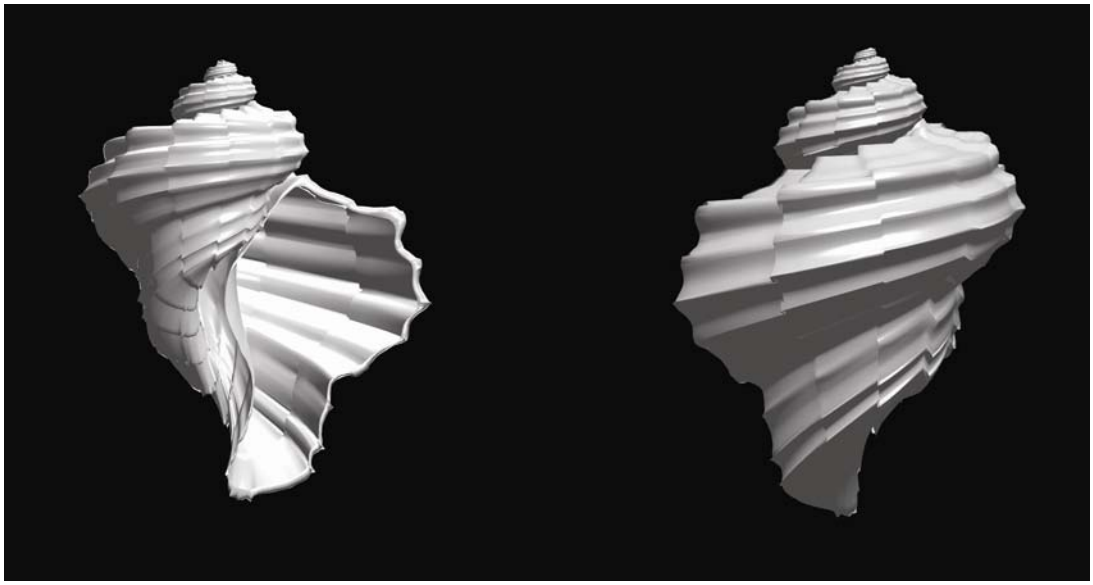

Figure 1: Example of a simulation of growth halts.

REFERENCES

Bucher, H. 1997: Caractères périodiques et mode de croissance des ammonites: comparaison avec les gastéropodes. Geobios Mémoire Spécial, 20, 85-99.

Checa, A. G. & Jimenez-Jimenez, A. P. 1997: Regulation of spiral growth in planorbid gastropods. Lethaia 30(4), 257-269.

Checa, A. G., Okamoto, T. & Keupp, H. 2002: Abnormalities as natural experiments: a morphogenetic model for coiling regulation in planispiral ammonites. Paleobiology 28(1), 127-138.

Hammer, O. & Bucher, H. 2005a: Buckman's first law of covariation: a case of proportionality. Lethaia 38, 67-72.

Urdy, S., Goudemand, N., Bucher, H. & Chirat, R. 2009: Allometries and the morphogenesis of the molluscan shell: a quantitative and theoretical model. Journal of Experimental Zoology, Part B (accepted).

7. Future horizons in marine and continental research drilling

Flavio Anselmetti, Othmar Müntener, Daniel Ariztegui

Commission of Oceanography and Limnology (COL)

7.1

Exploring 200'000 years of climate and environmental history with ICDP drill cores from Lago Petén Itzá, Northern Guatemala

Anselmetti Flavio S.[1], Ariztegui Daniel[2], Hodell David[3], Brenner Mark[4], Gilli Adrian[5], Mueller Andreas[5] & PISDP scientific team members

[1]*Eawag, Swiss Federal Institute of Aquatic Science and Technology, Überlandstrasse 133, 8600 Dübendorf, Switzerland (flavio.anselmetti@eawag.ch)*
[2]*Section of Earth & Environmental Sciences, University of Geneva, Switzerland*
[3]*Department of Earth Science, University of Cambridge, UK*
[4]*LUECI, University of Florida, Gainesville, Florida, USA*
[5]*ETH, Swiss Federal Institute of Science and Technology, Zurich, Switzerland*

As part of a recent ICDP initiative, more than 1.3 km of lake sediment were recovered at seven sites of varying water depths in Lago Petén Itzá, northern Guatemala. Multiple holes with a maximum depth of 133 m were drilled at each core site using the GLAD800 drill-rig mounted on the RV/Kerry Kelts superbarge. This ensured complete recovery of lacustrine sediment sequences that contain a long, continuous record of continental climate change from the lowland Neotropics. Radiocarbon and tephrochronologic dating indicates that the record spans the last ~200 kyr, permitting to study the long-term tropical hydrologic and temperature changes as well as the correlation to other regional and global paleoclimate records.

Lake Petén Itzá is the deepest lake in the lowlands of Central America, with a maximum depth >160 m. It is hydrologically "closed," making it highly sensitive to past changes in the ratio of evaporation to precipitation. Pre-drilling seismic surveys and the new drill cores confirm that the lake sediments are sensitive recorders of past hydrologic changes as reflected by variations in lithology and physical properties.

Site PI-6 (water depth = 71 m) was drilled to a maximum sediment depth of 75.9 m. Radiocarbon dates on terrestrial organic matter are well ordered and indicate a mean sedimentation rate of ~1 mm/yr to ~44 kyr BP at a depth of ~49 m. The age of the basal section is constrained by an identified ash layer at 70.4 m, 1.5 meters above limestone bedrock. The elemental geochemical fingerprint of this rhyolitic tephra layer is consistent with the Los Chocoyos eruption of the Atitlán Caldera around 84 kyr BP. This age of the tephra layer results in a sedimentation rate of 0.6 mm/yr for the lower section and chronologically confines a transgressional sequence, which represents the onset of lacustrine sedimentation in the basin at this site. At Site PI-6, the top 10.8 m were deposited during the Holocene and consist primarily of gray carbonate clay with abundant charcoal. The Pleistocene/Holocene boundary is marked by a transition to Holocene clay from underlying, interbedded, dense gypsum sand and clay deposited during the Late Glacial (~17 to 9.3 kyr). This transition represents a switch from relatively arid conditions during the Late Glacial to moister climate during the early Holocene. In contrast to the Late Glacial period, the Last Glacial Maximum (LGM), from 23 to 17 kyr, consists of gray carbonate clay that is similar to Holocene deposits, suggesting high detrital input and high lake level, i.e. moist conditions. This finding contradicts previous results that suggested the LGM was dry in the Guatemalan lowlands. In Lake Petén Itzá, clay deposition during the LGM was preceded by interbedded gypsum and gray carbonate clay deposited before ~23 kyr during Marine Isotope Stage 3. This pattern of clay–gypsum (wet–dry) oscillations closely resembles the temperature records from Greenland ice cores and North Atlantic marine sediment cores and precipitation proxies from the Cariaco Basin. The most arid periods coincided with Heinrich Events when cold sea surface temperatures prevailed in the North Atlantic, meridional overturning circulation was reduced, and the Intertropical Convergence Zone (ITCZ) was displaced southward. Sediments deposited during MIS 4 and 5a consist of fine-grained clay-rich lithologies with variable content of carbonate and organic matter reflecting rather moist conditions.

The basal ~85 kyr horizon was penetrated in two drillsites, where a deeper and older stratigraphic succession was recovered. Tephrastratigraphic analysis document that this older lacustrine succession dates back to ~200 kyrs, providing thus an unprecedented long paleoclimatic/paleoenvironmental record of the Central American tropics

REFERENCES

Hodell, D.A., Anselmetti, F.S., Ariztegui, D., Brenner, M., Curtis, J.H., Escobar, J. Gilli, A., Grzesik, D.A., Guilderson, T.J., Kutterolf, S. and Müller. A.D., 2008, An 85-ka record of climate change in lowland Central America: Quaternary Science Reviews 27, 1152-1165.

Mueller, A.D., Anselmetti, F.S., Ariztegui, D.A., Brenner, M., Hodell, D.A., Curtis, J.H., Escobar, J., Gilli. A., Grzesik, D., Guilderson, T.P., Kutterolf, S., Plotze, M.L., subm., Late Quaternary paleoenvironment of Northern Guatemala: evidence from deep drill cores and seismic stratigraphy of Lake Petén Itzá: subm. to Sedimentology.

Mueller, A.D., Islebe, G.A., Hillesheim, M.B., Grzesik, D.A., Anselmetti, F.S., Ariztegui, D., Brenner, M., Curtis, J., Hodell, D., Venz, K.A., 2009, Climate drying and associated forest decline in the lowlands of northern Guatemala during the late Holocene: Quaternary Research 71, 133-141.

7.2

Potential and limits of drill cuttings for lithostratigraphical interpretations in siliciclastic environments: preliminary results from the IODP NanTroSEIZE Stage 2 Expedition 319 Site C0009 (Nankai Trough, Kumano Forearc Basin, Japan).

N. Efimenko[1], D. Buchs[2], C. Buret[3], K. Kawabata[4], A. Schleicher[5], M. Underwood[6] , E. Araki[7], T. Byrne[8], L. McNeill[9], D. Saffer[10], K. Takahashi[11], N. Eguchi[11], S. Toczko[11] and Expedition 319 Scientists[12]

[1]*Institut de Géologie et Paléontologie, Université de Lausanne, Switzerland e-mail: natalia.efimenko@unil.ch*
[2]*Research School of Earth Sciences, Australian National University*
[3]*Université de Picardie Jules Verne, 80025 Amiens, France*
[4]*National Central University, Taiwan*
[5]*Department of Geological Sciences, University of Michigan, Ann Arbor, Michigan, USA.*
[6]*Department of Geological Sciences, University of Missouri, Columbia, Missouri 65211*
[7]*Earthquake and Tsunami Research Project for Disaster Prevention, JAMSTEC, Japan*
[8]*University of Connecticut, Storrs, CT 06269, USA*
[9]*University of Southampton, Southampton, UK*
[10]*Dept. of Geosciences, Pennsylvania State University, USA*
[11]*Centre for Deep Earth Exploration, JAMSTEC, Japan*
[12]*D.Boutt, University of Massachusetts-Amherst, Amherst, USA; M.Conin, CEREGE, Collège de France, France; D.Cukur, Pukyong National University, Korea; M.-L.Doan, Université Joseph Fourier, France; P.Flemings, University of Texas, Austin, USA; K.Horiguchi, Osaka University, Japan; N.Hayman, University of Texas, Austin, USA; G.Huftile, Queensland University, Australia; T.Ito, Tohoku University, Japan; S.Jiang, Florida State University, USA; K.Kameo, Chiba University, Japan; Y.Kano, Kyoto University, Japan; G.Kimura, University of Tokyo, Japan; M. Kinoshita, JAMSTEC, Japan; K.Kitada, JAMSTEC, Japan; A.J.Kopf, University of Bremen, Germany; W.Lin, JAMSTEC, Japan; M.Kyaw Thu, JAMSTEC, Japan; C.Moore, University of California, Santa Crus, USA; G.Moore, University of Hawaii, USA; Y.Sanada, JAMSTEC, Japan; H. Tobin, University of Wisconsin-Madison, USA; K.Toshiya, JAMSTEC, Japan; G.Wheat, Monterey Bay Aquarium Research Institute, USA; T. Wiersberg, GFZ German Research Center for Geosciences, Germany*

During the IODP NanTroSeize Expedition 319 riser-drilling system was employed for the first time to collect cuttings and core for scientific purposes at Site C0009A (Nankai Trough, Kumano forearc basin). Cuttings are the mixture of rock fragments and sediments produced as the drill bit cuts through the formation. During riser drilling, the cuttings are transported via the circulation of drill mud with suspended cuttings material within riser pipe between the drill ship and the bottom of the hole.

We present first geologic results from riser drilling, coring, and cuttings collection at the Site C0009A in the Kumano forearc basin. One of the scientific objectives for this site was to characterise the lithology and deformation of the Kumano forearc basin sediments and underlying units through analysis and integration of (i) cuttings, (ii) core, (iii) measurements while drilling, and (iv) wireline logging data. Cuttings were retrieved from each 5 m intervals from 703.9 to 1604 m below sea floor and cores were recovered from 1509.7 to 1593.9 m below sea floor. As core availability was strongly limited by operational costs and time restrictions, the study of cuttings was important for the understanding of their potential and limits for lithostratigraphical interpretations compared to the core.

First, cuttings were described based on visual macroscopic description of the bulk material. We estimated (i) the relative amount of coarser (sand/silt) and finer (clay) material, (ii) the appearance, relative amount and size of hard rock chips, and (iii) the abundance of wood fragments. Then, we separated the grains of the size more than 45 μm by sieving in order to describe them under the binocular microscope and prepare smear slides. We distinguished specific minerals, volcanic glass and lithic fragments, made qualitative estimations of their relative abundance, roundness, sorting, and relative variation in grain size. The chips of hard rock of 1-4 mm size were separated and used for the preparation of thin-sections, X-ray diffraction and X-ray fluorescence analyses. We also compared cuttings and cores in the cored interval to determine possible artifacts and uncertainties related to the use of cuttings for lithostratigraphical interpretations.

Cuttings allowed us to recognise major lithological variations and trends in mineralogical and chemical data. We distinguished four lithological units composed of mud and mudstone with coarser silty and sandy interbeds, and volcanic ash/tuff. Based on the integration of cuttings description, measurements while drilling, wireline logging data, seismic data and biostratigraphy, first three lithological units are interpreted as fine-grained turbidite-rich deposits of the Kumano Basin accumulated during Pleistocene to Present. The lower part of Unit III (Subunit IIIB) had an increased amount of wood fragments and of rounded glauconite. This fact points to the increased terrigeneous input in transgressional settings. The Subunit IIIB is represented by the first sediments deposited above the angular uniconformity with slightly older deposits of Unit IV of Late Miocene age. The depth of the unconformity is 1285 mbsf. The Unit IV is composed of thin-bedded turbidites which are more fine-grained than overlying deposits. Compositional maturity of sediments is increased compared to the first three units. This Unit could be interpreted either as accreted trench sediments, or as trench slope deposits or as sediments deposited in

the distal reaches of the early Kumano Basin.
Consistency between unit boundaries determined from cuttings and those determined from log data is good in terms of depth, with typical mismatches of less than 10m. The lithological futures and variations at the scale smaller than 5m could not be recognised. Problems affecting the preservation of cuttings are (i) degree of lithification, (ii) mixing of cuttings/cavings, and (iii) possible contamination with drill-mud. Small size of cuttings (< 2 cm) and desegregation of poorly lithified sediments during the transport in the drilling mud makes difficult to obtain the information about lithofacies and sedimentary structures. Mineralogical and chemical analyses in cuttings are biased by the preferential consolidation of fine-grained sediments with respect to coarse-grained sediments. XRD and XRF analyses from cuttings are more homogeneous than those from core samples, and the composition of cuttings is similar to the samples of silty claystones from the cores.
In the future, more accurate quantitative characterisation of cuttings through the use of digital imaging can improve the description of lithofacies. Although the quality of cuttings is affected by caving and drilling mud contamination, our results clearly indicate that cuttings analysis in combination with seismic and logging data to coring in deep ocean drilling is a viable analogue to core for general lithostratigraphical interpretations when no scientific requirements for precise sedimentological analysis are required. To make precise lithostratigraphical description and interpretation in critical intervals, the study of core is needed.

7.3

Lithospheric heterogeneities, hydrothermal activity and serpentinization at slow spreading ridges: Insights through ocean drilling

Früh-Green Gretchen[1], Delacour Adéilie[1,2] & Boschi Chiara[1,3]

[1]*ETH Zurich, Institute for Mineralogy & Petrology, Clausiusstr. 25, CH-8092 Zurich (frueh-green@erdw.ethz.ch)*
[2]*IPGP, Equipe de Géoschiences Marines, F-75252 Paris Cedex 05*
[3] *Istituto di Geoscienze e Georisorse-CNR, Via Moruzzi 1, I-56124 Pisa*

The formation and alteration of the oceanic lithosphere are fundamental processes that determine the chemical and physical evolution of our planet. In the nearly 40-year history of the scientific ocean drilling programs, a limited number of sites have been drilled into oceanic basement; however, only two holes, ODP Hole 735B and IODP Hole 1309D, have been drilled to depths >1000m in lower crustal sequences. These have led to a better understanding of mid-ocean ridge processes and, in turn, have led to the recognition of fundamental differences in crustal accretion and alteration processes related to spreading rates. In contrast to the apparently more layered and spatially homogeneous oceanic lithosphere at fast-spreading ridges (e.g., ODP Hole 504B and Hole 1256D), slow- and ultra-slow spreading centres are markedly heterogeneous with respect to lithology, deformation and degree of alteration. These heterogeneities reflect profound variations in magmatic, tectonic and hydrothermal activity along- and across-isochrons.

At many sites on the Mid-Atlantic Ridge (MAR), the magmatic layer is discontinuous and mantle lithologies are exposed at or near the seafloor within oceanic core complexes (OCCs): the footwalls of long-lived low-angle detachment faults. IODP Expeditions 304 and 305 targeted the 1.5 to 2 Myr old dome-like Atlantis Massif, located just west of the MAR at 30° N. The Atlantis Massif forms the inside corner of the intersection between the MAR and the Atlantis Transform Fault and is now one of the best studied OCC comprised of lower crustal and upper mantle rocks. Three domains are distinguished on the basis of lithology and morphology: a central dome, a peridotite-dominated southern wall and a basaltic eastern bloc, interpreted as a hanging wall separated from the OCC by a detachment fault. Here we review recent results of drilling at Site 1309 on the central dome of the Atlantis Massif, and compare these with results from detailed submersible studies of the southern wall, 5 km to the south.

The main hole 1309D was drilled on the crest of the central dome of the massive at a water depth of 1656 mbsf and penetrated 1415.5 mbsf with an average core recovery 75%. Quite unexpectedly, the predominant lithology recovered was gabbroic rocks (91.4%) with minor intercalated ultramafic rocks (5.7%) and diabase (~3%). The gabbroic rocks are compositionally diverse and are the most primitive ever cored in slow-spreading ocean lithosphere (with high Mg# (74–90), low TiO_2 (<0.49 wt%) and Na_2O (0.1–3.7 wt%). Mantle peridotites are very rare (<0.3%) and are concentrated in the upper part of the hole. The gabbroic rocks are relatively undeformed and show limited seawater-rock interaction downhole, as indicated by relatively homogeneous and mantle-like Sr-, Nd-, and S-isotope compositions.

The dominance of primitive gabbroic rocks, the absence of significant amounts of serpentinized mantle peridotites, and the low degree of fluid-rock interaction at Site 1309 contrasts greatly with results of submersible studies of the southern wall of the massif. The southern wall of the AM is dominated by serpentinized harzburgites, intruded by minor gabbroic bodies, and hosts the recently discovered Lost City Hydrothermal Field (LCHF), a peridotite-hosted hydrothermal system composed

of spectacular, up to 60 m high, carbonate and brucite chimneys that vent low-temperature and high-pH fluids resulting from serpentinization reactions at depth. The Lost City fluids are enriched in hydrogen, methane and other hydrocarbons, produced abiotically through Fischer-Tropsch type reactions. Production of reduced volatiles and variable mixing with seawater in the subsurface and in near-vent environments are important processes in creating strong chemical gradients that provide micro-niches for distinct communities of hydrogen-, sulphur- and methane-utilizing archaea, bacteria as well as eubacteria. Geochemical investigations of the serpentinites hosting Lost City indicate long-lived seawater-peridotite interaction at 150-250°C and high fluid-rock ratios (>100 and up to 10^6), which produced enrichments in B, U and light REE, and systematic changes in Sr- and Nd-isotope ratios towards seawater values. Our multidisciplinary investigations of Lost City highlight the complex interplay between deformation, fluid flow, mass transfer and microbial activity within this long-lived system and are changing our views not only about the conditions under which life can thrive on our planet but, perhaps, on others as well.

The fact that IODP Hole U1309D on the Atlantis Massif (AM) on the MAR unexpectedly yielded 1400m of gabbro adjacent to where peridotite had previously been recovered, and close to the peridotite-hosted Lost City vent field, is testament to how laterally variable magmatic accretion processes and hydrothermal activity are at slow spreading ridge environments. Through studies of the Atlantis Massif and drilling at ODP Site 209 (along the MAR from 14° to 16°N on both sides of the Fifteen-Twenty Fracture Zone), a new model for the structure and formation of slow-spread ridges has emerged. Slow spreading ridges are probably less magma starved than previously believed, but melt is retained in the upwelling mantle as it ascends, and becomes incorporated into a relative thick lithosphere. The latter deforms and extends along localized zones of deformation, some of which become major detachment faults operating via a rolling hinge model. Such detachment faults may therefore at least locally constitute the de facto plate boundary. Drilling has also contributed to modifying our notions of ophiolites as analogues for ocean crust formation and has shown that slow-spread crust cannot be considered comparable to dismembered ophiolitic crust.

7.4

Scientific drilling in the ocean lithosphere : what's next?

Benoît Ildefonse

Géosciences Montpellier, CNRS-Université Montpellier 2, CC60, 34095 Montpellier cedex 05, France (benoit.ildefonse@um2.fr)

The mid-ocean ridges and the new oceanic lithosphere that they create are the principal pathway for thermal exchange and physical/chemical interactions between the earth's interior, the hydrosphere, and the biosphere. Hence the ocean lithosphere records the inventory of global thermal, chemical and associated biological fluxes.

A key outcome of the InterRidge-IODP "Melting, Magma, Fluids and Life" workshop (Southampton, 27-29 July, 2009; www.interridge.org/WG/DeepEarthSampling/workshop2009) was the formulation of integrative scientific questions and implementation approaches that will elucidate the role of ocean lithosphere processes within the broader Earth System. There are three, equally important main themes, each comprising geological, hydrological, chemical, and biological processes that are closely interdependent.

- Understanding the accretion of ocean crust. This goal requires full section characterization of minimally-disrupted ocean crust and a sufficient portion of underlying uppermost mantle, and detailed understanding of active processes within the axial zone;
- Understanding lithospheric heterogeneity in slow- and ultraslow spread crust, in particular the impact of serpentinization on global biogeochemical cycles and plate rheology.
- Following the maturation process of lithosphere from the axis to the ridge flanks and investigating the hydrological-geochemical-microbiological feedbacks during the aging of the oceanic basement.

Focussing in on the first theme, sampling a complete section of the ocean crust, from the ocean floor to the uppermost mantle through the seismic Mohorovi i discontinuity (the 'Moho'), was the original inspiration for scientific ocean drilling, and remains the main goal of the 21st Century Mohole Initiative in the IODP Science Plan. Fundamental questions about the composition, structure, and geophysical characteristics of the ocean lithosphere, and about the magnitude of chemical exchanges between the mantle, crust and oceans remain unanswered due to the absence of in-situ samples and measurements. The geological nature of the Moho itself remains poorly constrained.
The "Mission Moho" proposal submitted to IODP in April 2007, sets the ambitious goal to drill completely through intact oceanic crust, across the Moho and into the uppermost mantle, in lithosphere formed at a fast spreading rate. Although, no

long-term mission has been adopted by IODP, the scientific objectives related to deep drilling in the ocean crust remain essential to our understanding of the Earth. Our current knowledge if in-situ ocean crust remains limited; much will be learned on the way to the mantle. The journey and the destination are equally important.

Fundamental scientific goals include:

- Determine the bulk composition of the oceanic crust to establish the chemical links between erupted lavas and primary mantle melts, understand the extent and intensity of seawater hydrothermal exchange with the lithosphere, and estimate the chemical fluxes returned to the mantle by subduction,
- Test competing hypotheses of the ocean crust accretion at fast spreading mid-ocean ridges, and quantify the linkages and feedbacks between magma intrusion, hydrothermal circulation and tectonic activity,
- Determine the geological meaning of the Moho in different oceanic settings,
- Determine the in situ composition, structure and physical properties of the uppermost mantle (and its variability), and understand mantle melt migration,
- Calibrate regional seismic measurements against recovered cores and borehole measurements, and understand the origin of marine magnetic anomalies,
- Establish the depth limit of deep biosphere and hydrological/geobiological processes in the lithosphere.

The “MoHole” was planned as the final stage of Mission Moho. At the recent InterRIDGE-IODP Workshop "Melting, Magma, Fluids, Life", scientists re-iterated their enthusiasm and support for an ultra-deep hole in intact oceanic crust and into the uppermost mantle. This project would provide major inspiration for the next generation of scientists and engineers. The challenge is formidable, and requires as soon as feasible careful site selection, geophysical site survey, and the development of cutting edge technology including drilling capability to achieve +6000m of penetration in +4000m water depth. The next drilling program needs a mechanism to enable the community to move forward with planning, design and implementation in order to complete one of the major goals of scientific ocean drilling.

7.5
The age of sedimentary fillings of overdeepend valleys in the Alps

Frank Preusser

Institut für Geologie, Universität Bern, Baltzerstrasse 1+3, 3012 Bern, Switzerland (preusser@geo.unibe.ch)

Overdeepened basins and valleys are known from several areas within the Alps, in particular from Switzerland and northern Italy (e.g. Schlüchter, 1979). It is furthermore remarkable that glacial erosion partly left remains of older deposits in lateral valley positions such as Gnadenwaldterrasse of the Inn Valley (Fliri et al., 1973), Austria, or Thalgut in the Aare Valley (Schlüchter, 1989), Switzerland, that represent former valley bottoms. Several of the deep basins and relics contain complex sedimentary sequences that indicate deposition before the last glaciation of the Alps (Würmian). Recent results from palynology and luminescence dating indicate a complex deposition history for such sediments, for example for the complex sequence of Meikirch, Aare Valley (Preusser et al., 2005). The available data implies that deep erosion and shaping of the present subsurface occurred throughout several phases during the Quaternary. However, the exact timing of these processes is still poorly constrained as the number of sites available is rather limited. Since most of the valley fillings are deeply covered by sediments of later glaciations, further detailed information about this issue can only be achieved by recovering cores from such structures by deep drillings (down to some hundred metres). First results from a case study in the Wehntal (Züricher Unterland) will be presented.

REFERENCES

Fliri, F., 1973. Beiträge zur Geschichte der alpinen Würmvereisungen: Forschungen am Bänderton von Baumkirchen (Inntal, Nordtirol). Zeitschrift für Geomorphologie Supplement 16, 1-14.

Preusser, F., Drescher-Schneider, R., Fiebig, M., Schlüchter, Ch., 2005. Re-interpretation of the Meikirch pollen record, Swiss Alpine Foreland, and implications for Middle Pleistocene chronostratigraphy. Journal of Quaternary Science 20, 607-620.

Schlüchter, Ch., 1979. Übertiefte Talabschnitte im Berner Mittelland zwischen Alpen und Jura (Schweiz). Eiszeitalter und Gegenwart 29, 101-113.

Schlüchter, Ch., 1989. The most complete Quaternary record of the Swiss Alpine Foreland. Palaeogeography, Palaeoclimatology, Palaeoecology 72, 141-146.

7.6

New sights on Late Pleistocene climate variability in Southernmost Patagonia: An ICDP approach

C. Recasens[1], D. Ariztegui[1], N.I. Maidana[2], F.S. Anselmetti[3], A. Vuillemin[1], R. Farah[1] and the Pasado Scientific Team

[1]*Section of Earth and Environmental Science, Rue des Maraîchers 13, 1205 Geneva (cristina.recasens@unige.ch)*
[2] *Dpto de Biodiversidad y Biología Experimental, FCEyN-UBA, Buenos Aires, Argentina*
[3] *EAWAG, Überlandstrasse 133, 8600 Dübendorf*

Laguna Potrok Aike, at 52°S, 70°W in Southern Patagonia, contains a unique paleoclimatic record of southern South America. This ~770 ka old maar located in the province of Santa Cruz, Argentina, is one of the few permanent lakes in this steppe region, providing a continuous sedimentary record over an extended time span in this area of the world. Within the framework of the ICDP-sponsored Potrok Aike Maar Lake Sediment Archive Drilling Project (PASADO), three sites were cored during October and November 2008 by an international group of scientists using the GLAD800 drilling rig operated by DOSSEC (Figure 1).

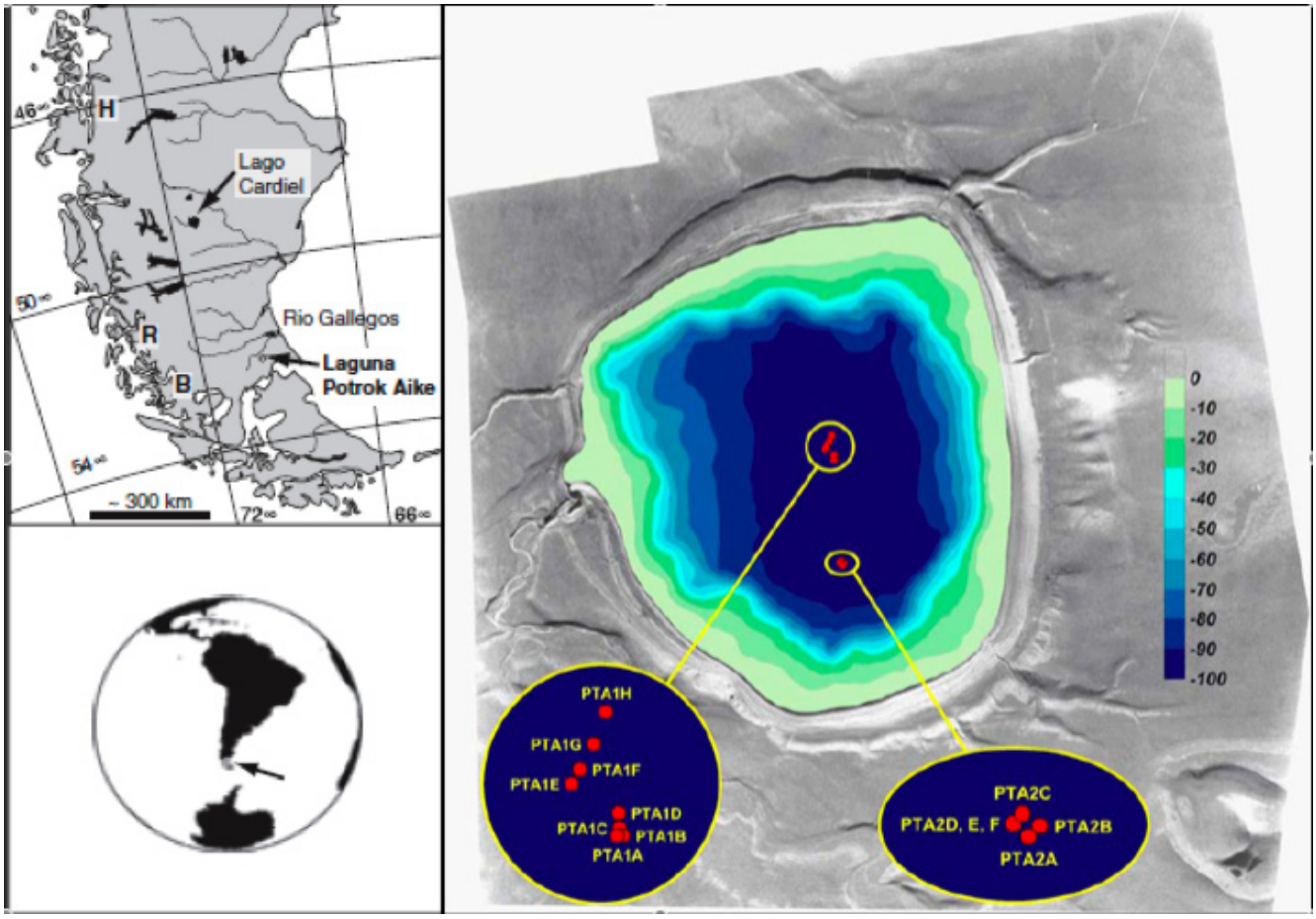

Figure 1. Bathymetric map of Laguna Potrok Aike with drill sites PTA1 and PTA2 and holes labeled alphabetically. PTA-1E to -1H and PTA-2D to -2F are gravity cores covering the sediment water interface. Inserts show location of the lake in southern South America. The volcanoes Reclús (R), Hudson (H) and Mt. Burney (B) are marked with capital letters.

The lake is located in the Pliocene to late Quaternary Pali Aike Volcanic Field, a northwest-southeast oriented tectono-volcanic belt that is ~50 km wide and more than 150 km long. The available geomorphological data indicate that Laguna Potrok Aike has neither been reached by the last glaciation nor by any other Pleistocene ice advance during the last 1 Ma. Thus, it is potentially the only site that has archived a continuous and high-resolution sediment record covering several glacial/interglacial cycles for the southern hemispheric mid-latitudes. Several drilling sites were chosen after the interpretation of the seismic profiles obtained in prior field campaigns, within the framework of the project "SALSA", South Argentinean Lake Sediment Archives and Modeling (Anselmetti et al. 2008, Wille et al., 2007). More than 500 m of sedimentary cores were recovered and the longest core reached over 100 m.

On-site laboratory analyses were carried out simultaneously to the drilling operations. All core sections were scanned for petrophysical properties prior to opening with a GeoTek® Multisensor Track Core Logger (MSCL). An in situ geochemical laboratory was also habilitated in order to achieve the first analysis on the recovered material. Core catchers (approximately one every three meters) were photographed and described, and then subsampled for water content, Ca and Cl contents as well as pH which were measured immediately in the camp. Samples were furthermore taken for stable isotopes, pollen and diatoms for subsequent analysis in the homebased laboratories. Smear slides were mounted for petrographic microscopic examination.

An international scientific team will work on the different sedimentary cores recovered at the three sites using a multidisciplinary approach. Several analyses are currently underway including more accurate MSCL scans of the cores and core catcher analysis for diatoms, pollen and stable isotopes. A sampling party at the core repository in Bremen, Germany, is actually on the go. Cores have been split and are being sampled at high resolution for all the planned analyses.
The Swiss scientific contribution to the project involves two main aspects: 1. the diatom record of the retrieved cores for paleoenvironmental reconstructions and collaboration in the development of a modern training set for diatoms in Patagonia; 2. the characterization of the deep biosphere investigating living microbial communities within the sediments, which is embedded in an integrated study including microbiology, geochemistry (interstitial waters), and mineral authigenesis/diagenesis.

REFERENCES

Anselmetti, F.S. et al., 2008: Environmental history of southern Patagonia unravelled by the seismic stratigraphy of Laguna Potrok Aike. Sedimentology, 53, 873-892.

Wille, M., et al., 2007: Vegetation and climate dynamics in southern South America: The microfossil record of Laguna Potrok Aike, Santa Cruz, Argentina. Review of Palaeobotany and Palynology, 146, 234–246.

7.7

PALEOVAN - The International Continental Scientific Drilling Program (ICDP) in Lake Van, Eastern Anatolia (Turkey)

Mona Stockhecke[1], Flavio S. Anselmetti[1], Aysegül F. Meydan[2], Paul Hammer[3], Rolf Kipfer[1], Daniel Odermatt[4], Mike Sturm[1], Yama Tomonaga[1] and PALEOVAN scientific team

[1]Eawag, Swiss Federal Institute of Aquatic Science and Technology, Überlandstrasse 133, 8600 Dübendorf, Switzerland (mona.stockhecke@eawag.ch)

[2] Yuzuncu Yil Universitesi, Muhendislik-Mimarlik Fakultesi, Jeoloji Muhendisligi Bolumu 65080, Van, Turkey

[3] Dept. of Earth Science, Haldenbachstrasse 44, 8092 Zurich, Switzerland

[4] Remote Sensing Laboratories, Dept. of Geography, University Zurich, Winterthurerstrasse 190, 8057 Zurich, Switzerland

Lake Van is the fourth largest terminal lake in the world (volume 607 km^3, area 3,570 km^2, maximum depth 460 m), extending over 130 km WSW-ENE on the Eastern Anatolian high-plateau, Turkey. The annually-laminated sedimentary record of Lake Van promises to be an excellent palaeoclimate archive because it potentially yields a long and continuous continental sequence that covers several glacial-interglacial cycles (~500 kyr). Therefore, Lake Van is a key site within the International Continental Scientific Drilling Program (ICDP) for the investigation of the Quaternary climate and paleoenvironmental evolution in the Near East .The ICDP drilling operations 'Paleovan' will be performed with active involvement of various Swiss research groups. Drilling is planned for 2010 and the technical preparations are currently underway.

As preparation for the drilling campaign, several site surveys were carried out during the past years consisting of ~850 km seismic profiles, multidisciplinary analysis of up to 9 m long cores extending back to the Last Glacial Maximum and water column analysis. Furthermore, recent investigations focused on modern particle dynamics and varve formation using sequential sediment traps, multispectral satellite images and short sediment cores (Stockhecke, 2008).

The sediment trap samples and satellite images of 2006 revealed that three annual phases of authigenic particle production occur, one in spring characterized by non-skeletal algae, one in summer with dominance of authigenic carbonate production, and one in autumn, which is characterized by diatoms and thus biogenic silica production. The sediment trap samples from 2007 to 2008 show the same organic spring-peak as the year before, but the biogenic silica concentration increased si-

gnificantly. The maxima of authigenic carbonate production in late autumn of 2008 is related to significant higher air temperatures and increased water mixing processes at the corresponding depth. Further investigations are planned that document the annual cycles with seasonal resolution and their preservation potential in the lake sediments, calibrating the sensitive climate-lake-sediment system.

All these investigations show the large potential of PALEOVAN for obtaining a continuous undisturbed and long continental palaeoclimate record. This will shed new lights on paleoenvironmental conditions, the dynamics of lake level fluctuations, noble gas concentration in pore waters, history of volcanism and and earthquake activities (Litt, 2008).

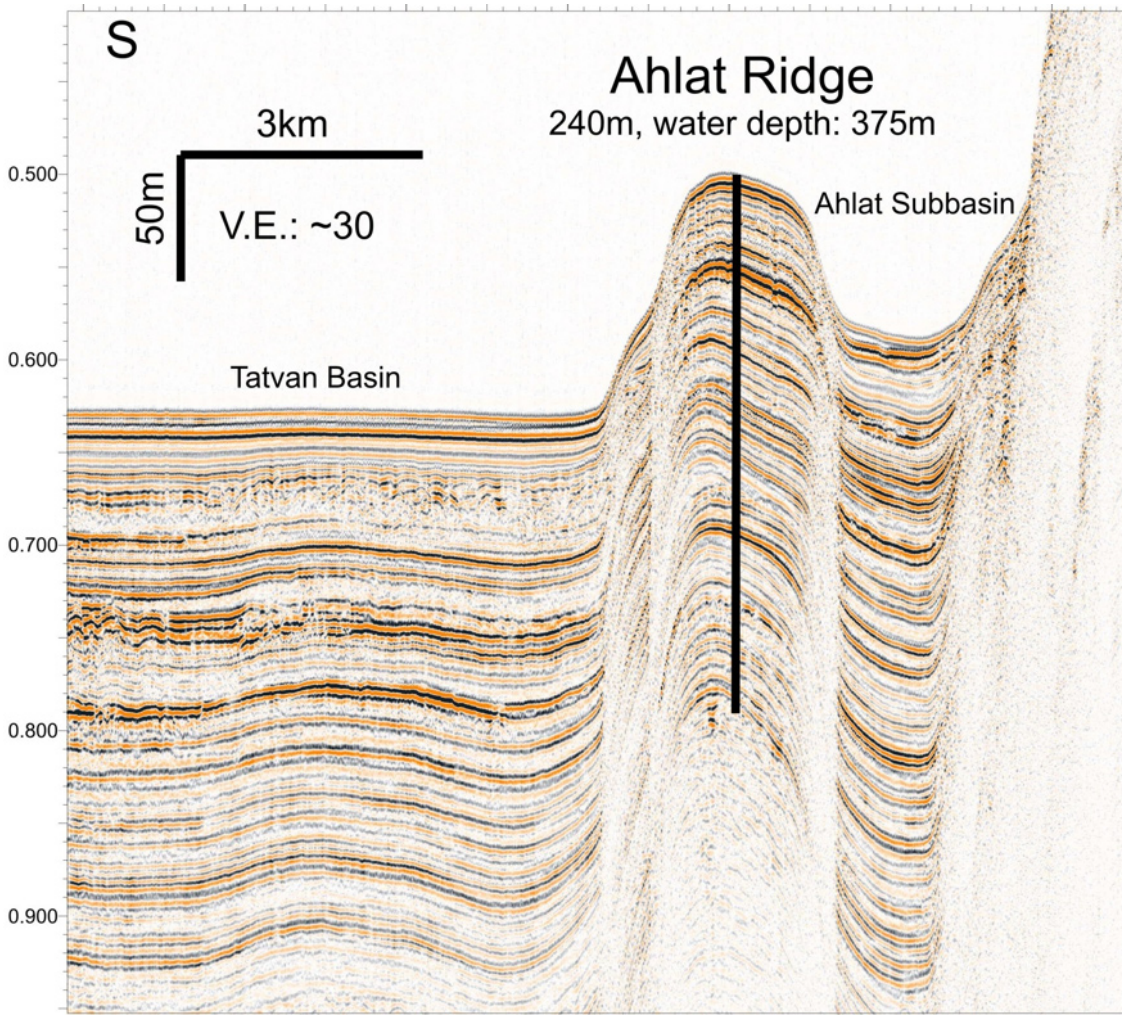

Figure 1. Part of seismic profile GEO04-007 crossing the Tatvan Basin and Ahlat Ridge in a S-N direction with the proposed ICDP drill site.

REFERENCES

Litt, T., Krastel, S., Sturm, M., Kipfer, R., Örcen, S., Heumann, G., Franz, S.O., Ülgen, U.B., Niessen, F., 2008, submitted: Lake Van Drilling Project "PALEOVAN", International Continental Scientific Drilling Program (ICDP): Results of a recent pre-site survey and perspectives. Quaternary Science Rewies.

Stockhecke, M. (2008). The Annual Particle Cycle of Lake Van: Insights from Space, Sediments and the Water Column. University of Zurich.

7.8

Addressing Geohazards from Submarine Slides through Ocean Drilling: The "Nankai Trough Submarine Landslide History" drilling Proposal

Strasser Michael[1], Moore Gregory F.[2], Ashi Juichiro[3], Camerlenghi Angelo[4], Dugan Brandon[5], Huhn Katrin[1], Kanamatsu Toshiya[6], Kawamura Kiichiro[7], McAdoo Brian G.[8], Panieri Giuliana[9], Pini Gian-Andrea[9], Urgeles Roger[4]

[1] *MARUM, Centre for Marine and Environmental Sciences, Univ. Bremen, Leobener Strasse, D-28359 Bremen (mstrasser@marum.de)*
[2] *Dept. of Geology and Geophysics, Univ. Hawaii, USA*
[3] *Ocean Research Institute, Univ.Tokyo, JPN*
[4] *ICREA – Univ. Barcelona, ESP*
[5] *Dept. of Earth Science, Rice Univ. USA*
[6] *Japan Agency for marine-earth science and technology JAMSTEC, JPN*
[7] *Fukada Geol. Inst. Tokyo, JPN*
[8] *Dept. of Earth Sciences & Geography Vassar College, NY, USA*
[9] *Dept. of Eartn and Geo-Environmental Sciences, Unv. Bologna, ITA*

With increasing awareness of oceanic geohazards (e.g. Morgan et al., 2009), also submarine landslides are wide gaining attention not only because of their catastrophic impacts (e.g. landslide-induced tsunamis, submarine infrastructure), but also because they can be directly related to primary trigger mechanisms including earthquakes, rapid sedimentation, gas release, or clathrate dissociation, many of which represent geohazards themselves (e.g. Camerlenghi et al., 2007). Scientific ocean drilling can be a key element in understanding such geohazards, given that the submarine geological record preserves structures and past occurrences. To improve our knowledge, quantitative constraints on frequency and magnitude on relevant timescales need to be related to trigger and failure mechanisms.

Towards this goal, the IODP - Ancillary Project Letter - Proposal "**Nan**kai **Tro**ugh Submarine Land**SLIDE** History – **NanTroSLIDE**" aims to add one site to the NanTroSEIZE (Nankai Trough Seismogenic Zone Experiment; Tobin and Kinoshita, 2007) study area to constrain timing, causes and consequences of submarine landslides in this well-studied accretionary complex. On the basis of new 3D seismic data interpretation in the NanTroSEIZE study area, we have identified an ideally suited slope basin sedimentary succession that is composed of stacked Pleistocene-to-recent mass transport deposits (MTDs) that includes one exceptionally large MTD up to 150m in thickness. A 350m thick succession, comprising the distal part of the mega deposit, is proposed to be completely drilled and logged within 3 days before, during or after any of the upcoming NanTroSEIZE operations on the Japanese drilling vessel *Chickyu*.

We expect to catalog a detailed submarine landslide event history along with clues on the depositional dynamics of each MTD as they relate to tsunamigenic potential. In conjunction with 3D seismic interpretation we will be able to constrain scales and landslide magnitude. The results obtained will be interpreted in terms of short-term trigger mechanisms and long-term pre-conditioning factors by correlating the magnitudes and frequencies of MTDs to the seismicity and tectonic evolution of the margin. Additionally, data from nearby NanTroSEIZE drill sites are expected to reveal quantitative constraints on slope stability conditions and submarine landslides initiation. In combination, the available data set will allow us to establish a better physical understanding of tectonic processes and slope failures, to gain a general understanding of failure-related sedimentation patterns and the significance of large episodic mass-transport events. Ultimately, this could help us to asses the tsunamigenic potential of submarine landslides. We thus expect this proposed project to become an important case study providing the base to improve our conceptual understanding of causes and consequences of submarine landslides.

The primary goals of drilling the proposed site (NTS-1A) are:

(i) To establish a well-dated Pleistocene-to-recent mass-movement event stratigraphy
(ii) To sample the distal part of an exceptionally thick MTD for analyzing its rheological behavior to constrain sliding dynamics and tsunamigenic potential

This aims at providing answers to following questions:

1) What is the frequency of submarine landslides
2) How are MTDs and earthquakes related and can we use the MTD-inventory to interpret paleoseismology
3) What controls type, size and magnitude of turbitides and MTDs and how do they change through time?
4) What are the dynamics of large submarine landslides and can we infer ther tsunamigenic potential?

By addressing these focused key questions, we aim to isolate tectonic processes influencing magnitude and occurrence of submarine landslides along active subduction zone margins and to understand their potential for triggering catastrophic consequences both in terms of hazard (tsunamigenic landslides) and of sediment mass-transfer and margin evolution.

REFERENCES

Camerlenghi, A., Urgeles, R., Ercilla, G., and Bruckmann, W., 2007. Scientific ocean drilling behind the assessment of geohazards from submarine slides, Scientific Drilling, 4, 45-47

Morgan , J.K., Silver, E., Camerlenghi, A., Dugan B., Kirby, S., Shipp, C., Suyehiro, K., 2009. Addressing Geohazards Through Ocean Drilling. Scientific Drilling, 7, 15-30

Tobin, H., and Kinoshita, M., 2007. The IODP Nankai Trough Seismogenic Zone Experiment. Scientific Drilling, 1, 39-41

7.9

Evidence for a middle Pliocene change in the ocean nitrate inventory based on foraminifera-bound δ15N in the Caribbean Sea

Straub Marietta[1], Haug Gerald[1], Daniel Sigman[2], Haojia Ren[2]

[1] *Geological Institute, Department of Earth Sciences, ETH Zurich, 8092 Zurich, Switzerland*
[2] *Department of Geosciences, Guyot Hall, Princeton University, Princeton, NJ 08544, USA*

The nitrate budget in the low-latitude surface ocean is mainly controlled by the typically opposing effects of denitrification and nitrate fixation. The state of the global ocean nitrate inventory affects primary production, which allows sequestering CO2 into the deep ocean. This may influence climate variability and control warm and cold periods in Earth history. Studies have shown that nitrogen isotopes reflect the nutrient status of the upper water column and therefore are a proxy for the state of the ocean's 'biological pump'.

So far, the N inventory has mostly been reconstructed based on bulk sedimentary N-isotope measurements, which can be affected by syn- and post-sedimentary processes. Promising approaches to circumvent these potential biases are based on measurements of foraminifera-bound $\delta^{15}N$. In the subtropical and tropical ocean, planktonic foraminifera are a main component of the sinking particle flux. The organic compounds encapsulated within the foraminiferal tests are protected from sedimentary diagenetic processes. As a result they record a pristine signal of the nitrate composition in the water column. The novel method used here employs denitrifying bacteria Pseudomonas chlororaphis and Pseudomonas aureofaciens to produce nitrous oxide (N_2O), recovered from the nitrate extracted from the organic matter sheltered within the foraminifera shell, which is analyzed for $\delta^{15}N$ with a Gas bench II – IRMS and produces results with reproducible isotopic measurements of samples down to 1 μM nitrate.

Previous data from the investigated site (ODP Leg 165, site 999A, Caribbean Sea), studying the last 30'000 yrs using the same method, indicate a systematic difference between glacial and interglacial values. The glacial state is characterized by high $\delta^{15}N$ values around ~ 5 ‰ (suggesting less N-fixation) and the interglacial state by low $\delta^{15}N$ values around ~ 3 ‰ (N-fixation increase). On contrary, our data from foraminifera-bound $\delta^{15}N$ of *G.ruber* and *G.sacculifer* reveals evidence for a change in the mean ocean nitrate compared to the last 30'000 yrs. The basic findings from the measured interval between 3.2 Ma to 2.4 Ma show glacial $\delta^{15}N$ values of ~ 4.5-7 ‰ for *G.sacculifer* and ~ 3-5.5 ‰ for *G.ruber*, interglacial values range between ~ 4-6 ‰ for *G.sacculifer* and between ~ 3-5.5 ‰ for *G.ruber*. Based on the obtained $\delta^{15}N$ values we could not differentiate between glacial and interglacial periods. This lead us to the conclusion that there probably was a general change of the ocean nitrate inventory and the dominating processes of N-fixation and denitrification performed in a different way than today. Further measurements will be necessary to understand the preliminary data and to interpret the possible changes in the ocean during late Pliocene.

REFERENCES

M.A. Altabet, R. Francois (1994): Sedimentary nitrogen isotopic ratio as a recorder for surface ocean nitrate utilization. Global biochemical cycles, Vol. 8, No. 1, Pages 103-116.

G.H. Haug, R. Tiedemann, R. Zahn, A.C. Ravelo (2001): Role of Panama uplift on oceanic freshwater balance. Geology, Vol. 29, Pages 207-210.

H. Ren, D.M. Sigman, A.N. Meckler, B. Plessen, R.S. Robinson, Y. Rosenthal, G.H. Haug (2009): Foraminiferal Isotope Evidence of Reduced Nitrogen Fixation in the Ice Age Atlantic Ocean. Science, Vol. 323, Pages 244-248.

D.M. Sigman, K.L. Casciotti, M. Andreani, C. Barford, M. Galanter, J.K. Bhlke (2009): A Bacterial Method for the Nitrogen Isotopic Analysis of Nitrate in Seawater and Freshwater. Analytical chemistry, Vol. 73, No. 17. Pages 4145-4153.

D.M. Sigman, S.L. Jaccard, G.H. Haug (2004): Polar ocean stratification in a cold climate. Nature, Vol. 428. Pages 59-63.

7.10

New prospects in ICDP research: investigating the subsurface biosphere in Lake Potrok-Aike sediments

A. Vuillemin[1], D. Ariztegui[1], J. Pawlowski[2], S. Templer[3] and the PASADO Scientific Team

[1] *Section of Earth & Environmental Sciences, University of Geneva, 13 rue des Maraîchers, 1205 Geneva, Switzerland (aurele.vuillemin@unige.ch)*
[2]*Section of Biology, University of Geneva, 30 quai Ernest Ansermet, 1211 Geneva, Switzerland*
[3]*Massachusetts Institute of Technology, Massachusetts Institute of Technology, 77 Massachusetts avenue, 02139 Cambridge, USA*

Microbial activity on recent sediments is fully recognized as a major player in lithification processes. These omnipresent organisms have the capacity of catalyzing and enhancing diagenetic reactions even in extreme environments from the very surface of the sediments to as deep as 4.5 km below the water column. Living bacterial communities have been tracked down into deep sediments and even into the deeper basaltic sub-seafloors. Although the distribution and diversity of microbes in marine sediments through depth have been studied for some years already, there is a lack of these investigations in the lacustrine realm.

Furthermore, geomicrobiology studies in modern lakes allow taking a closer look into early diagenetic processes linked to microbial activity in subrecent sediments. The foci of most of these studies, however, have been either very shallow sediments and/or the water column.

More than 500 meters of sedimentary cores were retrieved from Lake Portok Aike, a crater lake located in Southern Patagonia within the framework of the ICDP-sponsored PASADO project (Potrok Aike Maar Lake Sediment Archive Drilling Project). A 100 meters long core was dedicated to geomicrobiology sampling, allowing the inspection of undisturbed deep lacustrine sediments. Special windows were cut in the liners for direct sampling under the most sterile conditions possible immediately after core recovery. In situ ATP measurements are used as indication of living organisms within the sediments. Various samples were chemically fixed and/or frozen for methane determination, bacterial cell counting, DGGE (molecular fingerprinting technique) and cell cultivation.

In situ ATP data reveal a constant low microbial activity below 40 m sediment depth whereas three main peaks appear at 34, 10 and 5 meters respectively. Studying the microbial community based on 16S rDNA, we identified a broad, but conserved diversity pattern in the older sediments. In contrast, the diversity seems to decrease and change dramatically in the upper section. A preliminary interpretation of these results suggests that each ATP peak correlates with microbial community interphases. The latter together with the negative correlation between activity and diversity may indicate that nutrients are systematically depleted through bacterial activity cycles since each individual community may be at least partially fed by the metabolic products of the overlying community. Adaption becomes necessary for communities evolving in environments with decreasing trophic state.

The integration of these dataset with ongoing multiproxy studies in the same record will bring new light into microbial activity in lacustrine systems and their role on various diagenetic processes.

8. Geoscience and Geoinformation – From data acquisition to modelling and visualisation

Nils Oesterling, Adrian Wiget, Massimiliano Cannata, Erich Zechner

Swiss Geological Survey; Swiss Geodetic Commission; Swiss Geotechnical Commission; Swiss Geophysical Commission; Swiss Hydrogeological Society

8.1

GeoShield: a server side user permissions management to OGC services

Milan Antonovic

Institute of Earth Sciences – SUPSI

GeoShield is a project born to offer a centralized way to define security access-control to geo-services. It acts like a proxy, intercepting all the communications between clients and OGC compliant services (WMS, WFS, WPS, SOS).

GeoShield is able to manage users and groups, it handles authentication and privileges settings among groups and registered services. It is capable to analyse requests applying the filters setted to the user and manipulating the response.

For example handling WMS security, with GeoShield we can:
- define access privilege for each layer provided by the service,
- specify if a layer can be viewed or not,
- define geometrical extent of view permission.

All privileges on single layers are based on Common Query Language (CQL) filters, that allow interesting combination of permissions definition that operate in a hidden way to end-user.

Technical info
- The core of GeoShield is written in Java and rely on GeoTools.
- The database used for storing data is PostgreSQL.
- Authentication method is the “HTTP Authentication: Basic Access Authentication”, that guarantee compatibilities with most of the clients (like uDig, ArcGis, Google-Earth, etc.)
- Web interface build with ExtJS and OpenLayers

REFERENCES

GeoShield - http://istgeo.ist.supsi.ch/site/projects/geoshield
OGC (Open Geospatial Consortium) - www.opengeospatial.org
Geotools - http://geotools.codehaus.org/
ExtJs - extjs.com
OpenLayers - openlayers.org

8.2

Preliminary 3D fault model of the European geothermal site (Soultz-sous-Forêts, France)

Baillieux Paul[1], Schill Eva[1]

[1]*Laboratoire de Géothermie, Université de Neuchâte, Rue Emile Argand 11, CH-2009, Neuchâtel, Suisse (paul.baillieux@unine.ch)*

The geothermal resources at the European test site at Soultz-sous-Forêts are strongly related to approximately N-S striking normal fault systems (e.g. Bächler, 2003). Fluid circulation in general and in particular along fault systems is a very effective heat transport mechanism compared to conductive heat transport. In the areas of Landau (Germany) and Soultz (France), fluid convection has been used to explain the temperature distribution at depth. In the case of Landau, fluid convection has been simulated in a vertical fault in order to explain the distribution of relatively warm and cold zones along the Omega-fault (Bächler et al. 2003).

In the project "Geothermal resources of Rhineland-Palatine" (Schill et al., 2007, Schill et al., 2009), geological 3D models were performed for the areas Bad Bergzabern, Landau, and Speyer. It has been shown that the major thermal anomalies in the Rhine valley are related to horst structures. The inversion of the gravity data in the Soultz area reveals a low density anomaly, which coincides with the Soultz horst structure. Such low density can be related to high porosity. 2D Magnetotelluric measurements across the Soultz horst reveal a high electric conductivity in the western part of the horst between the Soultz and Kutzenhausen faults at the top granite. High electric conductivity can be related the geothermal brine with mean resistivity of about 0.1 Ohm m.

In order to investigate the formation of these types of geothermal reservoirs, a 3D geological model is set up using seismic reflection profiles to describe the structures in detail (Figure 1). Implicit 3D geological modeling provides a powerful tool extrapolate complex fault geometries derived from 2D cross sections such as seismic profiles and borehole data to unknown parts of the model, (e.g. Renard and Courrioux, 1994).

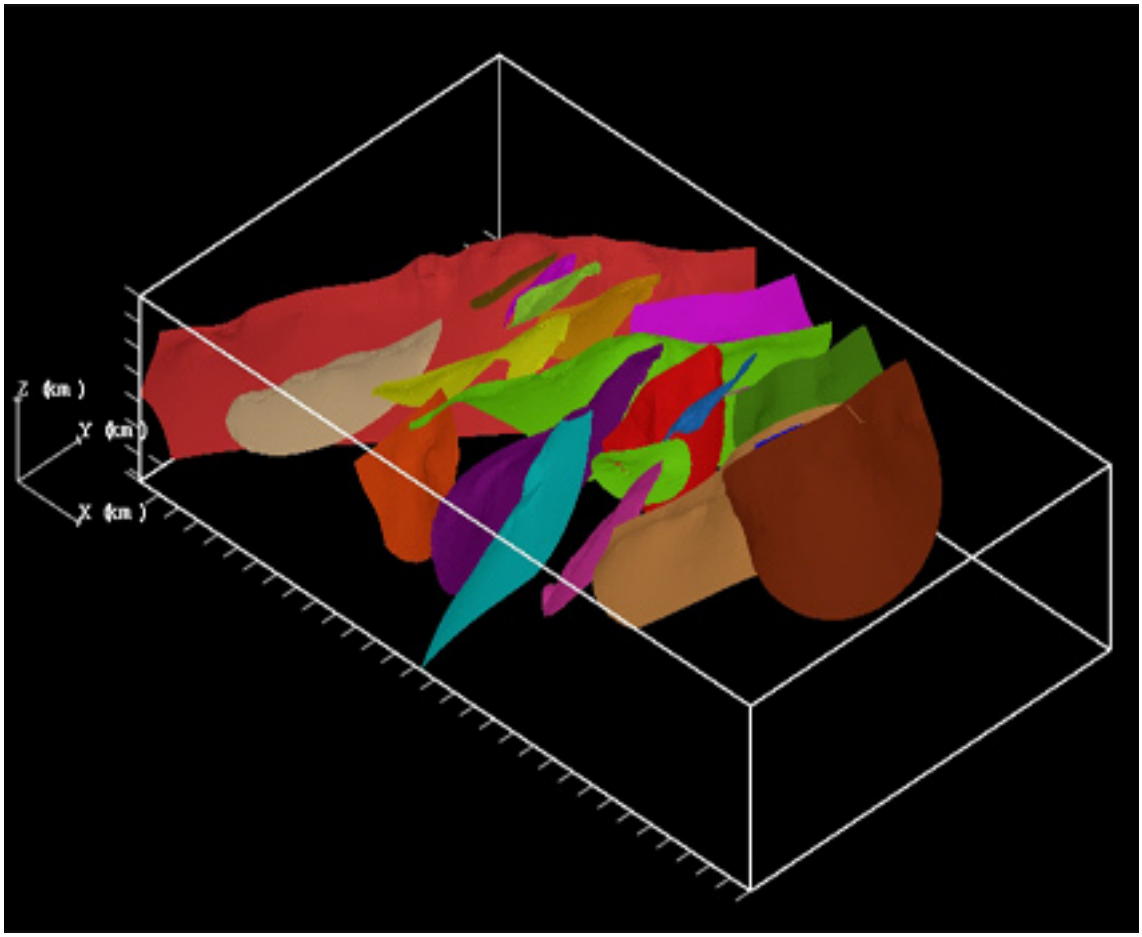

Figure 1: Preliminary 3D Model of the Fault Network at Soultz

The general aim of this study is to investigate the distribution and formation of permeability in these horst structures. This will be accomplished by meshing the geological regional 3D model for numerical simulation. A geodynamic model will established using different observables in the horst structure, such as the temperature anomaly, distribution of faults, fractures and porosity, and the specific morphological setting of a horst in the Rhine valley. In a second part of the project, the influence of the orientation small-scale structures such as the internal morphology of faults on the fluid dynamics will be investigated.

REFERENCES

Bächler, D., Kohl, Th., Rybach, L. 2003: Impact of graben-parallel faults on hydrothermal convection - Rhine Graben case study, Physics and Chemistry of the Earth, 28, 431-441.

Renard, P. & Courrioux, G. 1994: "3-Dimensional geometric modeling of a faulted domain – the soultz-horst example (Alsace, France)." Computers & Geosciences 20(9): 1379-1390.

Schill, E., Kohl, Th., Wellmann, J. F. 2007: First results of the Geothermal Resource Analysis in Rhineland-Palatine, First European Geothermal Review, Geothermal Energy for Electric Power Production, October 29-31, 2007, Mainz, Rhineland Palatinate, Germany, Abstracts and Papers.

Schill, E., Kohl, Th., Baujard, C., Kümmritz, J., Wellmann, J. F., 2009: Geothermischer Ressourcenatlas Rheinland-Pfalz – Süd- und Vorderpfalz. Report for the Ministerium für Umwelt, Forsten und Verbraucherschutz Rheinland-Pfalz, February, 2009

8.3

Converting geological maps to vector datasets – Completing the National Geological Information

Baland Pauline[1] & Möri Andreas[1]

[1]*Federal Office of Topograpy swisstopo, Swiss Geological Survey, Seftigenstrasse 264, CH-3084 Wabern (Pauline.Baland-Renaud@swisstopo.ch)*

The Swiss Geological Survey (SGS) has been producing geological maps for more than 80 years. Their main product is the Geological Atlas of Switzerland 1:25'000 (GA25). About 50% of the 220 map sheets are finished and available in printed and raster formats. Because the demand for geological vector data has increased strongly in recent years, the SGS started to convert the existing geological maps into vector datasets.

Depending on the available source format, one of two techniques is applied to convert map data into a GIS-format:

1) "Method Sion": Maps available "only" in raster format are directly vectorised in a GIS environment. This method was developed in cooperation with the Centre de recherche en environnement alpin (CREALP) and the actual transformation is performed at the Institute of Geomatics and Risk Analysis of the University of Lausanne (IGAR)

2) "Method Vallorbe": For recently printed maps, Adobe Illustrator vector data are available. Using these data as an input, "cartographic" data are converted by the aid of Avenza-Mapublisher to attributed GIS-data. This method is being developed in collaboration with the Swiss Geotechnical Commission.

Both methods are equivalent and are based on the geological data model, which is developed in a separated project (cf. Strasky et al., this volume). Presently about 40% of the existing maps of the GA25 (about 50 maps) were already converted. The "Method Sion" is now implemented by the SGS also on other published maps with different scales.

Since the SGS is not able to solely finance the entire vectorisation, collaboration with cantons and insurance companies has been initiated. This model of financing works quite well, but , the SGS is subject to the priorities and resources of the specific institutions.

The overall objective of the SGS is to build a Geographic Information System, which provides seamless vector datasets of Switzerland. To reach this aim, one of the main tasks will be to geometrically and semantically harmonise the existing vector datasets. The difficulty of this task is increased by the various "quality" of each map. During the 80-year period of map production, the scientific knowledge has changed many times and therefore the geological interpretation in the maps as well. The two methods are currently in full use and well integrated. Furthermore, constant updating of the applied methods ensures high data quality. These data are the basis for the future growth of the Geological Information System of Switzerland.

8.4

Risk, measured risk aversion and individual characteristics

Baruffini Moreno[1]

[1]*Istituto Scienze della Terra IST-SUPSI, C.P. 72, CH-6952 Canobbio (ist@supsi.ch)*

Risk and uncertainty play a key role in everyday life: during the past several years the world has witnessed some unprecedented disasters that heavily crushed societies and living systems.
Individuals, institutions, and communities have the ability to deflect, withstand, and rebound from serious shocks in terms of the course of their ordinary activities or through ingenuity and perseverance in the face of a crisis.
Is therefore very important to record and estimate risk aversion.

What is the impact of contexts on willingness to take risks? How do risk perception changes hazard perception and thereby risk?

Unfortunately this task is still extremely difficult: the individual behaviours depends on a lot of characteristics with elicitation bias, preference reversal and so on.
Using a question that asks about willingness to take risks (on a eleven points scale) we performed some tests on a cohort composed by young students.
Using questions about their risk perception in specific domains, as car driving or training, we analyzed the risk aversion and the impact of context.
We finally validated results though a lottery question for an hypothetic investment.

Aiming to improve our understanding of risk perception and how to represent it we found some evidences: distribution to take risks is quite heterogenic across individuals, females and old aged people are more risk averse than males and young people, a general risk question can actually be used to model a general risk behaviour.

The initial results, although still rough, can be very useful to represent actual risk aversion across a society or a group and can be used to validate risk management studies in the field of natural or technological hazards.

REFERENCES

Caliendo, M., Fossen, F. and Kritikos, A. 2007: Risk attitudes of nascent entrepreneurs: new evidence from an experimentally-validated survey. Discussion papers DIW Berlin.

Darmstadt University of Technology, Institute WAR; University of Bern, Department of Geography, Applied Geomorphology and Natural Risks, Spatial planning and supporting instruments for preventive flood management, Technische Universität Darmstadt, Darmstadt/ Bern

Dohmen, T. et al. 2005: Individual risk attitudes: new evidence from a large, representative, experimentally-validated survey. Discussion papers DIW n.511, Berlin.

Hartog, J., Ferrer-i-Carbonell, A. and Jonker, N. 2002: Linking measured risk aversion to individual characteristics. KYKLOS Vol. 5 - 2002 - Fasc. 1, 3-26.

8.5

Systematic analysis of natural hazards along infrastructure networks using a GIS-tool for risk assessment

Baruffini Mirko[1] & Thüring Manfred[1]

[1]*Istituto Scienze della Terra IST-SUPSI, C.P. 72, CH-6952 Canobbio (ist@supsi.ch)*

Infrastructure vulnerability is a raising topic of interest in the scientific literature for both the general increase of unexpected events and the extremely importance that certain links play in solving everyday needs.
In fact, due to the topographical conditions in Switzerland, the highways and the railway lines are frequently exposed to natural hazards as rockfalls, debris flows, landslides, avalanches and others.

To mitigate these associated losses, both traditional protective measures and land-use planning policies are to be developed and implemented to optimize future investments.
This asks for a high level of surveillance and preservation along the transalpine lines. Efficient protection alternatives can be obtained consequently considering the concept of integral risk management.

Risk analysis, as the central part of risk management, has become gradually a generally accepted approach for the assessment of current and future scenarios (Loat & Zimmermann 2004). The procedure aims at risk reduction which can be reached by conventional mitigation on one hand and the implementation of land-use planning on the other hand: a combination of active and passive mitigation measures is applied to prevent damage to buildings, people and infrastructures.

With a Geographical Information System adapted to run with a tool developed to manage Risk analysis it is possible to survey the data in time and space, obtaining an important system for managing natural risks.

As a framework, we adopt the Swiss system for risk analysis of gravitational natural hazards (BUWAL 1999). It offers a complete framework for the analysis and assessment of risks due to natural hazards, ranging from hazard assessment for gravitational natural hazards, such as landslides, collapses, rockfalls, floodings, debris flows and avalanches, to vulnerability assessment and risk analysis, and the integration into land use planning at the cantonal and municipality level. The scheme is limited to the direct consequences of natural hazards.

Thus, we develop a system which integrates the procedures for a complete risk analysis in a Geographic Information System (GIS) toolbox, in order to be applied to our testbed, the Alps-crossing corridor of St. Gotthard.
The simulation environment is developed within ArcObjects , the development platform for ArcGIS. The topic of ArcObjects usually emerges when users realize that programming ArcObjects can actually reduce the amount of ripetitive work, streamline the workflow, and even produce functionalities that are not easily available in ArcGIS. We have adopted Visual Basic for Applications (VBA) for programming ArcObjects. Because VBA is already embedded within ArcMap and ArcCatalog, it is convenient for ArcGIS users to program ArcObjects in VBA.

Our tool visualises the obtained data by an analysis of historical data (aerial photo imagery, field surveys, documentation of past events) or an environmental modeling (estimations of the area affected by a given event), and event such as route number and route position and thematic maps.

As a result of this step the record appears in WebGIS. The user can select a specific area to overview previous hazards in the region. After performing the analysis, a double click on the visualised infrastructures opens the corresponding results.
The constantly updated risk maps show all sites that require more protection against natural hazards.

The final goal of our work is to offer a versatile tool for risk analysis which can be applied to other situations. Today our GIS application mainly centralises the documentation of natural hazards. Additionally the system offers information about natural hazard at the Gotthard line.
The initial results of the experimental case study shows how useful a GIS-based system can be for effective and efficient disaster response management.
In the coming years our GIS application will be a data base containing all information needed for the evaluation of risk sites along the Gotthard line.
Our GIS application can help the technical management to decide about protection measures because of, in addition to the visualisation, tools for spatial data analysis will be available.

We present the concept and current state of development and an application to the testbed, the Alps-crossing corridor of St. Gotthard.

REFERENCES

Bründl M. (Ed.), 2009 : Risikokonzept für Naturgefahren - Leitfaden. Nationale Plattform für Naturgefahren PLANAT, Bern. 416 S.

BUWAL 1999: Risikoanalyse bei gravitativen Naturgefahren - Methode, Fallbeispiele und Daten (Risk analyses for gravitational natural hazards). Bundesamt für Umwelt, Wald und Landschaft (BUWAL). Umwelt-Materialen Nr. 107, 1-244.

Loat, R. & Zimmermann, M. 2004: La gestion des risques en Suisse (Risk Management in Switzerland). In: Veyret, Y., Garry, G., Meschinet de Richemont, N. & Armand Colin (eds) 2002: Colloque Arche de la Défense 22–24 octobre 2002, dans Risques naturels et aménagement en Europe, 108-120.

Maggi R. et al, 2009: Evaluation of the optimal resilience for vulnerable infrastructure networks. An interdisciplinary pilot study on the transalpine transportation corridors, NRP 54 “Sustainable Development of the Built Environment”, Projekt Nr. 405 440, Final Scientific Report, Lugano

8.6

Challenges for geological surveys in geological 3D model building and validation

Baumberger Roland & Oesterling Nils

Swiss Geological Survey, Federal Office of Topography swisstopo, Seftigenstrasse 264, CH-3084 Wabern, Switzerland
Contact: roland.baumberger@swisstopo.ch

Geological 3D models are always wrong to some extent. Therefore, while building up geological 3D models, special emphasis has to be made on efforts concerning data quality management, data assessment and model validation. In this context, the Swiss Geological Survey (SGS) assumes a special position, since its mission regarding geological 3D modelling is legally based. According to the federal law on geoinformation (GeoIG) and the federal act for the SGS (LGeolV), the SGS has to provide geological data and information to the federal administration and to third parties in analogue or digital formats. Additionally, the SGS is in charge of offering extensive geological data and therefore wants to build up national, regional and local geological 3D models at different resolutions and scales.

While producing the Geological Atlas of Switzerland, the SGS is generally committed to a high level of quality in order to meet the scientific and cartographic standards that are either set by the SGS itself or demanded by the partners and customers. Regarding the geological 3D modelling, it is the responsibility of the SGS to build up valid, geologically correct and consistent 3D models. Furthermore, this level of quality must comply with the quality requirements of the map production.
Driven by this guidelines, the SGS faces several technical and organisational challenges: (1) the required input data for 3D modelling is widely distributed and its existence is sometimes uncertain, (2) the quality of the existing input data depends on the producer and has highly variable resolution, accuracy, conceptual geological background and reliability, (3) the purpose and scale of the data sampling varies, (4) different concepts for data management (acquisition, storage, usage) have to be integrated and (5) the technical and conceptual backgrounds of already existing 3D models are diverging.

Facing these challenges, one has to be aware that the quality, information depth and density as well as the consistency provided by a geological 3D model show a direct correlation to the quality of the data sources. The information provided can only be as good as the quality of the input data.
As a consequence, the SGS has to perform extra efforts in the fields of data standardisation and harmonisation as well as quality management. These basic steps will be covered by the data model for geological data, which is currently being built by the SGS.
From the scientific point of view, it is necessary to use the latest proven geological concepts and to follow research trends in order to successfully provide the most accurate geological models in three dimensions.
Regarding the technical aspects, the SGS must use updated approaches regarding modelling concepts, methods and workflows, data storage, data exchangeability, model validation and distribution of the 3D models.
The challenges listed above have lead to the conception of the general architecture of geological 3D modelling at the SGS (ELFERS et al., 2004, adapted by SGS). Following this approach, the large number of input data is first of all stored in appropriate storage facilities. Secondly, these data are checked, adapted, interpreted, (re-)formatted, assessed and harmonised. Thirdly, the prepared and standardised data are fed into the geological 3D modelling software, and a 3D fault model and a 3D surface model are developed iteratively. Fourthly, these two models are stored as the basic geological 3D model, from which a large number of specialized and specific 3D models may be derived (Figure 1).

To perform the aforementioned process, the SGS applies the Move software suite from Midland Valley Exploration. Model validation is also performed with Move. By providing various tools for model building and validation, the Move software allows the SGS (1) to build up valid 3D models, (2) to achieve geological consistency in three dimensions and through time as well as (3) to account for the uncertainty regarding the data quality.
Using Move2009.2, the SGS is able to manage the scientific, organisational and technical challenges it is facing in the field of geological 3D modelling.

REFERENCES

ELFERS, H. et al. (2004): Wege zur 3D-Geologie, Krefeld, 2004
MOVE2009, Midland Valley Exploration, Glasgow (UK), http://www.mve.com

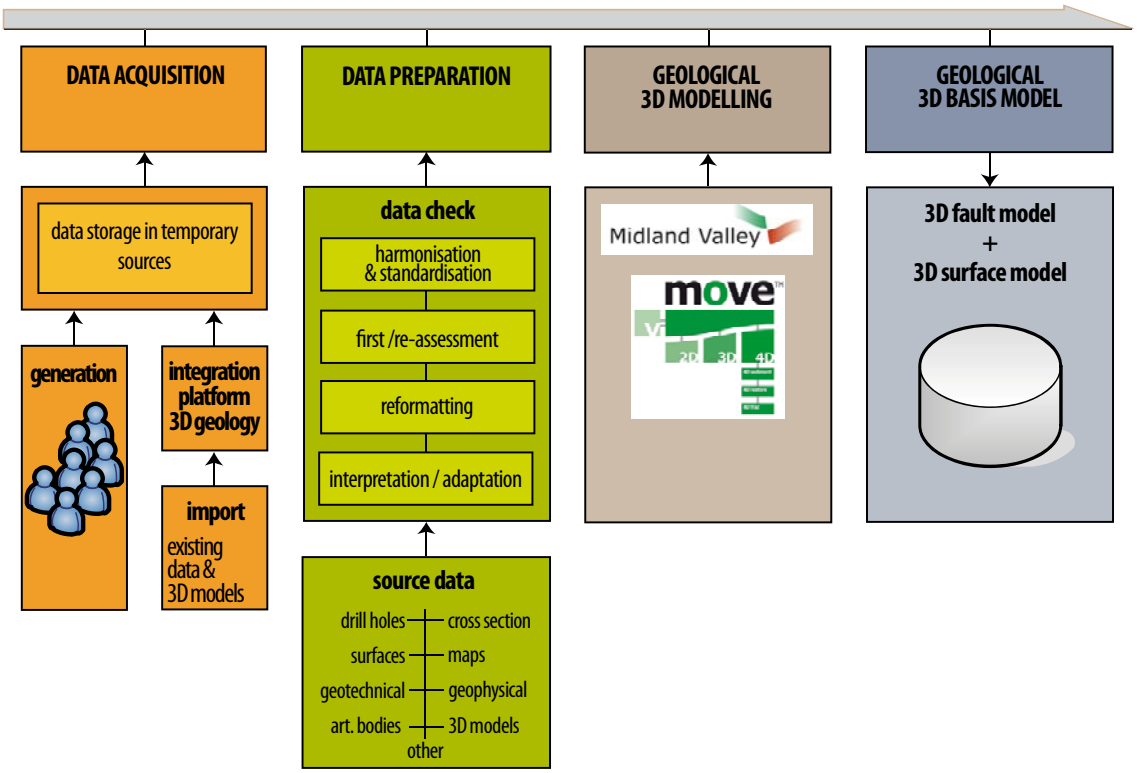

Figure 1: The architecture of the process of geological 3D modelling at the SGS (based on ELFERS et al. (2004), adapted by SGS)

8.7

Overview of available geoscience data in Switzerland

Beres Milan & Kühni Andreas

Swiss Geological Survey, Federal Office of Topography swisstopo, Seftigenstrasse 264, CH-3084 Wabern (milan.beres@swisstopo.ch)

Geoscience information is made available for the purposes of recognizing and reacting to environmental problems, evaluating construction projects and natural resources, planning excursions and simply enjoying nature. Many users of this information are also producers and include various federal and state agencies, the energy industry, universities and private consulting offices. In Switzerland the production of geoscience data and information is highly decentralised, signifying a wide variety of formats, qualities, accessibilities and visualisations. Furthermore, the users commonly do not know which datasets are available, where they can be obtained and what purposes they all serve.

To meet the challenges mentioned above, the Swiss Geological Survey and its collaborators are planning to publish an overview of all available datasets in Switzerland that are relevant to earth science (Beres et al. 2008, 2009). This overview is aimed at a diverse audience (e.g. politicians, interdisciplinary professionals, researchers, teachers, students, hobby geologists, tourists) and has the following goals:

- To give an overview: eye-catching figures and short texts, which describe the dataset theory, purpose, source and production methods, are envisaged for the publication.
- To sensitise the public: as many people as possible should be made aware of how the earth sciences touch our everyday life.
- To boost public relations: with such a publication, producers of geoscience data and information can advertise to decision makers and the general public.
- To build a network: the results ought to promote contacts and collaboration among producers and users of geoscience data and information.
- To integrate datasets: an overview serves as the basis for integrating datasets in the geological information system of Switzerland (Oesterling et al. 2009).

Recent publications (Jackson 2004; Hofmann & Schönlaub 2007) show that similar goals are best achieved by creating a printed, easily understandable document.

Production of the overview comprises clearly defined tasks. Contacting the data producers and establishing collaboration are part of the initial phase. This phase also includes determining exactly who has what and choosing the optimal representation for a particular theme. Presently, the overview contains 54 themes, which are categorised into the following four basic groups:

- Earth fundamentals, e.g. tectonics, stratigraphy, bathymetry, soil types, magnetic field, gravity anomalies, topography.
- Construction and resources, e.g. hydrogeology, land use, geothermal energy, various types of rock quarries.
- Hazards and environment, e.g. earthquakes, mass movements, radon risk, groundwater quality.
- Geotourism and geological heritage, e.g. show caves, thematic hiking trails, geotopes.

The layout stipulates two pages (A4 portrait) for each theme. On the left page, the dataset, in some cases generalised, is overlain on a map of the Swiss national boundary and major lakes. In the case of point data, a simplified tectonic map serves as an additional background. Logos and an extract of a more detailed dataset or an explanatory figure are located on the lower half of this page. On the right page, the title, the theme's category, explanatory text, data sources/ownership and a carefully chosen diagram or photograph are included. Since Switzerland is a multilingual country, a column of text in German and a second column of the same text in French are necessary. Providing a summary of the text in English would be particularly helpful for international readers.

In summary, there are many reasons to produce an attractive and informative overview of the available geoscience datasets in Switzerland. Such an overview not only will illustrate the highlights of the country's unique natural features, but it will also sensitise a broad audience and strengthen networking among members of the Swiss geo-scene. These reasons make it an important contribution to the planned geological information system of Switzerland.

REFERENCES

Beres, M., Kühni, A. & Schindler, U. 2008: Bringing geothematic maps to the public. Abstract of the 33rd International Geological Congress, August 6-14, Oslo, Session IEI-14.

Beres, M., Kühni, A. & Schindler, U. 2009: The geothematic atlas of Switzerland: An overview of geologically relevant maps for everyone. Extended Abstract of the 6th European Congress on Regional Geoscientific Cartography and Information Systems, Vol. II, June 9-12, Munich, 233-235.

Hofmann, T. & Schönlaub, H. P. (Eds.) 2007: Geo-Atlas Österreich, Die Vielfalt des geologischen Untergrundes. GBA, Böhlau, Vienna, 112 pp.

Jackson, I. (Ed.) 2004: Britain beneath our feet. BGS Occasional Publication 4, Keyworth, Nottingham, 120 pp.

Oesterling, N., Baumberger, R., Beres, M., Kühni, A. & Kündig, R. 2009: The geological information system Switzerland. Extended Abstract of the 6th European Congress on Regional Geoscientific Cartography and Information Systems, Vol. I, June 9-12, Munich, 254-256.

8.8

Exposure-based risk assessment for tephra accumulation: the example of Cotopaxi volcano (Ecuador)

Biass Sébastien[1], Parmigiani Andrea[1], Dell'Oro Luca[2], Senegas Olivier[2] & Bonadonna Costanza[1]

[1]*Départment de Minéralogie, Rue de Maraîchers 13, CH-1205 Genève, Switzerland (biasse3@etu.unige.ch)*
[2]*UNOSAT, International Environment House, Chemin des Anémones 11-13, CH-1219 Châtelaine, Switzerland*

Tephra is a major product of explosive eruptions and its dispersal and accumulation can cause significant disruption of human activities. Due to its capacity to reach widespread areas, various effects on the surrounding communities need to be considered. These can be classified as physical aspects (e.g. collapse of buildings, breakdown of electrical systems), economical aspects (e.g. damage to crops, death of cattle, effects on tourism), functional aspects (e.g. blockage of roads, airports and air traffic) and health aspects (e.g. breathing of fine particles, eye and skin irritation) (e.g. Blong 1984).

Due to the constant increase of population density around volcanoes (Sibert and Simkins 1994), governments and planners require knowledge of both the expected hazard and the elements at risk in order to produce efficient land-use and emergency planning prior a crisis. In this framework, we present a new methodology designed to help decision-makers to deal with tephra fallout. First, hazard maps are compiled based on the TEPHRA2 analytical model (Bonadonna et al. 2005). Second, exposure-based risk maps are produced by combining hazard maps and urban elements through GIS-based fuzzy modelling. Given that precise and up-to-date geographical data are typically difficult to access, we based our exposure assessment on free and global datasets, which include information on buildings, vegetation, agriculture, airports, road network and critical infrastructures.

We have tested our methodology on Cotopaxi volcano (Ecuador), which is located 60 km south of Quito and threatens a highly populated valley. We have produced exposure-based risk maps accounting for different eruption magnitudes typical of the last 2000 years of volcanic activity of Cotopaxi volcano.

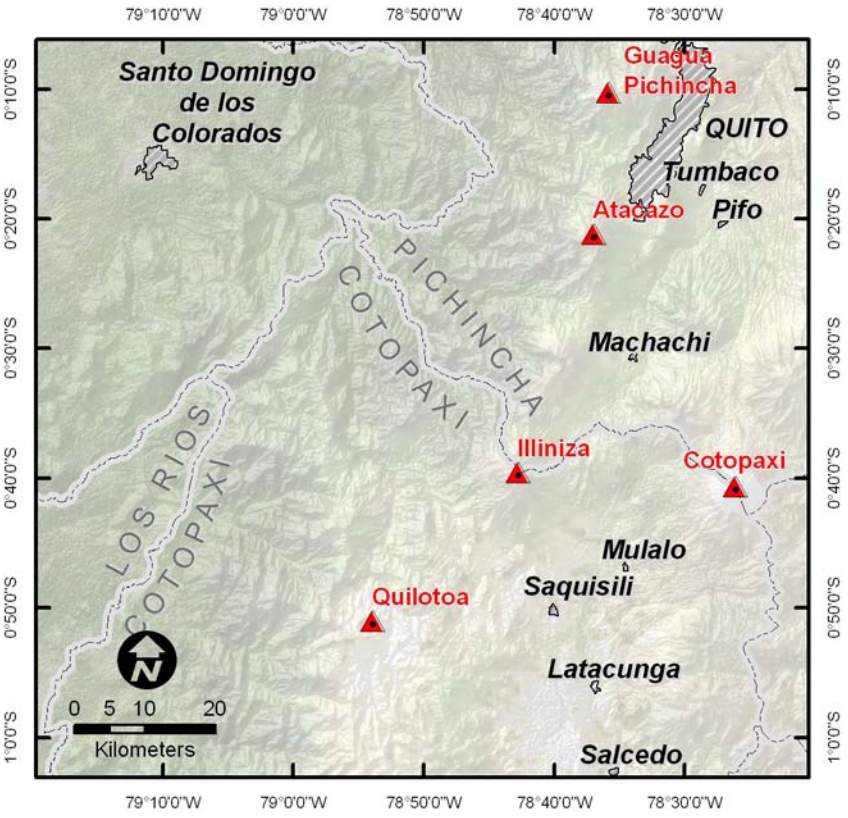

Figure 1. Situation map with main populated areas and principal volcanoes.

REFERENCES

Bonadonna, C., Connor, C.B., Houghton, B.F., Connor, L., Byrne, M., Laing, A., Hincks, T.K. 2005: Probabilistic modelling of tephra dispersal: Hazard assessment of a multiphase rhyolitic eruption at Tarawera, New Zealand, Journal of Geophysical Research, 110, B03203, doi:10.1029/2003JB002896.

Blong, R.J. 1984: Volcanic hazards: a sourcebook on the effects of eruptions. Academic Press, Sydney.

Simkin, T., Siebert, L. 1994: Volcanoes of the world, Geoscience press Inc. in association with Smithsonian Institution, 1-349.

8.9

GIS-based method for groundwater management and protection: geotypes serving 3D applications

Bilgot Séverine[1], Parriaux Aurèle[1]

[1] *EPFL ENAC IIC GEOLEP, Station 18, CH-1015 Lausanne (severine.bilgot@epfl.ch)*

Sustainable management of underground natural resources is more and more a worthwhile topic. In particular, worrying about groundwater protection becomes imperative. Taking into account the increase of incompatibilities between water conservation and the use of other underground resources, the Geolep laboratory brought one of its research axes around to new methods for groundwater resources assessment and management.
As these methods have to be as transparent as possible, we implemented a GIS to use standardized protocols to realize new maps of groundwater protection areas and resources index and, in a second step, to determine where it should be possible to install geothermal heat pumps without endangering drinkable water resources (OFEV, 2009).
These methodologies are both based on the use of the geotypes, which is a new classification for geological formations (Parriaux and Turberg, 2007); it involves the use of genetic standards for loose material (e.g. lodgement till) and lithologic standards for hard rock (e.g. sandstone). Forty-one geotypes and their properties in relation to groundwaters were thus integrated in a GIS and completed with geophysical and boreholes data.
The achievement of the new groundwater protection areas maps is currently in the pipeline for the whole canton of Vaud, while the implementation of the new methodology forgeothermal heat pump admissibility mapping (riquiring the building of a 3D geological model) is still being tested.

REFERENCES

OFEV : Exploitation de la chaleur tirée du sol et du sous-sol. Aide à l'exécution destinée aux autorités et aux spécialistes de géothermie. L'environnement pratique n°0910. Office fédéral de l'environnement, Berne, 51 p, 2009.

A. Parriaux and P. Turberg, Les géotypes, pour une représentation géologique du territoire, Tracés, Nr. 15/16, pp. 11-17, 2007.

8.10

A pseudo-genetic approach for the stochastic generation of karstic networks

Andrea Borghi[1], Philippe Renard[1] and Sandra Jenni[1]

[1] *University of Neuchâtel, Stochastic Hydrogeology Group, 11 Rue Emile Argand CP 158 2000 Neuchâtel, Switzerland. andrea.borghi@unine.ch, philippe.renard@unine.ch*

[1] *Schlumberger Water Services, Immeuble Madeleine D, 92057 Paris la Défense Cédex France, sjenni@la-defense.oilfield.slb.com*

Modelling karst systems is a challenge because of their extreme spatial heterogeneity which strongly influences the hydraulic and solute transport behaviour. For this reason it is necessary to take into account both the conduit system and the matrix. It becomes then necessary to develop methods to generate realistic karstic conduit systems even if their position is not known accurately.
The method presented in this poster simulates karst conduit systems taking into account on one hand field observations (that may be indirect) and on the other hand the conceptual geological knowledge controlling the conduit structures that might be displayed in a given geological environment.

The suggested methodology is based on the following steps:

1. 3D regional geology modelling: the position of the carbonate formations in 3D with respect to the other non karstifiable formations controls the locations where the karstic network can develop;
2. simulation of the internal properties of the karstifiable formation (e.g. fracturation, stratification joints): the internal properties of the formation strongly influence the local shape of the conduits;
3. identification of the recent or paleo hydrodynamic controls at a regional scale: this is achieved by identifying recharge and discharge mechanisms, location of the punctual or diffuse outlets and inlets (springs, dolines, shallow-holes etc), as it is known that the type of recharge or discharge controls the type of network that can develop;
4. for each possible phase of karstification:
   a. extrapolation of the corresponding paleo base level and simulation of the karstic conduits from the topographic surface toward the base level using a fast front tracking method (level set) and random walker method;
   b. using the same front tracking method, connect the paths that have been created in the unsaturated zone to the outlet through the saturated zone; in both steps a and b, the paths follow the geological structure and are controlled on one hand by the local heterogeneities generated in step 2 and on the other hand by the flow conditions;

The final result is a 3D karstic network that is controlled by the regional geology, the local heterogeneities and the regional flow conditions. The network can then be used to model flow and transport. Several levels of randomness can be considered (uncertainty on large scale geological structures, local heterogeneity, position of possible inlets and outlets, phases of karstification) allowing to investigate the uncertainty on the structure of the network and its consequences.

Compared to other techniques, this method presents the advantage to be fast, to account for the main factors controlling the 3D geometry of the network, and to allow conditioning from field observations when available.

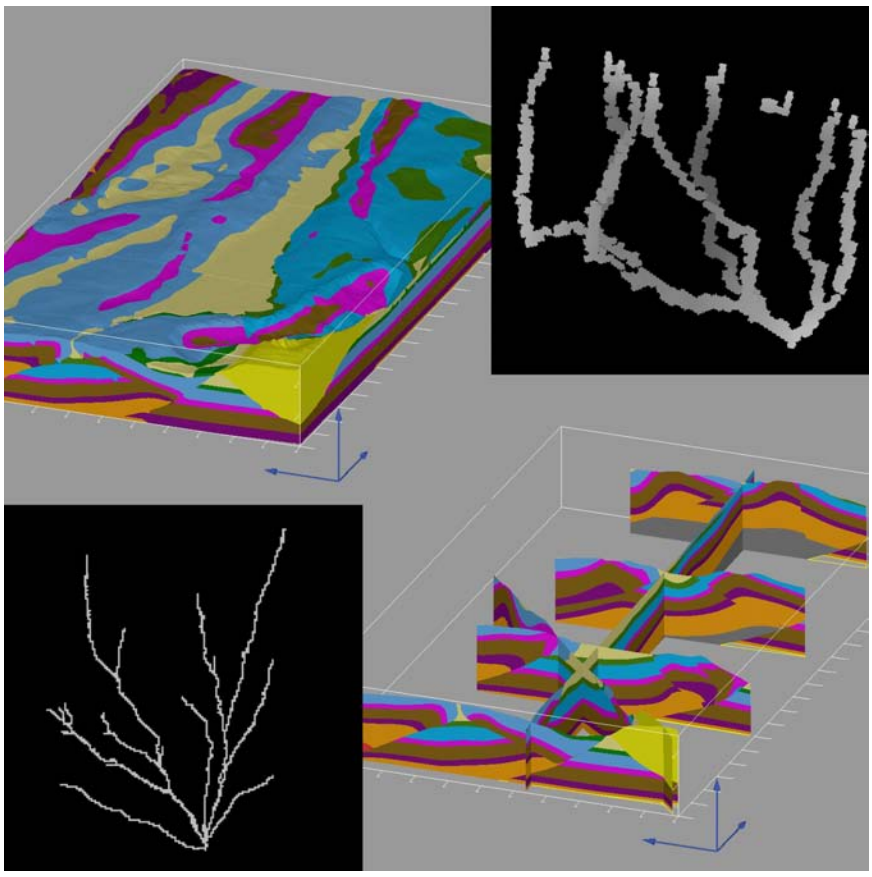

Figure 1.a) 3D geological model (volume view) b) 3D karstic network in a regular mesh c) 2D karstic network in 2D regular mesh d) 3D geological model (cross sections)

8.11

SAPHYR, the Swiss atlas of physical properties of rocks

Bruijn Rolf[1], Zappone Alba[1], Burlini Luigi[1], Tripoli Barbara[1], Holliger Klaus[2], Burg Jean-Pierre[1] & Kissling Eduard[1]

[1]ETH, Department of Earth Sciences, Sonneggstrasse 5, CH-8092 Zürich (rolf.bruijn@erdw.ethz.ch)
[2]UNIL, Institute of Geophysics, Amphipole – UNIL SORGE, CH-1015 Lausanne

Since 2006, a multi-year project runs under the umbrella of the Swiss Geophysical Commission (SGPK), with the aim to digitize all existing data on physical properties of rocks and to link them using a geographical frame (GIS).

The aim is to make those data accessible to a wide public such as in industrial context: construction and engineering companies, geothermal investigation and extraction, etc., for land use planners: water resource, waste disposal natural hazard etc.; and finally for academic studies (integrated geophysical, geological and petrological research, research in petrophysics etc).

The physical properties of interest are density and porosity, seismic, magnetic, thermal properties, permeability, electrical properties. For the time being data from literature has been collected extensively for seismic properties and only partially for the other physical properties. Here we present the first output: a map of Switzerland with sample locations combined with contoured values of Vp, see figure 1, extrapolated to room conditions from the high pressure laboratory measurements (matrix or crack free properties). The values are reported as contours and colour-coded. A sample location map for Vs measurements is also presented. Vs analysis and data processing is ongoing work in progress. We expect to publish the results on the Atlas of Switzerland (swisstopo), hopefully by the end of 2009.

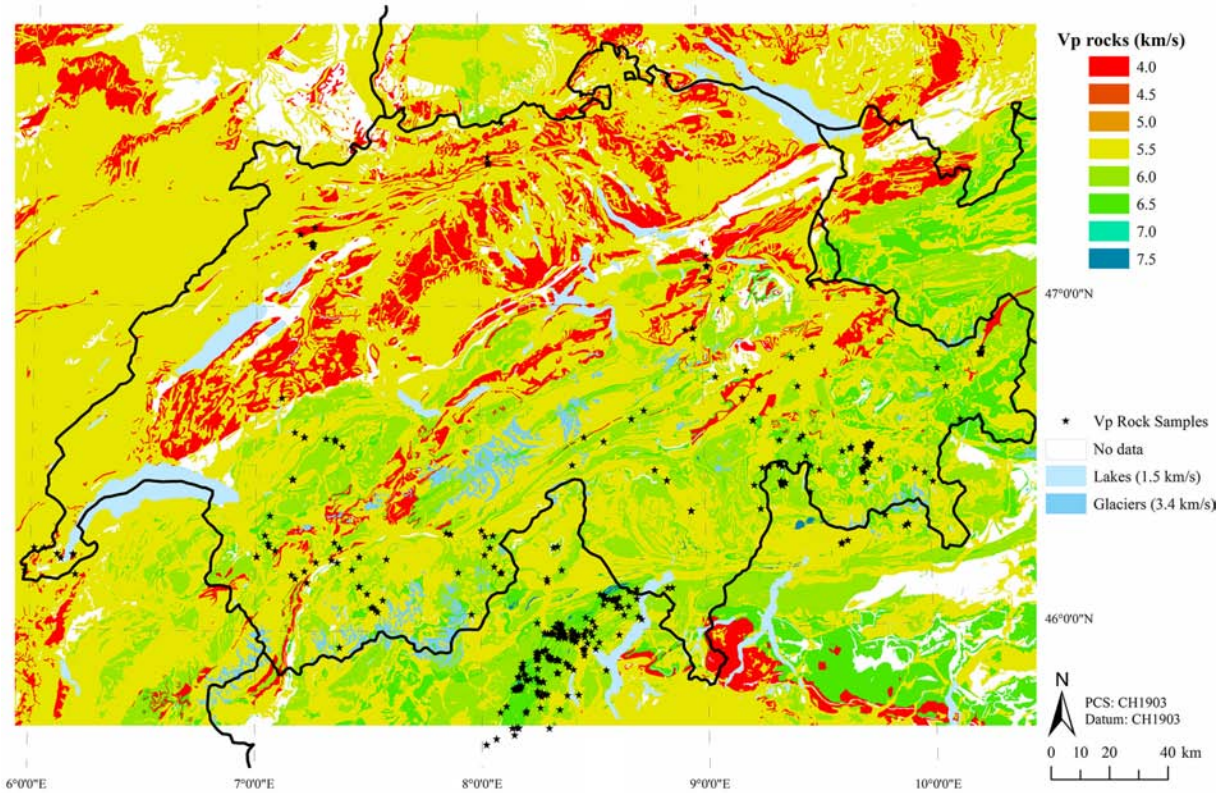

Figure 1. Map of Switzerland with compression wave velocity variations, originating from lithological heterogeneities. Vp colour groups were derived from individual Vp measurements on typical rock types found in the Alps. Locations of rock samples are marked by a black star. Literature values for water and ice are used to represent lakes and glaciers. Map polygons were taken from 'Digitale Geotechnische Karte der Schweiz 1:500000', produced by SGTK.

8.12

IstSOS: Sensor Observation Service in Python

Massimiliano Cannata, Milan Antonovic

Istituto Scienze della Terra, IST-SUPSI CH-6952 Canobbio, Tel. +41 (0)58 666 62 09

Approving the new federal low about goinformation (RS 510.62), the Switzerland gave a great impulse to the establishment of a national spatial data infrastructure, which in agreement with the European Commission directive INSPIRE (2007/2/CE), will be based on geo-services.

This approach has the advantage to give, local administration and data maintainer, the freedom to choose the desired formats, software and data model but impose the provision of the required data throughout a standard Web service. This simplify the process of data gathering (the user get the data on demand and not anymore the maintainer provide them on request) providing the basis for a real and practical accomplishment of the so much desired data interoperability.Geoscientists are particularly interested in this type of interoperability: in fact a considerably expensive common phase of most of the geo-projects involves the acquisition and integration of data in order to be further on processed and analyzed.

While some of the Geographical Web Services, like WMS and WFS, are today widely diffused and applied, others like SOS (Sensor Observation Service) are still a work in progress and need some revision for their correct application.

In order to investigate and provide such a kind of SDI for scientists, the IST (Istituto Scienze della Terra) is developing a new, fully OGC compliant, SOS in Python language that is able to distribute observation data and to provide a processing environment for developing researches.

During the development phase a series of considerations and practical solutions has been studied. As a conclusion, at this stage of development, the authors can underline the following open issues:

- The xml schemes used in the SOS are numerous, nested and often interchangeable. This leads to an SOS responses variable, depending on the software and the interpretation that the developer applied, and therefore a difficult automatic parsing.
- The SOS does not provide precise information on onthologies leading to misunderstanding definitions.
- The standards do not take into account the type of observation according to the sensor location (in-situ or remote), the observation type (point-wise or distributed), and the observation dynamic (static or mobile).

To override this lacks, we are developing a system that internally consider these issues still conserving the compliance with the current standard.
More information are available at: http://istgeo.ist.supsi.ch/site/projects/istsos

REFERENCES

510.62, Loi fédérale sur la géoinformation, http://www.admin.ch/ch/f/rs/510_62/index.html
OpenGIS® Sensor Observation Service (SOS), http://www.opengeospatial.org/standards/sos

8.13

Modeling heterogeneous geological reservoirs using multiple-point statistics simulations

Comunian Alessandro[1], Straubhaar Julien[1], Renard Philippe[1], Roland Froidevaux[2]

[1]*Centre for Hydrogeology (CHYN), University of Neuchâtel, Emile-Argand 11, CH - 2009 Neuchâtel (alessandro.comunian@unine.ch, julien.straubhaar@unine.ch, philippe.renard@unine.ch)*
[2]**Ephesia Consult**, *9, rue Boissonnas CH - 1227 Geneva, Switzerland (roland.froidevaux@ephesia-consult.com)*

3D models of heterogeneous geological reservoirs are important tools to understand and manage aquifers. When a conceptual geological model (analogue site, training image) of the structures is known, multiple-point statistics (MPS) (Strebelle, 2002, Mariethoz et al., 2009) can be used to simulate the reservoir geometry constrained to field observations.
The basic principles of MPS simulations consists of a sequential process visiting all nodes of the simulation grid. For each node, a conditional probability density function (cpdf) is computed using all pixel configurations within the training image (TI) and the configuration centred on the visited node in the simulation grid. This cpdf is then sampled in order to draw randomly a facies into the visited node.

In this work, we illustrate on two case studies the application of a newly developed MPS technique (Straubhaar et al, 2009). The corresponding software (Impala) is parallel and can account for the non stationarity of the geological formations.

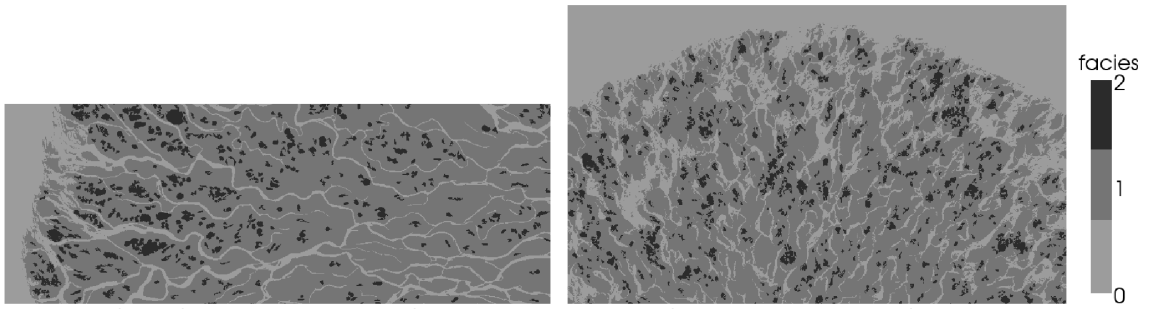

Figure 1. Left) TI of size 1501 x 501: delta of the Lena River (Russia) (ref.: Landsat 7 image, USGS/EROS project and NASA Landsat project); right) Simulated delta structure (size 1500 x 900) based on the TI on the left.

First, a 2D example with 3 facies (channels, lakes, land) is considered. A satellite image of a part of the Lena River delta is taken as a natural analogue (TI, Figure 1). The MPS technique allows to simulate similar structures with different orientations (Figure 1) in a place where no data are available. The distance to the coast, rotations, and conditioning data (in sea) are used to control the non stationarity.

MPS simulation can also be applied to reconstruct the three-dimensional structure of highly heterogeneous sedimentary deposits. This is illustrated using the Herten dataset (Bayer, 2009). The dataset contains six parallel outcrops of 16 by 7 meters recorded during the excavation of a quarry in the Rhine basin close to Basel; the facies described in the sections are used as conditioning data.

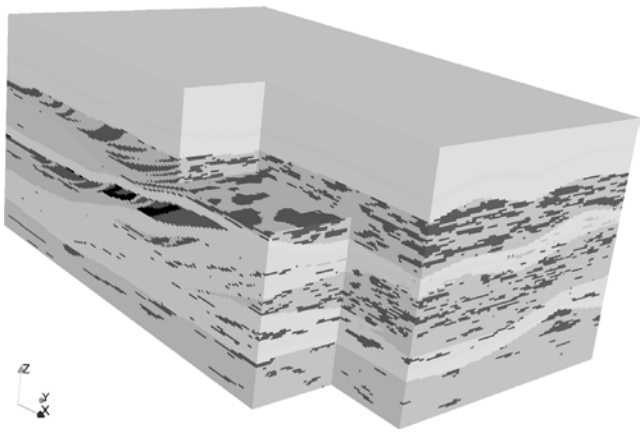

Figure 2. One simulation of the Herten aquifer analogue obtained using MPS and a hierarchical approach.

A hierarchical approach is used: the main sedimentary structures are simulated with ordinary Kriging; inside these large scale structures, small scale heterogeneities are simulated with the MPS technique. Figure 2 displays one realization of the 3D heterogeneities.

The two case studies described above illustrate how the MPS technique can be used to model realistic non stationary and highly heterogeneous structures with success. Those methods can then be applied to evaluate the impact of these heterogeneities on physical processes such as flow and transport and then help to improve management decisions in a context of uncertainty.

REFERENCES

Bayer, P. 2009: 3-D high-resolution characterization of a sedimentary gravel body for use in hydrogeological and reservoir modeling, Hydrogeology Journal, submitted.

Mariethoz, G., Renard, P. & Straubhaar J. 2009: The direct sampling method to perform multiple-points geostatistical simulations, Water Resources Research, submitted.

Straubhaar, J., G. Mariethoz, and P. Renard 2009: Multi-point reservoir modeling, International Patent nr. 2009WO-EP053614.

Strebelle, S. 2002: Conditional simulation of complex geological structures using multiple-points statistics, Mathematical Geology, 34, 1-21, 2002.

8.14

Different resolutions for different topics - the geological 3D-model of the Basel region

Dresmann Horst, Zechner Eric, Huggenberger Peter & Epting Jannis

Applied and Environmental Geology, Institute of Geology and Paleontology, Bernoullistrasse 32, CH-4056 Basel (Horst.Dresmann@unibas.ch)

Different problems related to the subsurface of an urban area such as the Basel region require detailed and up to date knowledge. Some of the most important address the use of groundwater resources for drinking water and industrial processes, the use of geothermal energy (deep and shallow), the exploration of natural resources (e.g. salt), construction of infrastructure (roads, railways or buildings in the subsurface) and earthquake hazard evaluation. Each of them has specific needs regarding a 3D-model of subsurface. In particular they need different scales of resolution to adequately represent relevant surfaces and volumes of the different thematic fields (e.g. geology, hydrology, geophysics). The presented 3D-model of the Basel region was continually developed in order to address the specific problems.

The growing complexity of 3D data requires a clear and up to date data storage concept. Ideally, the model should be easily adjustable with new data and a spatial extension, or a local refinement of the model should be possible at all time. Therefore, the aim is to develop a flexible tool, which offers the basis for the treatment of the most diverse questions in 3D spaces.

Within the scope of an INTERREG IV and a BFE (Bundesamt für Energie Switzerland) project, we started to completely revise the initial 3D-model of Basel (Zechner 2001). The main goal of these projects is to evaluate the possibilities and risks of the deeper underground (Geopotentiale), with a focus on issues related to the use of deep geothermal energy, earthquake risks and the sequestration of carbon dioxide. Therefore, the model was extended to a surface of 20 km by 30 km and to a depth of 6000 m. Data of about 9000 boreholes, 15 reflection seismic lines, as well as high-resolution DEM´s were imported. In a first step a geological 3D-surfaces-model is constructed, which contains about 20 geological horizons and all important fault structures. This surfaces-model offers the basis for a volume-model, which offers the possibility to assign various specific parameters (e.g. geophysical, hydraulical, geochemical) to a distinct body. Such a geometrically consistent and parameterised volume model serves as an ideal basis for numerical modelling approaches such as groundwater flow simulation.

To address the growing importance of urban influences to subsurface processes, models containing high resolution (1-5 m grids) surfaces are needed. Therefore, based on the presented geological 3D model of the Basel region we plan a model, which focuses on near surface objects typical for highly urbanized areas such as tunnels, water supply channels, subways, sewage system, cellars, parking garages, sites using shallow thermal energy and waste disposal sites.

REFERENCES

Zechner E., Kind F., Fäh D. & Huggenberger P. 2001: A 3D Geologic Model of the Southeastern Rhinegraben compiled on existing geologic data and geophysical reference modelling, 2nd EUCOR-URGENT Annual Workshop 2001, Abstract volume.

8.15

Use of digital terrain models and GIS for neotectonic studies: Analysing fluvial terrace morphology in northern Switzerland

Fraefel Marielle[1], Kock Stéphane[2], Schnellmann Michael[3]

[1] *ETH Zürich, Institute of Terrestrial Ecosystems, Universitätsstrasse 16, CH-8092 Zürich (marielle.fraefel@env.ethz.ch)*
[2] *SC+H AG Chur, Ringstrasse 203, CH-7000 Chur*
[3] *Nagra, Hardstrasse 73, 5430 Wettingen*

The tectonic evolution of Northern Switzerland is intensively studied by Nagra (National Cooperative for the Disposal of Radioactive Waste) in the search for a potential disposal site for nuclear waste. Tectonic stability is a key criterion for the location of a nuclear-waste repository to achieve safe and long-term containment. Recent tectonic deformation rates and associated seismic activity in northern Switzerland are very low, as shown by geodetic measurements (Nagra, 2008) and the seismotectonic record (Deichmann et al., 2000). In order to better describe the recent deformation field, we study young fluvial sediments (Niederterrasse) in the lower Aare and Rhine valleys that were deposited between ca. 32 and 11 ka ago (Bitterli et al., 2000; Kock et al., 2009). These alluvial gravel terraces record the position of the riverbed before one of several incision episodes. Due to their relatively smooth depositional surfaces, the terraces represent marker horizons for detecting tectonic movements during the last 10-30 ka. Without tectonic disturbance, their surfaces are expected to show a smooth shape and gentle downstream dip. Irregularities to this trend can be a sign for neotectonic activity.

The morphology of the Niederterrasse gravel surfaces is analysed in a GIS, using the high-resolution digital terrain model DTM-AV (Swisstopo, 2007). The individual terraces are mapped using elevation differences, slope, different hillshade illuminations and topographic relief. The projected traces of the terrace surfaces are then plotted in a longitudinal valley profile, allowing for the detection of along-stream steepness variations. The 3D orientation of the terraces is approximated using an automated planar trend function.

The results of this study help visualising the present-day position and orientation of the preserved terrace surfaces and can be analysed for effects of tectonic deformation.

The terrace distribution indicates a regional northward tilt in the lower Aare valley after the formation of the Niederterrasse gravel terraces, which is in agreement with geodetic measurements and thus seems to be ongoing today. North of the Jura mountains, in the Rhine valley between Koblenz and Basel, the terrace occurrence and dip directions give no indication of a consistent deformation pattern. This is probably due to the combination of a relatively complex accumulation and erosion history and low deformation rates. So far, no clear evidence of localised deformation around major faults could be found.

The digital terrain model analysis proves a helpful tool to systematically and reproducibly describe and interpret the morphology of fluvial terrace systems over large areas. It allows for the simultaneous investigation of the 3D shape of a large number of river terraces, the fast and reliable identification of morphological patterns, and a better differentiation of signals caused by geological processes from anthropogenic terrain modifications. While keeping in mind other possible influences on river terrace shape like sedimentary processes or data processing artifacts, the presented approach facilitates a fast and extensive investigation for the geomorphological expressions of neotectonic activity.

REFERENCES

Bitterli, T., Graf, H.R., Matousek, F., & Wanner, M. 2000: Geologischer Atlas der Schweiz: Zurzach (Blatt 1050), Erläuterungen. Bundesamt f. Wasser u. Geologie, Bern, Switzerland.

Deichmann, N., Dolfin, D.B., & Kastrup, U. 2000: Seismizität der Nord- und Zentralschweiz. Nagra Technischer Bericht, 00-05.

Kock, S., Kramers, J.D., Preusser, F., & Wetzel, A. 2009: Dating of Late Pleistocene terrace deposits of the River Rhine using uranium series and luminescence methods: potential and limitations. Quaternary Geochronology, 4: 363-373.

Nagra, 2008: Vorschlag geologischer Standortgebiete für ein SMA- und ein HAA-Lager: Geologische Grundlagen. Nagra Technischer Bericht NTB 08-04.

Swisstopo 2007: DTM-AV. geodata-news, 14, http://www.swisstopo.admin.ch/internet/swisstopo/de/home/products/height/dom_dtm-av.parsysrelated1.19059.downloadList.63245.DownloadFile.tmp/gn142007defr.pdf (accessed 07 April 2008).

8.16

Insights from two high-resolution bathymetric surveys in Swiss lakes

Michael Hilbe[1], Flavio S. Anselmetti[1], Raymond Eilertsen[2] & Louise Hansen[3]

[1]*Eawag, Swiss Federal Institute of Aquatic Science & Technology, Überlandstrasse 133, CH-8600 Dübendorf (michael.hilbe@eawag.ch)*
[2]*Geological Survey of Norway (NGU), N-9296 Tromsø*
[3]*Geological Survey of Norway (NGU), N-7491 Trondheim*

High-resolution digital terrain models (DTMs), generated by airborne laser scanning or other techniques, have been well established in Switzerland for a few years. Providing a typical horizontal resolution of a few meters or less, they are used for a variety of tasks such as geomorphological mapping or the monitoring of earth surface processes related to natural hazards. Bathymetric data (DTMs) for the Swiss lakes, however, so far do not provide a comparable level of detail due to limitations of the «traditional» survey techniques, i.e. single soundings or single-beam echosounders. Furthermore these techniques are labor-intensive and thus not suitable for monitoring programs involving frequently repeated surveys. State-of-the-art acoustic hydrographic survey systems (multibeam echosounders, swath bathymetry systems) allow a significant improvement of the horizontal resolution of subaquatic DTMs to values comparable with high-resolution terrestrial data. Such equipment was utilized for the first time in Switzerland in the framework of a pilot project started in 2007.

New data collected during two field campaigns on Lake Lucerne and on Lago Maggiore using a GeoAcoustics swath bathymetry system and accurate RTK-GPS positioning reveal a wealth of previously unknown features on the lake floor. Additionally, backscatter analysis allows for a classification of the acoustic properties of the lake floor, e.g. a differentiation between soft sediments and hard rock surfaces.

The submerged valley system of Lake Lucerne is characterized by a complex glacial morphology with a number of moraine ridges. Some of them are prominent and have been known for a long time, others are mostly covered with younger sediments and are only expressed by a low relief visible on the newly collected data. The Holocene sediments on the lateral slopes are affected by mass movements, the signatures of which can be accurately mapped and quantified. The northeastern part of Lago Maggiore is dominated by two major deltas of the Maggia, Ticino and Verzasca rivers. The slopes of these deltas are covered by ubiquitous small-scale undulating bedforms and incised channels, presumably reflecting the dynamics of river-borne turbidity currents.

As these examples indicate, the use of high-resolution bathymetric data is an appropriate and necessary approach to map otherwise invisible underwater morphologies. The data are the basis for subsequent investigations of the lake sediments and for other applications in coastal engineering and construction, natural hazard analysis and natural resources prospecting. Periodic repetitions of the surveys will allow monitoring and quantifying alterations of the lake floors related to natural processes as well as to human impact.

8.17

SyGEMe, Integrated Municipal Facilities Management of Water Ressources: Tool presentation, choice of technology, man-machine interface, business opportunities and prospects

F. Kuchler[1], G. Cherix[1], R. Sauvain[1], S. Storelli[1], D. Lindemann[2], E. Andrey[3]

[1] *Centre de Recherches Energétiques et Municipales (CREM), Av. du Grand-St-Bernard 4, CP 256, CH-1920 Martigny*
[2] *Depth SA, Chemin d'Arche 40 B, CH-1870 Monthey,*
[3] *Ecole Polytechnique Fédérale de Lausanne (EPFL), Laboratoire de Systèmes d'Information Géographique (LASIG), EPFL ENAC LASIG, Bâtiment GC, Station 18, CH-1015 Lausanne*

Nowadays, water management raises questions related to the global climate changes, the rising demand of resources in emerging economies and the decisions on energy policy about the exploitation of hydropower and water protection [1].
In Switzerland, the geographical differences cause a marked difference in availability of drinking water, both quantitatively and qualitatively. So, public municipalities, which are a few miles apart, can therefore be faced to an excess, respectively, a lack of water resource.

Meanwhile, the public authorities have the responsibility to manage the various energy flows that serve the cities (water / sewage, natural gas, electricity, district heating, TV network) and thus ensure the safety and quality of the services to customers.
Specific management tools already exist for each specific area but there is still no integrated tool which allows a global and comprehensive vision of the network steering and management.
Since 2007, experts from the Research Center in Energy and Municipalities (CREM) and the Ecole Polytechnique Fédérale de Lausanne (EPFL) in collaboration with the companies Depth SA, ESRI Switzerland SA, SD Ingénierie and SIG Genève have worked on the development of a management tool for integrated municipal urban technical networks, applied initially to the water cycle (SyGEMe).
The main objective of this project was to develop a new service for communities and network operators, which includes a monitoring system (with real-time flows measurements) and an expert system of knowledge management, both on a geographic information system (input interface of the tool).

For operators, this tool available through a web platform must allow:

- the real-time analysis of their network operation
- the reception of alarms which can detect non-standard situations
- the sustainability of their practical knowledge in network management with an access to a structured information system which facilitates registration and access to data and operational experiences.

The SyGEMe tool has entered its final phase. The system offers many features that will be developed in this article. But it is possible to mention especially the documentation and georeferencing of objects and events on the network, ie measuring devices, tasks and reports created by or for network operators, an access to real-time telemetry etc.
This article aims to present in details the SyGEMe tool, to document the choice of technology, to identify business opportunities and to imagine the prospects of the SyGEMe project.

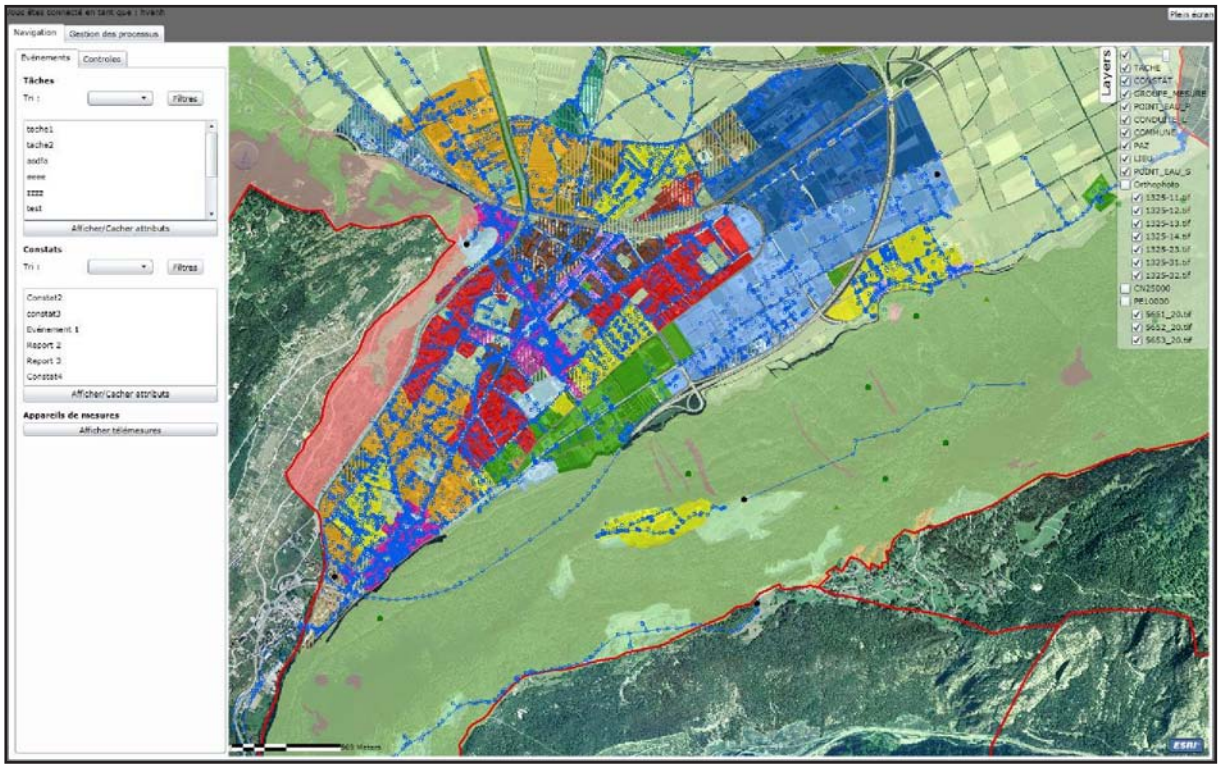

Figure 1 - SyGEMe, online view of the tool.

REFERENCES :

OFEN, Office fédéral de l'énergie, Suisse : « Plan d'action pour les énergies renouvelables », Fiche d'information 6, 2008
Bruno Schädler, Division Hydrologie, OFEV, Office fédéral de l'environnement, Suisse : « Dossier au fil de l'eau », Environnement – Avril 2006
Convention alpine, Italie : « L'eau dans les Alpes », Communiqué de presse : Sécheresse ou Crue? 2ème Rapport sur l'état des Alpes, 2009
Convention alpine, Italie : « L'eau et la gestion des ressources en eau : Rapport sur l'état des Alpes », Signaux alpins – Édition spéciale 2 – 2009

8.18

Towards a Swiss Geological Information System

Andreas Kühni, Nils Oesterling

Bundesamt für Landestopografie swisstopo, Landesgeologie, Seftigenstrasse 264, CH-3084 Wabern, andreas.kuehni@swisstopo.ch, nils.oesterling@swisstopo.ch

The main tasks of the Swiss Geological Survey (SGS, Federal Office of Topography swisstopo) are to produce geological, geophysical and geotechnical data and information and to facilitate the access to relevant data for our main customers. As the geological surveying activities in Switzerland – in contrast to most European countries – is organized in a federalistic and highly decentralized manner, particularly the second goal can only be accomplished by a high amount of coordination.

In response to the fast growing demand for digital geological data and information the SGS started some years ago to put a major effort in the production of harmonized digital data sets such as geological, geophysical and geotechnical maps as well as drill hole data and geological reports. A meta database and an interactive viewer for all the geological data available at swisstopo were created and made available on the swisstopo homepage in order to facilitate the accessibility to geological data to our customers. With the availability of the first geological vector data sets covering large areas at planning scale 1:25'000 (e.g. cantons VD, NE, JU), the demand for this kind of data increased as the use became evident to a large range of professionals who need geological information in interdisciplinary decision making processes, such as environmental and urban planning, civil engineering, risk assessment etc.
However, only a small fraction of the data needed by our main customers can be downloaded from the SGS homepage. The other required geological and geo-thematic data has to be searched for and procured at different cantonal, federal, scientific or private organizations.

In order to further facilitate the access to all of the relevant data and information the SGS plans to build up a Swiss Geological Information System in close collaboration with the main players in the Swiss geological community such as other cantonal and national governmental bodies, the scnat (including its earth-science commissions) and the Swiss Association of Geologists (representing the private economy sector).

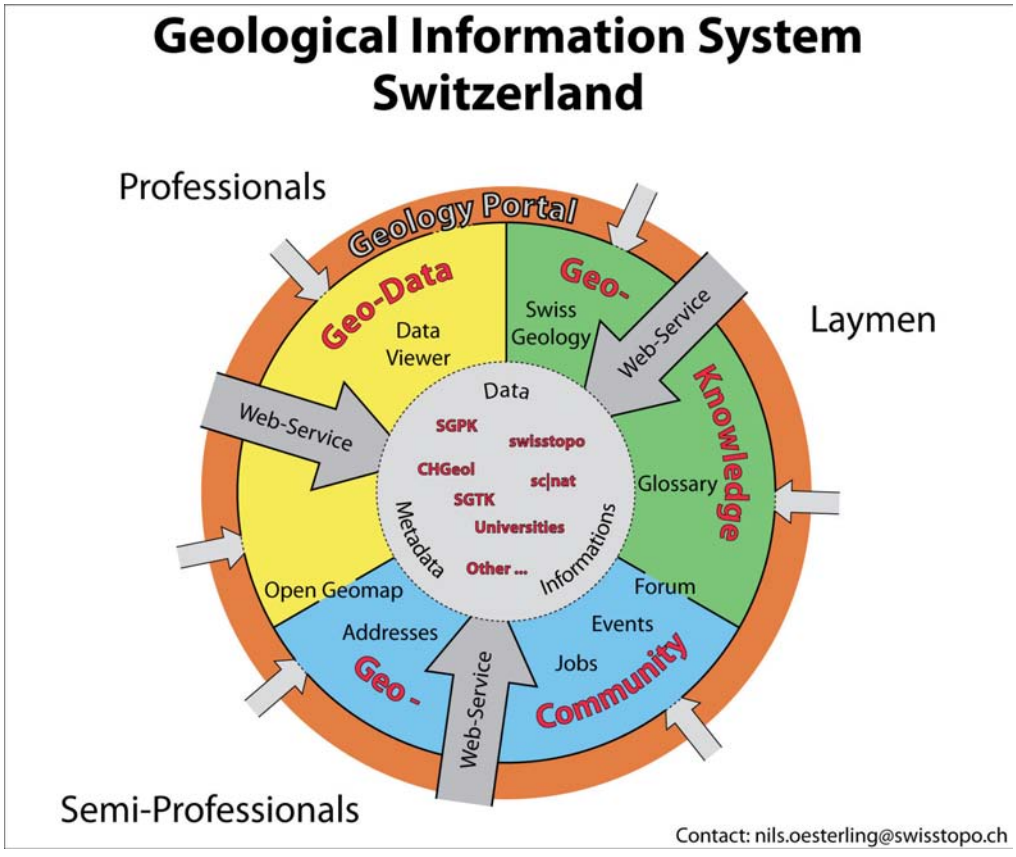

Figure 1: Schematic overview of the structure of the Swiss Geological Information System. The available geological data and information are at the core of the system. Access to the data is provided via a web-portal or directly via web-services. The entire system is divided into three sectors covering issues related to geo-data, geo-knowledge and the geo-community. Each sector contains different components, e.g. a data viewer for visualizing geological data or a discussion-forum for the communication between professionals and laymen. The target groups are professional geologists, semi-professionals in geology (e.g. teachers) as well as laymen from a broad public.

The Geological Information System (Oesterling 2008, Figure 1) aims to achieve three major goals in three different sectors of the national internet portal:

1. GEO-DATA: Improve accessibility to all data and information related to geology
2. GEO-COMMUNITY: Give an overview of the tasks, responsibilities, products and services of the institutions in the field of earth sciences in Switzerland
3. GEO-KNOWLEDGE: Increase awareness of the importance of geological data at political and public levels.

In order to reach these goals the SGS in working in **three main pillars**: technical infrastructure, data production/acquisition, coordination/legal aspects.

Technical Infrastructure: The technical implementation is based on the guidelines of the National Spatial Data Infrastructure of COGIS (Coordination, Geo-Information and Services, swisstopo), a platform aiming to link all spatial data relevant to the Swiss (public) economy at a national level. Thus the technical infrastructure is to a large extent already provided. In order to allow the homogeneous integration and the interoperability of geological data from different sources a general geological data model is being developed (Oesterling 2006; Strasky 2009)

Data Production and Acquisition: During the last decade the production of digital geological data has been increasingly pushed. All of the geological maps are available in pixel format and most in vector format. The newly initiated project GeoCover (Baland 2009) aims to make a seamless geological vector map (scale 1:25'000 – 1:50'000) available within three years. The internal production of the Geological Atlas 1:25'000 is currently of being transferred to a GIS production cycle based on the software 'Tool Map' (Schreiber 2009), which was developed in collaboration with crealp (Research center on alpine environment). The collaboration with the Swiss Geotechnical and the Swiss Geophysical Commissions have been intensified and the respective products are integrated into the Geological Data Viewer of swisstopo.

Coordination and Legal Aspects: Although the SGS has a strong legal base (Schweizerische Eidgenossenschaft 2008a, b) for its duties and especially for its coordination and turntable function since 2008, most of the external producers of geological data and information are not forced by law to integrate their data in a publicly accessible platform and to make geological data available to the public.
Therefore and because of very limited recourses the building up of a Geological Information System by the SGS depends to a large degree on the capacity of its potential partners to understand that such an information system will facilitate life for all the members of the Swiss geological community and strengthen the position of geology in the Swiss society in general.

REFERENCES

Baland, P. 2009: Converting geological maps to vector datasets – Completing the National Geological Information; SGM09, poster, this abstract volume

Oesterling, N., Jemelin, L., Kühni, A. 2006: The Geological Information System of Switzerland – Data Model and Data Viewer, 33rd International Geological Congress, Oslo, Proceedings, Volume 1, 235-237.

Oesterling, N., Kühni, A. and Kündig, R. 2008: The Geological Information System Switzerland, 6th EUREGEO Proceedings, Volume 1, 235-237.

Schreiber, L., Ornstein, P., Sartori, M., Kühni, A. 2009: TOOLMAP – 'Sion'method: development of a new GIS framework for digital geological mapping, 6th EUREGEO Proceedings, Volume 1, 89-90.

Schweizerische Eidgenossenschaft (2008a), Bundesgesetz über Geoinformation (Geoinformationsgesetz, GeolG), Stand: 1. Juli 2008, Bern

Schweizerische Eidgenossenschaft (2008b), Verordnung über die Landesgeologie (Landesgeologieverordnung, LGeolV), Stand: 1. Juli 2008, Bern

Strasky, S. 2009: Towards a Swiss geological data model; SGM09, oral presentation, this abstract volume

8.19

Rock glacier monitoring with low-cost GPS receivers

Limpach Philippe & David Grimm

Institute of Geodesy and Photogrammetry, ETH Zurich, Schafmattstrasse 34, CH-8093 Zurich (limpach@geod.baug.ethz.ch, grimm@geod.baug.ethz.ch)

To investigate the potential of low-cost GPS receivers for the precise monitoring of slope instabilities in mountain areas, a small GPS test-network was installed on the Dirru rock glacier near Randa, Mattertal, Swiss Alps. The site was selected by the Alpine Cryosphere and Geomorphology research group of the University of Fribourg and the Swiss Federal Office for the Environment, based on velocities detected by SAR interferometry and periodic GPS surveys (Delaloye et al. 2007).

The test-network was installed in June 2009 and consists of three permanent GPS stations (Figure 1), equipped with low-cost mono-frequency GPS receivers from the Swiss manufacturer μblox. Power is supplied by solar panels. To validate the results from the GPS network, parallel observations with an automated tachymeter system were carried out. A mini prism was installed next to each GPS antenna on the same boulder (Figure 2). The prisms were measured by the tachymeter every 30 minutes during two weeks.

The GPS data processing is based differential carrier phase techniques using the Bernese GPS software. Daily station coordinates, as well as kinematic coordinates with a sampling interval of 5 s are computed. The low-cost GPS system allowed to reliably observe velocities in the order of 2 cm/day. Station coordinates were obtained with accuracies (standard deviations) of 0.5 cm for the daily solutions and 1.5 cm for the kinematic solutions. A very good velocity agreement of better than 0.1 cm/day was obtained with respect to the tachymeter solutions.

By providing continuous observations of surface motion, independent of weather conditions, permanent monitoring based on low-cost GPS receivers can help to strengthen the understanding of processes linked to permafrost-related slope instabilities. In addition, it is a powerful tool to enhance existing monitoring and early-warning systems, in order to improve the prevention and mitigation of impacts of natural hazards on infrastructure and human life, and to support local decision-making processes.

Figure 1. GPS station installed on the rock glacier, including (from right to left) GPS antenna, solar panel and instrument box containing GPS receiver and battery.

Figure 2. GPS antenna and mini prism installed on the same boulder (left picture) and mini prism in detail (right picture).

REFERENCES

Delaloye, R., Strozzi, T., Lambiel, C., Perruchoud, E., Raetzo, H. 2007: Landslide-like development of rockglaciers detected with ERS-1/2 SAR interferometry. Proceedings of FRINGE 2007 Workshop, Frascati, Italy, 26-30 November 2007.

8.20

A GIS tool to create fluvial flooding maps. Interaction of 1D hydrodynamic model and GIS

Marzocchi Roberto[1], Federici Bianca[2], Sguerso Domenico[2]

[1] *IST – SUPSI Istituto scienze della Terra, CP 72, CH-6952 Canobbio (roberto.marzocchi@supsi.ch)*
[2]*DICAT, Università degli Studi di Genova, Via Montallegro 1, 16145, Genova (Italy) (bianca.federici@unige.it)*

Each year flooding happens worldwide posing at risk the life and the property of million people. An increment of the exposure to risk is caused by climate changes and population growth that leads to the development of infrastructures, buildings and business in the areas surrounding rivers. However, flooding is a natural phenomenon and is necessary for the survival and health of the ecosystem.

The identification of flood prone areas is of considerable importance either for emergency management and for planning activity, such as scheduling of works for the reduction of hydraulic risk or town planning finalized to the optimal land use. For this reason in recent years several flooding hazard models and risk assessment procedures were developed. Also a Geographic Information System (GIS) may be a tool that can assist floodplain managers as decision support system.
The present work proposes an automatic procedure implemented in GIS environment to create perifluvial flooding maps. The potentially fluvial inundated areas are obtained knowing *(i)* the conformation of the floodplain surrounding the river by an high resolution Digital Terrain Model (DTM) and *(ii)* a water surface profile along the river axis calculated for given discharge through a generic one-dimensional hydraulic model (HEC-RAS, Basement, MIKE 11, etc). The interest for the interaction between a GIS and common hydrodynamic models is shown by many works in literature and by the implementation of several software to this purpose (HEC-GeoRAS®, Mike 11 GIS and Surface water Modeling System).
The implemented procedure has innovating characteristics: in fact, even if it remains substantially one-dimensional, it takes into account the two-dimensionality of floodplain and inundation phenomena, adducing hypotheses that let to correct many errors typical of one-dimensional usually employed procedures. Hence, with respect to the use of an one-dimensional model without the GIS support, this procedure allows to obtain more realistic perifluvial flooding map (fig. 1). Moreover, with respect to a two-dimensional model, it needs a lower computational effort, that allows to apply it to river reaches very long (of the order of 100 km).

The procedure may be summarized in four phases that are automatically implemented (more detail in Marzocchi et al. 2009). In the first phase, the value of water level in the nearest point of fluvial axis is assigned to each cell of DTM, through the creation of Thiessen polygons; hence, a first flooding map is obtained making a comparison between elevation and water level in each cell. In the second phase, the procedure removes all the areas previously defined at hazard, but not connected with the river axis. In the third phase, the procedure takes into account levees or other obstructions to the water flow, under the hypothesis that water diffuses from river to the surrounding areas only in direction perpendicular to the river axis. In the fourth phase the previous hypothesis is removed and, only for the areas dried in the third phase, several two-dimensional water paths are analysed, obtaining the final flooding map.

A first validation of the procedure was performed (Federici et al., 2007) on a reach of the Tanaro River (about 120 Km, Italy): the historical inundated area and the potentially inundated area caused by the alluvial event in 1994 that interested the river through Alessandria city were compared with satisfactory results. Recently, the tool has been applied also to a little stream (Roggia Scairolo) in the Ticino Canton, for the flooding hazard valuation (Pozzoni et al., 2009) obtaining reliable results.

The procedure was implemented in the open source Geographic Resources Analysis Support System Software (GRASS, 2008) combining the use of the shell script and fortran languages. A new module (r.inund.fluv) with a user friendly graphical interface was created and now it is distributed under the terms of the GNU General Public License, free downloading from the web site http://grass.osgeo.org/wiki/GRASS_AddOns.

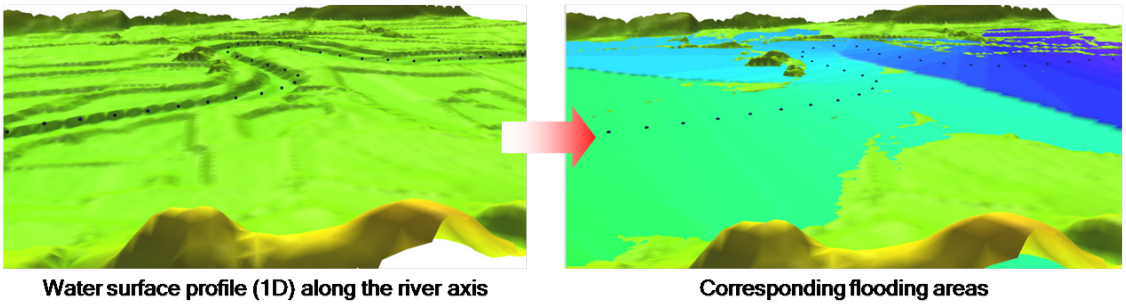

Figure 1. Working principle of the implemented GIS tool.

REFERENCES

Federici B., Sguerso D., 2007. Procedura automatica per la creazione di mappe di potenziale inondazione fluviale. Bollettino SIFET, ISSN: 1721-971X, n. 4, pp. 25-42.

Marzocchi, R., Federici, B. & Sguerso D. 2009 Procedura automatica per la creazione di mappe di potenziale inondazione fluviale in GRASS: il modulo r.inund.fluv, Atti del IX Meeting degli Utenti Italiani di GRASS - GFOSS, 21-22 febbraio 2008, pp. 161-178

GRASS Development Team 2008. Geographic Resources Analysis Support System (GRASS) Software. Open Source Geospatial Foundation Project. http://grass.osgeo.org

Pozzoni, M., Marzocchi, R. & Graf, A. 2009. Roggia Scairolo - Zonazione della pericolosità per alluvionamento, Technical report IST

8.21

A GIS embedded model for dam break

Marzocchi Roberto & Cannata Massimiliano

[1]*IST – SUPSI Istituto scienze della Terra, CP 72, CH-6952 Canobbio (roberto.marzocchi@supsi.ch)*

In the XXI century around 200 notable dam and reservoir failures happened worldwide causing massive fatalities and economic costs. Increasing energy demand and other benefits have caused the construction of many dam in mountainous regions; at the same time the intensive watershed urbanization has lead to a society exposed to risks like never before. For this reason, nowadays governments are looking into disaster mitigation strategies with higher attention. Within the process of strategies, design the spatial information plays an invaluable role. In fact is impossible to take effective and comprehensive decisions without understanding the extent of potential hazards and without localizing existing conditions of vulnerability that could pose a potential threat to harm people, properties, essential services and economy of regions. Therefore, in order to protect the society from a given type of hazard is of primary importance being able to assess the spatial distribution of the threatening phenomena and their intensities.

In order to perform risk analysis (fig. 1), GIS represent a needful instrument. Usually hazard areas are evaluated by using standalone hydrodynamic models, while GIS are used to manage inputs and to perform the risk analysis using outputs. This approach is time expensive, error prone, due to export/import requirements, and not user friendly, but necessary because of the lack of embedded GIS hazard models.

To this purpose, the Institute of Earth Science is developing a series of GIS embedded hazard models within the RiskBox project (Cannata & Molinari, 2008). The aim of this project is to provide a unique system offering all the capabilities required by risk assessment analyses. The chosen GIS system is the Geographic Resources Analysis Support System Software (GRASS, 2008). Its selection was based on the consideration that this software provides high quality, flexibility and interoperability, and, least but not last, that it is Open Source.

With this work, a new numerical model for the solution of the two-dimensional dam break problem has been implemented in the GRASS GIS as a embedded module. The model solves the conservative form of the 2D Shallow Water Equations (SWE) using a Finite Volume Method (FVM); the inter-cell flux is computed by one-side upwind conservative scheme (Ying et al., 2004) extended to a two-dimensional problem on a squared grid.

The command can generate raster time series of water depth and flow velocity with time resolution defined by the user, and a variety of output raster maps useful to obtain the maximum phenomenon intensity (BUWAL 1998).
The problem formulation and the new GRASS module are detailed presented in references (Marzocchi & Cannata, 2009). The model has been tested with two standard synthetic problems referenced in literature and verified in a real dam case where official flooding maps were available (fig. 2). A comparison with other existing dam break models will be conduct.

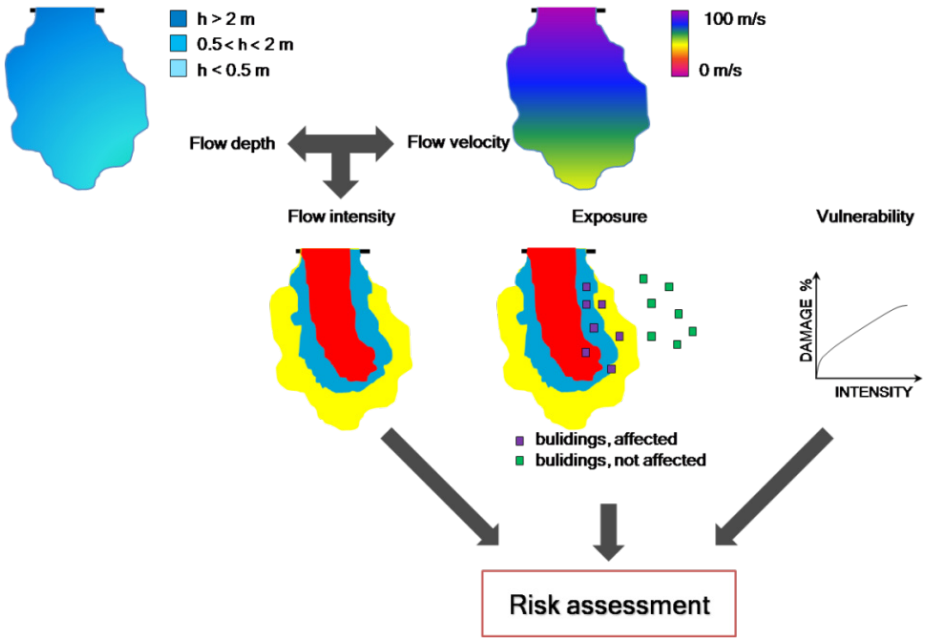

Figure 1. Risk assessment strategy in case of dam break

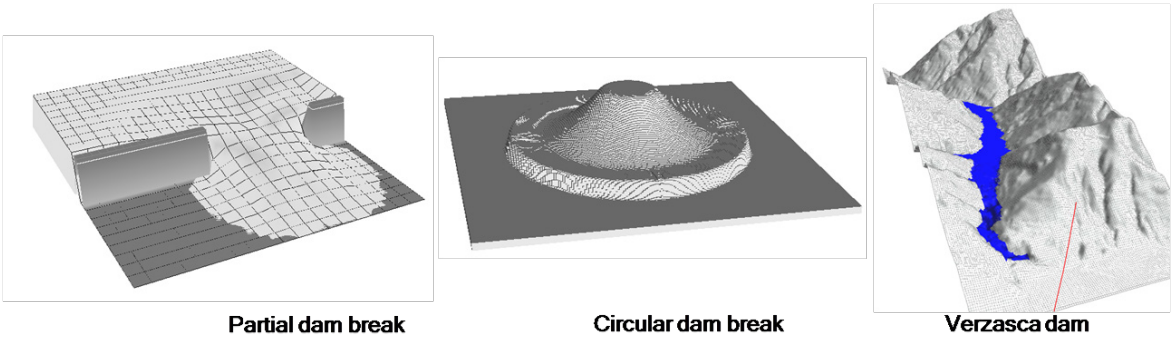

Figure 2. Test cases used for model validation

REFERENCES
BUWAL 1998 Methoden zur Analyse und Bewertung von Naturgefahren. Umwelt-Materialien Nr. 85, Bern, p. 229
Cannata M. & Molinari, M. 2008, Natural Hazards and Risk Assessment: the FOSS4G capabilities. Proceedings of the Free and Open Source Software for Geospatial (FOSS4G 2008) conference. Cape Town, South Africa.
GRASS Development Team 2008. Geographic Resources Analysis Support System (GRASS) Software. Open Source Geospatial Foundation Project. http://grass.osgeo.org
Marzocchi, R. & Cannata, M. 2009. Two-dimensional dam break flooding simulation: a GIS embedded approach. In press
Ying, X., Khan, A. &Wang, S.S.Y. 2004. Upwind conservative scheme for the Saint Venant Equations

8.22

Naturereignisse entlang der Bahnlinien: eine systematische Aufnahme

Meier Andreas & Willi Christina

SBB Infrastruktur, Umwelt, Naturrisiken, Mittelstrasse 43, 3000 Bern 65

Die Bahnlinien sind aufgrund der topografischen Gegebenheiten in der Schweiz häufig klimatischen und gravitativen Naturprozessen ausgesetzt. Sturzprozesse, Hochwasser, Hangrutsche, Murgänge, Lawinen, Sturmwinde und Starkniederschläge sind Naturgefahren, welche typischerweise die SBB-Linien gefährden.

Die systematische Erfassung der Naturereignisse ist aus fachlicher und betrieblicher Sicht von grosser Bedeutung. Die SBB strebt mit der Erstellung und Pflege eines netzweiten Ereigniskatasters Naturgefahren an, ein differenziertes Bild über die Auswirkungen von Naturereignissen auf Infrastruktur und Bahnbetrieb zu gewinnen.

Ereigniserfassung
Mit dem «Geographischen Informationssystem GIS NR» der SBB werden gravitative Naturgefahren sowie Einflüsse der Witterung auf die Infrastruktur in einem zweistufigen Prozess erfasst, dokumentiert und visualisiert. Die wichtigsten Informationen zu einem Ereignis umfassen:

- Ereignisdatum und –ort
- Ereignisart, -beschreibung und -bewertung
- Prozesskenngrössen, Prozessart, Wirkungspunkt, Auslöser, Ursachen, Auswirkungen
- Personen- (Verletzte, Tote), Sach- (CHF) und Betriebsschäden (Verspätungsminuten, Zugsausfälle, Störungen)
- Sicherheitsbezogener Ereignistyp
- Angaben zu Sofort- und Folgemassnahmen

Die Daten werden laufend aktualisiert und ergänzt. Sie bilden die Grundlage für die Ereignisanalyse und den Jahresrückblick.

Datenauswertung und Erstellung von Kenngrössen
GIS NR ermöglicht die Erstellung von definierten Abfragen aus dem Ereigniskataster und die raumbezogene Betrachtung von Ereignisabfolgen. Auf der Basis weiterer SBB-interner Daten dient die Analyse der Naturereignisse der Erstellung von

unternehmerischen Kenngrössen und Einschätzungen. Über diese Kenngrössen können die Auswirkungen auf den Bahnbetrieb verfolgt werden und entsprechende Massnahmen getroffen werden.

Folgende Fakten werden abgeleitet und jährlich verfolgt:

- Räumliche Verteilung der Ereignisse (Fig.1)
- Entwicklung der Ereignisse
- Anzahl Unfälle und Verspätungsminuten
- Summe der versicherten Schäden
- Typisierung von Schadensbildern
- Einschätzung der Risikolage
- Überblick der Stellen mit Massnahmenbedarf

Die Resultate der Ereignisanalysen werden im jährlichen internen Standbericht Naturrisiken und auf thematischen Kartendarstellungen präsentiert.

Langfristig werden auf Basis der über die Jahre gesammelten Daten Trendanalysen zur Entwicklung der Naturereignisse möglich sein.

Figur 1. Naturereignisse auf dem SBB-Netz seit 01.01.2008

Ausblick
Die Pflege und Analyse von Ereignisdaten wird weiter systematisiert und ausgebaut. Damit wird der Ereigniskataster zu einem integralen Bestandteil des Naturrisikomanagements der SBB.

Um die Schadensentwicklung und die Wirkung von Schutzausbauten zukünftig besser beurteilen zu können, werden Vergleiche zu nationalen und kantonalen Ereignis- und Schadenskatastern immer wichtiger.
Die SBB unterstützt die verschiedenen Bestrebungen in der Schweiz zur Verbesserung der Datenlage zu Naturereignissen. Eine Ausweitung des Nutzerkreises des «Geographischen Informationssystems Naturrisiken» der SBB auf weitere Bahnen könnte aus Sicht der Gefahrenprävention und der Bahnbetreiber notwendige Synergien schaffen.

REFERENZEN

Meier, A. 2008: Naturgefahren: Herausforderung für die SBB. Geomatik Schweiz 2008/5, 242-243.
Meier, A. & Willi, C. 2008: Systematic recording and analysis of natural hazards along railway lines using GIS. SGM 2008.

8.23

Shallow Landslide Vulnerability Assessment

Molinari Monia Elisa[1], Cannata Massimiliano[1], Troung Xuan Luan[2]

[1] *Institute of Earth Sciences – SUPSI, Trevano, C.P 72, CH-6952 Canobbio*
[2] *Hanoi University of Mining and Geology – Dong Ngac, Tu Liem, Hanoi, Vietnam*

The Philippines, Vietnam, Cambodia, Thailand, Laos, Sumatra and Indonesia are among the countries identified as climate change "hotspots"- countries particularly vulnerable to some of the worst manifestations of climate change including lan slides.

In particular, shallow landslides has a huge destruction power. Because of theirs high density and speed, damages are very severe and sometimes tragic: destroying houses, bridges and infrastructure and claiming people's lives.
The threat due to natural hazards can be reduced, by integrating them into land use management, urban planning, and population protection plans. Computer simulation is one of a few possibilities to objectively assess the hazard due to a process, by simulating its localization and expansion.

Two models already has been successfully applied in many cases:

- TRIGRS (Baum et al. 2008) for modeling the timing and distribution of shallow, rainfall-induced landslides, and
- DFWALK (Cannata & Molinari 2008) for modeling the expansion area and the intensity of the phenomena.

Unfortunately this two software are not linked together thus do not permit their usage for predicting when, where and with what intensity a phenomenon is going to occur.

This research aims to couple the two above mentioned models (TRIGRS and DFWALK) to derive a complete framework for shallow landslides modeling.
This achievement is very important for planning efficient countermeasures and in time disaster responses.
Moreover, this research aims also to embed this two models within a GIS able to be interfaced with the Internet through a Web Processing Service implementation in order to create a web-based application for spatial decision support systems on shallow landslide. This solution enable the usage of geospatial data for modeling and turns it into knowledgeable informtion (maps) which are much easier to understand and less expensive for better decision making.

REFERENCES

Baum R.L., Godt J.W., Savage W.Z., 2008: TRIGRS – A fortran program for transient rainfall infiltration and grid-based regional slope-stability analysis, Version 2.0. U.S. Geological Survey Open-File Report 08-1159.

Cannata M., Molinari M.E, 2008: Natural Hazard and Risk Assessment: the FOSS4G, Proceeding of the 2008 Free and Open Source Software for Geospatial Conference, Cape Town, South Africa.

8.24

3D modeling of geological heterogeneity: the direct sampling multiple-points simulation method

Philippe Renard, Grégoire Mariethoz, and Julien Straubhaar

Centre for Hydrogeology and Geothermics (CHYN), University of Neuchâtel, Emile-Argand 11, CH - 2009 Neuchâtel (philippe.renard@unine.ch, gregoire.mariethoz@unine.ch, julien.straubhaar@unine.ch)

Geological heterogeneity is a key factor controlling groundwater flow and transport processes. But because of the lack of exhaustive geological data, it is often necessary to model it and its impact in order to provide not only reliable forecasts but also reliable error bounds with the groundwater flow model forecasts. During the last 50 years, massive progresses have been made in this field but mostly in the context of relatively simple heterogeneity models (binary or multi-Gaussian models). However that there are a significant number of applications in which the underlying assumptions made when applying

those models are not valid. This is why a richer model should be used to describe the heterogeneity and integrate as much as possible geological, hydrological, and geophysical observations.

One technique that has these characteristics is the multiple-point statistics. It has become a prevalent subject in geostatistics over the last 5-10 years. Despite the existence of certain shortcomings, it is by now the most flexible method to integrate a conceptual model of heterogeneity in a stochastic framework. The concept behind the method is to use a training image to represent the desired spatial structure of the field. The training image is scanned and all pixels configurations of a certain size are stored in a catalogue of data events. This structure is then used to compute the conditional probabilities at each simulated node. Because of limited memory usage, the standard approach can only deal with categorical variables, in addition the memory load can be prohibitive for large 3D grids.

In this work, we show that there is no need to store and count the configurations found in the training image. Instead, it is more convenient to sample randomly the training image for a given data event. This technique is statistically equivalent to previous implementations but, because it relaxes the need to compute explicitly the conditional probabilities, it allows to extend the application of the standard theory from categorical to continuous and multivariate variables. This method (Mariethoz et al 2009) can be used for the simulation of geological heterogeneity, accounting or not for indirect observations such as geophysics, but it can also be used to simulate any variable that has non multi-Gaussian features which may have an important impact on hydrological processes. Computationally, it is fast, easy to parallelize, and parsimonious in memory needs. A comparison of its application for solute transport simulation with the application of standard multi-Gaussian techniques (Figure 1) shows that this new method is able to model correctly highly connected patterns that are impossible to model with the Sequential Gaussian Simulation technique (Fig. 1).

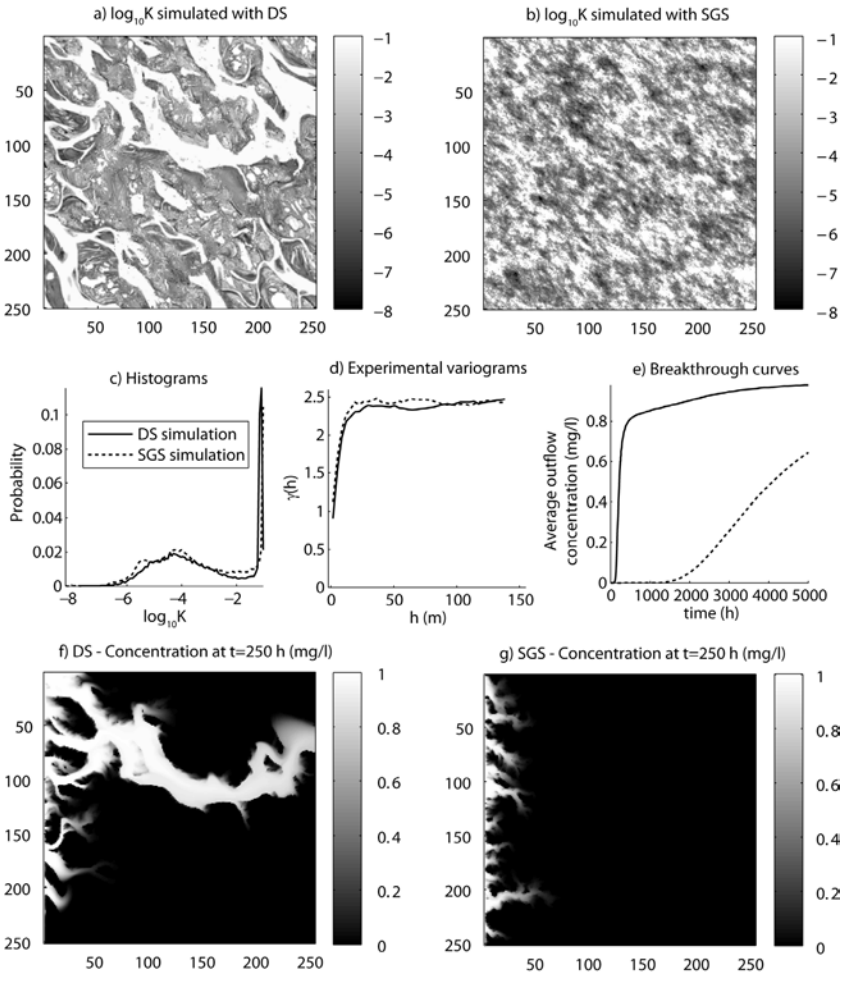

Figure 1: Influence on the connectivity patterns on transport behavior. a) One simulation obtained with Direct sampling. b) One simulation generated using SGS. c) Comparison of histograms of simulated values. d) Comparison of experimental omnidirectional variograms. e) Comparison of contaminant breakthrough curves on the outflow boundary. f) and g) comparison of the contaminant distribution at *t*=250 hours.

More generally, the multivariate framework offered by this method opens a wide range of perspectives for the integration of different data types. Possible applications are very diverse since categorical variables (e.g. geology, soil type, land cover category, vulnerability class) and continuous variables (e.g. porosity, concentration, recharge rate, rainfall) are often related and widely used in many fields of geosciences but are very seldom measured exhaustively. Therefore these variables often require to be interpolated or simulated and the DS method could then be used to simulate fields having a proper spatial structure.

REFERENCES
Mariethoz, G., Renard, P. & Straubhaar J. 2009: The direct sampling method to perform multiple-points geostatistical simulations, Water Resources Research, submitted.

8.25

Particle Swarm and Differential Evolution –Global Optimization for Geophysical Inversion

Saraswat Puneet

Indian School Of Mines University ,Dhanbad, Room 161 ,Topaz Hostel, Jharkhand-826004 (puneet.agpnasa@gmail.com)

The social behavior observed in a flock (swarm) of birds and in insects searching food has been simulated to develop a global optimization strategy popularly known as the Particle Swarm Optimization (PSO). Particle Swarm Optimization (PSO) emulates the social behaviors in a flock of birds (swarm) in solving an optimization problem. It utilizes both local and global properties of the swarm to formulate a novel search strategy that guides the swarm towards the best solution with constant updating of the cognitive and social knowledge of the particles in the swarm.

Differential Evolution (DE) is a novel parallel direct search method which utilizes NP parameter vectors

$$x_{i,G},\ i = 0, 1, 2, \ldots, NP-1. \quad (11)$$

as a population for each generation G. NP doesn't change during the minimization process. It is a Evolutionary algorithm suggested by Storn and Price(1996).It is based on swarm optimization along with genetic mutation , recombination and selection criteria to optimize a given problem.It also utilizes local and global properties of swarm along with their genetic development.

We used PSO and DE for Inverting the Seismic Log data (both real and synthetic) and comparing the computed and observed seismogram(generated using Convolution forward model), Inverted for Acoustic Impedance and results showed an appropriate match with the observed value one and was obtained within 1000 iterations and swarm of 100 in PSO and 10 times the unknown parameters in DE

For example -one of the problem we took for single trace vertical seismic log and inverted for acoustic impedance value for each layer and again computed seismogram using calculated impedance values and plotted the observed seismogram with computed one the results are shown in following figures:

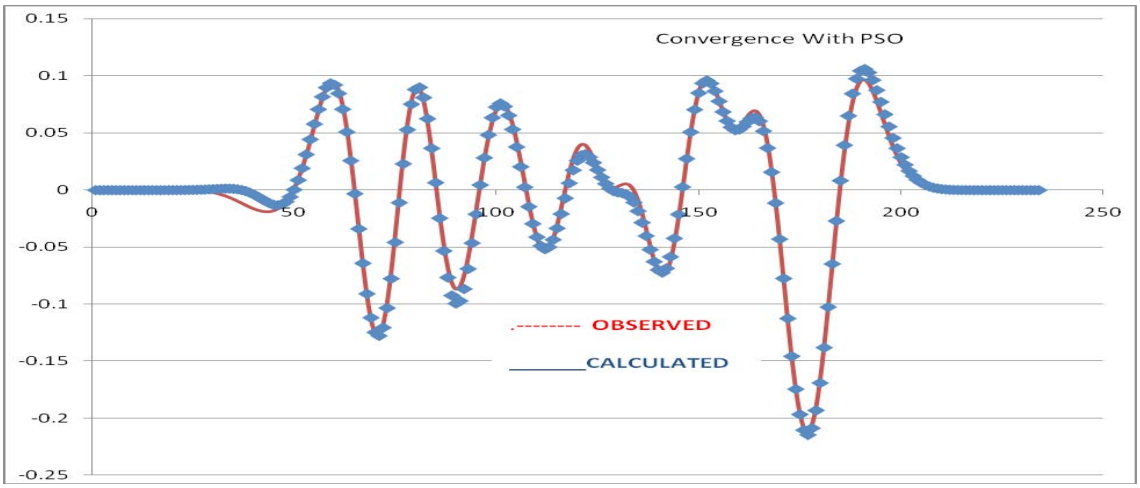

Figure1: Single Trace data fit using PSO with Virtical seismic log for Acoustic Impedance

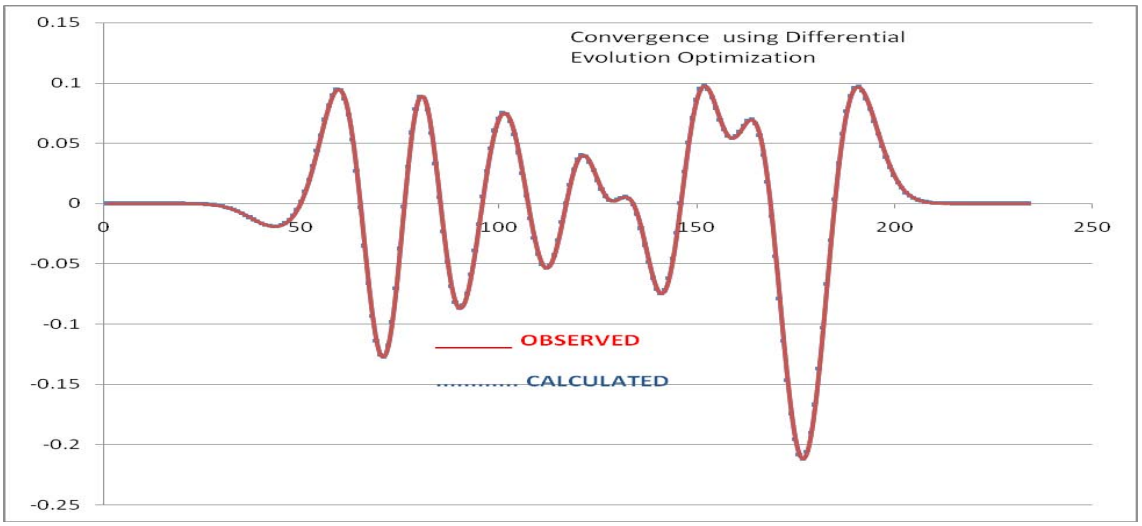

Figure 2: Data fit using Differential Evolution ,Inverted for Acoustic Impedance for 135 layered earth ,shows an exact fit of observed and computed value of seismogram.

Similarly we worked over large number of seismic data both real field (Oil and Natural Gas Corporation Of India seismic data) and synthetic data (single trace and multiple traces)and Inverted for Acoustic Impedance and found good results with very low error. Hence the two new techniques served as excellent tools for Geophysical Inversion
In this study we reported the utility of swarm intelligence in solving multi-parameter optimization problems in geophysics. Seismic data has been inverted using a classical particle swarm optimizer with 30-100 individuals in a swarm. For synthetic as well as field data sets, the solutions obtained explain the observed data satisfactorily besides exhibiting acceptable resolution for the model parameters.

REFERENCES

Rania Hassan 2004: Particle Swarm Optimization-methods and application, MIT esd 16.888,ESO.77
Rainer Storn & Kenneth Price 1995: Diffrential Evolution-a simple and efficient adaptive scheme for global optimization over continuous spaces,TR-95-012

8.26

Fast Colorization, Analyses and Visualization of Airborne Laser Data

Yannick Stebler, Philipp Schaer, Jan Skaloud

Swiss Federal Institute of Technology, Lausanne (Switzerland)

Airborne laser scanning (ALS) has become very popular for modeling topographic objects because of the high resolution and accuracy as well as the short acquisition time required for large study area. The digital elevation model (DEM) of the surveyed area is often represented by mean of point cloud triangulation considering a horizontal plane. This implies that only one single altitude value can be set for each point (2.5-dimensional) issued from the ALS data. Such a modeling is not suitable for very steep terrain and cliffs, which may be of high importance for understanding geological features or natural hazard causes.
Helicopter-based ALS system as that developed by EPFL (Skaloud et al., 2006) can be mounted obliquely to allow steep and vertical cliffs to be captured for an optimal scan angle. At the same time, oriented images are taken to produce ortho-rectified imagery. In order to get a realistic model of such terrain, rigorous 3D models need to be produced based on triangulation and image draping on the resulting mesh. This procedure is possible but rather involved computationally and in the absence of standardized data structures the results are often not portable across software applications (Buckley et al., 2008).

We present a lightweight, fast and robust alternative to the 3D modeling that directly explores the high density laser data and the high-resolution imagery (collected together or separately). The proposed method associates a RGB value for each laser pulse. It presumes good quality exterior-orientation (EO) for the camera data and its good calibration. The camera's EO is calculated by the CAMEO software (Skaloud and Legat, 2006) for each image in the same reference frame as that of laser data.

As one laser point can be visible within several images, a vector is reconstructed between the laser point coordinates and the camera position to choose the most optimal image for the RGB extraction. This choice is made according to the angle between this vector and the estimated surface normal. The pixel coordinates and thus the associated radiometric values corresponding to the laser point are computed by applying the classical colinearity equations and are finally corrected for radial lens distortions. For interoperability purposes, the obtained RGB values can be stored together with the laser data in standard formats such as LAS 1.2.

The visualization engine is based on C++/OpenGL approach and is optimized for simultaneous handling of tens of millions of points over steep terrain and cliffs. A smearing feature can be applied at each zoom level, so the user have an impression of seeing full 3D model instead of discrete values (Fig. 1).

Finally, the described software platform allows also analyses of the terrain. First, the laser points are indexed into a kd-tree data structure and then a terrain normal is estimated. The estimation of the terrain normal is achieved by local covariance analysis. This procedure includes an automated classification algorithm (Bae and Lichti, 2004) for removing the vegetation. Once the covariance analyzes is completed the laser data can be colored for slope (Fig. 2) and orientation (Fig. 3).

Figure 1: Point cloud colorization according to RGB values.

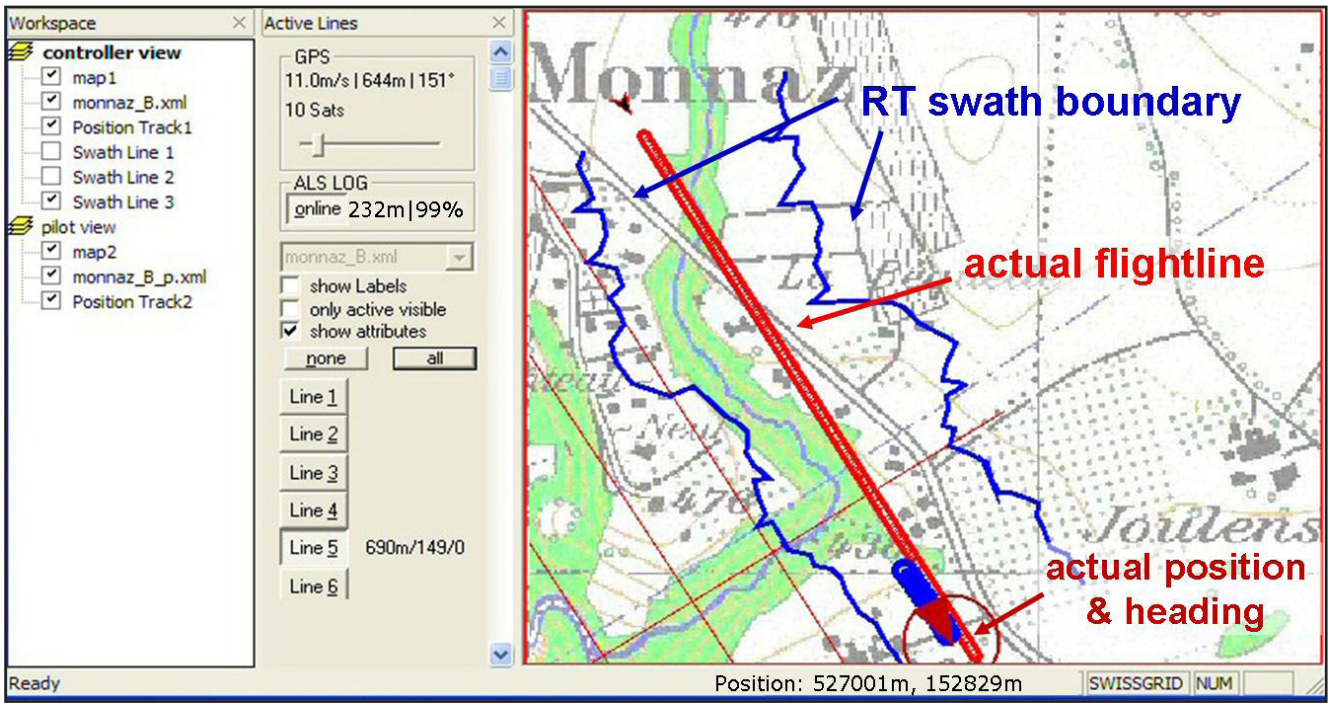

Figure 2: Point cloud colorization according to terrain slope.

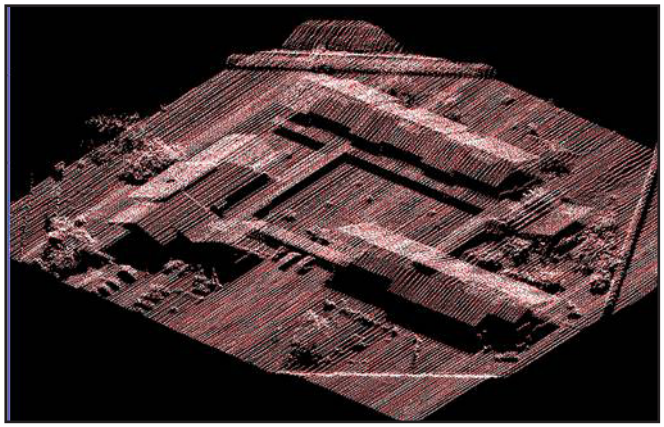

Figure 3: Software interface showing the terrain orientation displaying mode.

Acknowledgment
This project was partially financed by Alp-S project 1.14AB. This support is greatly appreciated.

REFERENCES

Bae, K.-H., and Lichti, D., 2004, Edge and Tree Detection from Three-dimensional Unorganised Point Clouds from Terrestrial Laser Scanners, 12th Australian Remote Sensing and Photogrammetry Conference: Fremantle, Australia.

Buckley, S.J., Wheeler, W, Braathen, A, Vallet, J, 2008. Oblique Helicopter-Based Laser Scanning for Digital Terrain Modelling and Visualisation of Geological Outcrops. The International Archives of the Photogrammetry, Remote Sensing and Spatial Information Sciences, Beijing, Vol. XXXVII, Part B5, Commission 5.

Skaloud, J., and Legat, K., 2006. CAMEO - Camera Exterior Orientation by Direct Georeferencing.: Swiss Federal Institute of Technology Lausanne (EPFL).

Skaloud J., Vallet, J., Keller, K. Veyssiere, G., Koelbl, O., 2006. An Eye for Landscape - Rapid Aerial Mapping with Handheld Sensors. GPS Word, May 2006.

8.27

Topography and surface processes in borderline ecotones

Strähl S. C.[1], Kuhn N. J. [2]

[1]*Geographisches Institut, Klingelbergstrasse 27, CH-4056 Basel (sarah.straehl@unibas.ch)*
[2]*Geographisches Institut, Klingelbergstrasse 27, CH-4056 Basel*

Climate, soil and human activity strongly affect the vegetation patterns in borderline ecotones. Vegetation borderlines are characterized by certain abiotic and biotic factors and differ between the ecosystems. Borderline ecotones represent areas of transition between abiotic and biotic factors controlling the borderline ecosystem. Borderline ecotones therefore contain a great number of ecologic niches and wide species diversity. Succession processes lead to the existence varying vegetation patterns. These subsiding succession processes are important for the vegetation dynamic and last generally over several 100 years. Climate and environmental changes have an important influence on vegetation density and diversity.

Borderline ecotones in two different climatic regions, cold and arid study area, are compared. The alpine study site is in the region of Grindelwald (Bernese Oberland), where vegetation patterns are influenced by temperature gradient: forest – dwarf shrubs – alpine grassland. The arid study area is situated in a side valley near Sede Boqer (Negev desert, Israel), where vegetation patterns are influenced by water supply. The Braun Blanquet vegetation mapping method was used to determine vegetation type and direction of succession. Results show, that not only temperature and precipitation influence surface processes in borderline ecotones. In both areas geo morph dynamic processes play an important role in the development of various vegetation patterns. An important question is the reaction of these systems in the coming 100 years with the influence of Global climate and environmental change.

REFERENCES
Burga, C.A., Perret, R. (2001): Monitoring of eastern and southern Swiss alpine timberline ecotenes. Tasks for vegetation science 35. In Burga, C.A., Kratochwil, A.. Biomonitoring: General and applied aspects on regional and global scales.
Holtmeier, F. Die Höhengrenze der Gebirgswälder. Arbeiten aus dem Institut für Landschaftsökologie. Westfälische Wilhelms-Universität. Band 8, Münster. Verlag Natur und Wissenschaft Harro Hieronismus und Dr. Jürgen Schmidt. Postfach 170209 Solingen. 2000.
Olsvig-Whittaker, Shachak, M. & Yair, A. (1983): Vegetation patterns related to environmental factors in a Negev Desert watershed. Accepted 30 May 1983.
Yair, A. & Raz-Yassif, N. (2003): Hydrological processes in a small arid catchment: scale effects of rainfall and slope length. Received 1 July 2003. Received in revised form 1 December 2003. Accepted 3 December 2003.

8.28

Towards a Swiss geological data model

Strasky Stefan[1], Baland Pauline[1], Oesterling Nils[1] & Kühni Andreas[1]

[1]*Federal Office of Topography swisstopo, Swiss Geological Survey, Seftigenstrasse 264, CH-3084 Wabern (stefan.strasky@swisstopo.ch)*

After ~80 years of traditional geological map production for the Geological Atlas of Switzerland 1:25000 (GA25), a growing need for vector datasets of this map series has evolved during the last decade. Considerable effort is therefore being spent by the Swiss Geological Survey to convert the existing printed GA25 into high-quality Geographical Information System (GIS) datasets. To speed up the conversion from raster to vector graphics and to meet the requirements of the geo-community, the Swiss Geological Survey recently initiated the GeoCover project, which aims to provide geological GIS-data at a scale of 1:25000 throughout Switzerland within the next three years.

However, a well-established data model to describe the structure of the geological data, with specific object and attribute definitions and their relationships, is still missing. An early attempt of a conceptual data model, based on the GA25 map of Zurzach, was presented by Jemelin & Beer (1999). Baland-Renaud & Oesterling (2007) extended the data model to all existing GA25 maps by using the catalogue of lines and symbols for the GA25, which was published by the Federal Office for Water and Geology (2002). Nevertheless, the model developed by Baland-Renaud & Oesterling is a beta version, and thus needs to be further refined in order to carefully structure the original heterogeneity of the current map data. The aim of our project is to establish a structural design for the geological data of the Swiss Geological Survey and to describe all relevant objects, attributes and relationships. Furthermore, the data model should serve as a fundamental basis for the compilation of a seamless, nationwide vector dataset of Switzerland. In collaboration with an external group of experts we approach the refinement of the model. Here we present some examples of the newest results as well as current challenges.

REFERENCES
Baland-Renaud, P. & Oesterling, N. 2007: Modèle de données géologiques. Partie: stockage des données, Version 1.0, 117 pp.
Federal Office for Water and Geology 2002: Line and Symbol Catalogue for the Geological Atlas of Switzerland 1:25 000. Version 1.1, 35 pp.
Jemelin, L. & Beer, C. 1999: Geologischer Atlas der Schweiz 1:25'000 Erfassungskonzept, GIS-Applikation und Struktur der Datenbank, Bull. angew. Geol., 4/2, 103–115.

8.29

The Swiss Atlas of Physical Properties of Rocks (SAPHYR)

Tripoli Barbara[1], Zappone Alba[1], Burlini Luigi[1], Burg Jean-Pierre[1], Hollinger Klaus[2] & Kissling Eduard[1]

[1]Departement of Earth Sciences, ETH Zürich, Sonnegstrasse 5, CH-8092 Zurich, Switzerland
[2]Institute of Geophysics, University of Lausanne Amphipole - UNIL SORGE , CH-1015 Lausanne

Physical properties of rocks are key parameters for several disciplines spanning from oil industry to engineering to geophysics, petrology, structural geology and water resources. They are therefore useful to several scientific disciplines as well as to industry and society.

Since 2006, a multiyear project runs under the umbrella of the Swiss Geophysical Commission (SGPK), with the aim to digitize all existing data on physical properties of rocks and to link them using a geographical frame (GIS), so that they can be ready accessible to a wide public. Moreover, where data are lacking or spare, campaigns of measurements on rock samples are promoted within this or other projects. The project is focused on data from the Swiss Alps but, is not limited to the borders of Switzerland.

The resultant maps will be integrated in the Atlas of Switzerland.
The future evolution of this program could be an extension to 3-D, using the structure of the exposed geology, the data from boreholes and from geophysical investigation.

8.30

Estimation of local tectonic movements using continuous GNSS network

Villiger Arturo[1], Heller Oliver[1], Geiger Alain [1], Kahle Hans-Gert[1] & Brockmann Elmar[2]

[1]Geodesy and Geodynamics Lab, Institute of Geodesy and Photogrammetry, ETH Zürich (arturo.villiger@geod.baug.ethz.ch)
[2]Swisstopo

The canton Valais is a seismic active area within Switzerland. However, compared to other regions like Greece the expected tectonic movements are at least one magnitude smaller. The predicted velocities are few millimetres per year. During the project TECVAL, initialized by HAZNET funds, five permanent GPS stations have been built covering the Wildstrubel area. The stations have been mounted on various buildings such as sewage plants which are well connected to the ground to reduce local effects such as slow landslips or other non-tectonic processes.

Combining stations from TECVAL, IGS, RGN, and AGNES yields to a better local velocity field directly processed into the ITRF 2005 reference frame. For this purpose the software bernese 5.0 has been used to process daily solutions of the measured points. As the main research task is the local tectonic, a locally adjusted rotational velocity field has been estimated and reduced. For every time series, under the assumption of a time constant velocity, the velocity has been estimated using a linear regression model. As they contain high amounts of outliers a robust estimator was chosen with a high breaking point (up to 50 percent). The evaluation has shown that the time series contain up to 23 percent of blunders which would decrease the reliability of velocity estimation.

9. Water and land resources in developing countries: towards innovative management and governance

Hans Hurni, Urs Wiesmann, Thomas Breu

NCCR North-South; Centre for Development and Environment; Swisspeace Foundation; Swiss National Science Foundation; Swiss Agency for Development and Cooperation; Commission for Research Partnerships with Developping Countries (KFPE)

9.1

Bioenergy in Africa: Opportunities and threats of Jatropha and related crops

Ehrensperger Albrecht[1]

[1] *Centre for Development and Environment, Universität Bern (albrecht.ehrensperger@cde.unibe.ch)*

The development of the bioenergy sector is pushed worldwide in face of climate change and the expected shortage of fossil fuels. Biofuels have the potential to raise export revenues, to create new jobs and to develop industries in developing countries, but also to reduce dependency on oil imports (KOJIMA and JOHNSON 2005, SIMS, HASTINGS et al. 2006). More biofuel also means less use of fossil fuels. Models show that this would help reduce the price of oil, to the benefit of other developing countries that cannot grow biofuel feedstock. As a consequence of these environmental and economic opportunities, production of bio-ethanol from corn and sugar cane and production of biodiesel from rape and soy oil rapidly grew over the last years. However, current research unveiled significant impacts of bioenergy on the environment (ZAH, HISCHIER,GAUCH, LEHMANN, BÖNI and WÄGER 2007; SCHARLEMANN and LAURANCE 2008), on land use competition between energy and food crops (REINHARD and ZAH 2008; SEARCHINGER, HEIMLICH et al. 2008), as well as a strong dependence of the biofuels market on subsidies (STEENBLIK 2007).

This Bioenergy in Africa (BIA) project addresses important issues of sustainable development in connection to the production of biofuels, like food security, poverty alleviation, rural development and natural resources. By using a systemic approach, the project will provide pathways towards realistic and sustainable production of bioenergy in Eastern Africa. The approaches by which the opportunities of biofuel production can be maximised and its threats minimised are at the core of this approach. They include land use, livelihood strategies, natural resources management and policies. Specifically, the project looks at four aspects of biofuel production (see figure next page):

1. **Crop growth and processing**: Assessing sustainable bioenergy production potentials and processing of Jatropha biomass in different production systems and under different environmental and cultural settings.
2. **Impacts of biofuel production**: Assessing the socio-economic and environmental impacts of biofuel production in local contexts with a focus on local livelihoods and natural resources dynamics.
3. **Global policy, trade and certification**: Assessing the influence of external socio-political and economic decision-making processes on the regional and local biofuel production processes in Eastern Africa.
4. **Potentials of biofuel in Eastern Africa**: Upscaling findings in view of providing relevant decision-making and planning tools at the national and regional levels in Eastern Africa.

The integration of project results at a regional scale will provide highly relevant baseline information for a broad range of potential users. Concrete impacts are expected as follows:

- At the local scale: Enhanced capacity of farmers in crop production and biofuel processing.
- At the sub-national scale: Enhanced capacity of concerned governmental offices at district and provincial levels, to be achieved again via support to the extension services.
- At the national and regional scales: Better and more sustainable planning and policy making in relation to bioenergy production. Strengthening of the Eastern African Region through advocacy of its needs, priorities and potentials.
- At the global level: Impact on the global discourse on biofuel

REFERENCES

Kojima, M. and T. Johnson (2005). Potential for Biofuels for Transport in Developing Countries. Washington, World Bank: 150

Reinhard, J. and R. Zah (2008). "Consequential Life Cycle Assessment of the Environmental Impacts of an Increased Rapemethylester (RME) Production in Switzerland." Biomass & Bioenergy.

Scharlemann, J. P. W. and W. F. Laurance (2008). "How green are biofuels?" Science 319: 43-44.

Searchinger, T., R. Heimlich, R. A. Houghton, F. Dong, A. Elobeid, J. Fabiosa, S. Tokgoz, D. Hayes and T.-H. Yu (2008). "Use of U. S. Croplands for Biofuels Increases Greenhouse Gases Through Emissions from Land Use Change." Science 319 (5867): 1238 - 1240.

Steenblik, R. (2007). Government support for ethanol and biodiesel in selected OECD countries - A synthesis of reports addressing subsidies for biofuels in Australia, Canada, the European Union, Switzerland and the United States, GSI - Global Subsidies Initiative: 82.

Sims, R., A. Hastings, B. Schlamadinger, G. Taylor and P. Smith (2006). Energy crops: current status and future prospects. Global Change Biology.

Zah, R., R. Hischier, M. Gauch, M. Lehmann, H. Böni and P. Wäger (2007). Life Cycle Assessment of Energy Products: Environmental Impact Assessment of Biofuels. Bern, Bundesamt für Energie, Bundesamt für Umwelt, Bundesamt für Landwirtschaft: 20.

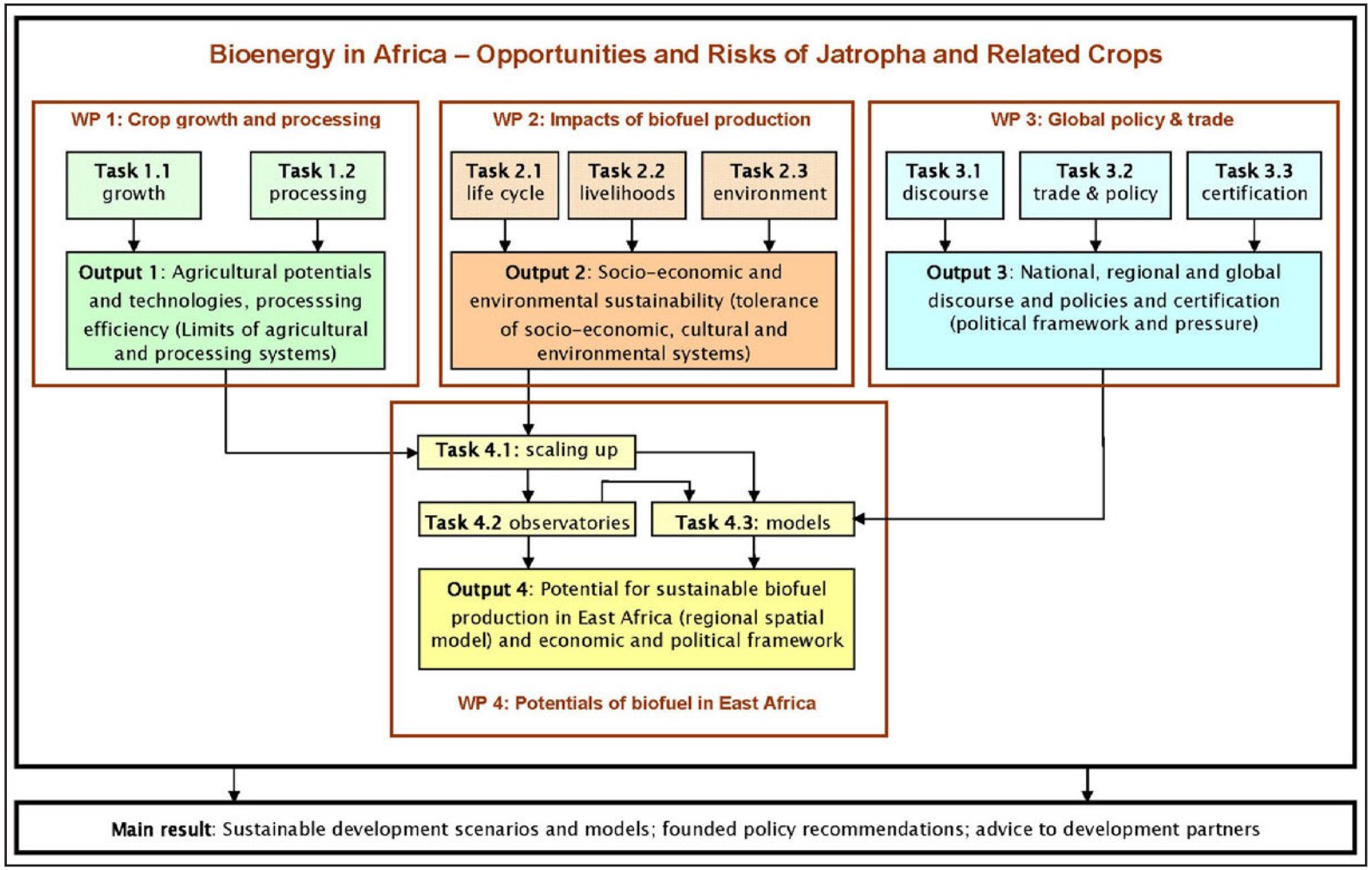
Bioenergy in Africa – Opportunities and Risks of Jatropha and Related Crops
WP 1: Crop growth and processing
Task 1.1 growth
Task 1.2 processing
Output 1: Agricultural potentials and technologies, processsing efficiency (Limits of agricultural and processing systems)
WP 2: Impacts of biofuel production
Task 2.1 life cycle
Task 2.2 livelihoods
Task 2.3 environment
Output 2: Socio-economic and environmental sustainability (tolerance of socio-economic, cultural and environmental systems)
WP 3: Global policy & trade
Task 3.1 discourse
Task 3.2 trade & policy
Task 3.3 certification
Output 3: National, regional and global discourse and policies and certification (political framework and pressure)
Task 4.1: scaling up
Task 4.2 observatories
Task 4.3: models
Output 4: Potential for sustainable biofuel production in East Africa (regional spatial model) and economic and political framework
WP 4: Potentials of biofuel in East Africa
Main result: Sustainable development scenarios and models; founded policy recommendations; advice to development partners

9.2

Water Governance as a tool to ensure sustainable and secure human development, in the Middle East

Exarchou Joanna[1], Salim Nidal[2]

[1] *Global Institute for Water Environment and Health (GIWEH), Geneva- Switzerland.www.giweh.ch*
[2] *Global Institute for Water Environment and Health (GIWEH), Geneva- Switzerland.www.giweh.ch*

A large proportion of the water resources in the Middle East is trans-boundary and final arrangements on water allocation between different countries in the region are not yet in place for “fair and equitable apportionment”. The Middle East region’s natural water is not only threatened, it is also threatening!

Water quality and quantity are the main challenges of the region. Beyond the challenges related to the management of resource scarcity there are hydro-political and trans-boundary considerations. The majority of the water resources in the region is rivers and aquifers that cut across borders. Other than the fact that this often hinders the efficient and equitable management of this water, the prospect of witnessing serious water conflicts in different parts of the region is very real.

When water resources in one community become scarce or threatened, the economic, social and environmental risks increase for everyone. Thus, a proactive integrated management approach is needed to balance the competing needs for this limited resource. “Water Sustainability” is a collaborative community-driven initiative, which requires the active participation of all members in the community. It seeks to establish new creative and coordinated water management strategies based on value addition and security for all stakeholders in the community.

The key aspects to be considered for the future prospective are the role of governance, while governance is considered as a process, so it is important to know 'how' it is done. Rules are brought in and decisions are made. From the other side, governance is a product (e.g. good governance, good decision making, bad governance).

One of the aims of the region is to improve sustainability through better water use efficiency and conservation. Water efficiency can be improved by adopting structural measures like improving technologies and non-structural measures such as water pricing, awareness raising, etc.
The second level of efficiency is related to the allocation and re-allocation of water resources to specific, higher-value uses and more equitable use by all stakeholders.
The highest level of efficiency is related to the inter-basin trade of water. As water is quite a bulky item to transport, trading water in its real form is costly, which is the reason why the concept of virtual water might comes into picture.

Governance in its several contexts such as (corporate governance, international governance, national governance and local governance) is needed in the area.

Cooperation in the management of scarcity and quality does not only occur at the government level but also that of corporations. The CEO Water Mandate within the Global Compact is an opportunity at the highest levels of management to commit to the improvement of water use efficiency.

9.3

Conflicts and Natural Resources. Research Results and Outlook

Laurent Goetschel[1], Didier Péclard[1]

[1] *Swisspeace Foundation, Sonnenbergstrasse 17, CH-3000 Bern 7 (laurent.goetschel@unibas.ch)*

The relations between natural resources and conflicts have a long history. For centuries, societies have used certain natural resources to pursue their interests and political goals. Until the end of the 18th century, for example, wood was of crucial importance to the sea powers. Today, oil is in the headlines of the media worldwide as an indispensable component of superpower politics, but also as a cause of conflict. This situation is referred to as geopolitics of conflicts connected with natural resources (so-called resource conflicts; see Le Billon 2005). However, states do not have the monopoly over appropriation of natural resources for political or military purposes. Control over natural resources or their use is also a significant factor with regard to tensions and even conflicts between societal groups – independently of whether the resources at stake are non-renewable (such as diamonds) or renewable (such as water or soil). Despite their long existence, the relations between natural resources and conflicts remain problematic and must be critically scrutinised. Based on various case studies we demonstrate that the notion of a direct causal link between the environment and conflicts, although widespread in the scientific literature, has no real empirical basis. Likewise, it is necessary to question the heuristic significance of this classical perspective: concentrating on ecological causal relations bears the risk of not paying due attention to the real historical, political and economic dimensions of these conflicts.

REFERENCES

Baechler G, Böge V, Klötzli S, Libiszewski S, Spillmann KR. 1996. *Kriegsursache Umweltzerstörung. Ökologische Konflikte in der Dritten Welt und Wege ihrer friedlichen Bearbeitung.* ENCOP Vol. 1. Zurich and Chur: Rüegger.

Bichsel C. 2006. *Dangerous Divides: Irrigation Disputes and Conflict Transformation in the Ferghana Valley* [PhD dissertation]. Bern: Institute of Geography, University of Bern.

Brock L. 1998. Umwelt und Konflikt im internationalen Forschungskontext. *In:* Carius A, Lietzmann KM, editors. *Umwelt und Sicherheit. Herausforderungen für die internationale Politik.* Berlin: Springer, pp 37–56.

Carius A, Baechler G, Pfahl S, March A, Biermann F. 1999. *Umwelt und Sicherheit: Forschungserfordernisse und Forschungsprioritäten.* Berlin: Ecologic.

Environmental Change and Security Project (ECSP). The Woodrow Wilson International Center for Scholars. http://www.wilsoncenter.org/ecsp; accessed on 9 September 2009.

Hagmann T. 2005. Confronting the concept of environmentally induced conflict. *Peace, Conflict and Development* 6:1–22.

Le Billon P. 2005. The geopolitical economy of 'resource wars'. *In:* Le Billon P, editor. *Geopolitics of Resource Wars.* London and New York: Frank Cass, pp 1–28.

Mason SA. 2004. *From Conflict to Cooperation in the Nile Basin: Interaction between Water Availability, Water Management in Egypt and Sudan, and International Relations in the Eastern Nile Basin.* Zurich: Center for Security Studies, Swiss Federal Institute of Technology Zurich

9.4

Local and regional sustainable land management options based on assessed experiences

Liniger Hanspeter[1], Schwilch Gudrun[1], Rima Mekdaschi Studer[1]

[1] *Centre for Development and Environment, University of Bern, Hallerstrasse 10, 3012 Bern, Switzerland (hanspeter.liniger@cde.unibe.ch; gudrun.schwilch@cde.unibe.ch; rima.mekdaschi_studer@cde.unibe.ch)*

Sustainable Land Management (SLM) uses all types of land resources (soils, water, animals and plants) for the production of goods to meet changing human needs, while simultaneously ensuring the long-term productive potential of these resources and ensuring their environmental functions. Water management cannot be separated from land use, thus all SLM technologies are related to water, by controlling surface runoff and increasing infiltration, and as a result, store more water in the soil. Without conservation measures the combined water loss through runoff and evaporation often leaves less than half of the rainfall – or irrigated water – available for crops or other vegetation.

Depending on the climate, two major categories can be differentiated: In humid environments soil erosion and soil fertility decline are common causes of land degradation. The implication is that conservation measures have to solve the problem of excess water and its safe drainage either through the soil profile or on the surface. Here, the main aim is to reduce the rapid runoff that causes sheet, rill and gully erosion on-site and flooding, sedimentation and pollution of rivers and water reservoirs off-site (downstream). Potential SLM technologies include vegetative measures such as grass strips, green cover, agroforestry systems or structural measures such as terraces, gully rehabilitation, etc. In sub-humid, semi-arid and arid regions, the same problems may occur through erratic rainfall, but the main focus is on water conservation and improved water use efficiency, e.g. through in situ accumulation of soil moisture and reduction of the water losses by runoff and direct evaporation from the soil, or through water harvesting. Examples here include conservation agriculture, improved cover, stone lines, planting pits and basins, area enclosure and assisted natural regeneration, etc. Successful SLM technologies often involve combined measures, for example structures to collect water as well as agronomic measures to reduce runoff and evaporation losses.

Worldwide, there are numerous positive experiences of sustainable land management. These counter the prevailing and pessimistic view that land and environmental degradation is inevitable and continuous. WOCAT has developed an internationally recognized, standardised methodology involving a set of three questionnaires to document relevant aspects of SLM technologies and approaches, including area coverage. A computer-based database system facilitates data entry, retrieval and evaluation. Apart from the cases documented through WOCAT (www.wocat.org) and elsewhere, the vast body of knowledge and wealth of experience in SLM made either by projects or through innovations and initiatives by the land users themselves remains scattered and localised. There is still a rich untapped SLM diversity that is not readily available to land users, those who advise them, or planners and decision makers. Thus the basis for sound decision making (for up-scaling) is lacking and mistakes are being repeated. The WOCAT tools provide a unique method for the comprehensive documentation, monitoring, evaluation and dissemination of SLM knowledge from land users, SLM specialists and researchers from different disciplines.

A new methodology has been developed for the selection of SLM strategies, combining a collective learning and decision approach with evaluated practices documented by WOCAT. A concise process of three parts involving all stakeholders starts with identifying land degradation and locally applied solutions in a stakeholder workshop. In the second part local solutions are assessed with the standardised WOCAT evaluation tool, and in the third part promising strategies for implementation are jointly selected with the help of a decision support tool. Facilitated by a moderator, participants conduct multi-criteria evaluation to rank existing and potential SLM strategies for field trials. This involves stakeholders identifying and weighing relevant criteria (e.g. technical requirements, costs and benefits, social acceptability, etc.). An option can only be considered sustainable if its evaluation is (more or less) positive with respect to all three dimensions of sustainability: economic, ecological, and socio-cultural. Thus, the negotiated SLM option has to pay off for land users implementing it, has to have positive impacts on land resources (including soil, water, vegetation, fauna), and has to be acceptable to local actors by fitting into their socio-cultural context and practices.

However, SLM is often beyond the means, responsibility and decision-making power of individual land users. Proper planning includes both local participation (by the stakeholders) and regional overall planning where on-site and off-site impacts and their interactions are considered and regulated. This is most important with regard to watersheds, where it can involve distant communities and affect their local land use planning. Too little consideration has been given to proper assessment of on-site and off-site land use interactions that lead to regional and global damage or benefits. Areas with land degradation and good SLM practices need to be identified and the impacts assessed, for which the WOCAT mapping tool was developed. It provides key information for decision making at local, regional and national level, about where investments can best be made, and about which SLM practices have the best potential to spread.

REFERENCES

WOCAT (World Overview of Conservation Approaches and Technologies). 2007: Where the Land is Greener. Case studies and analysis of soil and water conservation initiatives worldwide. Editors: Liniger, H. and Critchley, W. CTA, Wageningen (Netherlands).

Schwilch, G., Bachmann, F., Liniger, HP. 2009: Appraising and Selecting Conservation Measures to Mitigate Desertification and Land Degradation Based on Stakeholder Participation and Global Best Practices. Land Degradation & Development, 20, 308–326.

Liniger, HP. & Critchley, W., 2008: Safeguarding Water Resources by Making the Land Greener: Knowledge Management through WOCAT. In: Bossio, D. & Geheb, K. (eds): Conserving Land, Protecting Water. CABI Wallingford.

Liniger, HP. & Schwilch, G., 2002. Enhanced Decision-Making Based on Local Knowledge - WOCAT Method of Sustainable Soil and Water Management. Mountain Research and Development, 22(1) : 14-18.

9.5

From a Technocratic to a Custodianship Approach: Putting Herders at the Centre of Pasture Management in Kyrgyzstan

Daniel Maselli[1], Inam-ur-Rahim [2]

[1] *Centre for Development and Environment, Universität Bern, Hallerstrasse 10, CH-3012 Bern and University of Central Asia, Bishkek Kyrgyzstan, and Swiss Agency for Development and Cooperation, Bern (daniel.maselli@deza.admin.ch)*
[2] *Centre for Development and Environment, Universität Bern, Hallerstrasse 10, CH-3012 Bern, University of Central Asia, Bishkek Kyrgyzstan (irahim33@yahoo.com)*

In the context of research led by the NCCR North-South and the TPP 'Pastoral Production Systems' in Central Asia, a new participatory approach and methodology has been tested where local herders are actively involved in assessing, monitoring and managing pastures. So far the assessment of pasture conditions in Central Asia has been carried out by specialists employed by state entities. Based on periodic field visits, maps indicating the potential fodder production and carrying capacity have been established and were meant to be kept up-to-date. However, these maps appear to be hardly ever used by herders and village administrations and up-dating is being hampered by lack of financial and human resources since independence.

Based on experiences from northern Pakistan, a new approach has been tested in three different villages in Kyrgyzstan. The fundamental change is linked to the recognition of local herders as the real managers and future custodians of the pastures. The innovative methodology integrates biophysical, socio-economic and institutional elements into a participatory pasture management planning system. As these elements interact in a highly dynamic and interdependent manner, change in any one is bound to modify the resulting land-use strategy. This fact leads to a need for more appropriate context specific approaches for pasture management to secure the appropriate use of pastoral resources.

After an exploratory integrated survey meant to identify the appropriate planning units, the local herders are guided in selecting appropriate indicator species for pasture monitoring. In parallel the current seasonal occupation and utilization pattern is assessed. Herders are trained to evaluate grazing land conditions. During this process, the trained herders assess the relative availability of key indicator species, the calculated stocking capacity of different management units, and the current stocking. Based on this understanding a joint rehabilitation or sustainable management strategy can be devised using a multi-stakeholder process in which local authorities are integrated.

The main innovation resides in simplifying and modifying the classical conservation monitoring tools to a herder-monitoring tool in a transition context based on participation and taking into consideration local / traditional knowledge.

REFERENCES

Anna Carr and Roger Wilkinson (2005) Beyond Participation: Boundary Organizations as a New Space for Farmers and Scientists to Interact. Journal of Society & Natural Resources, Volume 18, Issue 3 February 2005 , pages 255 – 265

van Noordwijk, M., T. P. Tomich, and B. Verbist (2001) Negotiation support models for integrated natural resource management in tropical forest margins. Conservation Ecology 5(2): 21. [online] URL: http://www.consecol.org/vol5/iss2/art21/

Dale Dore (2001) Transforming Traditional Institutions for Sustainable Natural Resource Management: History, Narratives and Evidence from Zimbabwe's Communal Areas. African Studies Quarterly 5, no.3: [The online Journal for African Studies] URL: http://web.africa.ufl.edu/asq/v5/v5i3a1.htm

Rihoy E (1995) The Commons Without the Tragedy: Strategies for Community Based Natural Resources Management in Southern Africa. Proceedings of the Regional Natural Resources Management Programme Annual Conference. Lilongwe, Malawi: SADC Wildlife Technical Coordination Unit,.

Derek Armitage1 (2005)Adaptive Capacity and Community-Based Natural Resource Management. Journal of Environmental Management Volume 35, Number 6 / June, 2005 pp 703-715

Terry Hillman, Lin Crase1, Brian Furze1, Jayanath Ananda1 and Daryl Maybery1 (2005) Multidisciplinary Approaches to Natural Resource Management. Journal of Hydrobiologia. pp 99-108

Inam-ur-Rahim and Daniel Missili (2004) Improving sustainable grazing management in mountain rangelands of Hindukush Himalayas: An innovative participatory assessment method in Northern Pakistan. Mountain Research and Development, Vol 24 No: 2 (124-133)

9.6

Repartition Et Hydrochimie Des Aquiferes De L'extremite Nord Occidentales Flysch Numidien, (Tunisie Septentrionale)

MEJRI Zouhaier[1], BEN HAMZA Chedhly, HATIRA Nouri[2] et ABIDI Riadh ;

Unité de Recherche – Géologie des Ressources Naturelles, Département des sciences de la terre, Faculté des sciences de Bizerte, Jarzouna-Bizerte.7021. Tunisie. [1]mejrizouhair@yahoo.fr; [2]nouri_hatira@yahoo.fr

La region de Kromerie, située en rive gauche de l'Oued Mejerda, se carcterise par un réseau hydrographique dense et ramifié, une topographie très accidentée et une pluviométrie annuelle 1500mm
La série Numidienne de la région de Kroumerie (Tunisie septentrionale) est subdivisée en trois termes lithologiques distincts (Rouvier, 1977). Cette série représente un potentiel réservoir hydrogéologique important essentiellement dans le membre médian gréseux (Kroumerie).

La zone naturelle de la Kroumerie est découpée par un réseau d'accidents majeurs disposées en décrochements- chevauchements de direction NE-SW à NNE-SSW senestre et sub E-W dextre (Ben Ayed, 1994). Cette structuration est à l'origine, d'une part, de la compartimentation des grès et de l'isolement différentiel des réservoirs gréseux et d'autre part, de la création d'une fracturation multidirectionnelle tardive entraînant une augmentation préférentielle de la porosité et de la perméabilité des grés consolidés des flyschs numidiens du Maghreb (Johansson et al., 1998) (Fig.1).
Les réservoirs gréseux sont caractérisés par une dynamique sédimentaire représentée par des corps lenticulaires, des chenaux, slumps. Avec des bioturbations, des filons ; ont été perturbé par le replissement d'âge quaternaire ancien et d'extrusion de Trias salifère (Rouvier, 1977).
L'alimentation de réservoirs se fait par les filons gréseux qui assurent la jonction des différentes sills parcourant les grés de Kroumerie.

Les eaux souterraines issus de réservoir gréseux des Mogods montrent des faciès hydrochimiques de type chloruré et sulfaté calci-magnésien et de type chloruré et sulfaté sodique et potassique. des concentration élevais en sulfates et en sodium, avec un dégagement d'odeur fétides,a été manquées au niveau de certains captages implantés suivant une direction préférentielle orientée NNE-SSW.
Toutefois, la composition chimique des eau souterraines, mémoire des échanges eau-roches. Constitué un support fiable de lessivage et de dissolution des lithos faciès réservoirs. La richesse en chlorure et en sodium est difficile à expliquer sans admettre que set aquifère gréseux est connecté à des faciès évaporitique du Trias., notamment dus que un accident profond est injecté par un endroit par des pointements volcaniques.

REFERENCES

Ben Ayed, N. 1994. Les décrochements - chevauchements EW et NS convergents de la Tunisie septentrionale: Géométrie et essai de reconstitution des condition de deformations. Proceedings of the 4Th Tunisian petroleum Exploration conference. E.T.A.P, Tunisie, 25-35.

Johansson, M., Braakenburg, N.E., Stow A.V.D. and Faugères J. Cl. 1998. Deep-water massive sands: facies, processes and channel geometry in the Numidian Flysch, Sicily. Sedimentary geology .115, 233-265.

Rouvier, H. 1977. Géologie de l'extrême tunisien: tectoniques et paléogéographies superposes à l'extrémité orientale de la chaîne maghrébine, these Doctorat ès Sc., Univ. P et M. Curie, Paris, France.

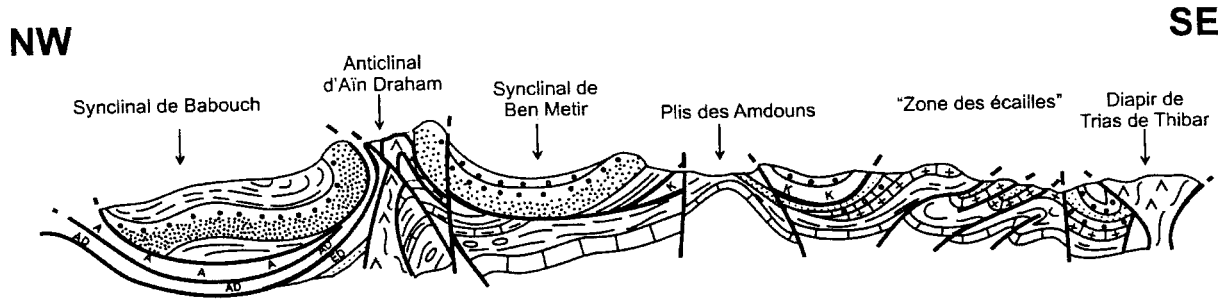

Fig .1. Coupe géologique simplifiée la structure des réservoirs hydrogéologiques de la région des Kroumerie (Rouvier, 1977)

9.7

Using the SWAT hydrological model to quantify water-related ecosystem services in a large East African watershed

Notter Benedikt[1], Hurni Hans[1], Abbaspour Karim[2]

[1] *Centre for Development and Environment, Universität Bern, Hallerstrasse 10, CH-3012 Bern (benedikt.notter@cde.unibe.ch)*
[2] *Eawag, Überlandstrasse 133, Postfach 611, CH-8600 Dübendorf*

The East African Pangani Basin, a watershed of about 43,000 km^2 located in Tanzania and straddling the border to Kenya, is characterized by an increasing demand for water-related ecosystem services. These include domestic use, agriculture, and hydropower production. The final aim of the study is to assess water availability to sustain ecosystem services for the current situation as well as possible future scenarios in the basin. We start from the assumption that an ecosystem service is realized if the availability of a resource (like water) matches an existing demand of any stakeholder in terms of quantity, quality, timing and location (Notter et al. [submitted]).

The SWAT model (Arnold et al. 1998) can be used to estimate water availability for unmeasured locations and for hypothetical situations, but under the given assumption needs to produce outputs for spatial and temporal units within which the ecosystem services of interest are transferrable. In the case of Pangani Basin, a monthly temporal resolution and spatial units corresponding to the intersection of climatic zones, subbasin boundaries, and administrative units at the Ward level is necessary. An additional challenge in our study was the lack of high quality data on climate, discharge, and water use, which makes uncertainty assessment an imperative. The mentioned challenges were met with a combination of five strategies:

a) Reducing data limitations by combining datasets from different sources, e.g. by using GIS tools to determine and implement the best possible technique for pre-processing climatic data taking into account elevation effects;
b) Implementing minor modifications to the SWAT2005 model code (corrections in the irrigation and dormancy routines, writing additional output variables, introduction of parameters that allow varying measured time-series inputs);
c) Developing a subbasin configuration procedure that takes into account administrative units and elevation zones while minimizing the number of subbasins created;
d) Applying the SUFI-2 algorithm (Abbaspour et al. 2007) for model calibration and uncertainty assessment, and additionally including uncertainty in measured time-series inputs like rainfall, temperature, point sources, and maximum allowed diversions in the uncertainty analysis;
e) Deriving proxies for water-related ecosystem services from SWAT outputs, e.g. water availability at the 95% reliability level as a proxy for domestic water, number of months per year without water stress as a proxy for agriculturally suitable land, or discharge at 75% and 95% reliability levels at topographically suitable locations as a proxy for hydropower production.

Calibration and validation of monthly discharge yields satisfactory results, with Nash-Sutcliffe coefficients of >= 0.5 reached at 8 of 12 stations, on average about 70% of measured data bracketed in the 95% prediction uncertainty, and an average width of this uncertainty range of about 1.13 standard deviations of measured data. Water quality parameters could not be calibrated for a lack of measured data, but uncertainty bands can be calculated based on the physically plausible ranges of parameters sensitive to water quality.

The calibrated model produces outputs for any required administrative unit, climatic zone, or subbasin, or any combination of these units. Preliminary results from ecosystem service quantification for the "current situation" (weather conditions from 1981-2005, land use and socio-economic data from 1997-2002) indicate that domestic, and to a lesser extent also industrial and livestock water demands are near satisfied at the 95% reliability level in those Districts that are better accessible by roads, probably because water infrastructure can be built and water rights can be obtained more easily in these areas. On agricultural land in the lowlands, where there is potential for expansion, periods without water stress are greatly prolonged where irrigation is applied, and productivity thus enhanced; however, irrigation directly impacts on hydropower potential by significantly reducing dry season discharge.
Evaluation of possible future scenarios and alternative management options has not been carried out yet but is planned for the coming months.

REFERENCES

Abbaspour, K.C. et al., 2007. Modelling hydrology and water quality in the pre-alpine/alpine Thur watershed using SWAT. Journal of Hydrology, 333: 413-430.

Arnold, J.G., Srinivasan, R., Muttiah, R.S. and Williams, J.R., 1998. Large Area Hydrologic Modeling and Assessment Part I: Model Development. Journal of the American Water Resources Association, 34(1): 73-89.

Notter, B., Hett, C., Hurni, H. and Wiesmann, U. [submitted]. Water- and Land Cover-Related Ecosystem Services: Approaches to Quantification in East Africa and Laos. Ecological Complexity: Manuscript Number ECOCOM-S-08-00227.

9.8

Caribbean Water Monitor: Small island states, water resources and climate change

Thüring Manfred[1], Trotman Adrian[2] & Moore Anthony[2]

[1] *Institute of Earth Sciences, University of Applied Sciences of Southern Switzerland, PO Box 72, CH-6952 Canobbio (manfred.thuering@supsi.ch)*
[2] *Caribbean Institute of Meteorology and Hydrology, Husbands, BB-23006 Barbados (atrotman@cimh.edu.bb, amoore@cimh.edu.bb)*

The sufficient availability of water resources is a key factor of success for any community. This project addresses the changes in the availability of water resources in the Caribbean today, and the impact of climate change. An internet-based monitoring tool – the Caribbean Water Monitor - is being developed, which indicates the current situation regarding the availability of water on two island states of the Caribbean (Barbados and Trinidad & Tobago). Based on the input of climate data – mainly precipitation and temperature – the tool assesses automatically the current situation and displays it in a comprehensive form, such as maps or trend graphs, as developed in a former project for the Caribbean island Saint Lucia (Figure 1).

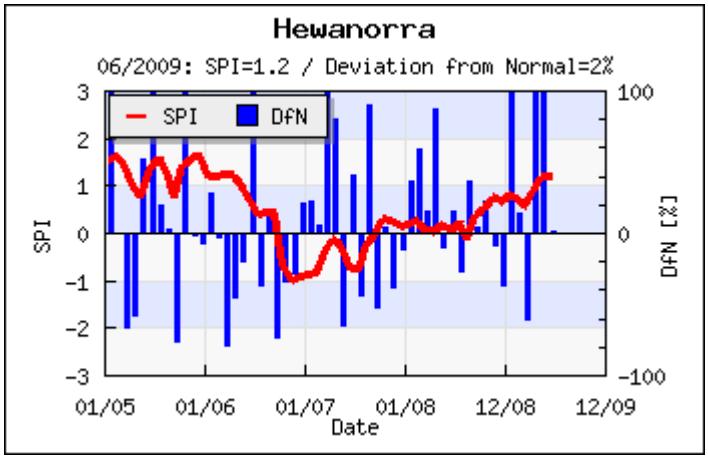

Figure 1. The usage of drought indices, such as Standard Precipitation Index or Deviation from Normal are used as support information in water resources management (www.droughtinfo.org).

The Caribbean Water Monitor is an essential tool for water resources management, and offers a help for decision support for planning and managing water resources. Climate change will require adaptation strategies. These strategies will have to be guided by assessment and monitoring tools, such as the proposed Caribbean Water Monitor.

This one-year project is developed in cooperation by a Swiss and Caribbean research partner with complementary competences, and financed by KFH-DEZA.

In our poster we show the current status of the project on the development of map based drought and water indices and the identification of climate change signatures in rainfall records of Barbados.

9.9

GIS-based Decision Support for Soil Conservation Planning in Tajikistan

Wolfgramm Bettina[1], Bühlmann Erik[1], Liniger Hanspeter[1] & Hurni Hans[1]

[1] *Centre for Development and Environment (CDE), University of Bern, Hallerstrasse 10, CH-3012 Bern (bettina.wolfgramm@cde.unibe.ch)*

Soil erosion on sloping agricultural land poses a serious problem for the environment as well as for production. In areas with highly erodible soils, such as those in loess zones, application of soil and water conservation measures is crucial to sustaining agricultural yields and preventing/reducing land degradation.

The present study, carried out in Faizabad, Tajikistan, was designed to evaluate the potential of local conservation measures on cropland to provide decision support for planning sustainable land use in a spatially explicit manner. A sampling design to support relative comparative analysis between well-conserved units and other field units was established in order to estimate factors that determine water erosion, according to the Revised Universal Soil Loss Equation (RUSLE). Such factor-based approaches allow ready application in a geographic information system (GIS) environment. Furthermore, the factor-based RUSLE model facilitates straightforward scenario modelling. High-resolution Quickbird satellite imagery was used to assess canopy cover – a major erosion control factor in the model. Standardised questionnaires designed by WOCAT (World Overview of Conservation Approaches and Technologies) were used to document local conservation measures.

The study showed first that assessment of erosion and conservation in an area with inhomogeneous vegetation cover necessitates the integration of plot-based cover derived from high-resolution satellite imagery in order to enable plot-wise conservation planning.

Furthermore, thorough field assessments showed that 25.7% of current total cropland is covered by conservation measures (terracing, agroforestry and perennial herbaceous fodder). Assessment of the effectiveness of these local measures, combined with the RUSLE calculations, revealed that current average soil loss could be reduced by low-cost measures such as contouring (by 11%), fodder plants (by 16%), and drainage ditches (by 55%). More expensive measures such as terracing and agroforestry can reduce erosion by as much as 63% (for terracing) and 93% (for agroforestry combined with terracing).

Indeed, scenario runs for different levels of tolerable erosion rates showed that more cost-intensive and technologically advanced measures would lead to greater reduction of soil loss. However, given the economic conditions in Tajikistan, it seems more advisable to support the spread of low-cost and labour-extensive measures.

REFERENCES

Bühlmann, E. 2006: Assessing Soil Erosion and Conservation in the Loess Area of Faizabad, Western Tajikistan. MSc, Centre of Development and Environment, University of Bern.

Liniger, H.P., and W. Critchley. 2007: Where the Land is Greener. Case studies and analysis of soil and water conservation initiatives worldwide. Wageningen: Technical Centre for Agricultural and Rural Cooperation.

Renard, K.G., G.R. Foster, G.A. Weesies, D.K. McCool, and D.C. Yoder. 1997: Predicting soil erosion by water: A guide to conservation planning with the Revised Universal Soil Loss Equation (RUSLE). Agriculture Handbook 703. Washington, DC: USDA.

Shi, Z.H., C.F. Cai, S.W. Ding, T.W. Wang, and T.L. Cho. 2004: Soil conservation planning at the small watershed level using RUSLE with GIS: A case study in the Three Gorge Area of China. Catena 55(1): 33-48.

10. Processes and environments influenced by water – boundaries crossed and encountered in the Quaternary research +

12. Biological, physical and chemical processes in soils

Judit Becze-Deak + Samuel Abiven, Pascal Boivin, Elena Havlicek, Claire Le Bayon

Swiss Society for Quaternary Research (CH-QUAT)
Société Suisse de Pédologie / Bodenkundliche Gesellschaft der Schweiz / Società Svizzera di Pedologia

10.18 Matile L., Achermann M., Krebs R. : Entwicklung und Anwendung einer Grobscreening-Methode zur Untersuchung des Abbauzustandes von Moorböden am Beispiel des Lobsigensees

10.19 Mavris Ch., Egli M., Plötze M., Blum J., Haeberli W. : Initial Stages Of Soil And Clay Minerals Formation In The Morteratsch Proglacial Area (Upper Engadine, Switzerland)

10.20 Meyer C., Lüscher P., Schulin R. : Regeneration of mechanically loaded soils under skid lanes by plantation of Alnus glutinosa

10.21 Pichler B., Schmidt H.-P., Boivin P., Abiven S. : Characterization of biochar and their impact on soil fertility

10.22 Prudat B., Adatte T., Hassouna M., Gobat J.-M., Verrecchia E. : Rock-Eval Pyrolysis to determine stable organic Matter in irrigated sandy Soils from Palm Orchards

10.23 Sastre V., Loizeau J.-L., Greinert J., Naudts L., Arpagaus P., Anselmetti F., Wildi W. : Morphology and recent history of the Rhone River Delta in Lake Geneva (Switzerland and France)

10.24 Schwanghart W., Frechen M., Klinger R., Schütt B. : Geomorphological drivers of Holocene environmental change in Mongolia

10.25 Singh N., Abiven S., Boivin P., Schmidt M.W.I. : Moisture and temperature effects of char in a forest soil

10.26 Studer M., Schneider M., Moreno J.M., Resco V., Abiven S. : A tool to estimate fire intensity and chemical structure of black carbon inputs into soil

10.27 Wang G., Or D. : Hydration effects on microbial motility and coexistence on unsaturated rough surfaces

10.1

Decomposability of pyrogenic carbon mixed to different organic substrates

Abiven Samuel[1], Andreoli Romano[1]

[1]Soil Science and Biogeography, Department of Geography, University of Zurich, Winterthurerstrasse 190, CH-8057 Zürich (Samuel.abiven@geo.uzh.ch)

In a recent study, Wardle and al. (2008) observed that the presence of pyrogenic carbon enhanced the decomposition of litter organic matter in a boreal ecosystem. The pyrogenic carbon (PyC) corresponds to the biomass residues after their incomplete combustion. It presents particular features regarding it biological, chemical and physical stability and might play a major role in the organic matter processes of soils.

The decomposition of organic substrates mixtures could be quite different from the decomposition of the same substrates considered individually. In most of the cases, the interactions within the mixture ends up with a higher decomposition (synergic effects). The cases when the decomposition is lower due to the mixture (antagonistic effects) or where no interaction effects (additive effects) were less reported (Gartner and Cardon, 2004).
These interactions can be explained by the presence of certain compounds that might influence the decomposition. For example, the degradation of rich-N organic substrates will make available mineral N that can be used by the micro-organisms to degrade more N-limited substrates and so will lead to a synergic effect (Handayanto et al., 1997). On the contrary, the release of biocide molecules like polyphenols might affect the decomposition of the mixture and cause an antagonistic effect (Palm and Rowland, 1997).

In this study, we followed the effects of the interactions between PyC and four different substrates containing different content in N and polyphenols.

The experimental design corresponds to an incubation under controlled conditions. We followed individually and in mixture the decomposition of Picea abies wood, char from this Picea abies wood and 4 types of fresh litter, Picea leaves, ashes leaves, oak bark and alder leaves, during 100 days at constant temperature (23°C) and moisture (field capacity). The 4 types of fresh litter had different contents in N (alder > ash > picea > oak) and in polyphenols (oak > alder > picea > ash).

The decomposition was estimated by the mineralised C-CO_2 measured by the conductivity method (Wollum and Gomez, 1970). The soil used in this incubation is a Cambisol (4 % C, 30 % clay, pH 6.0) sampled under forest (Laegern, Aargau).

The decomposition of the mixtures with N-rich content litter (alder and ash) was more important than the mixture containing oak bark and picea leaves (mineralization below 10 %).

In all the cases (example of the mixtures with Ash leaves, figure 1), we observed a more important decomposition of the mixture with wood (synergic effect) and a lower decomposition of the mixture with the char (antagonist effect). The differences between the different litters were relative to the general decomposition level of the initial substrates, rather than any interaction with particular compounds.

These results are challenging the study of Wardle et al. (2008) and show the need to take into account the initial quality of the decomposing substrates.

REFERENCES

Gartner, T.B. & Cardon, Z. G. 2004: Decomposition dynamics in mixed-species leaf litter. Oikos 104, 230-246.

Handayanto, E., Giller, K.E. & Cadisch, G., 1997: Regulating N release from legume tree prunnings by mixing residues of different quality. Soil Biology & Biochemistry. 29, 1417-1426.

Palm, C.A. & Rowland, A.P., 1997: A minimum dataset for characterization of plant quality for decomposition. Plant Litter Quality and Decomposition, Driven by Nature, eds G. Cadish and G.E. Giller, Ch. 28, 379-392

Wardle, D.A., Nilsson, M.C. & Zackrisson, O. 2008: Fire-Derived Charcoal Causes Loss of Forest Humus. Science. 320, 629.

Wollum, A. G. & Gomez J.E. 1970: A conductivity Method for Measuring Microbially Evolved Carbon Dioxide. Ecology. 51, 155-156.

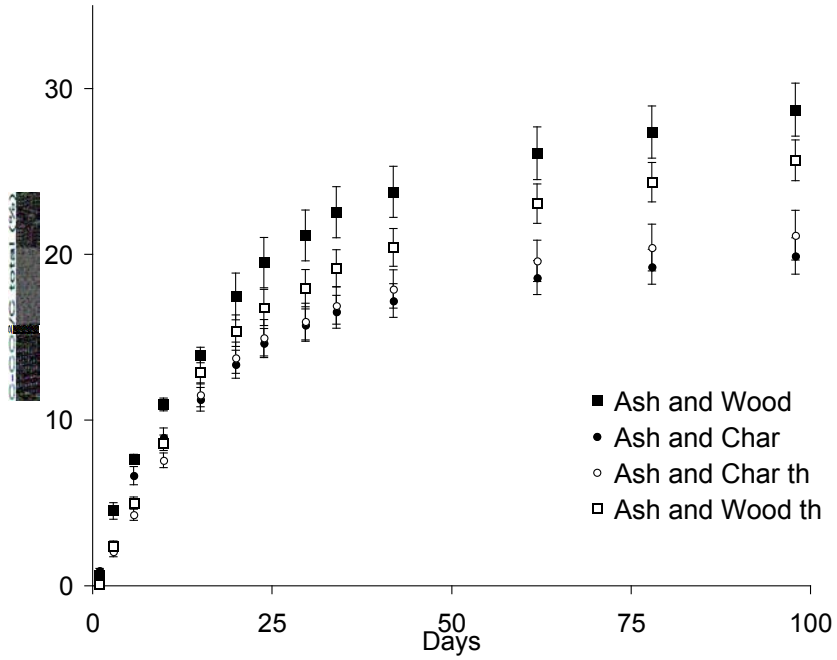

Figure 1. C mineralization (expressed as % C-CO_2 / Total C) of the mixture ash – wood (square) and ash – char (circle). The black symbols represent the measured values and the white symbols the arithmetic average of the mineralization of the organic substrates decomposing separetly (th: theoretical value).

10.2

Modelling of mechanisms affecting nitrogen and carbon cycles in soils subject to land use change

Batlle-Aguilar Jordi[1], Brovelli Alessandro[1], Porporato Amilcare[2], Barry D. Andrew[1]

[1]*Ecological Engineering Laboratory, Institute for Environmental Engineering, École Polytechnique Fédérale de Lausanne, Station 2, CH-1015, Switzerland (jordi.batlle@epfl.ch, alessandro.brovelli@epfl.ch, andrew.barry@epfl.ch)*
[2] *Civil and Environmental Engineering Department, Duke University, Durham, NC-27708, USA (amilcare@pratt.duke.edu)*

In order to meet demands for crops, pasture and firewood, the rate of land use change from forested to agricultural uses steadily increased over several decades, resulting in an increased release of nutrients towards groundwater and surface water bodies. In parallel, the continuous degradation of natural ecosystems such as riparian zones, contribute to diminish their capacity to provide ecological services, i.e. reduce the impacts of deleterious human activities on both surface and groundwater. Land use changes and restoration practices are known to affect both soil nutrient dynamics and their transport to neighbouring areas.

Biogeochemical transformations in soils are heavily influenced by microbial decomposition of soil organic matter. Carbon and nutrient cycles are in turn strongly sensitive to environmental conditions, primarily to soil moisture. This physical variable affects the reaction rate of almost all soil biogeochemical transformations, including microbial and fungal activity, nutrient uptake and release from plants, etc. Soil water saturation is not constant neither in time nor in space, thus further complicating the picture. In order to interpret field experiments and elucidate the different mechanisms taking place, numerical tools are beneficial.

The impact of hydroclimatic variability (soil moisture in particular) on soil carbon and nitrogen cycles was highlighted along with the consequences of land use changes from forest to pasture and/or agriculture. To this end, a mechanistic model based on the compartment model of Porporato *et al*. (2003) was developed. The predictive capabilities of the model to forecast the

effects of land use changes over carbon and nitrogen dynamics were shown, modelling four different scenarios, intertwining two different climate conditions (with and without seasonality) with two contrasting soils having physical properties that are representative of forest and agricultural soils. Synthetic time series of precipitation, and therefore soil moisture evolution in time, were generated using a stochastic approach. The model was subject to isothermal conditions and other considerations such as average values of carbon and nitrogen concentrations over the rooting depth. As well an average microbial organic decomposition rate was considered. Simulation results demonstrated higher concentrations of carbon and nitrogen in forests soils as a result of higher litter decomposition than in agricultural soils (Figure 1). High frequency changes in water saturation under seasonal climate scenarios were shown to be commensurate with carbon and nitrogen concentrations in agricultural soils. Forest soils have different properties to agricultural soils, leading to an attenuation of the seasonal climate-induced frequency changes in water saturation, with accompanying changes in carbon and nitrogen concentrations.

The model was shown to be capable of simulating the long term effects of modified physical properties of agricultural soils as a consequence of tillage, ploughing and harvesting. It is, thus, a promising tool to predict carbon and nitrogen turnover changes due to changes in land use. These results encourage further model improvements aimed at accounting for the complexity of the soil system and its processes for better understanding soil nutrients turnover.

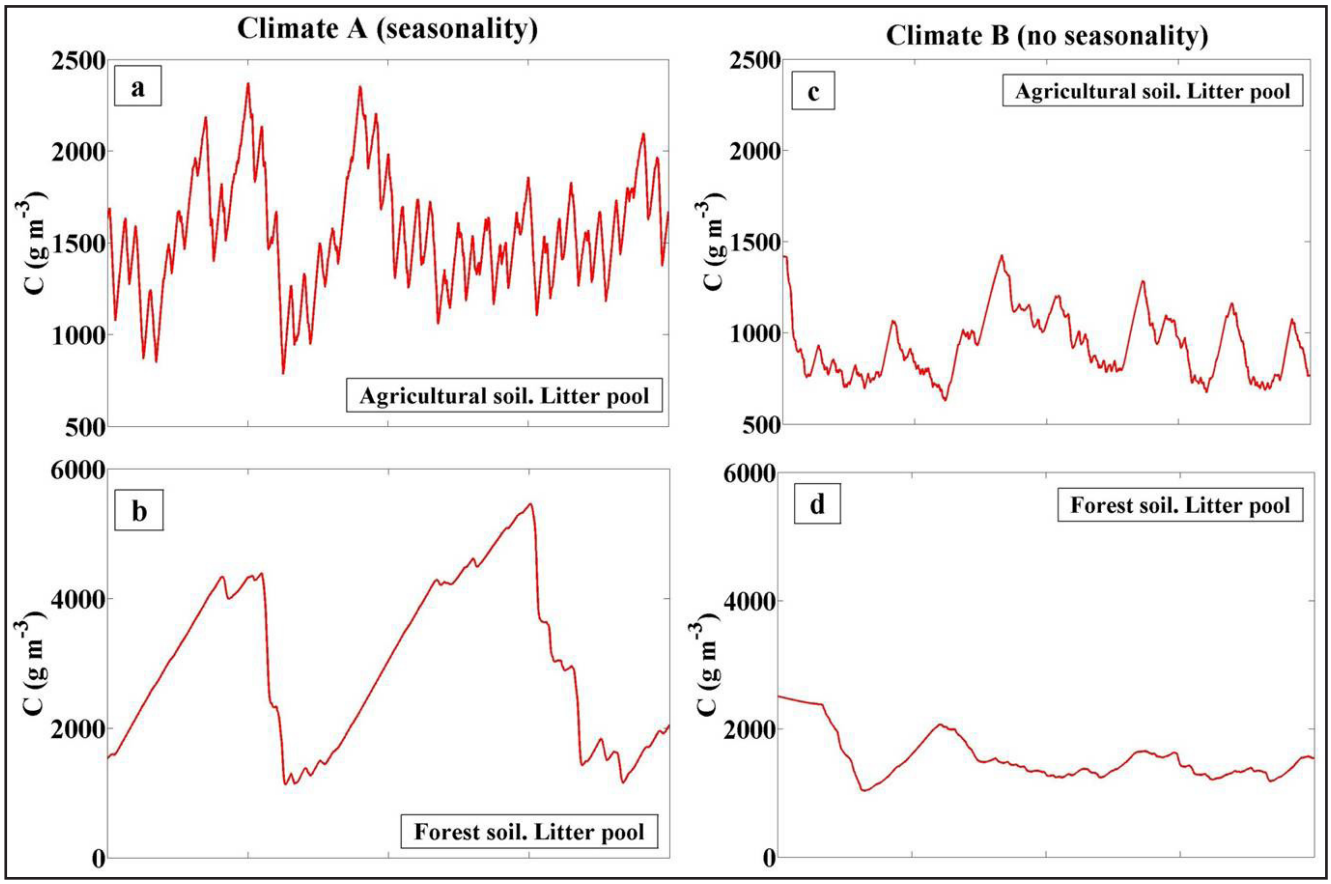

Figure 1. Simulated organic carbon concentrations in the litter pool for agricultural and forest soils under seasonal (left side) and no seasonal (right side) climate conditions.

REFERENCES

Porporato, A., D'Odorico, F., Laio, F. & Rodriguez-Iturbe, I. 2003: Hydrologic controls on soil carbon and nitrogen cycles. Adv. Water Resour., 26, 45-58.

10.3

Carbon isotope signature of biogeogenic trichloromethane: a tool to discriminate anthropogenic and natural sources in soils

Florian Breider[1], Christian Albers[2], Daniel Hunkeler[1] & Ole Stig Jacobsen[2]

[1]*Center of Hydrogeology, University of Neuchâtel, Rue Emile Argand 11, CH-2009 Neuchâtel (florian.breider@unine.ch)*
[2]*Geological Survey of Denmark and Greenland, Oster Voldgade 10, DK-1350 Copenhagen*

Trichloromethane (TCM, $CHCl_3$) has been for long time considered as an anthropogenic contaminant known for its cancerogenic effects. TCM is sometimes detected far from any anthropogenic sources without any other contaminants. To date more than 3800 natural halogenated organic compounds have been identified (Gribble, 2003). The presence of TCM in coniferous forest soils and groundwater has been widely demonstrated. Different studies suggest that TCM and other organohalogens such as chloromethane may be naturally produced in soils by enzymatic chlorination of the soil organic matter (Hoekstra et al., 1998). Chloroperoxidase excreted by some fungi may play a major role in the biosynthesis of organohalogens in soil (Hoekstra et al., 1998).

Isotope ratio mass spectrometry is a powerful tool to determine the origin and the fate of organic compounds in the environment (Harper et al., 2001). The aim of this study is to discriminate anthropogenic and biogeogenic TCM sources using compound specific isotope analysis. The isotopic signatures of TCM produced industrially and by chlorination of different humic substances and soil organic matter were measured by GC-C-IRMS. Moreover $\delta^{13}C$ values of TCM present in forest soils were also measured at different depth in three sites in Denmark.

All natural precursors used give comparable $\delta^{13}C$ values of TCM which are consistent with typical isotope signature of compounds derived from plant material (Fig.1). Industrial TCM is particularly depleted in ^{13}C ($\delta^{13}C$~49‰ vs. V-PDB) compared to TCM synthesized from natural precursors ($\delta^{13}C$~33‰ vs. V-PDB) (Fig.1). Therefore the isotopic ratio constitutes a good indicator of the origin of TCM.

The $\delta^{13}C$ values of TCM measured in forest soils are in the same range as TCM produced in laboratory from natural precursors. This confirms that TCM presents in soil air is biogeogenic (Fig.2). The variations of the $\delta^{13}C$ values with soil depth are inversely correlated with the TCM concentrations profiles. Indeed, when concentrations of TCM in the soil air are high, TCM is depleted in ^{13}C compared to soil layers presenting low TCM concentrations. These variations are likely due to the combination of production, degradation and transport processes in soils. Further investigations are currently carried out to know how climatic parameters such as precipitation, soil moisture and temperature can influence these processes and therefore the isotopic ratios of TCM.

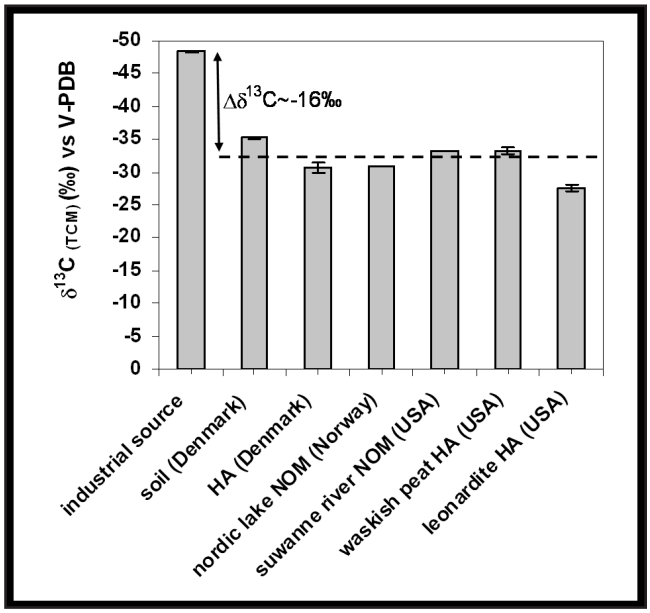

Figure 1. δ13C (‰) of industrial TCM and TCM synthesized from different natural precursors. HA: humic acid, NOM: natural organic matter

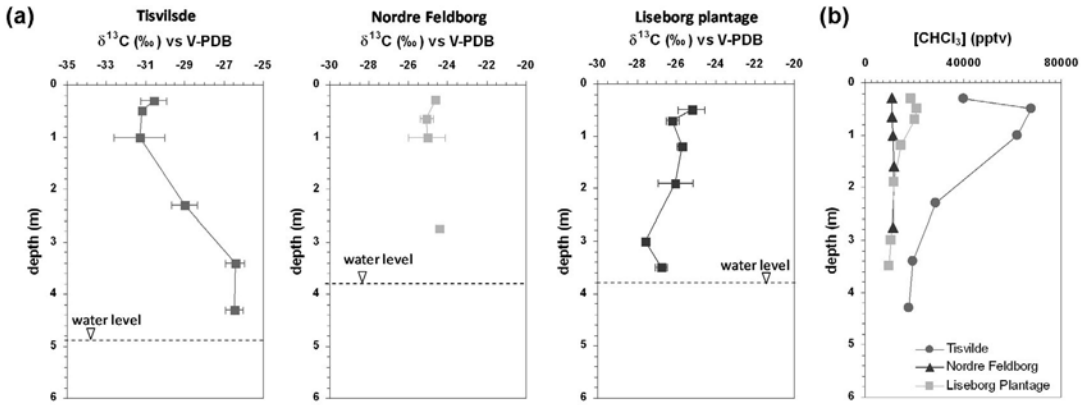

Figure 2. $\delta^{13}C$ (a) and concentration profiles (b) of TCM in soil air of three different sites.

REFERENCES

Gribble, G. W. 2003: The diversity of naturally produced organohalogens. Chemosphere, 52, 289-297.

Harper, D.B., Kalin, R.M., Hamilton, J.T.G. & Lamb, C. 2001. Carbon isotope ratios for chloromethane of biological origin: Potential tool in determining biological emissions, Environmental Science and Technology, 35, 3616-3619

Hoekstra, E.J., De Leer, E.W.B. & Brinkman, U.A.T. 1998: Natural formation of chloroform and brominated trihalomethanes in soil. Environmental Science and Technology, 32, 3724-3729.

10.4

Porewater pressure modelling in a rainfall triggered shallow landslide: the sprinkling experiment in Rüdlingen, Canton Schaffhausen

Broennimann Cornelia[1], Askarinejad Amin[2], Springman Sarah[2], Tacher Laurent[1]

[1]*GEOLEP, EPFL, Station 18, 1015 Lausanne (cornelia.broennimann@epfl.ch)*
[2]*Institut für Geotechnik, ETHZ, Wolfgang-Paulistr. 15, 8093 Zürich*

Heavy and long-term rainfall is well known as a major trigger of landslides at different scales. Nevertheless, often a lack of datasets complicates a detailed understanding of slope's hydrological regime. It is assumed that for shallow landslides the hydrogeological role of the bedrock is determinant for the slopes behaviour. In the presented study, two landslide triggering experiments were carried out on a densely equipped test site. Based on a large dataset, a finite element flow model was elaborated to reconstruct the evolution of pore water pressures in the slope during and after sprinkling tests.

The sprinkling experiment was located near the villages Rüdlingen and Buchberg in the canton Schaffhausen at the border of the river Rhine. With a slope inclination of locally up to 40° the area is rather steep and characterized by continuous regressive erosion processes (Figure 1). The experiment took place in a slope affected by former sliding processes which could be verified by several mass movement deposits of ~1 m thickness. During rainfall events, for example in May 2002, several shallow landslides occurred in the area and affected afforested soils as well as woodless areas.

The lithology in the area of the experiment is characterized by horizontally layered marls and sandstones from the lower freshwater (Aquitanien) and upper seawater molasse (Burdigalien) overlaid by 1 - 3 m of silty colluvium and soil. For more detailed lithological and hydrogeological reconnaissance, a 23 m deep borehole was drilled above the test site. The sandstone is poorly cemented and strongly altered. This explains the locally high hydraulic conductivity (10^{-2} m/s – 10^{-5} m/s) measured in various infiltration tests which were carried out in ~3 m deep hand auger boreholes. Furthermore, vertical joints in decametre scale oriented parallel to the Rhine affect locally the hydrogeological regime by draining effectively the slope. Seasonally controlled springs are observed along outcropping bedrock above the test site. This implies that at a local scale the bedrock water flows are highly heterogeneous.

The 10x30 m large test site with a mean inclination of 35° was equipped among others with pluviometers, tensiometers, decagons, piezometers, deformation probes, electric resistivity tomography instrumentation, acoustic sensors and video cameras. The site was irrigated artificially with an intensity of maximal 30 mm/h. During a first sprinkling period of 5 days in October 2008, the slope remained stable. However, in March 2009 it failed after an irrigation period of 15 hours.

The first experiment in October 2008 showed that heavy rainfall is not always sufficient to trigger a mass movement. The initial saturation of the soil plays an important role concerning the slopes stability. Also the hydrogeological character of the bedrock should be taken into account. The sandstone in the sprinkling area acted most likely as a drain due to its large joints. The initial conditions for the second experiment in fall 2009 were different because soil and bedrock were more saturated after rainy periods and snowmelt. This is most likely the reason for the rapid triggering of a ~180 m² large landslide.

Based on field and laboratory parameters, a 2D finite element flow model is created. It shows the relationship between surface water infiltration and the spatially and temporally evolution of porewater pressures before and during the slope failure. This gives new findings of the hydraulic conditions in the subsurface during the triggering of a shallow landslide. In future work, the modelled pore water pressure distribution can be combined with mechanical slope stability calculations.

This study was carried out in the frame of the TRAMM Project (Triggering of Rapid Mass Movements) financed by CCES (Competence Center Environment and Sustainability of the ETH Domain).

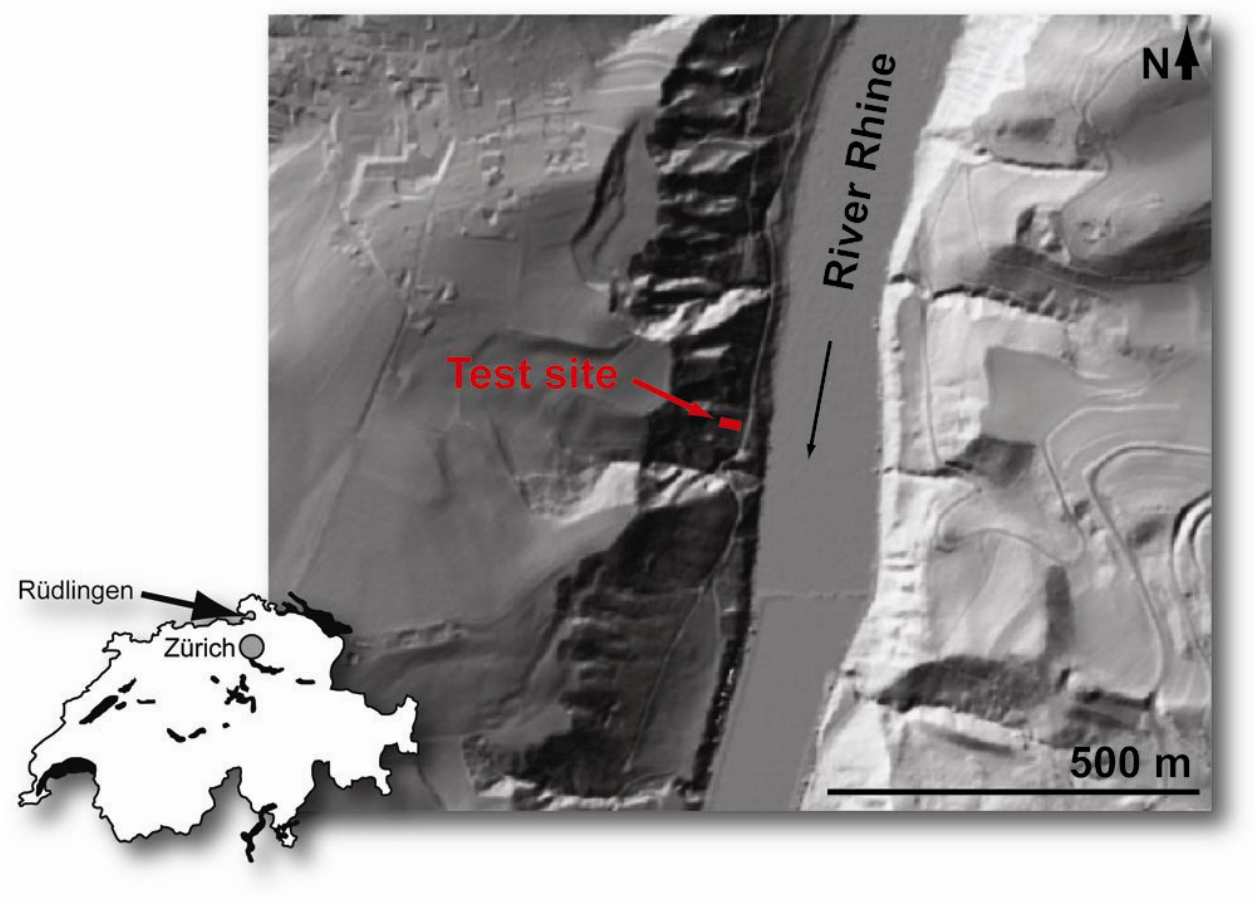

Figure 1: Location of the Rüdlingen sprinkling experiment. Notice the regressive erosion processes in the gullies and at the steep borders of the River Rhine (http://www.sh.ch).

10.5
Controls on the form of bars in braided rivers

Castelltort Sébastien[1] & Gredig Gaudenz[1]

[1]*ETH-Zürich, Earth Surface Dynamics, Sonneggstrasse 5, 8092 Zürich (sebastien.castelltort@erdw.ethz.ch)*

Despite the considerable amount of work completed on the morphology of braided rivers, the controls on the form of braid bars within channels and the processes that contribute to their formation are still unclear. Most studies have focused on the complexity of braiding and have tried to measure and characterize this complexity (see e.g. Egozi and Ashmore, 2008). Through different approaches it is shown clearly in these studies that the degree or intensity of braiding is controlled by the slope, discharge and quantity and quality of the sediment in transport. Many attempts have also been made at using these parameters in order to find threshold-separated fields of existence of the braided or meandering channel patterns. The sand or gravel bars that separate channels within a braided river reach have been given a different kind of attention: most studies interested in braid bars have explored and described the sedimentary processes acting upon their formation, their resulting sedimentary architecture and their sedimentology. The reason for this focus is that braid bars ultimately fill channels and thus represent the bulk of the coarse fill of continental environments related to braided systems s.l., potential reservoirs of crucial importance to resource geology.

However, are braid bars different in rivers with different slopes, grain size or discharge? No data has ever been collected before that can allow us to answer this question. In the present work we present new data that fill in this gap in knowledge.

Taking advantage of methods developed to study the shape of river networks in mountain ranges at ETH-Zürich (Castelltort et al., 2009) and image analysis methods developed for microscope petrography (JMicroVision©, University of Geneva), we study the characteristic angle between channels at multiple flow convergences in 10 braided rivers worldwide. We show that bars become more elongate and narrow as slope increases (Figure 1). This intuitively consistent result has important implications: 1) it confirms that the main processes that shape braid bars are erosive in nature (Murray and Paola, 1994). A braided river can be considered close to a succession of river networks incising a new surface after each flood. 2) if the form of braid bars can be inferred from fossil deposits, the paleoslope of the river can be deduced.

Slope however is not an independent parameter of river evolution. It is indeed controlled by the competition between water discharge and sediment flux and grain size which are the only independent variables at the upstream boundary of a river system. On given fluvial successions, given the sediment grain size distribution, the reconstruction of braid bars morphology and paleoslope can provide unique informations on river paleo-hydrology and climate.

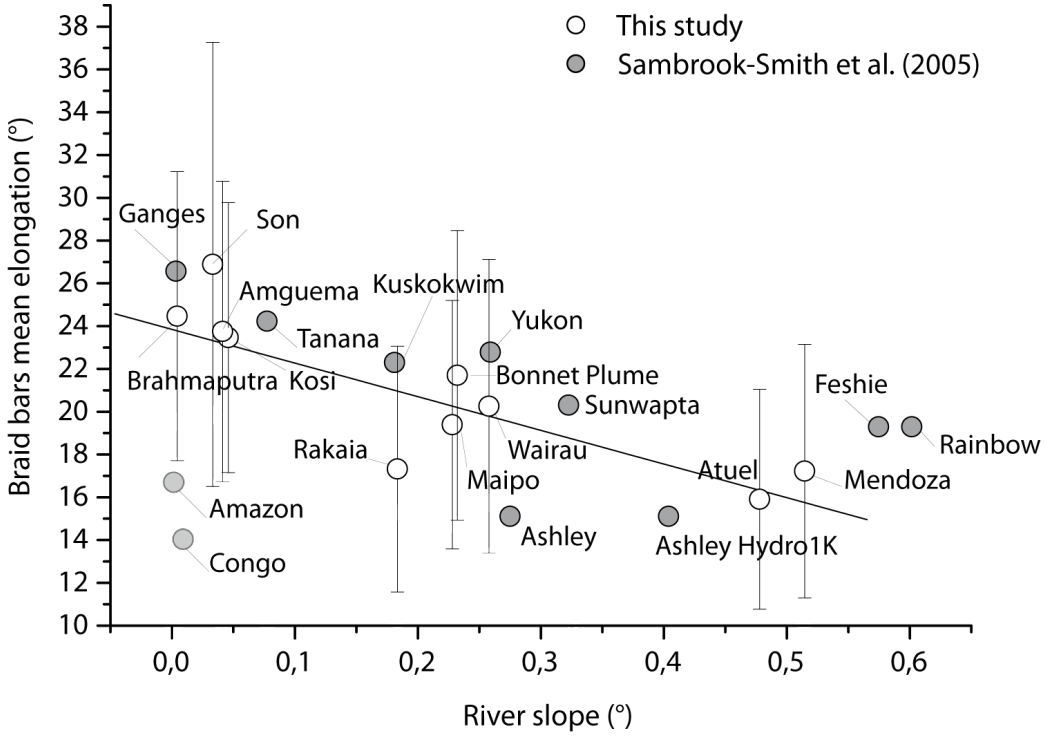

Figure 1. Braid bar mean elongation (equivalent confluence angle in degrees) versus river slope. The braid bars are broader (large confluence angle) on smaller slopes and more elongate (small confluence angle) on high slopes.

REFERENCES
Castelltort S., Simpson G. & Darrioulat A. (2009) – Slope-control on the form of river basins, Terra Nova, in press.
Egozi R. & Ashmore P. (2008) – Defining and measuring braiding intensity. Earth Surface Processes and Landforms, 33, 2121-2138.
Murray, A.B. & Paola, C. (1994) – A cellular model of braided streams, Nature, v. 371, 54-57.
Roduit, N. – JMicroVision: Image analysis toolbox for measuring and quantifying components of high-definition images. Version 1.2.2. http://www.jmicrovision.com (accessed May 2009).

10.6

Discrete simulation of biogeochemical exchanges in a microbial mat

Chappatte Damien[1], Verrecchia Eric[2]

[1]*Institut de Géologie et Paléontologie, Université de Lausanne, Anthropole, CH-1015 Lausanne, damien.chappatte@unil.ch*
[2]*Institut de Géologie et Paléontologie, Université de Lausanne, Anthropole, CH-1015 Lausanne, eric.verrecchia@unil.ch*

Microbial mats are complex ecosystems, which played and still play a major role in the Earth system. Their biogeochemical functioning is still not completely understood. Microbial mats are driven by several guilds of bacteria (with their own metabolisms), chemical substances, light, and many other external and internal parameters. Conventional approaches to computer simulate such a geo-ecosystem use numerical models, usually based on differential equations and their solutions. We propose to explore a different way by using another computer science tool, discrete simulation.

In discrete simulation, time and space are discretized in time steps and cells. Each cell contains the state of a small part of the mat. Time steps are iterated over the course of the simulation, and each cell state is updated.

In our simulations, cells contain information about chemical substances, chemical reactions, light, and bacteria characterized by their metabolisms. Simulations generate data similar to those obtained in a natural environment, such as chemical substance concentrations or light intensities. Such data can be obtained in any cell at any time step, the same way a natural scientist would get measurements in the field at different points in a mat and at different times of the day. Consequently, graphs and profiles can be plotted and simulation results compared to real microbial mat measurements.

Preliminary results show that this tool can mimic the diel cycles of main chemical substances found in microbial mats (such as O, S, or C). The goal is to extend the model capacity in order to precipitate calcium carbonate, leading to the simulation of stromatolite growth. In this way, we will have access to a virtual laboratory in which easy experiments could be run to check hypotheses regarding biogeochemical behaviour of microbial mats during the Earth's history.

10.7

Reconstruction of past vegetation succession on developping podzols using organic and mineral specific markers

Comment Nicolas[1], Pinard Gladys[1], Abiven Samuel[2], Adatte Thierry[3], Gobat Jean-Michel[1] & Verrecchia Eric[3]

[1]*Laboratoire Sol & Végétation, Université de Neuchâtel, Emile-Argand 11, CH-2009 Neuchâtel (nicolas.comment@unine.ch)*
[2]*Soil Science and Biogeography Unit, University of Zurich – Irchel, Winterthurerstr. 190, CH-8057 Zurich*
[3]*Laboratoire des Biogéosciences, Université de Lausanne, Anthropole, CH-1015 Lausanne*

Podzolisation is a pedogenetic process caracterised by different modifications of the organic matter and mineral material over time. This process occurs under specific biotic and abiotic conditions. The major one is the presence of an acidifying litter, which could be found under moorland or under coniferous litter. However, podzols are also found under meadows, which indicate that the vegetation changed during the podzolisation process.

The study site is located in Saint-Luc (VS) between 2100 and 2900 meter a.s.l. Soil profils were dug under different vegetation types, conifer forest, moorland and grassland. This study proposes to reconstruct past vegetation and associated podzolisation processes using specific bio- and mineral markers.

We used lignin as biomarkers of the vegetation, since this molecule is only originated from plants. Also, the lignin molecules are often considered as recalcitrant in the soil and so the chance to find traces of former vegetation is larger. The lignin was extracted using the cupric oxide oxidation procedure. Briefly, the soil samples were extracted using an alkaline solution under N_2 atmosphere. The solutions were cleaned and the concentration of 8 specific phenolic monomers for lignin were measured by GC – FID. The calculation of ratios allowed us to compare the actual composition of the soil lignin to the lignin of different vegetation types.

The podzolisation process was caracterised by (1) the mobilization of iron and (2) the destruction and neogenesis of clays. (1) During podzolisation, iron binds organic matter together in the form of chelates. This complexation enables iron to percolate through the soil. The eluvial horizon becomes depleted in iron. To estimate the losses of iron, two extractions on eluvial horizons were done (i) tetraborate of sodium and (ii) citrate-bicarbonate-dithionite (CBD). Tetraborate extracts the form of iron that is characteristic for podzolisation and CBD all forms of iron which are present in soil (excluding crystalized forms). Then, the ratio (Fe tetraborate/Fe CBD) is calculated. (2) Litter decomposition, roots and microorganisms release organic acids which attack phyllosilicates (mica and chlorite). This weathering leads to the neogenesis of new clay mineral following this order: mica-vermiculite mixed layers – vermiculite – mica-smectite mixed layers – kaolinite. Bulk rock and clay mineral assemblages were analyzed by X-ray diffraction (ARL X'TRA Diffractometer).

The first results of iron forms show the presence of two classes of eluvial horizon (Figure 1). Their distinction's limit is near 2550m a.s.l. It's interesting to underline that this height corresponds globaly to the higher limit that the forest had never reached in a nearby valley (Tinner et al., 2003).

The mineralogy of clays and mobilized iron from eluvials horizons estimate the degree of podzolisation of the different soils. These results will be correlected to the lignin data in order to trace the different kind of vegetation that might have been growing there. These results emphasize the role of combined organic and mineral matters in the podzolisation process through time.

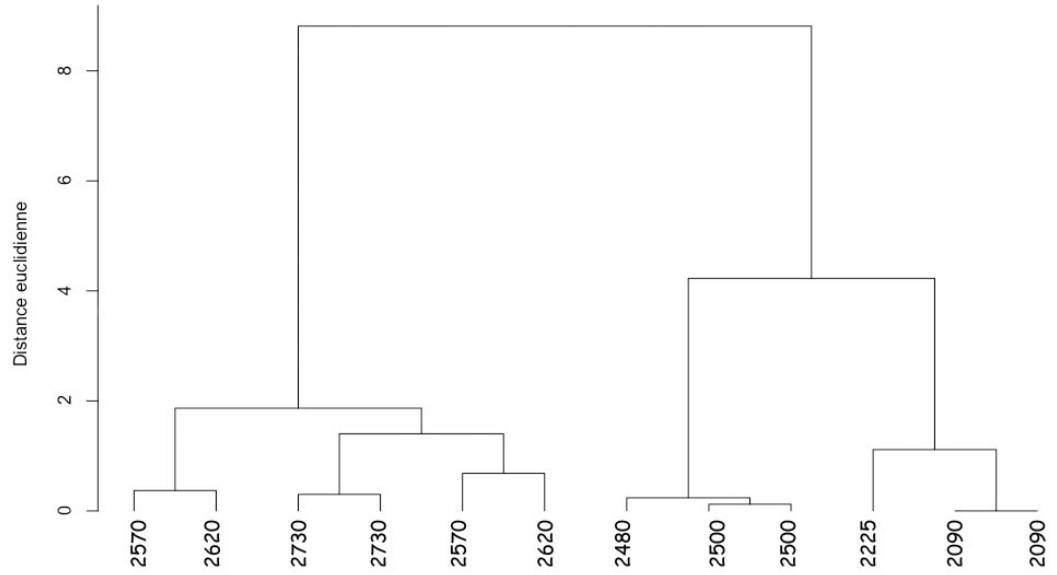

Figure 1: Dendrogram of eluvial horizons distribution according to euclidian distance (Ward agglomeration). The variables "altitude" and "ratio (Fe tetraborate/Fe CBD)" have been used to perform calculations. The number down below is the altitude of the studied soil.

REFERENCE

Tinner, W. & Theurillat, J.-P. 2003: Uppermost Limit, Extent, and Fluctuations of the Timberline and Treeline Ecocline in the Swiss Central Alps during the Past 11,500 Years. Arctic, Antarctic, and Alpine Research, 35, 158-169.

10.8

Etude de la dynamique des éléments traces métalliques en forêt périurbaine (Isle-Adam, Val d'Oise, France): approche écosystémique

Ehrhardt Fiona[1], Matera Virginie[2], Adatte Thierry[3], Verrecchia Eric[3]

[1]*Laboratoire Sol et Végétation, Université de Neuchâtel, Emile-Argand 11, CH-2009 Neuchâtel (fiona.ehrhardt@unine.ch)*
[2] *Institut d'Hydrogéologie et de Géothermie, Université de Neuchâtel, Emile-Argand 11, CH-2009 Neuchâtel*
[3]*Laboratoire des Biogéosciences, Université de Lausanne, Anthropole, CH-1015 Lausanne*

Cette étude se concentre sur la distribution et l'origine des éléments traces métalliques (ETM) dans une forêt péri-urbaine proche de Paris (L'Isle-Adam). Elle vise à intégrer différents compartiments de l'écosystème forestier afin de mieux comprendre les interrelations et les influences réciproques. Ainsi, le long d'un transect, dix stations ont été sélectionnées dans le but d'étudier fonctionnellement les sols et les formes d'humus associées, et de quantifier les ETM présents. Ceci complète certains travaux déjà effectués (Hernandez et al., 2003), et précise le lien entre ETM et phases porteuses.

Dans un premier temps, l'utilisation des analyses statistiques a permis de préciser les principaux facteurs de distribution (Bor vka, 2005), et ce, dès le dépôt des polluants atmosphériques en surface jusque dans l'ensemble des profils des sols étudiés. Les résultats montrent ainsi que l'analyse de la litière (OL) permet de déceler l'origine des éléments (en distinguant notamment les apports géogéniques des apports anthropiques) ainsi que leur mode de dépôt. Les horizons de fragmentation (OF) permettent ensuite la réorganisation des éléments en fonction des affinités pour les différentes phases porteuses du sol et le comportement chimique de chacun. Enfin, dans les horizons OH, qualité de la matière organique et degré d'humification semblent dicter la distribution des ETM.

S'agissant de la répartition globale des ETM dans l'ensemble des profils de sol étudiés, nous avons constaté que les facteurs de distribution sont principalement liés à deux gradients complémentaires (fig.1), l'un couplé à la présence de matière organique qui diminue avec la profondeur et l'autre, inverse, associé à l'augmentation de la proportion de matière minérale (notamment la proportion de phyllosilicates). Nous avons ainsi pu démontrer, grâce à une étude minéralogique, l'importance des smectites dans la migration des ETM.

L'étude du facteur d'enrichissement des ETM permet de préciser davantage la part de la contribution anthropique de celle d'origine géogène (Blaser, 2000) et de visualiser la migration des éléments anthropiques à travers le profil de sol. Ainsi le plomb, bien que réputé peu mobile, semble capable de migrer jusqu'à des profondeurs importantes dans ce type d'écosystème. La faune du sol contribue également à la dynamique des ETM en créant les formes d'humus et nous avons vu que la composition faunistique est propre à chaque grand type de forme d'humus. Elle permet l'intégration de la MO dans les sols, contribue à sa minéralisation et donc à la remise en circulation des ETM liés à la MO.
Les résultats expriment des valeurs relativement élevées pour le Pb (jusqu'à 130 ppm dans les sols et 210 ppm dans les horizons OH), le Cr (jusqu'à 342 ppm dans les horizons OF) et le Cd (jusqu'à 1.12 ppm dans les horizons OF et OH), mettant en avant l'importance des horizons humifères dans le stockage et la séquestration de ces éléments. Ces valeurs dépassent les valeurs limites définies par l'Osol (1998), à savoir 50 ppm pour le Pb, 50 ppm pour le Cr et 0.8 ppm pour le Cd.

En conclusion, les résultats obtenus montrent que le fonctionnement même du sol détermine la distribution des ETM selon les dynamiques de la MO et des phyllosilicates qui lui sont propres.

REFERENCES

Blaser, P. et al., 2000. Critical examination of trace element enrichments and depletions in soils : As, Cr, Cu, Ni, Pb, and Zn in Swiss forest soils. The Science of the Total Environment 249, 257-280.

Bor vka, L. et al., 2005. Principal component analysis as a tool to indicate the origin of potentially toxic elements in soils. Geoderma 128, 289-300.

Hernandez, L. et al., 2003. Heavy metal distribution in some French forest soils : evidence for atmospheric contamination. The Science of the Total Environment 312, 195-219.

Osol, 1998. Ordonnance sur les atteintes portées au sol. OFEV, confédération Suisse ; ordonnance du 1er juillet 1998, n° 814.12.

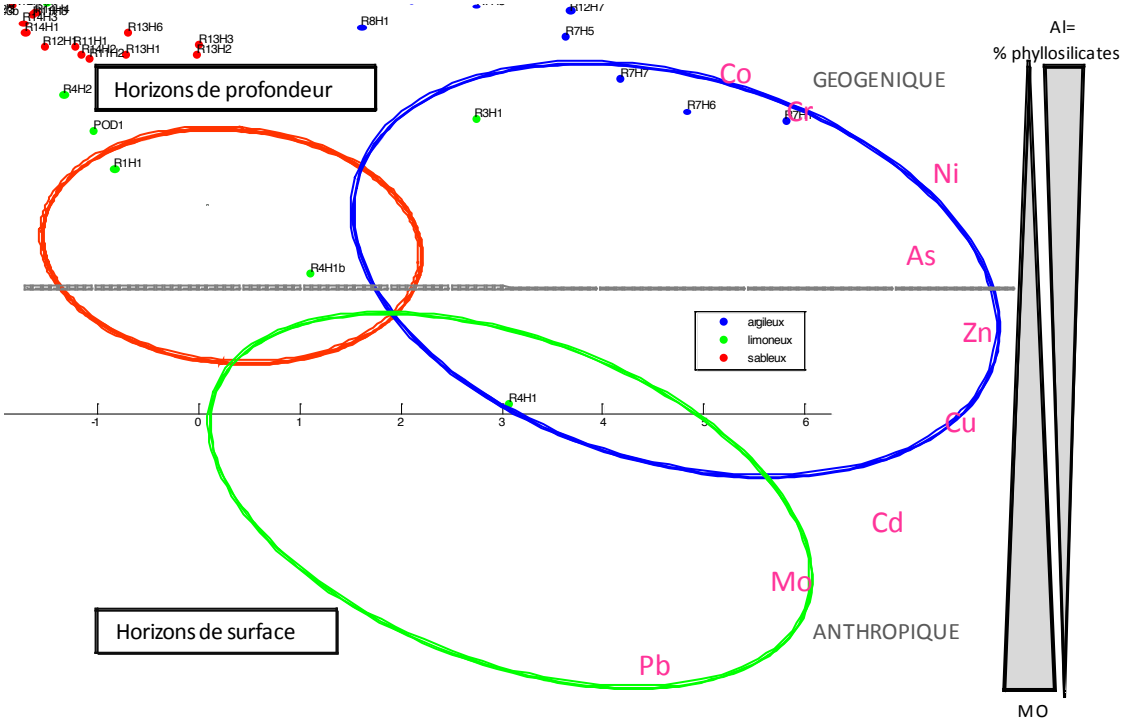

Fig.1 : Schéma synthétique de la répartition des ETM (Pb, Zn, Cu, Cd, Ni, Cr, Mo, As, Co) dans les horizons de sol (n=78), par une ACP. Variances expliquées sur CP1 : 58% et CP2 : 16%.

10.9

Soil porosities as engineered by earthworms microcosm experiment with tomography and shrinkage analysis assessment

François Füllemann[1 2], Roxane Milleret[2], Y. Capowiez[3], Renée-Claire Le Bayon[2], Jean-Michel-Gobat[2], & Pascal Boivin[1]

[1] *Laboratoire Sols et Substrat, hepia-Lullier, route de Presinge 150, 1254 Jussy, Genève (fullemann@gmail.com)*
[2] *Laboratoire Sol et Végétation, Université de Neuchâtel, rue Emile-Argand 11, CP 158, 2009 Neuchâtel.*
[3] *INRA Montfavet*

Earthworms are known to play a key role on soil ecological processes such as organic matter turnover, nutrient cycling and soil physical properties engineering. They are acknowledged as essential to soil fertility. However, their role on numerous soil physical properties is still poorly documented. The objectives of the present study were to test the effect of two earthworm ecological categories (*Nicrodrilus nocturnus* as anecic, *Alollobophora icterica* as endogeic species, and both as mixed population with 80% weight of *N nocturnus* and 20% of *A. icterica*) on two different soils. Shrinkage analysis and Computed Tomography were used to assess the impact of earthworms on soil porosities and bulk volume. The study was performed during 23 weeks on microcosms under controlled conditions (constant temperature and constant soil matrix potential). The soils were a silt loam Luvisol and a loamy Anthrosol. In addition, before the introduction of earthworms, all microcosms were set at two levels of soil compaction further called compacted and uncompacted soils.

The observed effects varied with the factors ‘soil type’, ‘initial soil bulk density’ and ‘earthworm species’, and with their interactions. The bulk soil volume was modified by earthworms, with decompaction of the compacted microcosms and compaction of the non compacted ones. The bulk volume changes were then split into worm gallery pores generated, and additional effect on smaller structural pores or plasma pores. A model of the changes induced by ‘anecic’, ‘endogeic’ and ‘mixed’ was then formulated. The impact are different according to the considered soil volume: bulk soil or soil matrix without pores due to galleries, structural porosity and plasmic porosity, respectively. Roughly, the decompaction effect of worms is due to the opening of galleries at bulk soil scale, but the matrix is either compacted (case of not compacted soil) or unchanged (case of compacted soil), and the compaction of the matrix is larger with endogeic species. The mixed-species treatment induced the same effects as monospecific ones in most cases, and the anecic effect was dominant, but the endogeic effect was effective on most considered soil volumes. Some cases showed an opposition between mixed activities and single treatments, pointing out particular ecological emergent properties.

10.10

FloodAlp! Frequency and intensity of extreme floods in the Alps through the Holocene

Glur Lukas[1], Wirth Stefanie B.[2], Anselmetti Flavio S.[1], Gilli Adrian[2] & Haug Gerald H.[2]

[1]Eawag, Swiss Federal Institut of Aquatic Science and Technology, CH-8600 Dübendorf (lukas.glur@eawag.ch)
[2]Geological Institute, ETH Zurich, Sonneggstr. 5, 8092 Zürich (stefanie.wirth@erdw.ethz.ch)

Floods caused by extreme precipitation events represent one of the major natural hazards in the Alpine realm. New climate models point to the possibility that flood frequency and intensities increase as a result of the upcoming climate changes. To scale these predicted changes of extreme events, knowledge of their natural variety is required.

The FloodAlp! project aims to reconstruct the frequency and intensities of Holocene flood events in the Alps by using lake sediments as natural geologic archives, which act as prehistoric recorders of extreme events. Lake basins record such events with characteristic sediment layers that contrast sharply to the regular background sediments. The high discharge values with large amounts of suspended particles trigger turbiditic underflows that focus the detrital particles in the deepest areas of the basins.

A total of twelve lakes along a north-south transect covering a wide range in altitude will be investigated during the project. Each targeted lake is first investigated by a high-resolution (3.5 kHz) reflection seismic survey, providing information on the sediment thickness, seismic stratigraphy, sediment distribution and ideal coring locations. After this first evaluation, long sediment cores (max. length 16 m) are taken in the deepest depression of the lake basin.

Precondition for establishing the flood record is a good age model, which is accomplished by ^{14}C and $^{137}Cs/^{210}Pb$ dating. Also crucial is the differentiation between background sedimentation and event layers as well as between mass-movement-related and flood-related event deposits. This characterisation of the sedimentary facies is achieved by chemical, physical and mineralogical analyses of the sediment material.

First results from two lakes (Lake Ledro, I, and Hinterer Schwendisee, CH) show already the potential of this approach. High-resolution reflection seismic profiles are able to image the geometry of the sediment filling and define the spatial focus of flood layer accumulation. Furthermore, over hundred flood-related turbidite deposits in each lake are sharply distinguishable from the background sediment. The age models of the two sediment-successions provide the means to construct a well-dated chronology of these potential hazardous events throughout the Holocene.

10.11

Effects of atmospheric deposition of acid compounds and nitrogen on soil solution in Swiss forests

Graf Pannatier Elisabeth[1], Schmitt Maria[1], Thimonier Anne[1] & Waldner Peter[1]

[1]Swiss Federal Institute for Forest, Snow and Landscape Research WSL, Zürcherstrasse 111, CH-8903 Birmensdorf (elisabeth.pannatier@wsl.ch)

In the framework of the Long-term Forest Ecosystem Research LWF, the chemistry of atmospheric deposition and soil solution have been analysed fortnightly since 1998 or later in seven forest plots in Switzerland. We aim to assess the soil response to the inputs of acid compounds and nitrogen (N) since they might alter the soil functions and represent potential stress factors for forest ecosystems. Acid deposition might accelerate soil acidification, leading to the leaching of nutrients and/or the mobilization of toxic aluminum for sensitive plants. Increased N concentrations in the soil solution may lead to nutrient imbalances for trees and changes in the composition of ground vegetation. Large nitrate leaching below the root zone might also threaten the quality of the ground- and surface-water.

Atmospheric deposition of the major elements was estimated from throughfall and bulk deposition measurements since 1995 or later. Soil solution has been measured since 1998 or later at four soil depths (below litter layer, 15 cm, 50 cm, 80 cm). The molar ratio of base nutrient cations to aluminum (BC/Al) in the soil solution was determined to assess soil acidification. This ratio is used as indicator in most critical load models in Europe, assuming BC/Al ratios smaller than 1 might cause adverse effect on tree roots. Nitrate leaching flux leaving the root zone was estimated from soil solution samples at 80 cm depth using nitrate concentrations and modelled infiltration rates.

Acid atmospheric deposition at the seven LWF plots ranged on average between -0.02 and 1.99 keq ha^{-1} a^{-1} with the lowest load in the Alps and the highest load in Southern Switzerland. Total nitrogen deposition varied between 2.4 kg ha^{-1} a^{-1} in the Alps to 31 kg ha^{-1} a^{-1} in the Southern Switzerland. The high acid and nitrogen loads in southern Switzerland come partly from the emissions of the industrialised and densely populated Po Basin.

The BC/Al ratios in the soil solution decreased in most plots during the two first years of the observation period, which might be caused by the installation of the lysimeters. After this period, BC/Al has stabilized in five plots, suggesting that acidification has proceeded very slowly during the last 10 years. At two sites, a further decrease in BC/Al was observed, suggesting a faster acidification.

Nitrate leaching ranging from about 2 and 13 kg N ha^{-1} a^{-1} was observed at sites subjected to moderate to high total N deposition (> 10 kg ha^{-1} a^{-1}). The C/N ratio of the soil organic layer, together with the pool of organic carbon in the soil and the humus type, played a critical role.

10.12

OSL-based chronology of the postglacial beach plain NE of Lake Neuchâtel on Swiss Plateau: Problems and possible solutions.

Heer Aleksandra[1], Hajdas Irka[2], Steffen Damian[3], Preusser Frank[3] & Veit Heinz[1]

[1] Institute of Geography, University of Bern, Hallerstrasse 12, CH-3012 Bern (heer@giub.unibe.ch)
[2] Ion Beam Physics, Swiss Federal Institute of Technology (ETH Zürich), Schafmattstr. 20, CH-8093 Zürich
[3] Institut für Geologiel, Universität Bern, Baltzerstrasse 1+3, CH-3012 Bern

With the aim of reconstructing the postglacial landscape evolution (~17'000 a BP till to presence), OSL has been used to date eight profiles from a fossil beach plain called Grosses Moos on the Swiss Plateau. For four profiles radiocarbon ages derived from underlying and intercalated organic horizons have also been calculated. OSL measurements were conducted on quartz sand-size grains applying the SAR-protocol after identifying the appropriate measurement conditions in a series of experiments (Wintle and Murray 2006). However, we recognised problems due to the intrinsic properties of the investigated quartz as well as due to the changing environmental conditions during the expected burial time.

The quartz grains are generally dim. Hence the measurements of 2 mm aliquots suffer from significant errors due to the signal intensity (Duller 2007, Li 2007). For most 2 mm aliquots the errors are higher then 10%. The consequence of accepting for errors higher then 10% leads to an overestimation of the true age. The dating of very young sediments also suffers from the limitation due to the dim signal. When the quartz is dim and one uses 2 mm aliquots, there will be preferential selection of aliquots that contain grains with higher doses. Possible causes for grains with high doses are radioactive hotspots such as zircon grains or K-feldspars and these have been identified in these samples. For 2 mm aliquots the CW-OSL signal amount of fast component varies between 24%-66%. The dim signal is probably responsible for those errors. However this signal may come from quartz with other properties. On the other hand, when using bigger sized aliquots (6 or 8 mm) the results improve significantly: the fast component amount rises up to more then 80% of the entire initial signal and the errors stay lower then 10%. I_{nat} – D_e - % D_e - error – plots have bin constructed to visualise this coherence and to check the independency of I_{nat} and % D_e – error as statistical variables influencing the D_e determination. For selected samples OSL signal properties and resulting consequences for dating will be presented. Also the thickness of the overlying deposit changed during the burial time. Especially for profile ISL6 the ^{14}C-data helped in determining the duration of the succeeding deposition. Otherwise the age of the basic palaeochannel would have been overestimated. Groundwater oscillations have been recognized while recording hydromorphic soil features. Therefore the reliability of the currently recorded water content for the whole expected burial time has been checked for each sample separately. Nevertheless, considering those problems a reliable and consistent chronology for Grosses Moos, applying OSL – and ^{14}C – data, has been developed.

REFERENCES

Duller, G.A.T., (2007), Assessing the error on equivalent dose estimates derived from single aliquot regenerative dose measur ements. Ancient, TL 25: 15-24.

Li, B., (2007), A note on estimating the error when subtracting background counts from weak OSL signals. Ancient TL 25/1, 9-14.

Wintle, A.G., Murray, A.S. (2006). A review of quartz optically stimulated luminescence characteristics and their relevance in single-aliquot regeneration dating protocols. Rad. Measurements 41, 369-391.

10.13

Is the mineral phase responsible for stabilizing lignin in soils?

Heim Alexander[1], Hofmann Anett[1], Miltner Anja[2], Christensen Bent T.[3] & Schmidt Michael W.I.[1]

[1] *Department of Geography, University of Zurich, Winterthurerstrasse 190, CH-8057 Zürich (alexander.heim@geo.uzh.ch)*
[2] *Department Environmental Biotechnology, Helmholtz Centre for Environmental Research - UFZ, Permoserstraße 15, D-04318 Leipzig*
[3] *Department of Agroecology and Environment, Faculty of Agricultural Sciences, University of Aarhus, DK-8830 Tjele*

Lignin is the second most abundant biopolymer in higher plants. Its fate in the soil is still largely obscure. On one hand, many litterbag studies point to a selective enrichment of lignin during the early phase of litter decomposition. On the other hand, compound specific isotope analysis of lignin-specific biomarkers has shown that the average turnover time of lignin in soils is similar or faster than that of bulk soil organic carbon. Mass balances combining annual input, soil lignin stocks and turnover rates inferred from isotope data, suggest the existence of at least two kinetic pools, one of which disappears very fast.
For bulk soil organic carbon (SOC), interactions of organic matter with the mineral phase in soil seem to be an important stabilization mechanism. However, very little data are available on the type of compounds that interact with the mineral phase.

Lignin monomers are biomarkers of relatively fresh plant inputs. The aim of this study is to trace these biomarkers into different soil fractions, answering the following questions: (I) Which soil fractions (size, density) contain most lignin? (II) Does the stability of lignin vary between these fractions? (III) Can differences in lignin content between soil fractions be explained by properties of the mineral phase (surface area, type of minerals)?

The study was conducted with arable soil from a long-term experiment that had been naturally ^{13}C-labelled by 18 years of maize cropping. We identified old lignin deriving from the time before maize cropping by compound-specific isotope analysis of lignin-derived phenolic biomarkers and compared its distribution within the soil to the initial distribution in an archived soil sample.
A large proportion of lignin was found in the coarse heavy fraction, suggesting inclusion into macroaggregates. However, isotope data clearly indicated that lignin in this fraction was less stable in the long-term than lignin in light fractions or in silt-size aggregates. The lignin/SOC ratio of the latter two fractions indicates that they contain less decomposed organic matter.

We suggest that the following mechanisms may control stability of lignin in arable soils: (1) Some lignin-containing cell structures (e.g. thick cell walls) seem to be indeed recalcitrant enough to persist for decades even under intensive cropping. Due to intensive cropping before the isotopic labeling started, the light fractions are already enriched in these recalcitrant structures, and therefore show very little degradation during the observation period. (2) Stable silt-size aggregates may preserve small fragments of relatively undecomposed plant residues. (3) Macroaggregates, by contrast, turn over more rapidly, so that inclusion into macroaggregates does not stabilize lignin as long as the other mechanisms.

10.14

Pyrogenic carbon solubility in the soils: quantitative and qualitative approaches

Hengartner Pascal[1], Abiven Samuel[1]

[1]*Soil Science and Biogeography, Department of Geography, University of Zurich, Winterthurerstrasse 190, CH-8057 Zürich (Samuel.abiven@geo.uzh.ch)*

The pyrogenic carbon (PyC) corresponds to the biomass residues after their incomplete combustion, mainly by wild fires. Until recent studies, this particular kind of soil organic matter was considered as passive, recalcitrant and so stable in the soils.

Recently, different authors highlighted significant biotic degradation (Baldock and Smernik, 2002; Hammer et al., 2004) and/or abiotic degradation (for example Smith and Chughtai, 1996) of these compounds. Moreover, specific PyC biomarkers were found in surface and marine waters and in sediments (Hockaday et al., 2006). These two findings might indicate that a fraction of this PyC is translocated though the soil.

However, the quantity and the characteristics of this PyC fraction as well as the mechanisms of their transports in the environment remain largely unknown.
In this study, we propose to estimate the quantity and the features of the soluble and colloidal fraction of PyC.

The PyC used in this study is the international standard as defined by the black carbon steering committee: Castanea sativa Mill. Wood, pyrolised at 450 °C during 16 h under a N_2 stream. The char was then grounded (< 1 mm).

The water-extractible fraction was first estimated in a batch experiment in the lab. The char was shake in deionised water at the rate of 160 g Char. l^{-1} and the fractions below 0.45 μm (soluble fraction) and below 5 μm (colloidal fraction) were collected by filtration. We repeated this batch design with 10 years old char pieces that we collected from a fire experiment in Tessin.
Then, we applied the standard char to a cambisol in the field (Laegern Hills, Aargau, CH) and we collected regularly the soil solution with suction plates.

The PyC quantity and characteristics were analysed using mass balance, C and N content and the Benzene PolyCarboxylic Acids method (BPCA, Browdowski, 2005). This method consists in an acid digestion of aromatic compounds, releasing polycarboxylic acids which are considered as specific PyC biomarkers. In this study, we adapted the method to small pyrogenic compounds.
In the batch experiment, the soluble fraction represented 1 per mil of the initial char mass (Fig. 1). The fraction only contained 38 % C (compared to 66 % for the initial char) and 0.66 % N (compared to 0.07 % in the initial char), indicating that the soluble fraction contains much other compounds than aromatic PyC moieties. The specific PyC biomarkers were only representing 1% of the dissolved C content.

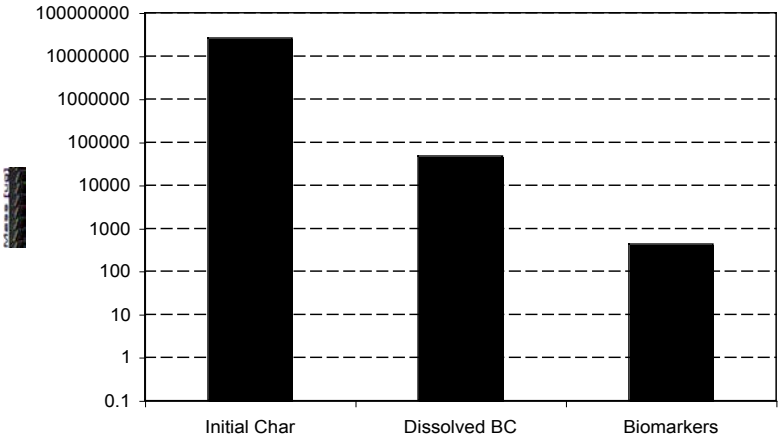

Figure 1. Mass recovery in the dissolved fraction (dissolved BC) and as specific PyC biomarkers (Biomarkers) from 25 g of standard char. Logarithmic scale.

REFERENCES

Baldock, J. A., and R. J. Smernik. 2002: Chemical composition and bioavailability of thermally altered Pinus resinosa (Red pine) wood. Organic Geochemistry, 33, 1093-1109.

Brodowski, S. 2005. Origin, function, and reactivity of black carbon in the arable soil environment. PhD Thesis, Bonner Bodenkundliche Abhandlungen, pp. 183.

Hamer, U., B. Marschner, S. Brodowski, and W. Amelung. 2004. Interactive priming of black carbon and glucose mineralization, Organic Geochemistry, 35, 823-830.

Hammes, K., Smernik, R.J., Skjemstad, J.O., Vogt, U.F., Schmidt, M.W.I. 2006: Synthesis and characterisation of laboratory-charred grass straw(Oryza sativa) and chestnut wood(Castanea sativa) as reference materials for black carbon quantification. Organic Geochemistry, 37, 1629-1633.

Hockaday, W. C., A. M. Grannas, S. Kim, and P. G. Hatcher, 2006: Direct molecular evidence for the degradation and mobility of black carbon in soils from ultrahigh-resolution mass spectral analysis of dissolved organic matter from a fire-impacted forest soil, Organic Geochemistry, 37, 501 – 510.

Smith, D. M., & A. R. Chughtai. 1996: Reaction kinetics of ozone at low concentrations with n-hexane soot, Journal of Geophysical Ressources, 101, 19,607 – 19,620.

10.15

Quantifying rates of surface denudation at the eastern Altiplano margin, La Paz region, Bolivia

K. Hippe1, F. Kober2, G. Zeilinger3, S. Ivy-Ochs4, P.W. Kubik4, C. Schlüchter5 & R. Wieler1

1 Isotope Geology and Mineral Resources, ETH Zürich, CH-8092 Zürich, Switzerland (hippe@erdw.ethz.ch)
2 Institute of Geology, ETH Zürich, CH-8092 Zürich, Switzerland
3 Institute of Geology, Univ. Potsdam, D-14476 Golm, Germany
4 Laboratory of Ion Beam Physics, ETH Zürich, CH-8093 Zürich, Switzerland
5 Institute of Geological Sciences, University of Bern, CH-3012 Bern, Switzerland

The Bolivian Altiplano is a large, flat plateau framed by the high peaks of the Western and Eastern Cordillera. Along its eastern margin the Rio La Paz has cut deeply across the Cordillera forming an eastward-draining river system that stands in sharp morphological contrast to the internally drained Altiplano. Landscape morphology, relief and surface processes change fundamentally across the drainage divide. A feedback mechanism between erosional unloading by focussed incision and flexural rebound has been proposed for the Rio La Paz drainage system (Zeilinger & Schlunegger 2007), but the effect of crustal bending on the adjacent Altiplano has not yet been evaluated. While denudation rates are known for the Rio La Paz system (Zeilinger et al. 2009) and the Eastern Cordillera (Safran et al. 2005), we have quantified rates of denudation on the Altiplano side. For catchments bordering the Rio La Paz drainage divide we have determined catchment wide denudation rates based on cosmogenic ^{10}Be in river sediments. For all catchments the landscape is flat with smooth hillslopes; precipitation is low with a strong interannual variability.

Cosmogenically determined denudation rates in the Rio La Paz system are 0.1-0.6 mm/yr (Zeilinger et al. 2009). Preliminary denudation rates for the Altiplano are one to two orders of magnitude lower between 0.002 and 0.029 mm/yr, with an integration time of 24-230 ky. This is in agreement with modern sediment yield rates (Guyot et al. 1992) although they integrate over only one to five years. For the Altiplano, denudation rates show no clear correlation with morphometric catchment parameters, but rather seem to be influenced by lithology (i.a. glacial deposits) and possibly also anthropogenic processes.

REFERENCES

Guyot, J.L., Wasson, J.G., Quintanilla, J. & Calle, H. 1992: Dissolved matter and suspended sediment loads in some inflow rivers and in the Rio Desaguadero. In: Lake Titicaca (Ed. by Dejoux, C. & Iltis, A.), 113-119.

Safran, E.B., Biermann, P.R., Aalto, R., Dunne, T., Whipple, K.X. & Caffee, M. 2005: Erosion rates driven by channel network incision in the Bolivian Andes. Earth Surf. Process. Landforms 30, 1007-1024.

Zeilinger, G., Kober, F., Strecker, M., Ivy-Ochs, S., Kubik, P.W. & Hippe, K. 2009: Erosion rates in the Rio La Paz drainage basin: evidence for spatially and temporally variable erosion processes. Geophys. Res. Abstracts, EGU General Assembly 2009.

Zeilinger, G. & Schlunegger, F. 2007: Possible flexural accomodation on the eastern edge of the Altiplano in relation to focussed erosion in the Rio La Paz drainage system. Terra Nova 19, 373-380.

10.16

The shape versus the processes of a landform – the Hörnli region, NE-Switzerland

Kober, F. [1], Abbühl, L.[2], Dürst, M.[2], Ivy-Ochs, S.[3], Schlunegger, F.[2], Kubik, P.W.[4]

[1]*Geological Institute, ETH Zürich, CH-8092 Zürich (kober@erdw.ethz.ch)*
[2] *University of Bern, Baltzerstrasse 1+3, CH-3012 Bern*
[3]*Ion Beam Physics, Particle Physics, ETH Zürich, CH-8093 Zürich and Department of Geography, University of Zürich, CH-8057 Zürich*
[4]*Ion Beam Physics, Particle Physics, ETH Zürich, CH-8093 Zürich*

Although the landscape of the Hörnli region in NE-Switzerland would, at first glance, imply that landscape processes and process rates must be different between the fluvially and glacially overprinted landform parts – there is no strong evidence for this argument in geomorphic parameters and spatially averaged catchment wide denudation rates obtained with cosmogenic 10Be. While glacially overprinted catchments tend to have lower average slopes and are at lower mean elevations, other parameters fail to show correlations. Slope-area plots suggest partial rejuvenation for glacial overprinted catchments, i.e., incision into accumulation planes in the lower river courses. This is also in accordance with observed knickpoints which are beyond the commonly lithologically controlled channel steps (Nagelfluh banks) that are observed everywhere. Spatially averaged catchment wide denudation rates vary between 30-2000mm/ky with a tendency towards lower values in catchments with glacial overprint, though not always.

It is suggested that glacially overprinted catchments with smoother topographies and accumulated glacial deposits in their lower reaches protect the landscape against faster erosion rates. Another option would be that glacially sourced sediments of the catchment with relatively higher cosmogenic nuclide concentrations control the lower denudation rates. In contrast, the fluvial catchments, with stepper slopes and exposed at higher elevations are controlled by more active processes, such as shallow landsliding, rock falls, debris flows and little soil development would promote shorter residence time in the catchment, hence higher denudation rates.

As such it is suggested, that the remnants of the glacial overprinting, i.e., sculpturing and deposition.

10.17

Earthworm, mycorrhiza and root interactions: effects on soil phosphorus nutrient status and soil structure

Kohler-Milleret Roxane[1], Le Bayon Claire[1], Boivin Pascal[2] & Gobat Jean-Michel[1]

[1]*Laboratory Soil & Vegetation, Institute of Biology, Emile-Argand 11, CH-2009 Neuchâtel (Roxane.Milleret@unine.ch)*
[2]*Laboratory of Soils and Substrates, HEPIA, Route de Pressinge 150, CH-1254 Jussy*

Biotic interactions in soils are known to influence the belowground and aboveground system by affecting soil fertility, i.e. its nutrient status and soil structure. Earthworms, arbuscular mycorrhiza fungi (AMF) and roots are especially important components of the belowground system. While AMF-plant symbiosis is essential for plant nutrition, they also modify soil structure in mechanical and chemical ways (soil particles enmeshment into bigger aggregates and glomalin secretion for AMF). Earthworms, as ecosystem engineers, are known to influence soil properties and plant production (soil structure and porosity modification by burial and feeding-casting activities, formation of the organo-mineral complex, microorganism dispersion or ingestion). However, little is known about the effects of earthworms and AMF on plant growth or soil chemical and physical properties. An experimental approach was therefore designed in order to assess separately or in combination the effects of earthworms (*Allolobophora chlorotica*, Savigny), AMF (*Glomus intraradic*es, Schenk and Smith), and plant roots (*Allium porrum*, L.) on i) soil structure, ii) availability of nutrients (mainly phosphorus, P) in the bulk soil as well as in both rhizosphere and drilosphere.

The results point out that plant roots improved soil stability at the level of macroaggregates (> 250 μm) and decreased the bulk soil density (as revealed by shrinkage analysis), whereas earthworms decreased soil stability and the bulk soil volume. AMF had no effect on soil structure stability but increased P transfer from the soil to the plant and consequently plant biomass. Earthworm had no direct influence on P uptake, but drilosphere soil contained a higher amount of available forms.

This study shows that under P limitation, AMF enhance plant growth *via* available phosphorous acquisition. In our experiment, earthworms have no direct effect on plant growth but drilosphere soil may serve as a nutrient pool that can be later mobilized. This experiment highlights the importance of a holistic approach measuring physical, chemical and biological soil parameters when studying soil organism interactions and their influence on plant performance.

10.18

Entwicklung und Anwendung einer Grobscreening-Methode zur Untersuchung des Abbauzustandes von Moorböden am Beispiel des Lobsigensees

Matile Luzius, Achermann Marco & Krebs Rolf

ZHAW, Institut Umwelt und Natürliche Ressourcen, Grüntal, CH- 8820 Wädenswil (luzius.matile@zhaw.ch)

Am Ufer des Lobsigensees (BE) befindet sich in einem ehemaligen Niedermoor die Fundstelle einer neolithischen Siedlung. Seit das Moor im Zusammenhang mit der landwirtschaftlichen Nutzung entwässert wird, findet der Torfabbau statt. Vom Abbau organischer Substanz ist dabei auch ein wesentlicher Teil der archäologischen Fundstelle betroffen. So hat ein Vergleich der Grabungen von 1953 und 2005 gezeigt, dass der Erhaltungsgrad der archäologischen Funde sehr stark abnahm.

Da die torfabbauenden Schrumpfungs- und Mineralisationsprozesse die physikalischen Eigenschaften des Bodens verändern, wurde untersucht, ob sich durch die Messung des Eindringwiderstandes grobe Aussagen über den Abbauzustand des organischen Bodens und damit auch der Fundstelle machen lassen. Um neben dem Abbauzustand auch die Abbaurate abzuschätzen, wurden Verrottungsversuche mit Baumwolltüchern durchgeführt.

Die mit einem dynamischen Rammpenetrometer (PANDA-Sonde) gemessenen Eindringwiderstände ergaben eine gute Korrelation mit bodenphysikalischen Parametern wie der Lagerungsdichte, mit dem Gehalt organischer Substanz und bestätigten den Befund der Profilansprache.

Durch die Messung des Eindringwiderstandes können somit dichtere (mineralische/antorfige) und lockerere Schichten (Torf) im Bodenprofil lokalisiert und in Zusammenhang zum Abbauzustand am untersuchten Standort gebracht werden. Diese einfache Methode würde eine grobe Übersicht über das Stadium der Moorsackung der jeweiligen organischen Böden im Tiefenprofil erlauben und damit Rückschlüsse auf den Zustand der betroffenen Fundstellen ermöglichen. Das Screeningverfahren wäre damit eine effiziente Methode zur Priorisierung gefährdeter Fundstellen.

10.19

INITIAL STAGES OF SOIL AND CLAY MINERALS FORMATION IN THE MORTERATSCH PROGLACIAL AREA (UPPER ENGADINE, SWITZERLAND)

Christian Mavris1[1], Markus Egli1, Michael Plötze2, Joel Blum3, Wilfred Haeberli1

1Department of Geography, University of Zurich, Zurich, 8057, Switzerland [1](christian.mavris@geo.uzh.ch)
2ETH Zurich, Institute for Geotechnical Engineering, Zurich, 8093, Switzerland
3Dept. of Geological Sciences, University of Michigan, Ann Arbor, MI 48109, USA

Investigations in Alpine soils indicate that mineral weathering is much faster in 'young' soils (< 1000 yr) than in 'old' soils (~10 000 yr). However, little is known about the initial stages of weathering and soil formation, i.e. during the first decades of soil genesis. In this study we investigated rock-forming minerals weathering at very early stages of soil formation. Due to the continuous retreat of the Morteratsch glacier (Upper Engadine, Swiss Alps), the proglacial area offers a full time sequence from 0 to 150 yr old surfaces. A low slope and the absence of glacier which might have interrupted soil formation processes, contributed to the choice of the Morteratsch proglacial valley for this case study. The area is well documented regarding vegetation and soils. The tectonic unit is the Bernina-crystalline, which is mainly constituted of granitoid rocks. Consequently, the glacial till has an acidic character. Mineralogical measurements were carried out on the bulk soil fraction (< 2mm) using XRD and DRIFT for qualitative and quantitative phase analysis. In addition, chemical analyses of the stream water from the main channel and, tributaries and of rainwater were performed with a special focus on Ca/Sr and Sr isotope ratios ($^{87}Sr/^{86}Sr$). Furthermore, the accumulation of organic matter within the time sequence and physical soil properties were assessed. Decreasing grain size with time shows active physical weathering processes. Soil organic matter has been accumulated during 150 yr at very high rates. Special emphasis has been given to chemical weathering and to the formation and transformation mechanisms of minerals. Of special interest were biotite, chlorite, epidote, plagioclase and calcite. Biotite has been continuously transformed into illite-like components. Within 150 years, the concentration of epidote significantly decreased. The high Ca/Sr as well as $^{87}Sr/^{86}Sr$ ratios in the stream and spring waters confirmed that Ca bearing minerals are weathering and transforming at very high rates in the proglacial area. Also in cryic, ice-free environments, chemical weathering rates are high leading to the formation and transformation of minerals. Disseminated calcite in granitoid rocks, not confined to sedimentary carbonate rocks, also plays a role in subglacial environments. It is, however, not known for how long such an influence is significant and measurable. The high Ca/Na and Ca/Sr ratio in the stream and tributary waters showed that calcite contributes to the supply of soluble Ca, although the ion activity product calculations clearly demonstrated that the waters were undersaturated with respect to this mineral.

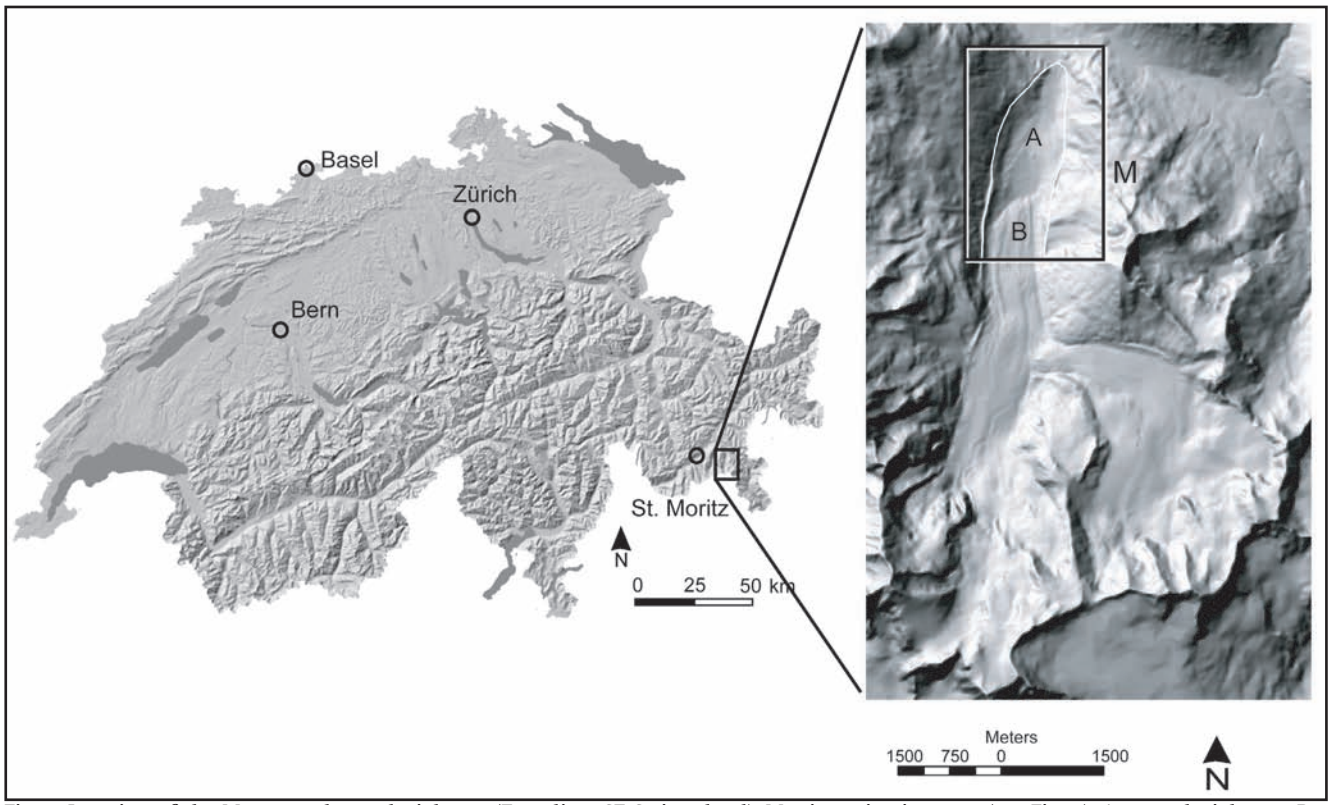

Fig. 1. Location of the Morteratsch proglacial area (Engadine, SE Switzerland). M = investigation area (see Fig. 2), A = proglacial area, B = Morteratsch glacier.

REFERENCES
Blum J.D., Klaue A., Nezat C.A., Driscoll C.T., Johnson C.E., Siccama T.G., Eagar C., Fahey T.j., Likens G.E. 2002: Mycorrhizal weathering of apatite as an important calcium source in base-poor forest ecosystems. Nature, 417, 729-731
Büchi H. 1994: Der variskische Magmatismus in der östlichen Bernina (Graubünden, Schweiz). Schweizerische Mineralogische und Petrographische Mitteilungen, 74, 359-371
Burga C. 1999: Vegetation development on the glacier forefield Morteratsch (Switzerland). Applied Vegetation Science, 2, 17-24
Egli M., Mirabella A., Fitze P. 2003: Formation rates of smectites derived from two Holocene chronosequences in the Swiss Alps. Geoderma, 117, 81-98
Mavris C., Egli M., Plötze M., Blum J.D., Mirabella A., Giaccai D., Haeberli W.: Initial stages of weathering ans soil formation in the Morteratsch proglacial area (Upper Engadine, Switzerland). Geoderma (submitted)

10.20

Regeneration of mechanically loaded soils under skid lanes by plantation of Alnus glutinosa

Meyer Christine[1], Lüscher Peter[1], Schulin Rainer[2]

[1] *Swiss Federal Institute for Forest, Snow and Landscape Research (WSL), Zürcherstrasse 111, CH-8903 Birmensdorf (christine.meyer@wsl.ch)*
[2]*Institute of Terrestrial Ecosystems (ITES), Universitätstrasse 22, CH-8092 Zürich*

After storm "Lothar" in 1999 serious soil damages resulted from clearance works with heavy timber machinery in many Swiss forests. In order to investigate how the regeneration of compacted soil could be enhanced, black alder (*Alnus glutinosa*) seedlings and willows (Fig. 1) were planted in 2003 in tracks of experimental skid lanes at three selected forest sites affected by storm “Lothar” (Habsburg, Messen and Brüttelen). As an additional treatment, compost was added to some of the planting sites.

This year we started to investigate root development and regeneration of soil structure at the Habsburg site, comparing planted plots with and without compost application with stocked reference sites. Next to selected trees we excavated a series of soil profiles (0.8 m depth, 1.5 m width), the first at 0.6 m distance to the stem, the second at 40 cm distance and the third at 20 cm distance, and the last directly at the stem base. On each profile, we recorded the numbers of fine and main roots, soil aggregate structure and hydromorphic soil features. Furthermore, we took soil samples with cylinders (1000 cc and 100 cc) for analysis of bulk density, precompaction stress, soil water content and air conductance.

The morphological evidence indicated that soil structure had considerably developed over the 6 years after the alders were planted. The alders planted in compacted soil had developed roots extending down to 80 cm depth and more, but also showing untypical morphological features such as flattened roots. Soil aggregation was enhanced in presence of trees, and soil hydromorphy reduced in comparison to control plots where no trees had been planted. In treatments with compost application the numbers of roots and their dry weights were highest and soil aggregation was enhanced most distinctly.

Next steps will be the analysis of soil physical, mechanical and chemical parameters. In combination with biological parameters we will use this information to identify the governing processes and limiting factors of soil structure regeneration, to evaluate the efficiency of the plantation and compost treatments and to derive estimates for the time required for full recovery.

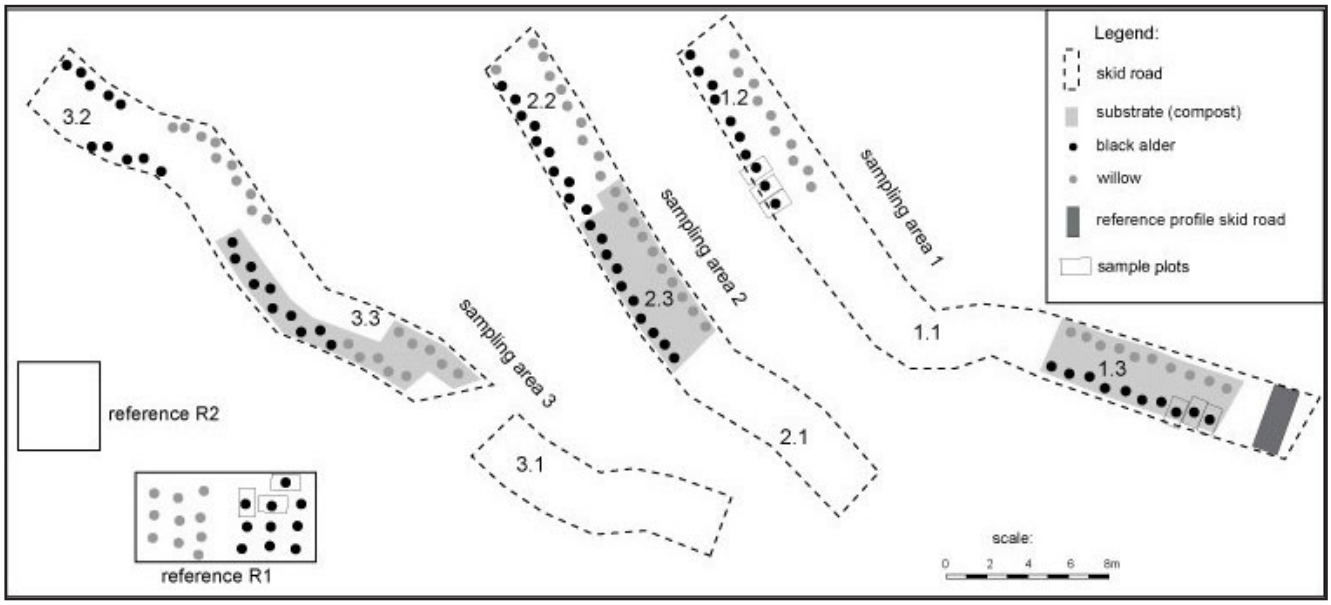

Figure 1. Schematic illustration of the experimental design at the study site Habsburg (Kt. Aargau).

Photograph 1. Black alders (left) and willows (right) planted in the tracks of a skid lane.

10.21

Characterization of biochar and their impact on soil fertility

Barbara Pichler[1], Hans-Peter Schmidt[2], Pascal Boivin[3] & Samuel Abiven[1]

[1]Geographisches Institut Universität Zürich, Winterthurerstrasse 190, CH-8057 Zürich (barbara.pichler@access.uzh.ch, samuel.abiven@geo.uzh.ch)
[2]Delinat-Institut, Ancienne Eglise 9, CH-1974 Arbaz (schmidt@delinat-institut.org)
[3]Laboratoire sols et substrats, Haute école du paysage, d'ingénierie et d'architecture de Genève, Rte de Presinge 150, CH-1254 Jussy (pascal.boivin@hesge.ch)

Biochar application to the soil has been proposed recently as a tool to improve soil fertility as well as to mitigate climate changes. Biochar is produced by the combustion of biomass under oxygen limited conditions. The production of biochar as well as their usage follows three main aims:

- The gas produced during the combustion can be used for energy (Syngas).
- The biochar will decompose very slowly into the soil and so might stabilise carbon on the long term.
- According to studies in Amazonian forest, the biochar might also improve soil fertility (nutrients and water retention).

In this study, we propose to investigate the effect of biochar on water retention.

Due to it porous structure, the biochar has a large specific surface area and might enhance for example water retention, soil aeration and the adsorption of nutrients and pesticides, thus limiting the leaching into the groundwater.

In March 2008 Delinat AG started a field study on SOC depleted vineyard soils in Valais (CH). 10 t biochar per hectar has been incorporated together with compost between the grape rows to a soil depth of 10 cm.
The compost has been applied with the aim to activate the biochar with organic matter. The application of biochar and compost was performed together with the sowing of legumes, in order to prevent erosion and serve as a N-source. Directly under the grape rows biochar has just been applied superficially.

Because of the poorly weathered, shallow soils, disturbed soil samples has been taken only from the upper 20 cm of the research patch mentioned above as well as from further reference patches, including:

- Bare vineyard soil without addition of biochar and compost and without coverage of legumes.
- Vineyard soil mixed with compost and covered with legumes.

Larger pieces of biochar particles, which have been found under the vine plants onto the soil surface also have been collected and analysed.
The soils of the different patches were sampled at the same altitude.

The water retention in soil was measured on disturbed samples of the fine fraction, following the procedure of Boivin et al., 2009: The dried soil samples were saturated to a water potential of -10 hPa. The saturated volume was measured using the plastic bag method. The samples were then dried in a shrinkage apparatus and their volume was measured again. At the end a shrinkage curve of the fine earth could be calculated to identify the pore-dependent water-storage capacity of the soil.
The biochar (pyrogenic carbon) content was estimated using the BPCA method (Brodowski et al., 2005). This method consists in an acid oxidation and determination of benzene polycarboxylic acids by chromatography. We also determined changes in soil organic matter quality using Diffuse Reflectance Infrared Fourier Transformation spectrometry. To determine the reactive surface area, BET specific surface area was measured using a gas absorber.

First results of the field study will be presented on the Swiss Geoscience Meeting 2009.

REFERENCES

Boivin, P., Schäffer, B. & Sturny, W. 2009: Quantification the relationship between soil organic carbon and soil physical properties using shrinkage modelling, European Journal of Soil Science, 60, 265-275.

Brodowski, S., Rodionov, A., Haumaier, L., Glaser, B. & Amelung, W. 2005: Revised black carbon assessment using benzene polycarboxylic acids, Organic Geochemistry, 36, 1299-1310.

10.22

Rock-Eval Pyrolysis to determine stable organic Matter in irrigated sandy Soils from Palm Orchards

Prudat Brice[1], Adatte Thierry[2], Hassouna Mohammad[2], Gobat Jean-Michel[1], Verrecchia Eric[2]

[1]*Laboratoire Sol & Végétation, Université de Neuchâtel, Rue Emile-Argand 11, CH-2009 Neuchâtel (brice.prudat@unine.ch)*
[2]*Laboratoire des Biogéosciences, Université de Lausanne, Anthropole, CH-1015 Lausanne*

Overuse of water resources is one of the most important problems in south Tunisia. In this area, palm orchards have the highest water consumption. Like in most soils, soil organic matter (SOM) in this irrigated agro-system has an important role in water efficiency, soil fertility and carbon storage. Consequently, understanding the way in which organic matter (OM) is integrated in sandy soils could be an approach to promote sustainable agriculture.
The aim of this study is to characterize stable SOM pools in sandy soils. Palm orchards constitute a pertinent experimental example because cultivators incorporate organic materials – mainly manure – into the soil every few years. Therefore, studying SOM in cultivated areas of different ages is interesting to estimate the stable OM pools present in these salty irrigated sandy soils.
Surface layer samples (0-20 cm) are sieved into different aggregate fractions in order to analyse OM. Then, SOM is extracted from all aggregate fractions as well as bulk soil, using a double extraction procedure - using 0.1M NaOH before and after treatment with 0.1M HCl - followed by an extraction on the residual fraction with a solution of DMSO/H_2SO_4. Finally, different analytical techniques are used to characterize (i) chemical extracts (Fourier Transform InfraRed spectroscopy (FTIR), Rock-Eval pyrolysis (RE), C/N ratio), (ii) the aggregate fractions (RE pyrolysis, C/N ratio) and (iii) the bulk soil (RE pyrolysis, C/N ratio).
Characteristics of peaks obtained using RE pyrolysis, coupled with FTIR spectra will give information on the structure of organic molecules present in the soils. The results obtained could help to understand the integration of OM in sandy soils. Understanding these processes would help to optimize the organic amendment quantities, qualities, and frequencies. Therefore, it would promote an increase in the farmers' incomes and the reduction of water losses in palm orchards.

10.23

Morphology and recent history of the Rhone River Delta in Lake Geneva (Switzerland and France)

Sastre Vincent[1], Loizeau Jean-Luc[1], Greinert Jens[2] , [3], Naudts Lieven[2], Arpagaus Philippe[1], Anselmetti Flavio[4] & Wildi Walter[1]

[1] *Institut F.-A. Forel, Université de Genève, 10, route de Suisse, CP 146, CH-1290 Versoix, Switzerland[1] .*
Corresponding author: walter.wildi@unige.ch
[2] *Renard Centre of Marine Geology, Department of Geology and Soil Science Ghent University, Krijgslaan 281 s.8 B-9000 Gent, Belgium*
[3] *New affiliation: Royal Netherlands Institute for Sea Research (NIOZ), P.O. Box 59, 1790 AB, Den Burg (Texel), The Netherlands*
[4] *Swiss Federal Institute of Aquatic Science & Technology (Eawag), Department of Surface Waters, Sedimentology Group, Überlandstrasse 133, CH-8600 Dübendorf, Switzerland*

The current topographic maps of the Rhone Delta - and of Lake Geneva in general - are mainly based on hydrographic data that were acquired during the time of F.-A. Forel at the end of the 19th century. In this paper we present results of a new bathymetric survey, based on single- and multibeam echosounder data. The new data, presented as a digital terrain model, show a well-structured lake bottom morphology, reflecting depositional and erosional processes that shape the lake floor. As a major geomorphologic element, the sub-aquatic Rhone Delta extends from the coastal platform to the depositional fans of the central plain of the lake at 310 m depth. The platform edge of the delta is cut by 9 canyons. These are sinuous ("meandering") channels formed by erosional and depositional processes, as indicated by the steep erosional canyon walls and the depositional levees on the canyon shoulders. The canyon bottoms and some slope areas are wrinkled by ripples or dune-like morphologies. Morphologies of the underlying bedrock and small local river deltas are located along the lateral slopes of Lake Geneva.
Based on historical maps, the recent history of the Rhone River connection to the sub-aquatic delta and the canyons is re-

constructed. The transition from three to two river branches dates to 1830 – 1840, when the river branch to the Le Bouveret lake bay was cut. The transition from two to one river branch corresponds to the achievement of the correction and dam construction work on the modern Rhone River channel between 1870 and 1880.

REFERENCE

Mallet, H. 1781 : Genève. Cote BPU 3 E 01/4.

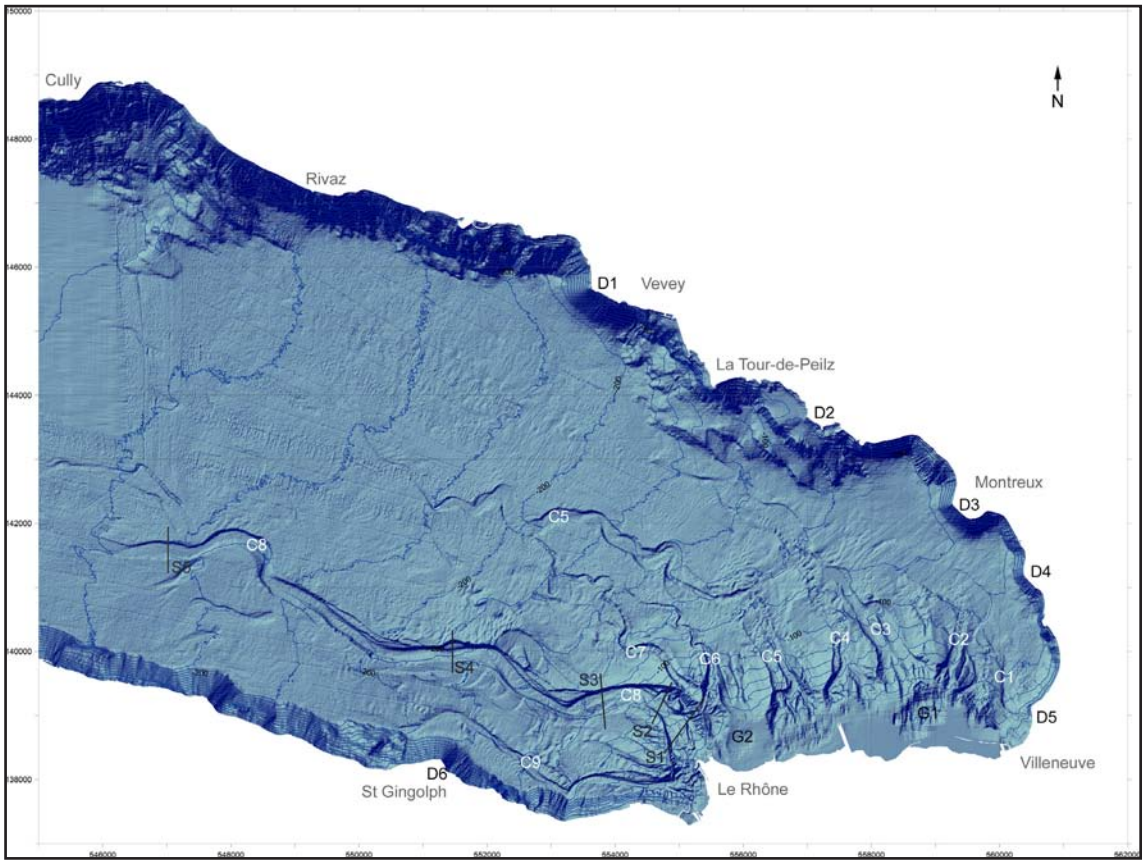

Figure 1. Topographic model of the Rhone River Delta in Lake Geneva, established by multi-beam and single-beam techniques.

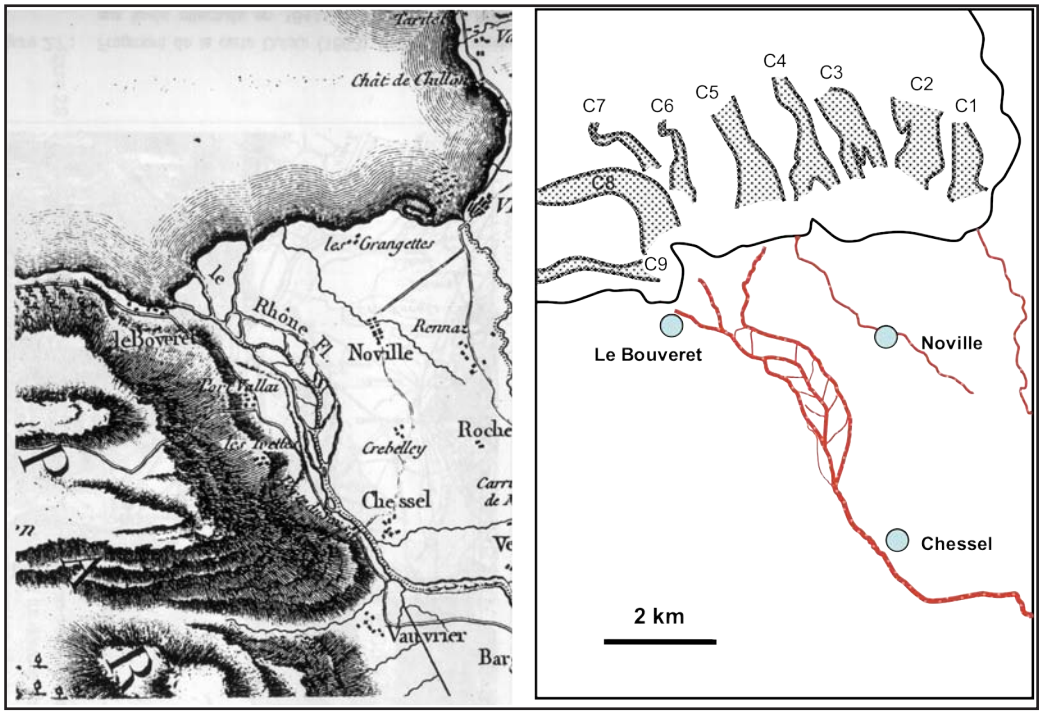

Figure 2: Map of the lower Rhone valley and the terrestrial part of the Rhone Delta by Mallet (1781), compared with modern coastline and canyons. EF: Eau Froide, FR: former bed of Rhone River flowing into the bay of Le Bouveret, RR: main Rhone River Bed, VR: Vieux Rhone.

10.24

Geomorphological drivers of Holocene environmental change in Mongolia

Wolfgang Schwanghart[1], Manfred Frechen[2], Riccardo Klinger[3] & Brigitta Schütt[3]

[1]*Department of Environmental Sciences, Physical Geography and Environmental Change, Klingelbergstr. 27, CH-4056 Basel (w.schwanghart@unibas.ch)*
[2]*Leibniz Institute for Applied Geosciences, Stilleweg 2, Section S3, Geochronology and Isotope Hydrology, D-30655 Hannover, Germany*
[3]*Department of Earth Sciences, Geographic Institute, Freie Universität Berlin, Malteserstr. 74-100, D-12249 Berlin, Germany*

Drylands are a major focus of palaeoclimatological and palaeoenvironmental research since the sensitivity of arid and semi-arid regions to climate change affects a large portion of the world's population. One of the most exciting regions in the world is Central Asia. Its situation in the triangle of the westerlies, the Indian and Southeast Asian Monsoon made it the playing field of the interactions of these windsystems (Fig. 1) during the Quaternary and beyond.

In this study we investigate the Holocene environmental evolution of the Ugii Nuur basin in the Orkhon Valley, central Mongolia, in order to gain a better understanding of the climate and landscape dynamics of the steppe region in Central Asia. We assessed terrestrial and lake sediments using mineralogical, geochemical and statistical techniques and provide absolute chronologies by radiocarbon and infra-red stimulated luminescence datings.

We provide a Holocene chronology of environmental changes and discuss these findings with regard to prehistoric and historic human activity, dominant geomorphological processes governing landscape evolution, and the regional environmental context (Schwanghart et al. 2009). Most prominently, loess deposition was intensified during the late Holocene. While the causes of wind blown dust need to be analyzed in a regional context, its hydrological and geomorphological implications are particularly strong at the local scale. These temporal and spatial interactions between aeolian and fluvial processes should be considered when reconstructing past environments in regions prone to loess deposition since they strongly affect the archives that we analyze.

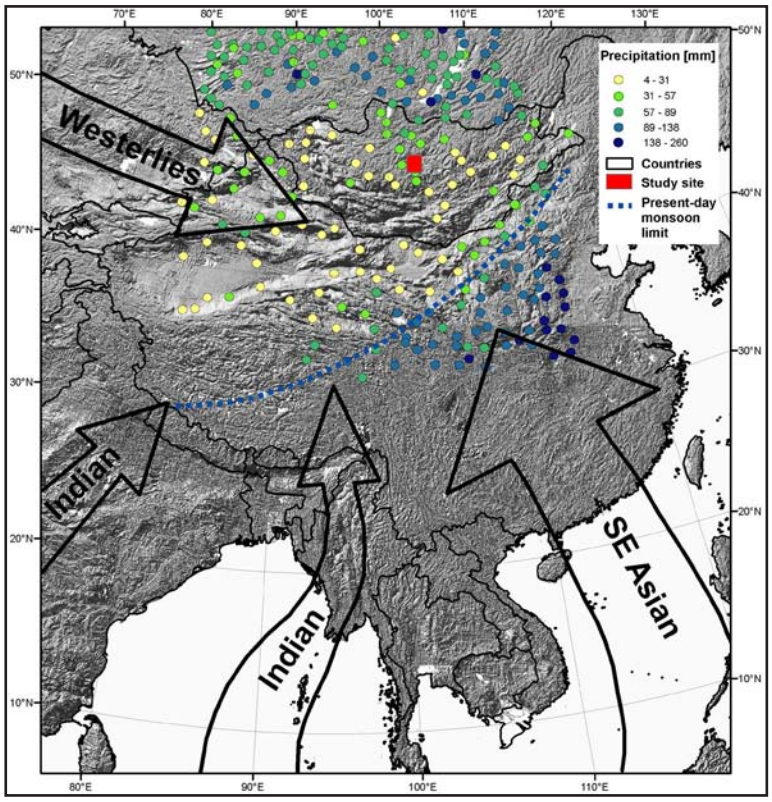

Fig. 1: Summer wind systems, mean july precipitation and present-day monsoon limit after Herzschuh (2006). Precipitation data is obtained from the GLOBALSOD database (1994-2004). Relief shading is based on GTOPO30.

REFERENCES

Schwanghart, W., Frechen, M., Kuhn, N.J. & Schütt, B. 2009: Holocene environmental changes in the Ugii Nuur basin, Mongolia. Palaeogeography, Palaeoclimatology, Palaeoecology, 279, 160-171.

Herzschuh, U. 2006: Palaeo-moisture evolution in monsoonal Central Asia during the last 50,000 years. Quaternary Science Reviews, 25, 1-2, 163-178.

10.25

Moisture and temperature effects of char in a forest soil

Singh Nimisha[1], Abiven Samuel[1], Boivin Pascal[2], & Schmidt Michael.W.I.[1]

[1]*Soil Science and Biogeography, Department of Geography, University of Zurich, Winterthurerstrasse 190, 8057 Zurich, Switzerland (nimisha.nimisha@geo.uzh.ch)*
[2] *hepia (haute ecole du paysage, de l'ingénierie et de l'architecture),150, route de Presinge CH-1254 Jussy/Geneve*

The application of fire-derived biomass (also called char or biochar) to soil is being considered as a long-term sink for atmospheric carbon dioxide in terrestrial ecosystems because of its slow turnover rate in the soil. The effect of char in increasing nutrient retention and crop production has been widely reported. Char is also known to affect physical properties of soil such as water retention and aggregation (Glaser et al., 2002), however, eventual significant changes in soil properties remains uncertain. Additionally, the adequate amount to positively impact soil quality without any serious environmental threats remains unknown (Lehmann et al., 2006). Nonetheless, it is important to realize that char stability and impact on soil properties depend on factors such as soil mineral composition, which is poorly understood. Thus, relating char amendments with soil properties requires careful evaluation (i) under field conditions in diverse soil types, (ii) under variable environmental conditions; and (iii) of the type of char used for achieving desired results.

We hypothesized that the water retention capacity of the soil would increase with increasing char content. Nevertheless, water retention capacity is dependent on soil mineralogy and could yield contradictory results (Tryon, 1948). Temperature and moisture are known important variables driving decomposition of soil organic matter and nutrient cycling among others. Consequently, any significant effect on these two soil properties might affect the C cycle on a global scale. The addition of char would darken the soil colour and could increase absorption of solar energy and soil temperatures (Krull et al., 2004); however, thermal property of soil is influenced by a combination of water content, soil texture and soil colour.

We are conducting a field-based study on the effect of different rates of application of char on the temperature and moisture content of the soil. The char used in the study is the reference char (initial substrate Castanea hardwood, pyrolysed at 450 °C under N_2 atmosphere) as used in the ring trial (Hammes et al., 2006). We use 15cm long (diameter = 10cm) mesocosms inserted in the soil, a Cambisol (clay 30%, org C. 4 %). The soil and char are well mixed and the rate of application of char to the mesocosms is 3, 6, 12, 24, 48 t C-char ha^{-1} respectively, in line with recent approaches for char mediated soil amendment.

The soil moisture content and temperature are monitored over a season (August to November) using sensors (ECH_2O-TE/EC-TM), installed at 5 cm depth inside the mesocosms and the data recorded every 30 minutes. At the end of the experiment, soil cores will be sampled and water retention curve will be determined on the undisturbed soil samples using exponential shrinkage model (Boivin et al., 2006).

This communication reports the first results of this study. The outcome of this study would facilitate in elucidating the quantitative assessment of the relationships between char application rate and the moisture content and temperature dynamics of the soil on a higher time resolution.

REFERENCES

Boivin, P., Garnier, P., and Vauclin, M. (2006). Modeling the soil shrinkage and water retention curves with the same equations. Soil Science Society of America Journal *70*, 1082-1093.

Glaser, B., Lehmann, J., and Zech, W. (2002). Ameliorating physical and chemical properties of highly weathered soils in the tropics with charcoal - a review. Biology and Fertility of Soils *35*, 219-230.

Hammes, K., Smernik, R.J., Skjemstad, J.O., Herzog, A., Vogt, U.F., and Schmidt, M.W.I. (2006). Synthesis and characterisation of laboratory-charred grass straw (Oryza saliva) and chestnut wood (Castanea sativa) as reference materials for black carbon quantification. Organic Geochemistry *37*, 1629-1633.

Krull, E.S., Skjemstad, J.O., and Baldock, J.A. (2004). Functions of soil organic matter and the effect on soil properties. In: Grains Research and development Corporation http://wwwgrdccomau/uploads/documents/cso000291pdf.

Lehmann, J., Gaunt, J., and Rondon, M. (2006). Bio-Char sequestration in terrestrial ecosystems- A review. Mitigation and Adaptation Strategies for Global Change *11*, 403-427.

Tryon, E.H. (1948). Effect of charcoal on certain physical, chemical, and biological properties of forest soils Ecological Monographs *18*, 81-115.

10.26

A tool to estimate fire intensity and chemical structure of black carbon inputs into soil

Studer Mirjam[1], Schneider Maximilian[1], Moreno José Manuel[2], Resco Victor [2] & Abiven Samuel [1]

[1]*Soil Science and Biogeography, Department of Geography, University of Zurich, Winterthurerstrasse 190 8057 Zürich, (samuel.abiven@geo.uzh.ch)*
[2] *Department of environmental science, University of Castilla – la Mancha, Toledo, Spain*

"Black Carbon" (BC) is becoming of increasing interest in soil science over the past few years. Black carbon is the residue of biomass pyrolysis, for example after a wildfire. Its contribution can represent up to 40 % of the organic matter in the soil (Preston & Schmidt, 2006). Global change models predict large increases in wildfire activity during the XXIst century, which would enhance BC contribution to the soil. BC was traditionally considered as an inert component of the soil carbon pool, until the recent observation that its decomposition and turnover are actually much higher than previously documented. Indeed, the chemical structure of BC largely depends on the conditions given during the combustion process. For example, higher temperature and lower oxygen content will lead to more condensed and probably more stable compounds.

The chemical structure of BC has been characterized by many different, often costly methods (Hammes et al., 2007). In this study we tried to develop a fast and cheap tool to characterize the black carbon chemical structure by predicting the burning temperature. This tool is based on an index calculated with Diffuse Reflectance Infrared Fourier Transform (DRIFT) spectroscopic measurements. First, we tried to propose an index based on lab-prepared samples. Then, we applied this index to samples from real wildfires.

Residues of pyrolysis from a woody (*Castanea sativa*) and a non-woody (*Oryza sativa*) species were used as standard to build up our index. The samples were pyrolised (N_2 fluxes without O_2) at temperatures of 200, 250, 275, 300, 350, 400, 500, 600, 700, 800, 900 and 1000 degree Celsius. The char was prepared according to the standard procedure described in Hammes et al. (2006). To relate the measurements to wildfires, residues of naturally burned Mediterranean shrubs (*Cistus ladanifer* and *Phillyrea latifolia*) were analysed (Pérez & Moreno 1998). The samples were collected across a gradient of fire intensity, estimated with the diameter of the remaining branches.
All samples were milled to a powder and mixed with dried KBr (3% sample). The analyses were performed with a Bruker TENSOR 27 DRIFT spectrometer. The spectra were normalized and peak regions, which varied with different burning temperatures, were identified (1510, 1420, 1320, 988 and 821cm^{-1}). To calculate the index the maximal peak height and the area of the peak regions were used.

Spectra of the lab-produced char showed a general flattening accompanied by rising absorbance with increasing burning temperatures. Samples >500°C have been shown to be highly condensed (Schneider, personal communication) and we hypothesised that the molecules might be too big and condensed for showing a strong and clear signal with DRIFT spectrometry. Within the spectra from 200 to 500°C changes of height in the selected peak regions could be observed. The resulting index predicted the burning temperature +/-50°C. Results were improved if the woody and non-woody species were analysed separately. The comparison of the lab-samples with the samples from the wildfires are ongoing and will be also presented.

REFERENCES

Hammes, K., Smernik, R.J., Skjemstad, J.O., Vogt, U.F., Schmidt, M.W.I. 2006: Synthesis and characterisation of laboratory-charred grass straw (Oryza sativa) and chestnut wood (Castanea sativa) as reference materials for black carbon quantification. Organic Geochemistry, 37, 1629-1633.

Hammes, K., Schmidt, M. W. I., Smernik, R. J., Currie, L. A., Ball, W. P., Nguyen, T. H., Louchouarn, P., Houel, S., Gustafsson, Ö., Elmquist, M., Cornelissen, G., Skjemstad, J. O., Masiello, C. A., Song, J., Peng, P., Mitra, S., Dunn, J. C., Hatcher, P. G., Hockaday, W. C., Smith, D. M., Hartkopf-Fröder, C., Böhmer, A., Lüer, B., Huebert, B. J., Amelung, W., Brodowski, S., Huang, L., Zhang, W., Gschwend, P. M., Flores-Cervantes, D. X., Largeau, C., Rouzaud, J.-N., Rumpel, C., Guggenberger, G., Kaiser, K., Rodionov, A., Gonzalez-Vila, F. J., Gonzalez-Perez, J. A., de la Rosa, J. M., Manning, D. A. C., López-Capél, E., Ding, L. 2007: Comparison of quantification methods to measure fire-derived (black/elemental) carbon in soils and sediments using reference materials from soil, water, sediment and the atmosphere, Global Biogeochemical Cycles, 21, GB2016.

Pérez, B. & Moreno J. M. 1998: Methods for quantifying fire severity in shrubland-fires. Plant Ecology, 139, 91-101.

Preston, C. M. & Schmidt, M. W. I. 2006: Black (pyrogenic) carbon: a synthesis of current knowledge and uncertainties with special consideration of boreal regions. Biogeosciences, 3, 397-420.

10.27

Hydration effects on microbial motility and coexistence on unsaturated rough surfaces

Gang Wang & Dani Or

Soil and Terrestrial Environmental Physics (STEP), Department of Environmental Sciences (D-UWIS), Swiss Federal Institute of Technology, Zurich (ETHZ), Universitaestrasse 16, CH-8092, Zurich
(gang.wang@env.ethz.ch)

Microbial motility is recognized as a key mechanism in biodiversity maintenance of ecosystem (Reichenbach et al. 2007), which plays a dominant role in most aspects of bioremediation, biochemical nutrient cycling, plant rhyzosphere, redox reactions and pathogen dispersal (Fenchel 2002; Madsen 2005). Quantitative description of microbial motility and other activities in soils is hindered by pore space complexity and hydration dynamics. Unsaturated conditions are common in nature (Barbara & Mitchell 2003), form fragmented aquatic habitats that are too small to support full immersion of microbes thereby forcing strong interactions with mineral surfaces, and result in significant restriction of microbial motility. A new hybrid model was developed to study the influence of surface hydration on microbial motility and its impact on species coexistence on unsaturated rough surfaces.

Simulations based on general parameter values from literature predict reduced colony expansion rates and correspondingly increased species coexistence time under drier conditions, which are in general agreement with experimental observations (Dechesne et al. 2008). Under matric potentials higher than -0.5 kPa (wet), microbial colonies grow fast at an average rate of colony expansion exceeding 421±94 μm/hr; the rate of colony expansion dropped to 31±10 μm/hr at -2 kPa and levelled at lower matric potentials; as expected, no significant colony expansion was observed at matric potential of -5 kPa because of the sub-micrometric and fragmented aquatic formation and the resulting capillary pinning forces. Drier conditions reduce motility and enhance coexistence of two competing species (indefinite coexistence for matric potentials lower than -2 kPa), conversely, no coexistence was found for matric potentials higher than -0.5 kPa. This study explores fundamental mechanisms of physical constraints of pore features and capillary pinning force on restricting microbial motility, hence affecting species coexistence on unsaturated rough surfaces. The finding of close dependence of species coexistence time on surface hydration (hence motility) also reflects the reduction of nutrient flux interception by the more competitive species, the restriction of spatial interactions and nutrient "shadowing" by rapidly expanding colonies under drier conditions that promote species co-existence on unsaturated rough surfaces.

REFERENCES

Barbara, G.M. & Mitchell, J.G. 2003: Marine bacterial organisation around point-like sources of amino acids. FEMS Microbiol. Ecol. 43, 99-109.

Dechesne, A., Or, D., Gulez, G. & Smets, B.F. 2008: The porous surface model, a novel experimental system for online quantitative observation of microbial processes under unsaturated conditions. Appl. Environ. Microb. 74, 5195-5200.

Fenchel, T. 2002: Microbial behavior in a heterogeneous world. Science 296, 1068-1071.

Madsen, E.L. 2005: Identifying microorganisms responsible for ecologically significant biogeochemical processes. Nat. Rev. Microbiol. 3, 439-446.

Reichenbach, T., Mobilia, M. & Frey, E. 2007: Mobility promotes and jeopardizes biodiversity in rock-paper-scissors games. Nature 448, 1046-1049.

11. Decision oriented modelling of the geosphere

H.-R. Egli, W. Haeberli, C. Hegg, O. Smrekar, M. Stauffacher

Swiss Academic Society for Environmental Research and Ecology (SAGUF)
Swiss Geographic Society, Swiss Geomorphological Society

11.1

Integrative hydro-geomorphologic modelling in alpine regions: scientific and operational challenges

Daniela Balin[1], Richard Metzger[2], Jean-Michel Fallot[1], Emmanuel Reynard[1]

[1] *Geography Institute, University of Lausanne, CH-1015 (daniela.balin@unil.ch)*
[2] *Geomatic and Risk Analysis Institute, University of Lausanne, CH-1015*

Hazard and risk assessment require, besides good data, good simulation capabilities to allow prediction of events and their consequences. Progresses have been done in building different modelling structures (conceptual and physically based, lumped and distributed) at different scales, with different amounts of input data and together with different calibration procedures.
Hazard assessment often requires involvement of decision makers and thus an important challenge is the evaluation of the credibility of the scientific results and the communication of the uncertainty.

The present study introduces an integrated approach based on the coupling of hydro-geomorphologic models, able to cope with uncertainty of input data and model parameters in order to perform a dynamic modelling in space and time of the main rainfall triggered hydro-geomorphologic processes.
The role of uncertainty as a tool to learn how input data could be used to evaluate different modelling structures at different scales has been also investigated.

The study region is represented by two small alpine catchments, the natural reserve of « Vallon de Nant » (13km^2) and the Tintaz catchment in the urbanised Verbier region. The hydrological model in this study is based on the Water Balance Simulation Model, WASIM-ETH (Schulla et al.,1997), a fully distributed hydrological model that has been successfully used previously in the alpine regions to simulate runoff, snowmelt, glacier melt, and soil erosion and impact of climate change on these. This model is intended to be coupled with slope stability methods to simulate the spatial distribution of the ini-

tiation areas of different geomorphic processes such as debris flows and rainfall triggered landslides.
To calibrate the WASIM-ETH model, the Monte Carlo Markov Chain Bayesian approach will be privileged (Balin, 2004, Schaefli et al., 200). Given that the spatial uncertainty of rainfall is an important factor of uncertainty in the hydrological modelling and given the high variability of the rainfall in alpine catchments, a quite dense network of meteorological stations has been implemented to better calibrate the hydrological model. Each step in the hydro-geomorphologic risk assessment undertakes uncertainty: evaluation of the main sources of uncertainty as well as the evaluation and communication of uncertainty is an important aspect of the proposed methodology. The Bayesian approach offers a good compromise between model efficiency and time consumption and represents a straightforward way to deal with different sources of uncertainty, as nowadays this is an important requirement of the decision makers involved in risk assessment.

REFERENCES

Balin, D. (2004). "Hydrological Behaviour through experimental and modelling approaches. Application to the Haute-Mentue catchment." Thèse EPFl n° 3007. Faculté Enac, EPFl, Lausanne, Suisse.

Schaefli B, Talamba Balin D., Musy A,.2007. "Quantifying hydrological modeling errors through a mixture of normal distributions" Journal of Hydrology 332 (3-4): 303-315

Schulla, J, Jasper, K. 1998/2000: „Modellbeschreibung WaSiM-ETH"; Institut für Geographie, ETH Zürich, 167 S.

11.2

Using predisposition factors for landslide hazard assessment: a new GIS-based methodology

Bilgot Séverine[1], Parriaux Aurèle[1]

[1] *EPFL ENAC IIC GEOLEP, Station 18, CH-1015 Lausanne (severine.bilgot@epfl.ch)*

Switzerland is exceptionally subjected to landslides; indeed, about 10% of its area is considered as unstable. Making this observation, its Department of the Environment (BAFU) introduced in 1997 a method to realize landslide hazard map. It is routinely used but, like most of the methods applied in Europe to map unstable areas, it is mainly based on the signs of previous or current phenomena (geomorphologic mapping, archive consultation, etc.) even though instabilities can appear where there is nothing to show that they existed earlier. Furthermore, the transcription from the geomorphologic map to the hazard map can vary according to the geologist or the geographer who realizes it: this method is affected by a certain lack of transparency and is not really efficient to forecast landslides.

The aim of this project is to introduce the bedrock of a new method for landslide hazard mapping; based on instability predisposition assessment, it involves the designation of main factors for landslide susceptibility, their integration in a GIS to calculate a landslide predisposition index and the implementation of new methods to evaluate these factors; to be competitive, these process will have to be both cheap and quick.

After showing that cohesion and hydraulic conductivity of loose materials were strongly linked to their granulometry and plasticity index, we implemented two new field tests, one based on teledetection and one coupled sedimentometric and blue methylen tests to evaluate these parameters. The hydraulic conductivity of fractured rocks was obtained from the analysis of their geometrical properties (fractures density, aperture size and orientation). The other factors were extracted from DEM and hydrologic mapping.

We added a last factor related to the predisposition of the geotype (new classification for geologic formations, based on genetic standards for loose material and on lithologic standards for hard rock) to slope instability process: the latter enabled us to integrate attributes proper to each geotypes (over-consolidation for ground moraines, stratifications for glaciolacustrine deposits, etc...) and which would be long and complex to integrate to a GIS.

Afterward, we implemented an ArcGis® toolbox allowing to lead to a landslide susceptibility index. Finally, we applied this methodology (from field survey to GIS operations) to ten sites in different contexts in Switzerland.
This new methodology can be considered as a cheap and efficient way to forecast landslides.

REFERENCES

Lateltin, O.: Prise en compte des dangers dus aux mouvements de terrain dans le cadre des activités de l'aménagement du

territoire. OFAT, OFEE, OFEFP, 1997.

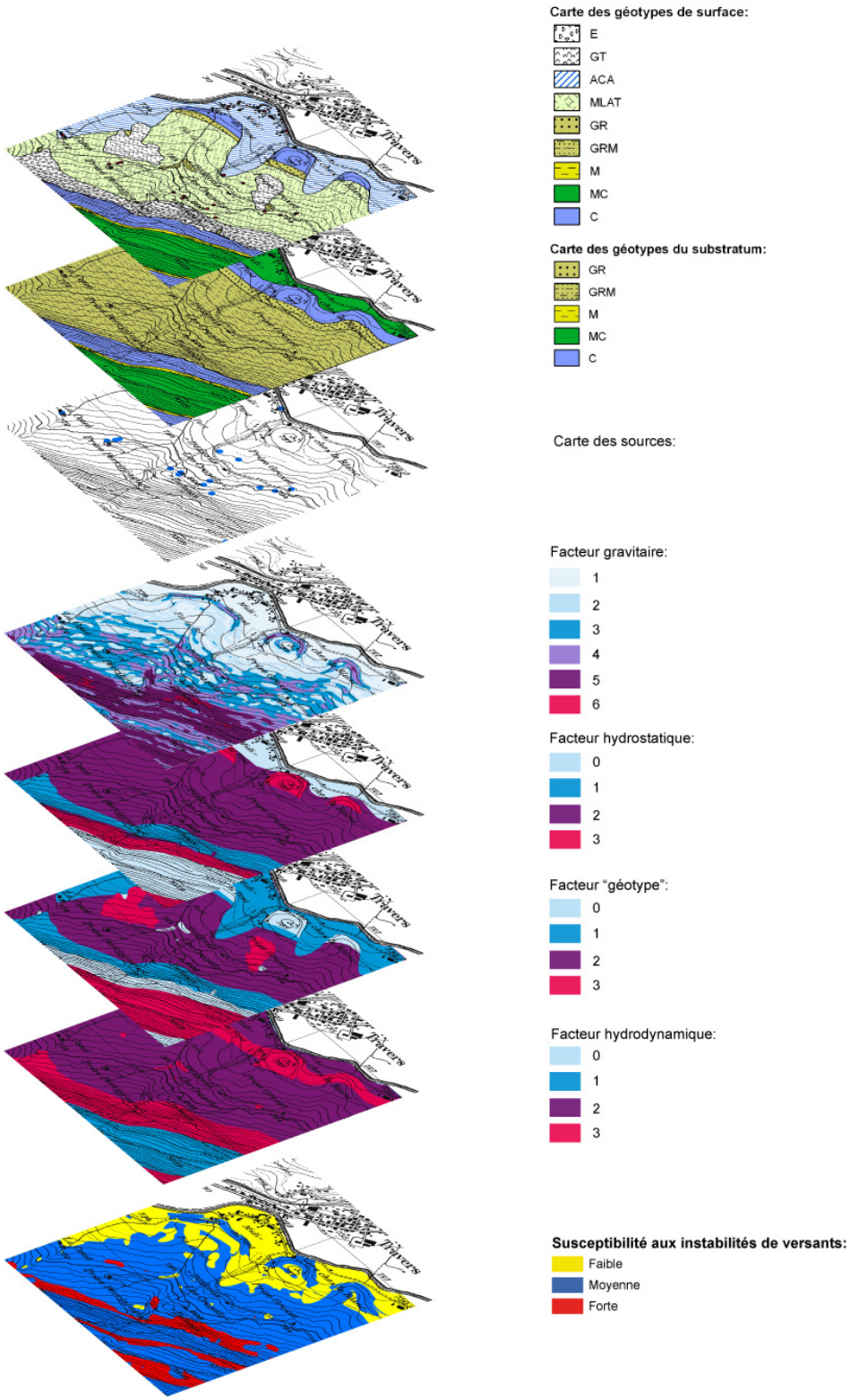

Figure 1. Application to the Travers landslide

11.3
Integrative modelling of pesticide use in developing countries

Binder Claudia R.[1 2], Feola Giuseppe[1], Garcia-Santos Glenda[1], Yang, Jing[1]

[1] *Department of Geography, University of Zurich*
[2] *Institute for System Science Innovation and Sustainability Research, University of Graz, Austria*

The livelihood of small farmers in developing countries depends on their ability to employ ecologically and economically sound production methods. While properly applied pesticides reduce yield losses up to 40% and improve product quality, their misuse might cause serious human health and environmental problems. The World Health Organization (WHO) (1990a) estimates an annual worldwide total of 3 million cases of acute poisoning with 220,000 deaths.
One of the central questions is why, despite all the efforts being made in research, no significant improvements in understanding and modeling farmers' decision-making and connecting it to environmental and human health impacts have been made. Antle et al. (2001) state that one of the reasons is the segregated disciplinary research which leads to the problem that different scientific investigations cannot be linked to provide a system understanding that includes social and natural science variables. However, this understanding is indispensable for science models that provide a sound system understanding and thus, results that are comprehensible and useful for policy makers.

This paper presents an integrative modelling approach to simulate and assess the effect of measures for reducing the human health and environmental risks from pesticide use. Figure 1 shows the conceptual approach underlying the model building process and the methods used thereby.

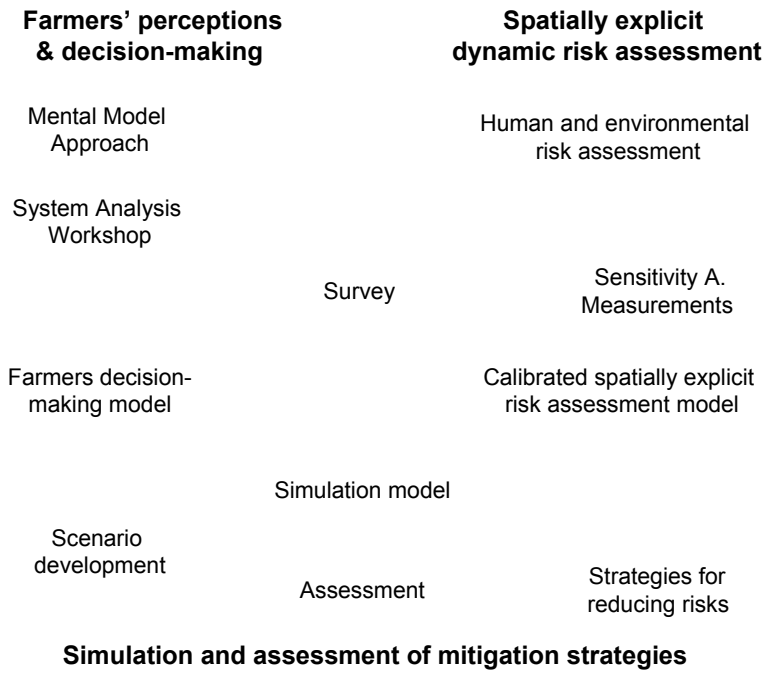

Figure 1. Methodological approach taken for designed the simulation model in the research project. Methods with [1] transdisciplinary methods

The simulation model is composed of two sub-models a farmers decision-making model and a spatially explicit risk assessment model. **Farmers' decision-making model** determines the amount and type of pesticide used and the type and frequency of usage of protective equipment during application. This model is based on a preliminary transdisciplinary analysis of farmers' perceptions on the potential risks of pesticide application and their system view (Schoell & Binder, 2009) and the Integrated Agent Centred (IAC) Framework (Feola & Binder, 2009). Results regarding the use or non use of protective equipment show that the variables mostly affecting this decision were (i) the perception of equipments' comfort, (ii) the practice of reading labels, (iii) the descriptive social norms and (iv) the perceived health impact (Feola and Binder, accepted). The third and fourth variable allow for defining a dynamic model which specifically includes feedback mechanisms as the effect of individual action on social norm.

The **spatially explicit risk assessment model** includes environmental as well as human health related processes and was developed to be spatially explicit. A combination of already existing models and their adaptation was chosen to simulate the fate and risk of the pesticides applied. The necessary input values for the model e.g. pesticide types, physical and chemical properties and pesticide application dates were obtained in the survey 2007. The survey included the spatially explicit application pattern by farmers, linking so the behavioural part with the spatially explicit risk assessment. Specific characteristics of the active ingredients were obtained from literature. The transfer-coefficients to the environmental compartments air, water, soil and plant as well as onto the farmer were obtained empirically using the WSP-uranine extraction.

The presentation will focus on the methodological approach taken highlighting the advantages of performing out-front transdisiplinary research to determine the main variables relevant for the system.

REFERENCES

Feola G. & Binder C.R. Theory paper – which do you want to cite??
Feola G. & Binder C.R. Why don't pesticide applicators protect themselves? Exploring the use of Personal Protective Equipment among Colombian smallholders. International Journal of Occupational and Environmental Health, in press.
Schöll R. &, Binder C.R., Comparing System Visions of Farmers and Experts, Futures, in press.
Schöll R. & Binder C.R., 2009, System perspectives of experts and farmers regarding the role of livelihood assets: Results from a Structured Mental Model Approach, Journal of Risk Analysis, 29 (2): 205-222.
WHO 1990b Safe use of pesticides. Fourteenth report of the WHO Expert Committee on Vector Biology andControl. Geneva, World Health Organization, 1990 (WHO Technical Report Series, No. 813).

11.4

A clustering method for uncertainty quantification applied to CO2 sequestration

Durrande Nicolas[1], Renard Philippe[2], Ginsbourger David[1],[2]

[1] Dep. of mathematics, Ecole des Mines de Saint-Etienne – 29 rue Ponchardier 42000 Saint-Etienne France, (durrande@emse.fr)
[2] Centre of hydrogeology and geothermics, University of Neuchâtel – Rue Emile-Argand 11, CH - 2009 Neuchâtel - Switzerland (philippe.renard@unine.ch, david.ginsbourger@unine.ch)

In order to reduce the atmospheric emission of CO_2 due to human activities, one possibility is to store CO_2 in geological reservoirs. The principle is to extract the CO_2 produced by a polluting factory (a coal fired power plant for instance) and to inject it into a geological reservoir such as a deep saline aquifer. If the caprock's quality is good, the CO_2 will be trapped and will progressively turn into sediments.

To decide upon the viability of such project, one of the main challenges is to quantify the risk of CO_2 leakage. As all the leakage scenarii depend on the growth of the CO_2 plume, it is necessary to study its expansion by numerical simulation (Fig. 1). However, the inputs of the simulation (permeability and porosity fields) are random, and simulating one single injection scheme with a finite volume method accounting the proper equation of states for supercritical CO2 takes around 2 days (20 years of injection with a 2 dimensional model).

As classical Monte-Carlo methods are unaffordable, the method we use here is as described by Caers in [1]. The aim is to select a limited number of simulation runs by applying a non intrusive method based on a proxy simulator (cheap-to-evaluate low-fidelity model). Following [2], kernel methods are used in order to linearize the data, which is supposed to improve the clustering procedure. The method consists of 5 steps:

- Generate *n* fields of permeability and porosity
- Use a proxy simulator to compute the n approximate solutions
- Define a distance between the solutions and create a mapping. This transformation may be based on kernel methods for greater linearity.
- Find *N* centres of clusters
- Run the simulator for the *N* selected points.

The flow simulation is performed using the software Tough2 with a 1 Mt/y injection rate during 20 years. The proxy simulator is a shorten Tough2 simulation of a 1 year injection. The number of initial fields generated is n=100 and the number of complete simulations is N=10. In order to evaluate the efficiency of our method, we perform a classical Monte-Carlo analysis using 100 complete simulations. The results are shown on Figure 2:

This work illustrates that proxy simulators can be used to efficiently select representative simulations. Here the CPU simulation time can be divided by one order of magnitude while keeping good estimates of the probability of presence of CO_2. However the distance definition seems to have a great impact on the final results. Future works may focus on the issue of selecting well-suited distances for importance sampling.

More generally, the proposed approach allows to improve the efficiency of large scale and complex modelling under uncertainty for decision making.

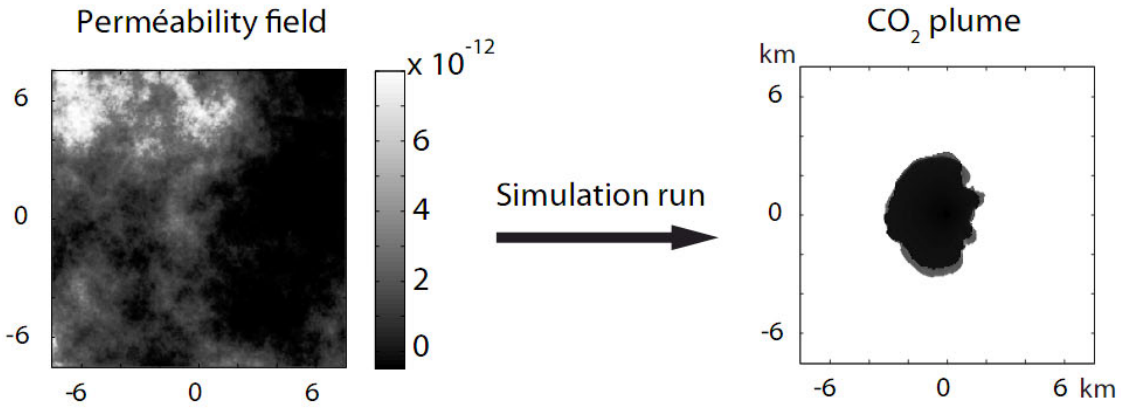

Figure 1. Example of permeability field and result of a 20 years injection

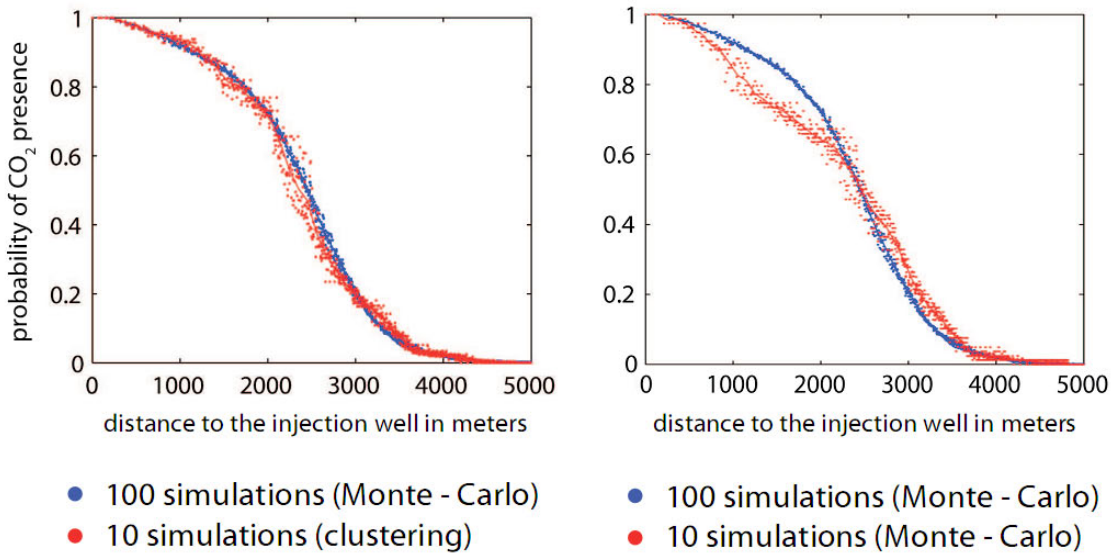

Figure 2. Comparison between clustering method and Monte – Carlo

REFERENCES

[1] J. Caers. 2008 - Distance-based stochastic modelling : theory and applications. Technical Report 21, Stanford University, Energy resources Engineering Dep

[2] C. Scheidt, J. Caers. 2008 - Uncertainty quantification using distances and kernel methods - application to a deepwater turbidite reservoir. Technical report, Stanford University, Energy resources Engineering Dep

[3] V. Vapnik. 1995 - The Nature of Statistical Learning Theory. Springer

11.5

4D information on climate-driven geosystem changes in high mountain areas - experiences and perspectives.

Wilfried Haeberli[1]

[1]Glaciology, Geomorphodynamics & Geochronology, Geography Department, University of Zurich

Integrated geoinformation systems combining data, models and scenarios are increasingly needed to anticipate developments of complex geosystems beyond the empirical knowledge basis from the past. Such geoinformation systems primarily provide an overview of the available knowledge and understanding concerning the most important processes, subsystems and their potential interactions. As a consequence of often incomplete or even missing (spatiotemporal) information, they must apply relatively simple and robust models, which need examination by more sophisticated process-oriented models. They render the corresponding scientific reflection (assumptions, hypotheses, scenarios) transparent, quantify results in the space and time domain and indicate knowledge gaps. Perhaps most importantly, they demonstrate the usefulness of, and the need for, considering complex systems and longer time scales. However, they are - and will always be - far from perfect and need continuous development in view of ongoing rapid changes in nature, technology and scientific understanding. Models of abiotic subsystems such as snow and ice conditions, water supply or hazards from rock falls, debris flows, avalanches and floods are already well advanced and useful. Biotic subsystems – especially vegetation as related to climate change, ice vanishing and effects of grazing – are less well covered by robust spatial models applicable in high-mountain topography: an urgent research need. Experiences are presented from a case study carried out in the Upper Engadin, eastern Swiss Alps, within the framework of the NRP48 and perspectives will be discussed in view of new lakes forming in rapidly deglaciating mountain ranges.

11.6

Simulation-based risk assessment of superimposed groundwater salinisation processes

Ellen Milnes[1]

[1]*Centre d'hydroéologie CHYN, Université de Neuchâtel, Rue Emile-Argand 11. CH- 2007-Neuchâtel*

Groundwater salinisation is a world-wide major groundwater contamination issue and is related to multiple processes, such as seawater intrusion, agrochemical pollution, geogenic contamination and irrigation-induced pollution. In salinity affected aquifers, the observed concentration of total dissolved solids may result from the superposition of several salinisation processes. In areas affected by groundwater salinisation, correct identification of the spatial distribution and dynamic interplay of the super-imposed salinity components is crucial, since the respective remedial or conservation measures may be entirely different.

Identification of different origins of salinisation can be considered a separate field in hydrogeological research and is efficiently addressed by means various hydrogeochemical techniques (e.g. Custodio, 1997; Vengosh et al., 1999). As opposed to simple salinity measurements, sophisticated techniques that yield clear information about the origin of salinity are often costly and usually only yield snap-shots in time and space. Combining information on the origins of salinity from such investigations with numerical simulations is therefore a promising strategy to investigate the interplay between different salinisation processes.

Vulnerability and risk assessments are becoming a standard approach in groundwater management when dealing with water quality and contamination issues. The most commonly used vulnerability mapping procedures are based on empirical point rating systems that bring together key factors. It has been found that the vulnerability and contamination risk can rarely be predicted with these key factors which is why there is a growing need for physically based risk and vulnerability assessments (Gogu & Dassargues 2000).

A simulation-based salinisation risk assessment methodology is proposed that allows mapping of areas at risk with respect to different salinisation processes. A numerical groundwater simulation procedure is presented which allows decomposition of a measured bulk salinity distribution into components derived from different salinisation processes. In a first step, a numerical groundwater flow and transport model accounting for all identified salinisation processes is calibrated, using the observed salinity distribution. Then, the observed salinity distribution is replaced by the simulated salinity distribution. By adapting the boundary conditions of the model each salinisation process can then be simulated separately. The simulation results are then used to obtain risk index distributions for each salinisation process, reflecting the spatial variation of possible future relative salinity increase with respect to a given process. In the last step, these risk index distributions are then overlain with defined threshold salinities, revealing areas requiring remediation or conservation measures.

The different steps of the salinisation risk mapping procedure are illustrated on a real aquifer system in Southern Cyprus (Akrotiri), where three major salinisation processes are superimposed (seawater intrusion, evaporation and irrigation-induced salinisation), revealing the possible usefulness in groundwater management decision-making process.

REFERENCES

Custodio, E. 1997 : Studying, monitoring and controlling seawater intrusion in coastal areas. In: Guidelines for Study, Monitoring and Control, FAO Water Reports 7-23, 11(1).

Gogu, R. C. & Dassargues, A., 2000 : Curent trends and future challenges in groundwater vulnerability assessment using overly and index methods. 549-559. Environmental Geology 39(6).

Vengosh, A., Spivack A., Artzi Y., Avner A. 1999: Geochemical and boron, strontium and oxygen isotopic constraints on the origin of the salinity in groundwater from the Mediterranean coast of Israel. Water Resources Research 35 (6), 1877-1894.

11.7

The Road to Climate Stabilization: Insights from Carbon Cycle - Climate Models

Gian-Kasper Plattner[1]

[1]*Climate and Environmental Physics, Physics Institute, University of Bern & IPCC WGI TSU, University of Bern*

The UN Framework Convention on Climate Change calls for "stabilization of greenhouse gas concentrations in the atmosphere at a level that would prevent dangerous interference with the climate system". Future climate stabilization will ultimately require stabilization of atmospheric greenhouse gas concentrations and substantial reductions in anthropogenic greenhouse gas emissions compared to present-day emissions. For CO2, the most important anthropogenic greenhouse gas, the amount of carbon emissions that can be released in order to reach a given CO2 stabilization target (i.e. the "allowable" emissions) will depend on how much of the extra CO2 will be removed from the atmosphere by natural CO2 sinks, mainly the oceans and the land biosphere. Ocean and land biosphere currently remove about 50% of the man-made annual CO2 emissions, and thereby substantially helped mitigating the rise in atmospheric CO2 over the last 200 years. Unfortunately, these natural sinks can not be expected to continue forever. Observational evidence and evidence from coupled climate - carbon cycle models suggest that increasing CO2 levels and climate change will likely decrease the ability of the natural system to take up extra CO2 in the future, leaving larger fractions of the anthropogenic CO2 emissions in the atmosphere, and therefore further raising CO2 levels and accelerating climate change. The reductions in global carbon emissions for a given CO2 stabilization target thus needs to be substantially larger if carbon cycle - climate feedbacks are accounted for. In my presentation, I will (1) quantify the impact of carbon cycle - climate feedbacks on the projected "allowable" emission for CO2/Climate stabilization in the current generation of carbon cycle - climate models and (2) highlight uncertainties in the model representation of carbon cycle processes resulting in substantial spread in both the model response to increasing atmospheric CO2 and climate change.

11.8

Seasonal climate predictions: From theory to end-user applications

Andreas Weigel[1]

[1]*Federal Department of Home Affairs FDHA Federal Office of Meteorology and Climatology MeteoSwiss, Zurich*

Seasonal forecasting, i.e. the provision of information on the expected tendency of the climate of the coming months and seasons, has become a well-established technique with applications world-wide. Indeed, seasonal forecasts are successfully applied for climate-risk management in many climate-sensitive sectors such as energy, health, water management, agriculture and the insurance industry.

Since 2005, MeteoSwiss issues seasonal forecasts on an operational basis, both for the public and for private customers. However, due to the wide range of uncertainties involved, seasonal climate predictions are inherently probabilistic, requiring significant efforts both from forecast providers and users. While the former need to make sure that the uncertainties are appropriately quantified and communicated, it is the task of the latter to make optimum use the uncertainty information provided. For applications in central Europe, these challenges are further aggravated by the fact that the prediction skill is very low in this region, i.e. that the predictable climate signal is often very weak in comparison to the unpredictable noise.

In this presentation, an overview of our experience gained in the field of seasonal forecasting will be presented. In particular, the following issues will be discussed and illustrated with examples: (i) How can the uncertainty range of climate predictions be accurately determined? (ii) How can the uncertainties and the prediction skill of seasonal forecasts be accurately communicated to the user community? And finally: (iii) How can seasonal forecasts be successfully applied, even if the prediction skill is very low?